JOURNAL OF
CHROMATOGRAPHY A
INCLUDING ELECTROPHORESIS AND OTHER SEPARATION METHODS

ELSEVIER

JOURNAL OF
CHROMATOGRAPHY A
INCLUDING ELECTROPHORESIS AND OTHER SEPARATION METHODS

ELSEVIER
Amsterdam – Lausanne – New York – Oxford – Shannon – Tokyo

SEVENTH INTERNATIONAL SYMPOSIUM ON HIGH PERFORMANCE CAPILLARY ELECTROPHORESIS

Würzburg (Germany), 29 January–2 February 1995

Guest Editor

H. ENGELHARDT

(Saarbrücken, Germany)

The articles submitted for the Symposium Volumes on the *7th International Symposium on High Performance Capillary Electrophoresis* are published in two consecutive Volumes of the *Journal of Chromatography A*, Vols. 716 and 717 (1995). The Foreword only appears in Vol. 716. A combined Author Index to both Vols. 716 and 717 only appears in Vol. 717.

JOURNAL OF CHROMATOGRAPHY A

CONTENTS

7TH INTERNATIONAL SYMPOSIUM ON HIGH PERFORMANCE CAPILLARY ELECTROPHORESIS, WÜRZBURG, 29 JANUARY–2 FEBRUARY 1995, PART II

PROTEINS

NUCLEIC ACIDS AND THEIR STRUCTURE

SYNTHETIC DYES

DRUGS, METABOLITES AND PHARMACOKINETIC STUDIES

CONTENTS

Capillary electrophoretic separation of proteins using stable, hydrophilic poly(acryloylaminoethoxyethanol)-coated columns

Marcella Chiari[a]*, Marina Nesi[a], Junior E. Sandoval[b], Joseph J. Pesek[b]

[a]Istituto di Chimica degli Ormoni CNR, Via Mario Bianco 9, 20131 Milan, Italy
[b]Department of Chemistry, San Jose State University, San Jose, CA 95192, USA

Abstract

Capillary electrophoretic separations of high efficiency and resolution were obtained using poly-(acryloylaminoethoxyethanol)-coated capillaries. The polymer was covalently attached to a silica surface previously modified with a α-methacryloxylpropyl functionality. The latter was realized by catalytic hydrosilylation of allyl methacrylate on an SiH-modified fused-silica capillary. The lifetime of the new type of coating used at pH 8.5 was more than twice that of conventional polyacrylamide.

1. Introduction

Capillary electrophoresis is becoming an important tool in the separation and characterization of macromolecules with potentially high efficiency and resolution and automation possibilities. However, the efficiency and reproducibility of capillary columns are in practice significantly lower than those predicted by theory [1,2]. Band-broadening effects occur when large macromolecules distribute themselves between the liquid and the wall; weak reversible interactions strongly affect efficiency while moderate adsorption can impair peak shapes, leading to poor reproducibility. Proteins, having more binding sites, tend to interact with surfaces in different ways and, in uncoated capillaries, characterized by a large surface-to-volume ratio, electrostatic interactions between the limited amount of injected samples and the large surface may play the most important role.

There are several ways to control electroosmotic flow and adsorption: (a) buffer changes, high or low pH [3–6], high salt concentrations [7,8] and additives [9–13], (b) adsorption of neutral or charged macromolecules on the wall [14,15] and (c) chemically bonded phases. Regarding the last point, capillaries with covalently bonded polymers are generally obtained by organosilanization, a surface modification procedure derived from the "silane coupling" methodology which has been successfully transferred to capillary electrophoresis. In a general reaction scheme, an organosilane reagent yields an Si–R functionality attached to the support through an Si–O–Si–C– (siloxane) linkage. The R group contains an active functionality which permits the covalent attachment of a polymeric coating. Bruin et al. [16] described glycidoxy-derivatized capillaries to which polyethylene glycol (PEG) 600 was anchored in order to decrease the influence of wall adsorption. PEG-600-modified

capillaries were used to separate alkaline proteins in acidic buffers, but they are not useful in the more interesting intermediate pH range.

Towns et al. [17] reported diol–epoxy coatings of sufficient thickness and hydrophilicity to reduce protein adsorption. These coatings are stable in both acidic and basic conditions and the electroosmotic flow (EOF) is strong enough to carry both cationic and anionic species past the detector. Although these coatings appear attractive, there are some problems related to the synthesis which limit their applicability. A gradual increase in the EOF was observed during their use; this problem is attributed to the formation of aldehyde groups during the BF_3-catalyzed cross-linking step. With time, these groups oxidize to a carboxyl group and increase the negative charge on the capillary wall. Another drawback is related to the nature of the catalyst: boron trifluoride in the form of vapor from an etherate solution is passed through the capillary in a stream of nitrogen to cross-link the oxiranes: delivery of the catalyst in the gas phase limits the length of capillary that can be prepared during the cross-linking step. Nashabeh and El Rassi [18] developed coatings having hydroxylated polyether functions bonded to the surface. These types of coatings, referred to as interlocked or fuzzy coatings, were used in the separation of alkaline proteins at pH 6 or 7.

Among the different types of polymeric phases, polyacrylamide-coated columns appear to be able to suppress electroosmosis to a negligible value. Columns with negligible electroosmosis have broad applicability in separations with polymer networks and in isoelectric focusing; migration times and efficiency are higher when electroosmotic flow is completely suppressed. As early as 1985, Hjertén [2] proposed coating the surface with covalently bonded polyacrylamide strings linked to the wall through γ-(methacryloxy)propylsilyl groups. There are, however, some limitations to the stability of this phase with time. In an effort to overcome this problem, Cobb et al. [19] reported a capillary procedure by which a direct Si–C linkage is formed by sequentially reacting silica with thionyl chloride and the Grignard reagent vinylmagnesium bromide. Linear polyacrylamide is attached to the silica via stable Si–C bonds. Sandoval and Pesek [20] proposed an alternative to a Grignard reagent for the formation of Si–C linkages on silica surfaces. They used catalytic hydrosilylation of olefins on a SiH-containing substrate. In addition to a superior hydrolytic stability, olefin hydrosilylation provides the option of preparing γ-methacryloxypropyl-modified surfaces [21,22] suitable for copolymerization with acrylamide and derivatives.

Excellent results in protein separations with regard to efficiency, peak symmetry and reproducibility were obtained by Schmalzing et al. [23] using a synthetic polyvinylmethylsiloxane diol with a cross-linker, the chemical structure of which is unfortunately unknown. They obtained a polymeric film containing vinyl double bonds, incorporated in polyacrylamide chains cross-linked with formaldehyde.

Polyacrylamide coatings when used at a pH higher than 8.5 show an increase in EOF with time, resulting from partial hydrolysis of the amido bonds. N-Mono- and -disubstituted acrylamide are known to be more stable to hydrolysis; the presence of a long, flexible alkyl chain is capable of protecting the amido plane as it can fluctuate in the nearby space and shroud the amido group. In addition, a number of papers have dealt with the problem of limited stability of siloxane linkages [24,25]. In order to overcome both problems, we have proposed a stable coating which combines the superior hydrolytic stability of an N-substituted acrylamide monomer, namely acryloylaminoethoxyethanol [26,27], with the enhanced surface attachment derived from direct Si–C linkages on the silica surface [19–22].

2. Experimental

2.1. Materials

3-(Morpholino)propanesulfonic acid (MOPS), tris(hydroxymethyl)aminomethane (Tris), N,N-bis(2-hydroxyethyl)glycine (bicine), α-chymotrypsinogen A, β-lactoglobulin from bovine

milk, trypsin from bovine pancreas, trypsin in-
hibitor from soybean, myoglobin from horse
skeletal muscle, trypsinogen from bovine pan-
creas and α-lactalbumin from bovine milk were
purchased from Sigma (St. Louis, MO, USA).
Lysozyme from hen egg white and ribonu-
clease A from bovine pancreas were obtained
from Boehringer (Mannheim, Germany), sper-
mine and 3-(trimethoxysilyl)propyl methacrylate
from Aldrich Chemie (Steinheim, Germany),
acrylamide, ammonium peroxodisulfate
and N,N,N',N'-tetramethylethylenediamine
(TEMED) from Bio-Rad Labs. (Hercules, CA,
USA) and methylcellulose of low molecular mass
(Methocel Premium Grade) from Dow Chemical
(Midland, MI, USA). Water and all the other
reagents were of analytical-reagent grade. N-
Acryloylaminoethoxyethanol (AAEE) was syn-
thesized as described by Chiari et al. [26].

2.2. Methods

CZE separations were performed in a Waters
Quanta 4000 capillary electrophoresis system
(Millipore, Milford, MA, USA) and in a Spec-
tra-Phoresis 1000 capillary system (Thermo
Separation Products, Freemont, CA, USA).
Data collection was performed on a PC com-
puter utilizing SW-Phoresis 1000 software. In all
the experiments, 75 μm I.D. fused-silica capil-
laries (Polymicro Technologies, Phoenix, AZ,
USA) coated by the methods described below
were used. Proteins and benzyl alcohol, used as
marker of electroosmosis, were detected at 214
nm. Protein stock solutions (10 mg/ml) were
prepared in water and diluted to the final con-
centration just before the injection. Between
runs the column was rinsed by hydrodynamic
pressure with the separation buffer for 2 min.
Electroosmotic flow was measured at 600 V/cm
in 25 mM bicine–Tris buffer (pH 8.5). The
samples were injected using hydrodynamic pres-
sure for 0.5 s.

2.3. Separation conditions

Separation of the alkaline proteins lysozyme
(0.5 mg/ml), ribonuclease A (0.6 mg/ml),

trypsinogen (0.5 mg/ml), α-chymotrypsinogen
(0.5 mg/ml) and myoglobin (0.5 mg/ml) were
performed at pH 3.0 and 4.4 in 20 mM phos-
phate buffer at 270 V/cm, 39 μA and in 50 mM
acetate–Tris at 540 V/cm, 26 μA, respectively.
The same mixture containing trypsin (0.5 mg/
ml) instead of myoglobin was analysed at pH 7.0
using 30 mM MOPS buffer and 1.5 mM sper-
mine at 400 V/cm, 29 μA; the polarity of the
power supply was positive (anodic injection).

The acidic proteins trypsin inhibitor, β-lacto-
globulin A and B and α-lactalbumin were re-
solved using 25 mM bicine–Tris (pH 8.5) buffer.
A field of 500 V/cm was applied and a current of
17 μA was produced. The polarity of the power
supply was negative (cathodic injection).

2.4. Coating procedure

Capillaries coated with linear polyacrylamide
bonded through methacryloxypropylsilyl moi-
eties were prepared as described by Hjertén [2]
with some modifications: the capillary was first
treated with 1 M NaOH for 5 h, then rinsed and
flushed with 0.1 M HCl followed by 0.1 M
NaOH. After 1 h it was rinsed with water and
tetrahydrofuran (THF). Residual water was
eliminated by connecting the capillary to a gas
chromatographic oven at 120°C for 45 min under
nitrogen pressure. A 50% solution of γ-metha-
cryloxypropyltrimethoxysilane in THF was then
pulled through the capillary under pressure for
20 min and allowed to stand for 12 h. After this
treatment, the capillary was flushed extensively
with THF and water and then filled with a 3%
acrylamide solution containing the appropriate
amount of catalyst (1 μl TEMED and 1 μl of
40% ammonium peroxodisulfate per ml of gel-
ling solution) and degassed under vacuum (20
mmHg) for 40 min. Polymerization was allowed
to proceed overnight at room temperature and
then the capillary was emptied by means of a
syringe.

Capillaries activated with γ-methacryloxy-
propyl bonded to the wall through a direct
silicon–carbon linkage were prepared as de-
scribed by Montes et al. [22]. Briefly, a hydride-
modified support was formed by reacting tri-

ethoxysilane (TES) with a silica substrate in the presence of water and hydrochloric acid using dioxane as the solvent. The γ-methacryloxy-propyl group residue was linked to the hydride-modified substrate by hydrosilylation of allyl methacrylate in the presence of a Pt catalyst.

Poly(AAEE)-coated capillaries were obtained by filling γ-methacryloxypropyl-activated capillaries with a 6% aqueous solution of AAEE containing the appropriate amount of catalyst (1 μl of TEMED and 1 μl of 40% ammonium peroxodisulfate per ml of gelling solution) and degassed under vacuum (20 mmHg) for 40 min. Polymerization was allowed to proceed overnight at room temperature and then the capillary was emptied by means of a syringe.

2.5. Stability test

A mixture of acidic proteins, trypsin inhibitor, β-lactoglobulin A and B and α-lactalbumin, each at a concentration of 0.5 mg/ml, was injected into both types of capillaries using 25 mM bicine–Tris (pH 8.5) buffer. The capillaries were washed with buffer for 2 min between the runs, the analyte was renewed before each run while the catholyte was changed every ten runs. A voltage of 500 V/cm was applied and the temperature was kept at 25°C. After every 15 h of use the ends of the capillary, up to 3 mm, were dipped in a 0.5% (w/v) solution of methyl-cellulose (MC) and after 20 min of contact the capillary was extensively rinsed with water (20
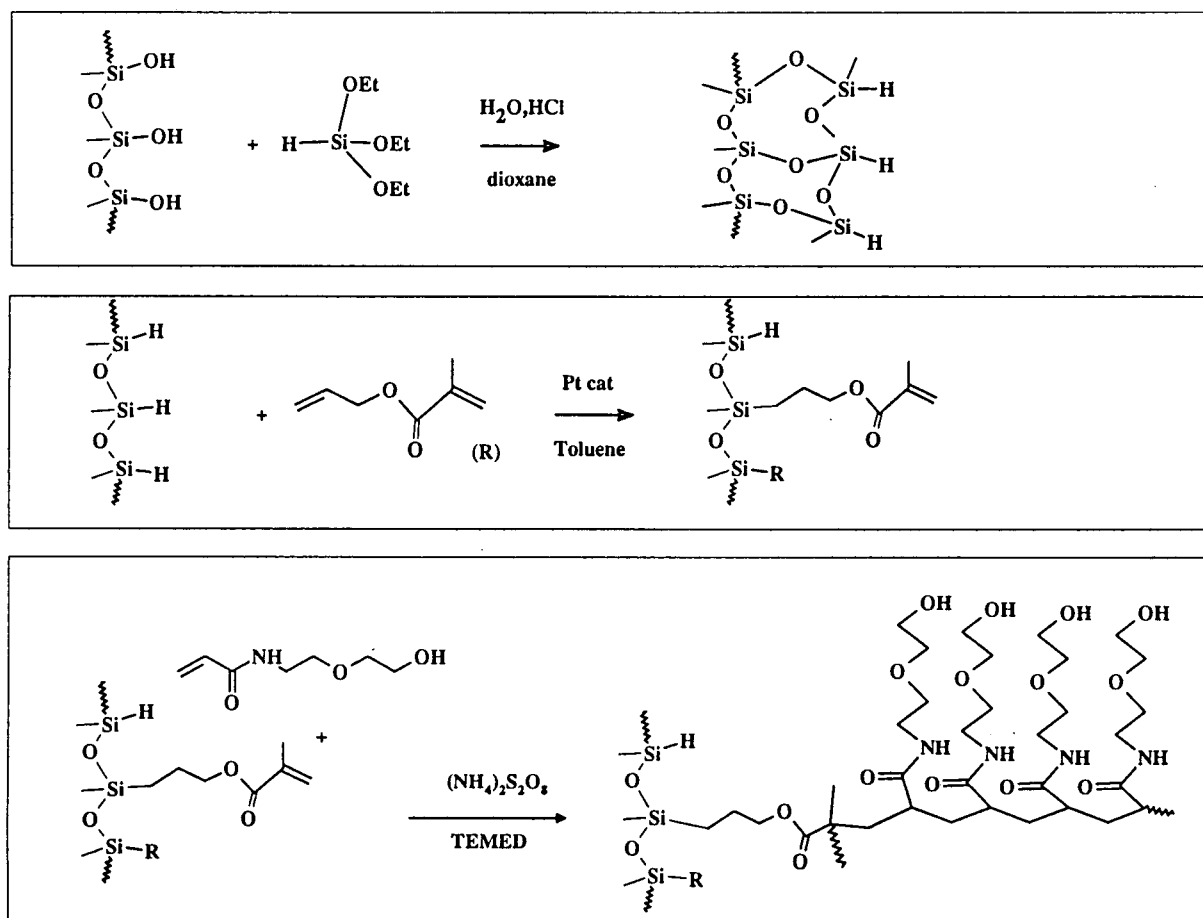
Fig. 1. Schematic representation of the coating procedure.

min) and reconditioned with the alkaline buffer. The EOF was measured at fixed intervals (every 15 h) during the entire test period.

3. Results and discussion

3.1. Surface modification

The overall scheme for preparing linear poly-(AAEE)-coated capillaries is illustrated in Fig. 1. The general process requires three steps. First, an intermediate hydride-modified substrate is produced by reaction of triethoxysilane (TES) with the silica substrate in the presence of water and an acid catalyst. Second, the methacryloxypropyl group is covalently linked to the hydride-modified substrate through an allyl double bond by hydrosilylation. In the third step, the methacryl group reacts with AAEE, yielding polymeric linear chains attached at multiple sites to the wall. The surface, after the first two steps, has a methacryloxypropyl functionality that is similar to that obtained after a conventional reaction with a trifunctional organosilane reagent. However, a stronger attachment is produced when a larger number of siloxane linkages are formed on reaction with TES.

By means of ^{29}Si cross-polarization NMR spectrometry it was demonstrated [22] that about 90% of the Si bearing hydride in the intermediate is fully condensed via formation of three siloxane linkages. In the light of these data, it is clear that in a conventional organosilanization reaction the extent of condensation is lower owing to the steric hindrance of the bulkyl alkyl groups.

When compared with acrylamide, the acryloylaminoethoxyethanol monomer offers the hydrolytic advantage derived from the N-substitution in acrylamide with the high hydrophilicity associated with a diethylene glycol group. N-Mono- and -disubstituted acrylamides are known to be generally more resistant to alkaline hydrolysis; flexible chains bound to the nitrogen are capable of protecting the amido plane as they can fluctuate in the nearby space and shroud the amido group. However, when alkyl chains are

linked to the nitrogen they should bear OH groups in order to lessen the hydrophobicity of the substituent. In the AAEE monomer the hydroxyl group is distant enough from the amido group to prevent the formation of five-, six- and seven-membered rings closing on to the amido linkage. Such rings favor hydrolysis of the amido bond via a mechanism of N,O-acyl transfer [28].

3.2. Stability test at basic pH

An investigation of the lifetime of the polyacrylamide- and poly(AAEE)-coated capillaries was performed by monitoring EOF variations, efficiency and migration time reproducibilities. Fig. 2 shows the separation of a mixture of four acidic proteins achieved at pH 8.5. This mixture was injected into both types of capillaries until the EOF reached a value incompatible with an efficient separation. The relative standard deviations of migration times of proteins were very high in the last series of 20 injections performed in polyacrylamide-coated capillaries, and the plate counts were ten times lower than the initial value.

When performing long-term stability tests at alkaline pH, one of the problems is the adsorption of proteins at the capillary inlet. In most of the capillaries that we have examined, after about 20 h of use at pH 8.5, the electroosmotic mobility was of the order of $3 \cdot 10^{-9}$ m^2/V·s. The EOF became negligible again after the removal of a few millimeters from the capillary ends.

Protein–wall interactions have been the subject of a number of previous studies [29,30] because this phenomenon leads to considerable peak broadening and asymmetry and causes migration time irresproducibility. Towns and Regnier [31] demonstrated that the adsorption of positively charged species which occurs preferentially at the capillary inlet produces a non-uniform axial distribution of the zeta potential within the column. Although proteins with an isoelectric point significantly lower than the pH of the running buffer were employed in this study in order to minimize electrostatic interactions with the wall surface, there are other
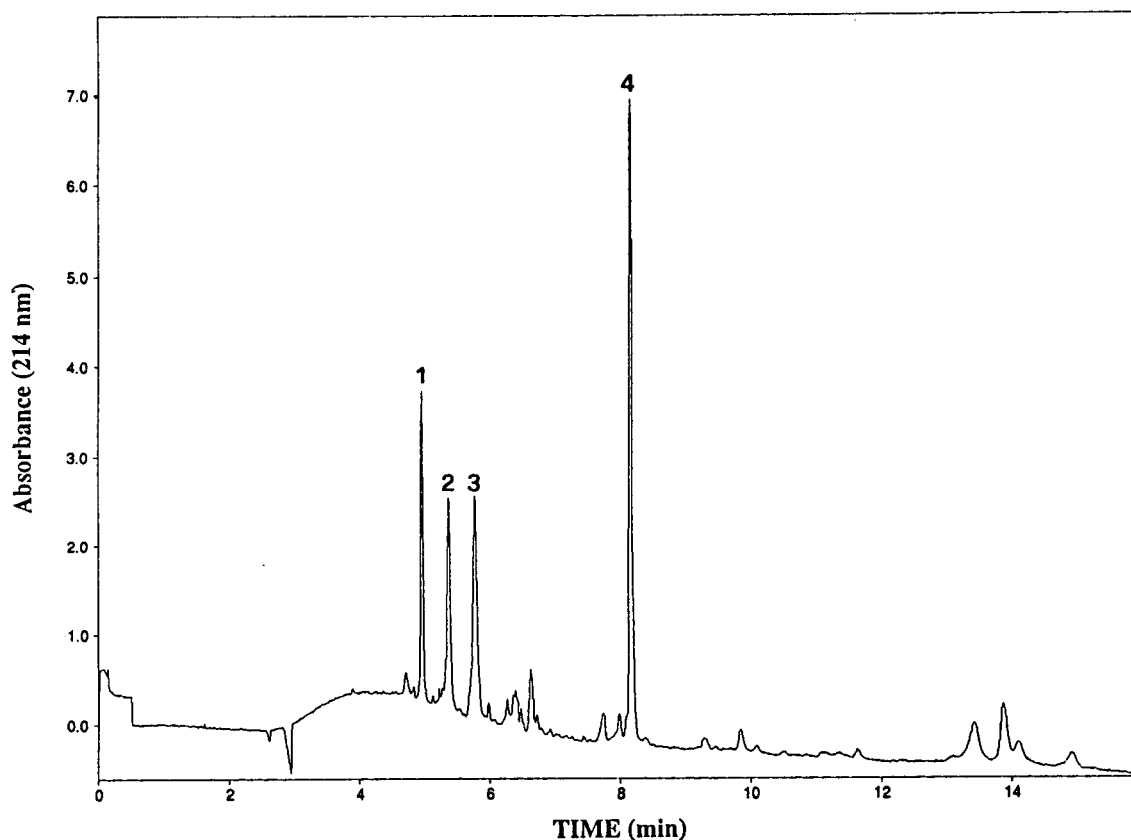
Fig. 2. Typical electropherogram of acidic proteins obtained in a poly(AAEE)-coated capillary (40 cm total length, 32 cm inlet to window) at 25°C, using 500 V/cm (17 μA), UV detection at 214 nm and 25 mM bicine–Tris (pH 8.5). Samples: 1 = trypsin inhibitor; 2 = β-lactoglobulin A; 3 = β-lactoglobulin B; 4 = α-lactalbumin. Reversed polarity, cathodic injection.

possible adsorption modes with the capillary such as hydrogen bonding and hydrophobic interactions which are known to play an important role in the process. In addition, degradation of the coating may occur preferentially at the capillary ends as a result of a possible heterogeneity of the electric field intensity, which increases in the vicinity of sharp corners. During electrophoresis, in particular when high voltage and an alkaline pH are employed, erosion of the coating may take place, thus exposing regions of uncoated silica surfaces in the proximity of the capillary inlet that could be responsible for poor peak shapes and generation of electroosmosis.

A simple solution to both problems, protein adsorption and degradation of the coating at the

capillary ends, is represented by dynamic coating of the ends with methylcellulose. Methylcellulose coatings have been used successfully in both capillary zone electrophoresis and isoelectric focusing and their use in combination with hydrophilic coatings has been reported [32,33]. In a dynamic coating, in order to prevent leakage of the polymer from the wall, a small amount of polymer, typically ranging from 0.01 to 0.4%, is added to the running buffer. In our case, the treatment with MC was limited to the ends of the capillary, since the aim of our investigations was stability of the polymeric coating covalently linked to the wall. Both types of capillaries, one coated conventionally with polyacrylamide and the other coated with poly(AAEE), both as described under Experimental, were subjected to

Table 1
Reproducibility of migration times

Protein	Poly(AAEE)		Polyacrylamide	
	Average (min)	R.S.D. (%)	Average (min)	R.S.D. (%)
Trypsin inhibitor from	5.12[a]	0.55	5.68[a]	1.10
soybean	4.95[b]	0.46	5.54[c]	3.60
β-Lactoglobulin A	5.42	0.78	6.26	1.86
	5.38	1.27	6.00	4.71
β-Lactoglobulin B	5.80	0.86	6.87	2.27
	5.85	1.9	6.52	5.00
α-lactalbumin	8.37	0.78	9.51	1.51
	8.24	0.75	9.43	6.27

25 mM bicine–Tris (pH 8.5) buffer; 500 V/cm.
[a] $n = 40$ (runs 1–40).
[b] $n = 40$ (runs 260–300).
[c] $n = 20$ (runs 130–150).

the MC treatment after every 15 h of use. In both cases this treatment improved the capillary performance. The dynamic coating of the ends physically shields any charges on the wall deriving either from adsorbed proteins or from exposed silanols. Poly(AAEE)-coated capillaries, owing to their higher stability, could be used in the separation of acidic proteins at pH 8.5 for 100 h, with 300 runs of 20 min each, whereas polyacrylamide-coated capillaries after 40 h (120 injections) of use showed strong variations in the migration times and a dramatic decrease in efficiency. In polyacrylamide-coated capillaries the treatment with MC restored the initial characteristics, but this effect was temporary and was lost after a few runs (typically less than ten).

Table 1 shows the reproducibility of migration times for consecutive runs at pH 8.5 in both types of capillaries. The average retention times of the first series of 40 injections are compared with the last series of 40 injections; in poly-(AAEE)-coated capillaries a total number of 300 injections (corresponding to 100 h of use) were performed, whereas in polyacrylamide-coated capillaries only 150 injections were carried out. In this case the first 40 injections were compared with the last 20, since the profile of the 150th run, which is the 15th run after the MC treatment, was not interpretable. The average migration times are lower in both cases in the last series of injections, probably as a consequence of the MC treatment. The efficiency (see Tables 2

Table 2
Efficiency for four basic proteins run at different pH values

Protein	Efficiency (plates/m)			Protein pI[a]
	pH 3.0	pH 4.4	pH 7.0	
Lysozyme (egg white)	356 000	614 000	316 000	11.0
Ribonuclease A	156 000	605 000	353 000	9.3
Trypsinogen	361 000	415 000	201 000	8.7
α-Chymotrypsinogen A	429 000	445 000	149 000	9.5

Separation conditions as in Figs. 4, 5 and 6.
[a] pI values from Refs. [11] and [19].

Table 3
Efficiency for four acidic proteins run at pH 8.5

Protein	Efficiency (plates/m)	pI^a
Trypsin inhibitor from soybean	370 000	4.5
β-Lactoglobulin A	187 000	5.13
β-Lactoglobulin B	131 000	5.23
α-Lactalbumin	585 000	4.8

Separation conditions as in Fig. 2.
[a] pI values from Refs. [11] and [19].

and 3) and the reproducibility of migration times between run numbers 1 and 300 in poly(AAEE)-coated capillaries (Fig. 3a) confirm the increased quality of the new phase, combining stable

attachment to the silica with a stable polymeric layer. In contrast, over a period of 150 h the conventional polyacrylamide-coated capillaries were seriously damaged (Fig. 3b). Even though the MC treatment restores the initial performance (see lane 2 in Fig. 3B, representing the ninth run after the treatment), the effects of such a treatment are quickly lost (lane 3) and in the last series of injections the R.S.D. is very high.

Another parameter which was evaluated as a quality criterion was electroosmosis. The EOF was determined with a buffer at high pH and low ionic strength to maximize silanol ionization. Notwithstanding this, the EOF was found to be reduced to a negligible value in columns coated with both linear poly(AAEE) and linear polyacrylmide. The initial EOF, calculated using an
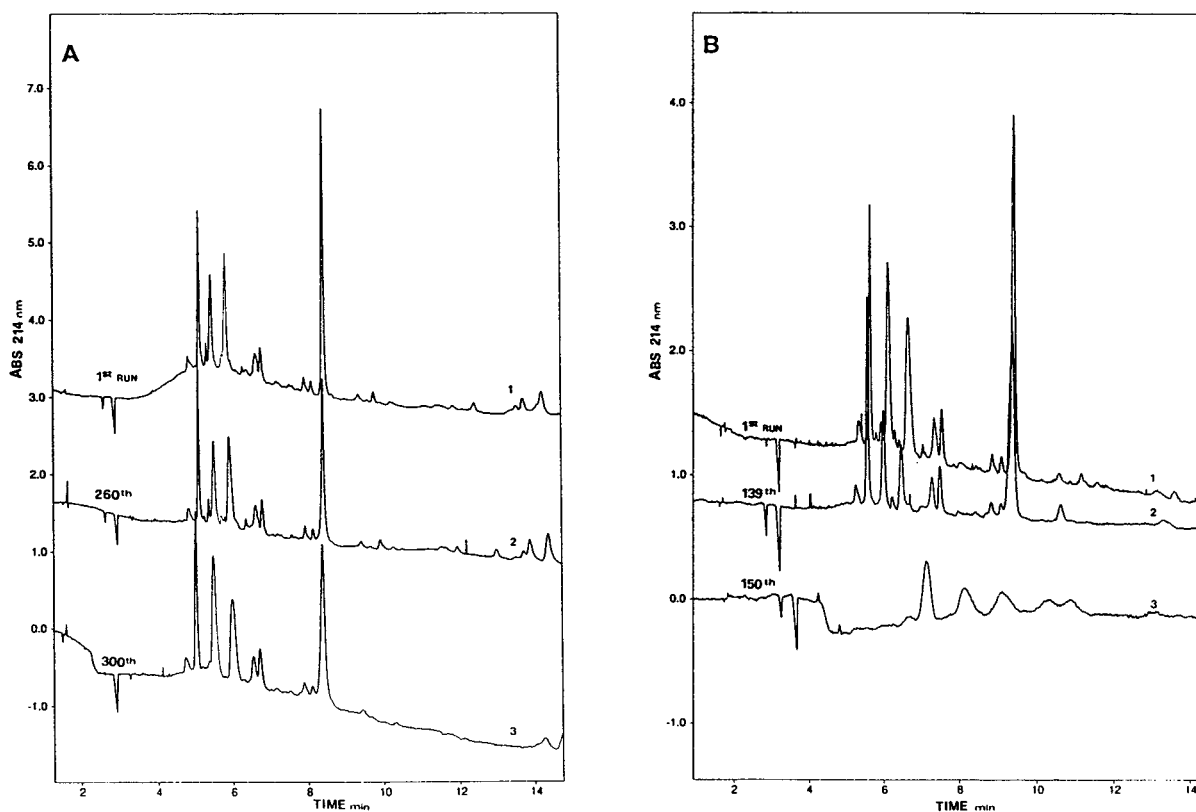
Fig. 3. (A) Protein separations in poly(AAEE)-coated capillary, 1st, 260th and 300th runs. Conditions as in Fig. 2. Samples, from the left: 1 = trypsin inhibitor; 2 = β-lactoglobulin A; 3 = β-lactoglobulin B; 4 = α-lactalbumin. (B) Protein separations in polyacrylamide-coated capillary, 1st, 139th and 150th runs (44 cm total length, 36 cm inlet to window), conditions as in Fig. 2. Samples, from the left: 1 = trypsin inhibitor; 2 = β-lactoglobulin A; 3 = β-lactoglobulin B; 4 = α-lactalbumin.

equation proposed by Jorgenson and Lukacs [1], was lower than $4 \cdot 10^{-10}$ m^2/V·s. Such a reduction was one of goals of this work as it influences other parameters characterizing the quality of a coating such as efficiency and transit time reproducibility. In evaluating such parameters we found that the performance of coated capillaries is acceptable as long as the EOF is lower than $1.2 \cdot 10^{-9}$ m^2/V·s. When the EOF reached such a limiting value the plate counts became at least ten times lower than the initial values and the R.S.D. of the migration times higher. This means that a low EOF can be associated with high efficiency and migration time reproducibility. The EOF variations as a function of hours of continuous use are summarized in Fig. 4. The electroosmotic mobility was measured every 15 h after the removal of 3 mm from the capillary ends in order to avoid the presence of degraded ends influencing the determination. With polyacrylamide coatings the EOF increased gradually with time and after 80 h it was found to be $3 \cdot 10^{-9}$ m^2/V·s, whereas with poly(AAEE) coatings, the EOF increased to $0.8 \cdot 10^{-9}$ m^2/V·s and after 100 h of use the plate count was still acceptable. The lifetime of the new of coating was more than twice that of conventional polyacrylamide.

3.3. Protein separations

The goals of this work were to produce capillaries with a stable hydrophillic coating capable of suppressing the EOF to a negligible value, and to investigate the variation of migration reproducibility and efficiency caused by an EOF increase after prolonged use. at pH 8.5 in the presence of an applied potential. Acceptable reproducibilities may be difficult to achieve without accurate control of the capillary temperature during CE separations. The instrument employed in the protein separations utilized a Peltier thermoelectric device to control the capillary temperature. When polyacrylamide-coated capillaries are used for the separation of proteins, a significant difference is observed between the number of theoretical plates effectively obtained and the values predicted by the theory, probably owing to insufficient masking of the silanol groups. Some workers have hypothesized that hydrophobic interactions [19] or hydrogen bonding [34] cause a reduction in efficiency. The high plate numbers that we achieved in the separation of basic and acidic proteins using poly(AAEE)-coated capillaries indicate that virtually no interactions occurred between proteins and the silica surface (Tables 2
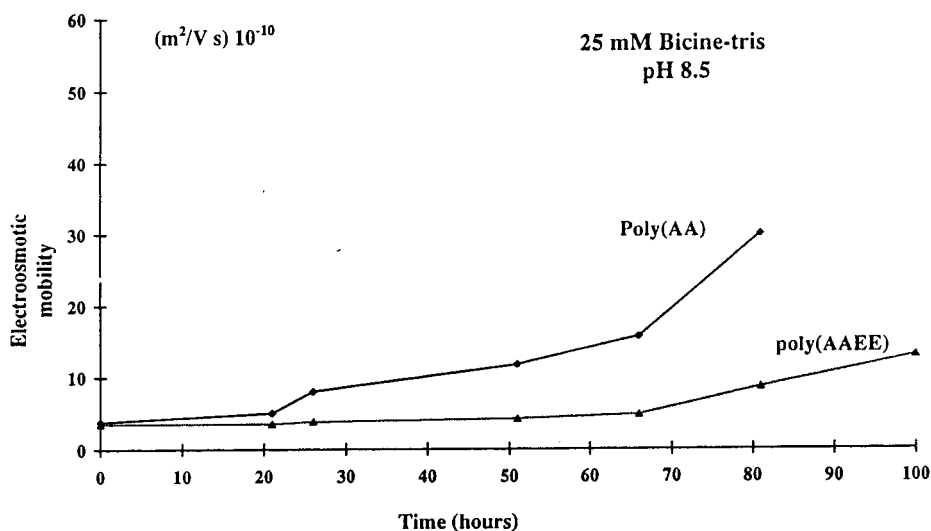
Fig. 4. Variation of electroosmosis as a function of hours of use in 25 mM bicine–Tris buffer (pH 8.5). EOF was measured using benzyl alcohol as a neutral marker in bicine–Tris buffer (25 mM, pH 8.5), 600 V/cm, 23 μA.

and 3). The coating procedure adopted here provides efficient shielding of the surface, thus precluding proteins from interacting with silanols. In addition, the hydrophilicity of the polymer reduces hydrophobic interactions. Alkaline proteins, being positively charged at most operative pH values, interact strongly with the wall. These proteins are often used to test the quality of a coating since in uncoated or inefficiently coated capillaries they are irreversibly adsorbed by the wall, leading to inefficient and irreproducible separations. In many cases no peaks are visible at the detector end. The features of this coating allow pH variations to optimize selectivity without a decrease in efficiency. A possible strategy to improve the

separation of basic proteins would be to work at acidic pH. In this way, silanol ionization is reduced and protein charges are maximized.

Fig. 5 shows the separation of five alkaline proteins performed at pH 3.0 in a poly(AAEE)-coated capillary. The peak shapes demonstrate that no interaction occurred between proteins and the surface but the resolution is poor. The lack of resolution is a typical drawback of the use of extreme pH. In Fig. 6, the same mixture was analyzed at pH 4.4. All peaks were resolved and the higher number of theoretical plates obtained in the separation (see Table 2) again indicates that no interactions with the wall were observed.

At extreme pH many proteins are significantly denatured and in their denatured state irrevers-
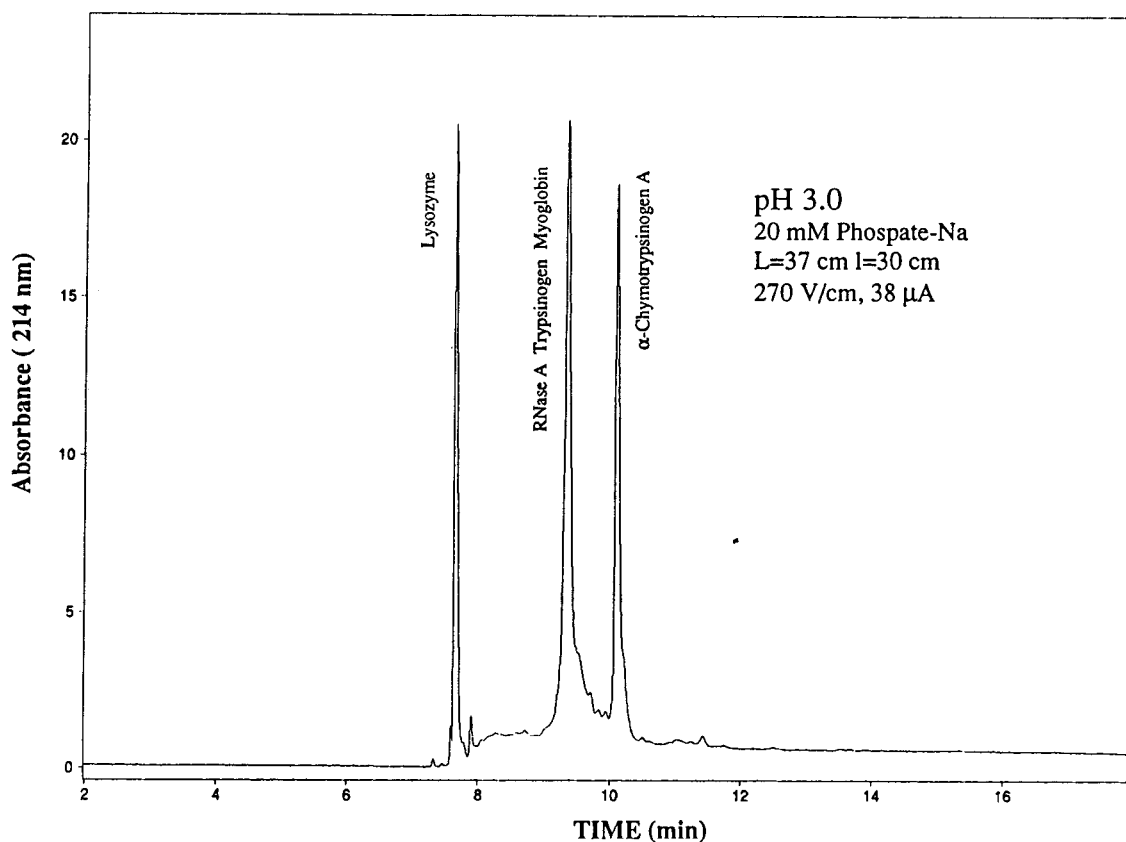
Fig. 5. Electropherogram of alkaline proteins obtained in a poly(AAEE)-coated capillary (36 cm total length, 28 cm inlet to window) at 25°C, using 270 V/cm (39 μA) applied field, UV detection at 214 nm and 20 mM sodium phosphate (pH 3.0). Samples: 1 = lysozyme; 2 = ribonuclease A, trypsinogen, myoglobin; 3 = α-chymotripsinogen A. Anodic injection.
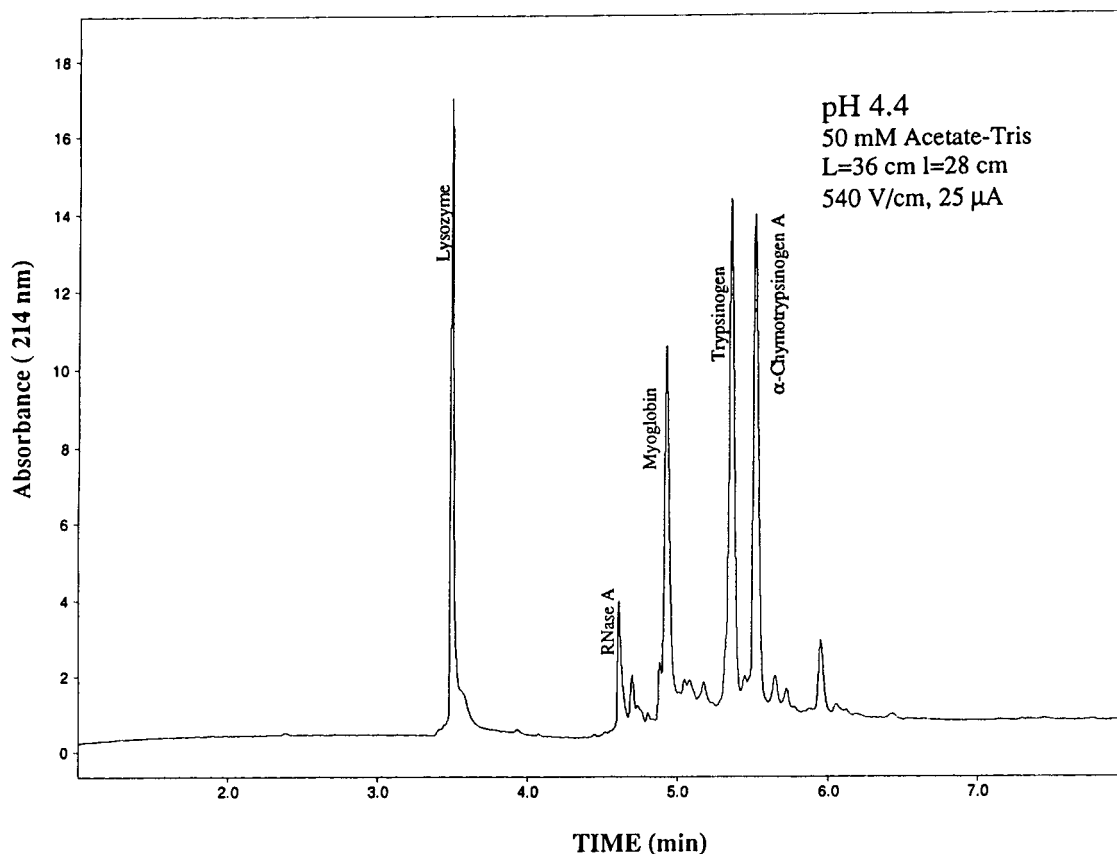
Fig. 6. Electropherogram of alkaline proteins obtained in a poly(AAEE)-coated capillary (36 cm total length, 28 cm inlet to window) at 25°C, using 540 V/cm (39 μA) applied field, UV detection at 214 nm and 50 mM acetate–Tris (pH 4.4). Samples: 1 = lysozyme; 2 = ribonuclease A; 3 = myoglobin; 4 = trypsinogen; 5 = α-chymotripsinogen A. Anodic injection.

ible adhesion to the wall may occur since proteins expose additional binding sites. We therefore tried to separate alkaline proteins at neutral pH in a buffer of low ionic strength. As indicated by the electrophoretic titration curves, the selectivity reaches a maximum value at this pH. It has been reported by Schmalzing et al. [23] that when alkaline model proteins are analyzed at pH 7.0, a small amount of cationic additives is necessary to provide highly efficient separations. Spermine at a concentration of 1.5 mM was used as an additive (Fig. 7) and, similarly to what was seen previously [23], with a poly(AAEE) coating too the addition of such a cationic additive does

not lead to a reversal of EOF as observed in uncoated capillaries.

4. Conclusion

From the foregoing experiments, it can be concluded that the lifetime of capillaries coated with poly(AAEE) bonded to the wall through direct Si–C linkages is at least doubled. With this new type of phase, the EOF was suppressed to a negligible value. Highly efficient separations of acidic and basic proteins were achieved at different pHs and low ionic strength, owing to efficient
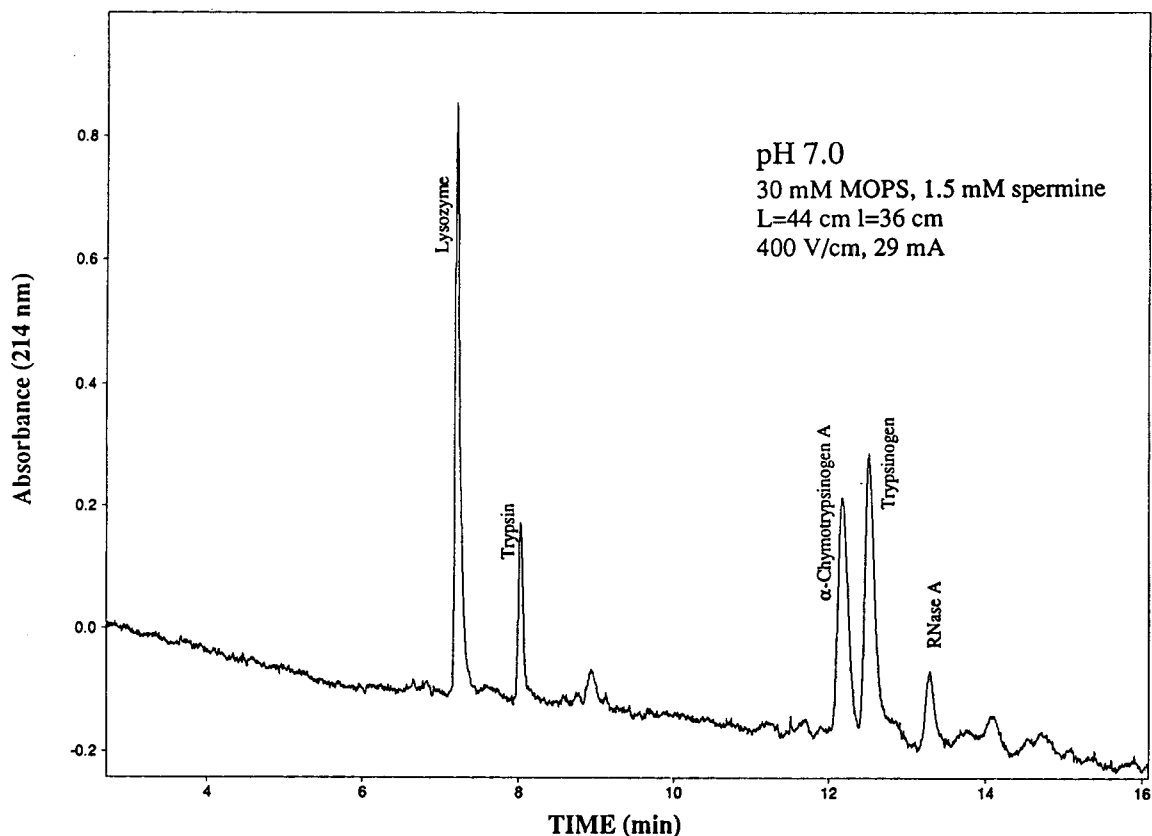
Fig. 7. Electropherogram of alkaline proteins obtained in a poly(AAEE)-coated capillary (44 cm total length, 36 cm inlet to window) at 25°C, using 400 V/cm (29 μA) applied field, UV detection at 214 nm and 30 mM MOPS–Na (pH 7.0) and 1.5 mM spermine. Samples: 1 = lysozyme; 2 = trypsin; 3 = α-chymotripsinogen A; 4 = trypsinogen; 5 = ribonuclease A. Anodic injection.

surface shielding and to the hydrophilic character of the polymer chains attached to the wall.

References

[1] J.W. Jorgenson and K.D. Lukacs, Anal. Chem., 53 (1981) 1298.

[2] S. Hjertén, J. Chromatogr., 347 (1985) 191.

[3] R.M. McCormick, Anal. Chem., 60 (1988) 2322.

[4] H.H. Lauer and D. McManigill, Anal. Chem., 58 (1986) 166.

[5] Y. Walbroehl and J.W. Jorgenson, J. Microcol. Sep., 1 (1989) 41.

[6] H. Lindner, W. Helliger, A. Dirschlmayer, M. Jaquemar and B. Puschendorf, Biochem. J., 283 (1992) 467.

[7] M.M. Bushey and J.W. Jorgenson, J. Chromatogr., 480 (1989) 301.

[8] F.A. Chen, L. Kelly, R. Palmieri, R. Biehler and H. Schwartz, J. Liq. Chromatogr., 15 (1992) 1143.

[9] M.J. Gordon, K.J. Lee, A.A. Arias and R.N. Zare, Anal. Chem., 63 (1991) 69.

[10] M. Zhu, R. Rodriguez, D. Hansen and T. Wehr, J. Chromatogr., 516 (1990) 123.

[11] A. Emmer, M. Jansson and J. Roeraade, J. High Resolut. Chromatogr., 14 (1991) 738.

[12] M.A. Strege and A.L. Lagu, J. Chromatogr., 630 (1993) 337.

[13] W.G.H.M. Muijselaar, C.H.M.M. de Bruijn and F.M. Everaerts, J. Chromatogr., 605 (1992) 317.

[14] J.E. Wiktorowicz and J.C. Colburn, Electrophoresis, 11 (1990) 769.

[15] K. Tsuji and R.J. Little, J. Chromatogr., 594 (1992) 317.

[16] G.C. Bruin, J.P. Chang, R.H. Kuhlman, K. Zegers, J.C. Kraak and H. Poppe, J. Chromatogr., 471 (1989) 429.

[17] J.K. Towns, J. Bao and Z. El Rassi, J. Chromatogr., 559 (1991) 227.

[18] W. Nashabeh and Z. El Rassi, J. Chromatogr., 559 (1991) 367.

[19] K.A. Cobb, V. Dolnik and M. Novotny, Anal. Chem., 62 (1990) 2478.

[20] J.E. Sandoval and J. Pesek, Anal. Chem., 63 (1991) 2634.

[21] C.H. Chu, E. Jinsson, M. Auvinen, J.J. Pesek and J.E. Sandoval, Anal. Chem., 65 (1993) 808.

[22] M.C. Montes, C. Van Amen, J.J. Pesek and J.E. Sandoval, J. Chromatogr., 688 (1994) 31.

[23] D. Schmalzing, C.A. Piggee, F. Foret, E. Carrilho and B.L. Karger, J. Chromatogr., 652 (1993) 149.

[24] N. Sogliano, T.R. Floyd, R.A. Hartwick, J.M. Dibussolo and N.T. Miller, J. Chromatogr., 443 (1988) 155.

[25] J.E. Glajch, J.J. Kirkland and J. Kohler, J. Chromatogr., 384 (1987) 81.

[26] M. Chiari, C. Micheletti, M. Nesi, M. Fazio and P.G. Righetti, Electrophoresis, 15 (1994) 177.

[27] M. Chiari, M. Nesi and P.G. Righetti Electrophoresis, 15 (1994) 616.

[28] A.P. Phillips and R. Baltzly, J. Am. Chem. Soc., 69 (1947) 200.

[29] Z. Zhao, A. Malik and M.L. Lee, Anal. Chem., 65 (1993) 2747.

[30] S. Hjertén and J. Kubo, Electrophoresis, 14 (1993) 394.

[31] J.K. Towns and F.E. Regnier, Anal. Chem., 64 (1992) 2473.

[32] S.M. Chen and J.E. Wiktorowicz, Anal. Chem., 206 (1992) 84.

[33] N. de Jong, S. Visser and C. Olieman, J. Chromatogr. A, 652 (1993) 207.

[34] M.A. Strege and A.L. Lagu, J. Liq. Chromatogr., 16 (1993) 51.

ELSEVIER

Use of plate numbers achieved in capillary electrophoretic protein separations for characterization of capillary coatings

H. Engelhardt*, M.A. Cuñat-Walter

Instrumentelle Analytik — Umwelt Analytik, Universität des Saarlandes, 66123 Saarbrücken, Germany

Abstract

The number of theoretical plates achievable in capillary electrophoresis has been proposed for the characterization of the quality of capillary coatings. It is shown that, as predicted by theory, the efficiency is independent of capillary inner diameter and increases with increasing field strength as long as dispersive effects can be neglected. On the other hand, in contrast to chromatography, there is no linear range within which the plate numbers are independent of the amount or volume of sample injected (from aqueous solutions). By optimization of the injection technique (use of dilute aqueous protein solutions, electrokinetic injection techniques, short injection times), up to $3 \cdot 10^6$ theoretical plates can be achieved. The plates generated by injection of similar amounts of sample from buffer solutions are lower by a factor of 20.

1. Introduction

The tremendous increase in capillary electrophoretic (CE) applications is partly due to the high efficiency achievable by this method. Extremely narrow peaks can be obtained even with high-molecular-mass solutes. One reason is the plug-shaped flow and migration profiles [1]. In pressure-driven liquid chromatography, the parabolic Hagen–Poiseuille flow profile is the main reason for peak dispersion, especially when the profile cannot be flattened owing to small diffusion coefficients. These effects have been described by the various equations for peak broadening in chromatography correlating peak dispersion, flow velocity and capillary diameter (particle diameter), such as the Taylor–Aris equation [2,3], the Golay equation for capillary gas chromatography [4], the Van Deemter equa-

tion for packed column chromatography [5] and the Giddings universal plate height equation [6].

Because no parabolic flow profile is present in CE, the equation for plate number contains only the longitudinal diffusion term [7] and can be reduced to

$$N = \frac{\mu V}{2D}$$

where N is the plate number, D the solute diffusion coefficient in the buffer, V the applied voltage and μ the overall mobility (electrophoretic and electroosmotic). The validity of this equation for CE has already been proved. Giddings [6] has also shown that in the usual range of voltages applied in CE (0–35 000 V) and 1–10 elementary charges for the solutes, the equation for the plate number can be approximated to

$$N = 20zV$$

This means that up to $10 \cdot 10^6$ theoretical plates

* Corresponding author.

can be generated in CE, a range extending that found in chromatographic systems. With DNA fragments in anti-convective systems such as gels these figures have been already verified and even exceeded [8].

Because of the absence of the mass transfer term in the mobile phase, the achievable plate numbers should be independent of capillary diameter and should increase with decreasing diffusion coefficient (increasing molecular mass) and increasing voltage. Observed plate numbers below those predicted by theory have been attributed to slow mass transfer and solute–wall interactions. Therefore, the plate numbers achievable with proteins in surface-coated capillaries have been proposed as a measure for characterizing coating quality. However, because of the extremely small volumes to be handled in CE, the injection technique has a significant influence on efficiency [9]. Additional contributions to peak broadening can be caused by overloading effects of the buffer, temperature effects [10–13] and mobility differences between buffer and analyte ions [14]. Because of on-column detection, the contribution of the detector to overall peak broadening can mainly be reduced to slow data conversion.

In this paper, the parameters governing efficiency in CE will be demonstrated for the separation of basic standard proteins. It will also be shown how the efficiency can be manipulated by applying the various injection techniques.

2. Experimental

2.1. Reagents and materials

Fused-silica capillary tubes were purchased from Polymicro (Laser 2000, Munich, Germany). Reagents for surface modification were purchased from different suppliers, such as acrylamide (Bio-Rad, Munich, Germany), ammonium peroxodisulfate and N,N,N′,N′-tetramethylethylenediamine (Electran, UK) and vinyltrichlorosilane (Fluka, Neu-Ulm, Germany). The proteins were obtained from different suppliers such as cytochrome c (Sigma, Deisen-

hofen, Germany), chymotrypsinogen (Serva, Heidelberg, Germany) and lysozyme and ribonuclease A (Fluka). All buffer components were obtained from Fluka.

2.2. Modification of fused-silica capillaries

Capillaries were coated with vinyltrichlorosilane and polacrylamide as described previously [15].

2.3. Apparatus

For all measurements a Beckman P/ACE System 2050 was used. Data acquisition was accomplished with Beckman Gold Software (V 7.12) and an IBM PS2 personal computer.

3. Results and discussion

3.1. Plates, capillary length and diameter

In chromatography, the plate numbers increase with decreasing particle (capillary) diameter. Decreasing diffusion coefficients always lead to smaller plate numbers, because the mass transfer term governs efficiency in liquid mobile phases. The plate numbers achievable are also dependent on the mobile phase flow-rate. The maximum plate numbers are achieved at a flow-rate depending on particle diameter and sample diffusion coefficient. Of course, the plate numbers also depend on the column length. This concept is only valid when all the other conditions, i.e., temperature, mobile phase composition, etc., are kept constant. In chromatography, the theoretical value is always the highest achievable. Owing to additional dispersive contributions (variance contributions from injection volume, connecting capillaries, detector cell volume, etc.), in reality smaller plate numbers are always obtained.

In CE, the plate numbers increase linearly with increase in effective capillary length as predicted by theory. This is shown in Fig. 1. It should be mentioned that for these measurements the field strength was kept constant; with
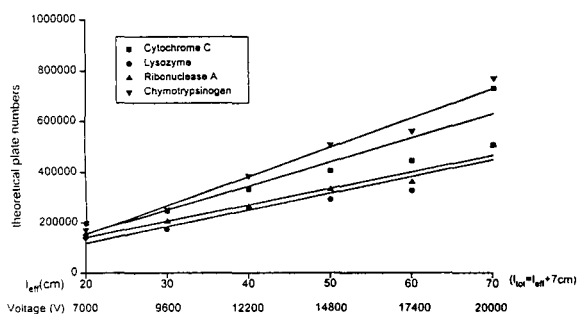
Fig. 1. Dependence of the number of theoretical plates on the effective capillary length with constant electrical field and injection plug length. Conditions: capillary, polyacrylamide–vinyltrichlorosilane, 75 μm I.D.; buffer, 50 mM phosphate (pH 3); field strength, 260 V/cm; samples dissolved in water; injection, pressure [3.45 · 10³ Pa (0.5 p.s.i.)], identical injection plug length in all capillaries (2.5 s with 60/67 cm capillary, 1 s with 20/27 cm capillary).

Fig. 2. Dependence of the number of theoretical plates on the applied electric field with different buffer concentrations and temperatures. Conditions: capillary, polyacrylamide–vinyltrichlorosilane, 20/27 cm × 75 μm I.D.; buffer, phosphate (pH 3); sample, lysozyme (100 ppm in water); injection, pressure [3.45 · 10³ Pa (0.5 p.s.i.)], 1 s with 50 mM buffer at 20°C and 2 s with 10 mM buffer at 20 and 50°C.

increasing capillary length the voltage was increased correspondingly. To exclude the contribution of the variance of the injection plug, the same portion of the capillary was always filled with sample. This means that the injection time was 1 s for the 20-cm capillary (total length 27 cm) and 2.5 s for the 60-cm capillary (total length 67 cm). With a polyacrylamide-coated capillary [15], between 6 · 10⁵ and 1 · 10⁶ plates per metre were achieved for proteins with molecular mass between 12 000 and 25 000. Surprisingly, but corresponding with theory, the protein with the highest molecular mass (α-chymotrypsinogen) gives the highest plate numbers.

The plate number should also increase linearly with increase in field strength at constant capillary length. However, this is only true if no additional zone dispersion due to secondary effects is present [10–13]. As can be seen in the upper part of Fig. 2, plate numbers increase with increase in field strength only if the latter does not exceed 300 V/cm. At higher field strengths, convective effects (temperature, viscosity and mobility gradients) caused by the Joule heat dissipation diminish the achievable plate numbers. This can be clearly seen for the 50 mM buffer. The lower part of Fig. 2, where the current is plotted vs. the field strength, shows

that at field strengths above 400 V/cm deviations from Ohm's law occur. These deviations are caused by insufficient heat transfer from the capillary.

Fig. 2 also shows that with lower buffer concentrations the influence of insufficient heat dissipation on plate number is less important. With the 10 mM phosphate buffer identical plate numbers can be achieved between 200 and 600 V/cm. However, peak distortion due to heat transfer problems is noticeable when the capillary is used at elevated temperatures. This is caused by problems with heat transfer in the equipment in thermostating the capillary. Of course, at elevated temperatures diffusion coefficients are higher, lower plate numbers are generated and only lower field strengths can be applied. The advantage of capillaries with smaller inner diameters (<50 μm) is that higher field
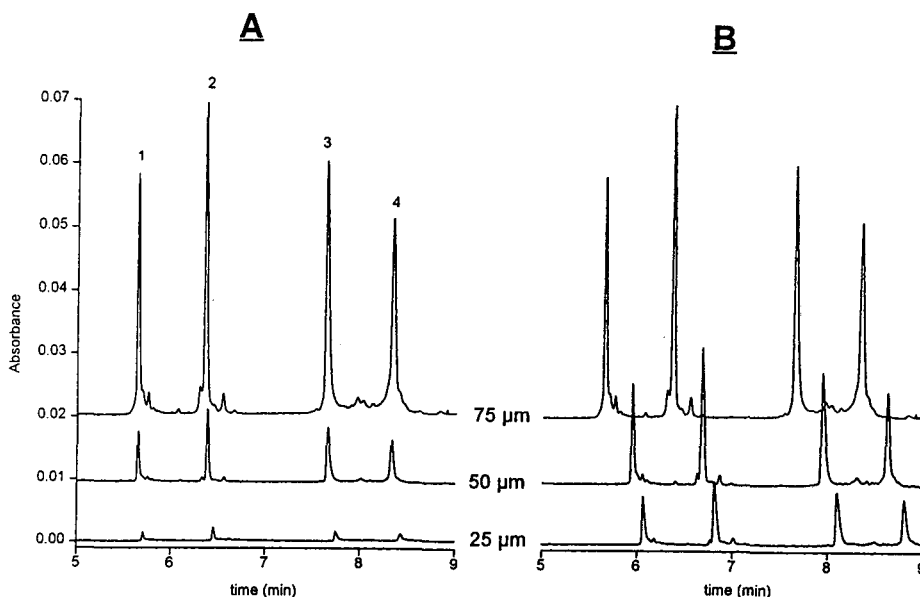
Fig. 3. Influence of the capillary inner diameter on the separation of basic standard proteins. Conditions: capillary, poly-acrylamide—vinyltrichlorosilane, 20/27 cm; buffer, 50 mM phosphate (pH 3); field strength, 260 V/cm; samples, 1 = cytochrome c, 2 = lysozyme, 3 = ribonuclease A, 4 = chymotrypsinogen (100 ppm in water); injection, pressure [3.45·10^3 Pa (0.5 p.s.i.)]; (A) identical injection time (2 s); (B) identical injection plug length (2 s with 75 μm I.D., 4.5 s with 50 μm I.D., 18 s with 25 μm I.D. = 0.45 cm).

strengths are applicable without a decrease in efficiency owing to more efficient heat dissipation.

Because only the longitudinal diffusion term contributes to peak broadening in CE, in theory the inner diameter of the capillary should not affect the plate numbers. In the right-hand part of Fig. 3 and in Table 1 it can be seen that plate numbers are independent of capillary inner diameter when the injection plug length is kept constant (contribution of injection volume vari-

ance to overall peak variance). A constant plug length of 0.45 cm was used, and consequently the injection time was varied between 2 s with the 75-μm capillary to 18 s for the 25-μm capillary. The error in the determination of plate numbers with these narrow peaks is up to 10%. As can be seen, it is possible to achieve 1·10^6 plates per metre without any problems. The decrease in peak height is due only to the decrease in the optical path length (Lambert–Beer law). The predictions of theory regarding

Table 1
Dependence of the number of theoretical plates per metre on the capillary inner diameter

I.D. (μm)	Injection (s)	Cytochrome c	Lysozyme	Ribonuclease A	Chymotrypsinogen
75	2	1 410 000	1 163 000	1 008 000	1 144 000
50	4.5	1 163 000	1 006 000	943 000	1 166 000
25	18	994 000	845 000	787 000	1 109 000
75	2	1 410 000	1 163 000	1 008 000	1 144 000
50	2	1 672 000	1 439 000	1 255 000	1 404 000
25	2	2 048 000	2 007 000	1 528 000	1 607 000

Conditions as in Fig. 3.

peak-broadening effects in CE are fulfilled: the plate number is independent of capillary inner diameter and increases with increase in field strength if secondary convection effects are negligible. Also, the number of plates is proportional to column length at constant field strength. It should be recalled that the variance contribution of the injection plug was identical in all cases.

On the other hand, when the same capillaries are used but the injection time is kept constant, of course in the 25-μm capillary only 11% of the amount is injected in comparison with the 75-μm capillary. As can be seen in the left-hand part of Fig. 3 and in Table 1, an increase in efficiency was observed when the capillary inner diameter was reduced from 75 to 25 μm. This is caused by the concomitant decrease in the amount of sample injected and the plug length (variance of injection volume). In comparing the two separations with the 25-μm capillaries, it can be seen that the efficiency can be varied by a factor of 1.5–2 just by changing the amount of sample injected. Of course, the plate number measured summarizes all contributions to peak broadening. Because of the extremely small volumes handled in CE, one should be very cautious about the contribution of dispersive effects other than the electromigration process. It should be stressed again that it is possible to compare and discuss efficiencies only when all parameters that contribute to peak broadening are kept constant. Because of the additional contributions of heat dissipation and the injection techniques of the various instruments (e.g., pressure profile in hydrodynamic injection), comparison of efficiencies of different capillaries can only be valid with the same instrument.

3.2. Overloading effects with hydrodynamic injection

So far either the plug length or the mass of the sample loaded to the capillary was kept constant. In Fig. 4, the influence of the injected sample concentration at constant plug length on efficiency is shown. As can be seen, the efficiency decreases tremendously when the mass of sample
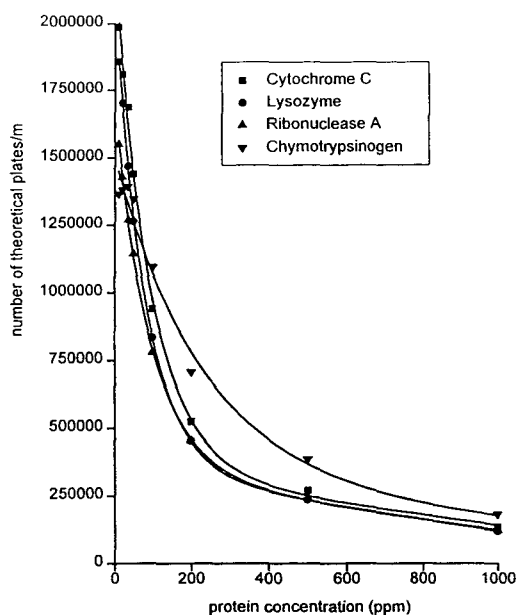
Fig. 4. Dependence of the number of theoretical plates on the protein concentration with a constant injection plug length. Conditions: capillary, polyacrylamide–vinyltrichlorosilane, 20/27 cm × 25 μm I.D.; buffer, 50 mM phosphate (pH 3); field strength, 260 V/cm; proteins dissolved in water; injection, 18 s pressure [3.45 · 10³ Pa (0.5 p.s.i.)].

increases. No linear region as in chromatography can be observed. Therefore, the efficiency achievable cannot be a measure for capillary characterization. It should be mentioned that the sample was dissolved in water, so that the injected plug length is less important owing to the stacking effect that occurs. The observed triangular peaks at sample concentrations above 100 ppm indicate that the capacity of the 50 mM buffer is insufficient for these sample loads. On the other hand, the lower the sample concentrations the more efficient the sample stacking effect becomes. As can be seen, decreasing the sample concentration from 200 to 20 ppm results in an improvement in plate numbers by a factor of three.

When the protein sample is injected from water, volume overloading does not contribute to a certain extent to peak broadening because the sample stacking effect concentrates the sample at the borderline of the injection solvent and
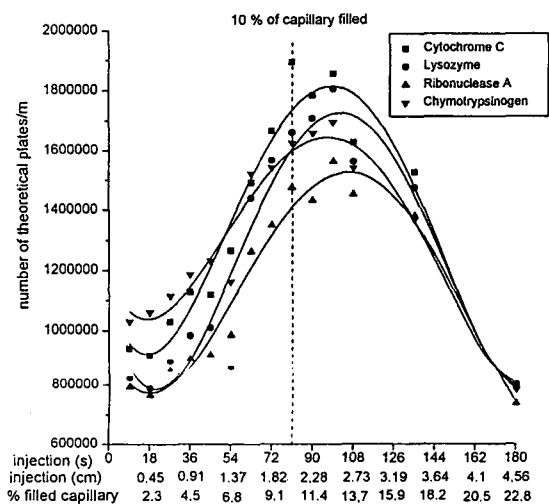
Fig. 5. Dependence of the number of theoretical plates on the injection plug length with constant injected sample mass. Conditions: capillary, polyacrylamide–vinyltrichlorosilane, 20/27 cm × 25 μm I.D.; buffer, 50 mM phosphate (pH 3); field strength, 260 V/cm; proteins dissolved in water; injection, pressure [3.45 · 10³ Pa (0.5 p.s.i.)], identical sample amount injected (18 s at 100 ppm = 180 s, at 10 ppm = 224 pg).

the buffer. As can be seen from Fig. 5, the plate number increases by a factor of around two when the plug length is increased from 0.45 to 2.73 cm and the mass of sample injected is kept constant. It should be mentioned that here 12% of the effective capillary length is filled with the sample solution. The increase in plate number is, of course, due to the lower sample concentrations injected (constant mass loaded), which improves the stacking effect. Only if the sample plug exceeds 12% of the capillary length is the volume variance no longer negligible and the plate numbers decrease again. The longer the part of the capillary filled with sample solution (water), the more the migration times increase because the field strength decreases mostly over the water plug [16].

The advantages of the stacking procedure are more clearly seen in Fig. 6, where this technique is compared with the conventional method, in which the sample dissolved in the separation buffer is injected. Comparable efficiencies are achieved only with the smallest plug length
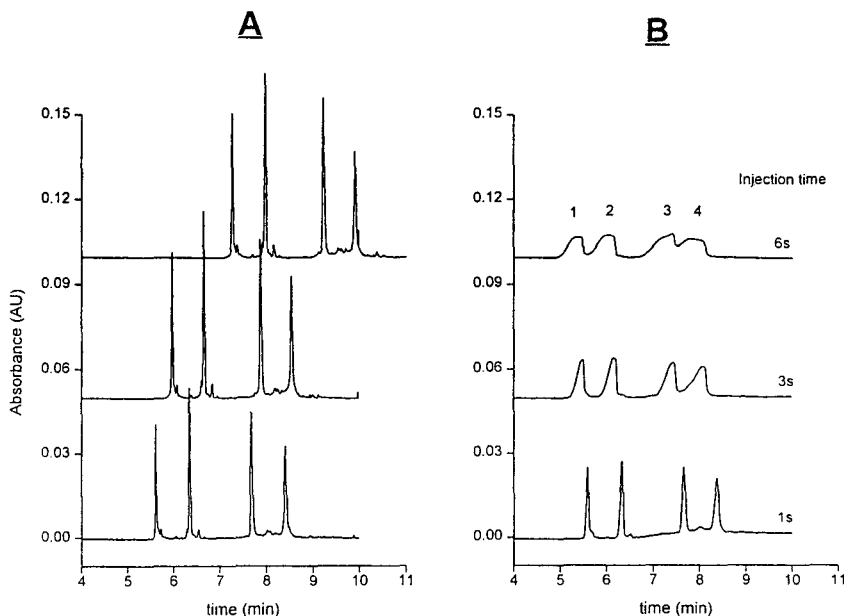
Fig. 6. Effect of injection plug length on peak performance for proteins from (A) aqueous solution or (B) separation buffer. Conditions: capillary, polyacrylamide–vinyltrichlorosilane, 20/27 cm × 75 μm I.D.; buffer, 50 mM phosphate (pH 3); field strength, 260 V/cm; samples, 1 = cytochrome c, 2 = lysozyme, 3 = ribonuclease A, 4 = chymotrypsinogen; injection, pressure [3.45 · 10³ Pa (0.5 p.s.i.)], identical sample amount injected (1 s at 200 ppm = 6 s, at 33.3 ppm = 224 pg).

injected (injection time 1 s). When longer plugs of the sample in buffer solution are injected (injection time >2 s), efficient and narrow peaks can no longer be observed. The peak width increases in proportion to the injection time because here the stacking effect is not working. On the other hand, with sample injection from water, highly efficient separations are observed even with an injection time of 6 s.

Stacking effects also play an important role in the case of mass overloading. However, when injected from buffer, generally fewer plate numbers are obtained and the efficiency is not greatly affected by increasing the sample concentration (constant plug length) with 50 mM phosphate buffer. However, the total plate number is only around 100 000 compared with 900 000 when the same amount (200 ppm) is injected from aqueous solution. Here one dilemma of CE becomes obvious: plate numbers are only defined when the separation conditions are kept constant, i.e., temperature, field strength and buffer composition. The use of the stacking procedure in combination with comparison of plate numbers is

a mistake similar to that which one can make in calculating plate numbers in gradient elution. On the other hand, to achieve efficient and reproducible separations, the injection time cannot be chosen too short, and therefore stacking procedures are required for efficient protein separations. Only with very short injection times from buffer solutions is comparison of capillary efficiencies possible and permitted.

3.3. Electrokinetic injection

The most efficient injection technique for proteins in order to achieve high plate numbers is the electrokinetic injection technique. In Fig. 7 and Table 2 the electrokinetic injection technique from water and from buffer solution is compared with the already described hydrodynamic injection techniques. In the case of electrokinetic injection there is almost no difference between injection from buffer and water solutions. However, at a constant injection time a smaller amount is injected from the buffer solution, because the buffer components also
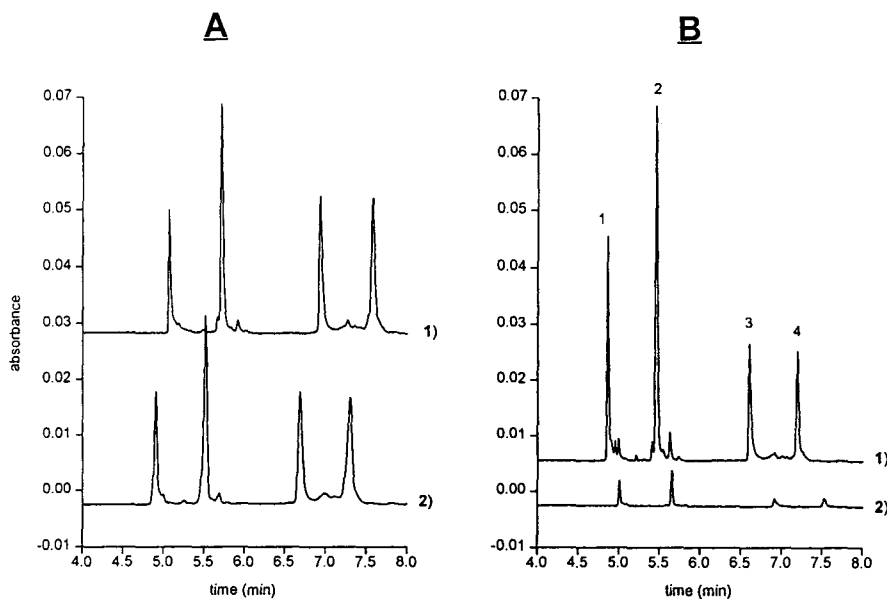
Fig. 7. Dependence of protein separation on injection technique. Conditions: capillary, polyacrylamide–vinyltrichlorosilane, 20/27 cm × 75 μm I.D.; buffer, 50 mM phosphate (pH 3); field strength, 260 V/cm; samples, 1 = cytochrome c, 2 = lysozyme, 3 = ribonuclease A, 4 = chymotrypsinogen; injection, (A1) pressure [3.45·10^3 Pa (0.5 p.s.i.)], 1 s, samples in water; (A2) pressure (0.5 p.s.i.), 1 s, samples in buffer; (B1) 1 kV, 5 s, samples in water; (B2) 1 kV, 5 s, samples in buffer.

Table 2
Influence of the injection technique on the number of theoretical plates per metre

Solvent	Injection	Cytochrome c	Lysozyme	Ribonuclease A	Chymotrypsinogen
Water	1 s, pressure	977 000	782 000	792 000	784 000
Buffer	1 s, pressure	463 000	436 000	382 000	329 000
Water	5 s, 1 kV	1 350 000	979 000	1 180 000	1 315 000
Buffer	5 s, 1 kV	1 437 000	1 309 000	750 000	982 000

Conditions as in Fig. 7.

migrate into the capillary. As no electroosmotic flow was present in the capillary used, the discrimination of sample components according their mobility differences can clearly be seen by comparing the relative peak heights obtained with hydrodynamic and electrokinetic injection from the same solutions. Although from aqueous solution higher sample amounts are introduced in the capillary, the highest efficiencies are always obtained with the electrokinetic injection techniques. This can be explained by the plug-shaped electromigration of the sample molecules into the capillary.

3.4. How to achieve record plate numbers

In chromatography, there is a linear range within which the plate number is independent of sample size. In linear chromatography one usually works in this region. Only when this region is exceeded do plate numbers decrease with increasing sample size. In CE, however, there is no such region in the case of injection from water. Only when proteins are injected from buffer solutions is a linear region obtained, but the plate numbers achievable are much lower, only around 100 000–200 000. With the same capillary, plate numbers up to $3 \cdot 10^6$ can be achieved just by optimization of the sample injection techniques. Such a highly efficient separation of standard proteins is shown in Fig. 8. The same samples were used as in all demonstrations in this paper. Hence it is obvious that it is possible to achieve plate numbers predicted by theory just by optimization of injection techniques. It should be mentioned, however, that for real protein samples the application of the different injection techniques is limited. There-

fore, it is hardly possible in the real world to achieve the plate numbers predicted by theory.

To obtain high plate numbers, the sample has to be injected elektrokinetically either from buffer or from water, or hydrodynamically from water with low sample concentrations and applying sample stacking techniques. Here either extremely short injection times should be used or the capillary should be filled up to 10% of its effective length with a very dilute aqueous sample solution. Generally the sample amount injected should be as low as possible. For reproducibility reasons it is better to inject a dilute solution for a longer time than a more concentrated solution for a relatively short period.
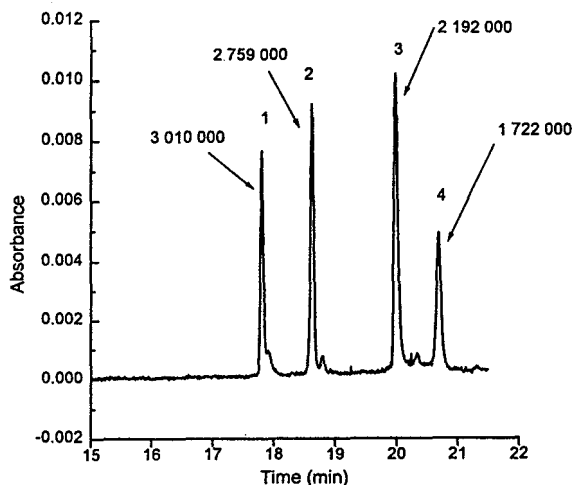
Fig. 8. Separation of basic standard proteins under optimized conditions. Conditions: capillary, polyacrylamide–vinyltrichlorosilane, 20/27 cm × 50 μm, I.D. buffer, 50 mM phosphate (pH 3); field strength, 260 V/cm; samples, 1 = cytochrome c, 2 = lysozyme, 3 = ribonuclease A, 4 = chymotrypsinogen (10 ppm each in water); injection, 33.8 s, pressure [3.45 · 10³ Pa (0.5 p.s.i.)].

Additionally, narrow capillaries (I.D. < 50 μm) have the advantage that higher field strengths can be used and zone dispersion by heat dissipation effects is negligible.

Consequently, plate numbers for proteins are not a good measure for comparing the efficacy of surface coatings in CE, and should be used only when all measurements are made under identical conditions with the same instrument.

References

[1] J.A. Taylor and E.S. Yeung, Anal. Chem., 65 (1993) 2928–2932.

[2] G.I. Taylor, Proc. R. Soc. London, Ser. A, 219 (1953) 196.

[3] R. Aris, Proc. R. Soc. London, Ser. A, 235 (1956) 67.

[4] M.J.E. Golay, in D.H. Desty (Editor), Gas Chromatography, Proceedings of 2nd Symposium (Amsterdam), Academic Press, New York, 1958.

[5] J.J. van Deemter, F.J. Zuiderweg and A. Klinkenberg, Chem. Eng. Sci., 5 (1956) 271.

[6] J.C. Giddings, Unified Separation Science, Wiley, New York, 1991.

[7] J.W. Jorgenson and K.D. Lukacs, Anal. Chem., 53 (1981) 1298–1302.

[8] A. Guttman, A.S. Cohen, D.N. Heiger and B.L. Karger, Anal. Chem., 62, (1990) 137.

[9] S. Terabe, K. Otsuka and T. Ando, Anal. Chem., 61 (1989) 251–260.

[10] J.H. Knox and K.A. McCormack, Chromatographia, 38 (1994) 207–221.

[11] S.L. Petersen and N.E. Ballou, Anal. Chem., 64 (1992) 1676–1681.

[12] E. Grushka, R.M. McCormick and J.J. Kirkland, Anal. Chem., 61 (1989) 241–246.

[13] J. Liu, V. Dolnik, Y.Z. Hsieh and M. Novotny, Anal. Chem., 64 (1992) 1328–1336.

[14] F.E.P. Mikkers, F.M. Everaerts and Th. P.E.M. Verheggen, J. Chromatogr., 169, (1979) 1–10.

[15] H. Engelhardt and M.A. Cuñat-Walter, J. Chromatogr. A, 716 (1995) 27.

[16] H.W. Zhang, X.G. Chen and Z.D. Hu, J. Chromatogr. A, 677 (1994) 159–167.

Capillary electrophoresis, a rapid and sensitive method for routine analysis of apolipoprotein A-I in clinical samples

Hartmut M. Liebich[a], Rainer Lehmann[a,*], Angelika E. Weiler[b], Gerald Grübler[b], Wolfgang Voelter[b]

[a]Abteilung IV Endokrinologie und Klinische Chemie, Medizinische Universitätsklinik und Poliklinik der Universität Tübingen, Otfried-Müller-Str. 10, D-72076 Tübingen, Germany
[b]Abteilung für Physikalische Biochemie, Physiologisch-chemisches Institut der Universität Tübingen, Hoppe-Seyler-Str. 4, D-72076 Tübingen, Germany

Abstract

A method for the determination of apolipoprotein A-I, the major protein compartment of HDL, in human serum is described. Rapid and easy serum sample preparation, well separated Apo A-I peaks in the human serum electropherogram and good linearity of the peak area vs. concentration plot, covering the range of the clinically relevant Apo A-I serum contents, suggest the introduction of this method routinely in clinical laboratories.

1. Introduction

Minimum sample and buffer requirements in combination with rapid and efficient separation have made capillary electrophoresis (CE) [1–5] one of the most attractive tools for the analysis of biopolymers such as peptides [6–10], proteins [11–16], glycoproteins [17,18] and oligonucleotides [19–21]. Recently, pharmaceutical and clinical analysis laboratories have started to develop routine CE methods for purity testing [22], determinations of the formulation contents [23–25], chiral analysis [26], monitoring of drugs in body fluids [27,28] and reliable and precise analyses of blood serum and its fractions [29–31]. Apolipoprotein A-I (Apo A-I) is the major protein constituent of human high-density lipoprotein (HDL). Decreased Apo A-I levels in

human serum are indicative of arteriosclerotic processes [32], acute hepatitis and hepatic cirrhosis [33]. The median serum concentrations for Apo A-I were determined to be 145 mg/dl for men and 160 mg/dl for women [34]. Today, immunonephelometric assay (INA) is the most common method applied in clinical laboratories for the routine determination of Apo A-I concentrations in human serum [35]; other methodologies used include radial immunodiffusion (RID), radioimmunoassay (RIA), electroimmunoassay (EIA), enzyme-linked immunosorbent assay (ELISA) and immunoturbidimetric assay (ITA). The major drawbacks of immunological methods for the determination Apo A-I are the inhomogeneity of HDL [36] and that masking lipids prevent antigenic sites being expressed [37,38]. Further, a serious problem of any INA or ITA is that hyperlipaemic samples may disturb the Apo A-I determination. A

* Corresponding author.

reliable Apo A-I assay to be performed via a simple serum sample work-up procedure and applying the advantages of CE is therefore of great interest for clinical chemists and such a method is presented in this paper.

2. Experimental

2.1. Materials and reagents

Fused-silica capillaries (50 cm × 50 μm I.D.) (Grom, Herrenberg, Germany) were used for all electrophoretic runs and pretreated with 1 M NaOH for 15 min, followed by 15 min rinsing with water before the electrophoretic separations. Using 30 mM borate buffer (pH 10), the capillary was rinsed for 60 s with water, followed by 120 s with 0.1 M NaOH, 120 s with water and finally 60 s with buffer after each run. After separations, performed with sodium dodecyl sulphate (SDS)-containing Bio-Rad (Munich, Germany) evaluation LLV buffer, the following rinsing sequence was applied by pressure 6.89 · 105 Pa (100 psi): water (60 s), LLV buffer (120 s), water (120 s) and LLV buffer (60 s). The Apo A-I standard sample was purchased from Sigma (St. Louis, MO, USA). The serum samples were prepared from blood from normal fasting male donors or clinical patients and allowed to clot. The serum was separated by low-speed centrifugation at 2000 g for 7 min and used immediately after recovery or stored at −70°C until used.

2.2. Electrophoretic apparatus

All separations were performed on a Bio-Rad BioFocus 3000 capillary electrophoresis system, equipped with an automatic constant-volume sample injection system, a temperature-control system for the capillary, sample and fraction collection compartment, a high sensitivity fast-scanning UV–Vis detector with wavelength programming and a dedicated computer system with a Microsoft Windows interface. During all runs, the capillary and the sample compartment was cooled to 15°C.

2.3. Immunonephelometric assay (INA)

For the INA we used a Behring nephelometer (Behringwerke, Marburg, Germany) and fixed-time kinetic analysis. The Apo A-I nephelometric determinations were performed according to the procedures provided by the manufacturers. After adding an aliquot of diluted sample (100 μl) and antibody (40 μl) to a cuvette containing the reaction buffer (80 μl), a background reading (zero time) was taken. After 6 min, the net increase in scattered light was calculated from a second reading. The scattered light value was compared with those on a calibration graph and the concentration was calculated. The manufacturer stated an assayable range from 18 to 580 mg/dl for Apo A-I, using a plasma or serum dilution of 1:20.

3. Results and discussion

As mentioned in the Introduction, INA is the most commonly used method for determining the content of Apo A-I in human serum in routine clinical laboratories. INA allows automated and rapid analysis, but nephelometric and turbidimetric methods are susceptible to factors that interfere with light transmission such as lipoproteins, dust and other plasma proteins [35]. Moreover, immunological procedures for Apo A-I determination in serum are complicated by the fact that it is a component of a large, heterogeneous particle, and some of the antigenetic sites are masked by lipids [37,38]. Consequently, the results are strongly influenced by variations in the specificity of antisera, the standardization procedure and the methodology used in a particular assay system. Therefore, our intention was to establish a CE method for determining the Apo A-I concentration in human serum which can be used conveniently in every routine clinical laboratory.

The feasibility of the routine analysis of human serum protein fractions by CE has been demonstrated [31,39–41], mostly using phosphate or borate buffers. Hence, our first attempt
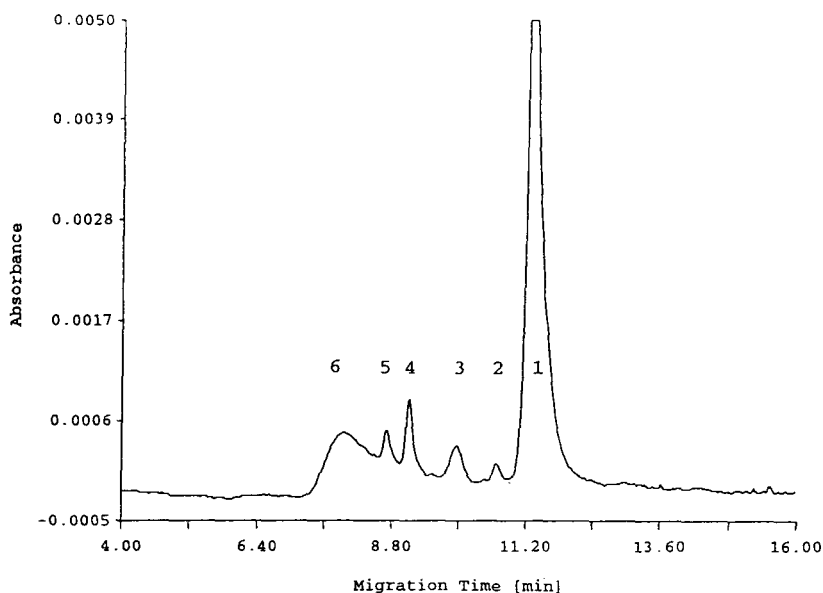
Fig. 1. Capillary electropherogram of a normal human serum sample (dilution: 1:30). Electrophoretic conditions: capillary, fused-silica (50 cm × 50 μm I.D.); loading, $2.75 \cdot 10^7$ Pa s; running conditions, 15 kV; buffer, 30 mM borate (pH 10); detection, UV at 220 nm; equipment, Bio-Rad CE 3000, BioFocus 3000. Peaks: 1 = albumin; 2 = α_1-globulin; 3 = α_2-globulin; 4 = β_1-globulin; 5 = β_2-globulin; 6 = γ-globulin.

to separate HDL, with Apo A-I as the main protein constituent, started with borate buffer (pH 10). Fig. 1 shows a capillary electropherogram of a diluted (1:30) serum sample obtained with a 50 cm × 50 μm I.D. fused-silica capillary and 30 mM borate running buffer (pH 10), demonstrating the well known separation profile of six fractions. Even using capillaries with different lengths and diameters and different buffer molarities, no lipoprotein fractions, in particular no specific HDL peak for quantitative evaluation, could be detected from normal human serum samples or HDL-spiked samples.

To determine Apo A-I concentrations in serum directly, a series of buffer systems with different additives were tested and it was found that the Bio-Rad LLV buffer allows the specific determination of Apo A-I in blood samples. Fig. 2 shows electropherograms of a diluted serum sample (1:30) spiked with 0.25 mg/ml of Apo A-I, recorded at wavelengths from 220 to 195 nm and using Bio-Rad LLV buffer. By adding an Apo A-I standard to the normal serum sample,

the well separated peak at a migration time of 21.10 min could be identified. As the sensitivity could be drastically increased by using a recording wavelength of 195 nm instead of 200–220 nm, which is commonly used, all further runs were performed at the lowest wavelength. Fig. 3 demonstrates that the electrophoretic conditions discussed above allow a clear separation of Apo A-I from serum proteins and quantitative peak evaluation even in highly lipaemic serum samples, whereas nephelometry gives doubtful results (see above).

The electropherogram of a patient's serum sample with an elevated level of Apo A-I is presented in Fig. 4, showing a major and an additional minor Apo A-I peak with a shorter migration time. Different polymorphic Apo A-I forms are responsible for this separation pattern, as revealed by analytical isoelectric focusing [42,43] and recently also by capillary electrophoresis [31,44]. Therefore, for Apo A-I determination the area of both peaks must be considered.
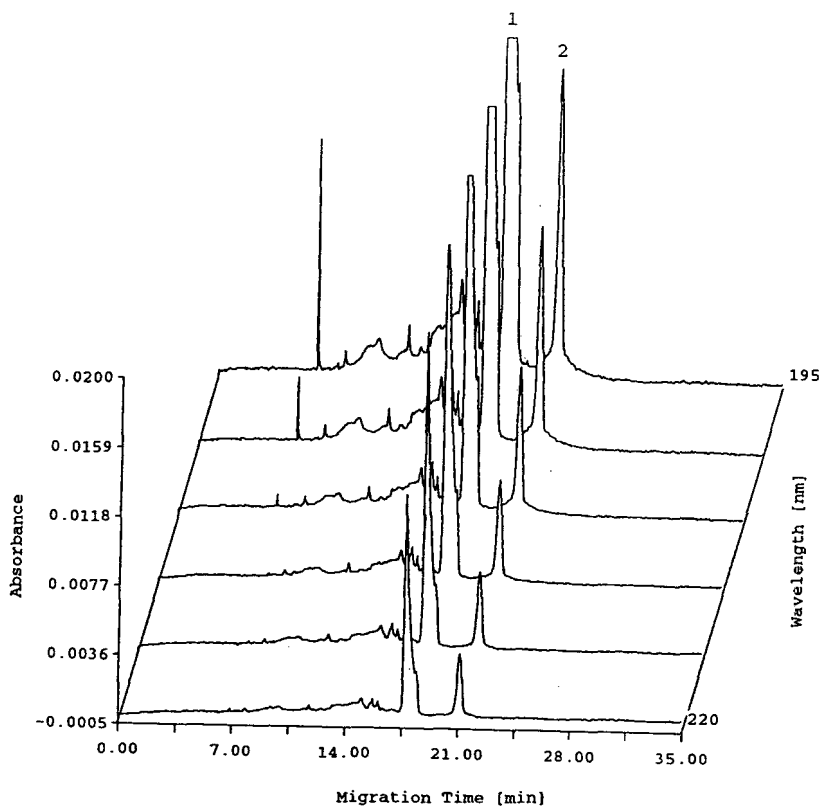
Fig. 2. Multi-wavelength electropherogram of a normal human serum sample (dilution 1:30) spiked with 0.25 mg/ml of Apo A-I. Electrophoretic conditions: capillary, fused-silica (50 cm × 50 μm I.D.); loading, 2.75·10^7 Pa s; running conditions, 20 kV; buffer, Bio-Rad evaluation LLV buffer; equipment, Bio-Rad CE 3000, BioFocus 3000. Peaks: 1 = albumin; 2 = Apo A-I.

Fig. 5 shows a linear plot of relative peak area vs. amount of Apo A-I standard (co-injected with a serum sample) obtained under the same conditions as in Fig. 2. The peak areas at each concentration were determined four times. As clinically relevant Apo A-I serum concentrations are 5–300 mg/dl, the detection limit and range of the CE method are suitable for routine analysis.

It is well known from the literature that protein sticking to the fused-silica capillary wall surface and basic washing buffers influence the migration time and peak areas [45–47], and both are undesirable in routine clinical analysis. However, when LLV buffer was used for washing between runs for 50 consecutively measured serum electropherograms, a relative standard deviation of 1.8% for the migration time (Fig. 6) and of 8.7% for the relative peak area (Fig. 7) were found, which are acceptable for routine analysis. The slightly increasing migration time of Apo A-I observed is a phenomenon well known for proteins separated with fused-silica capillary columns [15,39]. The slightly decreasing peak areas might well be a consequence of irreversible adsorption on the detector window, or protein adsorption could affect the efficiency of non-adsorbing species by setting up complex flow patterns within the capillary [48].

In Table 1, nephelometrically and capillary electrophoretically determined Apo A-I concentrations in sera from different patients are compared. If only the main Apo A-I peak fraction is considered, the concentrations determined by
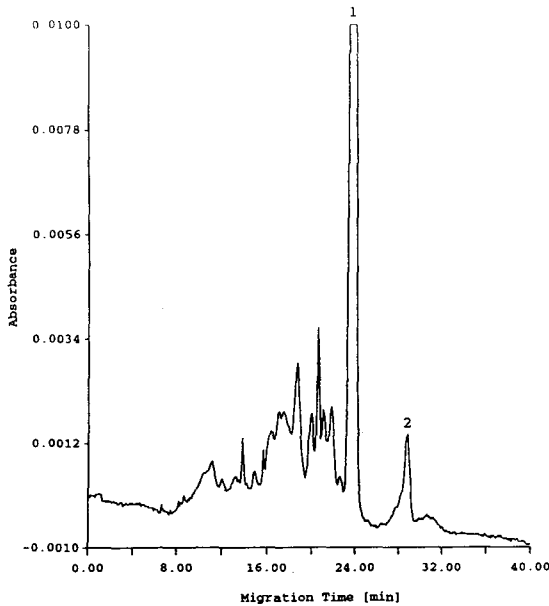
Fig. 3. Electropherogram of a lipaemic serum sample from a patient (triglycerides, 967 mg/dl; cholesterol, 298 mg/dl). Separation conditions as in Fig. 2; detection, UV at 195 nm. Peaks: 1 = albumin; 2 = Apo A-I. Results of determination of Apo A-I: CE, 167 mg/dl; nephelometry, 147 mg/dl.
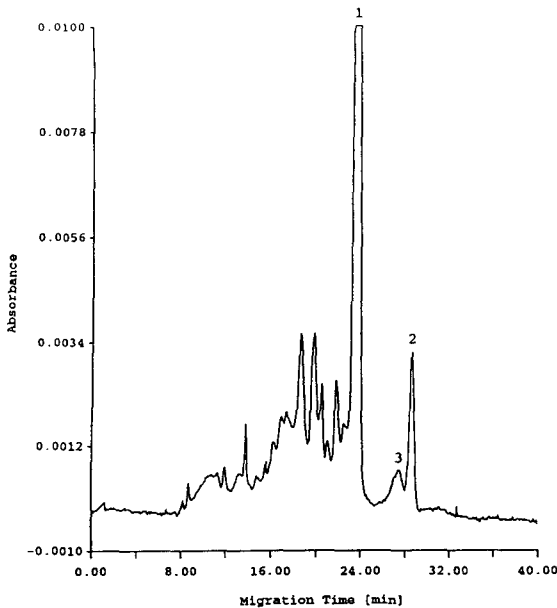
Fig. 4. Electropherogram of a patient's serum sample with an elevated level of Apo A-I. Separation conditions as in Fig. 2; detection, UV at 195 nm. Peaks: 1 = albumin; 2 + 3 = Apo A-I. Results of determination of Apo A-I: CE, 301 mg/dl; nephelometry, 244 mg/dl.
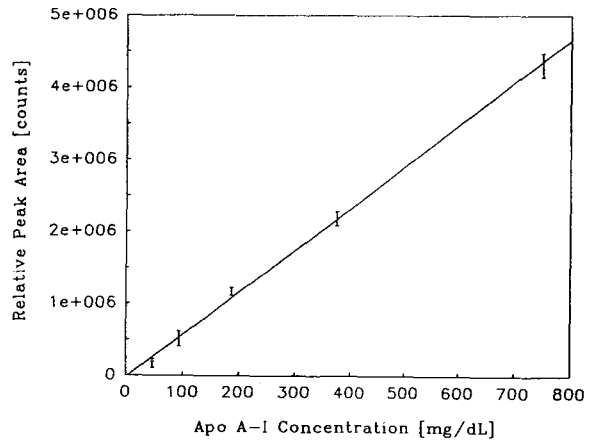
Fig. 5. Plot of relative peak area vs. amount of separated Apo A-I standard (co-injected with a serum sample). Electrophoretic conditions as in Fig. 2. All samples were analysed four times.

CE are about 50% lower than the nephelometric results. If the peak areas of the polymorphic Apo A-I forms are also included, there is a good agreement between nephelometry and CE, although on average about 10% higher values were found with CE, which may be caused by the above-mentioned drawbacks from which nephelometry suffers.
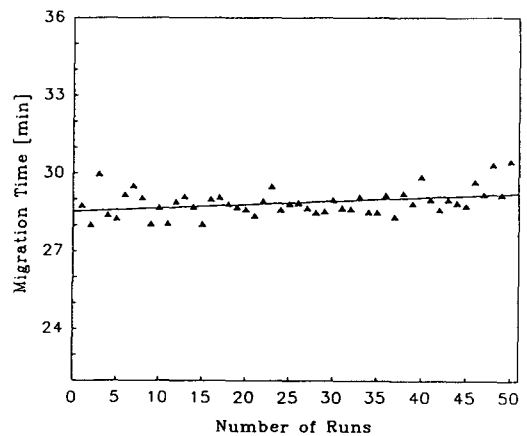
Fig. 6. Reproducibility of the migration time (50 runs) of the Apo A-I peak (intra-assay precision) for the electropherogram illustrated in Fig. 4. Mean, 28.88 min; S.D., 0.53 min; R.S.D., 1.84%.
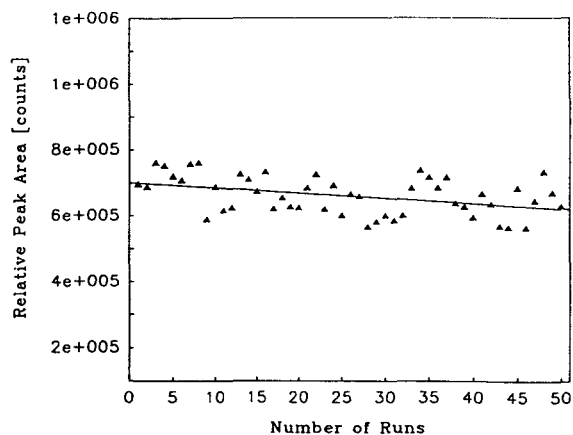
Fig. 7. Reproducibility of the relative peak area (50 runs) of the Apo A-I peak (intra-assay precision) for the electropherogram illustrated in Fig. 4. Mean, 660 441 counts; S.D., 57 812 counts; R.S.D., 8.75%.

4. Conclusions

The described buffer system makes possible the direct determination of Apo A-I concentrations in human serum samples. In contrast to nephelometry, CE also allows the detection of different polymorphic Apo A-I forms, the clinical relevance for which can now be investigated with our method. The ease of serum sample preparation, the good linearity of relative peak area vs. Apo A-I concentration, automation of the technique and low-cost reagents are advantages for application in routine clinical laboratories.

References

[1] H. Engelhardt, W. Beck, J. Kohr and T. Schmitt, Angew. Chem., 105 (1993) 659.
[2] W. Voelter, G. Grübler, H. Straubinger, H. Zimmermann, S. Stoeva, H. Echner, T. Kaiser and G. Paulus, LABO, 25 (1994) 40.
[3] C.A. Monnig and R.T. Kennedy, Anal. Chem., 66 (1994) 280R.
[4] H. Engelhardt, W. Beck and T. Schmitt, Kapillarelektrophorese, Vieweg, Braunschweig/Wiesbaden, 1994.
[5] J.P. Landers, Handbook of Capillary Electrophoresis, CRC Press, Boca Raton, FL, 1994.
[6] J.S. Green and J.W. Jorgenson, J. Chromatogr., 478 (1989) 63.
[7] J. Liu, K.A. Cobb and M. Novotny, J. Chromatogr., 519 (1990) 189.
[8] E. Yildiz, G. Grübler, S. Hörger, H. Zimmermann, H. Echner, S. Stoeva and W. Voelter, Electrophoresis, 13 (1992) 683.
[9] H.-J. Gaus, A.G. Beck-Sickinger and E. Bayer, Anal. Chem., 65 (1993) 1399.
[10] T. Kaiser, S. Stoeva, G. Grübler, H. Echner, A. Haritos and W. Voelter, in R.S. Hodges and J.A. Smith (Editors), Proceedings of the 13th American Peptide Symposium, Edmonton, June 1993, Escom, Leiden , 1994, p. 224.
[11] P.D. Grossman, J.C. Colburn, H.H. Lauer, R.G. Nielsen, R.M. Riggin, G.S. Sittampalam and E.C. Rickard, Anal. Chem., 61 (1989) 1186.
[12] E.C. Rickard, M.M. Strohl and R.G. Nielsen, Anal. Biochem., 197 (1991) 197.
[13] N.A. Guzman, M.A. Trebilcock and J.P. Advis, Anal. Chim. Acta, 249 (1991) 247.

Table 1

Comparison Apo A-I concentrations (mg/dl) in sera from different patients determined by nephelometry and capillary electrophoresis (conditions as in Fig. 2).

Patent	Nephelometry	CE[a]	
		Main peak	Both peaks
1	128	83 (−54%)	131 (+2%)
2 (lipaemic)	147	97 (−52%)	167 (+12%)
3	149	92 (−63%)	173 (+14%)
4	139	85 (−63%)	136 (−2%)
5	244	170 (−43%)	301 (+19%)

[a] The CE values are calculated on the basis of the peak area vs. concentration plot (Fig. 5).

[14] Z. Zhao, A. Malik and M.L. Lee, Anal. Chem., 65 (1993) 2747.

[15] M.A. Strege and A.L. Lagu, Anal. Biochem., 210 (1993) 402.

[16] W. Voelter, G. Grübler, S. Stoeva, T. Kaiser, H. Liebich and R. Lehmann, in Abstracts of the 2nd Symposium on Capillary Electrophoresis, Göttingen, September 1994, Bio-Rad, Richmond, CA, 1994, p. 8.

[17] S. Honda, A. Makino, S. Suzuki and K. Kakehi, Anal. Biochem., 191 (1990) 228.

[18] J.P. Landers, R.P. Oda, B.J. Madden and T.C. Spelsberg, Anal. Biochem., 205 (1992) 115.

[19] D. Demorest and R. Dubrow, J. Chromatogr., 559 (1991) 43.

[20] Y. Baba, J. Chromatogr., 618 (1993) 41.

[21] W. Voelter, G. Grübler, H. Straubinger, T.H. Al-Tel, A. Tippelt, M. Geiger and W. Reinig, Minerva Biotec, 5 (1993) 162.

[22] S. Fanali, M. Cristalli, A. Nardi, L. Ossicini and S.K. Shukla, Farmaco, 45 (1990) 693.

[23] S. Fanali, A. Nardi, M. G. Quaglia and A. Farina, Farmaco, 45 (1990) 703.

[24] G. Grübler, H. Mayer and W. Voelter, BIOforum, 3 (1992) 50.

[25] H. Wätzig, C. Dette and H. Uhl, Pharmazie, 48 (1993) 527.

[26] T. Schmitt and H. Engelhardt, J. High Resolut. Chromatogr., 16 (1993) 525.

[27] Z.K. Shihabi, Ann. Clin. Lab. Sci., 22 (1992) 398.

[28] W. Thormann, S. Molteni, J. Caslavska and A. Schmutz, Electrophoresis, 15 (1994) 3.

[29] O.W. Reif, R. Lausch and R. Freitag, Adv. Chromatogr., 34 (1994) 1.

[30] T. Tadey and W.C. Purdy, J. Chromatogr., 583 (1992) 111.

[31] R. Lehmann, H. Liebich, G. Grübler and W. Voelter, in Abstracts of Electrophoresis Forum '94, Munich, October 1994, Technical University, Munich, 1994, p. II/15.

[32] J.J. Maciejko, B.R. Holmes, D.A. Kottke, A.R. Zinsmeister, D.M. Dinh and S.J.T. Mao, N. Engl. J. Med., 309 (1983) 365.

[33] P. Alaupovic, Ann. Biol. Clin., 38 (1980) 83.

[34] F. Dati, M. Lammers, A. Adam, D. Sondag and L. Stienen, Lab. Med., 13 (1989) 87.

[35] J.L. Adolphson and J.J. Albers, J. Lipid Res., 30 (1989) 597.

[36] R.F. Atmeh, J. Shepherd and C.J. Packard, Biochim. Biophys. Acta, 751 (1983) 175.

[37] S.J.T. Mao, J.P. Miller, A.M. Gotto, Jr., and J.T. Sparrow, J. Biol. Chem., 255 (1980) 3448.

[38] G. Schonfeld, J.-S. Chen and R.G. Roy, J. Biol. Chem., 252 (1977) 6655.

[39] F.-T.A. Chen, C.-M. Liu, Y.-Z. Hsieh and J.C. Sternberg, Clin. Chem., 37 (1991) 14.

[40] M.J. Gordon, K.-J. Lee, A.A. Arias and R.N. Zare, Anal. Chem. 63 (1991) 69.

[41] F.-T.A. Chen and J.C. Sternberg, Electrophoresis, 15 (1994) 13.

[42] V.I. Zannis, J.L. Breslow and A.J. Katz, J. Biol. Chem., 255 (1980) 8612.

[43] G. Ghiselli, E.J. Schaefer, J.A. Light and H.B. Brewer, Jr., J. Lipid Res., 24 (1983) 731.

[44] A. Goux, A. Athias, L. Persegol, L. Lagrost, P. Gambert and C. Lallemant, Anal. Biochem., 218 (1994) 320.

[45] H.H. Lauer and D. McManigill, Anal. Chem., 58 (1986) 166.

[46] S. Hjertén, Electrophoresis, 11 (1990) 665.

[47] S.C. Smith, J.K. Strasters and M.G. Khaledi, J. Chromatogr., 559 (1991) 57.

[48] J.K. Towns and F.E. Regnier, Anal. Chem., 64 (1992) 2473.

Characterization of lipoprotein a by capillary zone electrophoresis

Alison Z. Hu, Ingrid D. Cruzado, Jeff W. Hill, Catherine J. McNeal, Ronald D. Macfarlane*

Department of Chemistry, Texas A&M University, College Station, TX 77843-3255, USA

Abstract

Lipoprotein a [Lp(a)] has been recognized as a significant marker for premature coronary heart disease (CHD). In this paper, we present the results of Lp(a) analysis based on capillary zone electrophoresis (CZE). CZE separation of Lp(a) and its reduced species, lipoprotein a$^-$ [Lp(a$^-$)] and apolipoprotein a [apo(a)], was accomplished using 50 mM borate buffer containing 3.5 mM sodium dodecyl sulfate (SDS) and 20% (v/v) acetonitrile (ACN). Low density lipoprotein (LDL) and high density lipoprotein (HDL) were separated under the same buffer conditions. The electrophoretic mobilities of both Lp(a) and Lp(a$^-$) were found to be different from that of LDL. Benzyl alcohol (BA) and methanol (MeOH) were used as electroosmotic flow markers. BA molecules associated with Lp(a$^-$) and LDL to enhance their UV absorbance, but did not change their effective electrophoretic mobilities. Our results show that CE is a very efficient and effective technique for lipoprotein analysis.

1. Introduction

Lipoproteins (LPs) are a class of large bio-molecules which are closely associated with CHD. Among them, lipoprotein a [Lp(a)] has been recognizd as a significant marker for predicting the risk of CHDs due to its genetic trait [1]. As a consequence, detection of elevated Lp(a) levels with rapid, efficient analytical methods could make a significant contribution to solving the problems of assaying Lp(a) in blood. Lp(a) has many of the features of low density lipoprotein (LDL). It consists of an LDL-like particle, lipoprotein a$^-$ [Lp(a$^-$)], and apolipoprotein a [apo(a)] [2]. Apo(a) is attached to

Lp(a$^-$) through a single disulfide bond which can be cleaved via chemical reduction.

Immunoassay [3,4] is the prevailing technique for measuring Lp(a) concentration in serum or plasma. However, because of the high heterogeneity of Lp(a) molecules detection methods with reliable standards and reference materials have long been sought [5]. Sodium dodecylsulfate polyacrylamide gel electrophoresis (SDS-PAGE) [6] is fundamental for characterization of Lp(a) polymorphism, but its performance is time-consuming.

Capillary electrophoresis (CE) has been used for the analysis of large biomolecules in many situations. Apoliproteins have been separated with capillary zone electrophoresis (CZE) [7–9] and lipoproteins with capillary isotachophoresis (ITP) [10]. In this paper, we present the results

---

* Corresponding author.

of a CZE method for the identification of Lp(a) and other lipoprotein species.

2. Experimental

2.1. Instrumentation

All CE data were collected with a Beckman P/ACE System 5510 (Beckman Instruments, Fullerton, CA, USA) equipped with System Gold software and a diode array detector. Fused-silica capillaries (Polymicro Technologies, Phoenix, AZ, USA) of 75 μm I.D. and 375 μm O.D. were used for the CE analysis. SDS-PAGE gels were casted with a gradient former (Jule, New Haven, CT, USA) and electrophoresis was performed with a vertical slab-gel unit SE 600 (Hoefer Science, San Francisco, CA, USA) and power supply FB 458 (Fisher Scientific, Pittsburg, PA, USA). A Beckman ultracentrifuge L7-65 with a 70Ti rotor was used for Lp(a) separation from plasma. Sample desalting was performed with Slide-A-lyzers (Pierce, Rockford, IL, USA).

2.2. Materials

Double distilled water, deionized with a Milli-Q system from Millipore (Bedford, MA, USA) and filtered with a 0.22-μm filter, was used in the preparation of all CE buffers. Sodium borate, sodium bromide, EDTA, and BA were obtained from Fisher Scientific (Fair Lawn, NJ, USA). Bovine serum albumin (BSA), fibrinogen, low density lipoprotein (LDL), high density lipoprotein (HDL), SDS (70% purity), dithiothreitol (DTT), and β-mecaptomethanol (ME), phenylmethyl-sulfonyl fluoride (PMSF), aprotinin, and coomassie brilliant blue R 250 were purchased from Sigma (St. Louis, MO, USA). Sodium azide was from Aldrich (Milwaukee, WS, USA). Acetonitrile (ACN), acetic acid, and methanol were purchased from EM Science (Gibbstown, NJ, USA). Acrylamide was obtained from Boehringer (Mannheim, Germany), and N′N′-methylenebisacrylamide from Life Technologies (Gaithersburg, MD, USA). Pre-

stained high-molecular-mass standards (M_r 49 000–194 000) for SDS-PAGE were obtained from Bio-Rad (Hercules, CA, USA). Lysine-Sepharose 4B gels were obtained from Pharmacia Biotech (Piscataway, NJ, USA). Lp(a) plasma concentration was determined by enzyme-linked immunosorbant assay (ELISA). Lp(a) ELISA kit was purchased from Strategic Diagnostic Industries (Newark, DE, USA). All chemicals were of analytical-reagent grade or electrophoresis grade and used without further purification.

2.3. Isolation of Lp(a) from blood

Lp(a) was isolated from blood plasma via ultracentrifugation [11] and purified by lysine-Sepharose affinity chromatography [12]. The subject selected had a Lp(a) plasma level of 1.08 g/l as determined by ELISA. The plasma was mixed with 0.15% EDTA, 0.01% sodium azide, 0.0001% PMSF, and 0.4 μM aprotinin. Its density was adjusted to 1.15 g/ml by adding sodium bromide. The density adjusted plasma was spun at 45 000 rpm for 24 h at 5°C. After fractionation, the top floating thick orange band was aspirated with Pasteur pipettes and its Lp(a) concentration was determined to be 4.75 g/l by ELISA. This fraction was dialyzed against phosphate buffered saline (PBS) solution for 20 min at 4°C. The fraction density was then readjusted to 1.05 with sodium bromide and subjected to spinning at 54 000 rpm for 20 h at 5°C. The bottom fraction [Lp(a) = 2.00 g/l by ELISA] was aspirated, dialyzed, and purified by lysine-Sepharose affinity chromatography.

2.4. SDS-PAGE

Gradient polyacrylamide gels of 3–10% were self-casted with a Jule gradient former. SDS (0.1%)–Tris (0.02 M)–glycine (0.2 M) buffer of pH 8.3 was used. Prestained SDS-PAGE standards and Lp(a) (15–20 ng each) were mixed with either nonreducing buffer for 30 min at room temperature or reducing buffer for 7 min at 100°C. The samples then were loaded on the gel wells and the gel was run for 8–10 h. The gel

was stained and destained following the established procedure [13].

2.5. CE methods

The fused-silica capillaries used had a total length of 57 cm and an effective length of 50 cm. Bared fused-silica capillaries were initially rinsed with 1 M NaOH and water and conditioned between runs with 0.1 M NaOH and water. Using 50 mM borate buffer containing 3.5 mM SDS and 20% (v/v) ACN, CE data were collected at 214 nm, 17.50 kV, 20°C, and pressure injection between 1–5 s. Lipoprotein samples were stored at 4°C in 0.15 M NaCl with 0.01% EDTA at pH 7.4. Each lipoprotein sample was diluted 10 times with run buffer before injection. Reduction of Lp(a) into apo(a) and Lp(a⁻) was performed by adding ME (0.09 M) to the diluted sample and boiling the sample for 7 min. The amount of lipoproteins injected was between 1–8 ng (0.5 fmol–4 fmol). Diluted BA (5 μl in 100 ml water) or methanol (1:1 in water) was used as the electroosmotic flow marker.

3. Results and discussion

3.1. Lp(a) reduction determined by SDS-PAGE

The ultracentrifugal separated and lysine-Sepharose 4B purified Lp(a) fraction was positively identified with Lp(a) ELISA. The Lp(a) was further analyzed by SDS-PAGE in non-reduced and reduced forms as shown in Fig. 1, where one and two bands were displayed correspondingly [14]. This result indicated that a fairly pure Lp(a) sample was isolated from plasma and Lp(a) reduction was complete.

3.2. Characterization of Lp(a) and its reduction products by CZE

Using 50 mM borate buffer of pH 10, Lp(a) produced very narrow peaks after it was premixed with 1% SDS–0.5 M Tris buffer (Fig. 2). The plate number of the Lp(a) peak was calculated to be higher than 10^7/m. However, the reduced
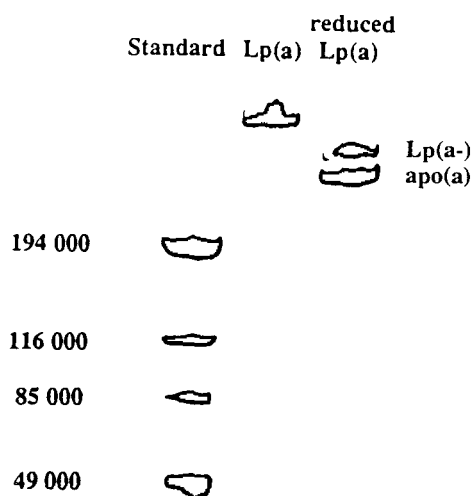
Fig. 1. Lp(a) in non-reduced and reduced forms determined by SDS-PAGE.

Lp(a) products, Lp(a⁻) and apo(a), were detected as one peak under the conditions used. The SDS concentration in the sample buffer (35 mM) was above the critical micellar concentration (CMC = 8 mM) and the running buffer was free of SDS. Therefore, the reduced Lp(a) particles formed micelles which migrated together and were detected as one peak. A similar result was observed for ovalbumin and conalbumin [15]. The loss of resolution and the peak sharpening effect were caused by the mobility gradients as indicated.
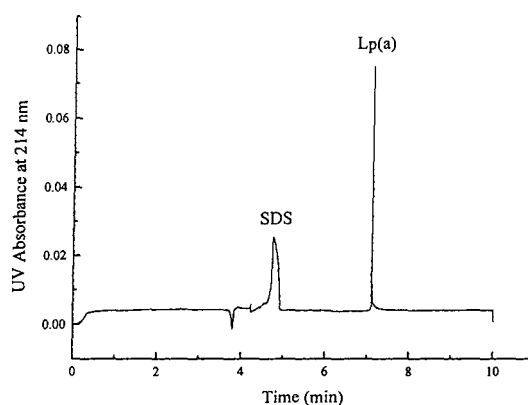
Fig. 2. Lp(a) in 50 mM sodium borate buffer at pH 10. The sample was premixed with 1% SDS–0.5 M Tris buffer. Running condition: 30 kV, 20°C, pressure injection for 5 s.

Using 20% acetonitrile (ACN), 3.5 mM SDS, 50 mM sodium borate (pH 9) as buffer and BA as electroosmotic flow marker, Lp(a) in its non-reduced and reduced form was examined as shown in Fig. 3. Comparing Fig. 3a and 3b, Lp(a) could be easily characterized. The LDL peak in Fig. 3a was identified using LDL samples purchased from Sigma. Two LDL samples from Sigma were tested, one isolated from plasma via size-exclusion chromatography and the other being lyophilized powder redissolved in phosphate-buffered saline (0.15 M NaCl, pH 7.4). The effective mobilities of these two LDL samples were very close. Unlike Lp(a), LDL remained intact after treatment with reducing buffer. Fig. 3 shows two interesting results. First, both Lp(a) and Lp(a$^-$) were different from LDL in terms of their effective electrophoretic mobilities (μ_{eff}). Second, LDL still existed in Lp(a) even after Lp(a) was purified by lysine-Sepharose affinity chromatography.

The LDL samples from Sigma were originally used to distinguish Lp(a$^-$) from apo(a), because Lp(a$^-$) has been assumed to be an LDL-like particle with regard of its lipid–protein ratio and particle size [16]. Our CE data revealed a significant difference in electrophoretic mobility between Lp(a$^-$) and LDL. We further examined LDL samples from different sources and ob-

Table 1
The effective electrophoretic mobilities of lipoproteins

Lipoproteins (sources)		$\mu_{eff} \times 10^{-5}$ (cm^2/V s)
Lp(a)	(subject's plasma)	15.9 ($\pm$0.2)
apo(a)	(subject's plasma)	14.5 ($\pm$0.2)
Lp(a$^-$)	(subject's plasma)	19.6 ($\pm$0.1)
LDL	(Sigma, liquid)	26.2 ($\pm$0.07)
	(Sigma, lyophilized powder)	24.1 ($\pm$0.1)
	(subject's plasma)	26.1 ($\pm$0.2)
HDL	(Sigma, liquid)	19.6 ($\pm$0.1)
	(Sigma, lyophilized powder)	19.5 ($\pm$0.1)

served fairly consistent μ_{eff} values (Table 1). Consistency of μ_{eff} values also applied to HDL samples (Fig. 4). Structurally, LDL consists of a lipid core with its surface partially covered by apo B-100 [2]. Cholesterol ester and triglyceride molecules, which are hydrophobic, are in the center of the lipid core, while the less hydrophobic free cholesterol and phospholipid molecules are on the surface layer. The apolipoproteins are hydrophilic and rest on the surface of the lipoproteins. Lp(a) is structurally different from LDL in having an additional apo(a). Our CE data indicate that both Lp(a) and Lp(a$^-$) are different from LDL in terms of their μ_{eff}. In CE, the μ_{eff} of a species is determined by its charge-to-size ratio. LDL and Lp(a) have comparable particle sizes [15]. SDS molecules can add nega-
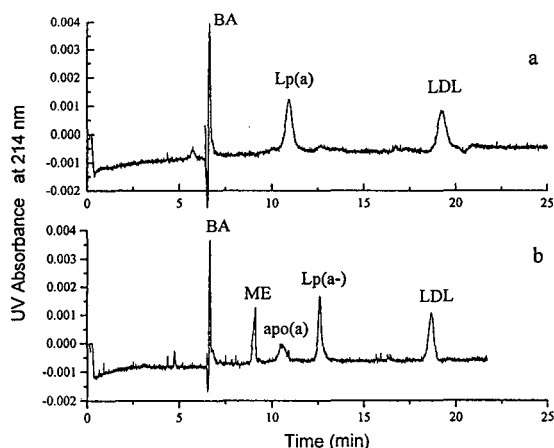
Fig. 3. Lp(a) in non-reduced (a) and reduced (b) forms. Running condition: 17.5 kV, 20°C, pressure injection for 1–2 s.
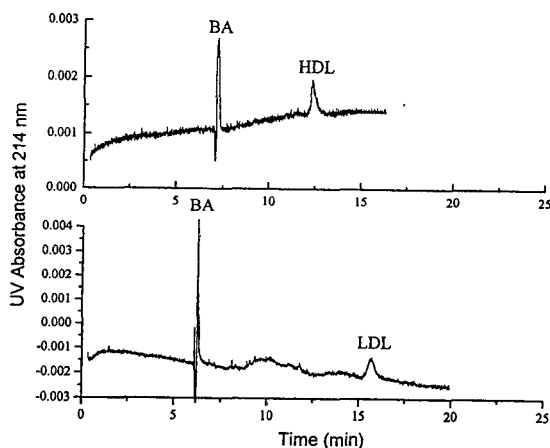
Fig. 4. HDL and LDL separation under the same conditions as in Fig. 3.

tive charges to lipoproteins by attaching to both lipid molecules and protein backbones. The average amount of lipid (w/w) in Lp(a) and LDL is 66 and 77%, respectively [16]. Because the surface of LDL is covered more by lipid than Lp(a), it is likely that more SDS molecules will attach to the LDL surface resulting in an increase of negative charges on the LDL particles. Hence, the charge-to-size ratio of LDL molecules exceeded that of Lp(a) and consequently a larger μ_{eff} was observed for LDL.

The existence of LDL in Lp(a) samples was clearly shown in Fig. 3 but could not be seen on the slab SDS-PAGE (Fig. 1). When Lp(a) was isolated as density fractions using ultracentrifugation, it was likely to be contaminated by LDL and HDL. Apo(a) in Lp(a) consists of many repeats of a unique structural domain, the kringle domain [2], which can specifically bind to lysine. Since kringle domains do not exist in LDL or HDL, it should be possible to purify Lp(a) from LDL and HDL by lysine-Sepharose affinity chromatography. Based on our CE data, HDL did not appear in the Lp(a) electrophoregrams. On the one hand, the detection of LDL in Lp(a) demonstrated the superior sensitivity of CE over slab SDS-PAGE; on the other hand, it implied that Lp(a)–LDL complexes exist in plasma because LDL could not have survived the affinity chromatographic separation unless it is tightly associated with Lp(a) via lipophilic interaction. Evidence for the high affinity of Lp(a) for LDL has been reported [17].

Both BA and methanol were used as neutral markers in our CE studies. Neutral marker was injected following each sample injection. Unexpectedly, the two markers caused considerable differences in the signal intensities of the LDL (Fig. 5) and Lp(a⁻) (Fig. 6) peaks. MeOH appeared as a positive peak in Figs. 5 and 6 because the background electrolyte buffer contained 20% ACN which showed a lower UV absorbance than MeOH. When methanol was used as the neutral marker, the LDL peak in the Lp(a) sample was either very small or non-observable. In contrast, the LDL peak was well detected simply by switching to BA as marker. The aqueous solubility of BA is limited due to its
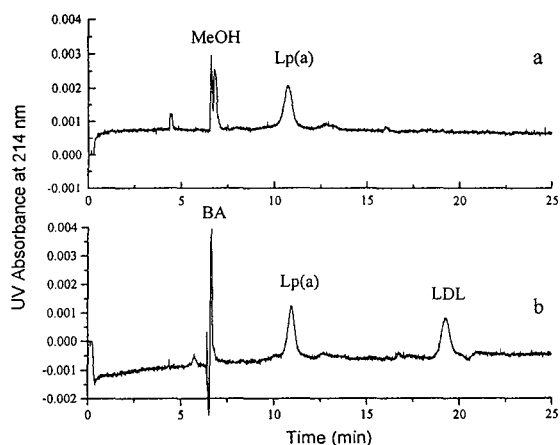
Fig. 5. UV enhancement effect of BA on LDL. The neutral markers used were (a) MeOH and (b) BA. The running conditions were the same as in Fig. 3.

hydrophobic aromatic ring which causes its intense UV absorbance. In LDL, the lipid molecules on the surface layer are hydrophobic and contribute little to the UV absorbance of the LDL particles. When BA was injected following the sample injection, it passed through the sample zone during migration. Presumably, part of the BA molecules became attached to the surface lipid portion to such an extent that the UV absorbance of the LDL molecules was no-
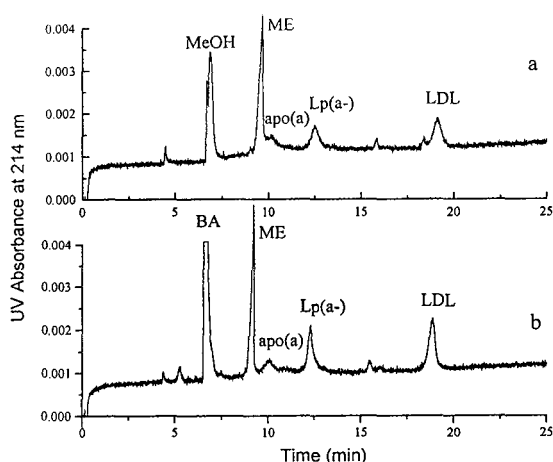
Fig. 6. UV enhancement effect on Lp(a⁻) and LDL. The neutral markers used were (a) MeOH and (b) BA. The running conditions were the same as in Fig. 3.

tably enhanced but its overall C/S ratio was not alternated. This UV-enhancement effect observed for LDL and Lp(a⁻) largely exceeded that of Lp(a) and HDL. It demonstrates that there is more lipid exposed on the surface of LDL and Lp(a⁻) compared with Lp(a) and HDL. In other words, Lp(a) and HDL are covered more by protein on their surfaces. Based on the literature, little is known about the nature of the interaction between apo(a) and Lp(a⁻) other than that the two components can be easily separated via chemical reduction. Our CE results indicate that apo(a) molecules have more interactive contacts with the Lp(a⁻) surface besides the disulfide bond linkage. In LDL particles, apo B-100 molecules are believed to be wrapped around the lipid core [2]. If we consider that the size of apo(a) molecules (300–800 kDa) is comparable to that of apo B-100 (500 kDa), it is conceivable that apo(a) covers a considerable part of the Lp(a⁻) surface.

The CZE method reported here is advantageous over the widely used ELISA and SDS-PAGE techniques. First, all immunoassays rely on specific antibody recognition of epitopes on the Lp(a) molecules. The nature and variety of the epitopes selected by Lp(a) antibodies is unknown. This feature causes the problems in reliable standardization and comparison [5]. In contrast, CZE detection of Lp(a) is based on the UV absorbance of the whole molecule. Therefore, it avoids the dependency on specific epitopes encountered in immunoassays. Secondly, Lp(a) and LDL show very low mobilities on SDS-PAGE due to their extremely large sizes as well as lipid contents, which makes the determination of molecular masses and isoforms difficult. On the other hand, all lipoproteins studied by us show very different electrophoretic mobilities. (iii) ELISA and SDS-PAGE require 3–10 h to accomplish, while all the measurements of Lp(a) and other lipoproteins presented above are achieved within 20 min. In addition, neither immunoassays nor SDS-PAGE can be used to simultaneously determine the concentration and isoforms of lipoproteins, whereas further development of CE methods will likely be successful in this respect.

4. Conclusions

Lp(a) and its reduction products, Lp(a⁻) and apo(a), can be separated and identified with sodium borate buffer containing SDS and ACN. LDL and HDL from different sources have consistent effective electrophoretic mobilities under the same conditions. Both Lp(a) and Lp(a⁻) are significantly different from LDL in their electrophoretic mobilities. Because of the lipophilic properties of Lp(a⁻) and LDL, they can absorb BA on their surface thereby enhancing their UV absorbance. Based on the different electrophoretic behaviors of Lp(a) and LDL, we speculate that Apo(a) does not simply attach to Lp(a⁻) via a disulfide bond, but has also other interactions with the Lp(a⁻) surface. All the CE data can be obtained within 20 min, which is very time efficient compared to immunoassay and SDS-PAGE.

References

[1] G. Utermann, J.J. Menzel, H.G. Kraft, H.C. Duba, H.G. Kemmler and C. Seitz, J. Clin. Invest., 80 (1987) 458.
[2] R.M. Lawn, Science, 266 (1992) 54.
[3] C. Labor, J. Shepherd and M. Racine, Clin. Chem., 36 (1990) 591.
[4] W.C. Taddei-Peters, B.T. Butman, G.R. Jones, T.M. Venetta, P.F. Macomber and J.H. Ransom, Clin. Chem., 39 (1993) 1382.
[5] J.J. Albers and S.M. Marcovina, Chem. Phys. Lipids, 67/68 (1994) 257.
[6] J.W. Gaubatz, K.I. Ghanem, J. Guevara, Jr., M.L. Nava, W. Patsch and J.D. Morrisett, J. Lipid Chem., 31 (1990) 603.
[7] T. Tadey and W. Purdy, J. Chromatogr., 583 (1992) 111.
[8] T. Tadey and W. Purdy, J. Chromatogr. A, 652 (1993) 131.

[9] A. Goux, A. Athias, L. Persegol, L. Lagrost, P. Gambert and C. Lallemant, Anal. Biochem., 218 (1994) 320.

[10] G. Schmitz and C. Möllers, Electrophoresis, 15 (1994) 31.

[11] J.W. Gaubatz, G.L. Cushing and J.D. Morrisett, Methods Enzymol., 129 (1986) 180.

[12] M.L. Snyder, D. Polacek, A.M. Scanu and G.M. Fless, J. Biol. Chem., 267 (1992) 339.

[13] J.F. Robot and B.J. White, Biochemical Techniques–Theory and Practice, Waveland Press, Prospect Heights, IL, 1990, p. 140.

[14] G.M. Fless, M.E. ZumMallen and A.M. Scanu, J. Lipid Res., 26 (1985) 1224.

[15] E. Kenndler and K. Schmidt-Beiwl, J. Chromatogr., 545 (1991) 397.

[16] G.M. Kostner, in A.M. Scanu (Editor), Lipoprotein a, Academic Press, San Diego, CA, 1990, p. 183.

[17] G.M. Kostner and H.K. Grillhofer, J. Biol. Chem., 266 (1991) 21287.

ELSEVIER

Application of capillary electrophoresis, high-performance liquid chromatography, on-line electrospray mass spectrometry and matrix-assisted laser desorption ionization–time of flight mass spectrometry to the characterization of single-chain plasminogen activator

A. Apffel[a],*, J. Chakel[a], S. Udiavar[a], W.S. Hancock[a], C. Souders[b], E. Pungor Jr.[b]

[a]Hewlett-Packard Laboratories, MS26U/R6, 3500 Deer Creek Road, Palo Alto, CA 94304, USA
[b]Berlex Biosciences, 430 Valley Dr., Brisbane, CA 94005, USA

Abstract

The analysis of recombinant *Desmodus* salivary plasminogen activator (DSPAα1), a heterogeneous glycoprotein, is demonstrated through the use of high-performance liquid chromatography (HPLC), high-performance capillary electrophoresis (HPCE), liquid chromatography–electrospray mass spectrometry (LC–ES-MS), and matrix-assisted laser desorption ionization–time of flight mass spectrometry (MALDI–TOF-MS). The protein is analyzed at three specific levels of detail: the intact protein, proteolytic digests of the protein, and fractions from the proteolytic digest. A method for "on-column" collection of HPLC fractions for subsequent transfer and analysis by HPCE and MALDI–TOF-MS is shown.

1. Introduction

The development of rDNA-derived protein pharmaceuticals has been facilitated by the introduction of new analytical methods that can be used to characterize proteins and/or to demonstrate consistency of manufacture of a protein. Peptide mapping is a key method for monitoring the amino acid sequence and is able to detect small changes in small to moderate size proteins, e.g. insulin and human growth hormone. The analysis of a much larger protein, e.g. fibrinogen (molecular mass of 350 000), or the heterogeneous glycoproteins, such as antibodies (molecu-

lar mass of 150 000), is hindered by the complexity of the range of peptides generated by an enzymatic digestion. Such complexity makes a single reversed-phase high-performance liquid chromatography (HPLC) separation combined with on-line UV detection of limited utility.

The advent of commercially available combined HPLC and electrospray ionization mass spectrometry (LC–ES-MS) systems compatible with conventional HPLC methodology has increased the power of peptide mapping considerably [1,2]. LC–ES-MS in combination with in-source collisionally induced dissociation (CID) has been used effectively to identify sites of N- and O-linked glycosylation [3–5]. However, even this technique is limited by insufficient resolution

* Corresponding author.

resulting from the large number of very similar peptides caused by variable protein glycosylation and enzymatic digests of moderately sized glycoproteins. It is therefore necessary to employ a range of techniques with orthogonal selectivity in order to characterize such samples. A significant issue is to efficiently utilize such multidimensional data in a way that multiple samples can be characterized for a product development program.

It is interesting to note the evolution of the terms "multidimensional" and "hyphenated". Ten years ago, these terms were routinely used to mean the (generally) on-line coupling of two single-stage analytical instruments, such as chromatography and mass spectrometry. Now, however, such a coupling is widely accepted and the multidimensionality of the analysis is of a higher order. The power of recent techniques lies in utilizing chromatography, high-performance capillary electrophoresis (HPCE), UV–Vis, mass spectrometric, and other spectrometric data in an integrated manner.

We have, therefore, investigated the use of combinations of HPCE, HPLC, LC–ES-MS, and MALDI–TOF-MS to allow for characterization of enzymatic digests of underivatized glycoprotein samples. The separation selectivity of HPLC and CE is sufficiently orthogonal to yield a great deal of comparative information. Although LC–ES-MS is extremely powerful for peptide mapping, when dealing with intact proteins the mass range is limited to simple mixtures and lower-molecular-mass fragments compared with MALDI–TOF-MS. Thus in combining data from the two techniques, highly complementary data are obtained.

As an example of a heterogeneous glycoprotein, DSPAα1, a single-chain plasminogen activator derived from *Desmodus rotundus* (vampire bat) salivary glands [6] was chosen. DSPAα1 is a serine protease that plays a role in clot lysis. The potential applications for the molecule are in the area of thrombotic myocardial and cerebral infarctions, deep vein thrombosis, lung embolism, and peripheral arterial occlusive diseases. DSPAα1 displays approximately 70% sequence homology with the double-chain serine protease, tissue plasminogen activator (tPA), and may have a fibrin specificity, with a strict dependence on polymeric fibrin as a co-factor [7]. DSPA is known to be heterogeneous when expressed in CHO cells [8]. It is a large (441 amino acids) complex molecule of calculated (non-glycosylated) average molecular mass 49 508, with six sites for potential glycosylation, four O-linked and two N-linked. It has been proposed, based on homology with other serine proteases [6] that there are 28 cysteines forming 14 disulfide bridges.

2. Experimental

2.1. Instrumental

HPLC

The HPLC separation was performed on a Hewlett-Packard 1090 liquid chromatography system equipped with DR5 ternary solvent delivery system, diode-array UV–Vis detector, autosampler, and heated column compartment (Hewlett-Packard, Wilmington, DE, USA). All HPLC separations were done using a Vydac C_{18} (Catalog No. 218TP54, Hesperia, CA, USA) 5-μm particle, 300-Å pore size reversed-phase column. A standard solvent system of water (solvent A) and acetonitrile (solvent B), both with 0.1% trifluoroacetic acid (TFA), was used with a flow-rate of 0.2 ml/min. The gradient for the separation was constructed as 0–60% B in 90 min. The column temperature was maintained at 45°C throughout the separation.

A schematic for "on-column" fraction collection is shown in Fig. 1. The effluent from the HPLC (at 200 μl/min) is mixed with a non-elutropic solvent, 0.1% TFA at 1000 μl/min delivered with an Eldex Model A-30-S metering pump (Eldex Laboratories, Napa, CA, USA). The resultant mixture was selectively directed to one of four possible collection columns, or a bypass, using a Valco Model CST6UW 6-position, 14-port, electrically actuated valve (Valco Instrument, Houston, TX, USA). The collection columns consisted of HP hydrophobic sequencing cartridge columns (P.N. G1073A) in a col-
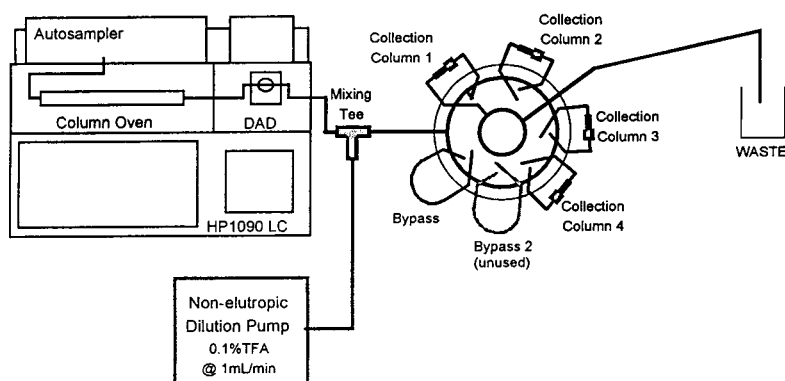
Fig. 1. Schematic of on-column fraction collection.

umn adapter (P.N. G1007A). Fractions were eluted from the collection columns using a gradient from 0 to 90% B in 5 min at a flow-rate of 0.2 ml/min and collected in Eppendorf vials. Four specific fractions were chosen to be collected from the endoproteinase ArgC digest of DSPAα1. The fraction collection process was repeated for four separations with 250 μl of sample at a concentration of 1.2 nmol/ml for a total sample consumption of 1.2 nmol. For each run, the specific fraction was directed to the appropriate cartridge. The samples were then eluted in approximately 200 μl and concentrated to a final volume of 100 μl. Thus approximately 1.2 nmol of each homogeneous peptide was collected while a lower amount is present for the heterogeneous glycoforms. Since in the original sample the 1.2 nmol was contained in 1000 μl, while the final fraction volume was 100 μl, an approximate ten-fold concentration was obtained along with isolation of the fractions.

High-performance capillary electrophoresis

HPCE was done on a Hewlett-Packard HP³ᴰCE system with a built-in UV–Vis diode-array detector (DAD) and MS Windows Chemstation 3D software. A phosphate deactivated [9] fused-silica capillary of 50 μm internal diameter and 56 cm effective length with a 150 μm extended light path (bubble cell) (P.N. G1600-62232) was used. The capillary was thermostatted at 35°C. Before each separation, the capillary

was conditioned by flushing with 0.1 M NaOH for 2 min at 50 mbar, followed by flushing with background electrolyte for 5 min at 50 mbar. The background electrolyte consisted of 100 mM sodium phosphate buffer at pH 2.4 and 100 mM NaCl. Injections were made by pressure for 10–30 s at 50 mbar. For peptide separations, the injection was followed by a trailing electrolyte consisting of 1 mM phosphoric acid at 5 kV for 2 min. The use of this discontinuous buffer system served to sharpen the peaks from the injection plug. The separation was monitored at 200 and 280 nm.

Mass spectrometry

LC–ES-MS. Mass spectrometry was done on a Hewlett-Packard 5989B quadrupole mass spectrometer equipped with extended mass range, high-energy dynode detector (HED), and a Hewlett-Packard 59987A API-electrospray source with high-flow nebulizer option. Both the HPLC and MS were controlled by the HP Chemstation software, allowing simultaneous instrument control, data acquisition, and data analysis. The high-flow nebulizer was operated in a standard manner with N_2 as nebulizing (1.5 l/min) and drying (15 l/min at 300°C) gas.

To counteract the signal suppressing effects on LC–electrospray MS of trifluoroacetic acid, a previously reported method [10], referred to as the "TFA fix" was employed. The "TFA fix" consisted of post-column addition of propionic

acid–isopropanol (75:25) at a flow-rate of 100 μl/min. The TFA fix was delivered using an HP 1050 HPLC pump and was mixed with a zero-dead-volume tee into the column effluent after the DAD detector and after the column-switching valve. Column effluent was diverted from the MS for the first 5 min of the chromatogram, during which time excess reagents and unretained components eluted.

For peptide mapping, MS data was acquired in scan mode, scanning from 200 to 1600 u at an acquisition rate of 1.35 Hz at 0.15 u step size. Unit resolution was maintained for all experiments. Data was filtered in the mass domain with a 0.03 u Gaussian mass filter and in the time domain with a 0.05 min Gaussian time filter. The fragment identification was done with the aid of HP G1048A protein and peptide analysis software, a software utility which assigns predicted fragments from a given sequence and digest with peak spectral characteristics.

For the in-source collisionally induced dissociation (CID) method for detecting fragments indicative of glycopeptides [3], the CapEx voltage was set to 200 V instead of the standard 100 V. Data acquisition was done in selected-ion monitoring (SIM) mode, monitoring ions at m/z 147, 204, 292, and 366, each with a 1 u window and a dwell time of 150 ms, resulting in an acquisition rate of 1.5 Hz. Data was filtered in the time domain with a 0.05 min Gaussian time filter.

MALDI–TOF-MS. Mass spectra were generated with a Hewlett-Packard 1700XP (predecessor to the Hewlett-Packard G2025A) MALDI–TOF-MS system. This system utilizes a N_2 laser (337 nm) for the desorption/ionization event coupled with a linear 1.7-m time-of-flight analyzer for mass analysis. Spectra were acquired at laser powers just above the ionization threshold using a matrix consisting of either 2,5-dimethoxy-4-hydroxycinnamic acid (sinapinic acid, HP P.N. G2055A) or 2,5-dihydroxybenzoic acid (DHBA, P.N. G2056A).

Intact protein: DSPAα1 (0.55 mg/ml) was mixed 1:1 with a 100 mM sinapinic acid matrix solution and two 1-μl aliquots (ca. 10 pmol total) were sequentially deposited onto the probe tip and vacuum dried in the HP G2024A sample prep accessory. Data were collected at a 100 MHz sampling rate and a total of 100 laser shots were summed. The mass scale was calibrated using a protein standard mixture (HP P.N. G2053A) as an external calibrant.

Protein digest mixture and HPLC pooled fractions: The entire digest mixture sample was prepared by two different methods. For each method, data were collected at a 400 MHz sampling rate and a total of 100 laser shots were summed. The standard preparation method comprised of diluting the digest mixture (0.35 mg/ml) 1:9 with 100 mM sinapinic acid. Two 0.5-μl aliquots (ca. 600 fmol total) were sequentially deposited onto the probe tip and vacuum dried. The alternative method involved generating a seed layer of polycrystalline DHBA on the probe tip and adding a sample–matrix solution to the bed of seed crystals [11]. In this technique, 1 μl of a saturated DHBA matrix solution (30% acetonitrile) is added to the probe tip, allowed to air dry, and mechanically crushed with a glass slide. Non-adhering crystals were then brushed off of the probe tip. The digest mixture sample was diluted 1:9 with the supernatant of the saturated DHBA solution. Then 1 μl of this solution (ca. 600 fmol) was applied to the bed of seed crystals where crystallization commenced immediately, allowed to sit for ca. 30 s, and rinsed with ca. 100 μl water prior to the sample–matrix deposit completely drying out. This method offers an approach that greatly increases the tolerance to contaminants which may interfere in the crystallization process.

The HPLC fractions were mixed 1:1 with a 100 mM sinapinic acid and two 0.5-μl aliquots were sequentially deposited onto the probe tip and vacuum dried. Data were collected at a 400 MHz sampling rate and a total of 75 laser shots were summed for each fraction.

The mass scale was calibrated using a peptide standard mixture (HP P.N. G2052A) as an external calibrant.

2.2. Chemicals and reagents

HPLC-grade acetonitrile and trifluoroacetic acid (TFA), as well as EDTA were obtained from J.T. Baker (J.T. Baker, Phillipsburg, NJ, USA). Distilled, deionized Milli-Q water (Millipore, Bedford, MA, USA) was used. Urea was obtained from GIBCO (Gaithersburg, MD, USA), D,L-dithiothreitol (DTT), iodoacetic acid, bicine, NaOH, and CaCl$_2$ were obtained from Sigma (Sigma, St. Louis, MO, USA). The enzyme endoproteinase Arg-C (Boehringer Mannheim, Indianapolis, IN, USA) was used for mapping. Recombinant DSPAα1 (from Berlex Biosciences, Richmond, CA, USA) was purified from CHO cells, and the starting concentration was 0.55 mg/ml.

2.3. Methods

Sample preparation

DSPAα1 (5 mg) was denatured in 6 M urea and titrated with 5 M NaOH to pH 8.3. The sample was then reduced using 32 mM DTT (molar excess to DSPA 1:300) by incubating at 55°C for 3 h. Alkylation of the reduced protein was done by a further 30 min incubation with 70 mM iodoacetic acid. The reduced and alkylated DSPAα1 was then desalted using size-exclusion chromatography.

Arg-C digestion

The reduced, alkylated, desalted DSPAα1 was digested in 200 mM bicine at 37°C with an enzyme-to-substrate (mass) ratio of 1:50 for 18 h in the presence of 20 mM DTT, 0.5 mM EDTA, and 8.5 mM CaCl$_2$. The digestion was quenched by titrating the sample to pH 1.5.

3. Results and discussion

3.1. Analytical strategy

The analytical approach used for the analysis of the DSPAα1 glycoprotein was to start at the gross level of the intact protein and use ana-

lytical techniques applicable to such a complex, high-molecular-mass sample. Following this characterization, the greater detail of the peptide map from an endoproteinase Arg-C digest was examined, followed by individual fractions from the digest. Thus the focus moved from more global properties of the sample to increasing degrees of detail. At each level, HPLC, LC–MS, HPCE, and MALDI–TOF-MS were applied. At the more global level, it is not possible to discern the detailed information of the specialized techniques. On the other hand, it is difficult to synthesize data from the more specific into a more global picture. This problem of context of scale of macromolecular analysis is at the heart of the need for multidimensional analysis. With samples of this complexity, no one technique yields the required depth of structure information combined with ready linkage to the overall structure of the macromolecule.

The intact glycoprotein

At the level of detail of the intact glycoprotein, information can be gathered concerning the gross chemical and structural characteristics of the protein as well as the purity of the sample preparation. In the current study, the DSPAα1 sample had already undergone a number of purification steps to isolate it from the cells in which it was cultured. With such a protein, there exist multiple opportunities for heterogeneity, including glycosylation, varying N-terminal sequence, amino acid modifications, and proteolytic clipping. The goal of the purification step for a recombinant DNA derived pharmaceutical glycoprotein such as DSPAα1 is to be combined with the production process to produce a high-purity product in a consistent manner. Such a product, however, may still contain substantial heterogeneity introduced by post-translational modifications such as glycosylation. Therefore, the analytical sample may consist of a mixture of not only potential contaminants, but heterogeneous glycoforms as well, which are an intrinsic part of the target molecule. It is the challenge of the analytical chemist to devise a suitable set of methods that

can be applied to such complex samples. Of course, in addition to separation methods discussed below, a wide range of tools including N- and C-terminal sequence analysis, X-ray crystallography, and biological activity tests can be applied.

The initial examination of the intact protein sample was performed by reversed-phase HPLC and is shown in Fig. 2. From the separation, it can be seen that the sample is quite pure, and at least in terms of hydrophobicity, relatively homogeneous, although product variants may not be separated under the applied conditions [12]. Through the use of UV–Vis diode-array detection, its UV spectra can be acquired throughout the separation (see Fig. 2, inset) and data can be obtained concerning the relative number of aromatic amino acids (tryptophan, tyrosine, and phenylalanine) present in the protein. In those cases for which the amino acid composition is known, this information can also be used as a partial identification for the peak in the presence of other proteins.

The capillary electrophoresis separation (see Fig. 3) is used to characterize the intact protein as well as to gather UV–Vis spectral information. In addition, the orthogonality of the separation mechanism, being based on charge rather than hydrophobicity, is useful in the further characterization of purity and homogeneity. In the case of a glycoprotein such as DSPAα1, the charge heterogeneity introduced from the variable sialic acid content due to the glycosylation results in a relatively broad peak, but the absence of other well-separated peaks is consistent with low levels of other contaminating proteins.

The analysis of the intact glycoprotein by MALDI–TOF-MS (shown in Fig. 4) yields information similar to that of HPCE. Although often a destructive technique, the separation is based on mass/charge, as is electrophoresis. Strictly speaking HPCE is based on size/charge, but for denatured peptides this is closely related to mass. The two major peaks in the spectrum represent singly and doubly charged ions from the protein. The mass of the protein, determined from the singly charged ion, is 54 111.6 ± 54 compared with the average molecular mass of 49 508.15 calculated from the amino acid sequence only. The difference in M_r of 4603 or approximately 9.3% indicates a mass increase due to glycosylation. The peak width of approximately M_r 5000 is related to the degree of microheterogeneity of glycosylation. Based on the expected resolution of the MALDI–TOF-MS experiment, if DSPAα1 were homogeneous, it would have a peak width at half height on the order of M_r 500 due, in part, to the isotopic
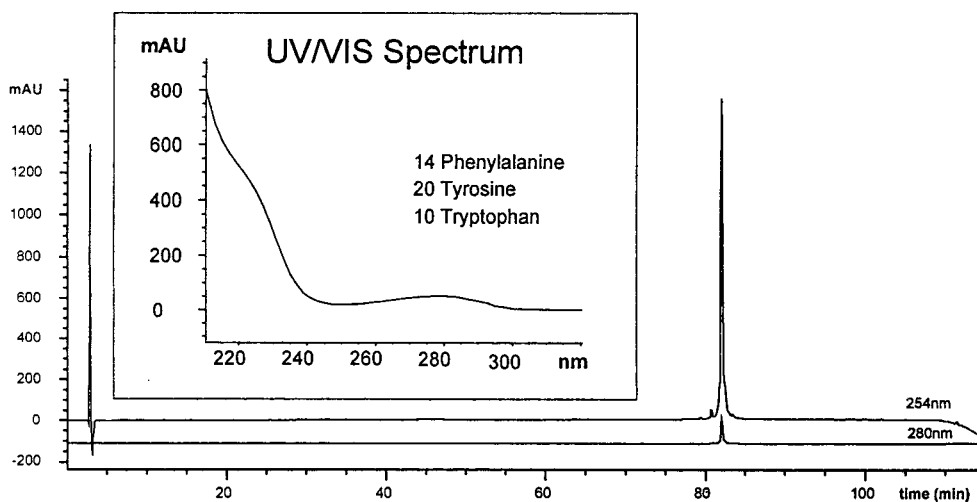
Fig. 2. HPLC of intact protein; 20 μg total protein injected. See text for conditions.
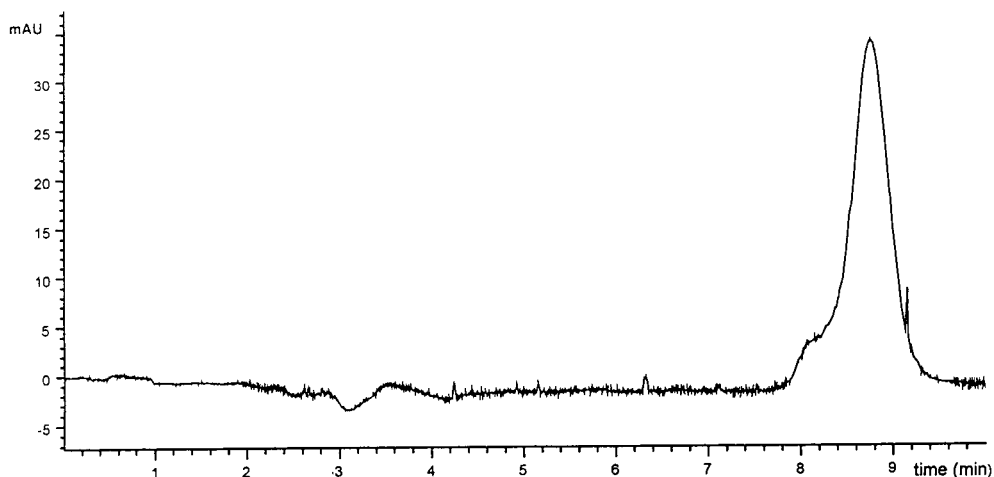
Fig. 3. CE of intact protein; 40 pmol total protein injected. See text for conditions.

distribution. In addition, there is some fine-structure of the $[M + 1]^+$ peak, which may indicate the presence of heterogeneous glycoforms.

It is useful at this level, as well as other levels of detail, to compare the relative sensitivity of the three techniques discussed above. In the case of HPLC, the total amount of sample applied was 20 μg injected in a volume of 10 μl, or a sample concentration of 2 mg/ml (40 mmol/ml). As can be seen from the chromatogram, the HPLC separation could be run at significantly lower concentration. In the case of the HPCE separation, a pressure injection of 1500 mbar s (50 mbar × 30 s) resulted in an injection volume of 10 nl, of an original sample concentration of 0.51 mg/ml, corresponding to 5 pg. While the mass sensitivity of HPCE is very good, due to the low injection volumes and short detection path lengths, the absolute concentration sensitivity is less impressive. In the case of MALDI–TOF-MS, a relatively small amount of sample is applied. The sensitivity is even more impressive
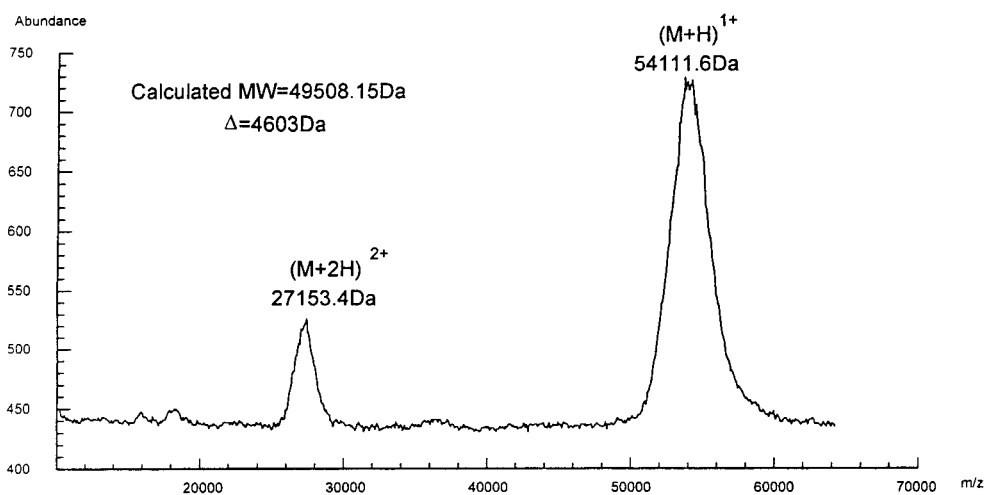
Fig. 4. MALDI–TOF-MS of intact protein; 10 pmol total protein applied. Matrix: sinapinic acid.

when one considers that of the 10 pmol applied, probably less than 100 fmol are consumed. The MALDI–TOF-MS technique generates useful data even when only 10–100 fmol of sample are applied.

The proteolytic digest

At the next level of detail, the intact glycoprotein is digested through the use of a proteolytic enzyme, resulting in a mixture of not only fragments due to the selectivity of cleavage, but of different glycoforms of specific glycosylated fragments as well. If, as is the case for DSPAα1, the cDNA sequence of the protein is known, the peptide map generated by the separation of the digest can be compared with the predicted sequence.

The generation of peptide maps through the chromatographic or electrophoretic separation of the proteolytic digest (as shown in Fig. 5) is extremely powerful in generating a "fingerprint" of the protein. However, when the separation is monitored with a UV–Vis detector, complete identification of the individual fragments is problematic. Although it has been shown that the individual fragments can be identified by comparing the UV spectra with those of standards, fragment identification usually requires fraction collection and subsequent analysis by mass spectrometry or N-terminal peptide sequencing.

The orthogonal separation mechanisms of reversed-phase HPLC and HPCE are evident in comparing the elution patterns of the two separations shown in Fig. 5. This can be exploited to resolve areas in one mode which co-elute in the other. The orthogonality of the separation mechanisms can also be used in a quality control environment as a fingerprint which can detect subtle changes in the protein product.

MALDI–TOF-MS can also be used to characterize enzymatic digest, as shown in Fig. 6. In this complex spectrum, a number of the predicted fragments can readily be identified. However, it is not possible to identify all the digest fragments present in the sample, due to a number of factors. The lack of chromatographic or
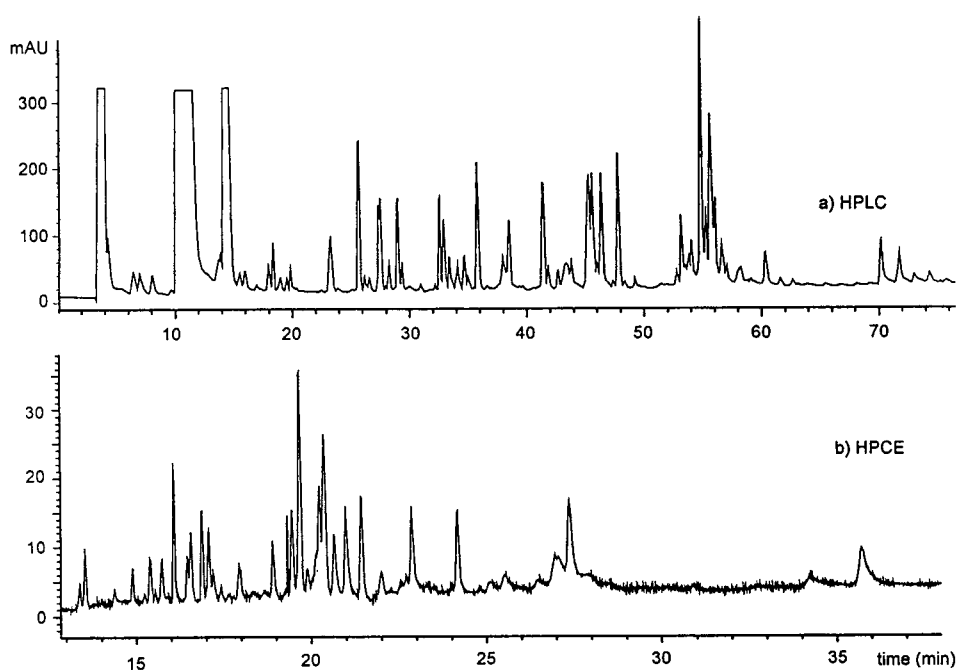
Fig. 5. HPLC and CE of digest. (a) HPLC monitored at 214 nm; 78 pmol injected. (b) HPCE monitored at 200 nm; 5 pmol applied. See text for other conditions.
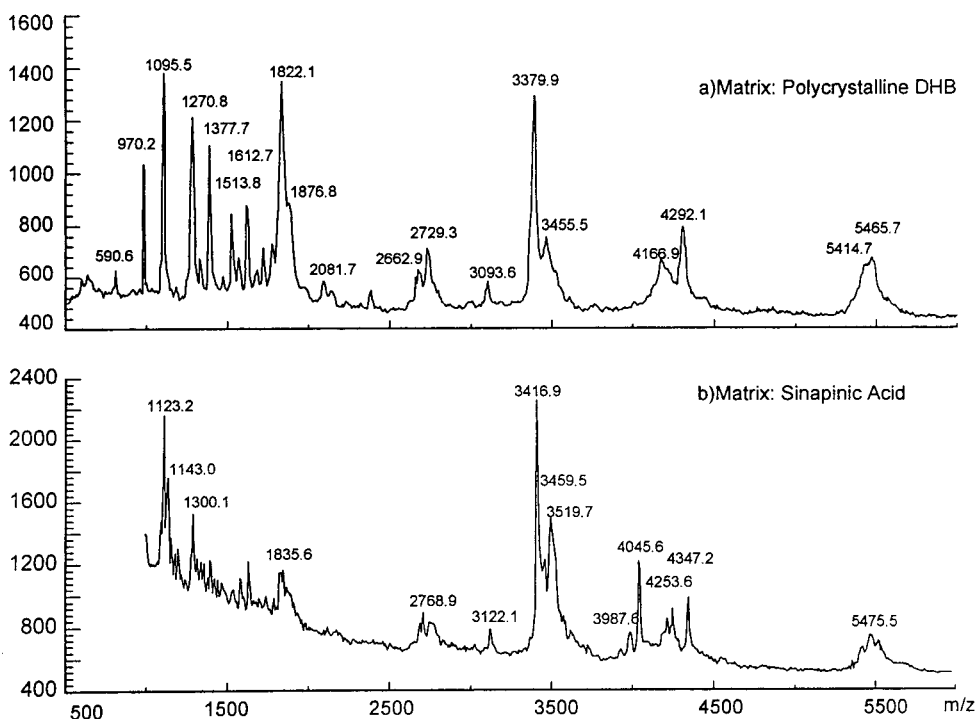
Fig. 6. MALDI–TOF-MS of digest; 500 fmol total protein applied. (a) Matrix: polycrystalline DHBA, (b) sinapinic acid.

electrophoretic separation hinders the ability to spot glycopeptides in complex mixtures. Furthermore, isobaric peptides cannot be resolved by mass spectrometric techniques alone. The complexity of the sample introduces selectivity in the ionization process which may suppress specific fragments. Often, 60–80% of the expected digest fragments are observed. The formation of matrix adducts may further complicate the mixture and may result in ions which are difficult to identify. In the lower mass range, matrix background ions are also present. For specific applications, selectivity can be optimized by judicious choice of matrix. In the data shown in Fig. 6, better detail is obtained in the lower mass range through the use of polycrystalline dihydroxybenzoic acid (DHBA) as a matrix than sinapinic acid. In general, lower-molecular-mass peptides (<2000) have higher desorption/ionization yields with DHBA than with sinapinic acid. More extensive coverage of a digest mixture can be realized via MALDI–TOF-MS analysis of prefractionated HPLC pools of the mixture. Even though the

single-dimensional analysis via MALDI–TOF-MS of enzyme digests is generally not comprehensive, it can be used to quickly generate a characteristic fingerprint similar to HPLC and HPCE.

The on-line combination of HPLC and electrospray ionization mass spectrometry adds a dimension to the analysis of peptide maps which makes it possible to identify most, if not all, of the predicted fragments. The LC–ES-MS analysis of the endoproteinase Arg-C digest of DSPAα1 is shown in Fig. 7. The UV signal at 220 nm is shown in the lower half of Fig. 7 for comparison. Note that the sensitivities of the two detectors (UV and MS) are similar and that most peaks show up in both traces, although the individual intensities may differ.

Electrospray ionization is particularly useful in the identification of relatively high-molecular-mass peptides because of its ability to generate a set of multiply charged ions [13] which can be used to determine the molecular mass of the peptide even when the molecular mass is far in
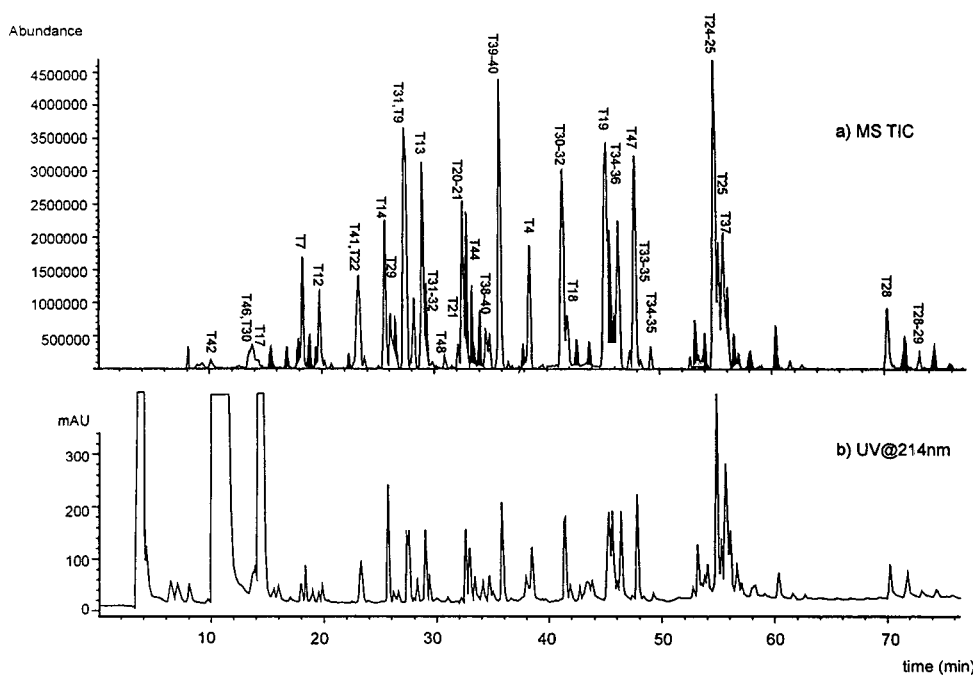
Fig. 7. LC–MS of digest; 78 pmol total protein injected. (a) Mass spectrometry total ion current, (b) 214 nm.

excess of the range available to the mass analyzer for singly charged molecules. For peptides found in enzymatic digests, molecular masses are typically below 5000 and the charge states are typically less than +5 (positive ion mode). The mass accuracy of the determination is typically better than 0.02%. In these experiments, mass spectral resolution was maintained at unit resolution across the scanned mass range and the sample was based on 78 pmol total protein. This is an important aid in assigning charge states to ions from peptides.

The identified fragments are listed in Table 1. The peaks which are unidentified are highlighted in Fig. 7. The interpretation of the peptide map was aided through the use of a software interpretation utility which greatly facilitates assignment of the predicted fragments to specific peaks in map. The software can also suggest anomalous sub-sequence fragments and modifications.

Although endoproteinase Arg-C was used as the proteolytic enzyme, there were a number of fragments which could not be explained by the cleavage selectivity of this enzyme. However,

most of the fragments could be accurately assigned as fragments produced by a tryptic digest. Trypsin cleaves peptide bonds on the C-terminal side of arginine or lysine residues. By contrast, endoproteinase Arg-C selectively cleaves only after arginine residues and, as such, the peptide fragment mixture which is generated by Arg-C can be considered a subset of a tryptic digest. All Arg-C fragments can be interpreted as single or multiple tryptic fragments. Future studies on DSPAα1 will use preparations of the endoproteinase that show a greater degree of arginine specificity.

Table 2 shows a list of predicted fragments which were not identified in the LC–ES-MS analysis. A number of predicted fragments were not identified because the mass of the singly charged ions falls below the scanned molecular-mass range (200–1800). Interestingly, those digest fragments which are expected to be glycosylated (O-linked: T25, T36, T39, T45; N-linked: T15, T43) are either missing or are found at low abundance relative to other fragments, and can be used as a rough predictor of glycosylation

Table 1
Found fragments

Retention time	Deconvoluted mass	Explanation
10.20	[475.2]	Fragment 42 (355–358) CAPK
13.57	[877.9]	Fragment 46 (420–427) DVPGV YTK
	[439.4]	Fragment 30 (254–256) TYR
18.29	[1104.4]	Fragment 7 (31–38) VEHCQ CDR
19.46	[1260.5]	Combination of fragments 6 to 7 (30–38) RVEHC QCDR
19.77	[780.3]	Fragment 12 (84–89) CEVDT R
23.25	[721.4]	Fragment 41 (349–354) LYPSS R
23.25	[677.3]	Fragment 22 (176–181) ATCGL R
25.59	[993.5]	Fragment 14 (102–110) GTWST AESR
26.52	[542.4]	Fragment 22 9249–253) VVLGR
28.89	[1404.6]	Fragment 13 (90–101) ATCYE GQGVT YR
29.86	[1520.2]	Combination of fragments 31 to 32 (257–267) VKPGE EEQTF KVK
30.91	[628.3]	Fragment 48 (437–441) DNMHL
32.11	[1488.6]	Fragment 21 (163–175) FTSES CSVPV CSK
32.84	[2440.1]	Combination of fragments 20 to 22 (163–181) AGKFT SESCS VPVCS KATCG LR
34.05	[1452.6]	Fragment 44 (364–376) TVTNN MLCAG DTR
35.75	[2151.1]	Combination of fragments 38 to 40 (283–348) HKSSS PFYSE QLKEG HVR
36.91	[1867.9]	Combination of fragments 39 to 40 (333–348) SSSPF YSEQL KEGHV R
38.44	[1298.7]	Fragment 4 (18–27) QESWL RPEVR
41.34	[1938.0]	Combination of fragments 30 to 32 (254–269) TYRVK PGEEE QTFKV K
41.82	[1879.8]	Fragment 18 (130–145) MPDAF NLGLG NHNYC R
45.21	[1645.9]	Fragment 19 (146–159) NPNGA PKPWC YVIK
46.31	[4216.1]	Combination of fragments 34–36 (271–306) YIVHK EFDDD TYNND IALLQ LKSDS PQCAQ ESDSV R
47.76	[1120.6]	Fragment 47 (428–436) VTNYL GWIR
48.31	[2795.4]	Combination of fragments 33 to 35 (270–292) KYIVH KEFDD DTYNN DIALL QLK
49.22	[2667.3]	Combination of fragments 34 to 35 (271–292) YIVHK EFDDD TYNND IALLQ LK
54.79	[3414.6]	Combination of fragment 24 to 25 (183–212) YKEPQ LHSTG GLFTD ITSHP WQAAI FAQNR
55.23	[3123.5]	Fragment 25 (185–212) EPQLH STGGL FTDIT SHPWQ AAIFA QNR
55.62	[2767.1]	Fragment 37 (307–330) AICLP EANLQ LDPWT ECELS GYGK
70.21	[3517.6]	Fragment 28 (219–248) FLCGG ILISS CWVLT AAHCF QESYL PDQLK
73.09	[4041.9]	Combination of fragments 28 to 29 (219–253) FLCGG ILISS CWVLT AAHCF QESYL PDQLK VVLGR

sites. This pattern was consistent with carbohydrate characterization studies [14] performed by others. There are also a number of lower-abundance fragments which were not identified at this stage, but based on previous studies it would be expected that secondary cleavages induced by the protease are the cause of many such fragments.

The characterization of enzymatic digests of glycoproteins by LC–ES-MS can be approached in three ways [15]. If the mass spectral data is presented as a contour map of m/z versus time versus intensity, series of unresolved glycopeptides will appear as diagonal bands, since for a given digest fragment, glycoforms with a greater degree of glycosylation will appear as slightly heavier and elute somewhat early [1]. A second method consists of using in-source collisionally induced dissociation to fragment glycopeptides, producing marker ions indicative of specific types of glycosylation [3]. Finally, if the sequence of the protein is known, fragments and their glycoforms can be predicted from knowledge of typical glycosylation patterns. One can then hunt for

Table 2
Not found fragments

Fragment	m/z	Sequence	Reason
T2[8–16]	1155.5	DEITQ MTYR	?
T3[17]	174.1	R	Low mass
T5[28–29]	233.1	SK	Low mass
T6[30]	174.1	R	Low mass
T8[31–38]	430.2	GQAR	?
T10[56–82]	3185.2	CHTVP VNSCS EPR	?
T11[38]	174.1	R	Low mass
T15[111–123]	1591.8	VECIN WNSSL LTR	Possible N-linked glycosylation
T16[124]	174.1	R	Low mass
T23[182]	146.1	K	Low mass
T26[213]	174.1	R	Low mass
T27[214–218]	534.2	SSGER	?
T33[270]	146.1	K	Low mass
T43[349–363]	667.4	FLFNK	Possible N-linked glycosylation
T45[377–419]	4649.0	SGEIY PNVHD ACQGD SGGPL	Possible O-linked glycosylation
		VCMND NHMTL LGIIS WGVGC	
		GEK	

the specific glycoforms through the use of extracted ion chromatograms [16].

In this study, specific N-linked glycosylation was identified in DSPAα1. The possible sites of N-linked glycosylation can be identified from the known sequence by the consensus sequence Asn–X–Ser(Thr). The N-linked structure is connected to the Asn residue. In DSPAα1, the two possible N-linked sites are at residue 117 in fragment T15[111–123] and residue 362 in fragment T43[359–363]. N-linked glycopeptides generated in mammalian cell lines often fall into three general classes: high-mannose, complex, and hybrid. The expected glycosylation patterns in DSPAα1 include high-mannose and complex structures, as illustrated in Fig. 8. All of these structures share the $GlcNAc_2Man_3$ backbone structure shown in the outlined triangle. The heterogeneity is introduced by the number of mannoses in high-mannose structures and the degree of branching in the complex structures. Branching in complex structures can be introduced by the HexNAc + Hex structure in the outlined rectangle. Further microheterogeneity can be introduced by the addition of fucose or sialic acid.

The choice of the proteolytic enzyme is im-

portant in the characterization of glycoproteins. The enzyme is typically chosen such that there is only one possible glycosylation site per fragment, as is the case for Arg-C digest of DSPAα1. Fortunately, the unexpected additional fragmentation encountered maintained this selectivity.
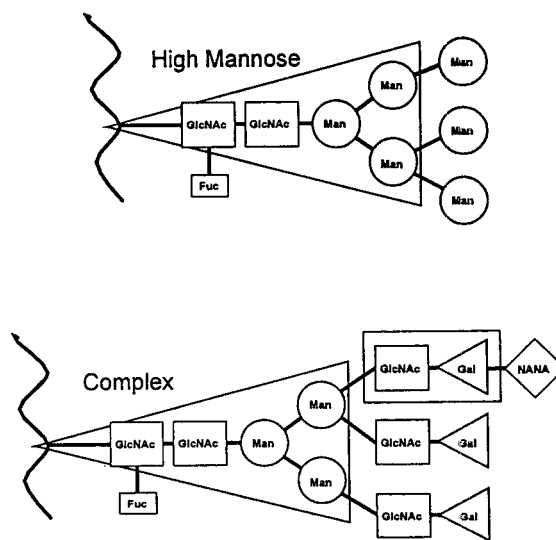
Fig. 8. Schematic of N-linked glycoforms.

Although the use of contour maps has been shown to be of utility in locating sites of glycosylation [2], the success of such an approach depends largely on the complexity of the glycosylation and the sensitivity of LC–MS analysis. If the sample is very heterogeneous, it will be difficult to differentiate the characteristic diagonal pattern from background signals. Fig. 9 shows a contour for a section of the Arg-C map of DSPAα1 from 40 to 50 min. The encircled area shows signal due to fragment T15[111–123] complex sialylated biantennary structures with two different charge states (+2 and +3) for different degrees of sialylation. Although the characteristic pattern is evident in this figure, in point of fact, these glycopeptides were identified through the use of extracted ions, as described below.

The use of in-source collisionally induced dissociation in the analysis of DSPAα1 is illustrated in Fig. 10. The CID mass spectral acquisition was carried out in selected-ion monitoring (SIM) mode to increase the sensitivity. The marker ions which were monitored are shown in Table 3. The reproducibility of the HPLC separation is sufficiently good that areas identified in the SIM analysis can be accurately compared with separate full spectral acquisitions conducted at lower fragmentation energy. This allows the parent glycopeptide to be identified. The success of this technique is limited by the complexity of the original glycoprotein and the sensitivity of the LC–MS system. In cases where there is a large degree of microheterogeneity due to glycosylation, there may not be an sufficient amount of an individual glycopeptide present to generate an interpretable low-energy spectrum. Note, however, that the sensitivity from the SIM CID data is sufficient since all of the different chromatographically unresolved glycoforms will contribute fragment ions to the electrospray signal. The summation of the signals due to the marker ions results in relatively broad looking chromatographic peaks. Based on the CID data, it is possible to infer some glycostructure differentiation. For example, all N-linked structures will generate a m/z 204 ion corresponding to the HexNAc in the backbone structure. All complex N-linked glycopeptides will generate a m/z 366 ion corresponding to the HexNAc + Hex structure indicative of the branching in multi-antennary structures. Only fucosylated glycopeptides will generate m/z 147 and only sialylated glycopeptides will generate a m/z 292 ion.

If the sequence is known and the glycosylation pattern of the host cell line is known, glycopeptides can be predicted and searched for in full scan mass spectral data via extracted ions. Individual glycopeptides which are present in such low amounts as to not generate an appreciable signal in the total ion current may be identified much more sensitively by looking only at the signals due to specific ions. An example is shown in Fig. 11, in which extracted ions corresponding to the T15 complex biantennary structure with different numbers of sialic acid are shown. Note that the region between 43.0 and 43.5 shows essentially no peaks in the total ion current. This is because the individual glycopeptides are present at significantly lower levels than a homogeneous non-glycosylated peptide fragment. From previous carbohydrate analysis, is known that DSPAα1 glycosylation is approximately 34.5%

Fig. 9. Detail of contour map for DSPAα1 Arg-C digest; 78 pmol total protein injected. CapEx voltage = 100 V. Data for signal >2000 counts shown.
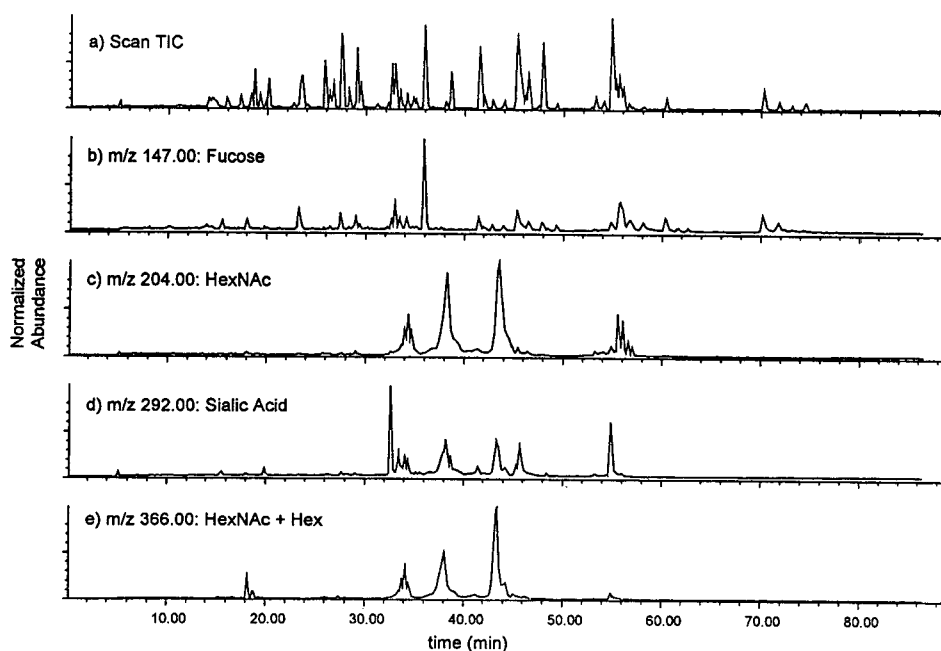
Fig. 10. CID detection of glycopeptides; 78 pmol total protein injected. (a) Total-ion chromatogram from scan acquisition (CapEx = 100 V), (b)–(e) from selected-ion monitoring acquisition (CapEx = 200 V): (b) m/z 147, (c) m/z 204, (d) m/z 292, (e) m/z 366 relative molecular mass.

high-mannose, 39.2% biantennary sialylated, 18.2% biantennary asialylated, 7.1% triantennary, and 1.1% tetraantennary [14]. In future work, in order to detect more of these structures, it will be necessary to utilize further preconcentration to improve the detection limits of the technique.

HPLC fractionation of the digest

In many cases, the complexity of the mixture generated by an enzymatic digest of a glycoprotein is too high for all components to be com-

pletely resolved by a single-dimensional analytical technique. Even two-dimensional techniques such as (LC or CE)–DAD UV–Vis or LC–MS have insufficient separation power to completely resolve the mixture. In these case, an orthogonal third dimension can be exploited. While three-dimensional systems have been employed on-line [17], we chose to transfer samples from an LC separation to subsequent analysis in a semi off-line technique. Fractions eluting from the reversed-phase HPLC separation were selectively transferred onto disposable hydrophobic collec-

Table 3
Glycomarkers

Sugar	Symbol	Chemical formula	Mass	Ion monitored [M + 1]$^+$
Fucose	Fuc	$C_6O_5H_{13}$	146.1	147.1
Hexose	Hex	$C_6O_6H_{12}$	162.1	163.1
N-Acetylhexosamine	HexNAc	$C_8O_6NH_{15}$	203.2	204.2
N-Acetylneuraminic acid	NANA	$C_{11}O_9NH_{19}$	291.3	292.1
Complex branch unit	HexNAc + Hex		365.3	366.3
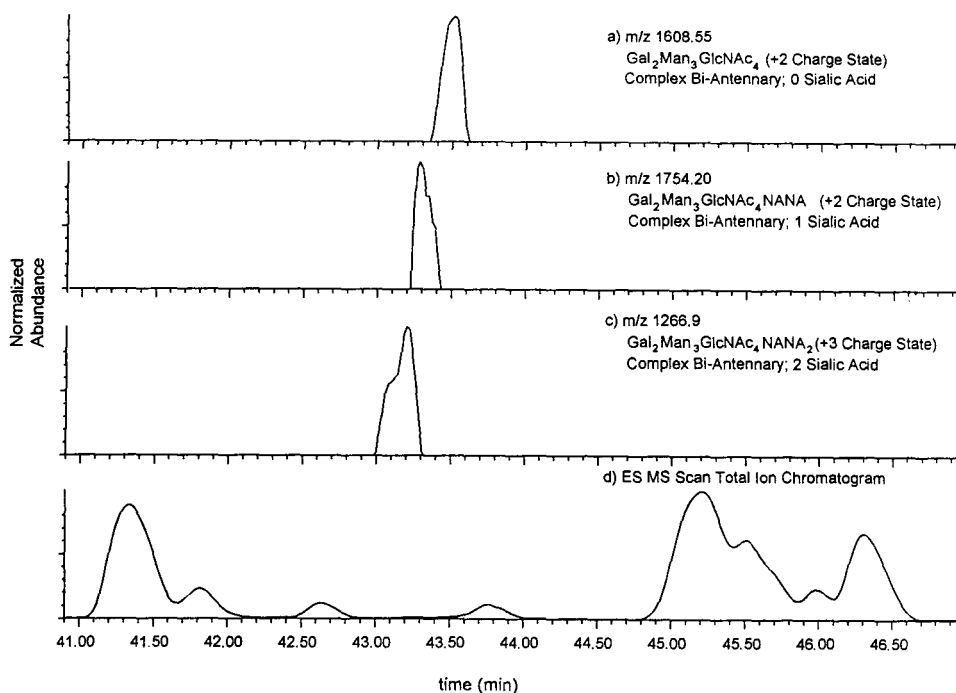
Fig. 11. Extracted ion detection of glycopeptides. Scan acquisition (CapEx = 100 V). (a) Extracted m/z 1608.55, $Gal_2Man_3GlcNAc_4NANA_0$ (+2 charge state). (b) Extracted m/z 1754.2, $Gal_2Man_3GlcNAc_4NANA_1$ (+2 charge state). (c) Extracted m/z 1266.9, $Gal_2Man_3GlcNAc_4NANA_2$ (+3 charge state). (d) Total-ion chromatogram.

tion columns after the effluent was diluted with a non-elutropic solvent. Because of the highly reproducible retention times of the LC separation, this process could be repeated, loading fractions from multiple LC runs on single collection columns. The hardware setup employed used a 14-port, 6-position valve which would allow four collection columns to be randomly accessed in addition to a bypass path. Following fraction collection, the fractions were eluted from the collection column with a rapid gradient. Since the fraction elution solvent does not have to be the same as the solvent system used in the peptide map, buffer transfer or desalting can also be accomplished in this step. This had the advantages of concentrating the samples for subsequent analysis and of great flexibility in transferring the sample fraction to subsequent analytical techniques.

This technique is particularly useful in transferring samples to subsequent HPCE separation.

As mentioned above, HPCE suffers from rather poor concentration sensitivity due to relatively small injection volumes and short-path-length UV detection. While on-line sample focusing and preconcentration techniques such as sample stacking [18] and capillary isotachophoresis (CITP) [19,20] are extremely useful in this respect, the low concentration of individual glycopeptides requires additional concentration to fully characterize the sample.

The technique is also useful for transferring samples to inherently static techniques such as MALDI–TOF-MS, in which an on-line flow-based approach would be difficult. The fractionation step itself is very important in reducing the complexity of the mixture to a point at which most of the components can be identified mass spectrally by MALDI–TOF-MS. The desalting characteristics of the fraction elution step can be very useful in increasing signal yields and the fraction of components observed.

Four fractions were collected from the HPLC peptide map, as illustrated in Fig. 12. Fractions 1 and 2 were chosen because of the high degree of glycosylation present in these areas as shown by the CID studies on glycomarkers. Fractions 3 and 4 were chosen because of the absence of glycoforms and because they represent fairly clean subsets of the entire map for subsequent evaluation. The benefits of the approach are not only the simplification of the analytical sample via fractionation, but a concentration step of approximately ten-fold as well.

The four fractions were analyzed by HPCE using the same method as had been used for the total digest. The electropherograms of the four fractions and the original digest are shown in Fig. 13. Referring to the HPLC fractions shown in Fig. 12, it can be seen that the first three HPLC fractions agree with this figure reasonably well in terms of number of peaks seen in the electropherograms. In the fourth fraction, how-

ever, no peaks are seen in the CE separation. It may be that these compounds, which elute late in the HPLC analysis, and therefore are hydrophobic, either are uncharged or are adsorbed to surfaces in the sample-transfer or separation process. The real strength of using CE to reanalyze HPLC fractions lies in the orthogonality of the separation mechanism. To fully exploit this separation power, a method is needed to couple the CE separation with mass spectrometry, either directly via CE–ES-MS or in an off-line manner running collected CE fractions by MALDI–TOF-MS. This approach has been used to characterize growth hormone tryptic peptides in a CE separation [21]. These approaches are currently under investigation, and will be reported in a future publication. Alternately, UV spectra could be used to track the elution order of a CE separation transferred from an HPLC fraction, analogously to peak tracking in HPLC peptide mapping [22]. This
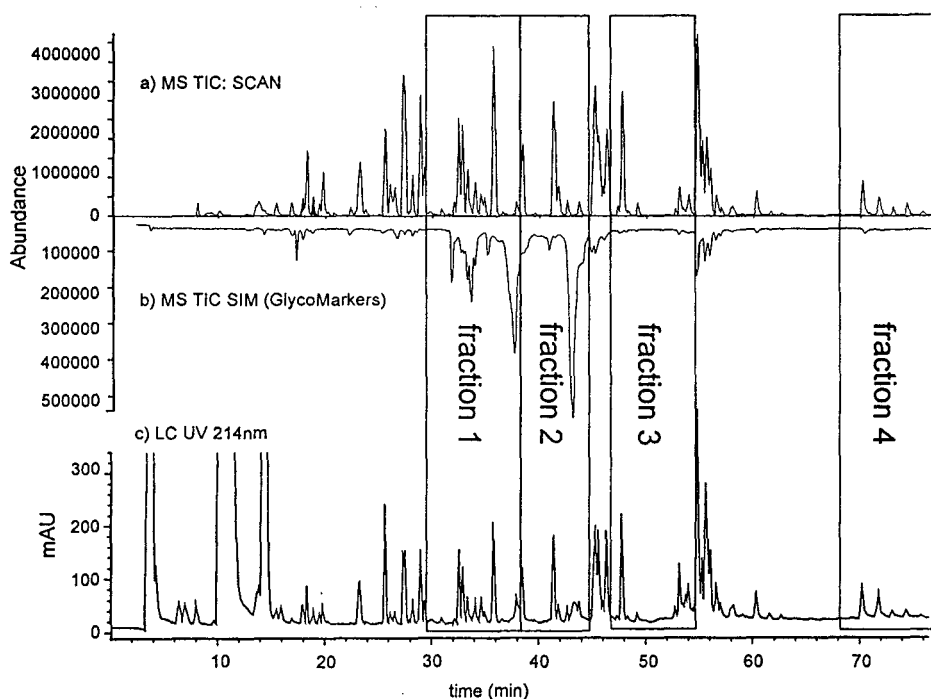
Fig. 12. Areas of HPLC fraction collection. Identification of regions from analytical separation (76 pmol). (a) Scan acquisition total-ion current (CapEx = 100 V). (b) CID SIM acquisition total-ion current (CapEx = 200 V). (c) UV at 214 nm. The actual fraction collections were done with 312 pmol injected.
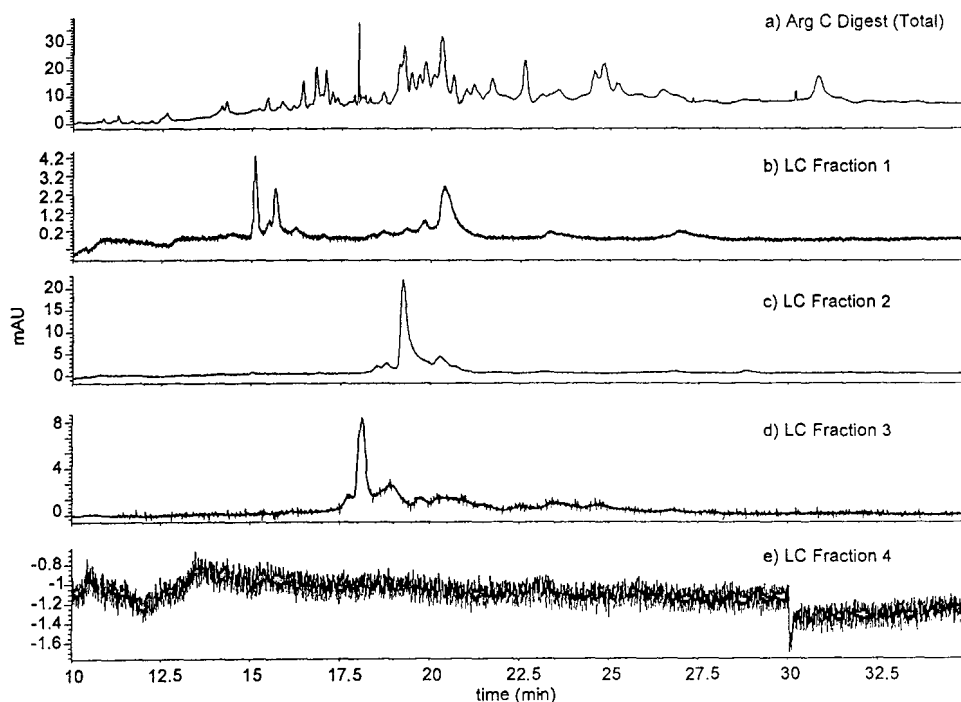
Fig. 13. HPCE of collected fractions; 30 nl injected. (a) Total Arg-C digest of DSPAα1. (b) HPLC fraction 1. (c) HPLC fraction 2. (d) HPLC fraction 3. (e) HPLC fraction 4.

approach requires that the HPLC separation is already sufficiently resolved to obtain pure spectra or that pure peptide standards exist.

The four collected fractions were also analyzed by MALDI–TOF-MS, as shown in Fig. 14. This is a particularly useful combination because the sensitivity of MALDI–TOF-MS allows clear unequivocal spectra which actually exhibit a selectivity closer to HPCE than HPLC, being based on mass/charge. The orthogonality of MALDI–TOF-MS relative to HPLC generates extremely useful information. In analyzing fractions collected from the total digest, the sample complexity has been reduced sufficiently so that the MALDI–TOF-MS spectrum is a good representation of the components present in the fraction. Contrast this with the data obtained for the total digest, in which only a fraction of the components are represented by strong signals in the spectrum. If one compares the MALDI–TOF-MS result with the analysis of the digest by LC–ES-MS, there are a number of peaks in each

fraction that are present in both the electrospray and MALDI–TOF-MS data (see Table 4). A number of the ions shown in Table 4 have not yet been identified. Thus one technique reinforces peak identification based on data from the other. There are also a number of peaks that occur in either one technique or the other, but not both. Thus a more complete and accurate picture is obtained by a combination of the two.

Future work

It should be noted that this multidimensional approach, does not, at this stage, replace more classical techniques of protein characterization. The classical approach would include preparative isolation and purification of the intact protein and enzymatic digestion followed by collection of each of the digest fragments for complete characterization by sequencing, mass spectrometry, UV–Vis, etc. However, it seems clear that, as our abilities to integrate and interpret the large amount of data which can be produced by newer

Fig. 14. MALDI–TOF-MS of collected fractions; 1 μl of collected fractions applied. Matrix: sinapinic acid. (a) HPLC fraction 1. (b) HPLC fraction 2. (c) HPLC fraction 3. (d) HPLC fraction 4.

orthogonal and complimentary selectivity of HPLC and HPCE. Currently, samples eluted and collected from HPLC columns are not very well suited to analysis by HPCE in terms of concentration. Although the 'on-column' fraction technique described above improves the situation, the ability to inject larger volumes into the HPCE capillary without sacrificing speed or resolution is needed. This situation is particularly exacerbated by the microheterogeneity of glycopeptide samples.

The on-line combination of HPCE and electrospray MS would simplify the identification of CE peaks and bring the power of MS to HPCE just as LC–ES-MS has done for HPLC. There are a number of instrumental approaches to this interface, and we are currently evaluating their use.

Although the coupling of MALDI–TOF-MS with separation techniques such as HPLC and HPCE has a great potential, as demonstrated in this work, there is a fundamental mismatch between the dynamic environment of the flow-based system and the static environment of the matrix crystal in which MALDI–TOF-MS samples are included. Sample collection from HPCE has been demonstrated in this context, and we will be evaluating this technique in the near future. Approaches for more efficiently using a greater amount of available sample for MALDI–TOF-MS also need to be developed.

4. Conclusions

In this work it has been shown that HPLC, HPCE, LC–ES-MS, and MALDI–TOF-MS are highly complimentary techniques for examining glycoproteins. In a problem of this complexity, different types of data can be integrated to get a more complete characterization of the analyte. LC–ES-MS is a powerful technique for the analysis of peptide maps and shows great potential in the identification of complex regions of glycosylation. Nonetheless, more work needs to be done to improve the power of this approach. High-yield concentration steps will be required due to extensive carbohydrate heterogeneity.

instrumental techniques improve, many of the more time and product consuming steps can be reduced or eliminated. This will have the overall effect of producing better data in a more timely manner.

This report represents a work in progress and there are a number of critical areas that have yet to be fully developed or exploited. Specifically:

Capillary isotachophoresis (CITP) used as a sample concentration method for HPCE is an important step in being able to exploit the

Table 4
Analysis of HPLC fractions ES-MALDI

LC fraction	ESI *m/z*	MALDI–TOF *m/z*	Sequence assignment	
1	1347.17	nd		
	1519.23	nd		
	629.21	623.1	T48[437–441]	DNMHL
	1205.3			
	745.7		T21[163–175]	FTSES CSVPV CSK
	1858.95	1851.9		
	1965.05	1966.2		
	1746.17	1729.3	T20–T21[160–175]	AGKFT SESCS VPVCS K
	1906.8	nd	T1–T2[1–16]	AYGVA CKDEI TQMTY R
	2116.77	2116.6	T38–40[331–348]	HKSSS PFYSE QLKEG HVR
	1850.92	1851.9	T39–40[333–348]	SSSPF YSEQL KEGHV R
	1876.84	1877.2		
	nd	1894.2		
	nd	2078.3		
	nd	2160.1		
2	1906.97			
	1299.2	1283.5	T4[18–27]	QESWL RPEVR
	1937.99	nd	T30–32[254–267]	KYIVH K
	1282.18	1283.5		
	1880.21	1881.3		
	966.23	nd		
	nd	1653.5		
	nd	1806.3		
	nd	1835.1		
	nd	1856		
	nd	1896.2		
	nd	1952.1		
3	1121.2	1121.5	T47[428–436]	VTNYL GWIR
	2796.14	2795.6	T33–35[270–292]	KYIVH KEFDD DTYNN DIALL QLK
	2668	2669.3	T34–35[271–292]	YIVH KEFDD DTYNN DIALL QLK
	4249.65	4249.2		
	3488.39	3487.2		
	3429	3429		
	3414.96	nd		
	nd	1136.8		
	nd	1142.2		
	nd	1163.6		
	nd	1179.1		
	nd	1327.7		
	nd	1345.9		
	nd	1387.9		
	nd	1593.3		
	nd	1688.8		
	nd	3031.7		
	nd	3444.2		
	nd	4343		
4	3518.56	3519	T28[219–248]	FLCGG ILISS CWVLT AAHCF QESYL PDQLK
	3460.31			
	3500.8	3500.8		
	4042.89	4046.9	T28–29/A21[219–253]	FLCGG ILISS CWVLT AAHCF QESYL PDQLKVVLGR
	3985.32	nd		
	3927.79	nd		
	nd	3535.8		
	nd	3630.2		
	nd	4056.9		

Finally, more effective techniques are required for the integration of information from the higher-dimensional data generated by the combination of these techniques.

Acknowledgements

References

[1] V. Ling, A.W. Guzzetta, E. Canova-Davis, J.T. Stults, W.S. Hancock, T.R. Covey and B.I. Shushan, Anal. Chem., 63 (1991) 2909–2915.

[2] A.W. Guzzetta, L.J. Basa, W.S. Hancock, B.A. Keyt and W.F. Bennet, Anal. Chem., 65 (1993) 2953–2962.

[3] S.A. Carr, M.J. Huddleston and M.F. Bean, Protein Sci., 2 (1993) 183–196.

[4] M.J. Huddleston, M.F. Bean and S.A. Carr, Anal. Chem., 65 (1993) 877–884.

[5] J.J. Conboy and J.D. Henion, J. Am. Soc. Mass Spectrom., 3 (1992) 804–814.

[6] J. Kraetschmar, B. Haendler, G. Langer, W. Boidol, P. Bringman, A. Alagon, P. Donner and W.D. Scheuning, Gene, 105 (1991) 229–237.

[7] W. Witt, B. Maass, B. Baldus, M. Hildebrand, P. Donner and W.D. Scheuning, Circulation, 90 (1994) 421–426.

[8] W. Witt, B. Baldus, P. Bringmann, L. Cashion, P. Donner and W.D. Scheuning, Blood, 79 (1992) 1213–1217.

[9] R.M. McCormick, Anal. Chem., 60 (1988) 2322.

[10] A. Apffel, S. Fischer, G. Goldberg, P.C. Goodley and F.E. Kuhlmann, J. Chromatogr. A, (1995) in press.

[11] F. Xiang and R.C. Beavis, Rapid Commun. Mass Spectrom., 8 (1994) 199.

[12] P. Oroszlan, S. Wicar, G. Teshima, S.-L. Wu, W.S. Hancock and B.L. Karger, Anal. Chem., 64 (1992) 1623–1631.

[13] J.B. Fenn, M. Mann, C.K. Meng, S.F. Wong and C.M. Whitehouse, Science, 246 (1989) 64–71.

[14] T. M'Timkulu, unpublished results.

[15] A.W. Guzzetta and W.S. Hancock, Recent Advances in Tryptic Mapping, CRC Series in Biotechnology, CRC Press, Boca Raton, FL, 1994, in press.

[16] M.W. Spellman, L.J. Basa, C.K. Leonard, J.A. Chakel, J.V. O'Connor, S.W. Wilson and H. van Halbeek, J. Biol. Chem., 264 (1989) 14100–14111.

[17] M.M. Bushey and J.W. Jorgenson, Anal. Chem., 62 (1990) 978–984.

[18] R.L. Chein and D.S. Burgi, J. Chromatogr., 559 (1991) 141–152.

[19] F.E.P. Mikkers, Thesis, Eindhoven University, Eindhoven, 1980.

[20] F. Foret, E. Szoko and B.L. Karger, J. Chromatogr., 608 (1992) 3–12.

[21] M. Herold and S.-L. Wu, LC · GC, 12 (1994) 531–533.

[22] H.-J.P. Sievert, S.-L. Wu, R. Chloupek and W.S. Hancock, J. Chromatogr., 499 (1990) 221–234.

Rapid one-step capillary isoelectric focusing method to monitor charged glycoforms of recombinant human tissue-type plasminogen activator

Kathryn G. Moorhouse*, Carina A. Eusebio, Glenn Hunt, Anthony B. Chen

Department of Quality Control Clinical Development, Genentech, S. San Francisco, CA 94080, USA

Abstract

A rapid (< 10 min) one-step capillary isoelectric focusing (cIEF) method was developed to monitor charged glycoforms of recombinant human tissue-type plasminogen activator (rt-PA). Focusing takes place between the detector and the anode and the electro-osmotic flow (EOF) sweeps the separated glycoforms past the detector, towards the cathode. The separation uses a neutral coated capillary and hydroxypropylmethylcellulose (HPMC) to reduce the EOF to a constant and reproducible value. The method uses an ampholyte mix with a 50:50 ratio of pH 5–8 and pH 3–10 ampholytes in 4 M urea and 0.1% HPMC to produce maximal resolution whilst maintaining protein solubility during focusing. The electropherograms were compared to isoelectric focusing (IEF) slab gels of samples of intact rt-PA. In both cases approximately ten charged species could be detected. Data analysis indicated that the intra-assay precision was < 5% for peak migration times and < 10% for normalized peak areas. The number of charged species detected by each of the two methods was consistent for samples of intact rt-PA, rt-PA types I and II and for neuraminidase-digested rt-PA. Overall the data indicate that the automated cIEF method can be an adjunct to slab-gel IEF in the characterization and routine analysis of recombinant glycoproteins.

1. Introduction

A major challenge in the quality control of recombinant glycoproteins is the analysis and monitoring of the heterogeneity of the constituent oligosaccharides. To date only hydrolytic assays for total neutral sugars and sialic acid content are routinely used, methods which are too simplistic to ensure the level of consistency required for a pharmaceutical product. The need for more specific methods has grown as the importance of the carbohydrate moiety of glycoproteins has become known. This is of particular importance with glycoproteins used as therapeutics with respect to their half-life and potency in vivo [1].

Recombinant human tissue-type plasminogen activator (rt-PA) is a fibrin-specific plasminogen activator which has been approved for the treatment of myocardial infarction. rt-PA is a glycoprotein consisting of 527 amino acids, with a polypeptide molecular weight of 59 000. The carbohydrate structures of the Chinese hamster ovary (CHO)-derived rt-PA have been elucidated [2]. The molecule has three N-glycosylation sites, positions 117, 184 and 448 and exists as two main variants, designated type I rt-PA and type II rt-PA. Type I contains N-linked oligosaccharides at all three sites while type II is

---

* Corresponding author.

only glycosylated at positions 117 and 448. Position 117 contains high mannose oligosaccharides exclusively, while positions 184 and 448 principally contain N-acetyllactosamine-type oligosaccharides. The N-acetyllactosamine-type oligosaccharides contain different amounts of sialic acid attached to the terminal galactose residues. Oligosaccharides at position 184 contain significant amounts of mono-, di-, and tri-sialyl residues while position 448 contains disialyl oligosaccharide as the predominant structure. The different numbers of sialic acid residues result in a number of different glycoforms of the parent molecule, or microheterogeneity, with corresponding variability in the isoelectric point (p*I*).

The traditional method for the analysis of charge heterogeneity of recombinant proteins has been by the techniques of ion-exchange chromatography and isoelectric focusing (IEF). In slab-gel IEF, glycoforms of the intact protein containing increasing amounts of sialic acid can be separated and visualized as discrete bands with increasingly acidic isoelectric points. Although this method can be used to characterize the heterogeneity and monitor the production consistency of recombinant proteins, it has the disadvantages of long and labor-intensive analysis times producing at best semi-quantitative data. A cIEF method for the fractionation of rt-PA glycoforms has previously been published using a two-step method (focusing followed by salt mobilization) [3]. However, this cIEF method gave poor peak shape, especially for the more basic glycoforms and was not compared to slab-gel isoelectric focusing patterns.

In this paper we based the successful development of a rapid capillary isoelectric focusing (cIEF) method on an existing slab-gel IEF method for rt-PA and on recently documented so-called one-step cIEF methodology [4,5]. In this one-step cIEF method focusing takes place between the detector and the anode, and the electro-osmotic flow (EOF) sweeps the separated glycoforms past the detector, towards the cathode. The two techniques were compared in order to demonstrate the applicability of the routine use of this cIEF method in addition to, or in place of, the traditional slab-gel IEF method.

2. Experimental

2.1. Materials

All chemicals were of analytical reagent grade. Hydroxypropylmethylcellulose (HPMC) and neuraminidase (E.C. 3.2.1.18, from *Clostridium perfringens*) were obtained from Sigma (St. Louis, MO, USA). Ampholytes (pharmalytes) ranges pH 3–10 and pH 5–8 and p*I* standards were obtained from Pharmacia LKB (Piscataway, NJ, USA). N,N,N′,N′-Tetramethylethylenediamine (TEMED), urea (electrophoresis grade) and 30% acrylamide/bis solution 19:1 (5% C) were obtained from Bio-Rad Laboratories (Hercules, CA, USA). Urea and acrylamide were deionized using a mixed-bed resin prior to use. rt-PA was manufactured in-house, types I and II rt-PA were separated by affinity chromatography using a lysine resin [6].

2.2. Capillaries

Unless otherwise stated the capillary routinely used was an eCAP™ neutral capillary from Beckman (Fullerton, CA, USA). μSIL® DB™-1, DB™-17 and DB™-WAX capillaries were from J&W Scientific (Folsom, CA, USA). CElect-H150 and CElect-P150 capillaries were from Supelco (Bellefonte, PA, USA). The BioCap capillary was from BioRad (Hercules, CA, USA).

2.3. Isoelectric focusing

Isoelectric focusing was performed using 0.4 mm thickness, 4% acrylamide gels containing 8 *M* urea and 2.4% (w/v) pH 3–10 and 5–8 ampholytes in the ratio of 65:35. A 20-μg amount of protein or 10 μl of standards (prepared according to the manufacturer's recommendation) were applied to paper applicators

placed 1–2 cm from the anode. The gel was focused for 2 h at 4°C, first at a constant power of 10 W until the voltage reached 1600 V, then at constant voltage. The anolyte was 1 M phosphoric acid and the catholyte 1 M NaOH. After focusing the gel was fixed with 5% sulfosalicylic acid–10% trichloroacetic acid (w/v) and then stained with Coomassie Brilliant Blue.

2.4. Capillary isoelectric focusing

cIEF was performed using a Beckman P/ACE 5510 (Fullerton, CA, USA). The internal diameter of the capillary was 50 μm, the total length was 27 cm; 20 cm from the inlet to the detector and 7 cm from the detector to the outlet. During analysis the temperature of the capillary was maintained at 20°C, the reagents and samples were at ambient temperature. The anolyte was 10 mM phosphoric acid and the catholyte 20 mM NaOH. The capillary was rinsed for 1 min with water then filled for 2 min with sample. The separation was achieved using reversed polarity, i.e. the anolyte at the outlet, at a constant voltage of 500 V/cm. The absorbance was measured at 280 nm with detection complete in less than 10 min. After each analysis the capillary was rinsed for 1 min with 0.1 M HCl, 1 min with 10 mM phosphoric acid and 1 min with water. For later experiments the post-separation HCl wash was excluded and the phosphoric acid wash extended to 2 min. In these cases a single 1-min HCl wash was performed at the beginning of each day. rt-PA samples were routinely diluted to give final concentrations of 125–250 μg protein/ml, 4 M urea, 0.1% (w/v) HPMC, 7.5% (v/v) TEMED and 3% (w/v) pH 3–10 and pH 5–8 ampholytes in the ratio 50:50. The final salt concentration of samples was 50 mM or less.

2.5. Removal of N-acetylneuraminic acid

Sialic acid residues were removed from rt-PA by treatment with neuraminidase. rt-PA was digested for 4 h with neuraminidase at 37°C in 0.2 M arginine-phosphate, 0.1% Tween 80, pH 7.2, with 0–0.003 units enzyme/ml rt-PA. After incubation samples were stored on ice before analysis.

3. Results and discussion

3.1. Development of cIEF

Development of the cIEF method for rt-PA consisted of an adaptation of the cIEF methods by Mazzeo et al. [4] and Pritchett [5] with consideration of known rt-PA slab-gel IEF requirements. rt-PA is a very hydrophobic protein and the loss of salt during either dilution or IEF causes extensive precipitation. For this reason IEF in both slab gels and capillaries must contain urea. For slab gels a final concentration of 8 M urea was used whereas for cIEF only 4 M was required. The urea concentration was kept to a minimum to avoid urea crystallization in the sample, or capillary during analysis. Original separations also included reduced Triton X-100 to aid solubilization, but this was found to be unnecessary. Later separations included HPMC to suppress any changes in EOF and aid the reproducibility of multiple injections using a single capillary. The choice of ampholytes (Pharmacia pharmalytes) was made to compare directly with the slab-gel method as a means of conserving the slab-gel IEF profile.

The effect of different ratios of ampholytes is shown in Fig. 1. The ratio giving optimal resolution and separation was determined to be a 50:50 mix of pH 5–8 and pH 3–10 ampholytes. This is close to the 65:35 ratio for these ampholytes used in the slab-gel IEF and is consistent with the known pI range of rt-PA measured in urea containing IEF gels as pH 6.2–7.9. A typical electropherogram is shown in Fig. 2.

Other factors investigated included the concentration of TEMED and the concentration of protein. TEMED acts as a basic blocker and upon focusing occupies the end of the capillary between the detector and the inlet. We found that altering the TEMED concentration in the range 3.75–7.5% (v/v) showed very little effect on either resolution or overall elution time. Use
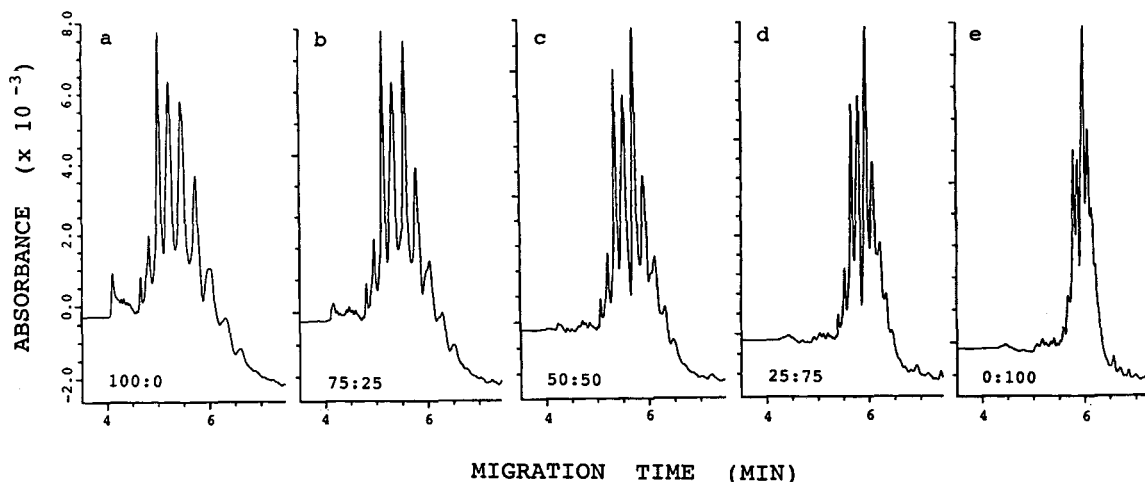
Fig. 1. Effect of changing the ratio of the ampholytes used from 100% pH 5–8 to 100% pH 3–10. The use of increasing amounts of pH 5–8 ampholytes, up to 50%, resulted in increasing resolution and separation of peaks. Values above 50% resulted in a loss of peak shape on the acidic side of the electropherogram (a–c). The use of increasing amounts of pH 3–10 ampholytes (c–e) resulted in decreasing resolution of the rt-PA peaks as the bands became compressed.

of concentrations in excess of 25% (v/v) lead to an overall loss of resolution and distortion of the pH gradient as evidenced by extremes in baseline response. Protein concentrations be-

tween 5 and 500 μg/ml were evaluated. Higher protein concentrations resulted in higher signals but also in loss of resolution. Lower concentrations gave the best resolution but suffered
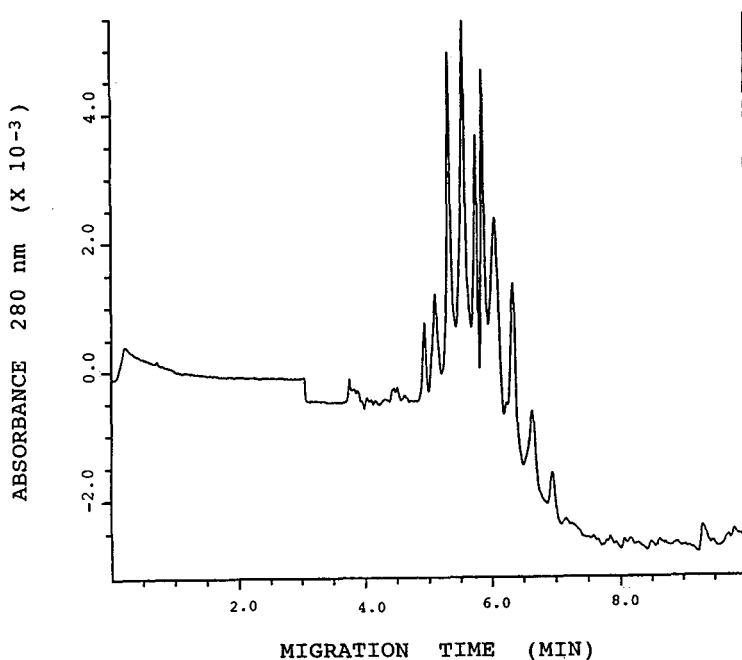
Fig. 2. A typical cIEF electropherogram of rt-PA showing the resolution and separation of ten peaks of increasing acidity. Analysis conditions were as described in Experimental.

from baseline noise, probably arising from residual absorbance by some of the ampholytes at 280 nm. Considering resolution and signal-to-noise ratio, the optimal protein concentration was determined to be in the range 125–250 μg/ml.

Using the optimal conditions intra-assay precision was calculated for six sequential injections of a single sample of rt-PA. The relative standard deviations (R.S.D.s) for the peak migration times and normalized peak areas of each of the ten peaks resolved are reported in Table 1. For migration time the R.S.D.s ranged from 2.3 to 3.1%, for area the R.S.D.s ranged from 0.6 to 10.4%, values within acceptable limits for a quality control assay.

A number of other coated capillaries were investigated for their resolving capabilities using this method, the results are shown in Fig 3. All of the capillaries, with the exception of the μSIL DB-WAX, gave equivalent or better resolution compared to the neutral coated capillary routinely used, indicating that the separation is very rugged. The success with so many alternate coatings could be credited to the presence of urea and HPMC in the separation buffer. The presence of urea seems to eliminate any solubility problems the protein may have, in particular at its isoelectric point that would lead to loss of resolution. The poorer resolution seen with the μSIL DB-WAX could be attributed to the coating which, even in the presence of 4 M urea, is able to exert some effect on the rt-PA molecule. The presence of HPMC depresses the inherent EOF which would otherwise cause loss of resolution, allowing the use of coatings which have greater EOF values than the neutral capillary.

3.2. Comparison of cIEF and slab-gel IEF methods

To validate the replacement of slab-gel IEF by cIEF a comparison of the data from the two methods was made using three sets of samples: intact rt-PA representing the most heterogeneous sample, purified type I and type II rt-PA representing the two major variants of rt-PA, and neuraminidase-digested rt-PA representing samples with a range of carbohydrate concentrations.

A typical cIEF electropherogram of intact rt-PA is shown in Fig. 2, while Fig. 4 shows the same sample analyzed by slab-gel IEF. Inspection of the gel shows that approximately ten major bands can be detected while the same number of peaks are resolved by cIEF. This data indicates that comparable resolution and separation was achieved by the two methods.

cIEF electropherograms of purified rt-PA types I and II are shown in Fig. 5, while Fig. 6 shows the same samples analyzed by slab-gel IEF. Glycosylation at the additional N-linked glycosylation site which occurs in type I rt-PA but not in type II rt-PA results in higher concentration of sialic acid for this variant. This difference can be seen by cIEF as a greater number of peaks of increasing acidity when compared to the number and acidity of peaks for type II rt-PA. Overall the number and relative pI of peaks detected by cIEF for the two samples was comparable with the number and relative pI of bands detected by slab-gel IEF.

When considering appropriate methodologies for the quality control analysis of charged glycoproteins one of the most important properties of

Table 1
Intra-assay precision for six replicate injections of rt-PA using CE-IEF

| Peak | R.S.D. | |
	Migration time (min)	Normalized area[a]
1	2.3	10.4
2	2.4	8.3
3	2.5	2.3
4	2.6	1.3
5	2.7	1.6
6	2.9	1.6
7	2.8	0.6
8	2.9	2.6
9	3.1	3.3
10	3.1	2.5

[a] Normalized peak areas were calculated as: (individual peak area/total peak area) · 100%.
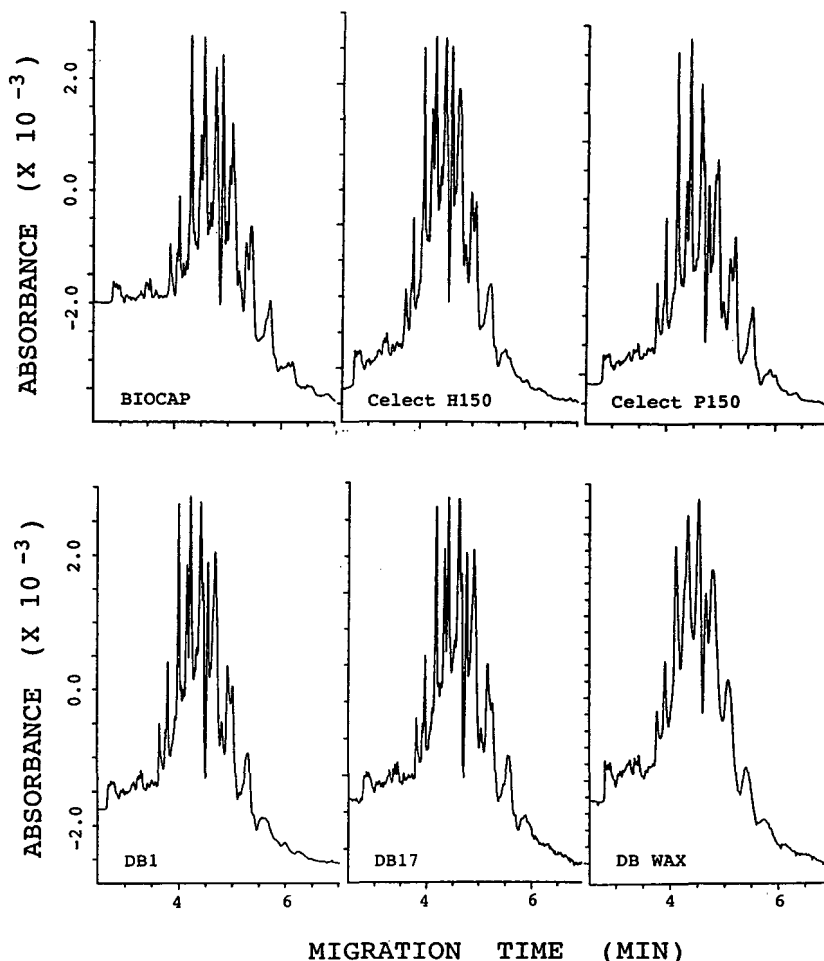
Fig. 3. The separation of rt-PA charged glycoforms was routinely performed using a neutral capillary (eCAP™). This figure shows that a number of other capillaries could also be used including: two neutral capillaries, the CElect-P150 with a hydrophillic phase and the BioCap, capillaries with a moderately hydrophobic phase, the CElect-H150 and the μSIL® DB™-17, and a capillary with a very hydrophobic phase the μSIL® DB™-1. Only a capillary with a high polarity, the μSIL® DB™-WAX gave an inadequate separation which may have resulted from the interaction of rt-PA with the polyethylene glycol phase used in this column.

the method is its demonstrated ability to differentiate samples which are known to be heterogeneous with respect to their charged carbohydrate content. To further demonstrate this for cIEF, samples greatly differing in their charged carbohydrate content were generated by the increasing removal of sialic acid residues by increasing concentrations of neuraminidase. A series of electropherograms of rt-PA digested with increasing concentrations of the enzyme is

shown in Fig. 7, while Fig. 8 shows the same samples analyzed by slab-gel IEF. As sialic acid residues are increasingly removed from the rt-PA molecule there is a concomitant decrease in the number and acidity of the peaks detected by cIEF and the number and acidity of bands detected by slab-gel IEF. The two major bands remaining after incubation with the highest concentration of neuraminidase did not appear to be related to sialic acid as incubation for extended
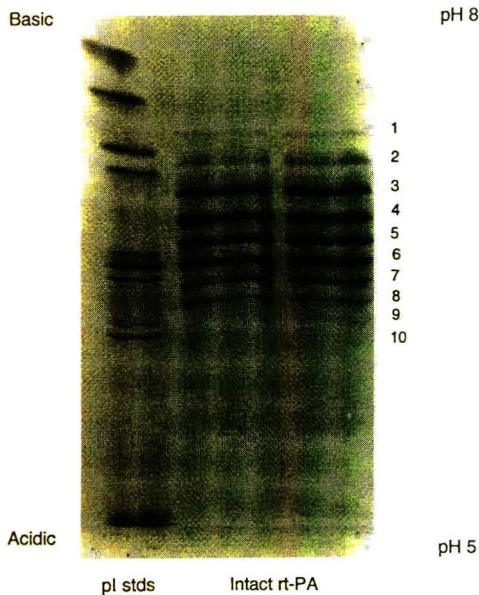
Fig. 4. An IEF slab gel of the same sample of rt-PA as analyzed in Fig. 2 showing the separation and resolution of ten major bands of increasing acidity. Analysis conditions were as described in Experimental.

periods of time at the highest concentration of enzyme used did not decrease their number (data not shown). Inspection of the data for the two methods indicated an excellent correlation with the same number of peaks or bands being detected by each method at every concentration of enzyme used.

4. Conclusion

Recent advances in CE methodology have allowed us to develop a fast and rugged cIEF method for the analysis of the charged carbohydrate heterogeneity exhibited by a recombinant glycoprotein, rt-PA. The ease of use, automation and short analysis time of this cIEF method offers great advantages over the current slab-gel IEF methodology. In addition to these advantages cIEF also offers a great reduction in the volume of reagents used, in particular the elimination of the use of the neurotoxin acrylamide
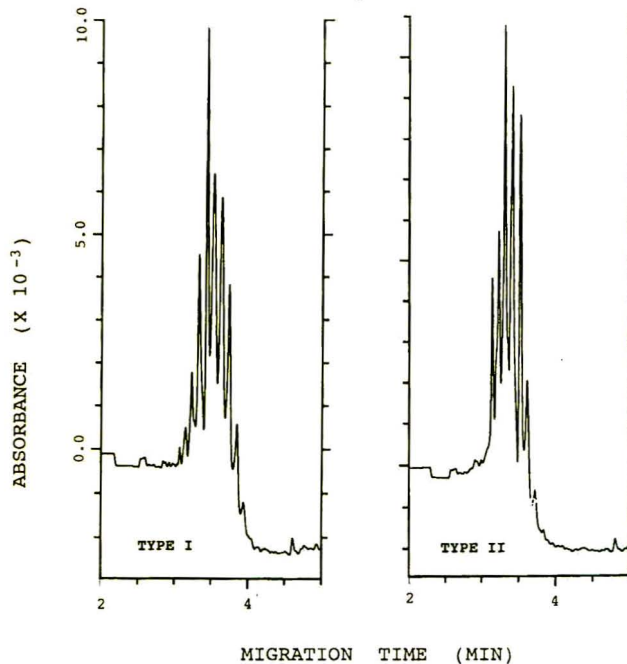
Fig. 5. cIEF electropherograms of the two major glycosylation variants of rt-PA, type I and type II. Type I rt-PA has sialic acid containing carbohydrate at two positions while type II has only one. The presence of additional sialic acid residues in rt-PA type I can be seen by cIEF as a greater number of peaks with increasing acidity compared to the number and acidity of the peaks for the rt-PA type II sample. Analysis conditions were as described in Experimental.
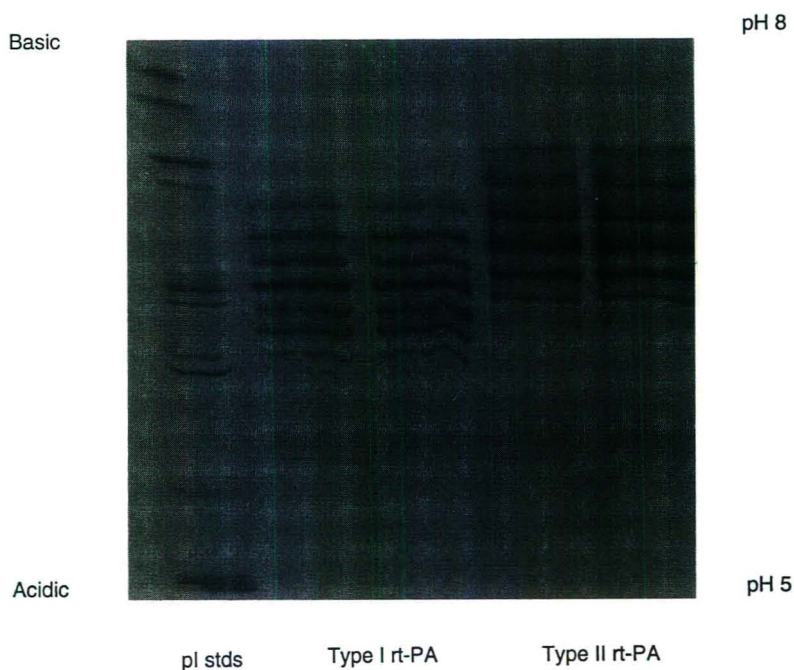
Fig. 6. An IEF slab gel of the same samples of rt-PA (in duplicate) as analyzed in Fig. 5. Type I rt-PA has sialic acid containing carbohydrate at two positions while type II only has it at one. The presence of additional sialic acid residues in rt-PA type I can be seen as a greater number of bands with increasing acidity compared to the number and acidity of bands for the rt-PA type II sample. Analysis conditions were as described in Experimental.
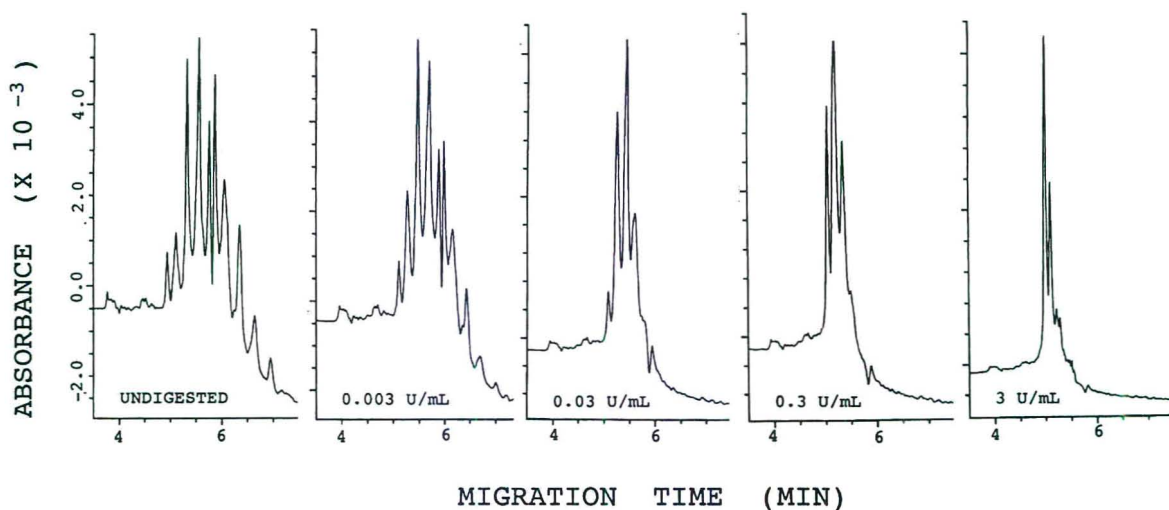
Fig. 7. cIEF electropherograms of rt-PA digested with increasing concentrations of neuraminidase. As sialic acid residues are sequentially removed there is a concomitant decrease in the number and acidity of peaks detected by cIEF. Enzyme incubation conditions and cIEF analysis conditions were as described in Experimental.
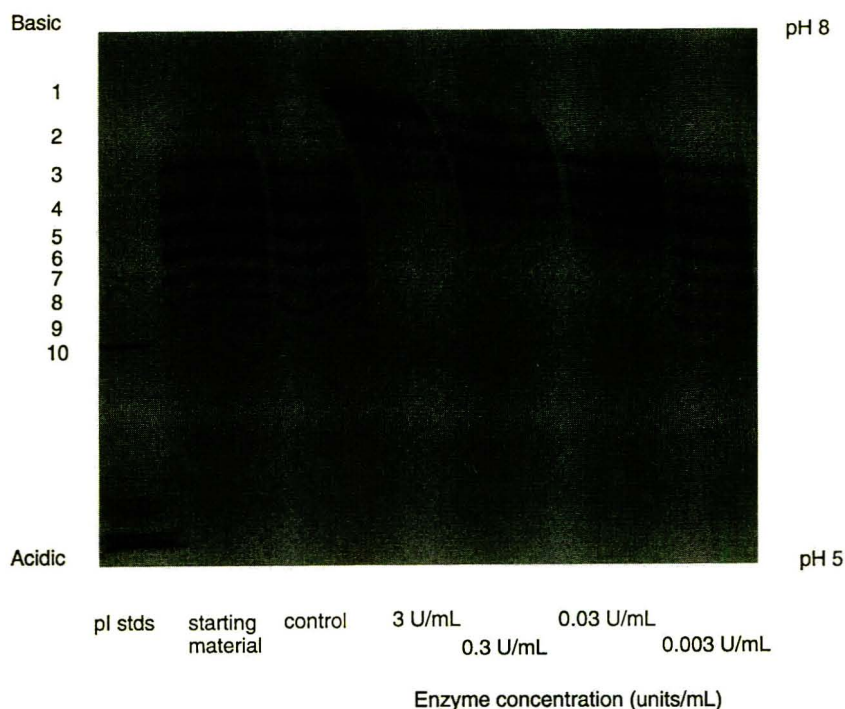
Fig. 8. IEF slab gel of the same samples of rt-PA as analyzed in Fig. 7. As sialic acid residues are sequentially removed there is a concomitant decrease in the number and acidity of bands detected by IEF. Enzyme incubation conditions and IEF analysis conditions were as described in Experimental.

and the large volumes of noxious stain/destain solutions required for slab-gel IEF methods. Most importantly the excellent correlation of cIEF to the slab-gel IEF, as demonstrated in this paper, provides a strong argument for its adoption for the routine quality control analysis of the consistency of recombinant glycoproteins.

Acknowledgements

The authors wish to thank M. Kaloostian, A. Jacobs, D. Arst and T. Pritchett at Beckman for all their help and advice.

References

[1] Garnick, N.J. Solli and P. Papa, Anal. Chem., 60 (1988) 2546.
[2] Spellman, L.J. Basa, C.K. Leonard, J.A. Chakel and J.V. O'Connor, J. Biol. Chem., 264 (1989) 14100.
[3] Yim, J. Chromatogr., 559 (1991) 401.
[4] Mazzeo, J.A. Martineau and I.S. Krull, Methods: A Companion to Methods in Enzymology, 4 (1992) 205.
[5] Pritchett, Sixth International Symposium on High Performance Capillary Electrophoresis, San Diego, CA, Jan 1994.
[6] Vehar, W.J. Kohr, W.F. Bennett, D. Pennica, C.A. Ward, R.N. Harkins and D. Collen, Biotechnology, 2 (1984) 1051.

Differences between natural and recombinant interleukin-2 revealed by gel electrophoresis and capillary electrophoresis

Joseph Knüver-Hopf*, Harald Mohr

German Red Cross Blood Transfusion Center of Lower Saxony, D-31832 Springe, Germany

Abstract

High-performance capillary electrophoresis (HPCE) is shown to be useful for analysis of interleukin-2 (IL-2) in its native state under non-reducing conditions. The results obtained were compared with those from analysis of IL-2 by protein blotting after sodium dodecylsulfate polyacrylamide gel electrophoresis (SDS-PAGE) under denaturing and reducing conditions. In addition, resolution of the different glycosylated and non-glycosylated natural IL-2 species was achieved by HPCE. The HPCE electropherogram of native IL-2 could easily generate quantitative amounts of the different naturally occurring IL-2 species. For HPCE of IL-2 run times of less than 10 min are sufficient, and only extremely small amounts of IL-2 are needed. In this report, human IL-2 expressed in bacteria has been analysed by HPCE and the existence of two recombinant IL-2 forms was demonstrated.

1. Introduction

High-performance capillary electrophoresis (HPCE) is a method with great potential for the high-resolution separation of biological substances [1]. The aim of this study was to compare this technique with sodium dodecylsulfate polyacrylamide gel electrophoresis (SDS-PAGE) for the characterisation of natural and recombinant interleukin-2 (IL-2).

Natural interleukin-2 (nIL-2) is a polypeptide which is synthesised and secreted by activated T-cells [2,3]. Previous investigations have demonstrated that the smallest nIL-2 component with a molecular mass of $15.0 \cdot 10^3$ is non-glycosylated, a $16.5 \cdot 10^3$ species is glycosylated and in addition mono-sialylated, and a $17.0 \cdot 10^3$ IL-2 component is glycosylated and di-sialylated [4].

In contrast, *Escherichia coli* derived recombinant interleukin-2 (rIL-2) is non-glycosylated. Additionally, in all genetically engineered IL-2 from *E. coli*, the cysteine residue at position 125 is substituted by a serine residue and the first amino acid alanine is missing [5].

2. Experimental

Human nIL-2 was prepared from the supernatants of human peripheral blood mononuclear cell (PBMC) cultures after activation with phorbol-12-myristate-13-acetate (PMA) and the calcium ionophore A 23187, and purified according to a scheme previously described [3]. Another nIL-2 was prepared from culture supernatants of concanavalin A (con A)-stimulated and propagated human PBMCs. The purification was done according to the same scheme. The rIL-2 used was produced by DNA technology. It was supplied by Euro Cetus (Frankfurt, Ger-

* Corresponding author.

many). The nIL-2 and rIL-2 samples used in the experiments were dissolved in 10 mM phosphate, pH 7.4, 0.9% sodium chloride. Capillary electrophoresis was performed in a Bio-Rad (Richmond, CA, USA) HPE 100, with data collection by a Hoefer Scientific GS 365 software package. Capillaries were supplied in cartridges with an integral flow cell for on-column optical detection. Proteins were introduced into the capillary by electromigration for 8 s at 8 kV. The samples were electrophoresed in a 100 mM pH 2.5 phosphate buffer at 10 kV in 20 cm × 25 μm I.D. coated capillaries.

SDS-PAGE was performed under reducing conditions using the method of Laemmli [6]. Stacking gel buffer: 0.062 M Tris, 0.062 M chloride, pH 6.7; separating gel buffer: 0.375 M Tris, 0.06 M chloride, pH 8.9; electrophoresis buffer: 0.05 M Tris, 0.38 M glycine, pH 8.3; sample buffer: 0.01 M Tris–HCl, 1% SDS, 5% β-mercaptoethanol, pH 8.0. For blotting, the slab gel was covered with a sheet of nitrocellulose membrane to which the proteins were electrophoretically transferred according to the procedure of Towbin et al. [7]. Transfer buffer: 25 mM Tris, 192 mM glycine, 20% methanol, pH 8.0. A voltage of 30 V for 16 h was used in a Trans blot cell at 10°C. To estimate the protein pattern after electroblotting of the gels, the transferred proteins were visualised by colloidal gold staining according to a modified method described by Moeremans et al. [8].

To check the reproducibility of the used methods all experiments were repeated three times.

3. Results and discussion

Fig. 1 shows the pattern of highly purified nIL-2 after separation by 15% SDS-PAGE, electroblotting and gold staining of the membrane. It shows the three different forms of nIL-2 migrating with different mobilities in SDS-PAGE, with molecular masses of $15.0 \cdot 10^3$, $16.5 \cdot 10^3$ and $17.0 \cdot 10^3$, respectively. The gold stain for protein blots has a very great sensitivity and therefore some artifactual bands are seen in the molecular-mass range $(40–70) \cdot 10^3$. These
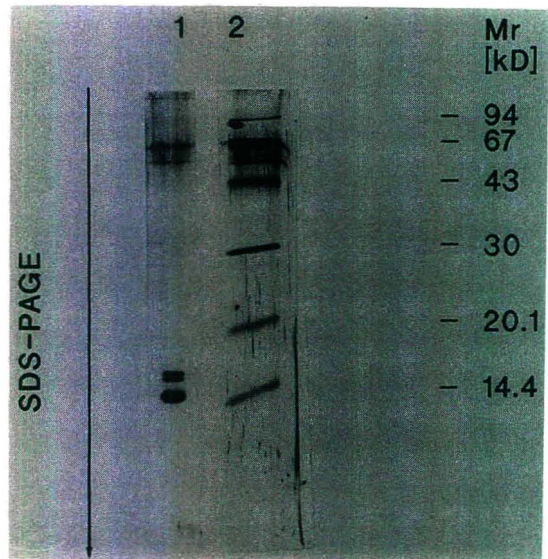
Fig. 1. Colloidal-gold stain on nitrocellulose of highly purified nIL-2. The protein was electrophoresed under reduced conditions. Lane 1: nIL-2; lane 2: molecular-mass marker proteins. An amount of 1 μg of the protein was applied per lane.

"ghost bands" simulate impurities, which could not be found in the electropherogram after HPCE (see below). To check further the purity and the composition of the nIL-2 preparations under non-denaturing conditions HPCE was used. The electrophoretic pattern of highly purified nIL-2 derived from A 23187/PMA-induced human lymphocytes is shown in Fig. 2. As
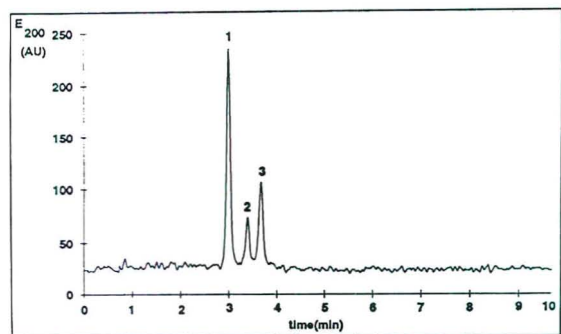
Fig. 2. High-performance capillary electrophoresis of nIL-2 (pIL-2 R435). Detection was by absorbance at 200 nm and the analog output to the collector was scaled 0.2 V and 0.005 AUFS.

can be seen, the three IL-2 species have different mobilities in HPCE. The first peak was detected at a retention time of 3 min, the second at 3.5 min and the third at ca. 4 min. Quantitation of the amounts of the three nIL-2 species was performed using the densitometer software GS 365. The percentage area for each peak is based on the total integrated area for the entire scan. For the first peak we measured 56% relative to the total area of the three peaks. The second protein peak takes 16% and the third protein peak takes 28% of the total peak area. Accordingly, in the nIL-2 preparation tested the proportion of the three peak areas was ca. 4:1:2. The ratio of the three IL-2 species was different in nIL-2 which was isolated from culture supernatants of A 23187/PMA-induced T-lymphoblasts which had been generated from T-lymphocytes by activation with concanavalin A 5–7 days prior to induction and purified using our standard procedure [3]. As shown in the electropherogram (Fig. 3), the first peak after 3 min represents 39% of the total protein, the second peak after 3.5 min 12% and the third peak after 4 min 50%, respectively. In this nIL-2 preparation the ratio of the three peak areas was 3:1:4. The results presented above demonstrate the high selectivity of the HPCE technique employed for separation of proteins with a single charge difference in polypeptides, like mono- and di-sialylated nIL-2. Fig. 4 shows recombinant IL-2 after 15% SDS-PAGE and electro-

Fig. 4. Colloidal-gold stain on nitrocellulose of highly purified rIL-2. The protein was electrophoresed under reduced conditions. Lane 1: rIL-2; lane 2: molecular-mass marker proteins. An amount of 1 μg of the protein was applied per lane.

blotting onto membranes. Under these denaturing and reducing conditions only one protein band was detected with a molecular mass of $15.0 \cdot 10^3$. Additionally, we again found ghost bands like those detected in the highly purified nIL-2 (Fig. 1). When the rIL-2 preparation was analysed by HPCE (Fig. 5), surprisingly, two protein peaks were detected instead of one, with approximately the same electrophoretic mobility as peak 1 in the electropherogram of nIL-2 in

Fig. 3. High-performance capillary electrophoresis of purified nIL-2 from propagated cells. Detection was by absorbance at 200 nm and the analog output to the collector was scaled 0.2 V and 0.005 AUFS.
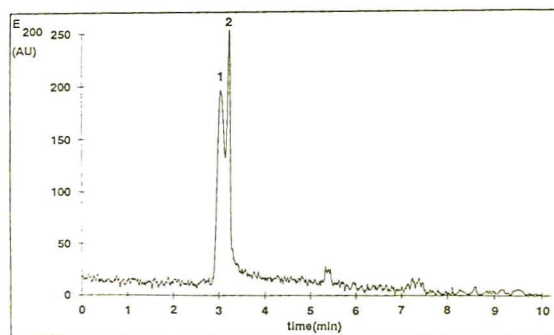
Fig. 5. High-performance capillary electrophoresis of rIL-2. Detection was by absorbance at 200 nm and the analog output to the collector was scaled 0.2 V and 0.005 AUFS.

Fig. 2. Up to now, it is not clear why in HPCE two protein peaks are found. We suggest that one of those peaks represents a rIL-2 form with a conformation slightly modified compared to the normal $15.0 \cdot 10^3$ species. More analytical work is required to confirm this supposition. One may speculate that the modified structure in the rIL-2 preparation could function as a neoantigen and thus may be the cause of the frequently observed relatively high antibody response during immunotherapy in cancer patients [9].

References

[1] B.L. Karger, A.S. Cohen and A. Guttman, J. Chromatogr., 492 (1989) 585–614.

[2] R.J. Robb, R.M. Kutny, M. Panico, H.R. Morris and V. Chowdnry, Proc. Natl. Acad. Sci. USA, 81 (1980) 6486–6490.

[3] H. Mohr and J.Knüver-Hopf, in M. Freund, H. Link and K. Welte (Editors), International Symposium on Cytokines in Hemopoiesis, Oncology, and AIDS, Vol. 1, Springer, Berlin, Heidelberg, 1990, pp. 351–358.

[4] H.S. Conradt, G. Geyer, J. Hoppe, L. Grotjahn. A. Plessing and H. Mohr, Eur. J. Biochem., 153 (1985) 255–261.

[5] F.E. Cohen, P.A. Kosen, I.D. Kuntz, L.B. Epstein, T.L. Ciardelli and K.A. Smith, Science, 234 (1986) 349–352..

[6] U. Laemmli, Nature, 227 (1970) 680–685.

[7] H. Towbin, T. Staehelin and J. Gordon, Proc. Natl. Acad. Sci. USA, 76 (1979) 4350–4354.

[8] M. Moeremans, G. Daneels and J. De Mey, Anal. Biochem., 145 (1985) 315.

[9] J. Knüver-Hopf, U. Pohl, M. Fischer, A. Großmann, J. Atzpodien, H. Kirchner and H. Mohr, in M. Freund, H. Link, R.E. Schmidt and K. Welte (Editors), International Symposium on Cytokines in Hemopoiesis, Oncology, and AIDS, Vol. 2, Springer, Berlin, Heidelberg, 1992, pp. 789–794.

Optimization of hapten–protein conjugation by high-performance capillary electrophoresis

Hanne Frøkiær[a], Hilmer Sørensen[b,*], Jens Christian Sørensen[a], Susanne Sørensen[a]

[a]*Department of Biochemistry and Nutrition, Technical University of Denmark, Building 224, DK-2800 Lyngby, Denmark*
[b]*Chemistry Department, Royal Veterinary and Agricultural University, 40 Thorvaldsensvej, DK-1871 Frederiksberg C, Denmark*

Abstract

HPCE has been found to be efficient for the optimization of conjugation procedures employed for coupling of the haptens p-nitrophenyl-α-D-galactopyranoside (PNPG) and soyasaponin I to a carrier protein, Kunitz soybean trypsin inhibitor (KSTI). The carbohydrate moieties of the haptens were oxidized with periodate followed by reaction with ϵ-amino groups of the carrier. For PNPG, the periodate oxidations (0.01–0.2 M NaIO$_4$) were followed by HPCE and 0.1 M periodate was chosen as the optimum concentration. The coupling of PNPG to KSTI was found to proceed at a constant rate for more than 250 min. The reaction rate for the soyasaponin conjugation to KSTI declined after 80 min of incubation. The coupling of soyasaponin to KSTI was confirmed by enzyme-linked immunosorbent assay with monoclonal antibodies directed against soyasaponin I. The method was found to be particularly powerful for the investigation of conjugates with low epitope densities that are difficult to determine otherwise.

1. Introduction

Haptens are small molecules incapable of eliciting immune responses without previous conjugation to immunogenic molecules, e.g., proteins. A wide variety of coupling reactions are available [1,2] and the choice of coupling reaction depends on the desired conjugate structure and the chemical structure of the hapten. Method adjustments and optimization are often required to obtain useful hapten–protein conjugates. The ease of method optimization is dependent on the methods available for evaluating the conjugation reaction. With haptens devoid of chromophoric groups or otherwise distinctive characteristics, method optimization may be dif-

ficult and sample consuming owing to the use of destructive methods, e.g., determination of free amino groups on the carrier protein by reaction with trinitrobenzenesulfonic acid [3]. There is, therefore, a need for generally applicable methods for analyses of hapten–carrier conjugation.

High-performance capillary electrophoresis (HPCE) offers a method with very low sample consumption (nl) and a high separation capacity, which can be utilized for separating uncoupled and conjugated carriers based on the differences in electrophoretic mobilities introduced by covalently coupling the hapten to the carrier. In addition, frequent on-line analyses from the sample vials are possible by HPCE, thus facilitating optimization of incubation times. The haptens used in the study were soyasaponin I and p-nitrophenyl-α-D-galactopyranoside (PNPG).

---

* Corresponding author.

The latter was chosen as a model hapten for soyasaponin I owing to its carbohydrate content and chromophoric group that allows traditional spectrophotometric characterization of the conjugation products.

Various leguminous plants have been shown to contain saponins [4,5], which comprise a group of glycosides. Many saponins have a bitter taste [4] and consequently saponins are considered to be important in relation to the production of high-quality legumes for food and feed and for the production of protein concentrates and isolates. The predominant saponin in extracts of pea has been shown to be soyasaponin I [6].

Current methods of analyses for soyasaponin I are hampered partly owing to the lack of an efficient detection system for soyasaponin I. Monoclonal antibodies (mAbs) against soysaponin I offer a specific detection system that can be employed in an enyme-linked immunosorbent assay (ELISA) method for analyses of large samples numbers. For this purpose, coupling of soyasaponin I to a carrier is necessary, as soyasaponin is too small a molecule to elicit an immune response.

The periodate oxidation method is applicable for coupling of carbohydrate moieties containing vicinal hydroxy groups to amino groups, e.g., lysine side-chains in carrier proteins. This method was chosen for coupling of soyasaponin I and PNPG to protein carriers. The drawbacks of the periodate oxidation method is that optimization may be necessary [2].

An HPCE method for protein analyses has been presented previously [7], and this method has been shown to be applicable for the characterization of hapten–protein conjugates [8]. The aim of this work was to show that HPCE is a valuable tool in the optimization of coupling reactions for generating immunogenic hapten–carrier conjugates.

2. Experimental

2.1. Materials

Kunitz soybean trypsin inhibitor (Type I-S) (KSTI), *p*-nitrophenyl-α-D-galactopyranoside

(PNPG), $NaIO_4$, taurine (2-aminoethanesulfonic acid) and cholic acid were obtained from Sigma (St. Louis, MO, USA), 3,3′,5,5′-tetramethylbenzidine (TMB) from Merck (Darmstadt, Germany), Triton X-100 from Serva (Heidelberg, Germany) and horseradish peroxidase (HRP)-labelled rabbit anti-mouse antibody from Dako (Glostrup, Denmark). Soyasaponin I and mAbs with soyasaponin I specificity were prepared as described elsewhere [8,9]. The structures of PNPG and soyasaponin I are shown in Fig. 1.

2.2. HPCE procedure

HPCE was performed using an HP[3D]CE system (Hewlett-Packard, Waldbronn, Germany) with a 614 mm × 0.05 mm I.D. fused-silica capillary. Detection was performed by on-column measurements of UV absorption at 200 nm at a position 530 mm from the injection end of the capillary. All measurements were made at 16 kV and 30°C. Buffer solutions of 75 mM Na_2HPO_4–50 mM taurine and with or without 35 mM cholic acid were prepared and filtered through a 0.2-μm membrane filter. The buffer pH was 8.0–8.1. Preconditioning of the capillary was performed prior to each run by flushing with 0.1 M NaOH for 1–2 min and run buffer for 1–3 min.

2.3. Hapten–carrier conjugation

PNPG (1.8 mg/ml in water; 133 μl) and 100 μl of water were incubated with $NaIO_4$ (0.1 M in water; 50 μl) in a buffer vial and on-line
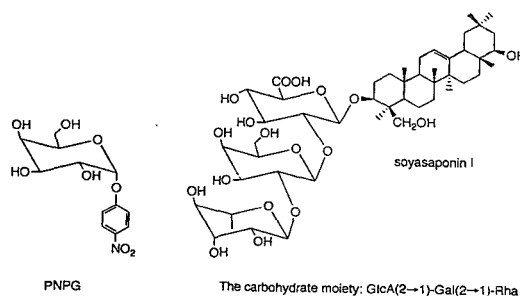
Fig. 1. Structures of PNPG and soyasaponin I. Periodate oxidation of the carbon–carbon bond at vicinal hydroxy groups on the carbohydrate moieties of the haptens results in the formation of aldehyde groups.

HPCE analyses were performed to follow the oxidation of vicinal hydroxy groups on PNPG.

For conjugation, PNPG (1.8 mg/ml in water; 133 μl) or water (133 μl; blank sample) and 100 μl of water were preincubated with NaIO$_4$ (0.1 *M* in water; 50 μl) for various periods followed by mixing with 70 μl of KSTI (10 mg/ml in 0.1 *M* NaHCO$_3$, pH 9.3). The mixture of PNPG and KSTI was analysed on-line by HPCE. Soyasaponin I (50 μl; 1.5 mg/ml in 10% MeOH) was preincubated with NaIO$_4$ (25 μl; 0.1 *M* in water) and mixed with 13 μl of KSTI (10 mg/ml in 0.1 *M* NaHCO$_3$, pH 9.3).

The conjugation products were finally reduced with NaBH$_4$ [8].

2.4. Coupling efficiency measured by ELISA

Wells of microtitre plates (MaxiSorp; Nunc, Roskilde, Denmark) were coated with 100 μl of saponin–KSTI conjugate (1 mg/ml) dissolved in carbonate buffer (50 m*M*; pH 9.6). The plates were incubated for 1 h at 20°C on a shaker and then washed with washing buffer containing detergent (0.5 *M* NaCl–27 m*M* KCl–15 m*M* KH$_2$PO$_4$–100 m*M* Na$_2$HPO$_4$·2H$_2$O–0.1% Triton X-100). Dilution rows of mAbs were incubated (150 ng/ml in the first well) for 1 h and the plates were washed four times. HRP-labelled rabbit anti-mouse antibody diluted 1:1000 in washing buffer was added to each well and incubation proceeded for 1 h. After washing, 100 μl of a substrate solution (0.2 *M* potassium citrate–3 m*M* H$_2$O$_2$–0.6 m*M* TMB) were added to each well. Colour development was stopped with addition of H$_3$PO$_4$ (100 μl per well; 2 *M*), and absorbance were read at 450 nm using an EL 312e microplate reader (BioTek Instruments, Winooski, VT, USA).

3. Results and discussion

The use of HPCE for on-line evaluation of coupling reactions was investigated. The coupling kinetics of two different molecules to carrier proteins were investigated by electrophoresis of the mixtures during conjugation.

3.1. PNPG periodate oxidation

Initially, the necessity for cholate in the buffer system was evaluated for the determination of PNPG by HPCE. In the absence of cholate, PNPG co-migrated with the solvent peak whereas increased cholate concentrations gradually increased the migration time of PNPG relative to the solvent peak. A concentration of 35 m*M* cholate was found to be appropriate for the determination of PNPG and the periodate oxidation product of PNPG.

The periodate oxidation of PNPG was investigated for various incubation periods (Fig. 2) at different periodate concentrations (0.01–0.2 *M*), as optimization of the periodate concentration has been reported to be important for obtaining a suitable degree of oxidation [2]. The oxidation of PNPG at vicinal hydroxy groups does not influence the chemical structure and the molar absorptivity of the chromophoric group of PNPG. Consequently, the total normalized area (NA) can be used as a measure of the amount of the chromophoric groups present in the sample.
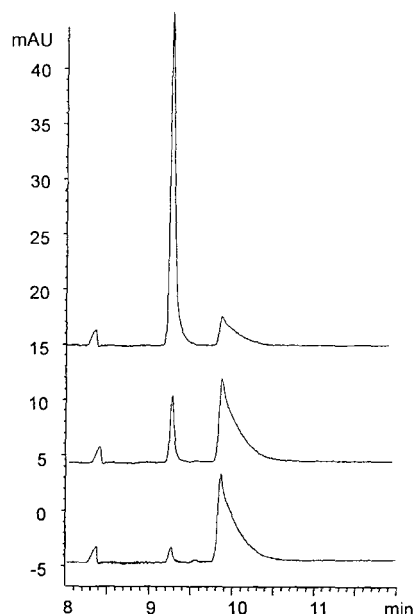
Fig. 2. Electropherograms recorded at 305 nm of PNPG incubated with NaIO$_4$ for 2 min (top), 15 min (middle) and 29 min (bottom). The peak at 9.3 min is PNPG and that at 9.9 min is the reaction product.
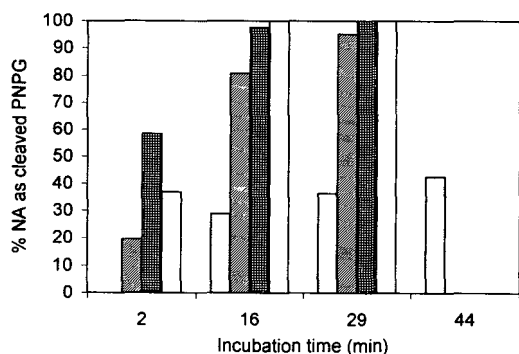
Fig. 3. Proportion of PNPG present as oxidized PNPG determined from NA at various periodate concentrations (grey, 0.01 M; diagonal hatched, 0.05 M; checked, 0.1 M; white, 0.2 M). At 44 min of incubation only the sample with 0.01 M NaIO$_4$ was analyzed.

In Fig. 3, the oxidation rate is illustrated as a percentage of total PNPG present as oxidized PNPG. With 0.01 M NaIO$_4$ the oxidation proceeds slowly, whereas NaIO$_4$ concentrations above 0.05 M result in complete oxidation after ca. 20 min. However, oxidation at high NaIO$_4$ concentrations and a prolonged incubation time markedly decreased the total NA measured (Fig. 4), implying that excessive oxidation destroys or changes the chromophoric group of PNPG. This was also seen by observations on the PNPG sample colour, which changed from colourless to

yellow, indicating that a more conjugated system was generated from the PNPG molecules. For further studies, preincubation with 0.1 M NaIO$_4$ was chosen.

3.2. Coupling of PNPG to KSTI

PNPG preincubated with periodate for different periods of time was mixed with KSTI and the formation of coupling products was determined from the normalized peak areas. The peaks of coupling products have higher migration times (MTs) than the MT of KSTI (17.5 min, Fig. 5) owing to hydrophobic interaction of the PNPG moieties with cholate micelles [8]. At 200 nm, the molar absorptivity of PNPG is diminished compared with that of KSTI, implying similarity of response factors of the KSTI conjugate and KSTI [8], thus allowing the determination of coupling densities from NA.

In parallel with the coupling experiments, corresponding blank samples without PNPG were mixed with KSTI to study the influence of IO$_4^-$ on the protein during incubation. The electropherograms of the blank samples showed that the electrophoresis pattern of KSTI was

Fig. 4. Degradation of PNPG measured as total NA in relation to the total NA found after 2 min of incubation at different periodate concentrations: ◇ = 0.01; △ = 0.05; ○ = 0.1; × = 0.2 M. Electropherograms for the NA determinations were recorded at 305 nm.
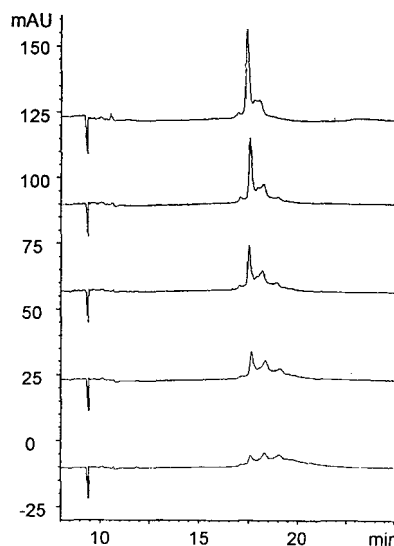
Fig. 5. Electropherograms of the reaction mixture from conjugation of PNPG with KSTI after (from top to bottom) 44, 112, 180, 247 and 382 min, recorded at 200 nm.

unchanged during the incubation periods. The additional peaks observed in the electropherogram are due to impurities present in the commercially available KSTI.

The coupling ratios of PNPG to KSTI were calculated as described previously [8] by using the NA for quantification. The control sample of KSTI without PNPG was used for correction of contributions from the unconjugated KSTI to the NA of the emerging KSTI conjugate due to co-migrating peaks.

Fig. 6 shows the coupling of PNPG to KSTI after various preincubation times of PNPG with periodate. The parameters studied did not result in substantial effects on the PNPG–KSTI coupling, implying that in the time intervals studied, activated PNPG was not a deficient component. In addition, the coupling reaction between PNPG and KSTI is apparently slow, as no coupling saturation was observed in the time interval studied.

3.3. Coupling of soyasaponin to KSTI

Soyasaponin was dissolved in a mixture of methanol and water, but the presence of methanol was found to cause denaturation of the carrier protein. Therefore, the solubility of soyasaponin I in mixtures with different ratios of methanol to water was investigated in order to minimize the use of methanol. This was evaluated from the NA obtained from HPCE of

soyasaponin I samples dissolved in different mixtures of methanol and water. The methanol concentration chosen for the saponin solubilization was 10%.

The conjugation of soyasaponin I to KSTI was followed after five different preincubation periods as shown in Fig. 7. The number of saponins per KSTI molecule was calculated from the normalized peak areas of the KSTI–saponin conjugates relative to the total NA of the protein present in the sample. Examples of electropherograms after various coupling periods are shown in Fig. 8. Similarly to the PNPG–KSTI conjugates, the coupling products have higher MTs than the MT of KSTI.

Although the methanol concentration had been reduced to 10%, some changes in the migration time of the KSTI control sample was observed during incubation, probably owing to denaturation in the presence of MeOH. Therefore, the NA obtained for the conjugation products were corrected for the NA contribution from co-migrating denatured KSTI.

From Fig. 7, it seems that the conjugation rate declined after 60–90 min of incubation of activated soyasaponin I with KSTI, although continued conjugation seemed to take place at a lower reaction rate. Preincubation for 17 h resulted in a lower epitope density, which may be due to excessive oxidation as proposed for the PNPG oxidation. Soyasaponin I was present in a twelvefold molar excess over KSTI, and during the conjugation the NA of saponin did not
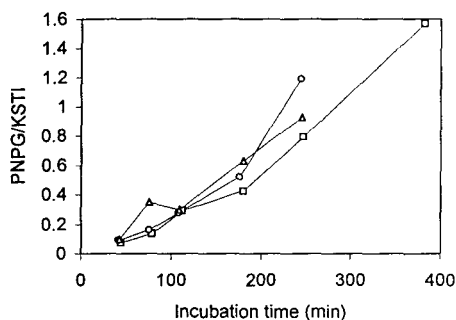
Fig. 6. Coupling density of PNPG to KSTI following preincubation with 0.1 M NaIO$_4$ for ($\square$) 10, ($\bigcirc$) 30 and ($\triangle$) 60 min.
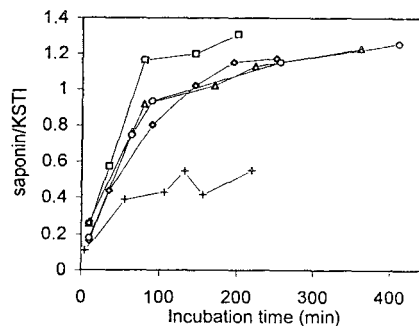
Fig. 7. Conjugation of soyasaponin I to KSTI following preincubation with 0.1 M IO$_4^-$ for ($\square$) 10, ($\diamond$) 30, ($\triangle$) 50 and ($\bigcirc$) 310 min and (+) 17 h.
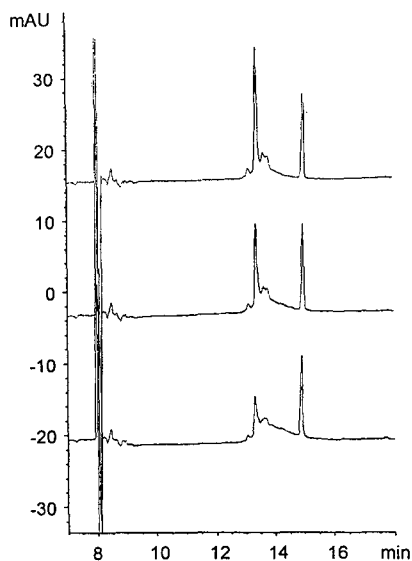
Fig. 8. Electropherograms of soyasaponin I conjugation to KSTI after 60 min of preincubation with 0.1 M $NaIO_4$. Coupling after 10 (top), 90 (middle) and 140 min (bottom). The MT of soyasaponin I is 14.8 min and that of KSTI is 13.5 min. Electropherograms were recorded at 200 nm.

decrease noticeably, thus supporting the contention that the epitope density is low.

Experiments were performed in duplicate in which oxidized saponin was reacted with KSTI for various lengths of time and then exposed to $NaBH_4$ and desalted [8]. Determination of degrees of conjugation from electropherograms of the reaction mixture and the reduced, desalted sample gave similar results, showing that the conjugation optimization can be performed directly on the reaction mixture.

The desalted samples were also investigated for their ability to bind monoclonal antibodies with specificity for soyasaponin I. For both experiments, samples incubated for 60, 90 and 150 min showed an increasing antibody binding as a function of reaction time. However, the sample incubated for 10 min showed an antibody binding capacity similar to that observed with 150 min of incubation. However, a correspondingly high epitope density was not found from the HPCE data of the samples, indicating that the high antibody binding capacity may be

due to higher accessibility of the epitopes instead of epitope density. This could be explained by the coupling reaction, an prolonged incubation may cause the coupling of the same saponin molecule at multiple sites, thereby reducing the epitope accessibility.

A sample incubated for 27 h showed a higher antibody binding capacity than found for samples incubated for 150 min, indicating that a prolonged incubation time results in an increase in coupling density. On HPCE this conjugation product showed a broad peak with an increased migration time.

In conclusion, HPCE has been shown to be a valuable tool for the investigation and optimization of the coupling of PNPG and soyasaponin I to KSTI. The HPCE method presented has several advantages over alternative methods and particularly important is the ability to measure low coupling densities, in contrast to spectrophotometric methods, e.g., TNBS conjugation to ϵ-amino groups on lysine. In addition, on-line HPCE of the conjugation mixture allows the optimization of the incubation time and concentrations of reactants with a minimum consumption of reactants owing to the low sample volumes necessary.

References

[1] B.F. Erlanger, Methods Enzymol., 70 (1980) 85.
[2] O. Mäkelä and I.J.T. Seppälä, in D.M. Weir (Editor), Handbook of Experimental Immunology, Vol. 1, Blackwell, Oxford, 1986, p. 3.1.
[3] A.F.S.A. Habeeb, Anal. Biochem., 14 (1966) 328.
[4] K.R. Price, I.T. Johnson and G.R. Fenwick, CRC Crit. Rev. Food Sci. Nutr., 26 (1987) 27.
[5] S.B. Mahato, S.P. Sarkar and G. Poddar, Phytochemistry, 27 (1988) 3037.

[6] K.R. Price, J. Eagles and G.R. Fenwick, J. Sci. Food
    Agric., 42 (1988) 183.
[7] A.M. Arentoft, H. Frøkiær, S. Michaelsen, H. Sørensen
    and S. Sørensen, J. Chromatogr. A, 652 (1993) 189.
[8] H. Frøkiær, P. Møller, H. Sørensen and S. Sørensen, J.
    Chromatogr. A, 680 (1994) 437.
[9] H. Frøkiær, L. Hørlyck, V. Barkholt, H. Sørensen and S.
    Sørensen, Food Agric. Immunol., 6 (1994) 63.

Demonstration of a heparin-binding site in serum amyloid P component using affinity capillary electrophoresis as an adjunct technique

Niels H.H. Heegaard[a,*], Hanne D. Mortensen[b], Peter Roepstorff[b]

[a]*Department of Autoimmunology, Statens Seruminstitut, DK-2300 Copenhagen S, Denmark*
[b]*Department of Molecular Biology, University of Odense, DK-5230 Odense M, Denmark*

Abstract

Linear heparin-binding sites in the DNA- and heparin-binding serum protein amyloid P component were investigated using affinity capillary electrophoresis and reversed-phase HPLC in conjunction with affinity chromatography. Peptide fragments were generated from amyloid P component by treatment with Glu-C and Asp-N endoproteinases. This peptide mixture was separated by HPLC before and after passage through a column of immobilized heparin. In addition, the proteolytic digest was separated by capillary electrophoresis in the presence of various amounts of heparin in solution. Migration shift patterns in the presence of heparin were in agreement with one of the components shown by HPLC to interact with immobilized heparin. The identity of this fragment was established by mass spectrometry after preparative HPLC and represents a novel heparin-binding sequence. The results illustrate the potential synergy in the combination of the two high-resolution separation techniques HPLC and CE. HPLC has the advantages of high recovery and preparative power while capillary electrophoresis is noted for highly efficient separations under physiological conditions. The possibility of using unmodified ligands in the study of biological activities of protein substructures while consuming very little material makes CE further attractive.

1. Introduction

Biomolecular interactions are often characterized using immobilized or otherwise modified (e.g., labelled) receptor proteins or ligands. In many cases, however, binding data may be obtained by means of various electrophoretic techniques using unmodified reactants [1]. The use of electrophoresis for the characterization of reversible binding is based on measurement of changes in electrophoretic parameters resulting from interactions that take place during electro-

phoresis. Accordingly, this type of interaction analysis is often called affinity electrophoresis [2]. Capillary electrophoresis (CE) has been used with advantage for affinity studies (affinity CE) in a growing number of specific cases [3–12] because of its merits of speed, versatility, low sample consumption and high resolving power.

Amyloid P component is a protein of unknown physiological function that is found in serum [serum amyloid P component (SAP)], from where it may readily be isolated by means of its Ca^{2+}-dependent affinity for DNA, heparin or residues in Sepharose. It seems to be an obligatory constituent of all amyloid lesions irrespec-

* Corresponding author.

tive of the nature of the amyloid core protein [13,14]. Owing to the persistent association of SAP and heparan sulfate proteoglycans with amyloid deposits, including those of Alzheimer's disease [13], there is interest in elucidating the structure of binding sites on SAP for heparin. The three-dimensional structure of SAP at pH 5.5 has been determined and a binding site for small anionic carbohydrates requiring Ca^{2+} and contributions from non-contiguous parts of the molecule was delineated [15]. However, there may well be other binding sites for larger anionic carbohydrates such as heparan sulfate and heparin. SAP is structurally closely related to C-reactive protein (CRP) [16] but, unlike CRP, it is not an acute-phase protein in man and is glycosylated. It has been shown that bioactive peptides may be generated from CRP on incubation with proteolytic enzymes from polymorphonuclear leukocytes (PMN) [17], and it was recently demonstrated that SAP in addition to CRP binds to PMN receptors and that peptides generated by subjecting intact SAP to proteolytic enzymes from PMNs inhibited this binding [18].

Hence, to identify linear binding sites possibly mimicking the binding of heparin by the parent protein, SAP was digested with various proteolytic enzymes and subjected to analysis by HPLC after absorption with immobilized heparin and by affinity CE using heparin in solution. Here we report the results of experiments carried out with SAP fragments generated by treatment with Asp-N and Glu-C endoproteinases. The study identified a novel heparin-binding sequence in SAP and illustrated the usefulness of CE as a complementary technique for the identification and characterization of ligand-binding sites.

2. Experimental

2.1. Chemicals

Bovine serum albumin, chondroitin sulfate, type C, from shark cartilage (C-4384), dithiothreitol, heparin from porcine mucosa (H-7005), Tris [tris(hydroxymethyl)aminomethane] and 4-vinylpyridine were obtained from Sigma (St.

Louis, MO, USA), *Staphylococcus aureus* V8 protease from Worthington (Freehold, NJ, USA), Asp-N endoproteinase from Boehringer (Mannheim, Germany), guanidinium hydrochloride, heparin-Eupergit C and trifluoroacetic acid (TFA) from Fluka (Buchs, Switzerland), DNA-agarose from Pharmacia–LKB (Uppsala, Sweden), formic acid from Aldrich (Steinheim, Germany) and HPLC-grade water and acetonitrile and all other chemicals (analytical-reagent grade) from Merck (Darmstadt, Germany).

2.2. Serum amyloid P component fragmentation

Serum amyloid P component (SAP) was purified from human plasma by affinity chromatography on DNA-agarose followed by ion-exchange HPLC as described [19]. Aliquots of 1 mg of SAP were dialysed against water at 4°C and evaporated to dryness in a centrifugal evaporator (SpeedVac). Reduction and S-pyridylethylation was performed by adding 500 µl of 6 M guanidinium hydrochloride in Tris-buffered saline [TBS: 5 mM Tris–HCl (pH 7.4)– 150 mM NaCl] to 1 mg of dried SAP followed by 2 mg of dithiothreitol. After stirring for 2 h under helium, 5 ml of 4-vinylpyridine was reacted with the sample at room temperature for 3 h, then 2 ml of formic acid were added and the solution was dialysed against water at 4°C overnight and dried.

The V8 protease was used for digesting the reduced and S-pyridylethylated SAP at a ratio of 10 µg of enzyme to 1 mg of SAP in 500 µl of 20 mM NH_4HCO_3–10% CH_3CN–1 M guanidinium hydrochloride. Under these conditions, the Glu-C endoproteinase activity of the enzyme predominates. The digestion was allowed to proceed at room temperature with stirring for 48 h. The digest was then mixed with an equal volume of formic acid and desalted on a C_{18} column (see below). All material that eluted with 70% CH_3CN in 0.1% TFA was collected, dried and resuspended in 400 µl of 45 mM phosphate (pH 7.5) containing 7.5% CH_3CN and 2 µg of Asp-N endoproteinase (corresponding to ca. 1% by mass of dried material). The sample was incubated at room temperature overnight with stir-

ring and then used for affinity chromatographic experiments. Chosen peptide fragments were collected manually from the HPLC system using a 150-μl injection volume. Another 150 μl were desalted on the HPLC column as described above. Purified material and desalted digest were dried by centrifugal evaporation.

2.3. Reversed-phase HPLC

HPLC was performed on an analytical C_{18} column (218TP54, 5 μm, 250 × 4.6 mm I.D.) from Vydac (Hesperia, CA, USA), eluted with a gradient at 1 ml/min of 5–65% acetonitrile in 0.1% TFA over 60 min. Detection took place at 210 and 280 nm.

2.4. Absorption with immobilized heparin

SAP-derived peptides in a volume of 50 μl in digestion buffer were mixed with 0.2 ml of heparin-Eupergit C matrix that had been previously washed with 10-ml volumes of water, tenfold concentrated TBS and TBS. After 10 min on the column at room temperature, the matrix was washed with 0.4 ml of TBS and all effluent was collected and analysed by reversed-phase HPLC as described above.

2.5. Plasma desorption mass spectrometry (PDMS) and amino acid sequencing

PDMS was performed on a BioIon 20 time-of-flight mass spectrometer (BioIon, Uppsala, Sweden). Peptide material was dissolved in 0.1% TFA–20% methanol to a concentration of ca. 50 pmol/μl and 2 μl were applied on a spin-cast nitrocellulose target [20].

Amino acid sequencing was done by Edman degradation using a Model 910 pulsed-liquid sequencer from Knauer (Berlin, Germany).

2.6. Capillary electrophoresis

The CE instrument was a P/ACE 2050 from Beckman Instruments (Fullerton, CA, USA) with data collection, storage, analysis and report-ing performed by System Gold Software (Beckman Instruments).

Throughout, uncoated fused-silica 50 μm I.D. capillaries of 57 cm length (50 cm to the detector) and an electrophoresis buffer of 0.1 M phosphate (pH 7.5) (filtered through a 0.22-μm filter) were used. Sample injections took place by pressure at the anode end of the capillary. A 1-s injection corresponds to a sample volume of 0.9 nl according to the specifications of the manufacturer. Detection was effected at 200 nm and the field strength used for the separations was 15 or 20 kV as indicated. The liquid cooling system was set to 19°C.

2.7. Affinity capillary electrophoresis

The dried material was subjected to capillary electrophoresis experiments after resuspension in HPLC-grade water (purified fragments in 50 μl and the digest mixture in 100 μl). Electrophoresis took place as described above in phosphate buffers with various additions of heparin or chondroitin sulfate from stock solutions at 20 mg/ml of glycosaminoglycan in 0.05 M phosphate (pH 7.5). Identification of individual peptides took place by co-injection of SAP digests with purified peptide from a second injection vial.

3. Results and discussion

After treatment of reduced and S-pyridylethylated SAP with Glu-C and Asp-N endoproteinases, a mixture of peptide fragments was obtained. The analysis of this by reversed-phase HPLC is shown in Fig. 1A. The digest was examined for heparin-binding components by absorption on immobilized heparin followed by HPLC (Fig. 1B). Affinity chromatography was performed using heparin immobilized on acrylamide instead of Sepharose because SAP is known to bind to components of the latter matrix [21]. Several fragments decreased in amount after incubation with immobilized heparin, indicating retention on the matrix. The main heparin-interacting components are peaks
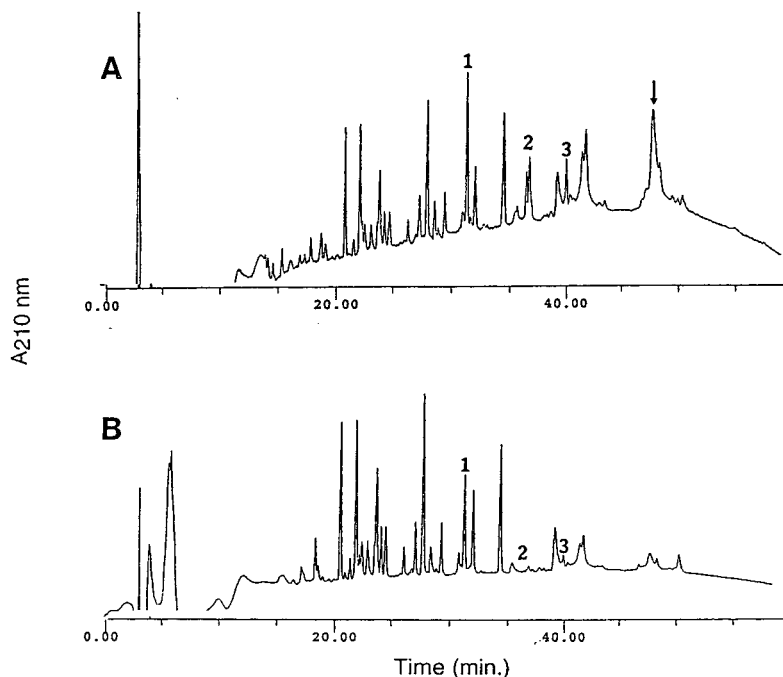
Fig. 1. HPLC analysis (detection at 210 nm) of an endoproteinase Asp-N-treated Glu-C digest of SAP. Heparin-binding SAP fragments characterized by absorption on immobilized heparin followed by HPLC. (A) Control (10 μl of material injected); (B) mixture after passage through a heparin-Eupergit C column (a volume of 400 μl was injected). Peaks 1–3 were collected separately and analysed further. Arrow marks a late complex that probably represents incompletely digested protein.

1–3 in Fig. 1A. The late complex observed after 45 min in Fig. 1A (arrow) probably represents intact and incompletely digested protein which is also retained on the heparin column. No material was eluted with 1.5 M NaCl (not shown). The late component was not investigated further but peaks 1–3 were isolated for characterization.

Analysis of the digest by CE after drying and resuspension in water is shown in Fig. 2. To characterize heparin binding under circumstances close to physiological conditions, the CE separations were performed using 0.1 M phosphate buffer at neutral pH as the electrophoresis buffer. Hence a 100% recovery of all the peptides seen in the HPLC separation was not expected. Approximately 20 components were separated by CE (Fig. 2A), and changes in the migration pattern were observed on incorporation of heparin into the electrophoresis buffer (Fig. 2B). Even through the whole population of peptides had an increased migration time when

heparin (Fig. 2B) or chondroitin sulfate (Fig. 2C) was added (due to a decrease in the electroosmotic flow), it was evident that the marked peptide peak (asterisks in Fig. 2) had a much more pronounced migration shift than the bulk of peptides in experiments with heparin (Fig. 2B), whereas this was not the case in experiments with additions of chondroitin sulfate to the electrophoresis buffer (Fig. 2C). Other, smaller, changes also occurred specifically in the heparin experiment, but these have not yet been investigated further. In accordance with these results, the parent protein, SAP, has been shown to exhibit a lower affinity for chondroitin 4-sulfate and chondroitin 6-sulfate than for heparin [22].

By spiking with purified components (not shown), the heparin-binding component identified by affinity CE was found to correspond to fragment 3 in Fig. 1A. In contrast, the material of peak 2 of Fig. 1A was not recovered under the CE conditions used in this study, and the materi-
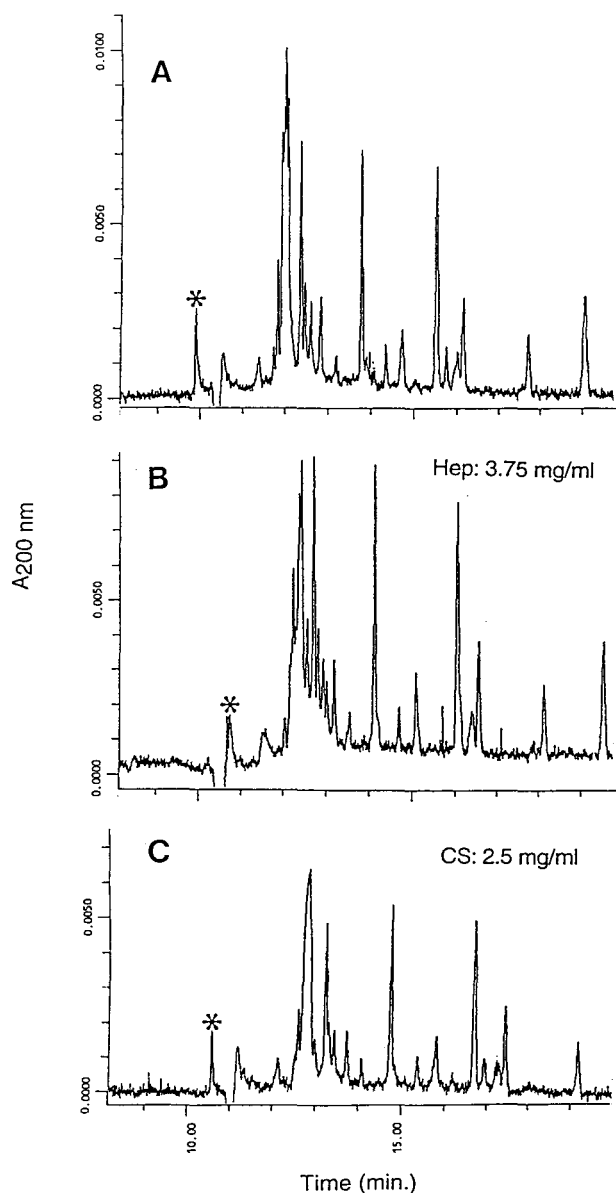
Fig. 2. Screening by affinity CE for interaction of SAP peptides with heparin in solution. An endoproteinase Asp-N-treated Glu-C digest of SAP solubilized in water was injected for 12 s and subjected to CE at 15 kV (detection at 200 nm) in the presence of heparin (Hep) (B) or chrondroitin sulfate (CS) (C) added to the electrophoresis buffer (0.1 M phosphate, pH 7.5) at the concentrations indicated. The peptide marked with asterisks was identified by spiking with HPLC-purified fragments and corresponds to fragment 3 in Fig. 1.

al of peak 1 yielded two components that did not seem to be influenced by heparin in affinity CE (not shown).

Fragment 3 was subjected to mass spec-trometry and amino acid sequencing. The first four residues were found to be H–Ile–Arg–Gly–Tyr and this and the measured mass of 1555.7 (expected, 1556) corresponded to a C-terminal

peptide: -Ile−Arg−Gly−Tyr−Val−Ile−Ile−Lys−Pro−Leu−Val−Trp−Val−OH (amino acids 192–204 in the SAP structure [23]). This peptide, purified from the SAP digest, was analysed and examined for heparin binding in affinity CE (Fig. 3). As can be seen, there was a concentration-dependent decrease in the mobility of the peptide with increasing concentration of heparin in the ¯electrophoresis buffer without apparent changes in peak shape or size. This is taken to indicate binding of the peptide to heparin with a dynamic equilibrium existing in the course of the electrophoretic process between non-complexed and heparin-complexed peptide (with a lower mobility than the free peptide). The equilibrium shifts towards longer times spent in the complexed form (and thus a more slowly migrating but homogeneous peak) when more heparin is present [1,5].
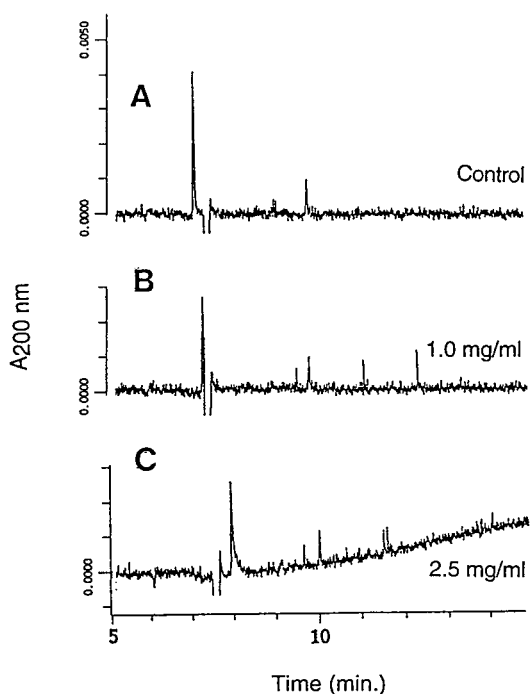
This pattern of behaviour is consistent with affinity interactions of intermediate strength characterized by fast association and dissociation rates [4,24].

A fundamental demand for the use of affinity CE to measure binding interactions is that complexed molecules must differ from unbound, free species in mobility. In the present study this was expected because heparin, by virtue of its high sulfation, is highly negatively charged. Thus, heparin-binding components would be predicted to reveal themselves in affinity CE by changing to a lower overall mobility or, for stronger interactions where the time for the electrophoresis is too short to ensure equal participation of all peptide molecules in complexes and in a free state, by decreases in peak size or by peak broadening or splitting [24]. For the peptide identified in this study, addition of heparin in sufficient amounts actually results in a reversal of its electrophoretic mobility from being towards the cathode to being towards the anode (Fig. 3B and C). In both cases, the observed mobility is due to the addition of the electroosmotic flow to the electrophoretic mobility and the consequence is that the molecule crosses the gap (water) representing the movement of neutral components in the system. Thus, on incorporation of heparin, the mobility of the peptide changes much more than the minor alterations in the electroosmotic flow account for.

Fig. 3. Purified heparin-binding fragment in affinity CE. Demonstration of interaction with heparin. Fragment 3 (cf., Fig. 1) was analysed at 20 kV (detection at 200 nm) after 5-s injection in the presence of the indicated concentrations of heparin in the electrophoresis buffer (0.1 *M* phosphate, pH 7.5).

4. Conclusions

A novel heparin-binding peptide from SAP has been demonstrated by a combination of HPLC and affinity CE methods. It does not contain the usual stretches of positively charged residues that are found in concensus sequences for glycosaminoglycan-binding peptides [25].

The observations in CE were supported by the results of reversed-phase HPLC separations of the same fragments incubated before chromatography with immobilized heparin, which demonstrated binding of this and other peptides.

Additional SAP-derived heparin-binding peptides generated utilizing other endoproteinases

and also synthetic peptides based on the activities discovered are now being characterized and related to the functions of the parent protein. This will be the subject of a forthcoming publication.

The problem of the recovery of potentially interesting molecules is illustrated in this study by fragment 2, which could not be analysed by CE at pH 7.5. The advantage of not being restricted to using an immobilized ligand was exemplified by peptide 1, which appeared to be retained on the heparin-Eupergit column but where neither of the two components that appeared in the CE analysis (not shown) interacted with free heparin in solution. Thus, the retention on the column for this peptide fraction may not be ligand specific or is due to a change in the ligand as a consequence of the coupling chemistry. The avoidance of artifacts due to modified ligands is one of the general advantages of methods such as affinity CE that use ligands in solution.

The solubilization and recovery of molecules are generally less problematic in reversed-phase HPLC than in CE. On the other hand, binding studies in solution are feasible in CE experiments in contrast to the meager opportunities to do this in the acidic organic environment of reversed-phase HPLC.

A final advantage of affinity CE analyses for the characterization of ligand-binding activities of components of proteolytic digests of proteins is the low consumption of material in comparison with solid-phase and equilibrium dialysis procedures, where the demands for material normally make it impossible to use components purified from enzyme digests. The present study is, to our knowledge, the first example of the use of CE to map directly binding sites in protein digests.

Thus, in summary, the potential for high-performance resolutions together with the preparative purification and the non-denaturing functional characterization of small amounts of material afforded by HPLC and CE, respectively, make the combination of the two techniques a potentially highly valuable tool in elucidating correlations between structure and function in proteins and other biomolecules. Peptides with binding activity may be demonstrated, identified in the sequence and characterized to an extent that none of the individual techniques can afford on its own.

References

[1] N.H.H. Heegaard, Appl. Theor. Electrophoresis, 4 (1994) 43.
[2] K. Takeo and E.A. Kabat, J. Immunol., 121 (1978) 2305.
[3] H. Kajiwara, H. Hirano and K. Oono, J. Biochem. Biophys. Methods, 22 (1991) 263.
[4] Y.-H. Chu, L.Z. Avila, H.A. Biebuyck and G.M. Whitesides, J. Org. Chem., 58 (1993) 648.
[5] L.Z. Avila, Y.-H. Chu, E.C. Blossey and G.M. Whitesides, J. Med. Chem., 36 (1993) 126.
[6] Y.-H. Chu and G.M. Whitesides, J. Org. Chem., 57 (1992) 3524.
[7] Y.-H. Chu, L.Z. Avila, H.A. Biebuyck and G.M. Whitesides, J. Med. Chem., 35 (1992) 2915.
[8] S. Honda, A. Taga, K. Suzuki, S. Suzuki and K. Kakehi, J. Chromatogr., 597 (1992) 377.
[9] N.H.H. Heegaard, Anal. Biochem., 208 (1993) 317.
[10] N.H.H. Heegaard and F.A. Robey, Anal. Chem., 64 (1992) 2479.
[11] N.H.H. Heegaard and F.A. Robey, J. Liq. Chromatogr., 16 (1993) 1923.
[12] N.H.H. Heegaard and F.A. Robey, J. Immunol. Methods, 166 (1993) 103.
[13] T. Duong, E.C. Pommier and A.B. Scheibel, Acta Neuropathol., 78 (1989) 429.
[14] A.D. Snow and T.N. Wight, Neurobiol. Aging, 10 (1989) 481.
[15] J. Emsley, H.E. White, B.P. O'Hara, G. Oliva, N. Srinivasan, I.J. Tickle, T.L. Blundell, M.B. Pepys and S.P. Wood, Nature, 367 (1994) 338.
[16] F. Prelli, M. Pras and B. Frangione, J. Biol. Chem., 260 (1985) 12895.
[17] F.A. Robey, K. Ohura, S. Futaki, N. Fujii, H. Yajima, N. Goldman, K.D. Jones and S. Wahl, J. Biol. Chem., 262 (1987) 7053.

[18] P. Landsmann, O. Rosen, M. Pontet, M. Pras, D. Levartowsky, E.G. Shephard and M. Fridkin, Eur. J. Biochem., 223 (1994) 805.

[19] S. Dhawan, R.L. Fields and F.A. Robey, Biochem. Biophys. Res. Commun., 171 (1990) 1284.

[20] P. Roepstorff, in A. Celis (Editor), Cell Biology: a Laboratory Handbook, Academic Press, Orlando, FL, 1994, p. 399.

[21] C.R.K. Hind, P.M. Collins, D. Renn, R.B. Cook, D. Caspi, M.L. Baltz and M.B. Pepys, J. Exp. Med., 159 (1984) 1058.

[22] H. Hamazaki, J. Biol. Chem., 262 (1987) 1456.

[23] S. Onishi, S. Maeda, K. Shimada and T. Arao, J. Biochem., 100 (1986) 849.

[24] N.H.H. Heegaard, J. Chromatogr. A, 680 (1994) 405.

[25] A.D. Cardin and H.J.R. Weintraub, Arteriosclerosis, 9 (1989) 21.

Low-molecular-mass RNA fingerprinting of bacteria by capillary electrophoresis using entangled polymer solutions

Eleftheria Katsivela*, Manfred G. Höfle

GBF—National Research Centre for Biotechnology, Division of Microbiology, Mascheroder Weg 1, D-38124 Braunschweig,
Germany

Abstract

Low-molecular-mass RNA (LMM RNA) fingerprinting uses the stable LMM RNA fraction (transfer RNA and 5S ribosomal RNA), with a size range of 70–135 nucleotides, from single bacterial strains for a genotypic identification and classification of bacteria. A novel application of capillary electrophoresis (CE) using entangled polymer solutions to separate LMM RNA to generate LMM RNA fingerprints was developed. Buffers containing 0.5% hydroxypropylmethylcellulose (HPMC) as sieving additive were employed to obtain improved peak resolution and good reproducibility. CE using 0.5% HPMC was suitable for routine analysis of LMM RNA, providing high resolution, reproducibility, system automation and high stability of the buffer. The relative standard deviation of the migration time for twenty successive runs was 0.5%. In addition, the variation of the resolution reproducibility of two separate buffer preparations was not greater than 5%. The limit of detection of RNA is ca. 0.02 μg per peak and separations can be performed using RNA samples as dilute as 10 μg/ml. One disadvantage of this system in the short lifetime of the capillary coating; DB-1 capillaries can be used for only 30–50 runs. LMM RNA fingerprints obtained with this system were compared with samples separated by polyacrylamide slab gel electrophoresis. The use of CE has the potential to provide a rapid and convenient way of identifying bacterial strains.

1. Introduction

The automation of conventional electrophoresis techniques is currently of great importance and interest owing to their universal use in a range of scientific applications. The classical manual separation methods applied in medical, molecular biological and genetic studies almost exclusively use slab polyacrylamide and agarose gel electrophoresis. Capillary electrophoresis (CE) employs the separation mechanisms of conventional electrophoresis in a capillary for-

mat and offers the possibility of quantitative analysis and automation. Recently, instead of classical electrophoresis, CE has been applied in many applications owing to its many advantages such as automated sample handling, reduced analysis time, improved on-line detectability without the need for staining procedures, small buffer requirements and samples and ease of use [1].

Initially, the use of capillary gel electrophoresis (CGE) was expected to offer a realistic alternative to the conventional slab gel electrophoresis [2–4]. Although excellent resolution has been demonstrated using CGE in the separation

---

* Corresponding author.

of DNA molecules and synthetic oligonucleo-
tides [2–4], the manipulations required to cast
gels in capillaries, the short capillary lifetimes
and their low reproducibility would appear to
limit the use of CGE for routine analysis.

In this respect, a possible alternative to CGE
employs the use of CE using entangled polymer
solutions [5–11]. The inclusion of linear poly-
mers in the separation electrolyte generates a
molecular sieving effect. The resolution of DNA
fragments in the example of ΦX-174 RF DNA/
HaeIII by CE using entangled polymer solutions
is comparable to that of CGE [10]. Additionally,
CE using entangled polymer solutions represents
a simple and inexpensive separation technique,
suitable for routine analysis, owing to replace-
able polymer separation matrices, and provides
reproducible separations on columns that are
easily refilled.

Many workers have reported the increasing
applicability of CE using entangled polymer
solutions for the analysis of synthetic oligonu-
cleotides, PCR products and DNA restriction
fragments [5–11]. Analysis of polymerase chain
reaction heteroduplex polymorphism [9] and
restriction fragment length polymorphism [10]
are carried out using this method as diagnostic
tools for clinical assays. Good results have also
been reported in the automated ribosomal DNA
fingerprinting of PCR products for taxonomic
studies of fungi [11].

We have previously reported [12] the sepa-
ration of low-molecular-mass (LMM) RNA by
CE using entangled polymer solutions. LMM
RNA profiling provides a genotypic fingerprint
technique for identifying bacteria [13]. This
technique is of particular importance for molecu-
lar ecology and taxonomic studies, and can also
be applied directly to analyses of environmental
samples [14]. This RNA fingerprinting method
uses the bacterial LMM RNA (small tRNAs,
large tRNAs and 5S rRNA in a size range
between 70 and 135 nucleotides), enabling
strains to be classified to the genus and species
level on the basis of species- and genus-specific
tRNA bands [13,15].

The standard established technique for LMM
RNA profiling employs slab polyacrylamide gel
electrophoresis (PAGE) using 55 cm length gels
with high resolution [15]. However, a more
rapid, automated technique is needed for LMM
RNA profiling in ecological studies. The use of
CE with 0.5% HPMC as sieving additive in
buffers resolved 5S rRNA and tRNAs, even
when they possessed only different secondary
structure or small differences in length (1–5
nucleotides) [12]. In order to determine the
reliability of this methodology, we investigated
the optimum conditions in terms of sample size,
detectability, reproducibility and stability of the
sieving buffer, as well as of the DB-1 capillaries.
We report on the first analysis of LMM RNA
fingerprints using a CE-based identification of
bacterial strains from different genera and we
compare them with LMM RNA fingerprints
obtained by conventional slab PAGE.

2. Experimental

2.1. Organisms and growth conditions

The following strains were obtained through
culture collections (listed as strain source and
catalogue number): *Alcaligenes eutrophus* DSM
531[T], *Hypomicrobium facilis* ATCC 27485[T],
Escherichia coli DSM 30083[T], *Pseudomonas
alcaligenes* LMG 1224[T] and *Pseudomonas
fluorescens* DSM 50090[T] (T = type strain of the
species). Strains were grown on relevant stan-
dard culture media, harvested by centrifugation
at 18 000 g for 5 min and stored at −20°C prior
to RNA extraction.

2.2. Materials

All chemicals were of analytical-reagent grade
or of high purity. All water used was ultra-pure,
doubly distilled and deionized. Tris(hydroxy-
methyl)aminomethane (Tris), ammonium per-
oxodisulphate and N,N,N′,N′-tetramethyl-
ethylenediamine (TEMED) were obtained from
Sigma (St. Louis, MO, USA). Acrylamide was
purchased from Amresco (Solon, OH, USA)
and 3-(trimethyoxysilyl)propylmethacrylate
(Bind Silane) from LKB (Bromma, Sweden).

Ethylenediaminetetraacetic acid (EDTA) and boric acid were obtained from Riedel-de Haën (Deelze, Germany). The polymer hydroxypropylmethylcellulose (HPMC), with a viscosity rating of 4000 cP for a 2% solution at 25°C, was obtained from Sigma.

A tRNA mixture from *Escherichia coli* MRE 600, containing 5S rRNA and tRNAs, was purchased from Boehringer (Mannheim, Germany). This tRNA mixture was used as a standard LMM RNA mixture.

Open-tubular capillaries coated with DB-1 were purchased from J&W Scientific (Folsom, CA, USA).

2.3. Equipment

A SpectraPhoresis 500 CE system (Spectra-Physics, Fremont, CA, USA) was used in the negative polarity mode (anode at the detection side) for all separations. Temperature control was achieved with a Peltier cooling system on the SpectraPhoresis 500. Electrokinetic injections were carried out for RNA-containing samples. The internal standard 2'-deoxyadenosine 5'-triphosphate (dATP) was injected hydrodynamically for 0.1 min in a double injection mode before sample injection. Nucleic acids were detected at 260 nm using a UV detector.

2.4. RNA extraction

Total RNA was extracted as described previously [15] from 10 mg of bacterial biomass (dry mass) with hot sodium dodecyl sulphate–phenol, purified in several steps and finally precipitated with ethanol.

2.5. Sample treatment

Crude extracts of total bacterial RNA were treated either by ultrafiltration or by Qiagen column chromatography for removal of large RNA fragments (16S rRNA and 23S rRNA) and other high-molecular-mass components (such as polysaccharides).

Ultrafiltration

Ultrafiltered samples were obtained by centrifugation at 6000 g for 35 min at 4°C in Centricon-100 concentrators (Amicon, Beverly, MA, USA) to remove the high-molecular-mass RNAs.

Qiagen column chromatography

Crude extracts containing 60 μg of total RNA were subjected to Qiagen column chromatography (Qiagen tip 20; Qiagen, Chatsworth, USA), as recommended by the manufacturer.

2.6. Capillary electrophoresis using entangled polymer solutions

DB-1 open-tubular capillaries, 70 cm long (62 cm effective length) × 100 μm I.D. with a coating of 0.1 μm dimethylpolysiloxane, were used without modification. DB-1 capillaries (70 cm) were filled automatically with the appropriate polymer sieving buffer for 20 min. Between runs, the capillaries were washed for 3 min at 60°C in the following sequence: water, methanol, 2-propanol, methanol, water. For monitoring the coating quality we have used the LMM RNA mixture from *E. coli* MRE 600. Depending on the conditions employed, capillaries were used for 30–50 runs.

The polymer sieving buffer contained 350 mM Tris–borate, 2 mM EDTA, 7 M urea (pH 8.6) and 0.5% (w/w) HPMC, prepared as reported previously [12].

RNA samples were prepared at a concentration of 100 μg/ml in 40 mM Tris–HCl buffer–1 mM EDTA (pH 5.0). Typically, the entire available volume of samples was 20 μl and many runs could be carried out. The crude extract (500 μg/ml) was five times more concentrated than the partially purified samples and was injected at −5 kV for 20 s. Partially purified samples were injected at −15 kV for 20 s at a concentration of 100 μg/ml. dATP was used as an internal standard for analysis of LMM RNA profiles. Before sample injection, the injection side of the capillary was washed twice with water for 0.1 min. All separations were performed at 20°C.

To determinate the electroendosmotic flow

(EOF), a neutral marker (0.5% mesityl oxide) was injected for 0.1 min hydrodynamically. The separation was carried out in the positive polarity model.

2.7. Conventional gel electrophoresis

Separation of LMM RNA was carried out under high power by denaturing PAGE [16]. Dried samples of LMM RNA (3 μg) were suspended in 4 μl of a loading solution (300 mg/ml sucrose, 460 mg/ml urea, 10 μl/ml 20% SDS, 1 mg/ml bromophenol blue, 1 mg/ml xylene cyanol, all substances dissolved in TBE buffer) and loaded on polyacrylamide gels {gel size 550 × 170 × 0.4 mm, 10% acrylamide [acrylamide–N,N-methylenebisacrylamide (28.8:1, w/w), 7 M urea, in TBE buffer [100 mM Tris–83 mM boric acid–1 mM EDTA (pH 8.5)]} that were bound to a carrier glass plate and run in a high-power electrophoresis unit (2010 Macrophor electrophoresis unit and 2297 Macrodrive 5 power supply; LKB–Pharmacia, Bromma, Sweden). Gels were run at 60°C and at constant power that was increased stepwise from 40 to 160 W during the 3-h run. RNA bands were revealed by a modified ammoniac silver staining procedure [15]. Gel scans were performed using a transmission densitometer (Elscript 400; Analysentechnik Hirschmann, Taufkirchen, Germany) at a wavelength of 546 nm. A detailed description of the conventional electrophoresis of LMM RNA has been given previously [15].

3. Results and discussion

3.1. Optimization of sample injection and detectability

To determine the optimum amount of LMM RNA that gives the best detectability using electrokinetic injection, a LMM RNA mixture from *E. coli* MRE 600 (1–100 μg/ml) was injected at either −10 kV for 15 s or −20 kV for 30 s and analysed using 0.5% HPMC sieving buffer in DB-1 capillaries. Compared with the classical gel electrophoresis method, electro-

kinetic injection uses relatively small amounts of sample. Sample loading is dependent on the electroosmotic flow, sample concentration and sample mobility. Variations in conductivity, which can be due to matrix effects, result in differences in voltage drop and amount loaded. In this experiment, we examined the response between sample concentration and peak area without considering the other factors mentioned above. Determination of the absolute amount of sample used for each run was not carried out. A linear relationship was obtained between peak area and sample concentration in the range 10–100 μg/ml RNA (Fig. 1A).

Using electrokinetic injection at −10 kV for 15 s, no distinct profile was produced at concentrations up to 10 μg/ml (Fig. 1B). Therefore, the injection parameters were altered to −20 kV for 30 s for low concentrations of LMM RNA in the range 5–10 μg/ml (Fig. 2). Additionally, the profile resolution using sample concentrations of 5 μg/ml was not satisfactory because of the high signal-to-noise ratio. Increasing the voltage and injection time (−30 kV for 30 s) did not improve the detectability of the RNA at concentrations lower than 5 μg/ml.

The limit of detection with injection at −20 kV for 30 s at the lowest detectable concentration (10 μg/ml) is ca. 0.02 μg of total RNA per peak (Fig. 2). However, concentrations between 20 and 50 μg/ml are recommended for good resolution with injection at −10 kV for 15 s. In comparison with CE, 2 μg of total RNA per sample are normally used in conventional slab gels per run. Hence CE is more sensitive than slab gel electrophoresis. A further increase in sensitivity could be obtained using fluorescence detection (limit of detection ca. 1 pg DNA per band), as often reported [8,17–19]. This could be of particular importance when analysing environmental samples that contain low concentrations of RNA.

3.2. Coating stability

The stability of the coating of DB-1 capillaries in CE using a sieving buffer containing 0.5%
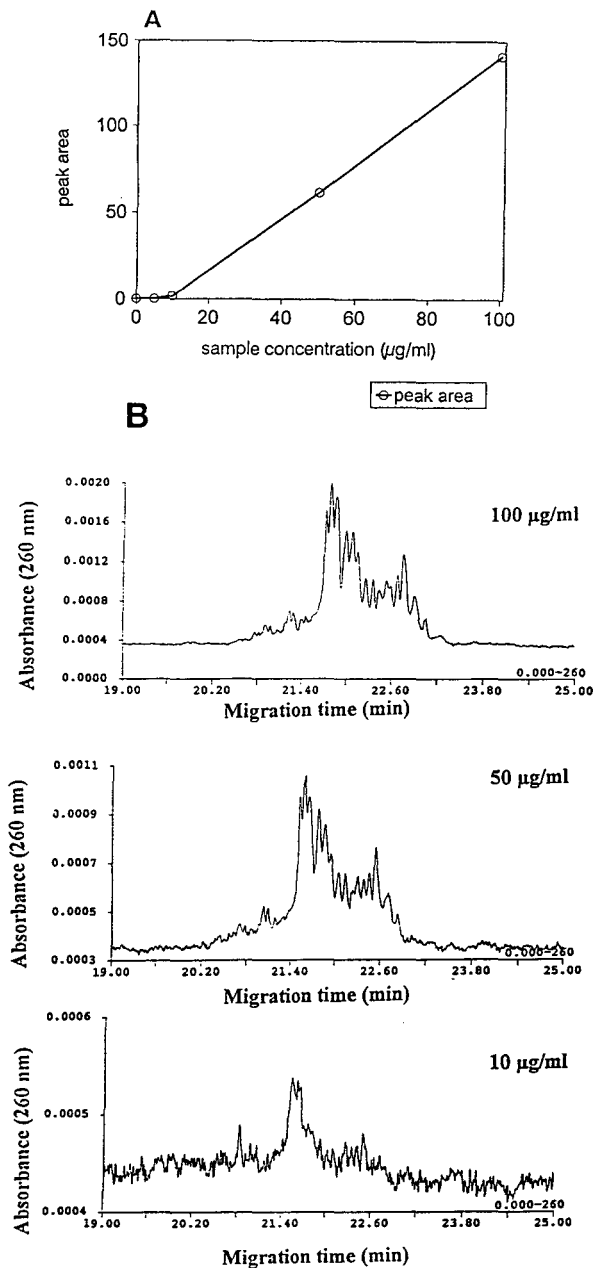
Fig. 1. (A) Sample concentration of LMM RNA plotted versus peak area. (B) Effect of total LMM RNA concentration on detectability of LMM RNA profiles analysed by CE using entangled polymer solutions. Sample, LMM RNA mixture from *E. coli* MRE 600; buffer, 350 m*M* Tris–borate–2 m*M* EDTA–7 *M* urea–0.5% HPMC (pH 8.6); capillary, DB-1, 70 cm (62 cm effective length) × 100 μm I.D., 0.1 μm thickness; injection, −10 kV, 15 s; field strength, 330 V/cm; detection, 260 nm.

HPMC was determined over the course of 150 runs using a standard LMM RNA mixture from *E. coli* MRE 600. Despite extensive washing (see Experimental) between runs, a gradual loss of resolution was observed in the LMM RNA profile. The first loss of resolution was observed (Fig. 3) after 50–70 successive runs and total loss after 150 successive runs and, despite extensive washing, regeneration of the column was not possible. In contrast to washing the capillary between runs, when the capillary was not washed the resolution decreased gradually up to 30–40 runs and then rapidly decreased, with a total irreversible loss of resolution occurring between 40 and 50 runs. Irreversible loss of resolution with DB-1 capillaries after 30–50 successive injections has also been reported in the separation of unpurified PCR products [11].

In contrast to samples containing complex RNA mixtures, samples with only one or two components (e.g., LMM RNAs or oligonucleotides) are well resolved, and for these small biomolecules (20–120 nucleotides long) a capillary could be used for over 150 injections (data not shown). However, the migration times of the components decreased and the relative standard deviations (R.S.D.s) increased with successive runs, indicating changes to the coating.

Similar results (not presented) were also obtained using other DB capillaries (DB-17, DB-Wax) that are coated with different phases relative to their matrix, polarity and hydrophobicity. These other DB capillaries produced LMM RNA profiles similar to that of DB-1, and a first loss of resolution was obtained after 50–70 successive runs in all cases.

Because none of the capillaries gave a detectable EOF (a measure of coating instability), even after 150 successive runs, the observed loss of resolution in the separation of LMM RNA profiles is presumably not dependent on coating deterioration or loosening from the capillary wall. Additionally, when negatively charged samples (such as RNA) are loaded, no detection should be possible when the column coating is detached or degraded owing to the negative polarity, suggesting that resolution is detrimentally affected, probably by the successive ac-

10 μg/ml

5 μg/ml
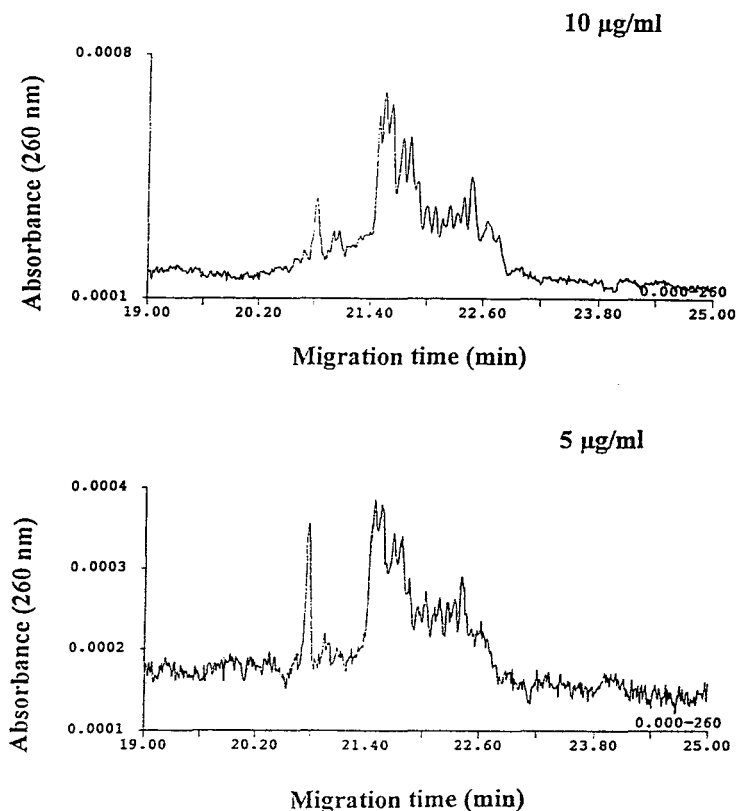
Fig. 2. Effect of total LMM RNA concentration on detectability of LMM RNA profiles analysed by CE using entangled polymer solutions fro the separation of the LMM RNA mixture from *E. coli* MRE 600. Injection, −20 kV, 30 s; other conditions as in Fig. 1.

cumulation of HPMC on the coated capillary wall.

The successive accumulation of HPMC was previously described by Bello et al. [20] as a "dynamic coating", a successive non-covalent coating of methylcellulose on the capillary wall of uncoated capillary columns. The polymer molecules in the layer of the "dynamic coating" near the capillary wall undergo an orientation or conformation change, which results in a reduced fluid viscosity in this region, relative to the bulk [20]. In the case of the DB-1-, DB-17- and DB-Wax-coated capillaries, a similar behaviour of "dynamic coating" may also be the cause of the progressive loss of resolution with each successive run, the possible decrease in polymer viscosity resulting in a decrease in the resistance

of the separated RNA molecules through the polymer network.

3.3. Reproducibility

In order to define the reproducibility of CE using entangled polymer solutions containing 0.5% HPMC in the separation of LMM RNA profiles, 55 successive runs were performed with a new DB-1 capillary. The reproducibility of relative migration time was determined by the migration times of the first and last peak of the standard LMM RNA mixture of *E. coli* MRE 600 (Fig. 4). The run-to-run reproducibility decreases with increasing run number. The R.S.D.s of the migration time of the first and last fragments were for 20 successive runs 0.51 and
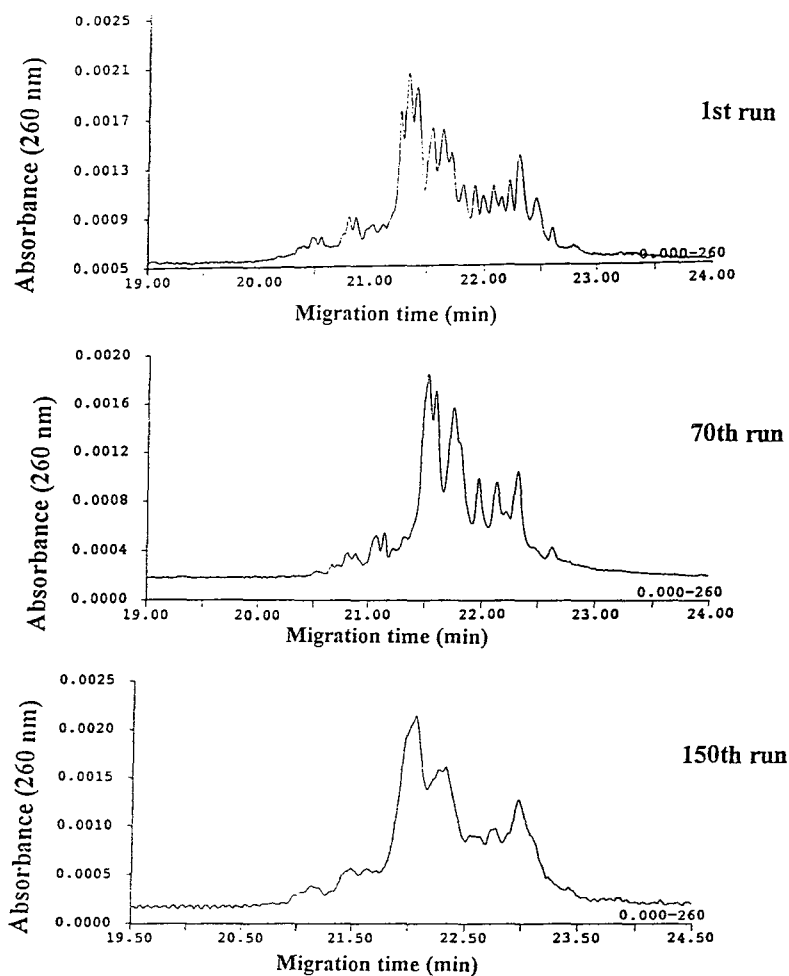
Fig. 3. Loss of resolution through capillary instability determined after 150 successive runs by CE using entangled polymer solutions. Sample, LMM RNA mixture from *E. coli* MRE 600 (100 µg/ml); conditions as in Fig. 1.

0.5%, for 30 runs 0.86 and 0.76% and for 55 runs 1.3 and 1.25% (Table 1). The loss of migration time reproducibility is consistent with the previously mentioned deterioration in coating stability with successive runs (see above).

3.4. Buffer stability and reproducibility in terms of profile resolution

Reproducibility in terms of profile resolution is paramount in separations of LMM RNA fingerprints because the primary goal is the identification of bacteria using a database. In order to

determine the reproducibility of buffer preparation in terms of profile resolution and migration time variation, two separate preparations of the 0.5% HPMC sieving buffer [HPMC (1) and HPMC (2); Fig. 5] were tested. The buffer reproducibility was determined for the separation of the LMM profile of *Pseudomonas alcaligenes* LMG 1224[T] over a period of 1 month during 30 runs. Runs were carried out daily using the same DB-1 capillary. In order to ensure coating stability, a new DB-1 capillary was used.

The stability of the resolution of the profiles was evaluated with software designed for capil-

A

number of runs

```
⊝ first peak
⊷ last peak
```

B

LMW RNA profile from E. coli MRE 600
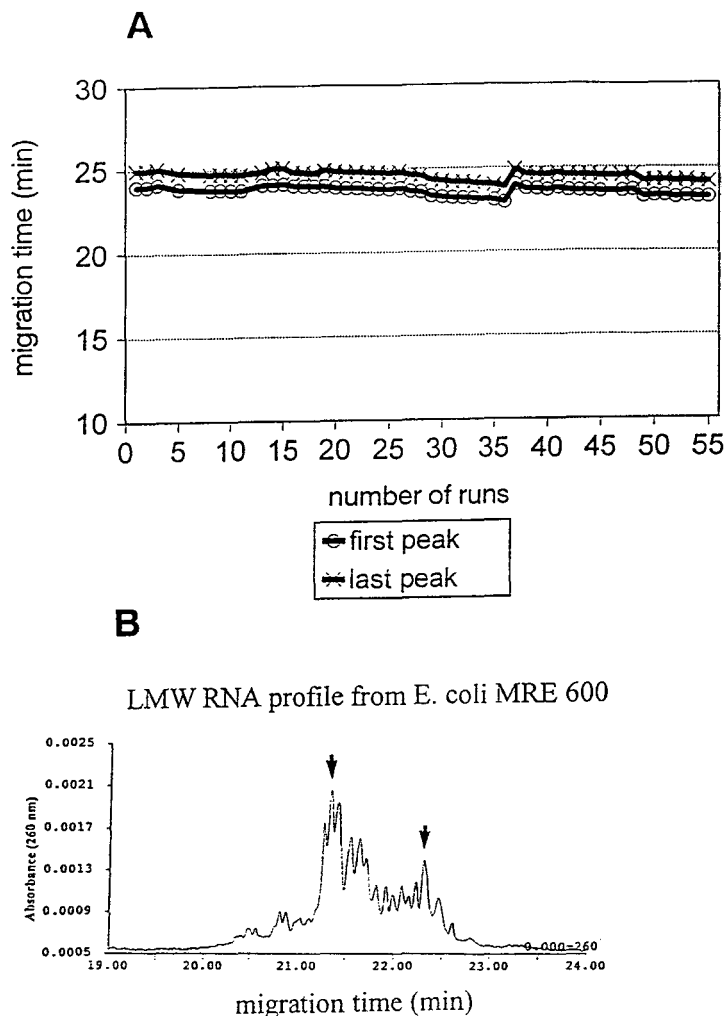
migration time (min)

Fig. 4. (A) Migration time reproducibility of two fragments [arrowed, see (B)] of the standard LMM RNA mixture from *E. coli* MRE 600 by CE using entangled polymer solutions. The mobility has not been corrected with an internal standard. Sample, 100 μg/ml; experimental conditions as in Fig. 1.

lary files (GelManager for CE files V.1.5; Bio-Systematica, Devon, UK). The CE files were imported into the GelManager software after conversion into ASCII files. Similarity of the profiles was calculated by the correlation of whole profiles by the Unweighted Pair Group Method Using Averages (UPGMA).

The 0.5% HPMC sieving buffer, prepared at different times over a 1-month period gives a high reproducibility with correlation coefficients in the range 0.94–1.0 between different runs with the same sample using the same capillary over a period of 1 month (Fig. 5). The correlation between two different buffer preparations is 0.94 by the second day after preparation and 1.00 by the 30th day after preparation (Fig. 5). Increasing storage of the 0.5% HPMC sieving buffer seems to reduce small differences in the

Table 1
Reproducibility of migration time of two peaks in the LMM RNA mixture from *E. coli* MRE 600 by capillary electrophoresis using entangled polymer solutions containing 0.5% HPMC as sieving additive

No. of runs	Migration time (min)	
	First peak	Last peak
1	23.98	24.95
5	23.85	24.81
10	23.78	24.74
15	24.12	25.09
20	23.89	24.86
Average	23.95	24.87
S.D.	0.123	0.125
R.S.D. (%)	0.51	0.50
25	23.75	24.73
30	23.29	24.26
Average	23.84	24.78
S.D.	0.205	0.189
R.S.D. (%)	0.86	0.76
35	23.08	23.99
40	23.65	24.56
45	23.56	24.50
50	23.28	24.21
55	23.21	24.14
Average	23.65	24.58
S.D.	0.312	0.308
R.S.D. (%)	1.3	1.25

Sample, 100 μg/ml; buffer, 350 mM Tris–borate–2 mM EDTA–7 M urea–0.5% HPMC (pH 8.6); capillary, DB-1, 70 cm (62 cm effective length) $\times$ 100 μm I.D., 0.1 μm thickness; injection, -10 kV, 15 s; field strength, 330 V/cm; detection, 260 nm.

resolution of separate buffer preparations. According to the instructions of the GelManager software program, the correlation values should be >0.95 between repeated runs with the same sample.

In addition, the R.S.D. of the migration times of the components of the same sample was in the range of 1.5–1.85% between two separately prepared buffers. The 0.5% HPMC sieving buffer seems to be reproducible in terms of profile resolution but with small variations in terms of migration times.

3.5. Sample preparation

The influence of sample preparation and purity of the extracts on the LMM RNA profile from *E. coli* DSM 30083[T] was investigated. Fig. 6 shows the profiles obtained from (A) crude extract, (B) an ultrafiltered sample and (C) a sample treated by Qiagen column chromatography. Profiles obtained from crude extracts or ultrafiltrated samples (Fig. 6A and B) do not show any major differences. However, the Qiagen-treated sample (Fig. 6C) shows some differences in resolution in terms of peak height and partial overlapping of peaks (Fig. 6C). The differences obtained may be due to the absence of some components in the Qiagen-treated sample that would otherwise influence the changes in conformation of the LMM RNA in the electric field and their interaction with the polymer network. In contrast, the same samples (crude extract, ultrafiltered and Qiagen-treated samples) when analysed by conventional gel electrophoresis did not show any differences in res-.olution (data not shown).

In summary, profiles produced from crude extracts and ultrafiltered samples could be obtained with high resolution using CE. However, the use of crude extracts could have an adverse effect on the coating lifetime because of the large RNA fragment (16S and 23S rRNA) present, or other impurities (e.g., polysaccharides).

3.6. Comparison of CE and slab PAGE using LMM RNA from bacteria of different genera

LMM RNA profiles of four type strains from different genera of bacteria belonging to three different subgroups of the Proteobacteria, *Alcaligenes* (beta), *Hyphomicrobium* (alpha), *Escherichia* (gamma) and *Pseudomonas* (gamma subgroup) were generated by CE using entangled polymer solutions (Fig. 7) and by slab PAGE (Fig. 8).

Consistent with a previous report [12], profiles generally produced by CE using entangled polymer solutions differed from those obtained by slab gel electrophoresis (compare Figs. 7 and 8). The differences between CE and conventional

Dendrogram of clustered pattern

0	0.1	0.2	0.3	0.4	0.5	0.6	0.7	0.8	0.9	1.0

0.5% HPMC (1)-2, 2nd day
0.5% HPMC (1)-1, 2nd day
0.5% HPMC (2), 2nd day
0.5% HPMC (2), 30th day
0.5% HPMC (1), 30th day
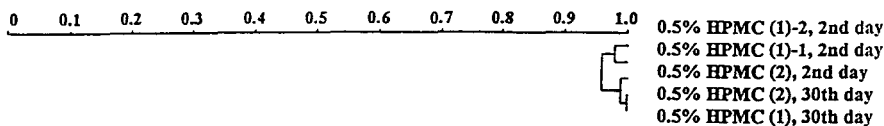
Correlation of profiles

0.5% HPMC (1)-2, 2nd day	100				
0.5% HPMC (2), 2nd day	96	100			
0.5% HPMC (1)-1, 2nd day	98	94	100		
0.5% HPMC (2), 30th day	96	99	95	100	
0.5% HPMC (1), 30th day	97	98	97	100	100

<u>*Sample:*</u> LMW RNA profile from *Ps. alcaligenes* t1 LMG 1224[T]
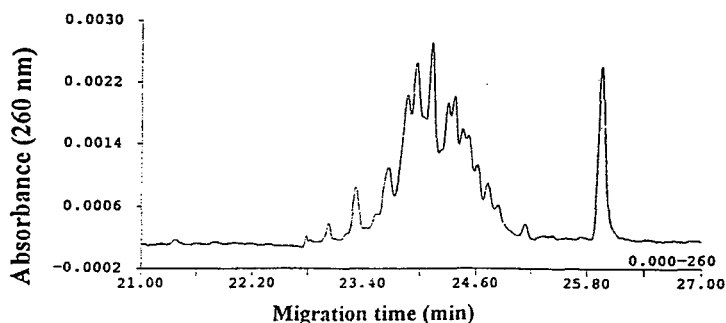
Fig. 5. Stability and reproducibility of the 0.5% HPMC polymer buffer over a period of 1 month in terms of profile resolution by the separation of LMM RNA profile from *Pseudomonas alcaligenes* LMG 1224[T]. Sample, 100 μg/ml; injection, −20 kV, 30 s; other conditions as in Fig. 1. Calculation of clusters and correlation of profiles using GelManager software. 0.5% HPMC (1) and (2), two separate buffer preparations; 0.5% HPMC (1)-1 and (1)-2, repeated runs with the same buffer preparation.

electrophoresis are expected, since conventional gel electrophoresis functions under denaturing conditions and separation is based on differences in size and charge, whereas in CE using entangled polymer solutions, electrophoresis is carried out under non-denaturing conditions and molecules are separated on the basis of size, spatial structure, changes in conformation and interactions with the polymer network [12,21]. One notable example is that, in contrast to PAGE, 5S rRNA molecules analysed by CE with the same length (120 nucleotides) from *E. coli* and *Ps. fluorescens* show different separation behaviours, probably because of their spatial structures and the interactions with the polymer network under the non-denaturing separation conditions.

In the RNA profiles produced by CE, 5S rRNA migrates very differently to the other tRNA molecules. Typically, for 5S rRNA, a distinguishable separation from other tRNA molecules is observed as a single peak (Fig. 7). This is not surprising, since in most bacteria only one kind of molecule is expected, and 5S rRNA molecules have a different size to the bulk of residual tRNA molecules in the cell of at least more than 10 nt [15].

In contrast to 5S rRNA, in any given strain,
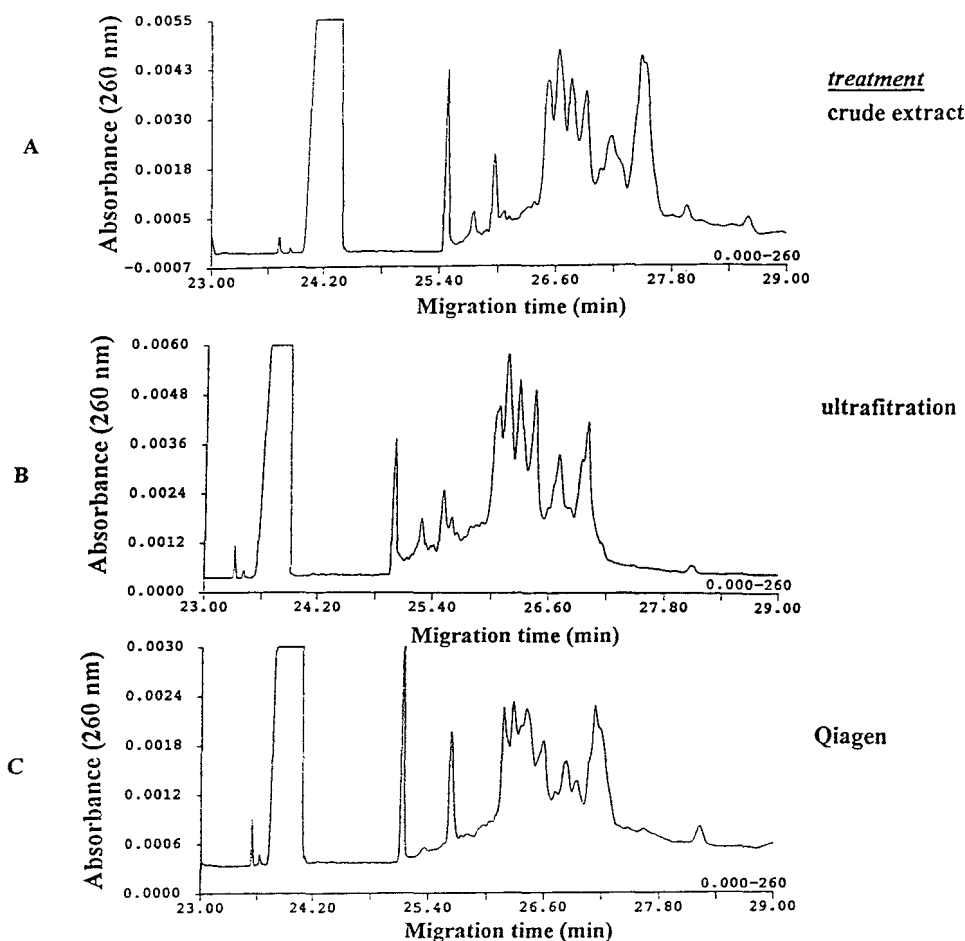
Fig. 6. Influence of sample treatment on LMM RNA profiles produced by CE using entangled polymer solutions. Sample, LMM RNA profile from *E. coli* DSM 30083[T]; (A) crude extract (500 μg/ml); (B) ultrafiltered sample (100 μg/ml); (C) Qiagen-treated sample (100 μg/ml). Injection, (A) −5 kV, 20 s; (B) and (C) −15 kV, 20 s. Other conditions as in Fig. 1.

tRNA constitutes a heterogeneous population (60 different tRNA molecules are possible) and, not surprisingly, CE produces a complex multipeak profile. However, there is not complete resolution of the different tRNA moities, probably owing to the tRNAs often having the same or similar nucleotide length.

Despite the differences in the way RNA is separated by CE and PAGE, there are some similarities in the profiles produced by these techniques, particularly for the 5S rRNA region. For example, the CE-separated profile of *H. facilis* exhibits a double band in the 5S rRNA region (Fig. 7) and this is also observed in the slab gel electrophoresis profile from *H. facilis* (Fig. 8).

Because the tRNA composition is individual for every bacterial strain [15], an analysis of a strain's tRNA composition can provide a fingerprint to aid in the identification of that strain. The tRNA analysis of four strains presented in Figs. 7 and 8 produced different tRNA profiles for each strain (fingerprints) by both conventional slab PAGE and CE. It is notable, however, that the CE-generated tRNA profiles (fingerprints) of the four strains are more dissimilar
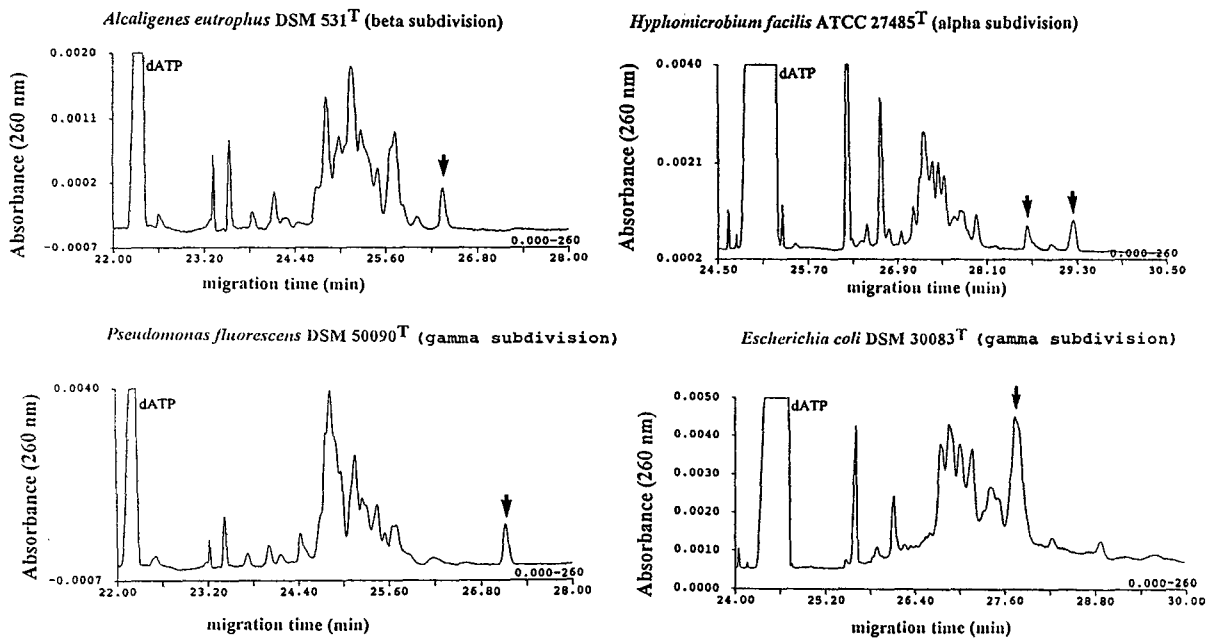
Fig. 7. CE-based LMM RNA fingerprints of bacteria from different genera. 5S rRNA peaks are arrowed. Experimental conditions as in Fig. 1.
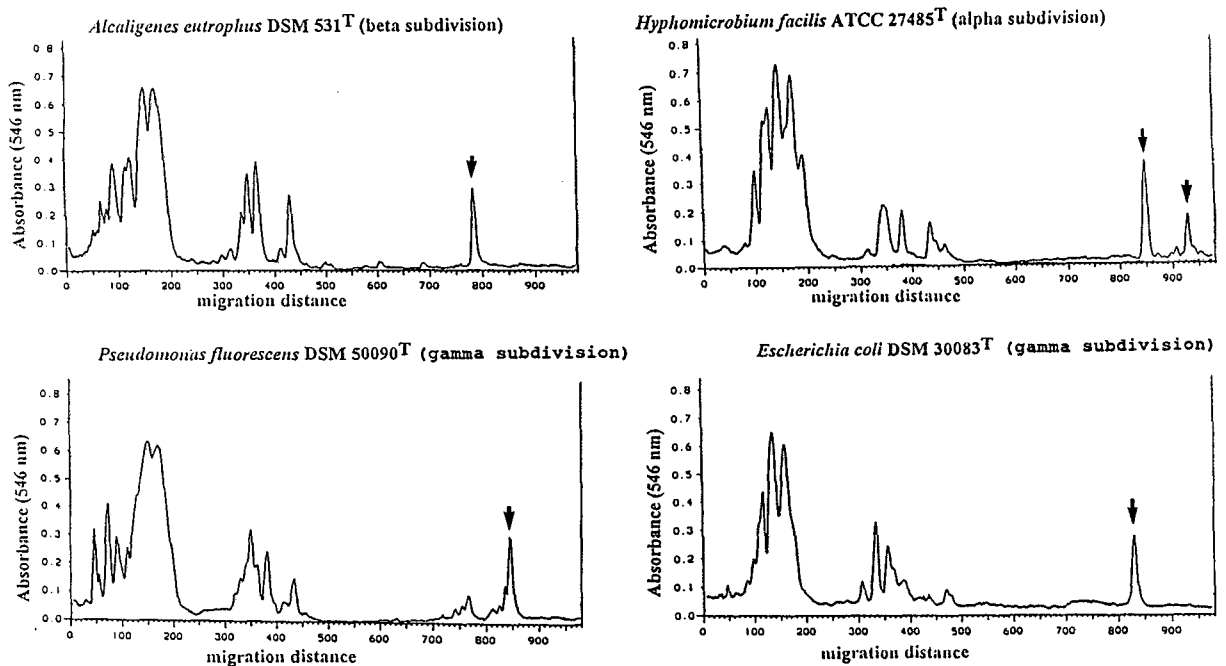
Fig. 8. Gel scans obtained from slab PAGE of LMM RNA fingerprints of bacteria from different genera. 5S rRNA peaks are arrowed.

than those produced by PAGE, indicating that CE is a more powerful means of distinguishing between individual strains.

Because CE using entangled polymers separates RNA molecules on the basis not only of size, but also other factors, such as spatial structure, this technique has potential advantages over PAGE in distinguishing similar strains that would have tRNA molecules of similar sizes. Additionally, the capacity of this technique to be automated lends itself to the analysis of a large number of strains, especially important in the field of ecology.

4. Conclusions

The use of CE with entangled polymer solutions represents an important technique for the rapid separation of bacterial LMM RNA producing a potentially useful genotypic fingerprint. These fingerprints may prove useful in the identification of single bacterial strains. CE generation of fingerprints offers a number of advantages over conventional PAGE techniques, including high sensitivity corresponding to very small sample size requirements (orders of magnitude less than conventional electrophoresis), good reproducibility, automated and easy handling, rapid run time (30 min) and on-line data collection. In addition to classical slab PAGE, CE using entangled polymer solutions can represent a convenient alternative method that uses non-denaturing separation conditions. The separation of the LMM RNA by CE is based on the size, the spatial structure, the changes in conformation of molecules and their interaction with the polymer network. Therefore, the profiles obtained by CE can give information additional to that obtained from conventional slab gel electrophoresis. In this context, the combined information from both methods could be of particular importance for future taxonomic studies.

Acknowledgements

References

[1] R. Kuhn and S. Hoffstetter-Kuhn (Editors), Capillary Electrophoresis: Principles and Practice, Springer, Berlin, 1993, p. 251.
[2] D.N. Heiger, A.S. Cohen and B.L. Karger, J. Chromatogr., 516 (1990) 33.
[3] A. Paulus, E. Gassmann and M.J. Field, Electrophoresis, 11 (1990) 702.
[4] J.A. Luckey and L.M. Smith, Electrophoresis, 14 (1993) 492.
[5] P.D. Grossman and D.S. Soane, J. Chromatogr., 559 (1991) 257.
[6] M.H. Kleemiss, M. Gilges and G. Schomburg, Electrophoresis, 14 (1993) 515.
[7] B.R. McCord, J.M. Jung and E.A. Holleran, J. Liq. Chromatogr., 16 (1993) 1963.
[8] S.M. Clark and R.A. Mathies, Anal. Biochem., 215 (1993) 163.
[9] J. Cheng, T. Kasuga, K.R. Mitchelson, E.R.T. Lightly, N.D. Watson, W.J. Martin and D. Atkinson, J. Chromatogr. A, 677 (1994) 169.
[10] K.J. Ulfelder, H.E. Schwartz, J.M. Hall and F.J. Sunzeri, Anal. Biochem., 200 (1992) 260.
[11] F. Martin, D. Vairelles and B. Henrion, Anal. Biochem., 214 (1993) 182.
[12] E. Katsivela and M.G. Höfle, J. Chromatogr. A, 700 (1995) 125.
[13] M.G. Höfle, Arch. Microbiol., 153 (1990) 299.
[14] M.G. Höfle, Appl. Environ. Microbiol., 58 (1992) 3387.
[15] M.G. Höfle, J. Microbiol. Methods, 8 (1988) 235.
[16] D. Rickwood and B.D. Hames (Editors), Gel Electrophoesis of Nucleic Acids, IRL Press Oxford, 1982, p. 1.
[17] H.E. Schwartz, K.J. Ulfelder, F.J. Sunzeri, M.P. Busch and R.G. Brownlee J. Chromatogr., 559 (1991) 267.
[18] P.D. Grossman, J. Chromatogr. A, 663 (1994) 219.
[19] B.R. McCord, D.L. McClure and J.M. Jung, J. Chromatogr. A, 652 (1993) 75.
[20] M.S. Bello, P. de Besi, R. Rezzonico, P.G. Righetti and E. Casiraghi, Electrophoresis, 15 (1994) 623.
[21] Y.C. Bae and D. Soane, J. Chromatogr. A, 652 (1993) 17.

Effect of the age of non-cross-linked polyacrylamide on the separation of DNA sequencing samples

Daniel Figeys, Norman J. Dovichi*

Department of Chemistry, University of Alberta, Edmonton, Alb. T6G 2G2, Canada

Abstract

Capillaries filled with non-cross-linked polyacrylamide and 7 M urea are stable for at least 4 months when stored at room temperature and exposed to the atmosphere. The stability of these capillaries when subjected to four successive DNA sequencing runs at an electric field of 300 V/cm was studied. Capillaries used the day after polymerization showed a dramatic increase in elution time with successive separations. Capillaries used at least 1 week after polymerization showed very reproducible elution times with successive separations. This effect was observed with capillaries where polymerization occurred in situ. Identical results were observed when poly-acrylamide was formed in an external vessel and the polymerized material was pumped into the capillary. In all cases, there was a gradual loss in resolution with successive separations; this loss of resolution was independent of the length of time since polymerization. Separations may be made successfully up to at least 115 days after polymerization for fragments less than 300 bases in length.

1. Introduction

Capillary electrophoresis has become a major analytical tool in the field of biological sample analysis. The high separation efficiency of and rapid separations by capillary electrophoresis are particularly powerful in the analysis of DNA sequencing samples [1–22].

Cross-linked polyacrylamide is used to obtain high-resolution separation of sequencing samples. Only a few reports are available on the effect of different parameters (%T, %C) on the separation of DNA [9,10,17]. Usually, only 2–3 separations can be performed on the same gel without a major change in the retention time or the occurrence of bubbles that damage the gel [14].

_____
* Corresponding author.

Non-cross-linked polyacrylamide has been used for the separation of DNA sequencing samples [12,15,20,22]. Non-cross-linked poly-acrylamide seems to be less affected by bubble formation than cross-linked polyacrylamide; however, the resolution obtained with non-cross-linked polyacrylamide is lower than that with cross-linked polyacrylamide [17]. At low concentrations, this material can be replaced in a capillary by applying a suitable pressure [23,24]. Refilling the capillary removes the step of realigning the system usually done when changing a capillary. However, after each refill, the capillary needs to be pre-run to remove unpoly-merized acrylamide and other small ions. This pre-run time depends on the viscosity of the polymer, and is typically 20–30 min for a 5 %T at 300 V/cm.

Fifty runs or more were reported with the

same capillary for samples consisting of double-stranded oligonucleotides [25–27]. However, there are only a few reports on multiple runs of DNA sequencing samples on the same capillary. Pentoney et al. [12] used 10 %T 7 M urea non-cross-linked polyacrylamide to perform 5–10 separations of DNA sequencing samples. To obtain useful separations, they had to trim 2 mm of the column a few minutes after each injection. This approach has also been used with cross-linked polyacrylamide to reduce the effect of bubbles at the injection end and to perform multiple runs [1,3,25]. Unfortunately, it appears difficult to automate this trimming procedure.

We have studied the effect of ionic depletion at the injection end of non-cross-linked polyacrylamide capillaries [28]. We noticed that the effect of ionic depletion decreases with older gels, which suggests that aged polyacrylamide may be more stable than freshly polymerized material for sequencing applications. In this paper, we describe DNA sequencing with non-cross-linked polyacrylamide (5 %T 7 M urea)-filled capillaries used up to 115 days after polymerization. The effects of the age of polyacrylamide on the separation of a DNA sequencing standard were analyzed.

2. Experimental

The Sequitherm Cycle Sequencing kit (Cedarlane Laboratories, Hornby, Canada) and the ΔTaq Cycle Sequencing kit (USB, Cleveland, OH, USA) were used to prepare sequencing samples of fluorescently labeled DNA. The kits' procedures for cycle sequencing were used with the following changes: ROX-labeled M13 universal (−21) primer (ABI, Foster City, CA, USA) was used with M13mp18 single-stranded DNA (USB). Samples were ddATP terminated. The samples were covered with mineral oil and heated for 5 min at 95°C. Cycle sequencing was performed using 30 cycles; each cycle consisting of 45 s at 95°C, 45 s at 47°C and 90 s at 70°C. Samples were precipitated with ethanol, washed and resuspended in 15–25 μl of formamide-

EDTA (49:1). Each sample was divided into 5–10 aliquots.

Non-cross-linked polyacrylamide (5 %T) was prepared by taking 1.25 ml of a 20% acrylamide (Bio-Rad, Richmond, CA, USA) stock solution, adding 1.0 ml of 5 × TBE buffer [2.7 g of Tris (ICN Biomedicals, Cleveland, OH, USA), 1.37 g of boric acid (BDH, Toronto, Ontario, Canada) and 1.0 ml of 0.5 M EDTA diluted to 50 ml in deionized, filtered water)] and 2.1 g of urea (Gibco BRL, Gaithersburg, MD, USA), and diluting the solution to 5.0 ml with deionized, filtered water. This solution was degassed for at least 20 min by bubbling argon gas through it. The polymerization reaction was initiated and catalyzed by adding 2 μl of N,N,N′,N′-tetramethylethylenediamine (TEMED) (Gibco BRL) and 20 μl of 10% ammonium peroxodisulfate (Boehringer Mannheim, Indianapolis, IN, USA). For in situ polymerization, immediately following the addition of initiators, the solution was injected into fused-silica capillaries (Polymicro Technologies, Phoenix, AZ, USA) with typical dimensions of 33 cm × 32 μm I.D. × 143 μm O.D. Capillaries were pretreated for 1 h with a silanizing solution. This solution was freshly prepared by mixing 0.5 ml of water, 0.5 ml of glacial acetic acid and 20 μl of γ-methacryloxypropyltrimethoxysilane (Sigma, St. Louis, MO, USA). All chemicals were of electrophoretic grade. The day of preparation was taken as day zero. Non-cross-linked polyacrylamide-filled capillaries older than day zero were left to age on the bench and trimmed before use.

For capillaries that were refilled with polyacrylamide, the polymerization occurred in a disposable centrifuge tube. On the day of analysis, the polymerized material was pumped into a capillary using a gas–tight syringe and a locally constructed connector.

The capillary electrophoresis system and fluorescence detection system used for these experiments were an in-house design [6,17]. The high-voltage power supply used in this experiment was a Spellman (Plainview, NY, USA) CZE1000R. Fluorescence was excited with a yellow (8 mW, $\lambda = 594$ nm) He–Ne laser (PMS, Electro-Optics, Boulder, CO, USA). Fluores-

cence was collected at right-angles to the laser beam with a 125 × microscope objective (Leitz, Weizlar, Germany). The fluorescence was imaged on to an iris, passed through a 630DF30 band pass filter (Omega Optical, Brattleboro, VT, USA) and detected with an R1477 photomultiplier tube (Hamamatsu, Middlesex, NJ, USA).

3. Results and discussion

Separation of sequencing samples was performed on non-cross-linked polyacrylamide-filled capillaries from 1 to 115 days after polymerization. Fig. 1 presents four subsequent sequencing runs done on a 1-day-old non-cross-linked

Fig. 1. Four subsequent separations of M13mp18 ddATP-terminated sequencing samples at −300 V/cm on a 35 cm long capillary filled with 1-day-old non-cross-linked polyacrylamide. The same, arbitrary, intensity scale was used for all runs. Fragments 91, 109–111 and 164–166 bases in length are noted.

polyacrylamide-filled capillary at −300 V/cm. The migration times increased from run to run; from the first to the fourth run, the migration time for base 91 increased from 23.7 to 39.4 min (66% increase in retention time), and the migration time for base 252 moved from 43.3 to 70.8 min (63% increase in retention time). Also, the peak heights decreased by a factor of 10 after four sequencing runs, despite the use of a fresh sample for each run. At the same time, the current in the capillary decreased from 1.21 μA for the first run to 0.70 μA for the fourth sequencing run.

The decrease in current is due to depletion of ions at the injection end [28]. This depletion of ions causes a localized increase in the electric field near the injection end, and a decrease of the electric field in the rest of the capillary. In addition, this depletion of ions extends further into the capillary with time, thus increasing the asymmetry of the electric field in the capillary. Depletion of ions causes the migration times to increase from run to run and also decreases the amount of sample loaded on to the capillary. Depletion of ions has been described by various workers for conventional slab gel experiments [29–34].

Fig. 2 presents separations performed with a capillary used 20 days after polymerization. After four runs, the migration time for base 91 changes from 22.2 to 22.3 min (0.04% increase in retention time), and for base 252 from 38.9 to 39.1 min (0.6% increase in retention time). The current was consistently 1.55 μA for the four runs. The peak heights change by less than 10%. While we have noted earlier the current stability for aged polyacrylamide capillaries [28], this is the first observation of highly stable migration times in aged non-cross-linked polyacrylamide capillaries.

The improved stability of polyacrylamide with age was also noticed in a different set of experiments, in which the polyacrylamide was polymerized in an external vessel and then pumped into the capillary. A capillary was refilled with a 1-day-old non-cross-linked polyacrylamide and three subsequent sequencing runs were performed (Fig. 3). The change in migration time is
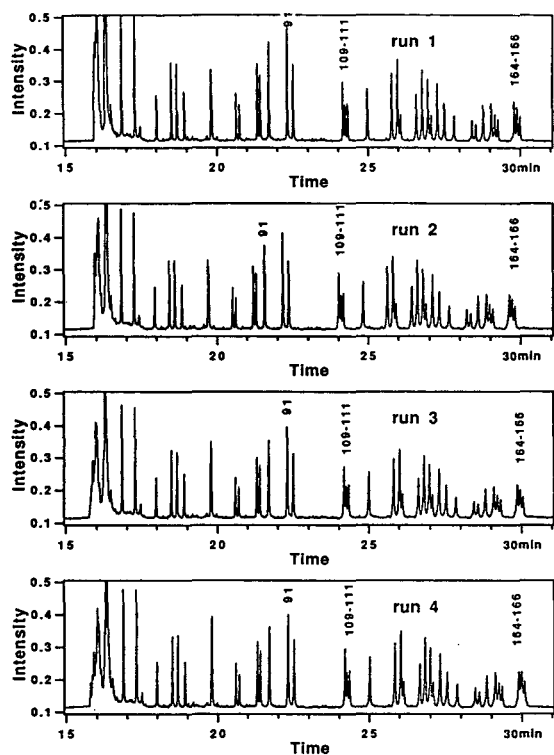
Fig. 2. Four subsequent separations of M13mp18 ddATP-terminated sequencing samples at −300 V/cm on a 32.1 cm long capillary filled with 20-day-old non-cross-linked polyacrylamide.

Fig. 3. Three subsequent separations of M13mp18 ddATP-terminated sequencing sample at −300 V/cm on a 36 cm long capillary. The capillary was filled with 1-day-old non-cross-linked polyacrylamide before the first run, using a gas-tight syringe.

similar to Fig. 1. When the capillary was refilled with a 20-day-old non-cross-linked polyacrylamide and four subsequent sequencing runs were performed (Fig. 4), the migration time was stable to 5% R.S.D. These results indicate that the change in the migration times with age is not due to a problem with the capillary wall. Instead, the change in migration time is due to changes in the properties of aging polyacrylamide.

Migration times were measured for bases 91 and 252 for capillaries ranging from 1 to 115 days old. Four successive runs were performed on each capillary. For non-cross-linked polyacrylamide less than about 2 days old, the mobilities (Fig. 5), there was a decrease by 40% for base 91 and 39% for base 252 from the first to the fourth sequencing run. In the case of non-cross-linked polyacrylamide 7 to 34 days old, the mobilities decreased by an average of

6.2% for base 91 and 4.5% for base 252 from the first to the fourth run. In the case of the 115-day-old non-cross-linked polyacrylamide-filled capillary, the mobilities increased by 29% for base 91 and 35% for base 252 from the first to the fourth run.

There was no detectable electro-osmosis in these capillaries. Because of the design of our system, any electro-osmotic pumping will displace the polyacrylamide matrix into the path of the laser beam of our detector. No such displacement was noted in any of our experiments.

A non-linear least-squares routine was used to fit a four-parameter Gaussian function to the peaks. From the values of migration time and peak width, the resolution, R, is calculated for peaks separated by a single base. The resolution (Fig. 6) for any particular run was weakly dependent on the age of the capillary; however, the resolution decreased significantly with the number of sequencing runs. This decrease could be caused by a decrease in peak spacing and/or an increase in peak width from run to run. Mobility, and hence peak spacing, are stable
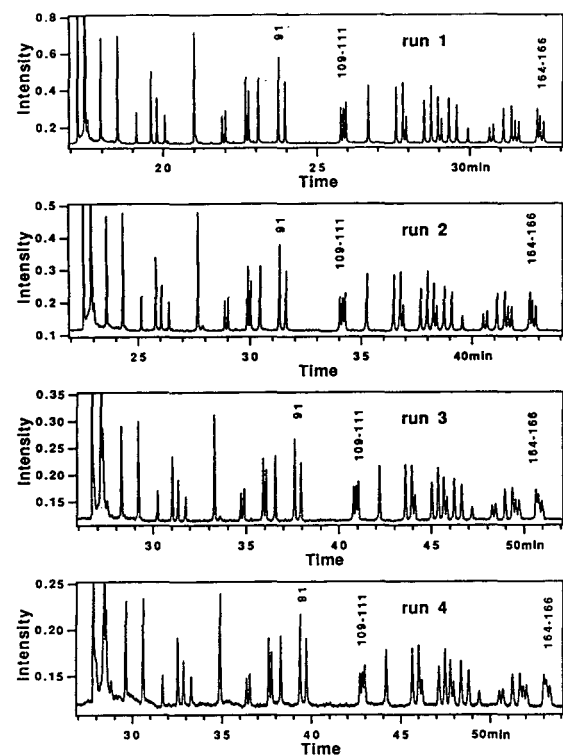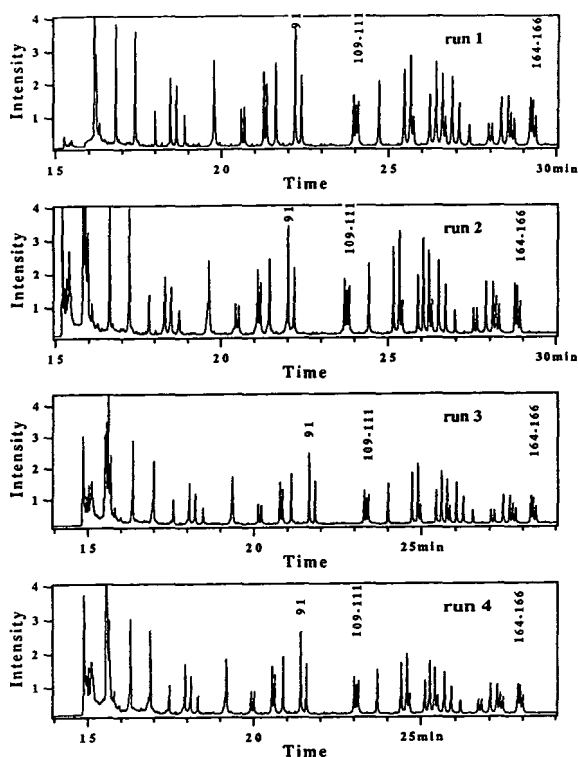
Fig. 4. Four subsequent separations of M13mp18 ddATP-terminated sequencing sample at −300 V/cm on a 36 cm long capillary. The capillary was filled with 20-day-old non-cross-linked polyacrylamide before the first run, using a gas-tight syringe.

Fig. 5. Mobilities for bases 91 and 252 versus the age of non-cross-linked polyacrylamide for four subsequent sequencing runs. The run number is indicated beside each line.

within the four runs for most of the different ages of non-cross-linked polyacrylamide; however, in the case of the 115-day-old non-cross-linked polyacrylamide, there is a decrease in peak spacing from the sequencing run one to four, and in the case of capillaries less than 2 days old, there is an increase in peak spacing from the sequencing run one to four.

Fig. 7 shows the number of theoretical plates for base 91 versus the age of non-cross-linked polyacrylamide. In all cases, except for the 115-day-old polyacrylamide, the plate count decreases from run to run. In the case of fresh non-cross-linked polyacrylamide (less than about 2 days old), the migration time increases by 66% and the peak widths increase by 200%, resulting in a decrease by a factor of three in the number of theoretical plates from the first to the fourth

sequencing run. Non-cross-linked polyacrylamide between 6 and 34 days old has migration times that increase by an average of 8% and peak widths that increase by 70%. This results in a decrease by a factor of 2.5 in the number of theoretical plates. Finally, in the case of the 115-day-old non-cross-linked polyacrylamide, the migration times decrease by an average of 25% and the peak widths increase by 1%, resulting in a decrease by a factor of 1.8 in the number of theoretical plates.

4. Conclusion

Non-cross-linked polyacrylamide can be used to perform subsequent sequencing runs on the same capillary if the non-cross-linked poly-
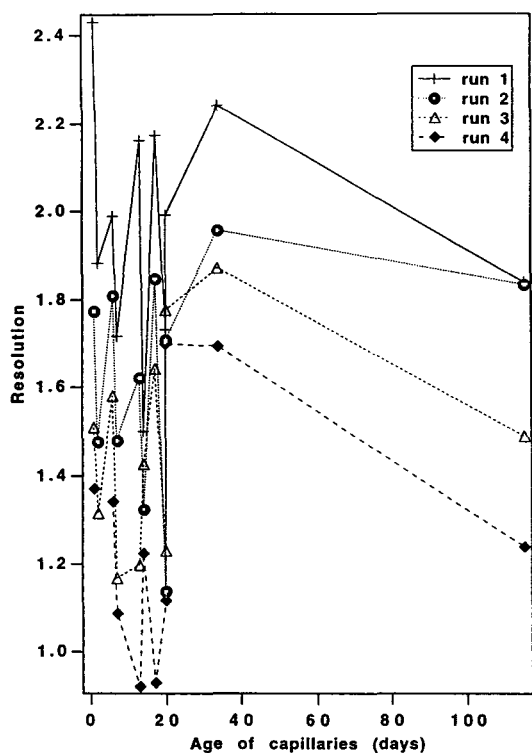
Fig. 6. Resolution for base 91-2 versus the age of non-cross-linked polyacrylamide for four subsequent sequencing runs. The run number is indicated beside each line.

Fig. 7. Theoretical plates for base 91 versus age of poly-acrylamide for four subsequent sequencing runs. The run number is indicated beside each line.

acrylamide is aged properly before use. This behavior occurs whether polymerization is performed in situ or if polymerization occurs in an external vessel and the polymerized material is pumped into the capillary. The migration times for aged non-cross-linked polyacrylamide change by less than 8% for base 91 and 5.5% for base 252 within four sequencing runs. Sufficient resolution was obtained for DNA sequence determination for fragments less than 300 bases in length for at least four sequencing runs and for capillaries containing polyacrylamide that was used at least 2 weeks after polymerization. This sequence read length is similar to that observed earlier at 300 V/cm; we have demonstrated that operation of these capillaries at lower electric fields leads to longer sequencing read length.

In an accompanying paper [35], we describe how aged non-cross-linked polyacrylamide may be used to obtain many separations of sequencing samples. This approach requires the minimization of template concentration in the sequencing sample, the use of aged polyacrylamide and the reversal of the electric field between separations to relax ionic depletion at the injection end of the capillary.

Acknowledgements

References

[1] H. Swerdlow and R. Gesteland, Nucleic Acids Res., 18 (1990) 1415.

[2] H. Drossman, J.A. Luckey, A.J. Kostichka, J. D'Cunha and L.M. Smith, Anal. Chem., 62 (1990) 900.

[3] A.S. Cohen, D.R. Najarian and B.L. Karger, J. Chromatogr., 516 (1990) 49.

[4] H. Swerdlow, S. Wu, H. Harke and N.J. Dovichi, J. Chromatogr., 516 (1990) 61.

[5] J.A. Luckey, H. Drossman, A.J. Kostichka, D.A. Mead, J. D'Cunha, T.B. Norris and L.M. Smith, Nucleic Acids Res., 18 (1990) 4417.

[6] D.Y. Chen, H.P. Swerdlow, H.R. Harke, J.Z. Zhang and N.J. Dovichi, J. Chromatogr., 559 (1991) 237.

[7] A.E. Karger, J.M. Harris and R.F. Gesteland, Nucleic Acids Res., 19 (1991) 4955.

[8] H. Swerdlow, J.Z. Zhang, D.Y. Chen, H.R. Harke, R. Grey, S. Wu, N.J. Dovichi and C. Fuller, Anal. Chem., 63 (1991) 2835.

[9] H.R. Harke, S. Bay, J.Z. Zhang, M.J. Rocheleau and N.J. Dovichi, J. Chromatogr., 608 (1992) 143.

[10] M.J. Rocheleau and N.J. Dovichi, J. Microcol. Sep., 4 (1992) 449.

[11] D.Y. Chen, H.R. Harke and N.J. Dovichi, Nucleic Acids Res., 20 (1992) 4873.

[12] S.L. Pentoney, K.D. Konrad and W. Kaye, Electrophoresis, 13 (1992) 467.

[13] X.C. Huang, M.A. Quesada and R.A. Mathies, Anal. Chem., 64 (1992) 2149.

[14] H. Swerdlow, K.E. Dew-Jager, K. Brady, R. Grey, N.J. Dovichi and R. Gesteland, Electrophoresis, 13 (1992) 475.

[15] M.C. Ruiz-Martinez, J. Berka A. Belenkii, F. Foret, A.W. Miller and B.L. Karger, Anal. Chem., 65 (1993) 2851.

[16] N.J. Dovichi, in J.P. Landers (Editor), Handbook of Capillary Electrophoresis, CRC Press, Boca Raton, FL, 1993, Ch. 14.

[17] D. Figeys and N.J. Dovichi, J. Chromatogr., 645 (1993) 311.

[18] S. Bay, H. Starke, J.Z. Zhang, J.F. Elliott, L.D. Coulson and N.J. Dovichi, J. Capillary Electrophoresis, 1 (1994) 121.

[19] H.R. Starke, J.Y. Yan, J.Z. Zhang, K. Muhlegger and N.J. Dovichi, Nucleic Acids Res., 22 (1994) 3997.

[20] N. Best, E. Arriaga, D.Y. Chen and N.J. Dovichi, Anal. Chem. 66 (1994) 4063.

[21] H. Lu, E. Arriaga, D.Y. Chen, H. Starke and N.J. Dovichi, J. Chromatogr., 680 (1994) 497.

[22] N. Chen, T. Manabe, S. Terabe, M. Yohda and I. Endo, J. Microcol. Sep., 6 (1994) 539.

[23] J. Sudor, F. Foret and P. Bocek, Electrophoresis, 12 (1991) 1056.

[24] M. Chiari, M. Nesi, M. Fazio and P.G. Righetti, Electrophoresis, 13 (1992) 690.

[25] Y. Baba, T. Matsuura, K. Wakamoto, Y. Morita, Y. Nishitsu and M. Tsuhako, Anal. Chem., 64 (1992) 1221.

[26] Y. Baba, T. Matsuura, K. Wakamoto and M. Tsuhako, Chem. Lett., (1991) 371.

[27] A. Guttman, B. Wanders and N. Cooke, Anal. Chem., 64 (1992) 2348.

[28] D. Figeys, A. Renborg and N.J. Dovichi, Electrophoresis, in press.

[29] M. Spencer, Electrophoresis, 4 (1983) 36.

[30] M. Spencer, Electrophoresis, 4 (1983) 41.

[31] M. Spencer, Electrophoresis, 4 (1983) 46.

[32] G.W. Slater, P. Mayer and G. Drouin, Analusis Mag., 21 (1993) M25.

[33] G.W. Slater, P. Mayer and G. Drouin, Electrophoresis, 14 (1993) 962.

[34] Y. Seida, Y. Nakano, J. Chem. Eng. Jpn., 24 (1991) 755.

[35] D. Figeys and N.J. Dovichi, J. Chromatogr. A, 717 (1995) 113.

Multiple separations of DNA sequencing fragments with a non-cross-linked polyacrylamide-filled capillary: capillary electrophoresis at 300 V/cm

Daniel Figeys, Norman J. Dovichi*

Department of Chemistry, University of Alberta, Edmonton, Alb. T6G 2G2, Canada

Abstract

The use of non-cross-linked polyacrylamide for multiple DNA sequencing runs on the same capillary is demonstrated. To minimize template loading, cycle sequencing was used to prepare fluorescently labeled samples. To minimize ion depletion, the current was reversed for several minutes between runs. To achieve stable operation, non-cross-linked polyacrylamide was aged for several days before use. This procedure allowed the successful generation of at least nineteen sequencing runs from the same capillary without replacement of the polyacrylamide and without trimming of the capillary tip. These separations were performed at an electric field of 300 V/cm.

1. Introduction

Non-cross-linked polyacrylamide is a useful medium for DNA sequencing by capillary electrophoresis. The material has been used to separate DNA sequencing fragments over 500 bases in length. An important issue in DNA sequencing is repeated separations in the same capillary; replacement of the capillary can require a tedious realignment step. While replacement of the separation medium is possible, it requires relatively high pressures, which is not convenient in certain situations [1].

The same capillary can be used for replicate analysis of synthetic DNA standards and restriction fragment digests in non-cross-linked polyacrylamide-filled capillaries [2]. However, replicate injections of DNA sequencing fragments have not proved successful; either the capillary performance degrades unacceptably or a portion of the capillary tip must be trimmed after each injection [3,4]. On the other hand, freshly prepared capillaries can separate sequencing fragment much longer than 500 bases in length when operated in a pristine condition [5,6].

It appears that two phenomena are important in limiting re-use of the capillary. First, depletion of ions from the injection tip of the capillary is caused by the mismatch in transport numbers across the buffer–polyacrylamide interface [7,8]. This ionic depletion leads to a large current drop at the injection tip, which leads to damage of the material. Second, the large template migrates with relatively low mobility. Conventional sequencing protocols generate at most one sequencing fragment per template molecule; as a result, the template is present in higher concentration than all sequencing fragments combined. This high concentration, along with the

---

* Corresponding author.

low mobility but high charge of the template, probably leads to gel damage at the injection tip of the capillary.

One simple solution to polyacrylamide degradation is found by replacing the separation medium after each run. Low-concentration non-cross-linked polyacrylamide can be replaced by pumping the material from the capillary. However, pumping the material requires high pressures, particularly when dealing with capillaries of small inner diameter [1]. Further, it is common to apply an electric field across the separation medium before operation to flush small ions from the capillary; this pre-electrophoresis run can account for a significant fraction of the time necessary for separation, leading to an undesirable extension of the analysis time.

Rather than replacing the separation medium, this paper reports repeated separations of DNA sequencing fragments without replacement of the separation medium. Successful re-use of a capillary relies on three steps. First, as noted in a companion paper [9], it is necessary to use polyacrylamide several days after polymerization; freshly prepared material leads to an unacceptable decrease in migration time reproducibility. Second, we rely on cycle sequencing for sample preparation. In cycle sequencing, thermal cycling allows repeated generation of sequencing fragments from the same template. This procedure is a variant of the polymerase chain reaction that produces a linear increase in sequencing template with the number of cycles. As a result, much less template is loaded on to the capillary. Third, we reverse the polarity of the electric field for a few minutes between each run. This field reversal decreases ionic depletion, yielding a homogeneous electric field in the capillary and more reproducible migration times for the sequencing fragments.

2. Experimental

The instrument and sample preparation method have been described in a companion paper [9]. The capillary used for this experiment had aged for 3 days before use.

3. Results and discussion

As noted [9], non-cross-linked polyacrylamide more than a few days old generates reproducible retention times for four subsequent injections. However, after more injections there is a gradual loss of current in the capillaries, presumably due to depletion of ions from the injection tip of the capillary. To decrease the effect of the depletion of ions, we reversed the electric field between each sequencing run. This voltage reversal allowed the depleted ions at the injection end to recover. The polarity was reversed for 10–20 min at +400 V/cm between each run. Up to 0.4 μA in current was recovered by this technique. Reversing the polarity was previously proposed by Swerdlow et al. [7] to eliminate the plugging of the gel pores by the DNA template.

To generate samples with low amounts of template, cycle sequencing was used. Fig. 1
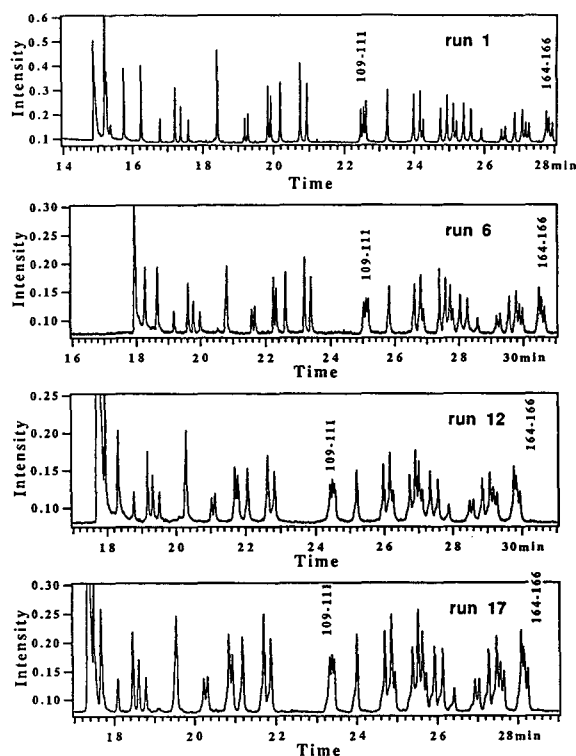
Fig. 1. Multiple runs of DNA sequencing samples on the same capillary at −3000 V/cm. The samples were prepared from M13mp18 and terminated with ddATP.

shows the sequence from the primer up to base 166 for runs 1, 6, 12 and 17 on the same capillary. By reversing the polarity between runs, a total of nineteen sequential runs were obtained on the same capillary without refilling the capillary. The mobility increases and the resolution decreases from the first to the last run; however, acceptable resolution remains even after nineteen runs.

Fig. 2 shows the change in current versus the run number. There is still a slight decrease in current (from 1.49 to 1.29 μA), which is not compensated for by reversing the polarity. This current drop could be due to incomplete deplugging of the pore. These experiments were performed over a 3-day period; an increase in current from run 7 to 8 and run 13 to 14 occurred during the overnight rest between these runs.

Fig. 3 shows the change in mobility versus the run number. The relative standard deviation of the mobility ranges from 3% to 6% for base 91 to base 350. Thus, the mobility of the sequencing samples is fairly stable within nineteen runs.

The peaks for bases 91, 142, 252 and 350 were

Fig. 3. Mobility versus number of runs for different peaks.

fitted with a Gaussian model. Fig. 4 shows the resolution for adjacent bases versus number of runs. The main decrease in the resolution occurs in the first four runs; however, after nineteen runs, the resolution had dropped by only a factor of two compared with a pristine capillary. We believe that the general decrease in resolution with increasing fragment length is associated with the effects of biased reptation [10]; operation of the capillary at lower electric field reduces this effect, generating longer sequencing reads [5]. The general loss of resolution with replicate runs must be associated with a change in the physical make-up of the non-cross-linked polyacrylamide. In principle, damage to the matrix could result in the formation of channels within the polymer, which leads to a band broadening mechanism that is similar to eddy diffusion in chromatography.

4. Conclusion

We have shown that it is possible to perform multiple separations of DNA sequencing samples

Fig. 2. Current versus number of runs.
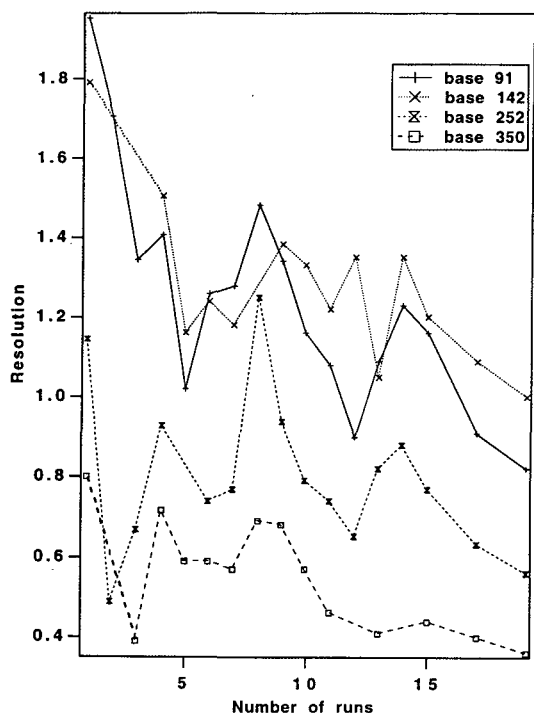
Fig. 4. Resolution versus number of runs for different peaks.

on the same capillary without replacing the separation medium. Up to nineteen sequential runs were obtained on the same capillary; this number of replicate analyses was limited by the operator's patience and not by failure of the separation medium; it appears that non-cross-linked polyacrylamide may be re-used virtually indefinitely. As a result, the tedious replacement of separation medium between runs may be eliminated, which will speed up large-scale sequencing efforts.

Acknowledgments

References

[1] M. Chiari, M. Nesi, M. Fazio, M. and P.G. Righetti, Electrophoresis, 13 (1992) 690–697.
[2] Y. Baba, T. Matsuura, K. Wakamoto, Y. Morita, Y. Nishitsu and M. Tsuhako, Anal. Chem., 64 (1992) 1221–1225.
[3] M.C. Ruiz-Martinez, J. Berka A. Belenkii, F. Foret, A.W. Miller and B.L. Karger, Anal. Chem., 65 (1993) 2851.
[4] S.L. Pentoney, K.D. Konrad and W. Kaye, Electrophoresis, 13 (1992) 467.
[5] N. Best, E. Arriaga, D.Y. Chen and N.J. Dovichi, Anal. Chem., 66 (1994) 4063–4067.
[6] N. Chen, T. Manabe, S. Terabe, M. Yohda and I. Endo, J. Microcol. Sep., 6 (1994) 539–543.
[7] H. Swerdlow, K.E. Dew-Jager, K. Brady, R. Grey, N.J. Dovichi and R. Gesteland, Electrophoresis, 13 (1992) 475–483.
[8] D. Figeys, A. Renborg and N.J. Dovichi, Electrophoresis, in press.
[9] D. Figeys and N.J. Dovichi, J. Chromatogr. A, 717 (1995) 105.
[10] T.A. Duke, A.N. Semenov and J.L. Viovy, Phys. Rev. Lett., 69 (1992) 3260–3263.

ELSEVIER

Determination of styrene oxide adducts in DNA and DNA components

W. Schrader, M. Linscheid*

ISAS, Institut für Spektrochemie und Angewandte Spektroskopie, P.O. Box 101352, D-44013 Dortmund, Germany

Abstract

The reaction of styrene oxide with DNA components was studied using separation by capillary zone electrophoresis (CZE) and detection by negative-ion electrospray mass spectrometry (MS). The CZE–MS interface was built for a sector field mass spectrometer. The reaction of styrene oxide with mononucleotides (dGMP, dAMP) was used to optimize the relevant separation parameters and to gather the first information about the behaviour of the possible products. With these mixtures, sample stacking procedures were developed and the scope of collision-induced dissociations were studied. From the fragments recorded, information about the reaction sites in the nucleotides was obtained. Further, the reaction with intact calf thymus DNA was investigated. The DNA was digested into oligonucleotides using the previously described approach with Benzonase, an unspecific nuclease, and alkaline phosphatase. Styrene oxide mono-adducts in dinucleotides, trinucleotides and tetranucleotides were detected, whereas pentanucleotides exhibit mono- and discernible amounts of di-adducts. The hexanucleotides were generally modified twice. The alkylated species moved faster than the unmodified oligomers.

1. Introduction

Adduct formation of alkylating or oxidizing carcinogenic compounds with DNA has reportedly been a crucial step in the initiation of tumours [1]. Especially some synthetic chemicals are enzymatically oxidized, yielding very reactive electrophiles. One of these chemicals is styrene. Stryene is among the most important chemicals with its major use for the production of plastics and polymeric resins. Since the monomer can be liberated from such materials during industrial application of the polymers, occupational exposure of workers in such work places occurs. It finds its way into the body generally through

inhalation. In the lung, it is easily absorbed in blood and metabolized primarily in the liver by the cytochrome P-450 pathway to styrene-7,8-oxide, an epoxide which is mutagenic in both procaryotic and eucaryotic test systems and carcinogenic in rodents. Workers occupationally exposed to styrene oxide has been found with increased chromosome aberration levels [2,3]. Hence styrene is considered a potential carcinogen and its allowed concentration in occupational situations is restricted.

With such a background, several in vitro studies addressing the genotoxic effects of styrene and particularly styrene oxide were performed using DNA or DNA components as models [4]. For the determination of the different reaction products, post-labelling and co-chro-

---

* Corresponding author.

matography with synthetic standards proved to be most successful [5]. The results indicate that alkylation through the epoxide takes place predominantly at the N-7-, N^2- and O^6-positions of guanine (Fig. 1).

Several attempts have been made to use mass spectrometric techniques also, since the identification of unknowns would be possible; the general problem is the lack of sufficient detection power. It could be demonstrated, however, that with appropriate derivatization the detection limits for modified nucleobases using GC–MS can be low enough to study biological samples [6,7].

Since the introduction of capillary zone electrophoresis (CZE) by Jorgenson and Lukacs [8], the technique has been used in high-resolution separation analyses for polar and particularly ionic substances at very low levels employing UV or fluorescence detection, the first studies in DNA adduct research have been described [9]. To increase the detection capabilities further, interfacing CZE with mass spectrometry (MS) was introduced using fast atom bombardment (FAB) [10] or electrospray ionization (ESI) [11]. Electrospray is the most often used means of detection since the detection capabilities of ESI are superior owing to much lower chemical backgrounds, but the greatest advantage is the ability to detect high molecular masses due to higher charge numbers per molecule giving access to mass spectra of large bioorganic compounds. For the detection of modifications in DNA, such a combination appeared most promising and we have constructed a capillary electro-

phoresis system interfaced to an electrospray ion source for a double-focusing sector field mass spectrometer built in this laboratory [12].

Here we demonstrate the application of the technique to the analysis of styrene oxide adducts obtained in in vitro reactions with mononucleotides and calf thymus DNA.

2. Experimental

2.1. Materials

Chemicals were purchased from the following suppliers: NH_4HCO_3, Sigma (Deisenhofen, Germany); alkaline phosphatase [1500 U suspension in $(NH_4)_2SO_2$], nucleotides (Böhringer, Mannheim, Germany); calf thymus DNA (lyophilized, research grade), Serva (Heidelberg, Germany); $Mg(OAc)_2$ (analytical-reagent grade), Benzonase (250 U/μl, purity I, 100 000 E per vessel), epoxystyrene (styrene-7,8-oxide), diethyl ether, 2-propanol, NaOH (analytical-reagent grade), Merck (Darmstadt, Germany); methanol (HPLC grade), Promochem (Wesel, Germany).

2.2. Capillary electrophoresis–mass spectrometry

A schematic diagram of the CZE–MS system is given in Fig. 2. A laboratory-constructed CE apparatus is interfaced with an electrospray ion source designed for a Finnigan MAT (Bremen, Germany) Model 90 double-focusing sector field mass spectrometer. The CE system is equipped with a pneumatically actuated sample tray providing space for eight sample reservoirs. Injection can be made electrokinetically or with pressure. The instrument is controlled by means of a single-board computer (Intel 8052). The CE potential is applied at the injection port via a gold electrode inserted in the buffer solution and the other end of the capillary is at electrospray potential. The use of titanium reservoirs [12] was discontinued since gas bubbles evolving during the separations occasionally caused breakdowns of the current. With PTFE cups this problem was solved. The CE apparatus is equipped with a 30
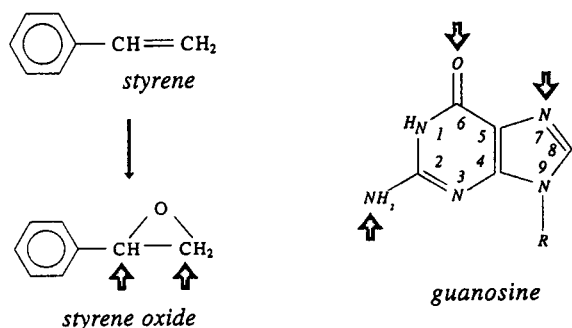
Fig. 1. Reaction sites of styrene oxide and deoxyguanosine.
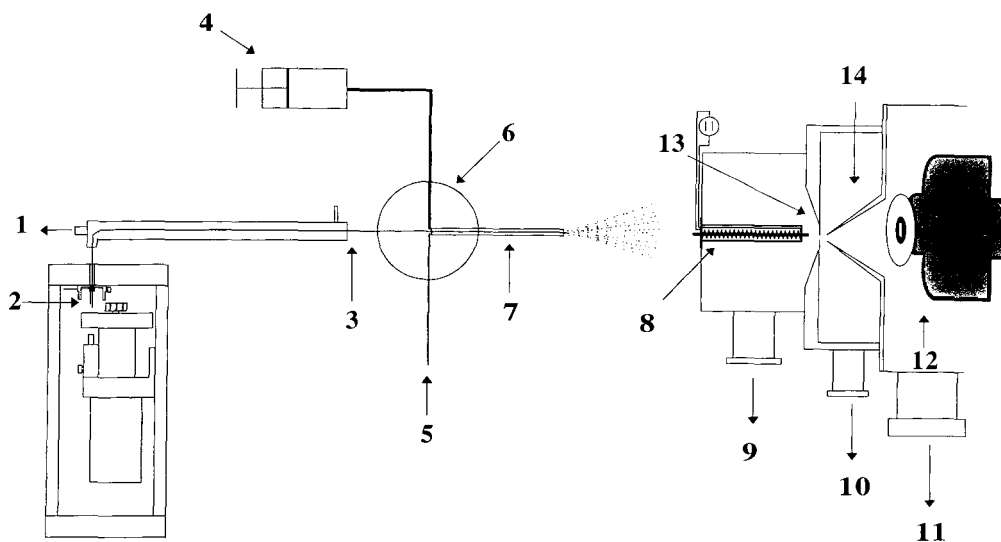
Fig. 2. Schematic diagram of the CZE–MS interface. 1 = air cooling using membrane pump; 2 = high-voltage CZE; 3 = CZE capillary; 4 = liquid sheath flow; 5 = high-voltage ESI; 6 = four-way junction at ESI potential (−8.3 kV); 7 = stainless-steel capillary (sprayer); 8 = indirectly heated capillary; 9 = first pumping stage; 10 = second pumping stage; 11 = source vacuum; 12 = ion optics with draw lens (−2.8 kV) and static quadrupoles; 13 = sampling orifice (0.6 mm); 14 = skimmer (0.8 mm).

kV power supply (Heinzinger, Rosenheim, Germany), which can be floated up to 5 kV.

Capillaries with a thinner silica wall (75 μm I.D., 190 μm O.D.) (SGE, Weiterstadt, Germany) caused difficulties owing to very small hair leaks resulting in gas bubbles inside the capillary. Similar effects have been reported by Moseley et al. [13] and termed electrodrilling. It could be reduced by using capillaries with thicker capillary walls (360 μm O.D., 75, 50 and 25 μm I.D.) (Analyt, Müllheim, Germany). However, even then keeping a constant CZE current for prolonged periods is one of the limiting problems in this interface and the reasons are not yet understood. As a liquid sheath we used 2-propanol and methanol at flow-rates of 5–15 μl/min. The separation capillary ended in a stainless-steel capillary (gauge 22 = 410 μm I.D.) (Hamilton, Darmstadt, Germany), which both ended in a four-way HPLC tee that was used as ESI sprayer. The capillary for liquid sheath was connected to a syringe pump (TSE Systems, Bad Homburg, Germany) and the fourth inlet was used as an electrode connection to the ESI potential.

In our set-up, it seems to be necessary to adjust the separation (inner) capillary so that the end is in line with the outer stainless-steel capillary; otherwise the spray may not be stable. A sheath flow of typically 5 μl also appeared essential to stabilize both the end potential of the CE voltage and the spray, because fluctuations in the eluting salt concentrations may destabilize the performance of the ESI spray, lowering the ion yield. Generally, support by additional air flow using nitrogen was not required.

For desolvation we replaced the earlier used resistively heated capillary with an indirectly heated capillary, providing a uniform temperature profile. The nozzle–skimmer system of the ESI ion source [14] was redesigned using SIMION calculations [15]. The "nozzle" is now conical towards the source with a hole of 600 μm, while the skimmer has an 800 μm entrance at a distance of 4 mm from the nozzle. The distance from the end of the desolvation capillary to the nozzle is 10 mm. Recently, the nozzle was redesigned to a dish-shaped form with a flat base of 2 mm and a hole of 600 μm to avoid contamination reducing ion transmission.

The ion optics design employing two sets of static quadrupoles has been reported for thermo-

spray [16], fast atom bombardment [17] and inductively coupled plasma MS [18] ion sources; with electrospray it gives much better ion transmission when the acceleration potential of the draw lens was held at 2.8 kV, allowing the ions to accelerate in the high-pressure region more moderately.

2.3. Sample preparation

One milligram each of 2′-deoxyadenosine-5′-monophosphate (dAMP), 2′-deoxyguanosine-5′-monophosphate (dGMP) and calf thymus DNA were dissolved in 1 ml of doubly distilled, deionized water and 10 μl of styrene-7,8-oxide were added. The reaction mixture was incubated at 37°C for 48 h. The DNA mixtures were extracted twice with 300 μl of diethyl ether to remove unreacted styrene oxide. The DNA mixtures were digested enzymatically using Benzonase and alkaline phosphatase. The solutions were used without further treatment for electrophoresis using 30 mM NH$_4$HCO$_3$ buffer, (pH 6.5–7.0).

2.4. Hydrolysis of styrene oxide in water

A 10-μl volume of styrene oxide was dissolved in 1 ml of water and kept for 48 h at 37°C. The solution was subjected directly to Raman Spectroscopy (Raman 2000 R spectrometer; Perkin-Elmer, Überlingen, Germany).

2.5. Sample stacking in the CE capillary

For this procedure the capillary was filled completely with the sample and by inverting the injection port potential of the CZE from positive to negative voltage, the sample migrated from the end of the capillary to the front, increasing the sample concentration. A precondition for this method is that the buffers at both ends have a higher ionic strength than the sample at the beginning. Usually, with CZE–MS there is no buffer reservoir at the sprayer end of the capillary. Therefore, an Eppendorf vessel filled with buffer solution was held in place over the sprayer

needle until the preconcentration was finished. The zones were compressed and concentrated, which was indicated by reaching 95% of the normal CZE current. Then the potential was reversed from negative to positive and the CZE–MS run was started.

3. Results

3.1. Mononucleotides

In first experiments, the reaction of styrene oxide with mononucleotides was studied. On that basis a typical reaction product pattern could be established and the electrophoretic separation parameters were optimized. The electrophoretic separation of reaction products of dAMP incubated with styrene oxide shows three peaks in the reconstructed ion mass electropherogram (Fig. 3, bottom).The corresponding mass electropherograms of m/z 330 (Fig. 3, top) identifies peak 3 as unreacted dAMP, while peaks 1 and 2 both contain two different species of styrene oxide adducts to dAMP (m/z 450; Fig. 3, middle).

Similar results were obtained by the reaction between the other mononucleotides and styrene oxide, with the exception that dGMP shows two additional compounds at m/z 586, probably doubly alkylated dGMP. Both bi-adducts migrate slightly faster than the corresponding mono-adducts, while unmodified dGMP migrates last. In Fig. 4, the separation of the products is shown using sample stacking. Since the absolute amount of sample is always of concern in CZE–MS, sample stacking [19] (on-column preconcentration) techniques were applied. The gain in detection power is approximately one order of magnitude, but there is obviously a loss of resolution, particularly for the main components; the reason for this is that the stacking procedure was terminated before the optimum current was reached to avoid sample loss. Without stacking the di-adducts were not detectable since their concentration is lower by at least two orders of magnitude compared with the starting material,
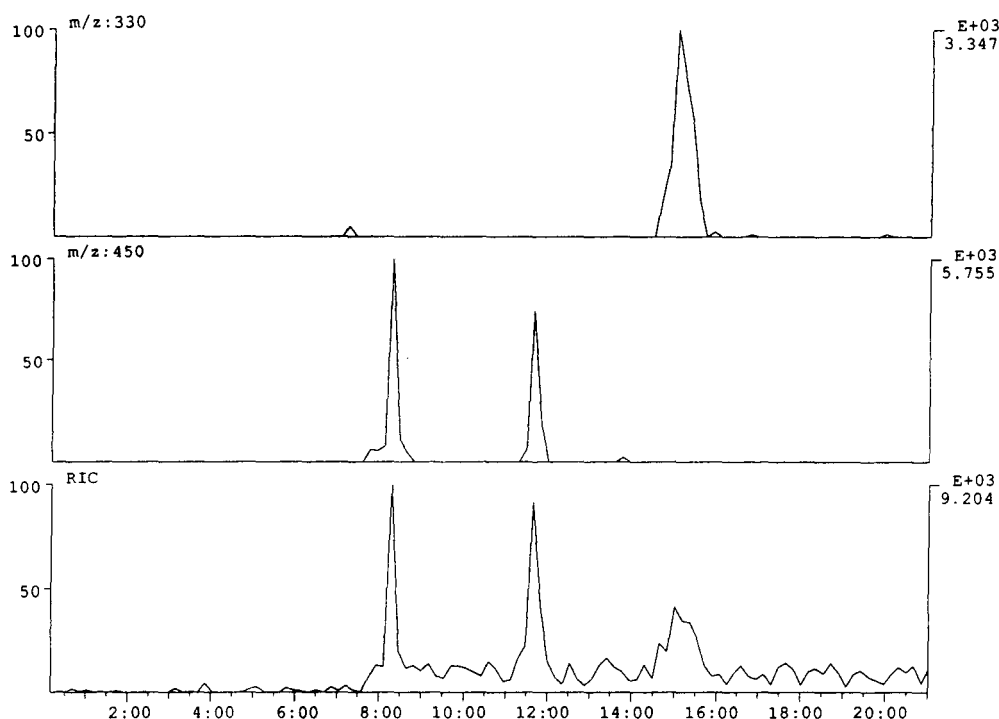
Fig. 3. CZE–MS of dAMP after reaction with styrene oxide. Top trace, electropherogram, m/z 330 (dAMP); middle trace, m/z 450 (mono-adducts dAMP–stryrene oxide); bottom trace, RIC. Separation conditions: capillary, 82 cm × 75 μm I.D.; buffer, 30 mM NH$_4$HCO$_3$ (pH 6.8); 280 V/cm.

as can be seen from the absolute intensities of the signals.

Since so far only the molecular ions $[M - H]^-$ were observed without relevant fragments, preliminary experiments using collisionally induced dissociation (CID) were made. A mixture of incubated dGMP was continuously infused at a flow-rate of 5 μl/min. The fragmentation was induced by a potential of -40 V between the nozzle and skimmer in the first pumping stage. Fig. 5 shows a mass spectrum of 20 accumulated scans from an experiment with incubated dGMP. At m/z 150 the negative ion of guanine appears, while m/z 195 indicates the loss of guanine from dGMP $[M -$ guanine]. Two peaks in the spectrum are significant for two different types of adducts: the signal at m/z 270 belongs to a guanine–styrene oxide adduct, whereas that at m/z 216 is styrene oxide phosphate. This means that one of the adducts is a phosphate derivative,

an artifact not common in DNA. From the two adducts in the electropherogram (Fig. 4, middle trace) the first is the phosphate adduct, since it is less polar, thus eluting first.

3.2. DNA digestion

The attempt to identify modifications of DNA at the oligonucleotide level was made by means of digested calf thymus DNA after styrene oxide incubation using two enzymes. The unspecific endonuclease Benzonase cleaves the DNA into oligonucleotides while the 5'-phosphates were removed with alkaline phosphatase. This digestion steps produce oligonucleotides of the type n-nucleotide–$(n - 1)$-phosphate with chain lengths of 2–8 nucleotides, irrespective of modification. Under the separation conditions used here, the oligonucleotides were separated into groups according to the same chain length.
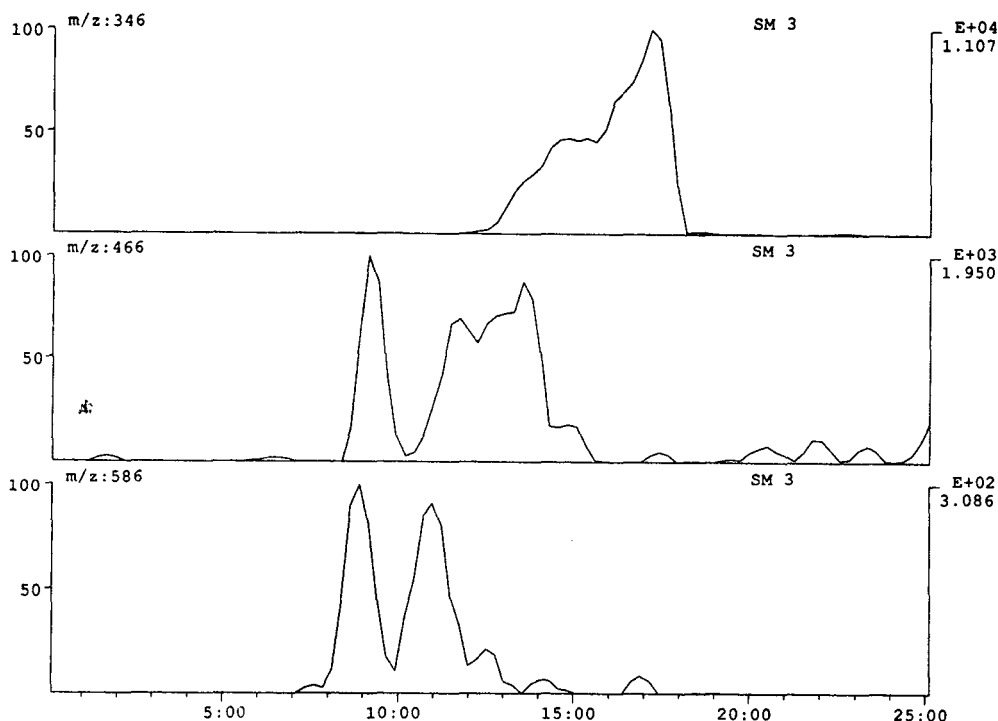
Fig. 4. CZE–MS of dGMP reacted with styrene oxide; sample stacking (capillary was filled completely). Top trace, m/z 346 (dGMP); middle trace, m/z 466 (two mono-adducts); bottom trace, m/z 586 (two di-adducts). Separation conditions: capillary, 82 cm × 75 μm I.D.; buffer, 30 mM NH$_4$HCO$_3$ (pH 6.8); 280 V/cm.

Fig. 6 shows a total ion electropherogram indicating four peaks. The first peak contains all dinucleotide monophosphates, the second the trinucleotide diphosphates and so on up to pentanucleotide tetraphosphate in this particular electropherogram; in other digestion experiments we have found the oligomers up to octanucleotides.

In Fig. 7 a CZE–MS separation is shown as an "eagle's view" [20], which allows the facile recognition of modified and unmodified oligomers by their separation in time and mass. The modified oligomers migrate slightly faster than the unmodified counterparts; hence it is difficult to separate them in different scans. It should be noted, however, that it is not possible on the basis of these data to distinguish between the 3'- and 5'-isomers of the same sequence, since they are not separated electrophoretically. From Fig. 7 it is evident that styrene oxide produces a variety of adducts under these in vitro conditions. All the oligomers with the exception only of thymine-containing sequences were found to be modified at least once. Di-, tri- and tetranucleotides were found to be modified once, while pentanucleotides showed mono- and di-adducts. Hexanucleotides were found only in doubly modified form and no unmodified oligomers remained. Since the reaction is possible at each nucleobase in the polymer, the probability of modification increases with increase in chain length.

To verify that the modification reaction has occurred before digestion of DNA and not with the oligonucleotides, the reaction was stopped with extraction of styrene oxide using diethyl
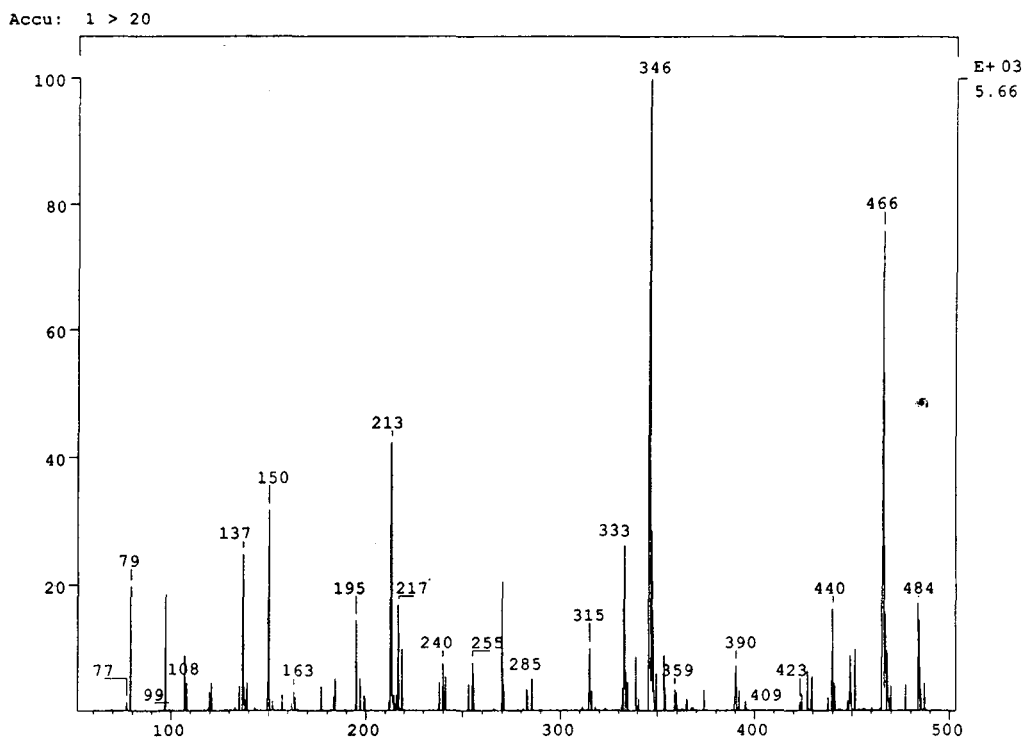
Fig. 5. CID in the skimmer region of reacted dGMP. Mass spectrum, 20 scans accumulated; nozzle voltage, −40 V.
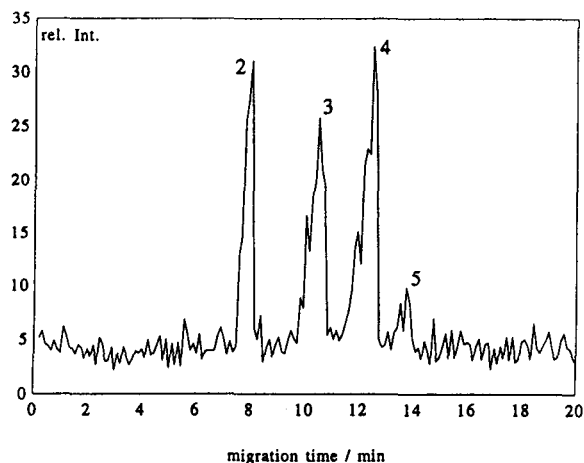
Fig. 6. CZE–MS of oligonucleotides: total ion electrophero-gram of oligonucleotides from enzymatically digested DNA. Separation conditions as in Fig. 3.

ether, but no differences to the reaction scheme without extraction were observed. Further, we have shown by Raman spectroscopy that after 48 h the epoxide is completely hydrolysed.

4. Discussion

The results shown here indicate that this approach to detecting modifications in DNA may be used to determine the frequency at which a particular reaction occurs in DNA and addition-ally any sequence specificity. The styrene oxide model seems not to exhibit sequence specificity, at least not at the high concentration level used for the orienting experiments. The observation that thymine does not react with styrene oxide shows the potential to detect such reactions in appropriate model systems. Additionally, at the
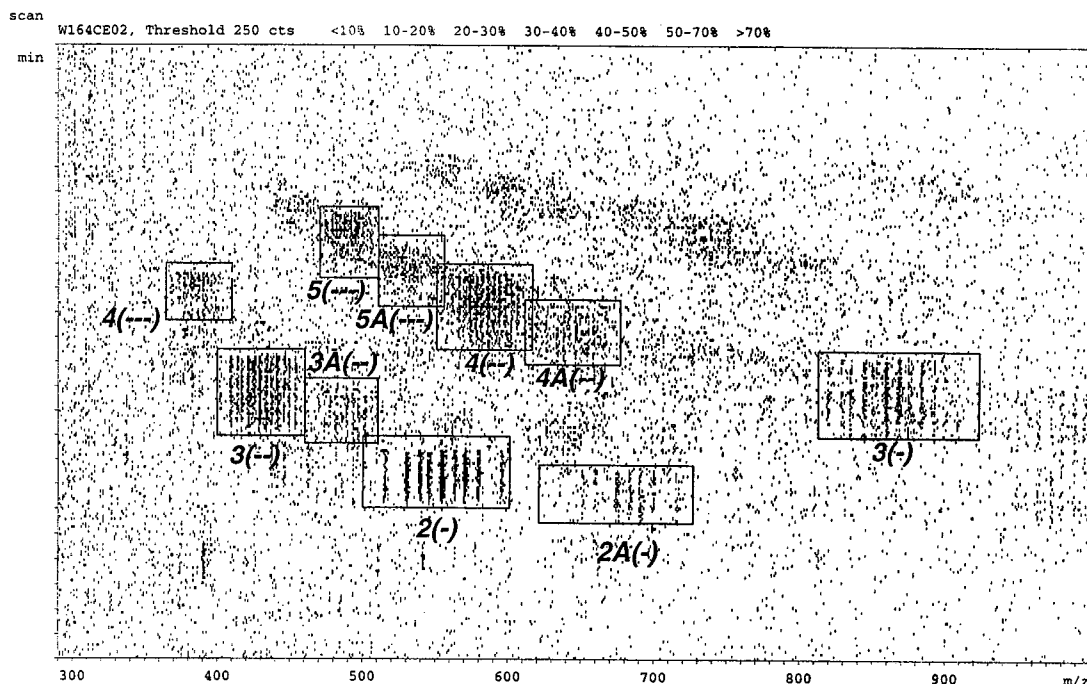
Fig. 7. "Eagle's view" of CZE–MS of oligonucleotides from calf thymus DNA incubated with styrene oxide. Experimental conditions: scan range, 300–1000, 15 s per decade; U(nozzle) = −70 V; T(capillary) = 120°C; separation capillary length, 82 cm; U(CZE) = 15 kV; U(ESI) = −8 kV; U(separation) = 23 kV (280 V/cm). The chain length and the charge state are given; A indicates the styrene oxide adducts.

dinucleotide level the adduct of d(CpC)[1] appears just above the background noise and the intensity of d(GpG) is only slightly higher. All other adducts of dinucleotides are readily detected.

At the trinucleotide level again only d(TpTpT) remains unmodified, whereas the adducts of d(TpTpC), d(ApApT) and d(ApApA) are barely visible. All other possible adducts of the trinucleotides appear with adequate intensities.

Two constraints need further attention. One is the insufficient separation of oligonucleotides of the same chain length, but preliminary results with different buffer systems are very promising. It seems possible to separate at least the different species [21], if not the isomers within the groups. Second, the level of detailed information about the reaction sites at the nucleobases could be optimized using CID either by means of skimmer CID or with MS–MS experiments. The

preliminary results discussed here are promising. The adducts formed at N-7 of the guanine yielding a cation should cleave the glycosidic bond anyhow, releasing the modified nucleobase, and we found indications that this indeed happens. This means, on the other hand, that the guanine adducts in the oligomers are adducts to the exocyclic N^2 or O^6, which are chemically stable. This is further indicated by the low intensity of d(GpG) adduct found in the spectra.

Quantitative considerations are impossible as yet owing to the lack of any standard. This makes even simple estimations of the detection power of the technique nearly impossible. With simple dinucleotides such as TpT it is possible to detect nucleotides in the femtomole range. The development of standards and comparison or the combination with other, known methods for the determination of modifications, e.g., GC–MS and post-labeling, are prerequisites for future work.

Considering the toxicological relevance, we

---

[1] Abbreviations: d = deoxy; A = adenosine; G = guanosine; C = cytidine; T = thymidine; p = phosphate.

have already started to isolate DNA from various sources, particularly from liver homogenates and cell cultures, and have successfully applied the same analytical protocol.

5. Conclusion

We have been able to separate the reaction products of styrene oxide with DNA constituents by means of CZE and to detect the molecular ions $[M - H]^-$ by ESI–MS in a laboratory-built CZE–MS instrument. With CID, fragments were obtained giving some indications about the reaction sites in the molecules, but this approach is in a very preliminary stage.

The same reaction was studied with calf thymus DNA. The DNA was subsequently digested into a mixture of oligonucleotides, which could then be separated into groups of the same chain lengths, but modified species were clearly separated due to different electrophoretic mobility and mass. It seems that the procedure has the potential to detect the preferred reaction sites in DNA and even sequence specificity should be instantly recognized. Since the overall scheme is rapid and effective without the need for derivatization, it can be envisaged that this strategy could provide a valuable tool in the study of toxicologically relevant reactions and in the exploration of genotoxic effects of drugs and xenobiotics. With improved instrumentation, namely CZE injection schemes, stacking procedures and with mass spectrometers providing superior detection power, even biomonitoring could be accomplished.

Acknowledgements

[1] A.M. Jeffrey, Pharmacol. Ther., 28 (1985) 237.
[2] S. Kaur, M. Pongracz, W.J. Bodell and A.L. Burlingame, Chem. Res. Toxicol., 6 (1993) 125.
[3] J.A. Bond, CRC Crit. Rev. Toxicol., 19 (1989) 227.
[4] K. Pongracz, S. Kaur, A.L. Burlingame and W.J. Bodell, Carcinogenesis, 10 (1989) 1009.
[5] K. Randerath, M.V. Reddy and R.C. Gupta, Proc. Natl. Acad. Sci. USA, 78 (1981) 6126.
[6] G.B. Mohammed, A. Nazareth, M.J. Hayes, R.E. Giese and P. Vouros, J. Chromatogr., 314 (1984) 211.
[7] C. Randt and M. Linscheid, Fresenius' Z. Anal. Chem., 335 (1989) 865.
[8] J.W. Jorgenson and K.D. Lukacs, J. Chromatogr., 218 (1981) 209.
[9] C.B. Norwood, E. Jackim and S. Cheer, Anal. Biochem., 213 (1993) 194.
[10] M.J.F. Suter, B.B. DaGue, W.T. Moore, S.N. Lin and R.M. Caprioli, J. Chromatogr., 553 (1991) 101.
[11] R.D. Smith, J.A. Olivares, N.T. Nguyen and H.R. Udseth, Anal. Chem., 60 (1988) 436.
[12] P. Janning, W. Schrader and M. Linscheid, Rapid Commun. Mass Spectrom., 8 (1994) 1035.
[13] M.A. Moseley, L.J. Deterding, K.B. Tomer and J.W. Jorgenson, Anal. Chem., 63 (1991) 109.
[14] J. Hau, C. Siethoff, W. Schrader and M. Linscheid, presented at the 13th International Mass Spectrometry Conference, Budapest, Hungary, 26 August–2 September, 1994.
[15] D.A. Dahl, Simion PC/PS2 Ion lens Program, Overlay Version 4.01, Idaho National Engineering Development/US DOE, 1988.
[16] J. Hau, W. Nigge and M. Linscheid, Org. Mass Spectrom., 28 (1993) 223.
[17] J. Hau, W. Schrader and M. Linscheid, Org. Mass Spectrom., 28 (1993) 216.
[18] M. Morita, H. Ito, M. Linscheid and K. Otsuka, Anal. Chem., 66 (1994) 1588.
[19] R.-L. Chien and D.S. Burgi, Anal. Chem., 64 (1992) 1046.
[20] J. Hau and M. Linscheid, Spectrochim. Acta Part B, 48 (1993) E1047.
[21] W. Schrader, P. Janning, C. Siethoff and M. Linscheid, unpublished results.

Capillary electrophoresis of DNA
Potential utility for clinical diagnoses

T.A. Felmlee[a], R.P. Oda[b], D.A. Persing[a], J.P. Landers[b,*]

[a]Clinical Microbiology, Department of Laboratory Medicine and Pathology, Mayo Foundation/Mayo Clinic, Rochester, MN 55905, USA

[b]Clinical Capillary Electrophoresis Facility, Department of Laboratory Medicine and Pathology, Mayo Foundation/Mayo Clinic, Rochester, MN 55905, USA

Abstract

The last few years have witnessed a tremendous shift in the use of capillary electrophoresis for clinical applications, particularly with DNA analysis. As a result of the large number of DNA-based clinical assays, there is an intense interest in making DNA analysis faster, less expensive and more automated. We describe the evaluation of CE-based single-strand conformation polymorphism (SSCP) and dideoxy fingerprinting (ddF) analysis for the detection of single-point mutations within a *Mycobacterium tuberculosis*-specific amplified DNA fragment. Both were found to be capable of detecting the mutation in the resistant isolate but ddF showed the most promise with respect to specificity and ease of implementation. In addition, initial results with a CE-based sizing method is shown to be competitive and, perhaps, superior to a Southern blot analysis for the detection of hepatitis C viral (HCV) infection.

1. Introduction

The potential application of capillary electrophoresis (CE) for both routine and esoteric clinical assays is rapidly being realized [1]. CE has been shown to be a viable alternative to many of the standard clinical techniques as a result of its ability to perform rapid, efficient, reproducible analyses in an automated format. CE analyses have been documented for a variety of analytes of biological importance; ranging from small organic ions to large macromolecules (see Ref. [1] and references therein).

The last decade has seen a tremendous shift

toward the development of deoxyribonucleic acid (DNA)-based assays for use in the clinical laboratory. The analysis of polymerase chain reaction (PCR)-amplified DNA products is the basis for an ever-increasing number of diagnostic assays, in which the amplified fragments are typically sized by agarose gel electrophoresis followed by DNA–DNA hybridization analysis (i.e., Southern blot evaluation). Alternatively, post-amplification analysis can be accomplished by using DNA sequencing, with the ultimate goal being the identification of specific nucleotide base changes. Since DNA sequencing analysis is a lengthy and more technically-involved process, screening methods have developed to identify those samples possessing a mutation. Single-strand conformation polymorphism (SSCP) [2], dideoxy fingerprinting (ddF)

---

* Corresponding author.

[3] and heteroduplex analyses [2], assess the DNA fragment for mutations without having to sequence it. All three of these methods detect mutations based on the migration of the single or double stranded DNA under non-denaturing conditions. The presence of a single-point (or multiple-point) mutation affects the secondary structure of the molecule and, hence, its electrophoretic migration. Differences observed in comparison with the electrophoretic behavior of the wild type provide the basis for identification of the mutation.

A substantial number of reports have highlighted the utility of CE for the analysis of DNA. The speed, efficiency, sensitivity (with laser-induced fluorescence detection) and potential for automation make CE a particularly attractive analytical method for the clinical laboratory, especially in light of the fact that the number of DNA-based analyses used for diagnoses is growing rapidly. CE is proving to be a promising tool for effectively replacing standard gel electrophoretic techniques for DNA analysis, particularly for use with the aforementioned methods. Recent literature describes the use of CE to size DNA fragments generated by restriction endonuclease digestion (RFLP analysis) [4], or fragments produced by using PCR [5]. The characteristics that make CE attractive for methods such as SSCP and DNA-sizing analysis include its speed, sensitivity, efficiency, not to mention its potential for providing qualitative and quantitative results under native or denaturing conditions.

In the present study, we describe preliminary results from attempts to exploit CE as a means of analyzing DNA for clinical diagnostic purposes. CE analysis using both fixed (crosslinked) gels (CGE) and polymer networks (pnCE) are used for the detection of single-base mutations within a *Mycobacterium tuberculosis*-specific amplified DNA fragment by using two approaches: SSCP and ddF. The significance of these analyses is to rapidly identify those organisms harboring a mutation that may be associated with resistance to the drug, rifampin. In addition, DNA sizing by pnCE is exploited for the quantitative and qualitative analysis of PCR products indicative of hepatitis C viral (HCV) infection.

2. Materials and methods

2.1. CE instrumentation

HPCE separation was carried out on a Beckman P/ACE System 5510 equipped with either a laser-induced fluorescence detector or a UV detector and a sample cooling tray. The laser system was a single-wavelength (488 nm) argon ion laser (3–4 mW) with detection at 510 nm (using YO-PRO-1; Molecular Probes, Eugene, OR, USA) or 520 nm (using fluorescein). The UV detector monitored absorbance at 254 nm. An IBM 486 ValuePoint computer utilizing System Gold software (V. 8.1) was used for instrument control and data collection. All peak information (migration time, peak areas and height) was obtained through the System Gold software.

2.2. SSCP-CE

The sample was *rpo*B amplicon-derived from a clinical isolate of *M. tuberculosis* as described by Whelen et al. [6]. The amplified DNA (1–10 μg), suspended in water, was diluted in PCR buffer ($1 \times$ buffer was 10 mM Tris pH 8.3, 50 mM KCl, 1.5 mM MgCl$_2$) such that the PCR buffer was at $0.25 \times$ strength. The samples were boiled for 3 min and immediately put on ice. Separation was carried out using a polymer network obtained from Dionex (Sunnyvale, CA, USA), using a 50 cm (resolving length) $\times$ 50 μm capillary. The temperature of the sample holding tray was maintained at 8°C using an external chiller while the capillary was maintained at 18°C. Ethidium bromide (EtBr) was added to the buffer system at a final concentration of 10 μg/ml. The sample was applied to the capillary by electrokinetic injection (45 s $\times$ 5 kV) and separated with 150 V/cm. A DNA standard (ϕX174 Rf digested with *Hae*III; BRL-Gibco) was run as a control to ascertain performance of the pnCE system.

2.3. ddF-CE

Samples for ddF-CE were generated using a ddG cycle sequencing reaction [7]. The template

for the cycle sequencing reaction was the same
*rpo*B gene fragment generated for SSCP analy-
sis. The primer used for gel electrophoresis ddF
analysis was a ^{32}P-5'-labeled oligonucleotide,
and the same primer was 5'-labeled with fluores-
cein for ddF-CE. The ^{32}P-labeled DNA frag-
ments were directly analyzed by using a non-
denaturing polyacrylamide gel electrophoresis
system [7] and visualized by autoradiography.
The fluorescein-labeled DNA fragments were
precipitated with alcohol, and suspended in
deionized water. The fluorescent ddF reaction
products were first analyzed using an automated
DNA sequencer [7] to establish the existence of
the chain terminated products. The sample was
then analyzed by using a CGE system (3%T–
3%C polyacrylamide fixed gel capillary, Scien-
tific Resources, Eatontown, NJ, USA) with 50
μm I.D., an effective length of 50 cm, and a
TBE (0.089 M Tris pH 8.3, 0.089 M borate, 2
mM EDTA) buffer system. The samples were
injected electrokinetically (60 s × 3.5 kV) and
separated with 150 V/cm. The fragments were
detected by laser-induced fluorescence of the
fluorescein fluorophore (Ex 488 nm, Em 520
nm).

2.4. HCV amplicon analysis

The samples used for this analysis were am-
plified DNA products using an HCV-specific
reverse transcription and PCR amplification [8].
The oligonucleotide primers were specific for the
HCV 5' untranslated region and generated a 308
bp product. The template for PCR were nucleic
acid extracts obtained from patient serum. The
amplified DNA fragments were treated with
isopsoralen [9] to prevent re-amplification, which
serves to eliminate false positive PCR results.
The pnCE conditions used were essentially those
of Butler et al. [5] and were as follows: 20 cm
(effective length) × 50 μm I.D. DB-17 coated
μ-Sil capillary (J&W Scientific, Folsom, CA,
USA). The polymer network was TBE (same as
above), 1% (w/v) hydroxyethyl cellulose (HEC),
0.06 mg/ml YO-PRO-1. The DNA fragment
standard used was a *Hae*III digest of pBR322
(Boehringer Mannheim Biochemicals, In-
dianapolis, IN, USA). The samples were ana-

lyzed directly from the PCR mixture, such that
the capillary was pre-injected with water (3 s ×
3.5 kV) before the electrokinetic introduction of
the sample (90 s × 3.5 kV) [10]. The separation
conditions were adjusted to 260 V/cm. Southern
blot results were generated by using standard
agarose slab-gel electrophoresis and blotting
procedures [11]. The Southern blot was probed
by using a DNA fragment internal to the am-
plified sequence and the ECL labeling kit
(Amersham, Arlington Heights, IL, USA) [8].

3. Results

3.1. SSCP-CE

Fig. 1 illustrates the comparison of standard
non-denaturing polyacrylamide gel electropho-
resis and pnCE as used to perform SSCP analysis
on the *M. tuberculosis*-specific *rpo*B-directed
PCR product. SSCP distinguishes DNA frag-
ments by virtue of secondary structural differ-
ences generated by the single strands (ssDNA) of
the DNA fragments [12]. In this example, organ-
isms resistant to rifampin harbor a mutation
within the sequence of the amplified fragment
being studied. As illustrated using standard non-
denaturing gel polyacrylamide electrophoresis
conditions [5] (Fig. 1A), the amplified DNA
derived from the genomes of rifampin sensitive
and resistant organisms can be differentiated.
However, only a slight migration difference was
detectable between the ssDNA derived from
wild type (rifampin sensitive clinical isolate) and
L363 (rifampin resistant due to one base change;
[7]). As a contrast, isolate L219 provided an
example were the ssDNA migration differences
were readily detected by routine gel electro-
phoresis. We chose to challenge the CE analysis
with amplified DNA from these two isolates to
determine if CE could better resolve the ssDNA
fragments. Initial experiments were aimed at
differentiating these two isolates from each other
and DNA fragments derived from a wild-type
isolate.

Various capillary and polymer network sys-
tems were employed to identify the system that
would provide the best resolution and repro-

ducibility for the SSCP-CE analysis. The polymer network systems tested included both a 3% and 4% linear polyacrylamide system in TBE, and 0.5 to 0.75% HEC in TBE. The Dionex pnCE system yielded the highest level of resolution for the *rpo*B-derived DNA fragments.

A)

Acrylamide (MDE) Gel Electrophoresis

B)

Time (minutes)
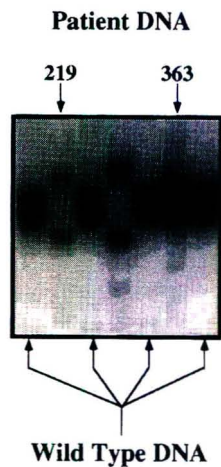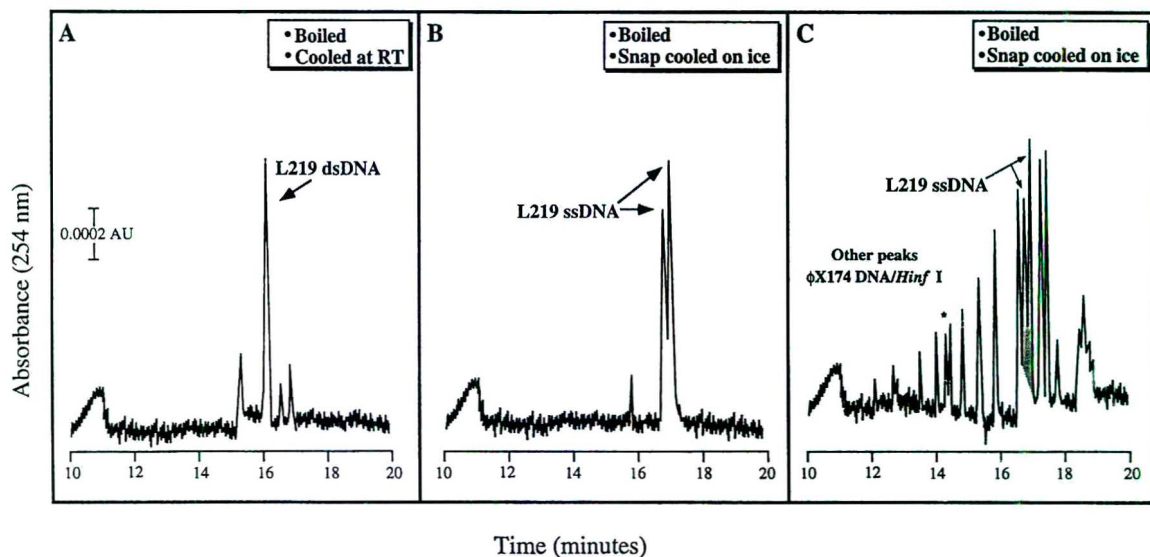
Fig. 1. (*Continued on p. 131*)

C)
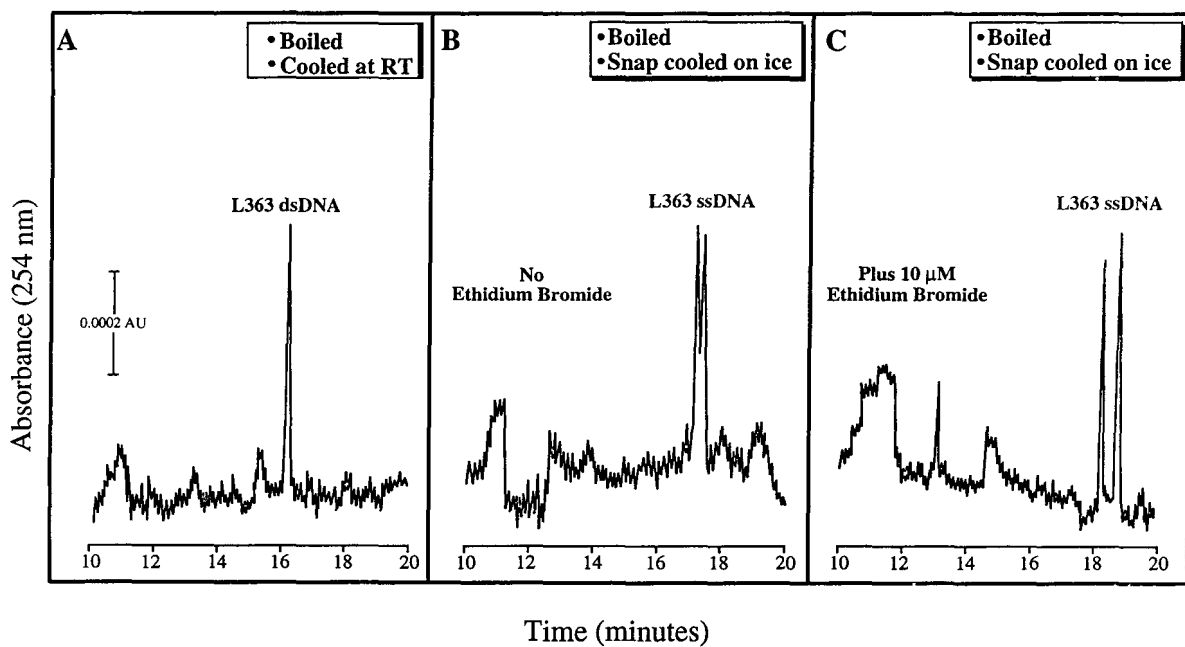
Fig. 1. SSCP analysis comparing electrophoretic separations using a standard acrylamide gel or pnCE. (A) Illustration typifying non-denaturing MDE (mutation detection enhancement) gel separation as described in Ref. [4]. The isolates used were either rifampin-sensitive wild-type DNA (lanes marked at the bottom of the autoradiogram), or rifampin-resistant isolates (lanes between the wild-type samples). Isolates L219 and L363 (designated at the top of the figure) were used to generate the SSCP-CE results that follow. (B) Panel A is the electropherogram resulting from boiling the amplified DNA from isolate L219 and allowing the sample to cool slowly, as indicated by the detection of re-annealed dsDNA. Panel B is the same sample as panel A, except the DNA was snap cooled by quickly placing the boiled sample on ice. The ssDNA species are noted in this panel. Panel C illustrates mixing the snap cooled, ssDNA from L219 with a ϕX174-*Hinf*I DNA fragment standard (Boehringer Mannheim Biochemical, Indianapolis, IN, USA). The peaks derived from L219 are filled in. (C) The first panel illustrates the re-annealed amplified DNA derived from L363. The middle panel illustrates the ssDNA migration pattern obtained from the same amplified DNA that has been snap cooled. The final panel illustrates the effects of adding ethidium bromide (10 μM final concentration) to the buffer system. The ssDNA peaks are labeled as such.

Fig. 1B illustrates the initial SSCP results using L219. The first two panels contrast cooling the heat denatured DNA slowly (first panel) or rapidly (middle panel). There was just a trace of single stranded material detected upon slowly cooling the DNA, whereas all of the DNA was in the single stranded state in the rapidly cooled sample. The ssDNA migrated at a slower rate through the matrix, which was consistent with standard non-denaturing polyacrylamide gel electrophoresis. We also mixed the snap-cooled

sample with ϕX174-HaeIII DNA fragment standards to determine if the separation of ssDNA was achievable within a mixture of dsDNA fragments. The third panel of Fig. 1B illustrates the ability to include dsDNA fragments as internal markers for this analysis without affecting the resolution.

The next sample analyzed was L363, which produced an SSCP pattern that was barely distinguishable from wild type using standard non-denaturing polyacrylamide gel electrophoresis

(Fig. 1A). CE was able to separate the ssDNA of L363, as illustrated in the first two panels of Fig. 1C. The degree of separation between the ssDNA fragments was similar to that of the L219 separation; however, the migration time was different for the two isolates (compare Fig. 1B and 1C). Ethidium bromide was added to the buffer system in an attempt to increase the resolution [13,14]. An enhanced (baseline) resolution of the ssDNA fragments was achieved with sample L363 (Fig. 1C, third panel), with a corresponding increase in peak height and with only a slight increase in analysis time. Consistent with the observations of others, EtBr-ssDNA strands migrated more slowly than that observed in the absence of the intercalator. Ethidium bromide did not produce the same effect with sample L219 (no significant change in strand migration and resolution).

The wild-type sequence was analyzed along with L363 and the level of resolution was insufficient to differentiate the two samples (data not shown). This result was comparable to what was detected by non-denaturing polyacrylamide gel electrophoresis in that the DNA strands of wild type and L363 amplified products almost co-migrated.

3.2. ddF-CE

As with the SSCP analysis, evaluation of the ddF method was conducted by comparing standard non-denaturing polyacrylamide gel electrophoresis and CGE. The theory and development of the ddF technique have been described in detail elsewhere [3,15]. Briefly, the ddF analysis involved non-denaturing polyacrylamide gel electrophoretic separation of dideoxy terminated fragments generated by a typical Sanger sequencing reaction using one dideoxy chain terminating nucleotide (Fig. 2). Thus, the fragments were essentially analyzed based on the chain termination differences (similar to DNA sequencing) and secondary structural differences (similar to SSCP). Fig. 3 illustrates the ddF results from an *rpo*B-specific amplicon derived from clinical isolates of *M. tuberculosis*. Using standard non-denaturing polyacrylamide acryl-

amide gel electrophoresis, strand migration differences were readily discernible between the products generated from the wild-type sequence and those derived from a rifampin resistant strain harboring a single C→T base mutation (Fig. 3A). This sample typified the degree of strand migration differences expected in a ddF analysis.

For ddF-CE analysis, the same samples were analyzed by using a fluorescein-labeled oligonucleotide primer. These reactions were first analyzed using an automated DNA sequencer to assure the production of chain-terminated products. Of the systems tested, the best resolution was obtained using a chemically cross-linked acrylamide gel system (Fig. 3B). The resolution was equivalent to that obtained with the non-denaturing slab-gel system. The reproducibility of the shift was established by running the samples in triplicate. The current associated with running the fixed gel system (at 15 kV) was initially 6.0 μA and decreased with subsequent runs. Use of the capillary was discontinued when the system current was < 5.2 μA.

3.3. dsDNA sizing analysis

As seen in Fig. 4, and as described by others [3], physical gel capillary electrophoretic separation has proven to be an excellent means of sizing amplified DNA. The PCR assay used was sensitive and specific for HCV [8], such that a fragment detected by agarose gel electrophoresis was considered to be a diagnostic marker for the presence of the HCV genome. The HCV-specific amplified DNA was easily detected with LIF-CE using a polymer network and YO-PRO-1 as a fluorescent intercalator (Fig. 4C). Routinely, Southern blot analysis is carried only to increase the sensitivity of detecting the amplified DNA fragment as shown in Fig. 4A. The signals observed with Southern blot analysis typified the range of responses from negative to strong positive. These results correlated well with the electropherograms shown in Fig. 4C. The resolution of the CGE system was assessed using a DNA fragment standard (Fig. 4B). Based on the
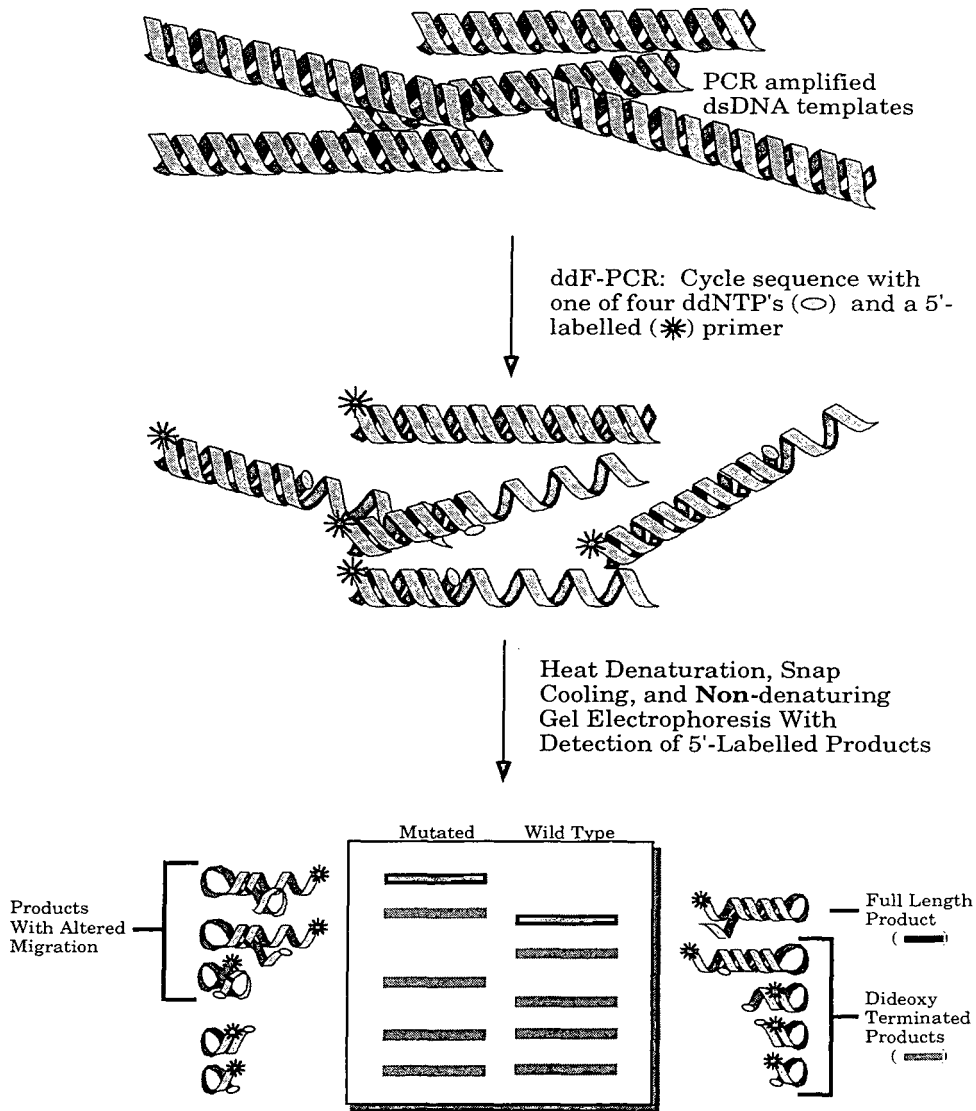
Fig. 2. The ddF theory is illustrated in this figure. The amplified DNA is used directly from the PCR mixture with no need to remove unincorporated deoxynucleotides (dNTPs) or unextended primers (top). The amplified DNA is added to a ddF reaction mixture containing a 5'-labelled oligonucleotide (32P or fluorescein) and one dideoxy nucleotide (ddNTP). The reaction is catalyzed by Taq DNA polymerase to generate a series of chain terminated products whenever the ddNTP is inserted (middle). The dNTPs added with the amplified DNA help fuel the extension of the 5'-labelled priming oligonucleotide. The chain terminated products are boiled, snap cooled and separated using non-denaturing polyacrylamide gel electrophoresis (32P 5'-labeled products) or CE (fluorescein 5'-labelled products), and the labeled ssDNA fragments are detected with autoradiography or laser-induced fluorescence, respectively. Nucleotide base changes (mutations) are detected by (1) the secondary structural differences generated by the various chain terminated fragments and (2) the position of chain termination, if it has been altered by a mutation (bottom).

migration times for the standard fragments, the 308 bp amplified fragment migrated as expected between 6.9 and 7.1 min. A small shoulder was observed on the early part of the fragment peak and was the result of isopsoralen treatment [9]. CE analysis of this amplified DNA gave clear

A

Acrylamide (MDE) Gel Electrophoresis

B

Capillary Gel Electrophoresis
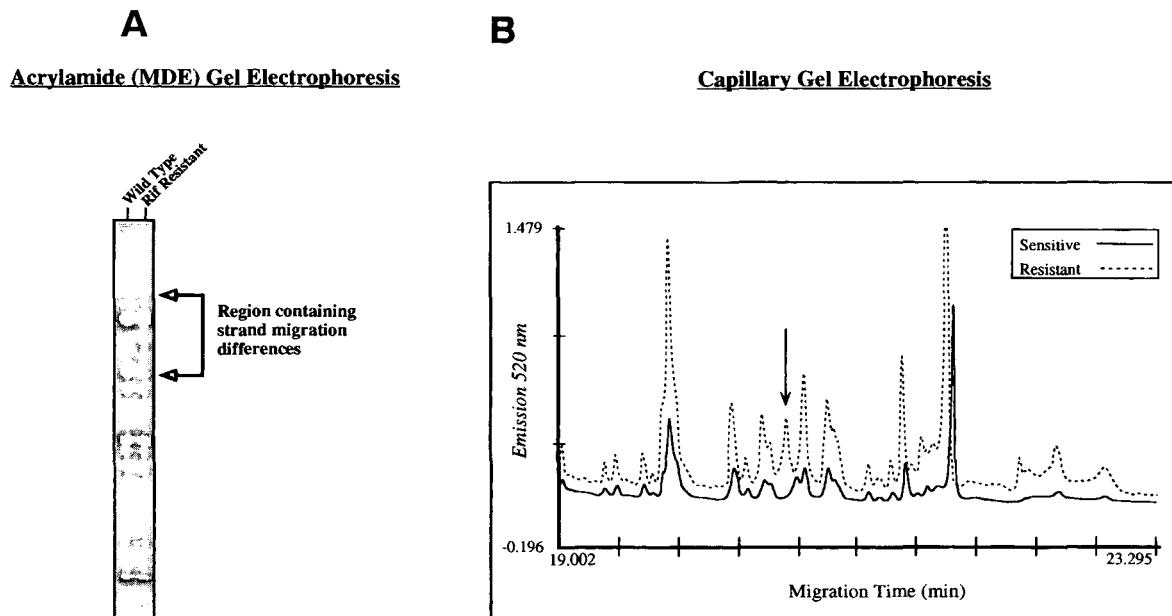
Fig. 3. ddF analysis comparing electrophoretic separations using an acrylamide gel method or CGE. (A) Illustration typifying non-denaturing gel separation as described in Ref. [4]. The top of the autoradiogram is labeled to indicate rifampin susceptibility of the isolate used to generate the amplified fragment. The rifampin resistant isolate harbored a single C to T mutation. The ddF reaction included a ^{32}P-5′-labeled oligonucleotide primer, and ddGTP as the chain terminating nucleotide. The region where strand migration differences can be detected is marked to the right of the autoradiogram. The arrow indicates the beginning of peak migration differences between the rifampin resistant and sensitive isolates. (B) The amplified DNA from the same isolates used in (A) was analyzed using a fluorescein-labeled oligonucleotide and ddGTP as the chain terminating nucleotide. The CGE separation of the fluorescein labeled fragments is illustrated in this figure. The arrow in B represents the detected mutation.

results for 39 clinical samples with a 100% correlation with Southern blot analysis [16].

4. Discussion

A recent trend in the development of clinical diagnostic procedures is to exploit molecular methods of analysis for the rapid detection of pathogens directly from patient specimens. It is clear that the most prominent molecular technique currently used is PCR, which can be developed to detect a pathogen with a high degree of specificity and sensitivity. Post-amplification analysis of DNA fragments produced by PCR is routinely carried out by agarose gel electrophoresis. Enhanced resolution can be obtained with the use of an acrylamide gel matrix, however, these gels can be more difficult to cast and require a longer separation time.

When information regarding the DNA sequence is required, the use of the acrylamide format is essential. Subsequently, all of the disadvantages associated with the use of these cumbersome systems compound the labor-intensity of the clinical diagnostic procedure. It is for this reason that CE in fixed gels and polymer networks has been embraced with intense interest and that, as in this study, critical comparisons between agarose/acrylamide (standard) gel electrophoresis systems and various CE systems are being carried out. In the present study, our ultimate goal was to establish the feasibility of using CE in the clinical molecular diagnostic laboratory setting. The advantages of CE are many, but the potential for rapid analysis and the ability to automate the CE system are among the most appealing to the clinical laboratory.

We investigated two different, yet related, methods of detecting mutations using an am-

Capillary Gel Electrophoresis

A   AGE/Southern Blot Analysis
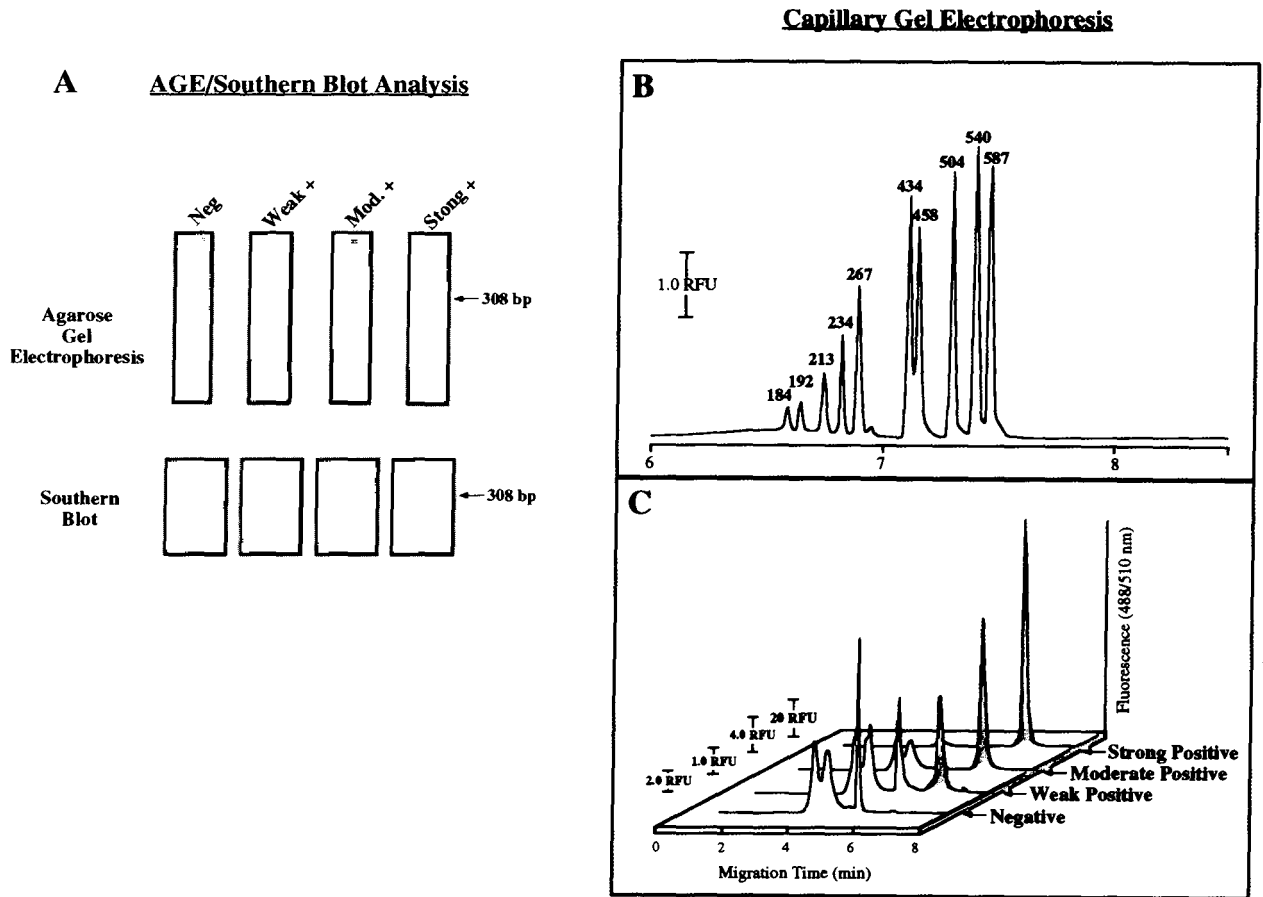
Fig. 4. DNA fragment sizing comparing electrophoretic separation and detection using standard agarose gel and Southern blotting methods, or LIF-pnCE. (A) Illustration of a typical agarose gel and Southern blot results. (B) The degree of resolution obtained with the pnCE system used is illustrated by the separation of a DNA fragment standards (2.5 ng/μl). The size of the DNA fragements is indicated at the top of each peak as the number of base pairs. (C) A stacked figure of electropherograms is illustrated, with the magnitude of the ordinate axis (emission detected at 510 nm) indicated to the left of the figure. The shaded peak represents the amplified DNA product and the range of detected signal for the various samples is indicated to the right of the figure.

plified DNA fragment: SSCP and ddF. Both methods rely on analyzing the ssDNA of a fragment, where the wild type and mutated strands can be differentiated by secondary structural differences formed during non-denaturing polyacrylamide gel electrophoresis. The standard means of analysis requires ^{32}P-labeled material and a non-denaturing polyacrylamide gel separation time of at least 3 h followed by autoradiography (typically overnight exposures). In light of this, the rapid nature of CGE becomes attractive. CE in polymer networks has previous-

ly been shown to be amenable to SSCP analysis [17]. The present results confirm these original findings since CGE was able to separate the ssDNA species of all the DNA fragments tested. However, use of the conditions defined in the present study allowed for separation in a shorter period of time. Furthermore, the addition of ethidium bromide was found to enhance the separation allowing for baseline resolution of some single strands. We can only speculate that this results from intercalator-induced secondary structural changes in the partially duplexed

ssDNA [18]. However, it is unclear why the same effect was not observed with the other sample tested. It is possible that the magnitude of the EtBr-induced structural changes is influenced by the nature of the mutation. Although this pnCE system performed best among those tested, it did not provide the level of resolution needed to differentiate various mutated DNA fragments from the wild-type sequence. This was particularly true for the L363 sample; unlike previous pnCE analyses using SSCP [17]. While there appears to be potential for SSCP-CE analysis as described by others [17], the CGE system described here is of limited application for the rpoB system. Clearly, the resolution achievable with CGE may be improved by altering the parameters affecting the secondary structure formation, namely the ionic strength conditions, temperature and fragment size [19] as well as the inclusion of various intercalating agents. Additionally, resolution may be increased to a functional level through altering the concentration and/or type of polymer utilized as a sieving matrix for the rpoB-derived amplicon.

Dideoxy fingerprinting-CE has not been previously reported in the literature and, based on the preliminary data described in this study, has potential for application in clinical analysis of amplified DNA fragments. The CE conditions described clearly allow for the detection of a single nucleotide base change. As with SSCP-CE, the use of ddF-CE analysis may prove to be advantageous for clinical screening of amplified DNA for mutations. A clear benefit to the use of the ddF analysis is that it is less influenced by the same factors affecting SSCP; therefore, ddF-CE may be the better choice for the post-amplification analysis of some DNA fragments. From the perspective of analysis time, ddF-CE analysis can be accomplished in ≈25 min per sample. As a result, 30 samples could be analyzed in 15 h in comparison with 36 h by acrylamide gel electrophoresis. The development of a clinical ddF-CE approach could include (1) the co-injection of internal markers, which could be used to normalize migration times and (2) the stream-lining of sample preparation techniques to minimize sample handling. With the ddF-CE system described here, this may be accomplished by using a formamide- or urea-based sample buffer which would allow for the ddF reaction products to be mixed directly with sample buffer, boiled, snap-cooled, and analyzed by CGE.

Finally, post-amplification sizing of DNA fragments is a ready-made application for CE and this is supported by the numerous reports in the literature (e.g., Refs. [5,14]). PCR assays that specifically amplify one DNA species, and require a sensitive post-amplification analysis are especially suited to pnCE analysis. The results of the present study illustrate that CE provides qualitative and quantitative information about the amplicon. CE not only affords a rapid analysis time but the inclusion of an intercalator in the buffer can increase the sensitivity dramatically over Southern blot analysis. We are currently conducting a prospective analysis to further compare the routine agarose gel and Southern blot analysis to the CE system described in this study. There is little doubt that the automated CE system will soon replace the currently used agarose and blot system for those amplified products that are specific for a template DNA. Simply altering the format of the CE sample loading tray to accept the 96 well format currently used with some commercial thermocyclers, will allow for tubes to be removed from the thermocycler and placed directly on to the CE for amplicon detection.

In summary, we envision many applications for CE in the clinical setting, especially those that involve the analysis of DNA. The attributes of CE, namely speed and automation, only encourage further investigations into clinical applications. DNA is a ready made analyte, whose potential as an agent in diagnostic evaluation of a patient is being exploited daily. It is clear that routine CE analysis of DNA in the clinical setting is rapidly becoming a reality.

References

[1] J.P. Landers, Clin. Chem., 41 (1995) 495–509.

[2] E.P. Lessa and G. Applebaum, Molec. Ecol., 2 (1993) 119–129.

[3] G. Sarkar, H. Yoon and S.S. Sommer, Genomics, 13 (1992) 441–443.

[4] E. Avaniss-Aghajani, K. Jones, D. Chapman and C. Brunk, BioTechniques, 17 (1994) 144–149.

[5] J.M. Butler, B. McCord, J. Jung, M. Wilson, B. Budowle and R. Allen, J. Chromatogr. B. , 658 (1994) 271–280.

[6] A.C. Whelen, T.A. Felmlee, J. Hunt, D. Williams, G.D. Roberts, L. Stockman and D.H. Persing, J. Clin. Microbiol., 33 (1995) 556–561.

[7] T.A. Felmlee, Q. Lui, A.C. Whelen, D. Williams, S.S. Sommer and D.H. Persing, J. Clin. Microbiol., 33 (1995) 1617–1623.

[8] T.A. Cha, J. Kolberg, B. Irvine, M. Stempien, E. Beall, M. Yano, Q. Choo, M. Houghton, G. Kuo, J. Han and M. Urdea, J. Clin. Microbiol., 29 (1991) 2528–2534.

[9] P.N. Rys and D.H. Persing, J. Clin. Microbiol., 31 (1993) 2356–2360.

[10] A. Guttman, K.U. Ulfelder and H.E. Schwartz, Presented at the 7th International Symposium on High Performance Capillary Electrophoresis, Würzburg, Germany, 1995, Poster £ P428.

[11] J. Sambrook, E.F. Fritsch and T. Maniatis, in Molecular Cloning: A laboratory manual, 1989, Cold Spring Harbor.

[12] A. Guttman, R.J. Nelson and N. Cooke, J. Chromatogr., 593 (1992) 297–303.

[13] A. Guttman and N. Cooke, Anal. Chem., 63 (1991) 2038–2042.

[14] H.E. Schwartz, K. Ulfelder, F.J. Sunzeri, M.P. Busch and R.G. Brownlee, J. Chromatogr., 559 (1991) 267–83.

[15] Q. Liu and S.S. Sommer, PCR Methods and Applications, 4 (1994) 97–108.

[16] T. Felmlee, P.S. Mitchell, K.J. Ulfelder, D.H. Persing and J.P. Landers, J. Cap. Elec., 2 (1995) 125–130.

[17] A.W. Kuypers, P. Williams, M. vander Schans, P. Linssen, H. Wessels, C. de Bruijn, F. Everaerts and D. Mensink, J. Chromatogr., 621 (1993) 149–156.

[18] P.R. Selvin, D.N. Cook, N.G. Pon, W.R. Baurer, M.P. Klein and J.E. Hearst, Science, 255 (1992) 82–85.

[19] K. Hayashi and D. Yandell, Human Mutation, 2 (1993) 338–346.

ELSEVIER

Intrinsic isotachophoretic preconcentration in capillary gel electrophoresis of DNA restriction fragments

M.J. van der Schans*, J.L. Beckers, M.C. Molling, F.M. Everaerts

Laboratory of Instrumental Analysis, Eindhoven University of Technology, P.O. Box 513, 5600 MB Eindhoven, Netherlands

Abstract

Reproducible migration times are required for accurate base-pair assignment of polymerase chain reaction (PCR) products in capillary gel electrophoresis (CGE). However, migration times are influenced by injection plug length and ionic strength of the sample. In this paper we introduce a new isotachophoresis (ITP)–CGE system where the transition from ITP to CGE is achieved by the mobility shift of DNA from free solution (ITP) to sieving gel buffer (CGE). With intrinsic isotachophoretic preconcentration in capillary gel electrophoresis (IICGE) large volume injections (up to 700 nl) are possible with accurate migration times in CGE independent of injection plug length or sample ionic strength.

1. Introduction

Although in capillary zone electrophoresis (CZE) only very small amounts of sample are required, the rather high concentration detection limits are a severe drawback. In order to be able to detect low sample concentrations, large sample volumes have to be injected, and sample analytes have to be concentrated to maintain a high resolution. A popular solution can be sample stacking whereby analytes are introduced at a very low ionic strength compared to that of the background electrolyte (BGE) [1]. Due to the relatively high local electric field, analytes migrate very quickly out of the sample zone and stack down in the BGE.

Field-amplified injection techniques for DNA analyses in capillary gel electrophoresis (CGE) have already been described. For example, a

* Corresponding author.

presample injection of a water plug creates a large field strength at the beginning of the capillary. This enhances the sample introduction into the capillary [2,3].

Another method is the introduction of an isotachophoretic (ITP) preconcentration step followed by separation in zone electrophoresis. In ITP–CZE the sample analytes are initially stacked between leading and terminating electrolytes. The concentration of the sample components are adapted to the concentration of the leading ion according to the Kohlrausch regulation function [4]. After the preconcentration ITP step the terminating ions pass the analyte ions and the analysis changes into zone electrophoresis. Several ITP–CZE combinations have been described. One possibility is the column coupling system described by Mikkers [5] and Everaerts et al. [6]. However, column coupling systems require rather complicated equipment. On-line versions of ITP–CZE can be performed in a

single capillary on a commercial CE instrument. Foret et al. [7] described the possibility of on-column transient preconcentration in CZE. Schwer and Lottspeich [8] presented presample injections of high ionic strength buffer followed by the sample plug. Recently, van der Schans et al. [9] showed roughly the same method to be applicable for the analysis of DNA restriction fragments. However, migration times of equal-sized DNA molecules are not constant because the length of the gel decreases for increasing injection plug lengths. Moreover, non-homogeneous electric field strength distribution induced by sample stacking or ITP preconcentration steps causes migration-time shifts. These shifts lead to inaccurate base-pair assignment of polymerase chain reaction (PCR) products. In this paper we will discuss an ITP–CZE procedure whereby the transition from ITP to CZE is achieved by the mobility shift from free solution to gel buffer. Constant reproducible migration times in the CGE are obtained by creating a constant length of the gel.

2. Experimental

All experiments were performed on a P/ACE 2200 from Beckman Instruments (Fullerton, CA, USA). The instrument was modified to enable pressure injections at 1.8 p.s.i. instead of the instrument's own 0.5 p.s.i. (3447 Pa). Detection was performed by UV absorbance at 254 nm.

Running temperature was kept at 20°C. The length of the polyacrylamide-coated capillary was 47 cm. The effective length to the detector was 40 cm. The voltage was 9.4 kV (200 V/cm) applied in the reversed mode (cathode on injection side) for the zone electrophoresis experiments. For the intrinsic isotachophoretic preconcentration in capillary gel electrophoresis (IICGE) experiments a constant current of 18 μA was established.

2.1. Chemicals

Tris(hydroxymethyl)aminomethane (Tris), acetic acid, boric acid, benzoic acid and hydro-

chloric acid were purchased from Merck (Darmstadt, Germany). Vinylmethoxysilane oligomer was purchased from ABCR (Karlsruhe, Germany). Butyric acid, propionic acid, acrylamide, ammonium persulphate and N,N,N',N'-tetramethylethylenediamine (TEMED) were purchased from Sigma Chemicals (Bornem, Belgium). ΦX174/*Hae*III was purchased from Beckman as supplied in the Beckman dsDNA 1000 kit. The PCR product of 118 bp was kindly donated by A.W.H.M. Kuypers (Nijmegen Academic Hospital, Nijmegen, Netherlands)

2.2. Coating procedure

Capillaries with an I.D. of 100 μm from Scientific Glass Engineering (Milton Keynes, UK) were rinsed with 1 M KOH (3 h), water (0.5 h) and methanol (0.5 h). The capillary was rinsed for 2 h with a mixture of 4 ml methanol, 200 μl acetic acid and 200 μl vinylmethoxysiloxane oligomer. During this treatment vinyl groups were attached to the capillary surface, after which the capillary was rinsed again with methanol and water. Then the capillary was filled with 0.1 M Tris–borate buffer (pH 8.3) containing 5% acrylamide, 0.1% TEMED and 0.1% ammonium persulphate. After 24 h the gel was pushed out of the capillary with water using a gas-tight syringe. The capillary was mounted in a capillary cartridge and rinsed with buffer. This procedure was based on the method described by Hjertèn [10]. However, methoxyvinylsiloxane oligomer was used instead of 3-methacryloylpropyltrimethoxysilane. The coating using 3-methacryloylpropyltrimethoxysilane seems to be less stable because of the presence of the weak ester bond [11]. Our experiences are that the coating using methoxyvinylsiloxane oligomer is more stable.

2.3. Gel buffer

Linear polyacrylamide gel buffers were prepared by polymerisation of 8% acrylamide dissolved in 0.1 M Tris buffer containing 0.5% TEMED and 0.08% ammonium persulphate for 48 h at 4°C [12]. The Tris buffer was adjusted to
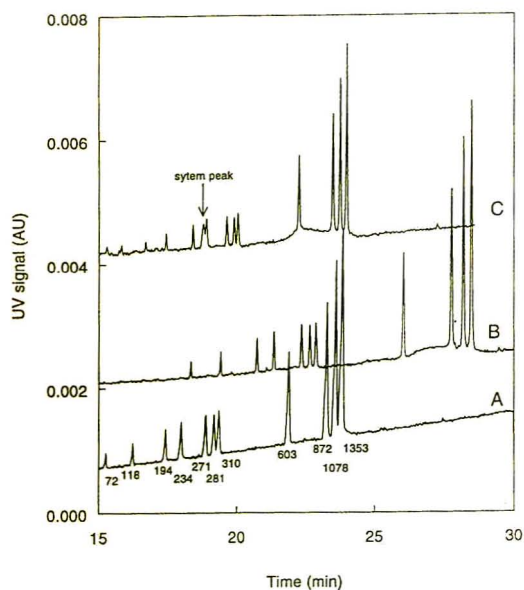
Fig. 1. Electropherogram of the separation of ΦX174/HaeIII. Buffer: 3% polyacrylamide in 50 mM Tris–borate at pH 8.3. Voltage: 9.4 kV. (A) 4-s pressure injection 100 μg DNA/ml. (B) 80-s pressure injection 5 μg DNA/ml. (C) 80-s pressure injection 5 μg DNA/ml in 50 mM KCl, 10 mM Tris–HCl, 1.5 mM MgCl$_2$. Numbers refer to the number of base pairs.

pH 8.3 with hydrochloric acid, boric acid or benzoic acid. After polymerisation the gel was diluted to 3% polyacrylamide with water and

buffer to achieve the appropriate concentration. The use of replaceable gels avoids sample carry over and sample-induced gel damage [13].

3. Results and discussion

3.1. DNA analysis in capillary zone electrophoresis

In Fig. 1 the electropherograms are given for the separations of the ΦX174/HaeIII digest where the sample was introduced at different injection times and different ionic strengths in a 3% polyacrylamide buffer (50 mM Tris–borate at pH 8.3). The viscosity of the gel buffer was 23 cP. A 4-s pressure injection results in a plug length of 2 mm and a 80-s injection in a plug length of 27 mm. Plug lengths and viscosity were determined according to formulas given by Bello et al. [14]. Fig. 1A refers to the 4-s pressure injection. Good resolution is achieved, where all peaks are baseline resolved throughout the range of 72 to 1353 base pairs. Fig. 1B refers to a 80-s pressure injection of ΦX174/HaeIII. The sample component concentration was 20 times lower than in the electropherogram representing the 4-s injection. Good resolution is still achieved due to the induced sample stacking conditions, because the ionic strength of the sample is low

Table 1
Migration times in minutes of DNA fragments analysed in zone electrophoresis in 50 mM Tris–borate buffer at pH 8.3

Injection time (s)	4	80	80	160	160
DNA conc. (μg/ml)	100	5	5	2.5	2.5
Matrix	Water	Water	Salt	Water	Salt
Basepairs					
72	15.3	18.3	15.8	20.2	17.7
118	16.2	19.4	16.7	21.5	18.2
194	17.4	20.8	17.4	23.1	18.9
234	18.0	21.4	18.4	23.8	19.3
271	18.9	22.4	19.6	25.0	19.9
281	19.2	22.7	19.9	25.3	20.1
310	19.4	22.9	20.0	25.6	20.2
603	21.9	26.0	22.3	29.5	22.0
872	23.3	27.8	23.5	31.7	23.1
1078	23.6	28.2	23.7	32.3	23.3
1353	23.9	28.5	24.0	32.7	23.5

and the voltage drop over the sample plug is high. The field strength in the rest of the capillary decreases, resulting in a lower velocity and longer migration times. However, real DNA samples do not have low ionic strengths. In particular, PCR products are delivered in electrolytes containing significant amounts of chloride [15]. Fig. 1C shows the result of 80-s pressure injection of ΦX174/HaeIII dissolved in 63 mM chloride. A system peak appears between 234 and 271 base pairs when large amounts of salt matrix are injected. Again the electropherogram shows good resolution, but this is not achieved by sample stacking. The high ionic strength sample induces a low electric field in the sample plug, but the excess of chloride acts as a leading ion and creates temporary ITP conditions resulting in rather sharp zones [16]. However, migration times of the small base-pair strands (<600 bp) are shifted because the excess of chloride must migrate away first. In Table 1 the migration times of the DNA fragments for different injection times and ionic strengths are given. It can be concluded that migration times are strongly affected by gel length and sample ionic strength.

3.2. Intrinsic isotachophoretic preconcentration capillary gel electrophoresis

Migration times are influenced by the length of the gel and field strength distribution. The solution to this problem therefore must be found in a constant length of the gel and constant electric field distribution during the DNA separation. A new approach to this is the intrinsic isotachophoretic preconcentration in capillary gel electrophoresis (IICGE). The outline of such a system is shown in Fig. 2. First the capillary is filled with gel buffer. Then a plug of free solution buffer with the same electrolyte composition (pre-sample injection) is injected, followed by the sample. The outlet is placed in the leading electrolyte, and the inlet is placed in a terminating electrolyte. The total length of the sample plug and free solution buffer is held constant to maintain a constant length of the gel. Since the polyacrylamide in the buffer is un-
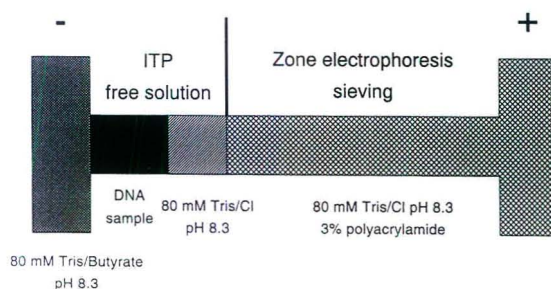
Fig. 2. Outline of the IICGE method. Preconcentration takes place in free solution. Separation takes place in sieving part of the capillary. For further information see text.

charged and the electric osmotic flow is suppressed, the polyacrylamide stays in this position. The pre-sample injection is necessary to create an ITP section, where the sample analytes are concentrated and separated from the excess of chloride. DNA fragments are not separated since they have equal mobility because of a constant charge to mass ratio in free solution [17]. If the ITP stack reaches the gel, the
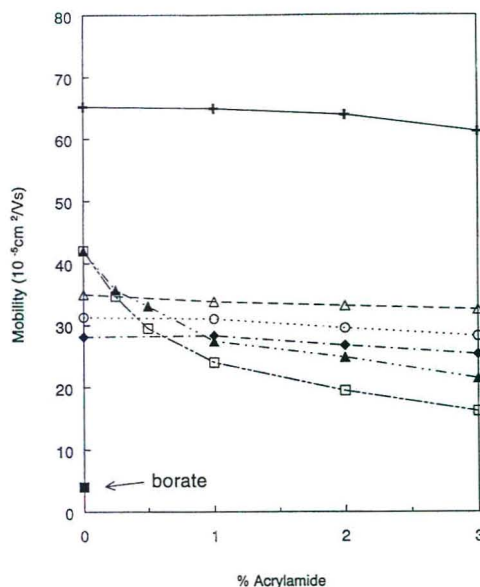
Fig. 3. Mobilities of different ions and DNA versus gel concentration. Mobility of ions are measured in indirect UV mode at 230 nm using a 10 mM Tris–benzoate buffer at pH 8.3. Symbols: + = chloride; △ = acetate; ○ = propionate; ◆ = butyrate; ▲ = 72 bp DNA; □ = 603 bp DNA; ■ = borate.

mobility of the DNA strongly decreases because it is size and gel-concentration dependent in gel [18]. If a suitable terminating ion is chosen, the DNA fragments migrate further in zone electrophoresis. A comparable system has already been described by Ornstein [19] and Davis [20] for proteins, where the transition from ITP to CZE is also achieved by a pH shift (see also Hjertén et al. [21]).

In order to choose a suitable terminating ion, we measured the effective mobilities of several ions in free solution and gel buffer. In Fig. 3 the mobilities of different ions and dsDNA fragments are given for different polyacrylamide concentrations. The mobility could be calculated using field strength, migration time and capillary length. The ions were analysed in a gel buffer using indirect UV detection at 230 nm. The buffer contained 10 mM of Tris adjusted to pH 8.3 with benzoic acid. Sulphate ions from the initiator ammonium persulphate were also present in the sieving buffer. These co-ions can lead to artifacts and system peaks in the electropherogram when indirect UV detection is used and make the electropherogram difficult to inter-

pret [22]. Therefore, the capillary was filled with gel buffer containing Tris–benzoate, whereafter the capillary ends were placed in free solution buffer. A 10-kV voltage was applied for 7 min allowing the sulphate ions to migrate out of the capillary. Then the sample ions were injected and analysed.

Ions like chloride, acetate and propionate are only slightly retarded in gel because of their small size. Chloride is always faster than DNA and can act as leading ion. Acetate, propionate and butyrate have lower mobility in free solution but higher than DNA in a 3% polyacrylamide gel. This means that in free solution these ions will act as a terminator, but they will overtake DNA as DNA will migrate further in a zone electrophoretic way. It is clear that borate does not fulfil this requirement. Borate has a lower mobility than DNA in free solution. The mobility of borate in gel buffer will be lower than the mobility of DNA, too. The injection of sample between chloride and borate would result in a isotachopherogram where no separation of the DNA takes place at all, because DNA remains stacked between chloride and borate (Fig. 4).

Fig. 4. Electropherogram for the separation of ΦX174/HaeIII applying borate as terminator. Capillary and outlet vial: 3% polyacrylamide in 80 mM Tris–HCl at pH 8.3. Inlet vial: 100 mM Tris–borate at pH 8.3. Pre-sample injection: 300 s by pressure 80 mM Tris–HCl at pH 8.3. Sample injection: 10 s by pressure, sample as in Fig. 1A. Current: 18 μA. Solid line = UV signal, dashed line = voltage.

Butyrate was chosen as terminator because of the large difference in mobility between DNA and butyrate in free solution. A large mobility difference will have a more effective zone-sharpening effect.

3.3. DNA analysis using intrinsic isotachophoretic preconcentration in CGE

Fig. 5 shows an electropherogram of ΦX174/HaeIII using IICGE conditions. Tris–chloride buffer was injected for 300 s followed by 100 s injection of sample (sample plug length = 52 mm; total ITP length = 182 mm). The voltage over the capillary is plotted on the right axis. Butyrate ions enter the capillary and must have the same velocity as the chloride ions to fulfil the isotachophoretic condition. This means that the voltage over the capillary increases during the run because of the lower mobility of the terminator. The field strength in the butyrate zone will be constant and therefore also the velocity of the DNA during the separation. The voltage curve shows a smaller slope at the beginning.

The system regulates the concentration of the chloride according to the Kohlrausch regulation function. The chloride concentration in the sample was 63 mM, while the chloride concentration in the buffer was 32 mM. (Dissociation degree of Tris at pH 8.3 is 0.40. Total concentration Tris is 80 mM, so the concentration chloride is 32 mM.) The voltage becomes constant when the last chloride ions leave the capillary and the capillary is totally filled with butyrate. An extra peak is observed when the last chloride ions pass the detector. This peak is caused by impurities in the butyrate electrolyte which are concentrated to very sharp zones and are not retarded by the sieving buffer. It acts as a nice reference peak for the leading–terminator transition and can be used to correct for the amount of chloride introduced in the capillary by the sample. Fig. 6 shows the electropherogram of 50 μg/ml sample injected for 12 s and a 5 μg/ml sample injected for 100 s. With the longer injection time also a long high ionic strength sample plug is introduced, resulting in different migration times for the equal-sized DNA fragments. However, the
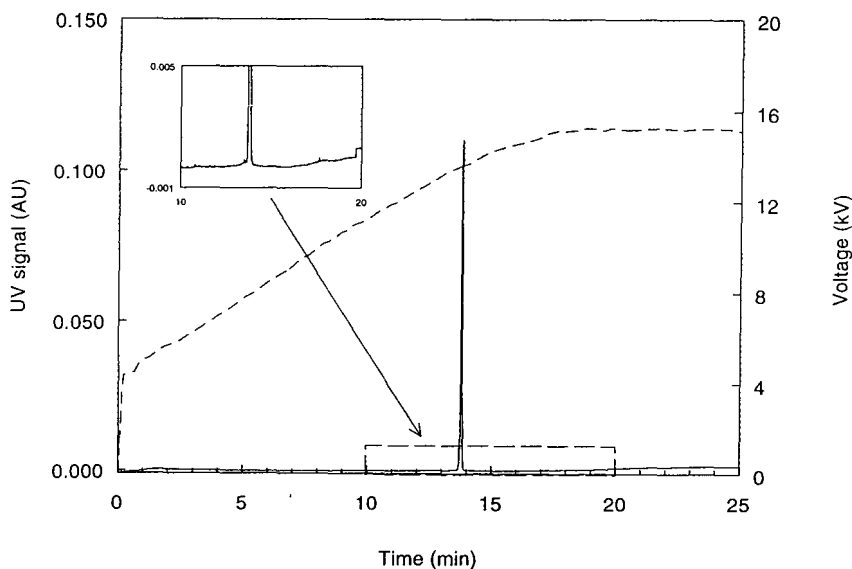

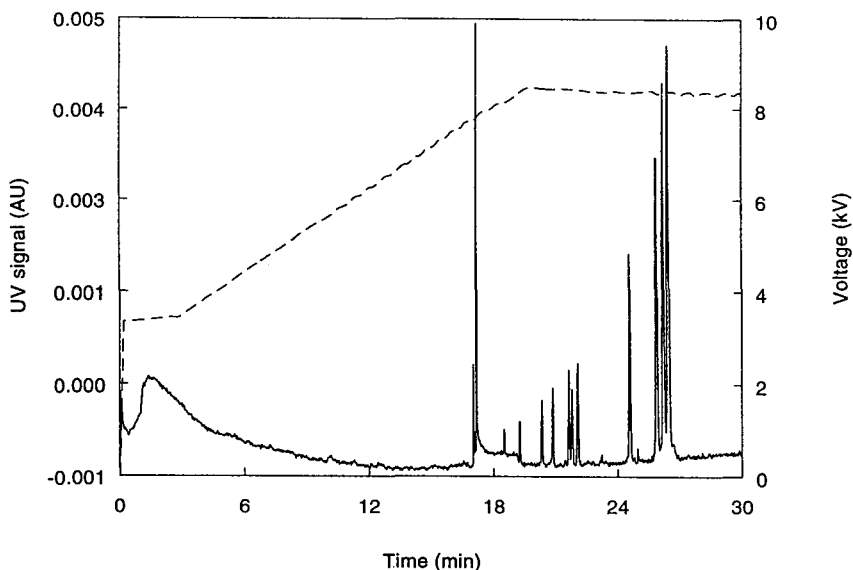Fig. 5. Electropherogram for the separation of ΦX174/HaeIII applying butyrate as terminator. Capillary and outlet vial: 3% polyacrylamide in 80 mM Tris–HCl at pH 8.3. Inlet vial: 100 mM Tris–butyrate at pH 8.3. Pre-sample injection: 300-s 80 mM Tris–HCl at pH 8.3 by pressure. Sample injection: 100 s by pressure, sample as in Fig. 1C. Current: 18 μA. Solid line = UV signal, dashed line = voltage.
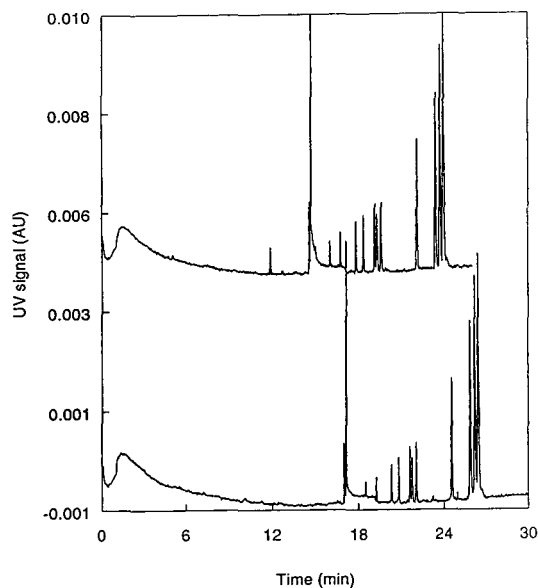
Fig. 6. Electropherograms for the separation of ΦX174/*Hae*III at different injection times. Upper electropherogram: 388-s pre-sample pressure injection of 80 mM Tris–HCl at pH 8.3; 12-s pressure injection of sample 50 μg/ml ΦX174/*Hae*III. Lower electropherogram: 300-s pre-sample pressure injection of 80 mM Tris–HCl at pH 8.3; 100 s pressure injection as in Fig. 1C. Further conditions as in Fig. 5

Fig. 7. Overlay of electropherograms with matched ITP peaks. Further conditions as in Fig. 6

reduced migration times are constant when the two electropherograms are overlaid and the ITP peaks are matched (Fig. 7). Table 2 shows the results of the migration times at different sample injection times. The migration times can be corrected for chloride amount by subtracting the time of the ITP peak from the DNA migration times. The migration times referring to the 210-s pressure injection in water matrix are an exception. A large part of the capillary was filled with very low ionic strength sample, and the ITP steady-state was never reached.

Fig. 8 shows the separation of an ΦX174/*Hae*III and a 118-bp PCR product in a Tris–borate zone electrophoretic system. PCR product and ΦX174/*Hae*III were injected in different runs for 100 s under pressure. Base-pair assignment of the PCR product fails because of differing ionic strengths of the sample. The PCR product has 118 base pairs but migrates like 200 bp compared with the standard. Fig. 9 shows the

same analysis but under IICGE conditions. When the ITP peaks are overlaid, it is clear that the PCR peak of 118 bp migrates exactly like the 118-bp peak of the ΦX174/*Hae*III.

4. Conclusion

Large sample volume injection in CGE leads to inaccurate migration times for equal-sized DNA molecules injected at different plug lengths and ionic strength. Also, stacking and ITP pre-concentration techniques induce heterogeneous field strength distribution, resulting in different migration times. IICGE is a method that makes use of the mobility shift of DNA from free solution to sieving buffer to achieve the transition from ITP to CZE. This can only be realised by the choice of a correct terminator (in this case butyrate), which must be slower than DNA in free solution but faster in the sieving buffer. This method enables the injection of a large sample volume (up to 700 nl) in a capillary of 47 cm. Constant reduced migration times are achieved

Table 2
Migration times and reduced migration times of DNA fragments as achieved in IICGE (reduced migration times are printed bold)

Injection time (s)	12	12	100	100	100	100	210	210	210	210
DNA conc. (μg/ml)	50	50	5	5	5	5	2.5	2.5	2.5	2.5
Matrix	Water	Water	Water	Water	Salt	Salt	Water	Water	Salt	Salt
Basepairs										
ITP	14.6	**0.00**	13.3	**0.00**	17.0	**0.00**	14.2	**0.00**	19.0	**0.00**
72	16.0	**1.47**	14.8	**1.46**	18.5	**1.50**	15.7	**1.54**	20.6	**1.54**
118	16.8	**2.21**	15.6	**2.23**	19.3	**2.25**	16.5	**2.32**	21.4	**2.29**
194	17.8	**3.29**	16.6	**3.31**	20.3	**3.32**	17.7	**3.47**	22.4	**3.37**
234	18.4	**3.81**	17.2	**3.85**	20.9	**3.84**	18.2	**4.00**	23.0	**3.90**
271	19.2	**4.60**	18.0	**4.64**	21.6	**4.61**	19.1	**4.83**	23.8	**4.69**
281	19.3	**4.76**	18.1	**4.80**	21.8	**4.77**	19.2	**5.00**	23.9	**4.84**
310	19.6	**5.04**	18.4	**5.08**	22.1	**5.05**	19.5	**5.30**	24.2	**5.12**
603	22.1	**7.55**	20.9	**7.62**	24.8	**7.56**	22.2	**7.97**	26.7	**7.63**
872	23.4	**8.85**	22.3	**8.95**	25.9	**8.85**	23.6	**9.39**	28.0	**8.95**
1078	23.7	**9.17**	22.6	**9.26**	26.2	**9.16**	23.9	**9.71**	28.3	**9.27**
1353	24.0.	**9.41**	22.8	**9.59**	26.4	**9.39**	24.2	**9.98**	28.6	**9.51**

because the gel length is kept constant, and migration-time shifts caused by different ionic strengths can be easily corrected. This method makes CE more applicable for real sample analysis with a minimum of sample preparation for PCR products.
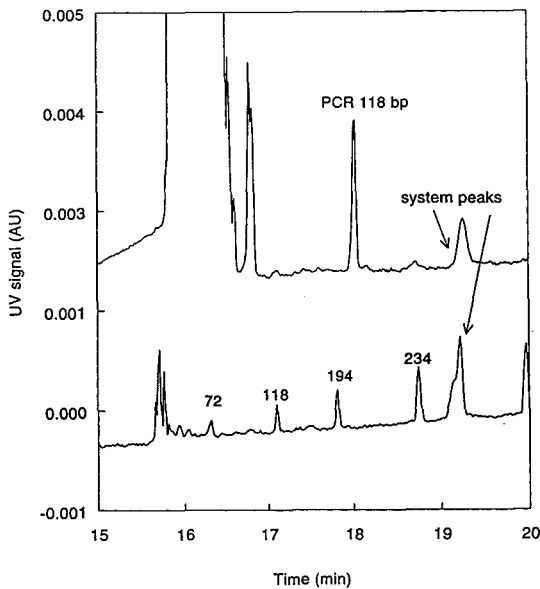
Fig. 8. Base-pair assignment of PCR products fails in CGE using Tris–borate buffer. Upper electropherogram: PCR 118 bp injected for 100 s. Lower electropherogram: sample as in Fig. 1C injected for 100 s. Further conditions as in Fig. 1
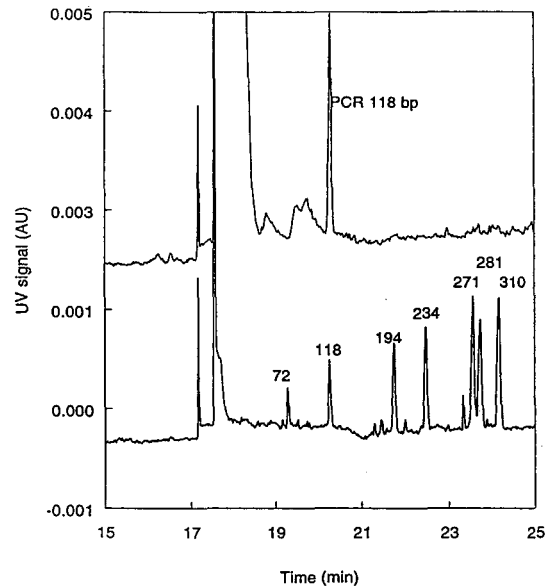
Fig. 9. Correct base-pair assignment of PCR product in IICGE. Upper electropherogram: PCR 118 bp injected for 100 s. Lower electropherogram: sample as in Fig. 1C injected for 100 s under pressure. Further conditions as in Fig. 5

References

[1] D.S. Burgi and R.L. Chien, Anal. Chem., 63 (1991) 2042.

[2] K.J. Ulfelder, H.E. Schwartz, J.M. Hall and F.J. Sunzeri, Anal. Biochem., 200 (1992) 260.

[3] J.M. Butler, B.R. McCord, J.M. Jung, M.R. Wilson, B. Budowle and R.O. Allen, J. Chromatogr. B, 658 (1994) 271.

[4] F.M. Everaerts, J.L. Beckers and T.P.E.M. Verheggen, Isotachophoresis: Theory, Instrumentation and Practice, Elsevier, Amsterdam, 1976.

[5] F.E.P. Mikkers, Thesis, Eindhoven University of Technology, Eindhoven, Netherlands, 1979.

[6] F.M. Everaerts, T.P.E.M. Verheggen and F.E.P. Mikkers, J. Chromatogr., 169 (1979) 21.

[7] F.Foret, E. Szoko and B.L. Karger, J. Chromatogr., 608 (1992) 3.

[8] C. Schwer and F. Lottspeich, J. Chromatogr., 623 (1992) 345.

[9] M.J. van der Schans, J.K. Allen, B.J. Wanders and A. Guttman, J. Chromatogr. A, 680 (1994) 511.

[10] S. Hjertèn, J. Chromatogr., 347 (1985) 191.

[11] M. Huang, W.P. Vorkink and M.L. Lee, J. Microcol. Sep., 4 (1992) 233.

[12] Y.F. Pariat, J. Berka, D.N. Heiger, T. Schmitt, M. Vilenchik, A.S. Cohen, F. Foret and B.L. Karger, J. Chromatogr. A, 652 (1993) 57.

[13] M.H. Kleemiss, M. Gilges and G. Schomburg, Electrophoresis, 14, No. 5–6 (1993) 515.

[14] M.S. Bello, R. Rezzonico and P.G. Righetti, J. Chromatogr. A, 659 (1994) 199.

[15] M.A. Innis and D.H. Gelfland, PCR Protocols — A Guide to Methods and Applications, Academic Press, San Diego, CA, 1990.

[16] J.L. Beckers and F.M. Everaerts, J. Chromatogr., 508 (1990) 19.

[17] B.M. Olivera, P.Baine and N. Davidson, Biopolymers, 2 (1984) 245.

[18] D.N. Heiger, A.S. Cohen and B.L. Karger, J. Chromatogr., 516 (1990) 33.

[19] L.Ornstein, Ann. N.Y. Acad. Sci., 121 (1964) 404.

[20] B.J. Davis, Ann. N.Y. Acad. Sci., 121 (1964) 321.

[21] S. Hjertèn, J.-L. Liao and R. Zhang, J. Chromatogr. A, 676 (1994) 409.

[22] J.L. Beckers, J. Chromatogr. A, 679 (1994) 153.

Determination of black dyes from cotton and wool fibres by capillary zone electrophoresis with UV detection: application of marker technique

H. Sirén[a,*], R. Sulkava[b]

[a]Laboratory of Analytical Chemistry, Chemistry Department, University of Helsinki, P.O. Box 55, University of Helsinki, FIN-00014 Helsinki, Finland
[b]National Bureau of Investigation, Crime Laboratory, P.O. Box 285, FIN-01301 Vantaa, Finland

Abstract

The development of capillary zone electrophoresis (CZE) for routine screening of black reactive dyes and black acid dyes, isolated from cotton and wool materials, is described. Detection was based on UV absorption. The electrolyte solution used was 3-(cyclohexylamino)-1-propanesulphonic acid buffer (pH 10.8), which was chosen to maintain the current at a low level under high voltages. Pretreatment of the cotton and wool samples involved extraction with NaOH or NH_3, respectively. With the CZE technique the dyes were detected at very low concentration levels. The dye components were identified by using a newly developed marker technique. The marker components for the calculations were UV-absorbing phenylacetic acid, benzoic acid and meso-2,3-diphenylsuccinic acid. The marker technique proved effective in determining the electrophoretic mobilities of the analytes, since the relative standard deviations of the migration indices and the electrophoretic mobilities for the analytes were below 0.6%.

1. Introduction

Recently, there have been numerous publications on the determination analysis of dyes and other components in the dye-manufacturing and dye-using industries [1–3]. The methods described have mainly been applied to pure standard dye components.

The excellent separation efficiency of capillary zone electrophoresis (CZE) has created possibilities for the separation and determination of many dyes and other components employed in the dye industry [4–7]. The dyes must be isolated from the matrix and be detectable by ultraviolet

(UV) or fluorescence (FL) detection with routinely available instrumentation.

Acid (anionic) dyes contain hydrophilic groups. These dyes are mostly used for colouring polyamide and wool fibres and are usually substituted by sulphonic acid groups. The dyes are attached to the fibres with ionic interactions, Van der Waals forces and in special cases with coordination bonds. Reactive dyes, which are also anionic, form only covalent bonds with cotton fibres. The most important groups of reactive dyes are those which can form bonds with cellulose fibres containing hydroxyl groups or with protein fibres containing amines, sulphates and thiols or with polyamide fibres [8].

Anionic dyes are rapidly separated by capillary

* Corresponding author.

zone electrophoresis (CZE) [1]. This means that
in these systems electrolyte solutions which have
a high ionic strength and high pH must be used,
but the high ionic strength increases the current
and thus the Joule heating inside the capillary
increases. However, when organic buffers are
present the current remains low even when
electrolytes with high ionic strengths are used.

In this study, CZE was used for the separation
of black reactive dyes and black acid dyes
isolated from cotton and wool, respectively.
Dyeing industry laboratories often do not want
to give information about the dyes they used in
manufacturing processes and it is therefore
sometimes difficult to identify the colour mix-
tures used. However, in our work the marker
techniques developed in our laboratory [9,10]
improved the reliability of the migration values
of the dye components.

2. Experimental

2.1. Apparatus

In this study, two different capillary electro-
phoresis instruments were applied for separation
of the dye components. One consisted of a
ChemStation 3D Capillary Electrophoresis
Model G 1600 AX (Hewlett-Packard, Avondale,
PA, USA), an HP Ergo Ultra VGA monitor, an
HP Vectra 486/66 XM workstation and an HP
DeskJet 510 printer. The system was controlled
by Windows Soft, which was modified to the HP
system. Detection was performed by diode-array
detection (DAD), with collection of the spectra
of peaks in the electropherograms from 190 to
600 nm. The detection wavelengths were 195,
214, 225, 217 and 254 nm. Injection was per-
formed hydrostatically by pressure at 50 bar for
30 s. The voltage was 25 kV. The capillary
cassette was temperature controlled by air pres-
sure. The separation temperature was 22°C.

The other apparatus was a Model 2050 P/ACE
capillary electrophoresis system with UV–Vis
detection and a liquid cooling system for the
capillary (Beckman Instruments, Fullerton, CA,
USA). The detection wavelength was at 254 nm.

Injection was performed hydrodynamically by
pressure (0.500 p.s.i.) for 9 s. The voltage was 18
kV. The separation temperature was 22°C.

CZE runs were carried out in fused-silica
capillaries (50 μm I.D. and 360 μm O.D.)
(Composite Metal Services, Worcester, UK, or
Hewlett-Packard). The lengths of the uncoated
capillaries were 58 or 68 cm (50 or 60 cm to the
detector).

All calculations were carried out with MAT-
LAB (Mathworks, Sherborn, MA, USA). The
algorithms were described earlier [10].

2.2. Materials

3-(Cyclohexylamino)-1-propanesulphonic acid
(CAPS) was obtained from Sigma (Poole, UK),
NaOH, ammonia solution (25%), methanol and
benzoic acid from Merck (Darmstadt, Germany)
and phenylacetic acid (99%) from Aldrich
(Steinheim, Germany). meso-2,3-Diphenylsuc-
cinic acid (TCI, Trade Mark, Japan) was a gift
from Toyohashi University (Toyohashi, Japan).

Distilled water was purified with a Water-I
apparatus (Gelman Sciences, Ann Arbor, MI,
USA) and was further purified by filtering
through 0.45-μm membranes (Millipore, Mols-
heim, France). All chemicals and solvents were
used as received.

Black cotton and wool materials and yarns
were obtained from the Crime Laboratory (Van-
taa, Finland) or were purchased from drapery
shops in Helsinki.

2.3. pH adjustment

The pH of the electrolyte used was adjusted
with a Model 3030 pH meter connected to an
electrode (Jenway, Felsted, UK) containing 4 M
KCl and saturated calomel. The pH meter was
calibrated with standard buffer solutions (pH
7.0 and 10.0) purchased from Radiometer
(Copenhagen, Denmark).

2.4. Electrolyte solutions

A 0.14 M electrolyte solution for CZE sepa-
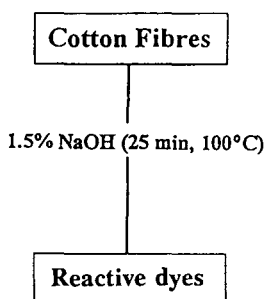rations was prepared from CAPS. The solution

Fig. 1. Extraction of black dyes from cotton materials.

was prepared by adding 3.0982 g of CAPS reagent to about 70 ml of Water-I purified water, adjusting the pH to 10.8 by adding about 5 ml of 0.1 M NaOH and diluting to 100 ml. The solution was filtered through 0.45-μm filters (Millipore) and degassed before use.

2.5. Pretreatment of the samples

The samples were 0.25–5.5 cm^2 of black cloth (cotton or wool) and 2.5 mm–1 cm thread (wool). The samples were pretreated according to Figs. 1 and 2. A 10% (v/v) concentration of methanol was added to the samples to obtain a better stacking effect by decreasing the ionic strength in the sample for narrower component zones. Most of the solvent was evaporated and the precipitate was dissolved into 300 μl of water–methanol (1:1, v/v).

Since the dyes were extracted into a very small

Fig. 2. Extraction of black dyes from wool materials.

volume of solvent, the ionic strengths were too high for direct injection of the sample into the capillary electrophoretic system. Therefore, the samples were always diluted with water (1:10) to improve the zone shapes and electropherograms. Before injection, each sample was filtered through 0.45-μm PTFE filters (Gelman Sciences, Ann Arbor, MI, USA).

3. Results

Usually, pyridine is used as a solvent to extract dyes. However, this study showed that it can be changed to ammonia solution, which is a more convenient solvent for routine work. For surface-treated materials, pyridine can extract those dyes which form salts when extracted with ammonia. It is suggested that pyridine has a catalytic effect, which ammonia does not have, because it only forms ammine complexes with the coloured components.

Figs. 3–5 show the electropherograms of dye components extracted from black cotton and wool fibres. Satisfactory separations were achieved after base extraction from the materials. When the sample sizes were large, the electropherograms were easily screened. However, when the material was surface-treated, the concentrations of the dye components were low, which made the screening of the electropherograms difficult.

The determination of dyes is usually very simple, but black dyes at low concentration levels are difficult to extract and screen with chromatographic separation techniques, since they have different solubilities in water. A high ionic strength was used to help the extraction. However, the extraction had a negative effect on the analysis using CZE. Therefore, the absolute migration times of the components changed from run to run, although the temperature was controlled (Figs. 3–5). Further, even the relative retention times calculated by dividing the absolute migration time of the unknown component by that of the reference component (benzoic acid) changed. The main reason was the high
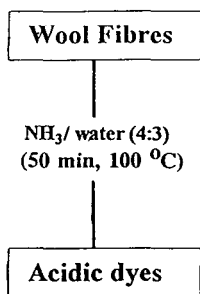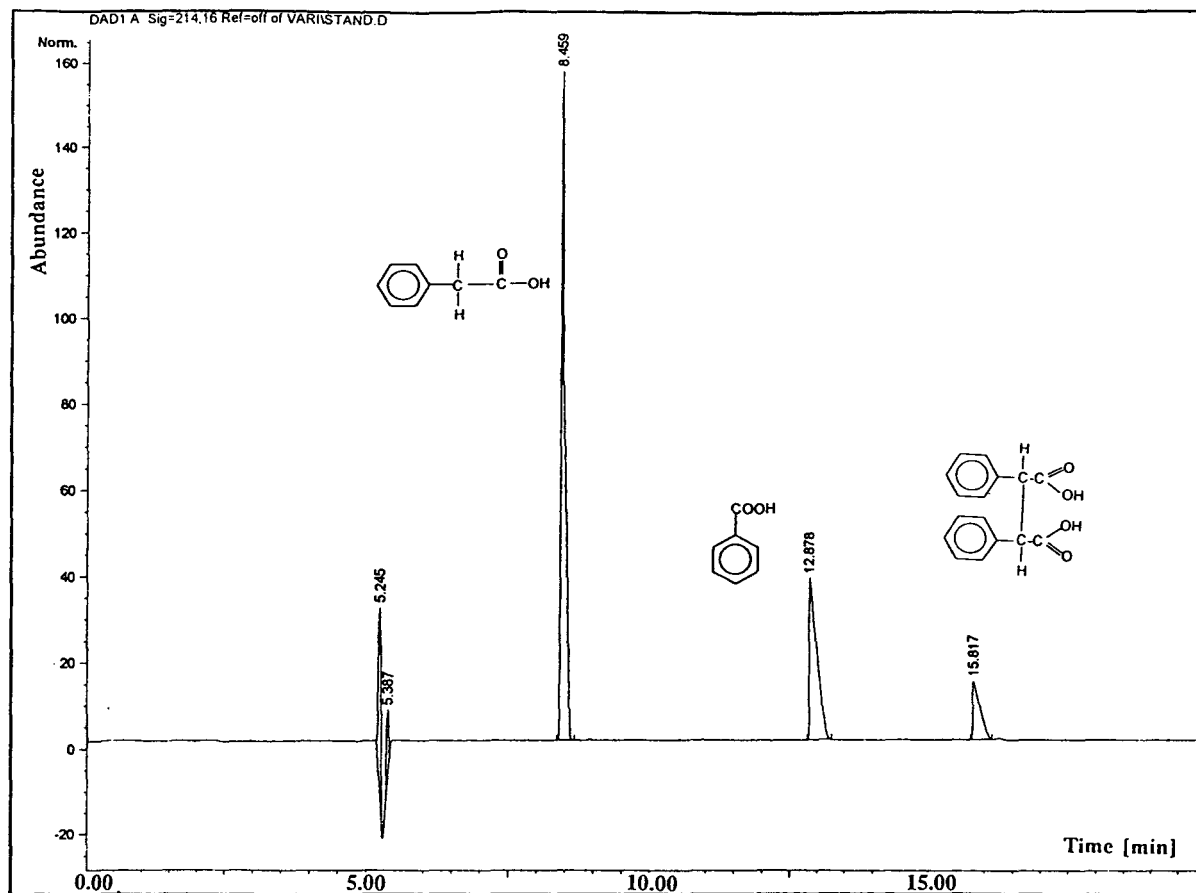
Fig. 3. Electropherogram of the marker compounds obtained with the HP ChemStation 3D capillary electrophoresis Model G 1600 AX instrument. Conditions as described under Experimental.

ionic strength in the sample and therefore the times of the separated component zones changed during the separation processes. This made the screening of the electropherograms very difficult, especially when the components were present at very low concentrations. For these reasons, two different marker techniques were introduced. The results showed that more reliable screening for the dye components could then be achieved. The technique was superior especially when two component zones were overlapped.

The repeatability of the CZE technique was tested by injecting the samples six times. Table 1 shows that the relative standard deviations of the migration indices [10] for two components are below 0.6% and for five components below 0.3%. Also, repeatabilities of electrophoretic mobilities [9] for the analytes (K.S.D. mostly below 0.3%) were superior to absolute migration times (Table 2). These values show that by using the two marker techniques the analyses are more repeatable than when using only absolute migration times (average relative standard deviations 1–2%). In this study, the limits of screening (wavelength 214 nm) were obtained by using 0.5 cm × 0.5 cm textile [signal-to-noise ratio (S/N) = 20] or 2.5 mm thread (S/N = 9), so that all the components present at high concentrations can still be monitored reliably in the electropherograms.

Fig. 4. Electropherogram of a reactive dye from black cotton material (Switzerland) obtained with the Beckman Model 2050 P/ACE instrument.

4. Conclusion

A CZE method with UV detection for screening black dyes from cotton and wool materials has been developed. The method is suitable for the separation processes because of the excellent separation efficiency of CZE. The advantages of the CZE technique could be exploited when the pH method stacking was used.

The recoveries of the black dyes were good (the colour was totally transferred into the solvent), although no reference materials from the manufacturers could be obtained. The repeatabilities of the extraction processes, which were detected for a reference with an UV–Vis dual-beam spectrophotometer, were also very good.

The calculated results were obtained by two marker techniques using phenylacetic acid, benzoic acid and *meso*-2,3-diphenylsuccinic acid as the marker compounds. The use of these carboxylic acids increases the reliability of the separation procedures. The migrations of the dye components were repeatable within a day. Therefore, the peaks in the electropherograms could be easily identified according to the index and the UV spectra taken from the two slopes and the apex of the peaks. No systematic changes in migration indices (Table 1) were found, which confirms that the method is accur-
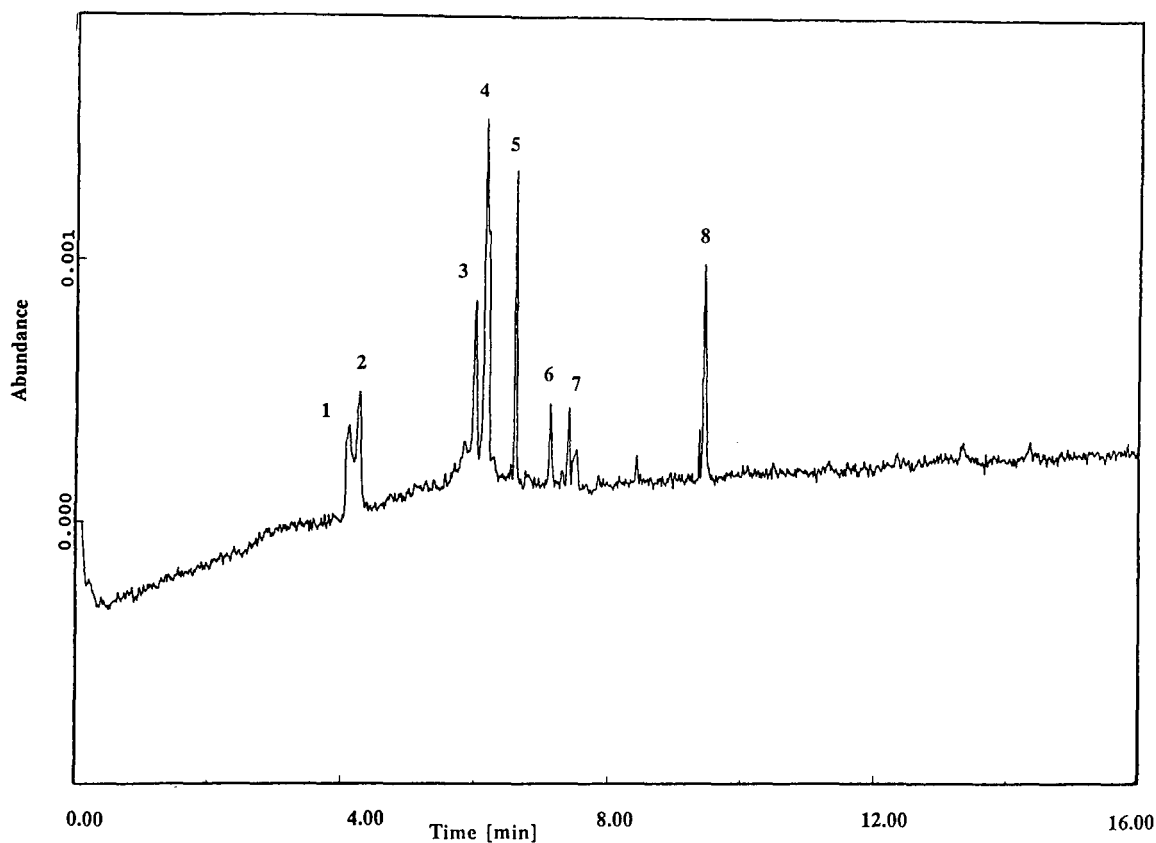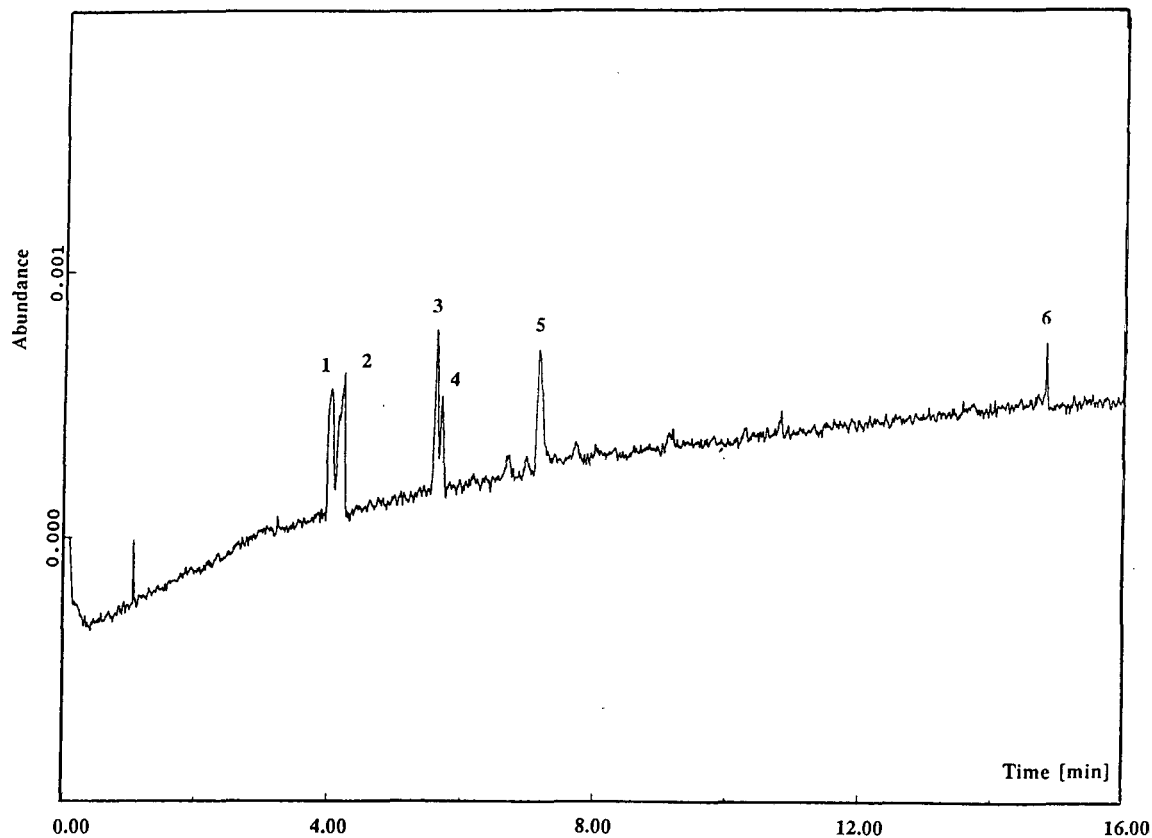
Fig. 5. Electropherogram of an acid dye from black wool material (Finland) obtained with the Beckman Model 2050 P/ACE instrument.

Table 1
Repeatability of the analysis in terms of absolute migration times and migration indices for dye components in black materials

Sample[a]	Compound No.	Absolute migration time (min)	R.S.D. (%)	Migration index	R.S.D. (%)
A	1	4.03	2.32	663.81	0.51
	2	4.20	2.35	691.46	0.22
	3	5.40	2.15	990.32	0.15
	4	6.12	2.02	1060.68	0.24
	5	7.00	0.78	1292.97	0.08
B	1	4.00	0.34	701.10	0.24
	2	4.19	0.38	733.39	0.11
	3	5.61	1.20	983.61	0.07
	4	6.01	0.38	1053.19	0.47
	5	6.73	0.71	1254.99	0.54
	7	7.20	0.35	1342.20	0.14
	8	9.76	0.46	1819.60	0.11

[a] Relative standard deviations within-day (six replicates). A, sample as in Fig. 5; B, sample as in Fig. 4.

Table 2
Average values and standard deviations for absolute migration times and electrophoretic mobilities determined with the marker technique using three aromatic carboxylic acids

Compound[a]	Migration time (min)			Mobility[b] (10^{-8} m^2 V^{-1} s^{-1})		
	$t_{a,ave}$	S.D.	R.S.D. (%)	μ_{ep}(ave)	S.D.	R.S.D. (%)
1	4.06	0.08	1.9	−1.1196	0.0552	0.321
2	4.23	0.06	1.5	−1.2726	0.0492	0.267
3	5.93	0.09	1.5	−1.9265	0.0108	0.258
4	6.10	0.10	1.4	−2.0276	0.0085	0.213
5	6.54	0.08	1.2	−2.3889	0.0072	0.202
6	7.05	0.08	1.1	−2.7296	0.0030	0.109
7	7.35	0.03	1.0	−2.9187	0.0265	0.091
8	9.93	0.07	0.78	−4.1461	0.0072	0.073

Sample as in Fig. 4.
[a] Data obtained with Beckman 2050 instrument.
[b] Calculations according to Ref. [9].

ate. However, good results were only obtained when the samples were analysed fresh within one day, to maintain the accuracy of the results.

Acknowledgement

References

[1] D. Hinks and D.M. Lewis, Eur. Chromatogr. Anal., (1993) 9.
[2] S.M.I. Burkinshaw, D. Hinks and D.M. Lewis, J. Chromatogr., 640 (1993) 413.
[3] T.A. Brettell and R. Sferstein, Anal. Chem., 65 (1993) 293R.
[4] S.N. Croft and D. Hinks, J. Soc. Dyers Colour, 108 (1992) 309.
[5] S.N. Croft and D.M. Lewis, Dyes Pigm., 18 (1992) 309.
[6] K.P. Evans and G.L. Beaumont, J. Chromatogr., 636 (1993) 153.
[7] P. Hänninen, P.J. Karttunen, H. Sirén and M.-L. Riekkola, in P. Sandra and G. Devos (Editors), Proceedings of the 16th International Symposium on Capillary Chromatography, Riva del Garda, 1994, p. 1920.
[8] J. Sundquist, Kemi. Kemi, 11 (1985) 937.
[9] J.H. Jumppanen and M.-L. Riekkola, Anal. Chem., 67 (1995) 1060.
[10] H. Sirén, J.H. Jumppanen, K. Manninen and M.-L. Riekkola, Electrophoresis, 15 (1994) 779.

ELSEVIER

Linear polymers applied as pseudo-phases in capillary zone electrophoresis of azo compounds used as textile dyes

Pavel Blatny[a], Christian-Herbert Fischer[b], Andreas Rizzi[a], Ernst Kenndler[a],*

[a]*Institute for Analytical Chemistry, University of Vienna, Währingerstr. 38, A-1090 Vienna, Austria*
[b]*Hahn-Meitner-Institut, Abt. Kleinteilchenforschung, Glienicker Strasse 100, D-14109 Berlin, Germany*

Abstract

Nine synthetic organic dyes, including seven azo compounds, used as colouring matter for textiles were separated as anions by capillary zone electrophoresis. As most of the solutes are sulfonic acids, the separation could not be effected by varying the pH of the buffer solution. Therefore, two methods were applied to adjust the electrophoretic mobility in a specific way: complexation by bis-tris-propane and interaction with linear polymers added to the buffer and acting as pseudo-phases. A buffer system containing polyethylene glycol and poly-vinylpyrrolidone permits the separation of all analytes. Retention of the dyes caused by the polymeric additives was related to the solute's structure. It was demonstrated by cluster analysis that the relative decrease in the electrophoretic mobility of the dyes correlates with the number of benzoaromatic rings in the solute molecules.

1. Introduction

After the first publication on azo compounds by Griess in 1858, extensive research started. In 1870, Kekulé discovered the coupling reaction of diazotized arylamines with phenols. Orange II (introduced by Roussin in 1876) belonged to the first acidic azo colorants, which dye wool directly and cotton by means of mordants. Acid 88 (synthesized by Caro in 1877) represented progress because of its deeper colour due to an additional aromatic ring [1].

Various techniques for the analysis of dyestuffs have been described [2,3]. Whenever the analytical question is the identification of known dyestuffs and not the structure elucidation of new compounds, separation methods are

superior to those based on spectrometry, because most often the samples consist of blends and/or mixtures with matrix material which interfere with the analytical information. Paper chromatography [4] and thin-layer chromatography [5,6] were the most frequently used techniques for the analysis of organic dyestuffs and still have merits. However, in the meantime new methods have been developed which have great advantages, especially for the compounds of interest. HPLC offers the possibility of applying reproducible solvent gradients and coupling the separation technique on-line with a diode-array spectrophotometer [7]. For acidic dyes, reversed phases (RP) are recommended. They provide some kind of structure–retention relationship, e.g., referring to the number of sulfuric acid groups or to the size of the aromatic skeleton [7].

On the other hand, this method often involves problems arising from the very small retention of

* Corresponding author.

tri- and higher sulfonated compounds, which are fairly common. In those cases ion-pair RP chromatography [8] or ion-exchange chromatography [9] could be applied. However, these methods do not allow one to derive easily structure–retention relationships, which are sometimes useful when there is a lack of reference substances.

Capillary zone electrophoresis (CZE) should be an efficient separation and identification method for the ionic analytes under consideration. In free solution the solutes are separated according to their effective mobilities. For weak acids or bases this property is most dominantly influenced by the pH of the buffer, which enables one to adjust the degree of dissociation of the analytes. This strategy will not succeed, however, for the analytes investigated in this work, because they are mainly strong electrolytes (sulfonic acids). In this case, other strategies must be developed.

One method is commonly used for this purpose: the application of micelles formed in the background electrolyte. This technique, termed micellar electrokinetic capillary chromatography (MECC), has been applied in this context for the separation of some synthetic dyes [10,11]. Another strategy was used in previous work for the separation of diastereometric derivatives of enantiomers [12–14] and also for the improvement of the separation of cationic synthetic dyes [15], namely the use of polymeric additives. These polymers seem to be able to introduce lipophilic interactions with the solutes, and are thus also termed pseudo-stationary phases, in analogy with RP chromatography. Polyethylene glycol (PE) and polyvinylpyrrolidone (PVP) were added to the buffer to adjust separation selectivity in this work.

The impact of the additive on electrophoretic migration was evaluated by cluster analysis [16–18] in order to obtain a better understanding of which analyte property is responsible for the retention of the solute on addition of the polymer. This chemometric method was applied in previous work on capillary electrophoresis to characterize the similarity of electrolyte systems [19–21] and that of solutes [22,23].

2. Experimental

2.1. Chemicals and reagents

The chemicals used for the preparation of the buffer were of analytical-reagent grade (Merck, Darmstadt, Germany). PVP (25; $M_r \sim 25\,000$, Serva, Heidelberg, Germany) and PEG (M_r $2 \cdot 10^6$, Serva) were added to the buffer solution without further purification. Water was doubly distilled before use. The buffer solution was filtered through a membrane filter of 0.2-μm pore size. The dyes and 1,3-bis[tris(hydroxymethyl)methylamino]propane [bis-tris-propane (BTP), 99%+ purity] were purchased from Aldrich (Steinheim, Germany). The dyes were dissolved in water at a concentration of 40 ppm.

2.2. Apparatus

CZE was carried out with a P/ACE System 2100 (Beckman, Palo Alto, CA, USA) equipped with a UV absorbance detector with fixed wavelength (214 nm). The separation capillary was made from fused silica (75 μm I.D., total length 0.269 m, effective length 0.202 m; Supelco, Bellefonte, CA, USA). The temperature was held constant at 25°C. Polyacrylamide-coated capillaries were prepared according to the procedure described by Kilar and Hjerten [24] and modified by Schützner et al. [12]. The conditions of the analysis are described in Table 1.

3. Results and discussion

3.1. Influence of a counter ion with complexing ability

The dyes under discussion (see Fig. 1) can form anions under the appropriate pH conditions. When the pH is not too low, the amino groups on the aromatic ring in compounds D5 and D9 will not be protonated, because the pK_a of such substituted anilines is about 5. In contrast to acidic conditions, at neutral pH the

D1
Natural Blue 2

D2
Acid Yellow 1, Naphthol Yellow

D3
Amaranth, Acid Red 27

D4
Ponceau 2R, Acid Red 26
Xylidine

D5
Methyl Orange, Acid orange 52

D6
Orange II, Acid orange7

D7
Crocein orange G, Acid orange 12

D8
Acid Red 88
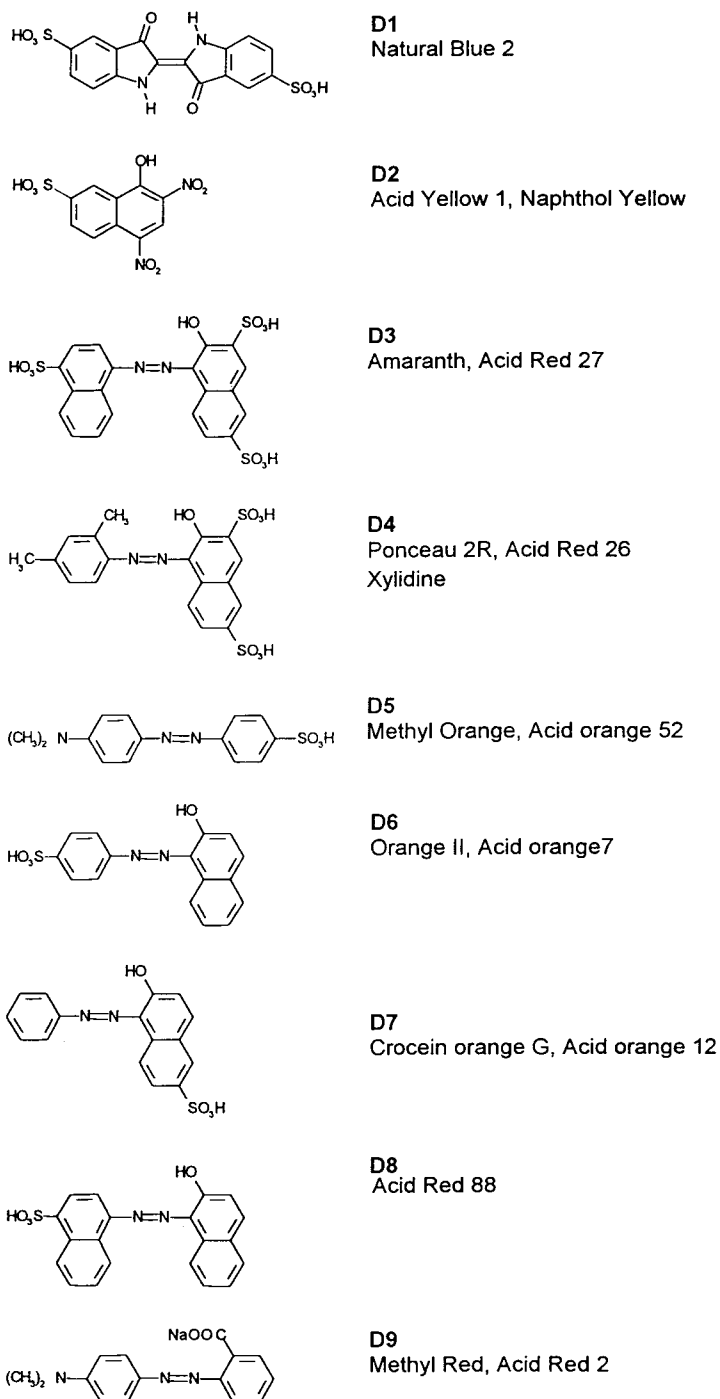
D9
Methyl Red, Acid Red 2

Fig. 1. Structural formulae, abbreviations and trivial names of the organic dyes investigated.

Table 1
Buffers, additives and separation conditions for the electrophoresis of the organic dyes shown in Fig. 1

System	Buffer	Additive	pH	Voltage	Capillary
I	5 mmol/l NaH$_2$PO$_4$–NaOH	None	7.0	−20	Coated
II	5 mmol/l NaH$_2$PO$_4$–NaOH	0.5% PVP	7.0	−10	Coated
III	5 mmol/l NaH$_2$PO$_4$–NaOH	1.0% PVP	7.0	−10	Coated
IV	10 mmol/l BTP–HCl	None	6.5	−20	Coated
V	10 mmol/l BTP–HCl	0.25% PEG	6.5	−10	Coated
VI	10 mmol/l BTP–HCl	0.5% PEG	6.5	−10	Coated
VII	10 mmol/l BTP–HCl	1.0% PEG	6.5	−10	Coated
VIII	10 mmol/l HCl–Ethanolamine	None	10.0	+20	Uncoated
IX	10 mmol/l HCl–Ethanolamine	0.1% PEG	10.0	+10	Uncoated
X	10 mmol/l HCl–ethanolamine	0.25% PEG	10.0	+10	Uncoated
XI	10 mmol/l BTP–HCl	0.5% PEG + 0.01% PVP	6.5	−10	Coated
XII	10 mmol/l BTP–HCl	0.5% PEG + 0.05% PVP	6.5	−10	Coated
XIII	10 mmol/l BTP–HCl	0.1% PVP	6.5	−10	Coated

BTP, bis-tris-propane.

compounds will not form zwitterions, but will migrate electrophoretically as anions owing to the dissociation of the strongly acidic sulfonic (dyes D1–D8) or the weakly acidic carboxylic (dye D9) groups.

However, it can be seen from Fig. 2 that a usual buffer with a neutral pH does not exhibit a sufficiently high selectivity for full separation. A separation according to a difference in pK values would not be efficient for the case of sulfonic acids (they have negative pK values). Some compounds have phenolic groups with pK_a values around 10, but it will be shown below that at high pH co-migration of most solutes is observed. Hence it must be assumed that varying the pH will not improve resolution.

For the oligosulfonic acids, the selectivity can probably be enhanced by using a counter ion with complexing ability, e.g., a higher charged metal cation (Ca, Mg, Cu, Al) or a bivalent organic base such as BTP. This complexing compound has recently been applied to resolve inositol phosphates by capillary isotachophoresis [25,26]. Separation in such a buffer is shown in Fig. 3. In ·comparison with phosphate buffer (with sodium as counter ion, Fig. 2), a significant improvement in the separation is observed, but also in this case some compounds are not separated and co-migrate. It can also be seen that in

this system Acid Red 88 (D8) is separated into two different components (indicated as D8A and D8B).
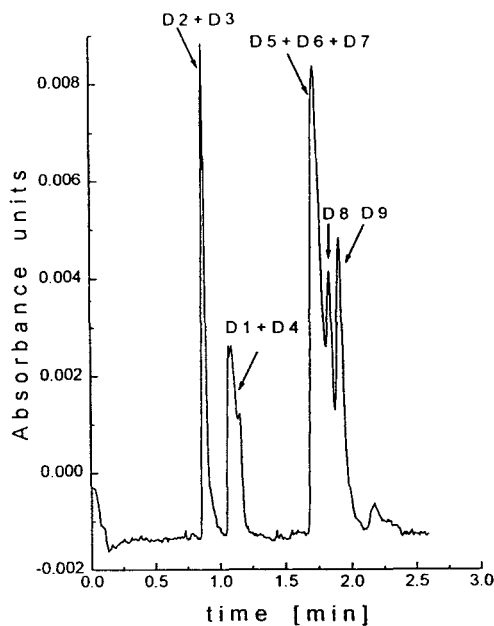

Fig. 2. Electropherogram of the dyes in a coated capillary at pH 7.0 without additive. Numbers as in Fig. 1; separation system I from Table 1 with sodium phosphate as buffer.
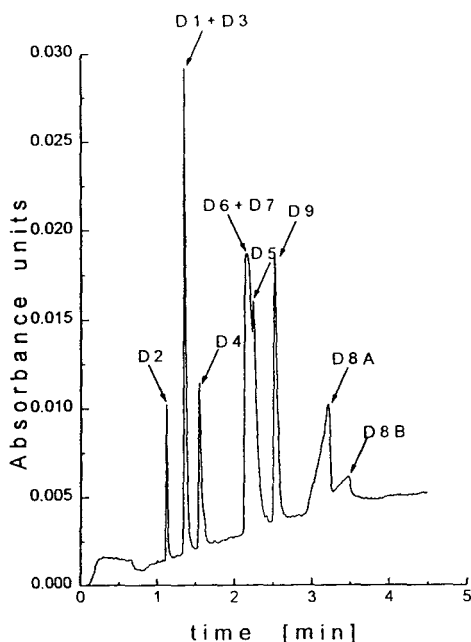
Fig. 3. Electropherogram of the dyes in a coated capillary at pH 6.5 with BTP as counter ion with complexing ability. Numbers as in Fig. 1; separation system IV in Table 1.
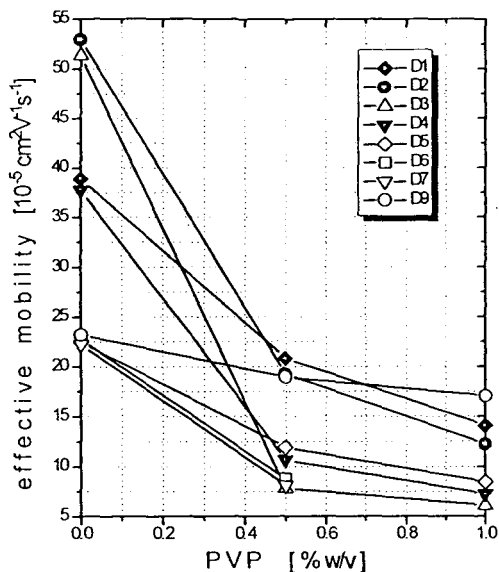

Fig. 4. Influence of the concentration of PVP on the effective mobility of the dyes in sodium phosphate buffer at pH 7.0. The mobilities of dyes D6 and D7 are less than $5 \cdot 10^{-5}$ cm^2 V^{-1} s^{-1} at 1% PVP and are therefore not indicated in the plot at this concentration. This is also the case for the dye D8 at a PVP concentration of 0.5% and higher. Numbers as in Fig. 1; separation systems I, II and III in Table 1.

3.2. Effect of linear polymers added as pseudo-phases

It was pointed out above that variation of the pH will not affect the separability of most of the analytes under consideration. For this reason, another approach was selected to enhance the selectivity, namely the use of linear polymers added as pseudo-phases to the background buffer. PVP and PEG were chosen as polymers. In Fig. 4, the influence of the concentration of PVP added to the phosphate buffer on the effective mobilities of the separands is depicted. It is apparent that PVP is a very efficient pseudo-phase for the dyes, because even 0.5% of the polymer reduces the effective mobilities by at least a factor of two and, moreover, it changes the migration sequence in a number of cases. The strongest affinity of PVP was found for Acid Red 88 (D8); 0.5% of PVP decreased the effective mobility of this compound to less than

$5 \cdot 10^{-5}$ cm^2 V^{-1} s^{-1} (this limiting value is given by the time of measurement, which was chosen as 20 min maximum). Such a low mobility was also found for Orange II and Crocein Orange G (D6 and D7) at a PVP concentration of 1%.

PEG was found to have less influence than PVP on the selectivity. The effect of the addition of PEG on the effective mobilities was investigated in buffers based on BTP, because it was expected that with the complexing counter ion even smaller changes in selectivities caused by the polymer would suffice to enhance the separation. The result of this investigation is depicted in Fig. 5. It can be seen that all mobilities decrease slightly with increasing concentration of PEG, and also some changes in the migration order are found. In Fig. 6 only a partial improvement of the separation is visible compared with the buffer without PEG (Fig. 3).

The influence of addition of PEG to the buffer on the mobilities of the dyes was investigated
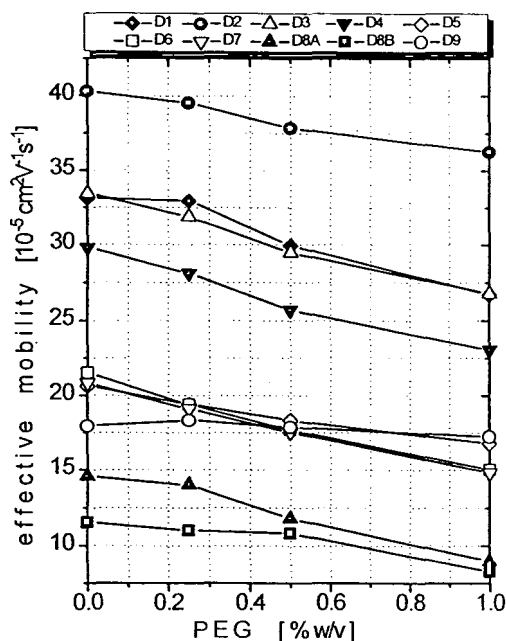
Fig. 5. Effect of the concentration of PEG on the effective mobilities of the dyes at pH 6.5 with BTP as complexing counter ion. Number as in Fig. 1; separation systems IV, V, VI and VII in Table 1.
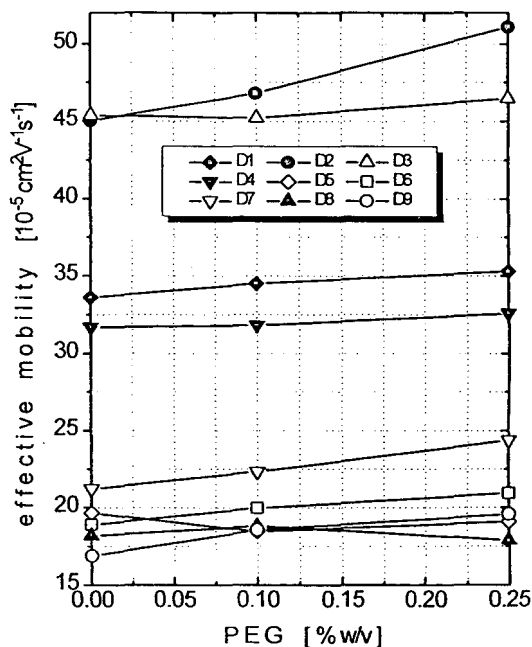

Fig. 7. Influence of PEG on the effective mobility of the dyes at pH 10. Numbers as in Fig. 1; separation systems VIII, IX and X in Table 1.
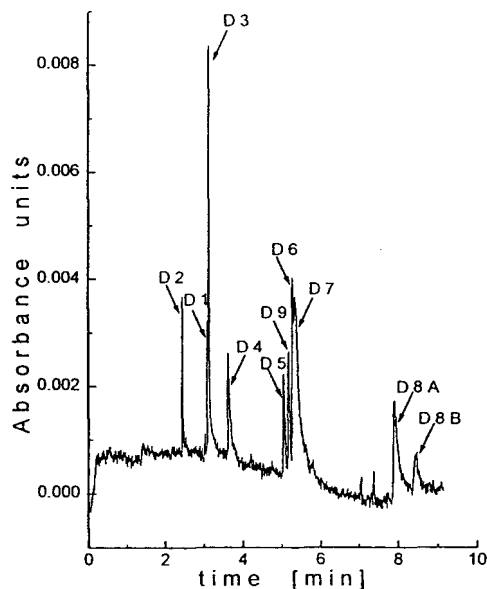

Fig. 6. Electropherogram of the dyes in a coated capillary at pH 6.5 with BTP as complexing counter ion and PEG as stationary pseudo-phase. Numbers as in Fig. 1; concentration of PEG, 0.5% (w/v) (separation system VI in Table 1).

also at high pH (10.0), as mentioned above. The result of this investigation is shown in Fig. 7. It can be seen that for a number of solutes the measured effective mobilities increase slightly with increasing PEG concentration, an unexpected effect, which can be possibly related to inconstancy of the temperature inside the capillary. Nevertheless, it can be concluded that a concentration of even 0.1% leads to a significant improvement in the separation. In Figs. 8 and 9 two systems are shown for comparison, one without PEG and the other with 0.1% of PEG. It can be seen that D1–D4 and D2–D3 become fully separated on addition of PEG, and also D6–D7 show baseline separation. However, three dyes (D5, D8 and D9) still co-migrate, because the selectivity is not sufficient using only PEG as a pseudo-phase.

For further optimization of the separation, the selective reduction of the effective mobility of dyes D3 and D5 by PVP was utilized. For this reason the migration behaviour of the solutes in
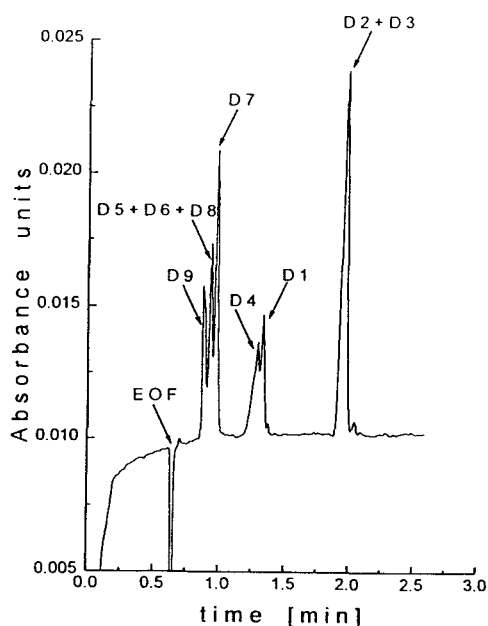
Fig. 8. Electropherogram of the dyes in an uncoated capillary at pH 10.0. Numbers as in Fig. 1; separation system VIII in Table 1.
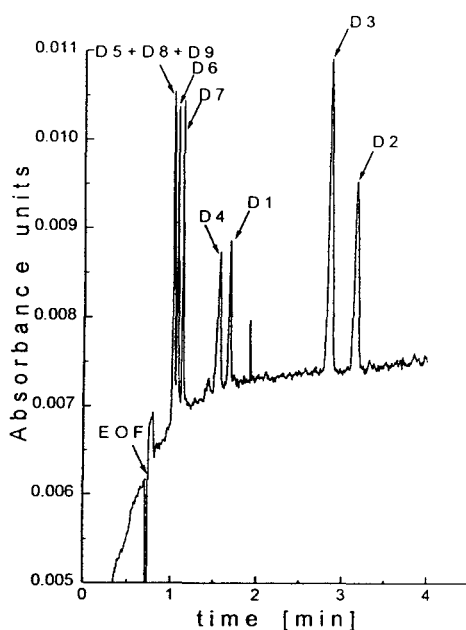
the buffer based on BTP with 0.5% of PEG was influenced by PVP added at very low concentration.

The results of this investigation are depicted in Fig. 10. The addition of 0.05% of PVP led to the separation of all compounds. Even such a low concentration of PVP leads to baseline drift, which was not observed in the buffer without PVP. This baseline drift was, on the other hand, well reproducible and could be compensated for easily by the use of the computer software by subtraction of the signal from the blank run (injection of water).

An electropherogram after such a subtraction is shown in Fig. 11. All compounds were separated in this mixed system. It should be mentioned, however, that Acid Red 88 (D8) migrates with an effective mobility of less than $5 \cdot 10^{-5}$ cm^2 V^{-1} s^{-1}, which leads not only to a long analysis time but also causes several problems with detection in this system, because the peak of this component is very broad under these conditions and can hardly be distinguished

Fig. 9. Electropherogram of the dyes at pH 10.0 in the presence of PEG (0.1%, w/v). Numbers as in Fig. 1; separation system IX in Table 1.
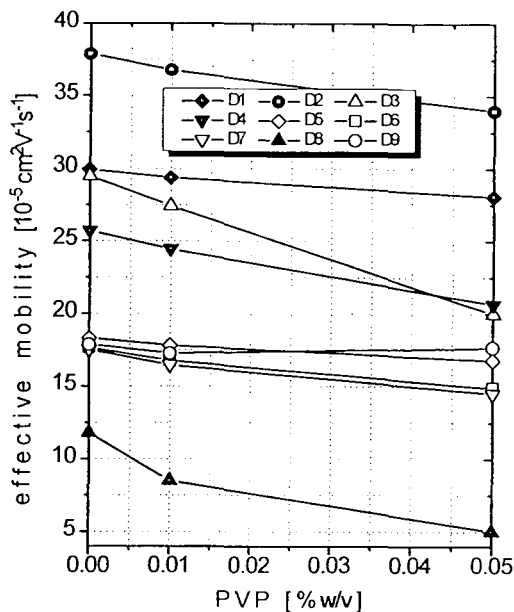

Fig. 10. Effect of the concentration of PVP on the effective mobility of the dyes in the separation system at pH 6.5 (BTP–HCl, 0.5% PEG). Numbers as in Fig. 1; separation systems VI, XI and XII in Table 1.
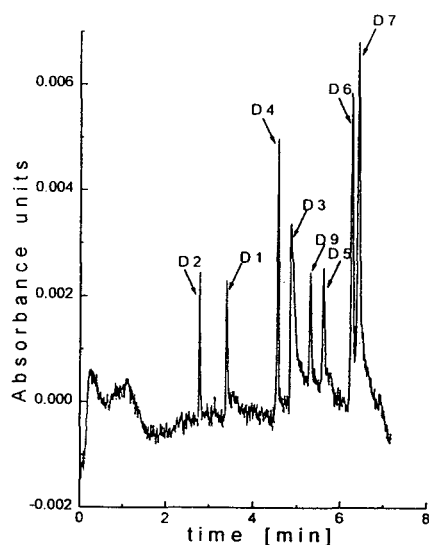
Fig. 11. Optimized electropherogram of the dyes in a coated capillary with a buffer at pH 6.5 with BTP as counter ion, 0.5% (w/v) PEG and 0.05% (w/v) PVP. Electropherogram of a blank run was subtracted. Numbers as in Fig. 1; separation system XII in Table 1.

from the noisy baseline, especially at low concentrations. If this component must be identified in the sample, the use of another separation system, IV in Table I, is therefore recommended, which allows the determination of Acid Red 88 in a much shorter time, within less than 4 min (see Fig. 3).

3.3. Relationship between solute structure and retention caused by the polymeric additive

The number of solutes studied is too small to allow a full interpretation of the relationship between the structure of the separands and the extent of interaction with the polymer. Some conclusions can be drawn, however, when the retarding effect of the polymer (PVP is considered because of its much stronger effect compared with PEG) on the dyes is expressed as the relative change in the solute mobility, as given in Table 2. It seems that within given buffer systems the relative retardation follows the number of benzoaromatic rings in the dye molecules. The solutes with two benzoaromatic rings exhibit the smallest retardation effect. Within this group, dye D9 is affected only to a minor extent by the polymer. Interestingly, D9 is the only component with a carboxylic function, in contrast to the other eight solutes, which are sulfonic acids. The dyes with four benzoaromatic rings, on the other hand, show the most pronounced retardation effect of all the compounds under consideration.

For better visualization, the azo-sulfonates are grouped by a sequential, hierarchical cluster analysis based on the average linkage algorithm, taking the solutes as the taxonomic units, and the relative mobility data from Table 2 as the features for constructing the corresponding simi-

Table 2
Effect of the polymer network on the retention of the solutes

Dye substance	No. of benzoaro-matric rings	$\dfrac{u^{(I)} - u^{(II)}}{u^{(I)}} \cdot 100$	$\dfrac{u^{(I)} - u^{(III)}}{u^{(I)}} \cdot 100$	$\dfrac{u^{(IV)} - u^{(XIII)}}{u^{(IV)}} \cdot 100$	$\dfrac{u^{(VI)} - u^{(XI)}}{u^{(VI)}} \cdot 100$	$\dfrac{u^{(VI)} - u^{(XII)}}{u^{(VI)}} \cdot 100$
D1	2	49	65	17	1.9	6.2
D2	2	59	75	21	2.9	10.2
D5	2	46	62	21	2.7	8.2
D9	2	15	25	4	3	1
D4	3	73	82	36	4.9	20
D6	3	62	>82	36	5	16
D7	3	64	>82	36	5.9	17
D3	4	82	87	48	7	32
D8	4	>80	>80	>69	28	57

The relative retention (%) is given by the difference between the effective mobility, u, of the solute in buffer without polymer to that with polymer, related to the former. Numbers of dye substances as in Fig. 1; buffers (indices of the mobilities) as in Table 1.
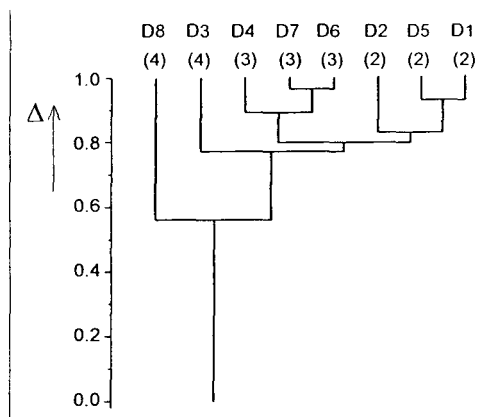
Fig. 12. Dendrogram as the result of the cluster analysis, demonstrating the relationship between the retarding influence of the polymeric additives and the structure of the dyes. Numbers of dyes as in Fig. 1. Numbers of benzoaromatic rings are given in the parentheses. Δ = normalized Euclidian distance.

larity matrix. The measure of (dis)similarity is the Euclidian distance between the taxonomic units in the five-dimensional vector space (five is the number of electrolyte systems).

The resulting dendrogram is shown in Fig. 12. The solutes with the same number of benzoaromatic rings are grouped in the subclusters formed. This result supports the assumption that the lipophilic interaction between the solutes and the polymeric additive is responsible for retardation.

4. Conclusions

It is possible to identify the dyes under discussion by CZE using different linear polymers as pseudo-phases to enhance the separation selectivity. The mobility of the solutes is not related to the viscosity, which is not surprising because Walden's rule (which states that the product of ionic conductivity and viscosity coefficient is a constant for different solvent systems) is not obeyed in many cases. This phenomenon can be related to the fact that the viscosity is a measure of the bulk phase, which clearly will be influenced when linear polymers are present in the solution. The charged dye molecules, on the

other hand, moving through the solvent encounter the local viscosity of the environment, which may be affected by the polymer to a much smaller extent; the latter, not the former, determines the electrophoretic migration properties of the analyte. The extent of interaction of the dye with the polymer and thus its retardation increase with increasing number of benzoaromatic rings in the solute molecule.

From the practical point of view, it can be concluded that the identification of synthetic dyes used as textile colorants is possible using a system with BTP as a buffering and complexing ion at pH 6.5, with 0.5% of PEG and 0.01% of PVP. For better detectibility of Acid Red 88 and to avoid too long run times, the identification of this single analyte can be performed in the same buffer without a polymeric additive in less than 4 min.

References

[1] W. Kratzert, R. Peicher, Farbstoffe, Quelle und Meyer, Heidelberg, 1981.
[2] K. Venkataraman (Editor), The Analytical Chemistry of Synthetic Dyes, Wiley, New York, 1977.
[3] Ch.-H. Fischer, in Encyclopedia of Analytical Science, Academic Press, London, 1995.
[4] J. Sramek, in K. Venkataraman (Editor), The Analytical Chemistry of Synthetic Dyes, Wiley, New York 1977.
[5] H. Schweppe, A. Brockes, A. Berger and D. Strocka, in Ullmanns Encyklopädie der Technischen Chemie, 4th ed., 1976.
[6] H. Schweppe, in K. Venkataraman (Editor), The Analytical Chemistry of Synthetic Dyes, Wiley, New York, 1977.
[7] Ch.-H. Fischer, M. Bischof and J.G. Rabe, J. Liq. Chromatogr., 13 (1990) 319–331.
[8] C. Prandi, 18th Fatipec-Congress, Vol. 3, 1987, pp. 521–529.
[9] I.L. Weatherall, J. Liq. Chromatogr., 14 (1991) 1903–1912.
[10] S.M. Burkinshaw, D. Hinks and D.M. Lewis, J. Chromatogr., 640 (1993) 413–417.
[11] S. Suzuki, M. Shirao, M. Aizawa, H. Nakazawa, K. Sasa and H. Sasagawa, J. Chromatogr. A, 680 (1994) 541–547.
[12] W. Schützner, G. Caponecchi, S. Fanali, A. Rizzi and E. Kenndler, Electrophoresis, 15 (1994) 769–773.
[13] W. Schützner, S. Fanali, A. Rizzi and E. Kenndler, J. Chromatogr., 639 (1993) 375–378.

[14] W. Schützner, S. Fanali, A. Rizzi and E. Kenndler, J. Chromatogr., in press.

[15] P. Blatny, Ch.-H. Fischer and E. Kenndler, Fresenius' J. Anal. Chem., in press.

[16] D.L. Massart, A. Dijkstra and L. Kaufman, Evaluation and Optimization of Laboratory Methods and Analytical Procedures, Elsevier, Amsterdam, 1978.

[17] D.L. Massart, B.G.M. Vandeginste, S.N. Deming, Y. Michotte and L. Kaufman, Chemometrics: A Textbook, Elsevier, Amsterdam, 1988.

[18] E. Kenndler, in N. Guzman (Editor), Capillary Electrophoresis Technology, Marcel Dekker, New York, 1993.

[19] E. Kenndler and G. Reich, Anal. Chem., 60 (1988) 120–124.

[20] E. Kenndler and B. Gassner, Anal. Chem., 62 (1990) 431–436.

[21] E. Kenndler and P. Jenner, J. Chromatogr., 390 (1987) 185.

[22] E. Kenndler and P. Jenner, J. Chromatogr., 390 (1987) 169.

[23] E. Kenndler, C. Schwer and P. Jenner, J. Chromatogr., 470 (1989) 57–68.

[24] F. Kilar and S. Hjerten, Electrophoresis, 10 (1989) 23–29.

[25] P. Blatny, F. Kvasnicka and E. Kenndler, J. Chromatogr. A, 679 (1994) 345–348.

[26] P. Blatny, F. Kvasnicka and E. Kenndler, J. Agric. Food Chem., 43 (1995) 129–133.

Separation of phenylenediamine, phenol and aminophenol derivatives by micellar electrokinetic chromatography Comparison of the role of anionic and cationic surfactants

C. Sainthorant[a], Ph. Morin[a,*], M. Dreux[a], A. Baudry[b], N. Goetz[b]

[a]*Laboratoire de Chimie Bioorganique et Analytique (LCBA), Université d'Orléans, BP 6759, 45067 Orléans, France*
[b]*L'Oréal, 1 Avenue Eugene Schueller, 93600 Aulnay-sous-Bois, France*

Abstract

A mixture of phenylenediamine, aminophenol and phenol derivatives was studied with capillary zone electrophoresis (CZE) at different pHs. The use of acidic or alkaline pH did not give separations with a good resolution. Next, separation was performed using micellar electrokinetic capillary chromatography (MEKC), first with the anionic surfactant sodium dodecyl sulfate (SDS) and second with the cationic surfactant cetyl trimethylammoniumchloride (CTACl). In both cases, a study of pH, surfactant concentration and ionic strength of the electrolyte as function of the capacity factor allowed for the determination of the optimum conditions.

Since separation was obtained with both surfactants, we studied the distribution coefficient to determine the affinities of the solutes for the aqueous medium and the different surfactants.

1. Introduction

Capillary electrophoresis (CE) is a modern analytical technique in rapid development. The high efficiencies and high resolution achieved allow for separations similar to those obtained with high-performance liquid chromatography (HPLC). CE has a large field of applications, e.g. the separation of ionizable solutes by capillary zone electrophoresis (CZE) [1] and the separation of neutral compounds by micellar electrokinetic capillary chromatography (MEKC), developed by Terabe et al. [2]. Most reports on MEKC use sodium dodecylsulphate (SDS) at concentrations higher than its critical

micellar concentration (CMC). Analytes are dissolved in the aqueous phase (moving at the electroosmotic flow velocity) and the pseudo-stationary phase (moving in the opposite direction as the electroosmotic flow of the negatively-charged micelles). Thus, the distribution of solutes over these two phases induces a difference in the migration velocities of the analytes which allows their resolution. One of the major advantages of capillary electrophoresis is the ability to resolve in the same run a mixture of anions, cations and neutral compounds.

Oxidative hair colorants are permanent hair colourers usually composed of a dye precursor and coupler in an alkaline medium and hydrogen peroxide. Hydrogen peroxide reacts with a primary intermediate (precursor, e.g. 1,4-diaminobenzene or 4-aminophenol) to produce an imine, which in its turn reacts rapidly with a

---

* Corresponding author.

second intermediate (coupler, e.g. 3-amino-phenol or resorcinol) to produce the dyes [3–5]. The groups which are responsible for the attractive forces of the oxidative dyes are the amino and hydroxy groups, the attractive behaviour also being dependent on the positions of these groups. As precursors phenylenediamines, diaminophenols and aminophenols are used which have their amino or hydroxy groups in *ortho* or *para* positions. The *meta*-diamines, the *meta*-aminophenols and the polyphenols are used as couplers. For a good colour quality, the composition of the dye has to be carefully controlled. Several selective analytical methods have been proposed for the identification and determination of this class of compounds, e.g. thin-layer chromatography [6], gas chromatography [7], mass spectrometry [8], high-performance liquid chromatography [9,10] and more recently capillary electrophoresis (isotachophoresis) [11]. Nowadays, the analysis of oxidative dyes is achieved by HPLC.

Our aim was to determine the ability of capillary electrophoresis to resolve such aromatic solutes by CZE, and next by MEKC using anionic (SDS) and cationic [cetyl trimethyl-ammoniumchloride (CTACl)] surfactants. To this end we selected the fourteen aromatic solutes (diamines, aminophenols, toluenediamines and phenols with different substituents) shown in Fig. 1.

2. Experimental

2.1. Apparatus

Part of the experiments were performed on a Spectraphoresis 2000 CE instrument (TSP, San José, CA, USA) equipped with a variable-wavelength UV–Vis absorbance detector, an automatic injector and an autosampler. It consists of a thermostated cartridge containing a silica capillary tube with an internal diameter of 50 μm, a total length of 70 cm (or 44 cm) and a injector–detector length of 63 cm (or 37 cm), respectively.

The other experiments were performed on a Beckman P/ACE 2100 (Beckman Instruments, Fullerton, CA, USA). The part of the capillary used for separation was kept at a constant temperature by immersion in a cooling circulation in the cartridge. The detection window was 100×800 μm. Fused-silica capillaries of 50 μm I.D. and 47 cm length (40 cm to the detector) were used. The UV detector was equipped with wavelength filters (190, 214, 254, 280 nm). In our experiments, the separation was carried out at 214 nm, using an applied voltage of $+20$ kV. A temperature of 25°C was selected to avoid dye oxidation. The pH of each electrolyte was checked using a Beckman pH meter (Model ϕ10, Beckman).

The capillaries were daily conditioned by rinsing first with 1 M sodium hydroxide (10 min) at 60°C, water (10 min) at 60°C, then 0.1 M sodium hydroxide (10 min) at 40°C, water (10 min) at 40°C, and finally the running electrolyte (30 min) at 25°C. The same washing procedure was used in MEKC, except for the last step where we used the electrolyte containing the surfactant (15 min) at 25°C. Between two analyses, the capillary tubes were flushed at 25°C with electrolyte (5 min) for CZE and with water (3 min) and electrolyte (5 min) at 25°C for MEKC, in order to improve reproducibility of the electroosmotic flow and migration times of the analytes.

2.2. Chemicals

All chemicals were of analytical reagent grade. Sodium dihydrogenphosphate (Fluka, Buchs, Switzerland), boric acid (Fluka), phosphoric acid (Carlo Erba, Milan, Italy), 1 M sodium hydroxide (Aldrich, Milwaukee, WI, USA), 0.1 M sodium hydroxide (Aldrich), sodium dodecylsulphate (SDS) (Fluka) and cetyl trimethylammoniumchloride (CTACl) (Aldrich) were used without further purification. Water used for dilutions or as electrolyte solution was of HPLC grade (Fison, Farmitalia, Milan, Italy).

Methanol and anthracene were used to determine the migration times of a neutral unretained solute and of micelle tracer, respectively.
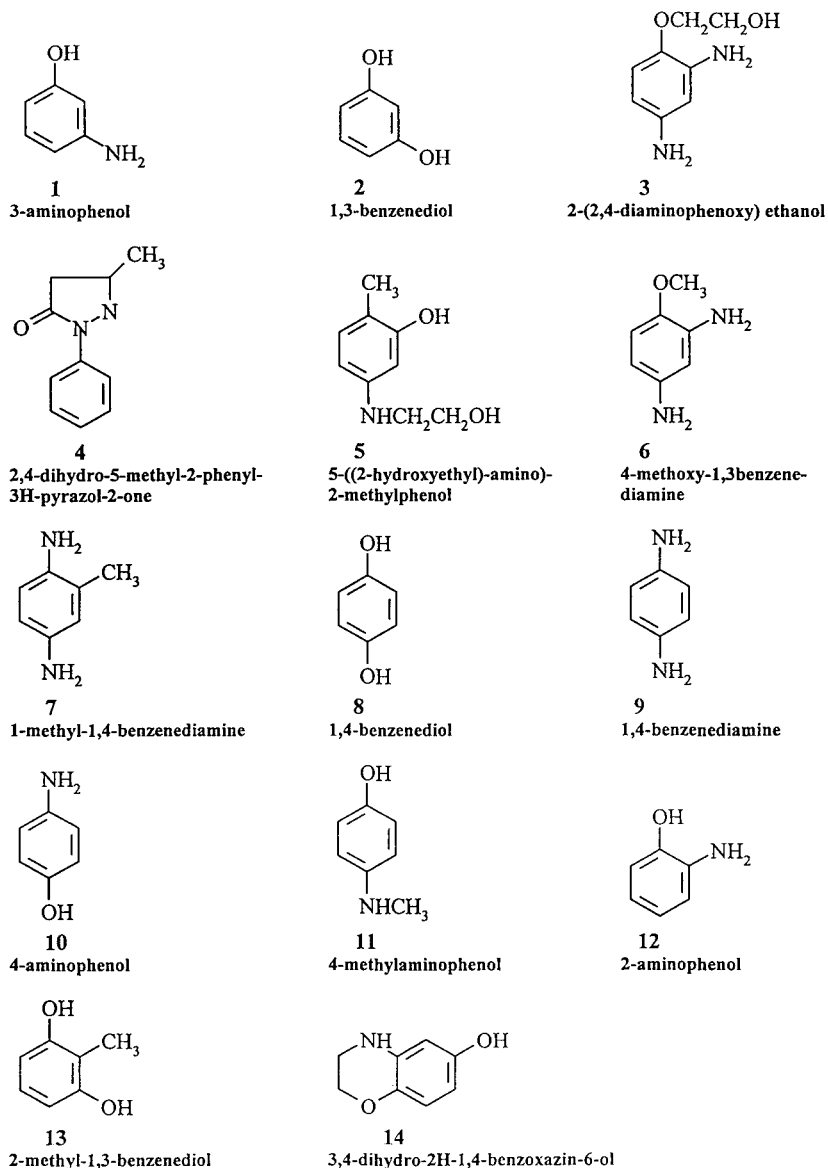
Fig. 1. Structures of the compounds analysed.

Authentic samples of oxidative dyes were a gift from Oreal (Aulnay-sous-Bois, France). The dye mixture was obtained by dissolving these solutes (50 mg/l) in the running buffer (pH 3)–methanol mixture (90:10, v/v). Finally, sodium sulphite (0.2%) was added to each sample to slow oxidation of the dyes.

3. Results and discussion

3.1. Capillary zone electrophoresis

Capillary zone electrophoresis (CZE) allows the separation of ionized molecules, which move according to their electrophoretic mobility [12]:

$$m_{ep} = \frac{L_d L_t}{V}\left(\frac{1}{t_m} - \frac{1}{t_0}\right) \qquad (1)$$

where m_{ep} is the electrophoretic mobility of the solute, V the applied voltage, L_d the injector-detector capillary length, L_t the total capillary length, t_m the migration time of solute and t_0 the migration time of neutral marker.

Neutral molecules would migrate at the electroosmotic flow (EOF) velocity, and the electroosmotic flow mobility (m_{eo}) is given by

$$m_{eo} = \frac{L_d L_t}{V}\left(\frac{1}{t_0}\right) \qquad (2)$$

The oxidative dyes contain amino groups (pK_a 3–5.5) or hydroxy groups (pK_a 9–11); the variation of their electrophoretic mobility with changes in running buffer pH is reported in Fig. 2.

The amino groups are ionized when the buffer pH is less than their pK_a values; in that case, the positive electrophoretic mobility of these organic cations is in the same direction as the electroosmotic flow. 3-Aminophenol (compound 1) has a positive m_{ep} at pH 4; when the buffer pH increases, its electrophoretic mobility decreases due to deprotonation of the amino group. At pH 6 the solute is neutral. When the pH is increased to the latter pK_a, the molecule moves with the electroosmotic flow. The hydroxy groups are ionized when the pH is higher than their pK_a values (pK_a 9–11), thus these anionic solutes have negative electrophoretic mobilities and migrate with the EOF. In contrast to the amino groups, the m_{ep} increases when the pH increases (because the solute gets more ionized hydroxy groups). For the aromatic solutes, the ionization constants of their amino and hydroxy groups may be determined by CZE. Figs. 3 and 4 show the results of the analysis of a mixture of the aromatic solutes using CZE. Under acidic pH the separation is better than at alkaline pH: pH
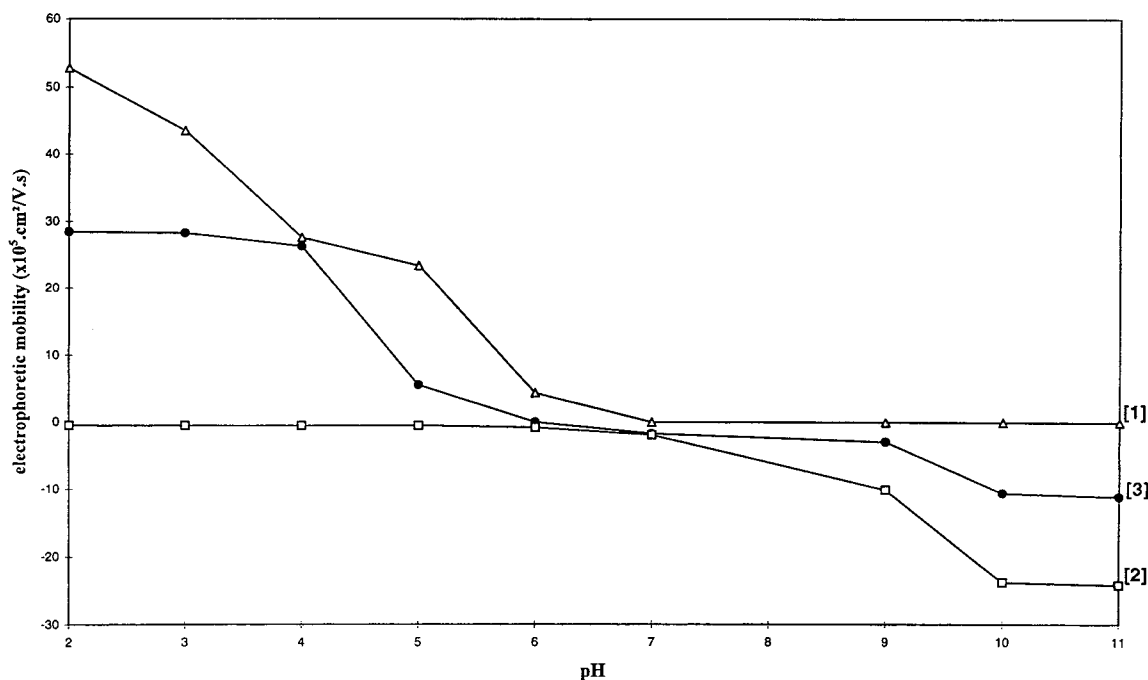

Fig. 2. Plot of electrophoretic mobility versus pH. Electrolyte, 25 mM phosphate–borate; capillary, 44 cm × 50 μm I.D.; UV detection, 214 nm; hydrodynamic injection, 2 s; voltage, 20 kV; temperature, 25°C. Compounds: [1] (△) 3-aminophenol (pK_a 4.3–9.4); [2] (□) 1,3-benzenediol (pK_a 9.1–11); [3] (●) 2-(2,4-diaminophenoxy)ethanol (pK_a 3.2–5.4).
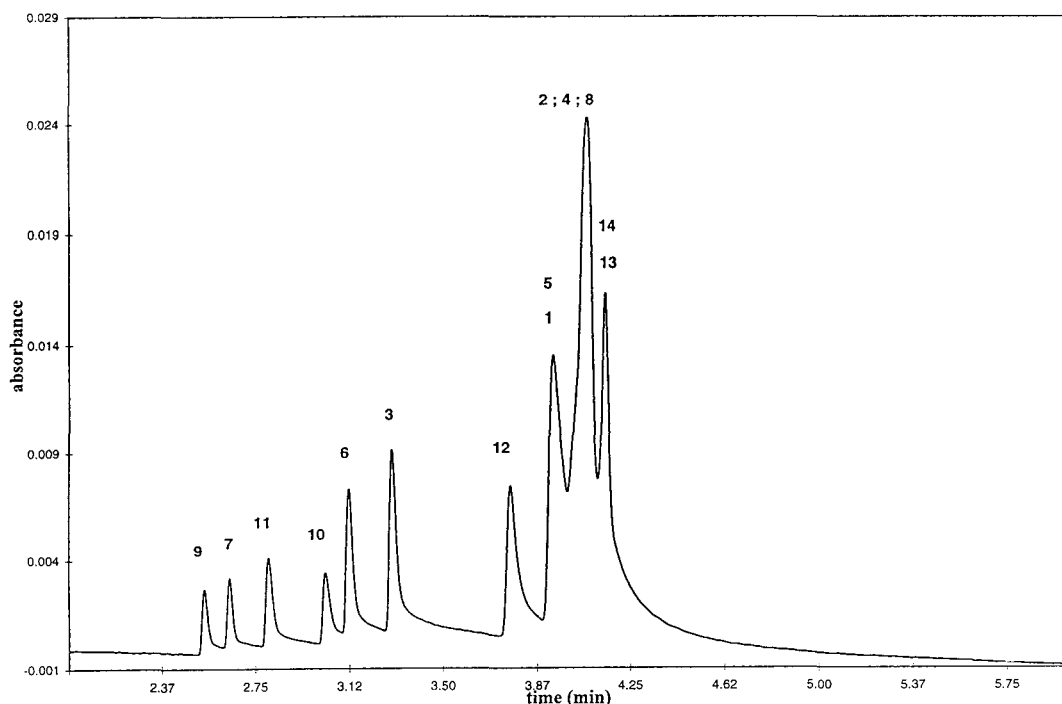
Fig. 3. Separation of oxidative dye mixture under acidic conditions (CZE). Electrolyte, 25 mM phosphate–borate, pH 5.5; capillary, 47 cm × 50 μm I.D.; UV detection, 214 nm; hydrodynamic injection 2 s; voltage, 20 kV; temperature, 25°C; concentration, 50 mM. For peak identification see Fig. 1.

increase causes deterioration of the resolution. The difficulties in realizing a separation with high resolution are caused by the pK_a of the molecules. Since these are small for the amino groups, the separation should be performed at low pH. In that case, the EOF is small and the neutral molecules (phenol) in the mixture will migrate only slowly. On the other hand, the pK_a of phenols are high and thus the pH must be increased to ionize those compounds (compounds 12, 13). However, reproducibility is rather low at alkaline pH due to increased dissolution of silica. At pH 5.5, the first peak corresponds with the aromatic diamines (di-cationic molecules). The diamine compounds (7, 9) are more ionized than the others, and thus their electrophoretic mobilities are higher. CZE separation depends on the ionic charge and the molecular mass of the analyte. Solute 7 migrates slower than solute 9 due to its higher molecular mass. This is also true for solutes 6 and 3. The

compounds 1, 10 and 12 are isomers, the pK_a of their amino groups being 4.3, 5.5 and 4.6, respectively. When the separation is performed at pH 5.5, compound 10 is more ionized than compounds 1 and 12. Their order of migration is 10, 12, 1. The elution order follows the decreasing pK_a order. These solutes have the same molecular mass, so they migrate in order of their ionization. The benzenediols migrate slowest due to their neutral character at pH 5.5, which results in migration with the electroosmotic flow. At pH 9.5, the solutes having two amino groups migrate at a velocity equal to the electroosmotic flow and are not resolved (compounds 9, 7, 6 and 3). On the other hand, when the buffer pH is not alkaline enough to ionize all phenol groups, we will not see the normal migration order diamines, aminophenols, phenols. For example, compound 2 is more ionized than its isomer 8 (only one group ionized) and thus solute 8 comigrates with the aminophenols.
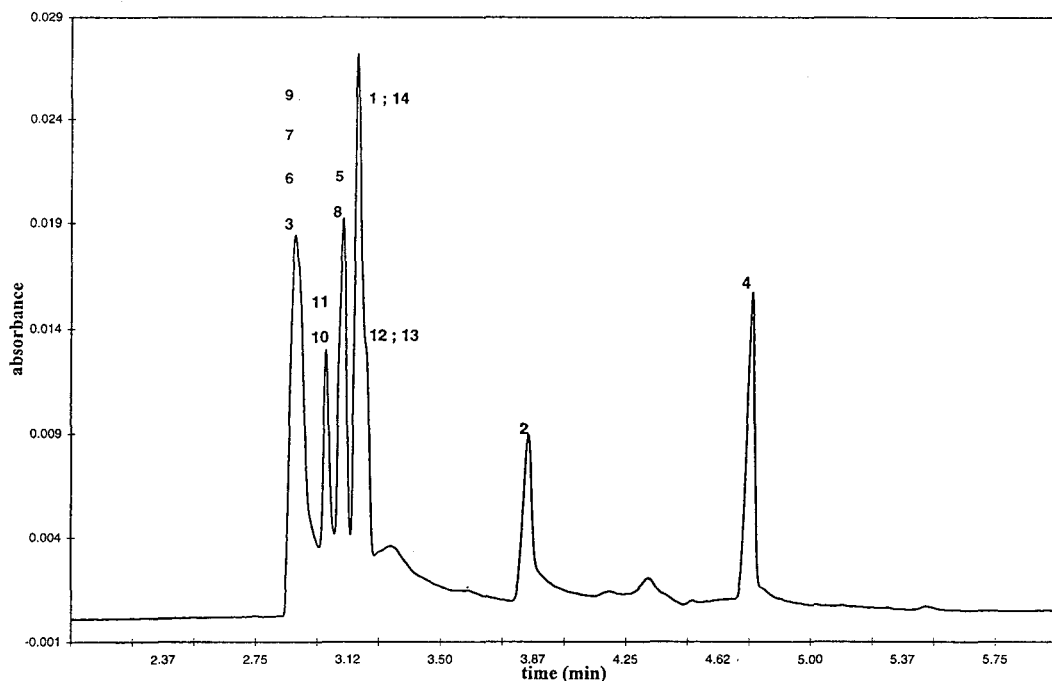
Fig. 4. Separation of oxidative dye mixture under alkaline conditions (CZE). Electrolyte, 25 mM phosphate–borate, pH 9.5; capillary, 47 cm × 50 μm I.D.; UV detection, 214 nm; hydrodynamic injection, 2 s; voltage, 20 kV; temperature, 25°C; concentration, 50 mM. For peak identification see Fig. 1.

3.2. Micellar electrokinetic chromatography

After the CZE experiments a more elaborate study was done using MEKC, first with SDS as surfactant, which is often used [13]. To determine the optimum conditions we do not calculate the m_{ep}, as in CZE, but instead we use the capacity factor, which takes the electrophoretic medium and the micelle interaction into consideration. The principle of separation in MEKC is based on the differential partition of the solute between the ionic micelles and the surrounding aqueous phase. In MEKC, the capacity factor of a neutral solute is given by [13]:

$$k' = \frac{t_r - t_0}{t_0(1 - t_r/t_{mc})} \qquad (3)$$

where t_r, t_0 and t_{mc} are the migration times for the solute, the neutral marker (methanol) and the micelle tracer (anthracene). Thus, the capacity factor of a neutral compound in first approxi-

mation is linearly related to the micelle concentration through

$$k' = K\bar{\nu}(C_{sf} - CMC) \qquad (4)$$

where K is the partition coefficient of the solute into the micelles, $\bar{\nu}$ the partial molar volume of the micelle, C_{sf} the total surfactant concentration and CMC the critical micellar concentration of the surfactant.

The migration behaviour of an anionic (or cationic) solute involves its own negative (or positive) electrophoretic mobility in the aqueous phase. Thus, in MEKC, the mobility of such an ionized solute is the weighted average of the mobility in the micellar phase and its mobility in the aqueous phase. Khaledi et al. [14] have derived the following equation:

$$k' = \frac{t_r - t_{r'}}{t_{r'}(1 - t_r/t_{mc})} \qquad (5)$$

where t_r, $t_{r'}$ and t_{mc} are the migration times of the solute in MEKC, CZE and of the micelle tracer in MEKC. Several assumptions have been made in deriving this equation: firstly, the mobility of the micelles is assumed to be unchanged when analytes are dissolved in them, and secondly, the EOF is the same with or without micelles. The latter means that changes in the zeta potential and the buffer viscosity caused by adding micelles to the electrolyte are negligible.

Our study started at pH 7, because below this pH the electroosmotic flow decreases rapidly and the separation shows broadening of the peaks. A variation of the buffer pH from 7 to 10 (Fig. 5) allowed to determine the optimum resolution (pH 7). In contrast to the experiment performed at pH 8.5, the compounds 5, 6, 7 and 8 are well separated while the others comigrate. At pH 10, only compound 6 is resolved. The ionization of hydroxy groups increases in going towards alkaline pH values. The appearance of negative
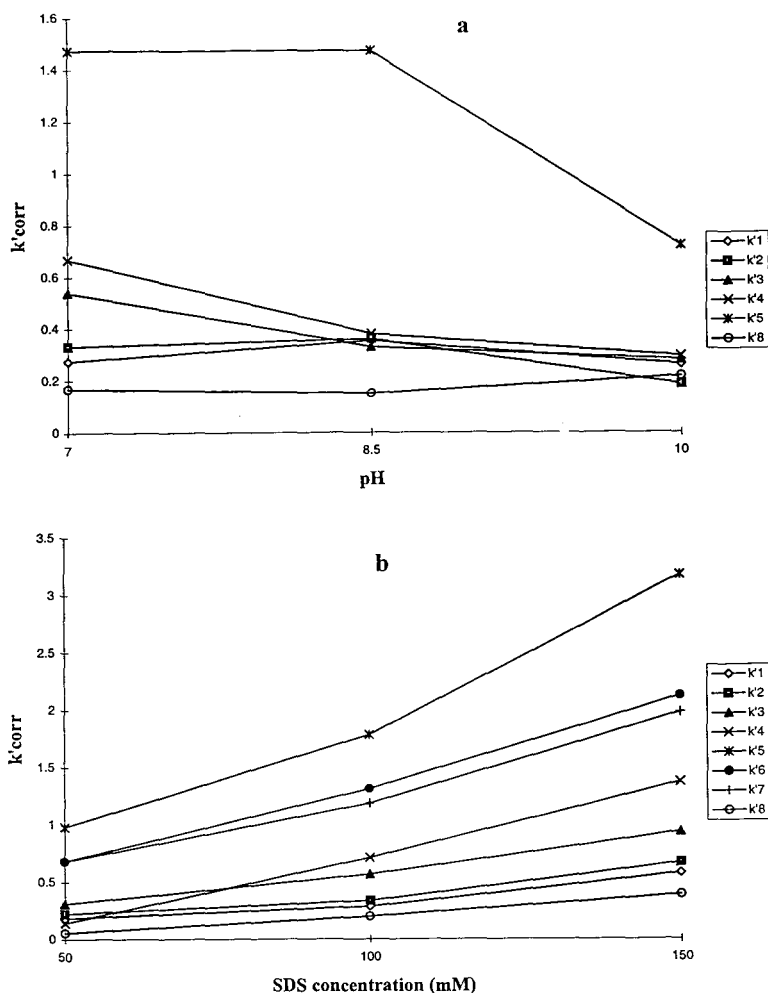

Fig. 5. (a) Influence of electrolyte pH in MEKC. Conditions: 75 mM SDS; capillary, 44 cm × 50 μm I.D. (b) Influence of SDS concentration in MEKC. Conditions: pH 7; capillary, 70 cm × 50 μm I.D. For (a) and (b): electrolyte, 25 mM phosphate–borate; UV detection, 214 nm; hydrodynamic injection, 2 s; voltage, 20 kV; temperature, 25°C.

charge on the compound decreases the micelle–compound interactions (as they are of similar sign), and thus resolution decreases. The same conclusion has been drawn by Takeda et al. [15] for the separation of aniline derivatives by MEKC. The capacity factor decreased significantly with increasing pH for p-anisidine and N-methylaniline due to a weaker protonation of amino groups; at alkaline pH the compounds interacted less with the micelles.

Next, the influence of the SDS concentration has been investigated. An increase of micelle volume improves the separation. However, it should be noted that the values of the capacity factors are rather low (under 3.5) even with an SDS concentration of 150 mM, in spite of a marked widening of the migration window. Comparing our results with those of Takeda et al. [15], we observed that the k'-values, which increase with the surfactant concentration, are always smaller than those reported for aniline derivatives. The aromatic solutes have pK_a values around 4–5 and consequently are partially ionized at pH 6.2. We cannot work below pH 7
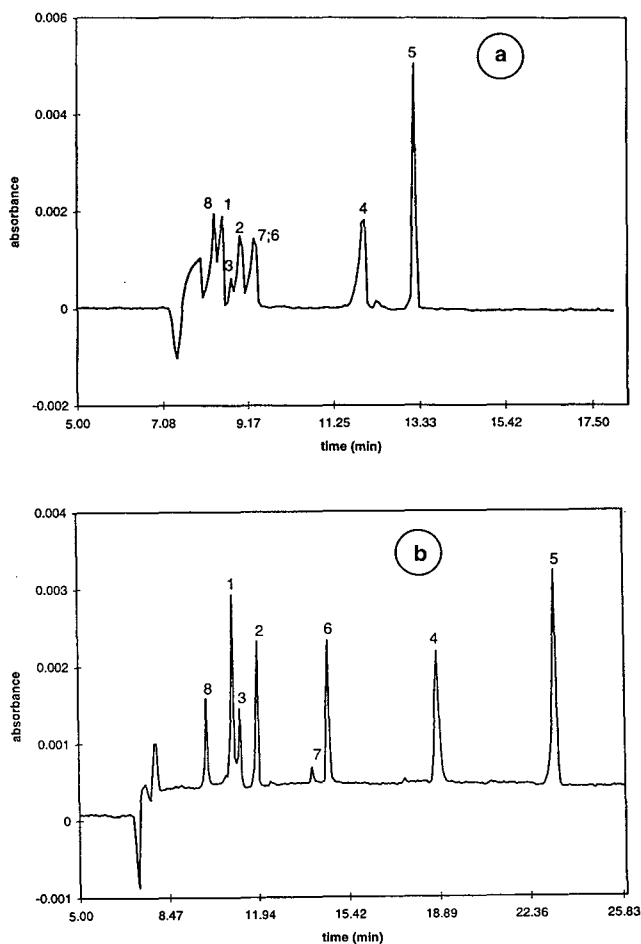

Fig. 6. Influence of ionic strength of electrolyte. (a) Electrolyte, 25 mM phosphate–borate, 150 mM SDS, pH 7. (b) Electrolyte, 75 mM phosphate–borate, 150 mM SDS, pH 7. Capillary, 70 cm × 50 μm I.D.; UV detection, 214 nm; hydrodynamic injection, 2 s; voltage, 20 kV; temperature, 25°C; concentration, 50 mM. For peak identification see Fig. 1.

with the oxidative dyes because the compounds have pK_a values smaller than those of the aniline derivatives. We can remark that diphenylamine and chloroaniline are more hydrophobic than aminophenol or phenylenediamine. Moreover, the mixture contains phenols which are neutral at this pH (compounds not present in the mixture of Takeda et al.).

For the mixture of oxidative dyes, improvement of the separation is obtained by increasing the electrolyte ionic strength. So the third parameter which has been changed, is the electrolyte ionic strength (Fig. 6). An increase of the buffer ionic strength induces a more hydrophilic aqueous medium, so a hydrophobic solute preferentially dissolves into the micelles. This fast mass transfer causes better peak efficiencies. The

migration time has doubled, so the solutes are better separated: compounds 7 and 6 are resolved with 75 mM but not with 25 mM of electrolyte. Compound 2 is better resolved from compounds 3, 6 and 7, and has a better efficiency. However, compound 3 is not completely resolved, because the increase in ionic strength has incited a decrease of the electrophoretic mobility which is smaller than that for solute 1. Upon further increase of the ionic strength, compound 3 elutes before compound 1.

This study allowed us to determine the optimum conditions to realize the analysis of the fourteen oxidative dyes (Fig. 7). Among the fourteen solutes resolved in 27 min, two compounds (compounds 2 and 9) are not well resolved. If we compare the electropherogram with
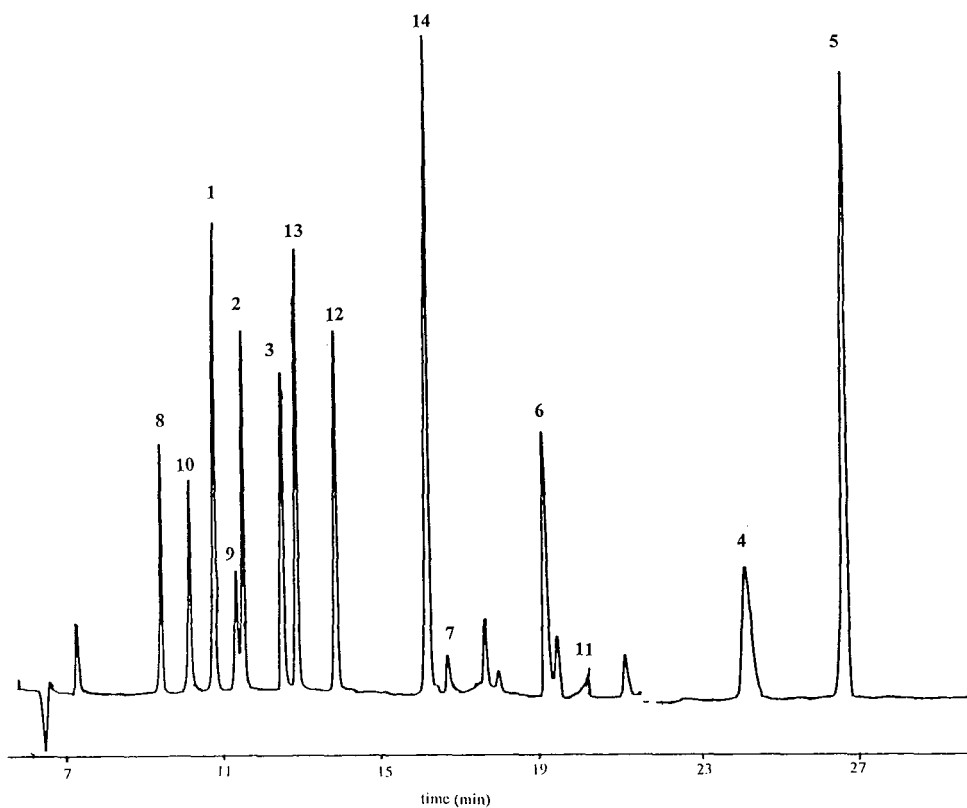

Fig. 7. MEKC separation with SDS surfactant under optimized conditions. Electrolyte, 75 mM phosphate–borate, 150 mM SDS, pH 7; capillary, 70 cm × 50 μm I.D.; UV detection, 214 nm; hydrodynamic injection, 2 s; voltage, 20 kV; temperature, 25°C; concentration, 50 mM. For peak identification see Fig. 1.

the HPLC chromatogram, the analysis time is similar but the MEKC resolution is better.

A similar study is realized using MEKC with the CTACl cationic surfactant. We selected CTACl because of its low Kraft temperature compared with CTABr. In the case of a cationic surfactant, ionic interactions exist between the ionized silanols and the CTA^+ cations. So, when the CTACl concentration increases, we note an evolution of the electroosmotic flow, which translates the modifications created at the silica capillary surface. At a given applied field strength and buffer system, the magnitude and the direction of the EOF is controlled solely by the capillary wall surface charge density. At pH 9.5, the ionization of Si–OH groups is very large at the wall surface. The addition of CTACl to the solution produces an EOF decrease, because the CTA^+ cations progressively cover the capillary surface due to attractive interactions with negative silanol groups. Then, a bilayer of CTACl molecules (hemimicelle) is formed at the capillary wall with a positive charge directed towards the centre of the capillary. So the direction of EOF is reversed [16–18].

In SDS-MEKC, few hydrophobic interactions exist between the aromatic molecules and the SDS micelles. So, we work at pH 9.5 to promote the ionization of hydroxy groups. Therefore, we will have hydrophobic interactions (same as SDS) and hydrophilic interactions [15].

Next, the variation in k' of each compound has been studied versus CTACl concentration. By increasing the CTACl concentration, the separation is improved (Fig. 8). To obtain a chromatogram of the mixture, we have chosen a CTACl concentration of 60 mM, since better separation will be obtained at higher concentrations. However, a high CTACl concentration produces a large current (100 μA) and results in
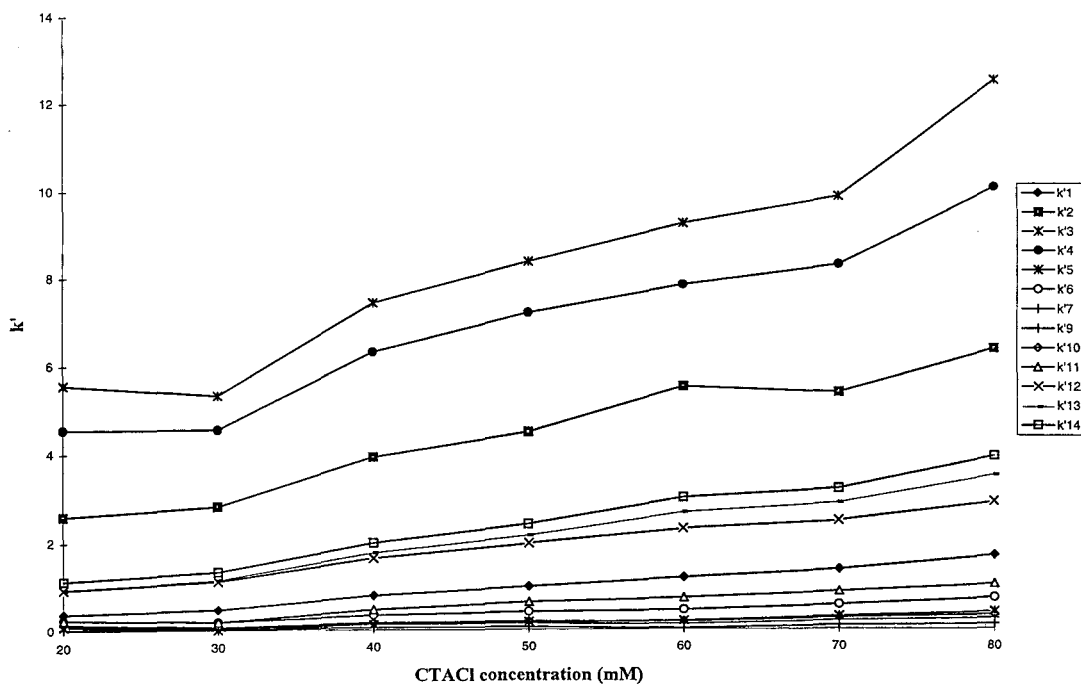

Fig. 8. Influence of CTACl concentration in MEKC. Electrolyte, 25 mM phosphate–borate, pH 9.5; capillary, 47 cm × 50 μm I.D.; UV detection, 214 nm; hydrodynamic injection, 2 s; voltage, 20 kV; temperature, 25°C.

a widening of peak 8 (and thus in loss of efficiency). A solution of phosphate–borate 30 mM, CTACl 60 mM, allows separation of the mixture with a good resolution; 14 peaks were obtained, which is better than the results obtained with HPLC, but less than obtained using MEKC with SDS. In MEKC, the analysis time using SDS is half of that found with CTACl, and thus separation could be improved. In the case of CTACl, the first migrating compounds are the phenylenediamines, which are neutral at pH 9.5 and have only hydrophobic interactions with the micelles. They are followed by the negative aminophenols (only one ionized group), having hydrophilic interactions with the positive Stern layer of the micelles. Lastly, we observe the migration of phenols (with two ionized groups), due to hydrophilic interactions with CTA$^+$ monomers (Fig. 9).

According to Kaneta et al. [19], we can calculate distribution coefficient of a compound between the aqueous medium and the micelles from Eq. 4. By plotting the variation of k'-values versus the surfactant concentration, we can graphically determine the CMC value (from the x-intercept) and K (from the slope $K\bar{v}$), as indicated in Fig. 10. The distribution coefficients for three solutes are reported in Table 1. The partial specific volumes given in the literature [20] are 0.977 ml/g for CTACl and 0.862 ml/g for SDS. The distribution coefficients are determined at pH 10, where hydroxy groups are ionized and amino groups are neutral. Finally, distribution coefficients are compared with the ionization degree of these three compounds. For the CTACl surfactant, decreasing order of the distribution coefficients is 1,3-benzenediol > 3-aminophenol > 2-(2,4-diaminophenoxy)ethanol,
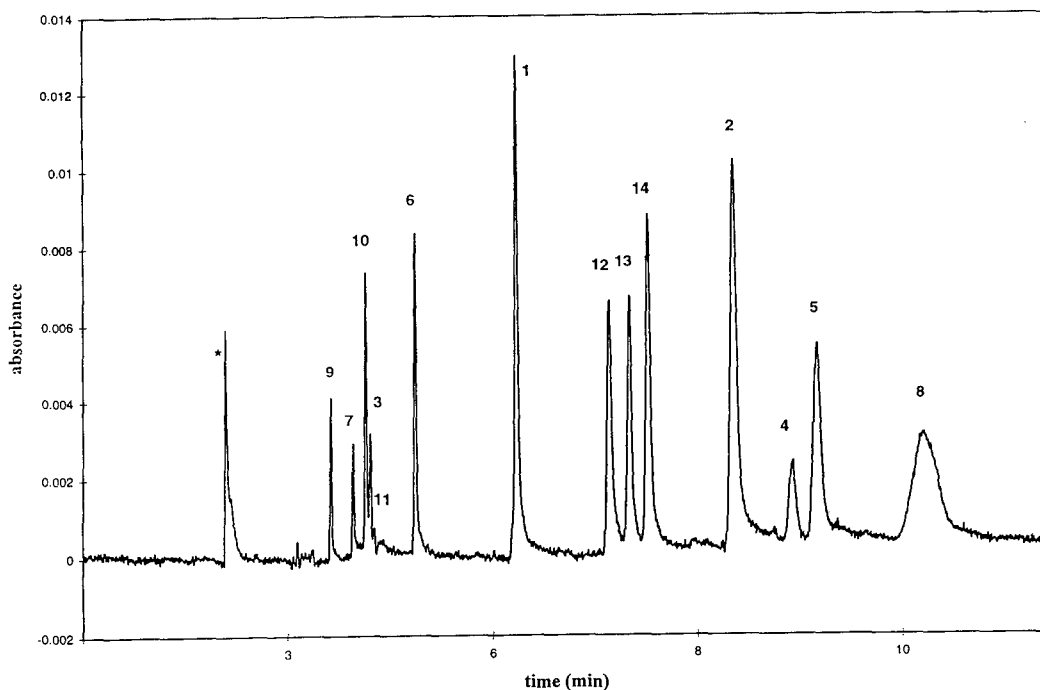

Fig. 9. MEKC separation with CTACl surfactant under optimized conditions. Electrolyte, 25 mM phosphate–borate, 60 mM CTACl, pH 9.5; capillary, 47 cm × 50 μm I.D.; UV detection, 214 nm; hydrodynamic injection, 2 s; voltage, 20 kV; temperature, 25°C; concentration, 50 mM. Asterisk indicates the peak of Na$_2$S$_2$O$_5$. For peak identification see Fig. 1.
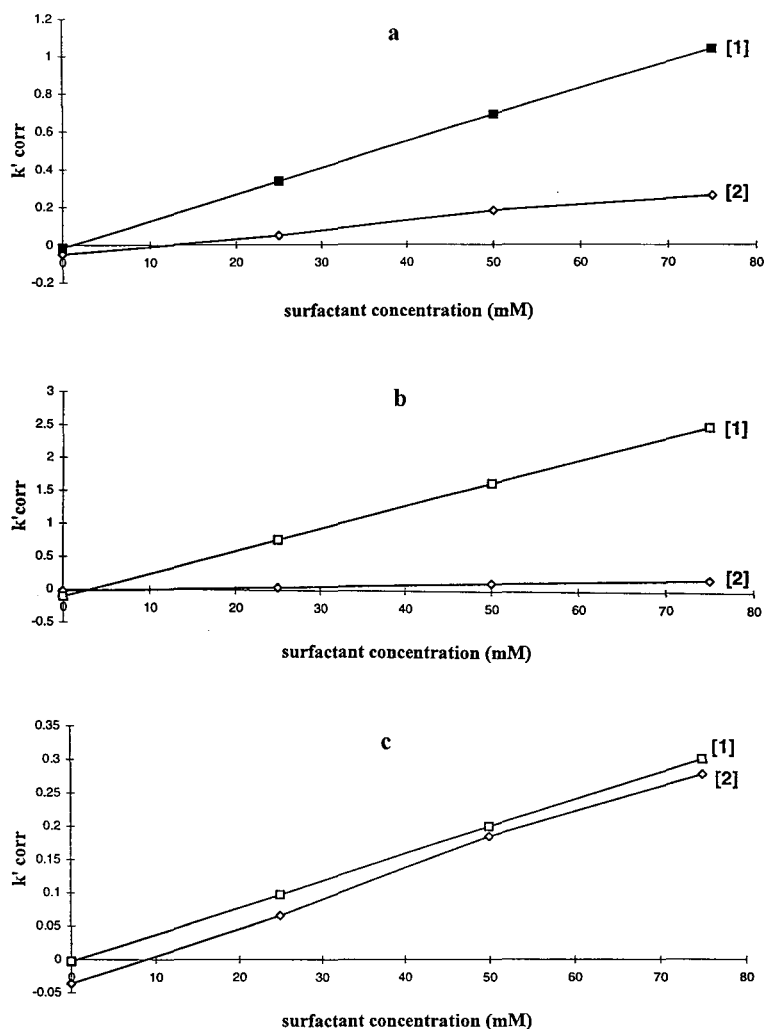
Fig. 10. Variation of corrected capacity factor versus CTACl surfactant concentration. Electrolyte, 25 mM phosphate–borate, pH 10; capillary, 47 cm × 50 μm I.D.; UV detection, 214 nm; hydrodynamic injection, 2 s; voltage, 20 kV; temperature, 25°C. Surfactant: [1] CTACl, [2] SDS. Compound: (a) 3-aminophenol, (b) 1,3-benzenediol, (c) 2-(2,4-diaminophenoxy)ethanol.

which is related with the decreasing interactions with the micelles. At pH 10, the neutral diamine group has a higher affinity for the aqueous phase than for the micellar phase. For hydroxy groups, the increase in K-value means an increase in the affinity with the micelles. Benzenediol has two groups ionized, and therefore it has a higher affinity for the micelle than aminophenol, which has only one hydroxy group.
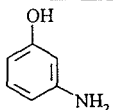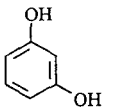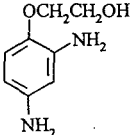
For the SDS surfactant all K-values are small,

because these compounds have less affinity for the micellar medium. The differences between K-values for anionic and neutral solutes are small.

4. Conclusion

The separation of oxidative dyes is realized by MEKC using two kinds of surfactant (SDS and

Table 1
Distribution coefficients of solutes for two surfactants

Solute			SDS surfactant			CTACl surfactant		
Structure	pK_a		K	CMC (mM)	r^2	K	CMC (mM)	r^2
OH ... NH$_2$	4.3 9.4		17.3	11.6	0.9812	45.1	1.13	0.9993
OH ... OH	9.1 11		10.2	9.1	0.9962	112.3	3.16	0.9880
OCH$_2$CH$_2$OH ... NH$_2$ ... NH$_2$	3.2 5.4		17.3	8.4	0.9954	13.1	1.39	0.9918

Electrolyte, 25 mM phosphate–borate, pH 10; capillary, 47 cm × 50 μm I.D.; UV detection, 214 nm; hydrodynamic injection, 2 s; voltage, 20 kV; temperature, 25°C.

CTACl). The separation of fourteen dyes has been satisfactorily achieved using 150 mM SDS at pH 7 or using 60 mM CTACl at pH 9.5. Thus with the method described here good resolution of the fourteen compounds was achieved. However, the analysis time differs from 30 min using SDS to 12 min using CTACl.

Acknowledgement

The authors thank Mrs D. Depernet for her technical assistance.

References

[1] S.F.Y. Li, Capillary Electrophoresis, Principles, Practices and Applications, Elsevier, Amsterdam, 1992.
[2] S. Terabe, K. Otsuka and T. Ando, Anal. Chem., 57 (1985) 834–841.
[3] Ch. Zviak, Science des Traitements Capillaires, Ed. Masson, Paris, 1988, Ch. 7.
[4] J.F. Corbett, J. Soc. Cosmet. Chem., 35 (1984) 297.
[5] C.R. Robbins, Chemical and Physical Behavior of Human Hair, Springer, New York, Berlin, Heidelberg, 1988, p. 171.
[6] H. Gottschalk and R. Machens, J. Soc. Cosmet. Chem., 33 (1982) 97.
[7] G. Chondhary, J. Chromatogr., 193 (1980) 277.
[8] N. Goetz, P. Lasserre, P. Boré and G. Kalopissis, Int. J. Cosmet. Sci., 10 (1988) 63.
[9] N. Goetz, J. Mauro, L. Bouleau and A. de Labbey, in P. Boré (Editor), Cosmetic Analysis, Cosmetic Science and Technology Series, Vol. 4, Marcel Dekker, New York, 1985, p. 245.
[10] V. Andrisano, R. Gotti, A.M. Di Pietra and V. Cavrini, Chromatographia, 39 (1994) 138.
[11] S. Fanali, J. Chromatogr., 470 (1989) 123–129.
[12] M.W.F. Nielen, J. Chromatogr., 625 (1992) 109–114.
[13] M. Sepaniak, D. Burton and M.P. Maskarinec, Micellar Electrokinetic Capillary Chromatography, American Chemical Society, Washington, DC, 1987, Ch. 6.
[14] M. Khaledi, S. Smith and J. Strasters, Anal. Chem., 63 (1991) 1820.
[15] S. Takeda, S. Wakida, M. Yamane, A. Kawahara and K. Higashi, J. Chromatogr. A, 653 (1993) 109–114.
[16] T. Kaneta, S. Tanaka and M. Taga, J. Chromatogr. A, 653 (1993) 313–319.
[17] G.M. Janini, K.C. Chan, J.A. Barnes, G.M. Mushik and H.J. Issaq, J. Chromatogr. A, 653 (1993) 321–327.
[18] A. Emmer, M. Jansson and J. Roeraade, J. Chromatogr., 547 (1991) 544–550.
[19] T. Kaneta, S. Tanaka and H. Yoshida, Anal. Chem. Soc., 64 (1992) 798–801.
[20] D.W. Armstrong and G.Y. Stine, J. Am. Chem. Soc., 105 (1983) 2962–2964.

Separation of enantiomers of drugs by capillary electrophoresis I. γ-Cyclodextrin as chiral solvating agent

B. Koppenhoefer[a,*], U. Epperlein[a], B. Christian[a], Ji Yibing[b], Chen Yuying[b], Lin Bingcheng[c]

[a]Institute of Organic Chemistry, Eberhard-Karls-University Tübingen, Auf der Morgenstelle 18, D-72076 Tübingen, Germany
[b]China Pharmaceutical University, 250009 Nanching, China
[c]Dalian Institute of Chemical Physics, Zhong Shan Road 161, 116012 Dalian, China

Abstract

Enantiomer separation was studied for a set of 57 chiral drugs. With γ-cyclodextrin as chiral solvating agent in capillary zone electrophoresis, seven enantiomeric pairs could be separated without recoursing to an optimization procedure. Possible interaction mechanisms between selector and selectand molecules are briefly discussed.

1. Introduction

The separation of enantiomers of chiral drugs deserves particular attention in view of the recent changes in regulation, by Japanese, Chinese, European and American institutions (e.g., Food and Drug Administration) [1]. Thus, in order to bring a new drug to the market, the main activity and possible side effects of both enantiomers of the drug must be established. This requires both preparative and analytical methods for the separation of enantiomers.

Due to its high resolution power, easy sample preparation and short analysis times, capillary electrophoresis has turned out as a favourable method in this field, in addition to high-performance liquid chromatography (HPLC) and gas chromatography (GC). As recorded in our molecular graphical database Chirbase/CE, different separation principles have been successfully applied. These include complexation by crown ethers

[2,3], micellar electrokinetic chromatography (MEKC) with bile salts [4–6] and amino acid derivatives [7,8], ligand exchange [9,10], and affinity interaction with proteins [11–13]. By far the most convenient approach, however, involves the addition of cyclodextrins and derivatives thereof, respectively, as complexing agents to the running buffer [14,15]; this method was applied in 120 out of 247 papers quoted in our database. Whereas most experiments quoted in the literature were performed with β-cyclodextrins, γ-cyclodextrin (Fig. 1) was less frequently used, basically because of its higher price. In this paper we report first results of an extensive screening of chiral drugs with regard to separability with cyclodextrins in CE under different conditions, starting with native γ-cyclodextrin.

2. Experimental

All experiments were carried out on a Bio-Focus 3000 automatic capillary electrophoresis
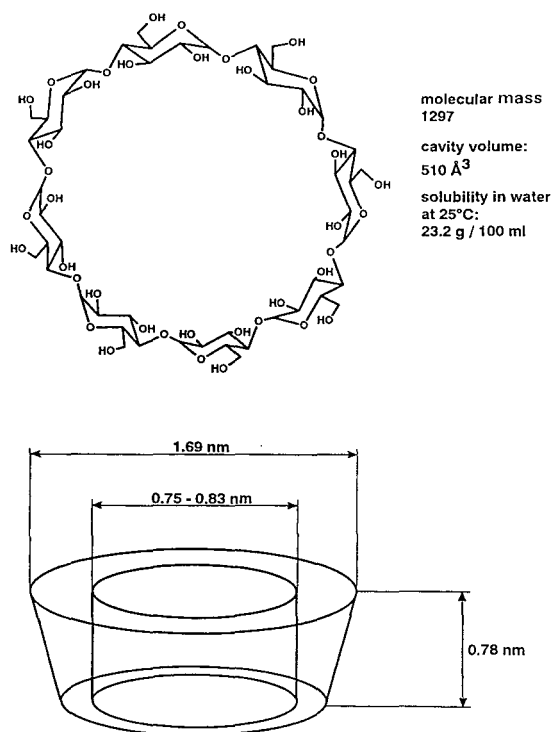
---

* Corresponding author.

molecular mass
1297

cavity volume:
510 Å³

solubility in water
at 25°C:
23.2 g / 100 ml

1.69 nm

0.75 - 0.83 nm

0.78 nm

Fig. 1. γ-Cyclodextrin: structure, shape, properties.

system (Bio-Rad Laboratories, Hercules, CA, USA) equipped with a variable-wavelength detector operated at 200 nm and an acrylamide-coated capillary from the same manufacturer. γ-Cyclodextrin was obtained from Wacker Chemie (Munich, Germany). Analytical samples of the chiral drugs were supplied by different pharmaceutical companies (3M Medica, Ankerpharm, Astra Chemicals, Arzneimittelwerk Dresden, Bayer, Boehringer Mannheim, Ciba, Durachemie, Gödecke, Hexal, Jenapharm, Klinge, Knoll, Krewel, Mann, Medice, Merck, Pfizer, Röhm Pharma, Rhône-Poulenc Rorer, Roche). All other chemicals were analytical grade.

The run buffer was prepared from a 0.1 M solution of sodium dihydrogenphosphate (NaH_2PO_4) and adjusted to pH 2.5 with phosphoric acid (H_3PO_4). As a chiral solvating agent (CSA), γ-cyclodextrin was dissolved in the plain phosphate buffer, to give a 15 mmol/l solution.

Stock solutions of the bulk drug samples (1 mg/ml) were prepared in deionized and distilled water. These were diluted ten-fold with a 1:1 mixture of purified water and the run buffer to give the sample solutions, which were transferred to the capillary by electrokinetic injection. The injection was carried out by applying a voltage of 8 kV for 6 s.
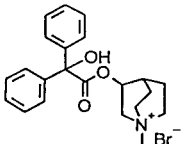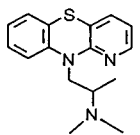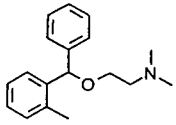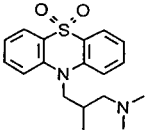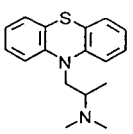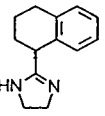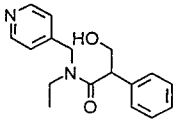
3. Results

Under standard conditions, kept as constant as possible throughout this study, seven enantiomeric pairs could be separated without recoursing to a time-consuming optimization procedure. In Table 1, these analytes are listed in alphabetical order of their names. All drug names used are international nonproprietary names of the pharmaceuticals assigned by the World Health Organization (WHO). The migration times in plain phosphate buffer were compared to the migration times in cyclodextrin-containing phosphate buffer. For all of the analytes separated, migration times were remarkably prolonged by the addition of γ-cyclodextrin to the running buffer, indicating a significant interaction between analyte and selector molecules.

The ratio of the migration times of the enantiomers, tm_2/tm_1, was taken as a measure of separation selectivity since no endoosmotic flow was observed [16]. The separation factors obtained range from 1.046 to 1.009. The enantiomers of oxomemazine, with a separation factor of 1.046, were completely resolved, as shown in Fig. 2. As demonstrated for tetryzoline in Fig. 3, a separation factor of 1.028 was still almost sufficient for baseline separation. Tropicamide with a separation factor of 1.009 was only partially resolved. This and other separations may be optimized further by adjusting both CSA concentration and pH individually for each analyte.

Table 2 compiles 50 racemates, in alphabetical order of their names, which failed to separate under standard conditions. Again, the molecular structures of all analytes are listed, along with their migration times in the CSA-containing

Table 1
Compounds successfully separated into the enantiomers, under standard conditions

Compound structure	Pharmaceutical name	tm_p [a] (min)	tm_1 [b] (min)	tm_2 [b] (min)	tm_2/tm_1 [c]
	Clidinium bromide	10.05	11.98	12.23	1.021
	Isothipendyl	8.83	11.17	11.33	1.014
	Orphenadrine	12.05	13.60	13.80	1.015
	Oxomemazine	8.98	11.95	12.50	1.046
	Promethazine	8.73	12.19	12.44	1.028
	Tetryzoline	7.57	8.35	8.58	1.028
	Tropicamide	8.60	10.46	10.55	1.009

[a] Migration time in plain phosphate buffer.
[b] Migration times in cyclodextrin containing phosphate buffer; first and second detected enantiomer, respectively.
[c] Separation factor of the enantiomers.
Conditions: instrument, Bio-Rad Bio-Focus 3000; capillary, fused-silica, coated, 44.5 cm × 50 μm; sample concentration, 0.1 mg/ml; buffer, phosphate, 100 mmol/l, pH 2.5; CSA, γ-cyclodextrin, 15 mmol/l; injection, 6 s, 8 kV; run, 14 kV + → −; detection, 200 nm/0.005 AUFS; capillary temperature, 30°C.

buffer. Although most analytes showed prolonged migration times as compared to plain buffer, some were not clearly retarded. In these cases, the limits of long-term reproducibility of the absolute migration times did not permit a quantitative treatment.
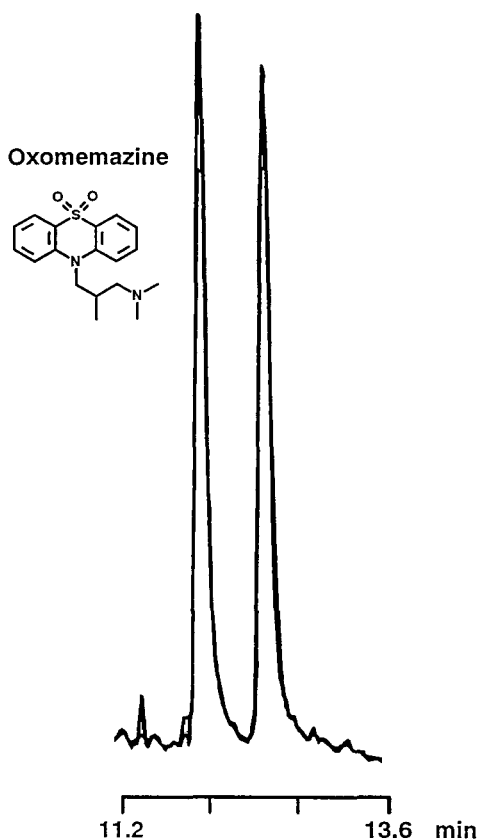
Fig. 2. Electropherogram of oxomemazine enantiomers. Conditions as quoted in Table 1. Detection at 200 nm, 0.005 AUFS.
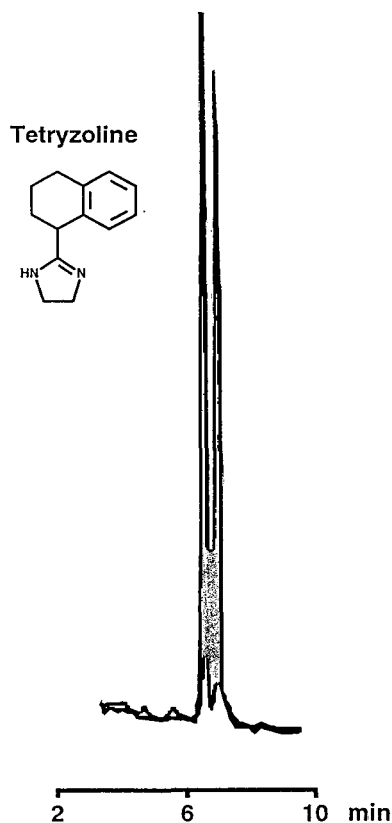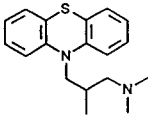

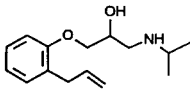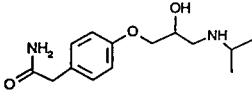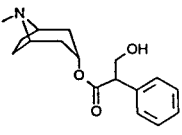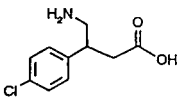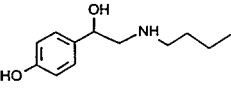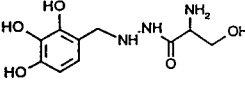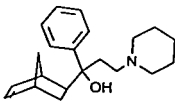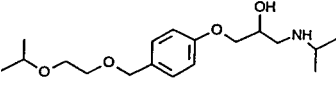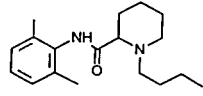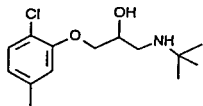Fig. 3. Electropherogram of tetryzoline enantiomers. Conditions as quoted in Table 1. Detection at 200 nm, 0.005 AUFS.

4. Discussion

As illustrated in Fig. 1, the γ-cyclodextrin molecule has a cavity of a diameter of 0.75–0.83 nm [17]. In α- and β-cyclodextrin, the diameter is approximately 0.30 and 0.15 nm smaller, respectively. Although the cavity in γ-cyclodextrin was occasionally considered too large for a significant enantiomer discrimination, there was a definite lack of experimental proof for this view. Indeed, an open mind might expect even improved recognition properties for the γ-cyclodextrin selector at least for large, bulky selectands. It should be mentioned that there are biological receptors with active sites larger than 80 nm, apt to include guests as large as a steroid molecule [18].
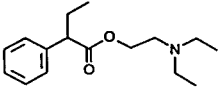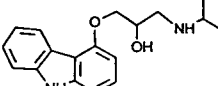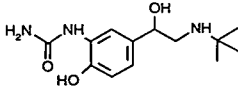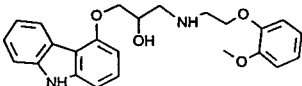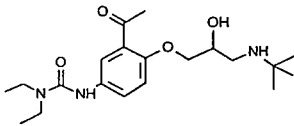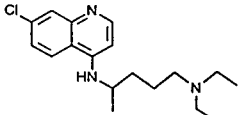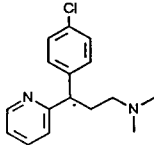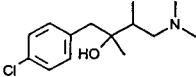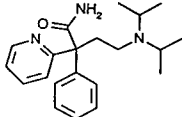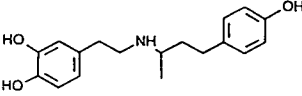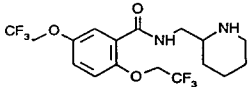
From these considerations, we expected to find several of the large tricyclic antihistaminic drugs among the seven at least partially separated analytes, as listed in Table 1. On the other hand, bicyclic and monocyclic sub-structures are also present among the molecules separated. Still these molecular structures are dominated by an extended, flat region. It may be assumed that these regions form an alignment with the upper rim of the cyclodextrin. The two enantiomers then differ significantly in their ability to stick their basic tail into the partially acidic cyclodextrin cavity. This model takes into consideration that possible interaction mechanisms do not only involve internal inclusion complex formation, but also external association [19]. An alternative model suggests to include the aromatic and

Table 2
Compounds not separated into the enantiomers, under standard conditions

Compound structure	Pharmaceutical name	tm [a] (min)
	Alimemazine	14.49
	Alprenolol	11.52
	Atenolol	9.61
	Atropine	11.59
	Baclofen	8.31
	Bamethan	9.14
	Benserazide	7.89
	Biperiden	14.04
	Bisoprolol	10.90
	Bupivacaine	8.75
	Bupranolol	13.97

Table 2 (continued)

Compound structure	Pharmaceutical name	tm [a] (min)
	Butetamate	9.96
	Carazolol	10.77
	Carbuterol	9.55
	Carvedilol	14.13
	Celiprolol	11.48
	Cloroquine	5.79
	Chlorphenamine	5.85
	Clobutinol	8.54
	Disopyramide	8.80
	Dobutamine	11.12
	Flecainide	9.99
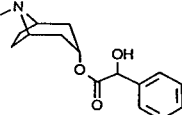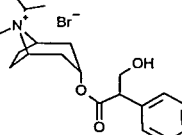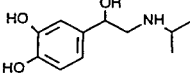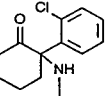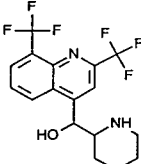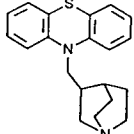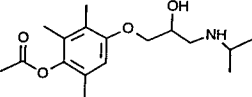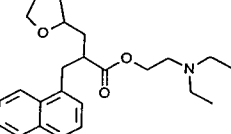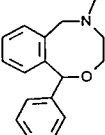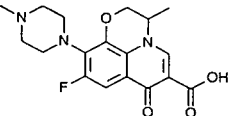
Table 2 (*continued*)

Compound structure	Pharmaceutical name	tm [a] (min)
	Homatropine	8.54
	Ipratropium bromide	10.97
	Isoprenaline	8.50
	Ketamine	10.01
	Mefloquine	10.10
	Mequitazine	14.49
	Metipranolol	10.35
	Naftidrofuryl	14.12
	Nefopam	9.38
	Ofloxacin	9.04

Table 2 (*continued*)
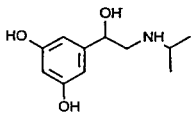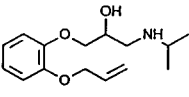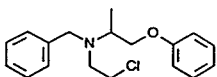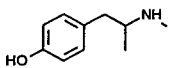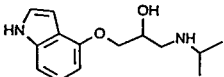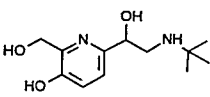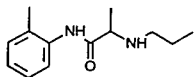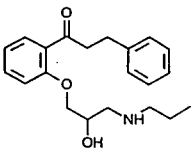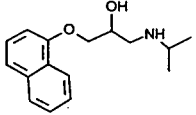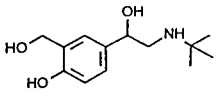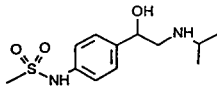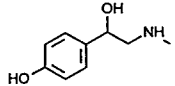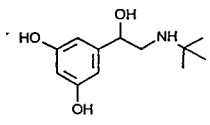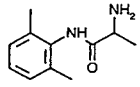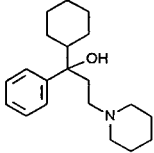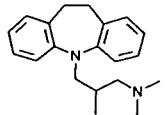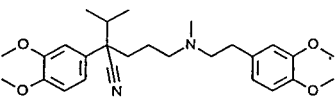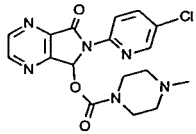
Compound structure	Pharmaceutical name	tm [a] (min)
	Orciprenaline	9.45
	Oxprenolol	9.09
	Phenoxybenzamine	11.17
	Pholedrine	7.45
	Pindolol	9.28
	Pirbuterol	6.74
	Prilocaine	8.70
	Propafenone	13.54
	Propranolol	10.75
	Salbutamol	9.01
	Sotalol	9.29
	Synephrine	7.57

Table 2 (continued)

Compound structure	Pharmaceutical name	tm [a] (min)
	Terbutaline	9.63
	Tocainide	8.53
	Trihexyphenidyl	12.79
	Trimipramine	20.13
	Verapamil	13.76
	Zopiclone	10.04

[a] Migration time in CSA containing buffer.
Conditions as quoted in Table 1.

heterocyclic portions, respectively, leaving the amino groups to external association. One may favour the first over the second model in view of the small retention increase of tetryzoline, bearing a bulky imidazoline side-chain, as compared to oxomemazine, promethazine and isothipendyl, each having an open chain side-chain (all structures are depicted in Table 1). On this basis, it may be readily explained why the even more bulky structure of mequitazine was not separated at all (see Table 2); however, the lack of separation of alimemazine (see Table 2), with a close similarity to both oxomemazine and promethazine (found in Table 1), appears rather

puzzling on first glance. This indicates clearly that further experimental evidence is required to decide on this question.

Moreover, not only the spatial conformation of the selectands should be considered, but also other properties, such as polarity and hydrogen-bonding capability. It will be one of our future aims to gather independent information on these questions by physicochemical studies of well-defined host–guest complexes of this type.

Throughout the study, the experimental conditions had been kept as constant as possible within the limits of this methodology. The given pair of CSA concentration and buffer pH is a

priori not optimal in this survey, because different complex formation constants and pK_a values of different selectands are expected to cause significant variations in the individual optimum separation conditions.

Such an individual optimization of the separation conditions for each analyte will certainly yield further progress in peak resolution, at least for the analytes listed in Table 1. The method development will also include the evaluation of reproducibility and detection limits. Last but not least, due to the higher solubility of γ-cyclodextrin compared to β-cyclodextrin, there is still a chance to find separation conditions for up to now unresolved enantiomeric pairs by choosing higher concentrations of γ-cyclodextrin as chiral solvating agent.

Acknowledgements

References

[1] S.C. Stinson, Chem. Eng. News, Sept. 19 (1994) 38.
[2] R. Kuhn, F. Erni, T. Bereuter and J. Häusler, Anal. Chem., 64 (1992) 2815.
[3] E. Höhne, G.-J. Krauss and G. Gübitz, J. High Resolut. Chromatogr., 15 (1992) 698.
[4] S. Terabe, M. Shibata and Y. Miyashita, J. Chromatogr., 480 (1989) 403.
[5] H. Nishi, T. Fukuyama, M. Matsuo and S. Terabe, J. Microcol. Sep., 1 (1989) 234.
[6] H. Nishi, T. Fukuyama, M. Matsuo and S. Terabe, Anal. Chim. Acta, 236 (1990) 281.
[7] A. Dobashi, T. Ono, S. Hara and J. Yamaguchi, J. Chromatogr., 480 (1989) 413.
[8] K. Otsuka, J. Kawahara, K. Tatekawa and S. Terabe, J. Chromatogr., 559 (1991) 209.
[9] E. Gassmann, J.E. Kuo and R.N. Zare, Science, 230 (1985) 813.
[10] S. Fanali, L. Ossicini, F. Foret and P. Bocek, J. Microcol. Sep., 1 (1989) 190.
[11] S. Birnbaum and S. Nilsson, Anal. Chem., 64 (1992) 2872–2874.
[12] S. Busch, J. Kraak and H. Poppe, J. Chromatogr., 635 (1993) 119.
[13] L. Valtcheva, J. Mohammad, G. Petterson and S. Hjerten, J. Chromatogr., 638 (1993) 263.
[14] A. Guttman, A. Paulus, A.S. Cohen, N. Grinberg and B.L. Karger, J. Chromatogr., 448 (1988) 41.
[15] S. Fanali, J. Chromatogr., 474 (1989) 441.
[16] M. Heuermann and G. Blaschke, J. Chromatogr., 648 (1993) 267.
[17] Song Li and W.C. Purdy, Chem. Rev., 92 (1992) 1457.
[18] W.L. Duax, J.F. Griffin and D. Ghosh, in H.-B. Bürgi and J.D. Dunitz (Editors), Structure Correlation, Vol. 2, VCH, Weinheim, 1994, Ch. 13, p. 605.
[19] A. Berthod, Weiyong Li and D.A. Armstrong, Anal. Chem., 64 (1992) 873.

Precision in capillary electrophoresis with respect to quantitative analysis of suramin

Kanthi Hettiarachchi*, Andrew P. Cheung

Life Sciences Division, SRI International, Menlo Park, CA 94025, USA

Abstract

Suramin is an important anti-tumor and anti-viral chemotherapeutic agent. We have previously presented a capillary electrophoresis (CE) method for its quantitative analysis, where its quantitation was linear over three orders of magnitude, with good precision (1.8%) and accuracy. The constantly varying electroosmotic properties of the capillary due to various causes such as analyte adsorption to the inner wall, affect the migration times of analytes during consecutive electrophoresis runs. This results in progressive changes in analyte peak areas, causing less desirable or unacceptable CE assay precision. This paper illustrates a strategy to overcome the problem of assay reproducibility by using an internal standard whose migration time is short and close to that of the analyte so that the relative change of migration time is minimized. Assay precisions as good as 0.3% were observed in these experiments. These results are in agreement with the theoretical basis of experimental capillary electrophoresis.

1. Introduction

Peak-area reproducibility is the most important criterion that leads to good precision in a separation-based assay. Usually, in high-performance liquid chromatography (HPLC), where the technique is very well understood and established, precisions of <1% are routinely achieved. Although capillary electrophoresis (CE) is much more efficient than HPLC, some obvious limitations tend to cause CE precisions to exceed 1%. One of these limitations is the sample loading size. CE is an inherent microanalytical technique, requiring the use of narrow-bore capillaries. The inner diameters of the

capillaries are between 25 and 75 μm [1] for optimum resolutions. Thus, total capillary volumes are in the microliter range, and sample loading volumes are usually at nanoliters or sub-nanoliters [1–3], whereas in HPLC, the sample volumes are in the microliter range. Together with the short detection path of 25 to 75 μm, CE peak areas usually have lower signal-to-noise ratios than those of HPLC. Thus, minute variation in sample loading, voltage, temperature, electrolyte, and capillary can cause considerable variation in the peak-area measurements. With the exception of the capillary, these variations can be eliminated with automation and internal standards. During electrophoresis, analyte molecules can adsorb to the capillary inner wall and affect the zeta potential, thereby changing the electroosmosis. This results in changes in migra-

* Corresponding author.

tion time from run to run and affects the reproducibility of the peak areas [4–6]. In order to minimize analyte adsorption, many coating technologies have been developed [7–11]. In our previous presentation on CE assays of quinobene and suramin [6] we discussed the effect of analyte adsorption on electroosmosis. Even with the use of an internal standard, the assay precision was 1.8%. Although this is an acceptable value for CE assays, we believe that it can be further improved.

Suramin, the hexasodium salt of 8,8'-[carbonylbis[imino - 3,1 - phenylenecarbonylim-

ino(4-methyl-3,1-phenylene)carbonylimino]]bis-1,3,5-naphthalenetrisulfonic acid (SU, Fig. 1) is an interesting and useful pharmaceutical. It has a wide range of therapeutic applications [12]. Its original synthesis dates back to 1916 and it was intended for the treatment of parasitic diseases. Later, as the literature reveals, suramin has been widely tested and used, including as an antitumor [12,13] and an anti-viral [14–17] drug.

Many HPLC procedures for the analysis of suramin have been reported [18–26]. In the work reported by Klecker and Collins [18] on human plasma and Stolzer et al. [19] on human plasma
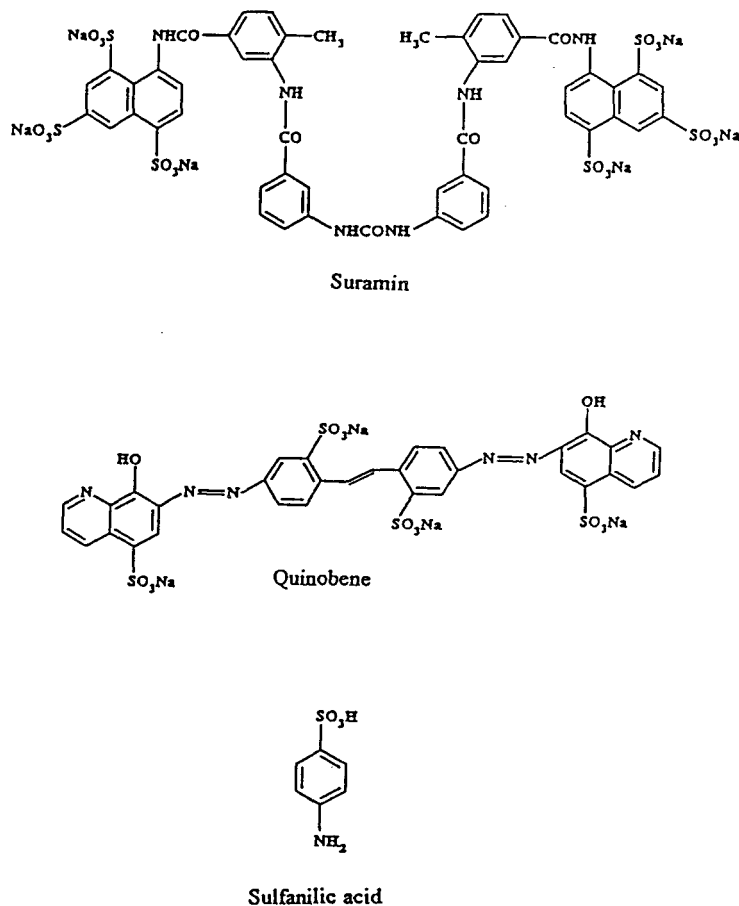
Fig. 1. Molecular structures of suramin, quinobene, and sulfanilic acid.

and urine, gradient and isocratic ion-pair HPLC assay methods were described, respectively. These authors have observed good linearities and recoveries in their work. Supko and Malspeis [20], Tong et al. [21], Tjaden et al. [22], and De Bruijn et al. [23] also describe ion-pair HPLC procedures using different types of columns. Fornstedt [24] described peak-distortion effects of suramin due to large system peaks in bioanalysis using ion-pair chromatography. Garcia and Shihabi [25] reported a rapid HPLC procedure for suramin by injecting diluted serum samples directly onto the column.

However, with respect to CE, only two reports appear in the literature on suramin analysis. Garcia and Shihabi [26] reported a rapid CE assay to measure suramin levels in serum using 3-isobutyl-1-methylxanthine as an internal standard. In that work, they have observed a good linearity of peak area versus concentration with a recovery of 93%. However, the precision of the assay was not reported. Hettiarachchi and Cheung [6] reported an internal standard CE assay with a precision of 1.8%. Due to the importance of suramin and the simplicity and separation efficiency of CE, it is beneficial to develop a more precise CE assay that is comparable to HPLC assays.

Our previous study [6] indicated that precision (R.S.D.) of the area of an analyte peak is about 2–3 times that of the migration time, which is inversely proportional to mobility (μ). Mobility of a chemical is a combination of its electrophoretic mobility (μ_{ep}) and the electroosmosis (μ_{eo}) of the capillary, and can be represented by

$$\mu = \mu_{ep} + \mu_{eo} \qquad (1)$$

Since μ_{ep} is an inherent property of the chemical, μ will remain constant if μ_{eo} is unchanged during the experiment. Irreversible adsorption of analyte molecules to the capillary wall, which results in μ_{eo} variation ($\Delta\mu_{eo}$), is not expected with the use of capillaries covalently coated with neutral organic polymers. However, experimental data indicated the opposite [6]. The adsorption was probably caused by the hydrophobic interaction

of the non-polar part of the analyte with the organic coating. Our efforts to desorb the adsorbed analyte molecules by washing the capillary in between electrophoresis with water and organic solvents were impractical or unsuccessful [27].

For analyte A and internal standard I.S., Eq. 1 can be written as:

$$\mu_A = \mu_{ep,A} + \mu_{eo} \qquad (2)$$

$$\mu_{I.S.} = \mu_{ep,I.S.} + \mu_{eo} \qquad (3)$$

$$\mu_A/\mu_{I.S.} = (\mu_{ep,A} + \mu_{eo})/(\mu_{ep,I.S.} + \mu_{eo}) \qquad (4)$$

Since irreversible adsorption of analytes to the capillary affects only μ_{eo}, Eq. 4 suggests that the ratio $\mu_A/\mu_{I.S.}$ is constant if (i) $\Delta\mu_{eo} \ll \mu_{ep,A}$ and $\mu_{ep,I.S.}$ or (ii) $\mu_{ep,A} \simeq \mu_{ep,I.S.}$. Since $\Delta\mu_{eo}$ is finite, condition (i) can be met if $\mu_{ep,A}$ and $\mu_{ep,I.S.}$ are large. Therefore, by choosing a CE condition and an internal standard that maximizes the mobilities of A and I.S. and minimizes the difference in their mobilities, reproducible peak-area ratio and hence good assay results can be achieved with CE. This paper demonstrates such an approach in the CE assay of suramin (SU), using quinobene, the tetrasodium salt of 4,4′-bis(8-hydroxy-5-sulfo-7-quinoline-azo)-stilbene-2,2′-disulfonic acid (QB) and sulfanilic acid (SA) as potential internal standards (Fig. 1).

2. Experimental

2.1. Reagents

Suramin and quinobene were received from the US National Cancer Institute. Sulfanilic acid was purchased from Eastman Organic Chemicals (Rochester, NY, USA). Sample solutions of 0.1 mg/ml were prepared with distilled water.

Tris(hydroxymethyl)aminomethane (Tris) and boric acid were purchased from Mallinkrodt (Paris, KY, USA). Ethylenediaminetetraacetic acid, disodium salt dihydrate (EDTA) was purchased from Aldrich (Milwaukee, WI, USA).

Polyethylene glycols (PEG) 6K, 12K, 20K, and 35K were from Fluka (Ronokonkoma, NY, USA). These chemicals were of reagent grade.

2.2. Electrolytes

Electrolytes were prepared by dissolving in 0.3 M Tris–boric acid–0.002 M EDTA (pH 8.6) buffer (TBE) (a) 4% each of 6K, 12K, 20K, and 36K PEG for a total of 16% PEG, (b) 0.5% each of 6K, 12K, 20K, and 36K PEG for a total of 2% PEG, (c) 0.25% each of 6K, 12K, 20K, and 36K

PEG for a total of 1% PEG. The TBE buffer was prepared with distilled water.

2.3. Equipment

CE was performed on a BioFocus 3000 electrophoresis system using 36 cm × 50 μm or 24 cm × 50 μm coated fused-silica capillary cartridges. All were purchased from BIO-RAD (Hercules, CA, USA). Electrophoresis was performed with pressure loading, 68.95–413.40 × 10^9 Pa (10–60 p.s.i.) per 1 s, and at 12–18 kV and with UV detection at 254 nm.
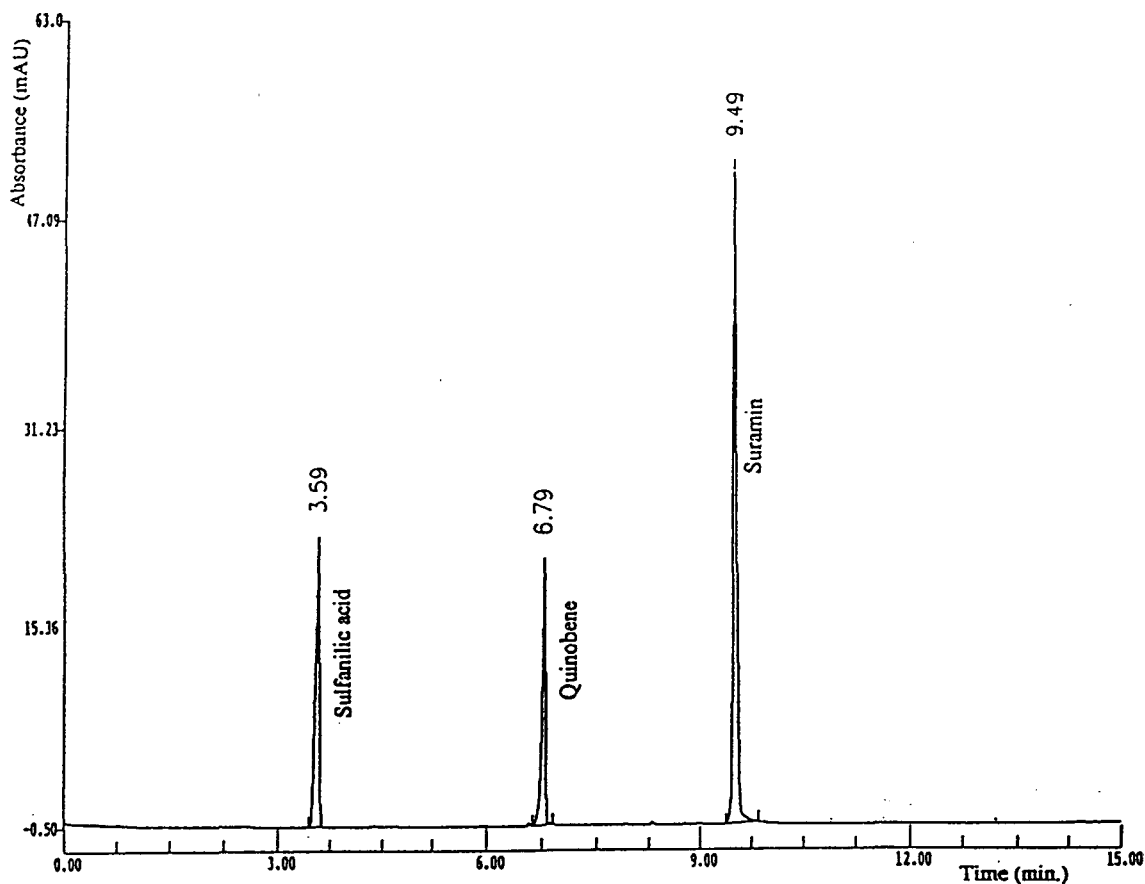
Fig. 2. Electropherogram of a mixture of suramin, quinobene, and sulfanilic acid. Conditions: 16% PEG electrolyte, 24 cm × 50 μm capillary, run voltage 15 kV, pressure injection, 2.67 · 10^9 Pa s (30 p.s.i. s), and detection at 254 nm.

3. Results and discussion

3.1. Reproducibility

To test the hypothesis that precision of an internal-standard CE assay can be improved by increasing mobility μ and decreasing the mobility difference between the analyte and the internal standard, we studied the electrophoresis data from a mixture of sulfanilic acid (SA), quinobene (QB), and suramin (SU). Multiple electrophoreses were performed with 24- and 36-cm coated capillaries and with electrolytes of different viscosity to create different mobilities for the analytes. Fig. 2 is a typical electropherogram of a mixture of SA, QB, and SU.

Consistent with our earlier observation [6], the mobilities of SA, QB, and SU decrease with each use of the capillary. Table 1 presents the mobility and peak-area data from 21 sequential electrophoreses of the mixture. For this experiment, the run voltage was set at 15 kV and loading was by pressure, 50 p.s.i. s. Using a 36-cm capillary and the most viscous electrolyte (16% PEG), the precisions (R.S.D.) of the peak-area ratios for all 21 runs are 2–4%. When they are calculated as seven run blocks, the R.S.D. of the first seven runs improved slightly, to 1–3%. Table 2 summarizes data obtained from a 24-cm capillary and the 16% PEG electrolyte. The run voltage was 15 kV and loading was by pressure at 30 p.s.i. s. In these CE

Table 1
Electrophoretic data from a 36-cm capillary

Run no.	Migration time (min)			Mobility (10^4 cm^2 V^{-1} s^{-1})			Peak-area ratio		
	SA	QB	SU	SA	QB	SU	SU–QB	QB–SA	SU–SA
1	11.62	23.93	33.00	1.08	0.52	0.38	3.42	0.90	3.08
2	11.58	23.85	32.90	1.08	0.53	0.38	3.50	0.93	3.26
3	11.63	23.98	33.12	1.08	0.52	0.38	3.51	0.89	3.13
4	11.70	24.17	33.36	1.07	0.52	0.38	3.52	0.94	3.30
5	11.76	24.31	33.61	1.07	0.52	0.37	3.48	0.91	3.18
6	11.82	24.47	33.85	1.06	0.51	0.37	3.54	0.92	3.26
7	11.97	24.78	34.24	1.05	0.51	0.37	3.42	0.89	3.06
8	12.00	24.91	34.45	1.05	0.50	0.36	3.52	0.93	3.27
9	12.04	25.03	34.66	1.04	0.50	0.36	3.45	0.84	2.89
10	12.08	25.17	34.84	1.04	0.50	0.36	3.52	0.93	3.27
11	12.11	25.27	34.99	1.04	0.50	0.36	3.36	0.91	3.06
12	12.17	25.43	35.26	1.03	0.49	0.36	3.54	0.93	3.29
13	12.37	25.76	35.67	1.02	0.49	0.35	3.50	0.93	3.26
14	12.39	25.86	35.83	1.01	0.49	0.35	3.54	0.94	3.32
15	12.42	25.90	35.90	1.01	0.48	0.35	3.55	0.90	3.21
16	12.42	25.97	36.01	1.01	0.48	0.35	3.57	0.99	3.53
17	12.44	26.04	36.14	1.01	0.48	0.35	3.30	0.98	3.25
18	12.44	26.04	36.16	1.01	0.48	0.35	3.55	0.90	3.19
19	12.47	26.03	36.11	1.01	0.48	0.35	3.40	0.98	3.33
20	12.42	25.96	36.05	1.01	0.48	0.35	3.52	0.92	3.23
21	12.46	26.05	36.19	1.01	0.48	0.35	3.46	0.93	3.92
R.S.D. (%): All 21 runs				2.6	3.1	3.3	2.0	3.6	3.9
Run 1–7				1.1	1.3	1.4	1.3	1.8	2.8
Run 8–14				1.2	1.3	1.4	1.7	3.5	4.6
Run 15–21				0.2	0.2	0.3	2.7	4.0	3.5

For conditions, see Experimental.

Table 2
Electrophoretic data from a 24-cm capillary

Run no.	Migration time (min)			Mobility (10^4 cm^2 V^{-1} s^{-1})			Peak-area ratio		
	SA	QB	SU	SA	QB	SU	SU–QB	QB–SA	SU–SA
1	3.69	7.06	9.81	1.40	0.73	0.53	1.88	0.73	1.38
2	3.55	6.80	9.52	1.46	0.76	0.54	1.91	0.73	1.39
3	3.50	6.70	9.39	1.48	0.77	0.55	1.91	0.74	1.42
4	3.57	6.80	9.51	1.45	0.76	0.54	1.92	0.74	1.42
5	3.52	6.74	9.46	1.47	0.77	0.55	1.93	0.74	1.44
6	3.50	6.72	9.44	1.48	0.77	0.55	1.90	0.75	1.42
7	3.50	6.69	9.40	1.48	0.77	0.55	1.91	0.76	1.44
R.S.D. (%):	All 7 runs			1.8	1.8	1.4	0.7	1.2	1.6

For conditions, see Experimental.

systems, migration of the analytes, from negative to positive electrode, ran counter to electroosmosis μ_{eo}. Mobility data in Table 2 are about 30–40% faster than those in Table 1, due to reduction in μ_{eo} in the shorter capillary. The R.S.D.s of the peak-area ratios from the 24-cm capillary were improved to 0.7–1.6%, about half of the result observed for the 36-cm capillary.

Improvements in the peak-area ratio precision are predictable and reproducible. Table 3 shows the summary of electrophoretic data from experiments performed on separate days and with 24-cm capillaries. Three electrolytes containing 16%, 2%, and 1% PEG in TBE buffer were used to create differences in mobility. As the viscosity of the electrolyte decreased from 16% to 1% PEG, an increase in the mobilities of the chemicals was observed. This is consistent with Stoke's law that electrophoretic mobility is inversely proportional to the viscosity of the electrolyte.

While by increasing the mobility of the analyte and internal standard the improvement of the precision of the CE assay has been demonstrated, decreasing the mobility difference between the analyte and the internal standard is equally effective in improving assay precision. Examine the peak-area ratio R.S.D. data versus normalized delta mobility, which is defined as the difference in mobility of the pair over its average

in Table 3. The peak-area ratio R.S.D. of the SU–QB pair, which has the least normalized delta mobility of 0.3, is significantly better than those of the other two pairs, even though SU and QB are the slower migrating ones. The normalized delta mobilities of the other two pairs, QB–SA and SU–SA, were respectively 0.6 and 0.9. Table 3 confirms that the R.S.D. of the peak-area ratio decreases with the normalized delta mobility. Thus, by choosing an internal standard (QB) which gives a small normalized delta mobility with the analyte, a CE assay of 0.6% R.S.D. can be routinely achieved for suramin.

3.2. Specificity

Using a 24-cm capillary, separation of suramin (SU) from the chosen internal standard (QB) was comparable for all three electrolytes discussed earlier (Fig. 3). When the 1% PEG electrolyte was used, the I.S. migrated closely with a significant decomposition product of SU (Fig. 4). While both 16% and 2% PEG electrolytes gave good separation for the I.S. and its decomposition products, the 2% PEG gave larger mobility for the analytes than the 16% PEG electrolyte and thus was chosen for the assay.

Table 3
Precision and "ruggedness" of peak-area ratio in an internal standard CE assay

Experiment no.	Run voltage (kV)	Electrolyte	Migration time (min)			Mobility (10^4 cm^2 V^{-1} s^{-1})			Normalized delta mobility			Peak-area ratio R.S.D.			n
			SA	QB	SU	SA	QB	SU	SU–QB	QB–SA	SU–SA	SU–QB	QB–SA	SU–SA	
1	15	16% PEG	3.55	6.79	9.50	1.46	0.76	0.54	0.33	0.63	0.91	0.72	1.18	1.56	7
2	15	16% PEG	3.58	6.92	9.78	1.44	0.75	0.53	0.34	0.64	0.93	0.84	1.14	1.10	5
3	15	16% PEG	3.68	7.08	9.91	1.41	0.73	0.52	0.33	0.63	0.92	0.52	1.22	1.54	7
4	13	16% PEG	4.28	8.21	11.50	1.39	0.73	0.52	0.33	0.63	0.92	0.62	0.85	1.22	7
5	15	2% PEG	3.73	5.91	7.80	1.39	0.88	0.66	0.28	0.45	0.71	0.69	1.07	1.56	9
6	12	2% PEG	4.46	7.67	10.23	1.45	0.84	0.63	0.29	0.53	0.79	0.58	1.59	1.99	9
7	15	2% PEG	3.55	6.07	8.11	1.46	0.85	0.64	0.29	0.52	0.78	0.31	0.53	0.65	9
8	18	2% PEG	2.89	4.92	6.58	1.49	0.88	0.66	0.29	0.52	0.78	0.61	0.66	1.13	11
9	18	1% PEG		2.51	3.14		1.72	1.37	0.22			0.51			6
											Average:	0.60	1.03	1.34	

For conditions, see Experimental.

3.3. Linearity

Table 4 presents the linearity data on the improved CE assay of suramin. The assay used a 24 cm × 50 μm coated capillary, 2% PEG elec-

trolyte, 15 kV, pressure loading at 15 p.s.i. s, and QB (0.25 mg/ml water) as the internal standard. In an analyte solution concentration range of 0.1 μg/ml to 1.0 mg/ml in I.S., the peak area-ratio of SU–QB (y) was linearly proportional to the
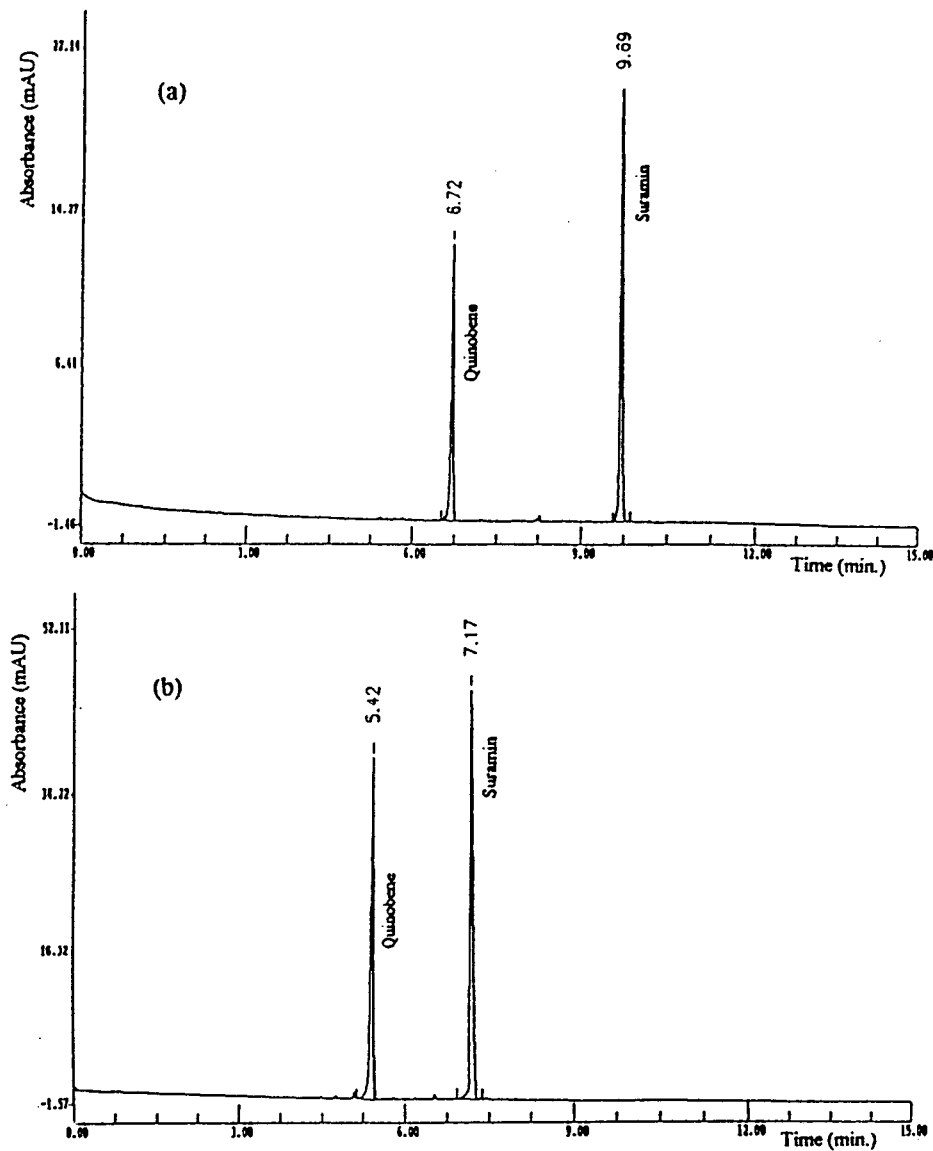
Fig. 3.
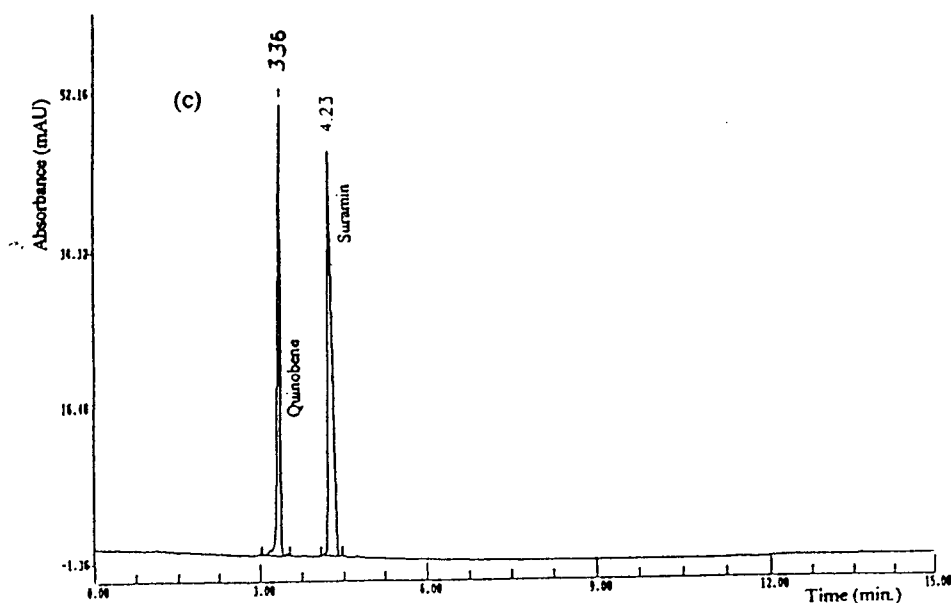
Fig. 3. Electropherograms of suramin and quinobene in (a) 16% PEG electrolyte, (b) 4% PEG electrolyte, and (c) 1% PEG electrolyte; other conditions: 24 cm × 50 μm capillary, run voltage 15 kV, pressure injection, $2.67 \cdot 10^9$ Pa s (30 p.s.i. s), and detection at 254 nm.

Table 4
Linearity data

Run no.	SU (mg/ml I.S.)	Peak-area ratio SU–QB
1	0.00013	0.00726
2	0.00126	0.04279
3	0.01256	0.42698
4	0.12560	4.11397
5	0.22130	7.17635
6	0.29080	9.41390
7	0.45430	14.48543
8	0.48380	15.37550
9	0.61700	19.43455
10	0.68580	21.64488
11	0.88350	27.32580
12	0.94500	29.25927
13	1.09500	33.56189
Slope	30.7913	
Std. error of slope	0.1836	
y-Intercept	0.2450	
Std. error of y est.	0.2403	
r^2	0.9996	

For conditions, see Experimental.

analyte concentration (x) according to the linear equation $y = 30.791x + 0.245$ with an r^2 of 0.9996.

4. Conclusion

Over the past few years, CE techniques have shown a tremendous growth in terms of efficiency, quantitation, and automation. By overcoming the systemic limitations and drawbacks, CE researchers are now achieving much better precisions. When the ease of operation and efficiency are considered, CE stands out in comparison to HPLC. Environmentally speaking, CE generates minute solvent waste in comparison to HPLC. Although many researchers [6,28–36] have shown that quantitation precision approaching that of HPLC was achievable, widespread use of CE assay in pharmaceutical analysis has not appeared yet. Due to a lack of full understanding of the quantitation limitation of a CE assay, many hesitate to use it as a routine
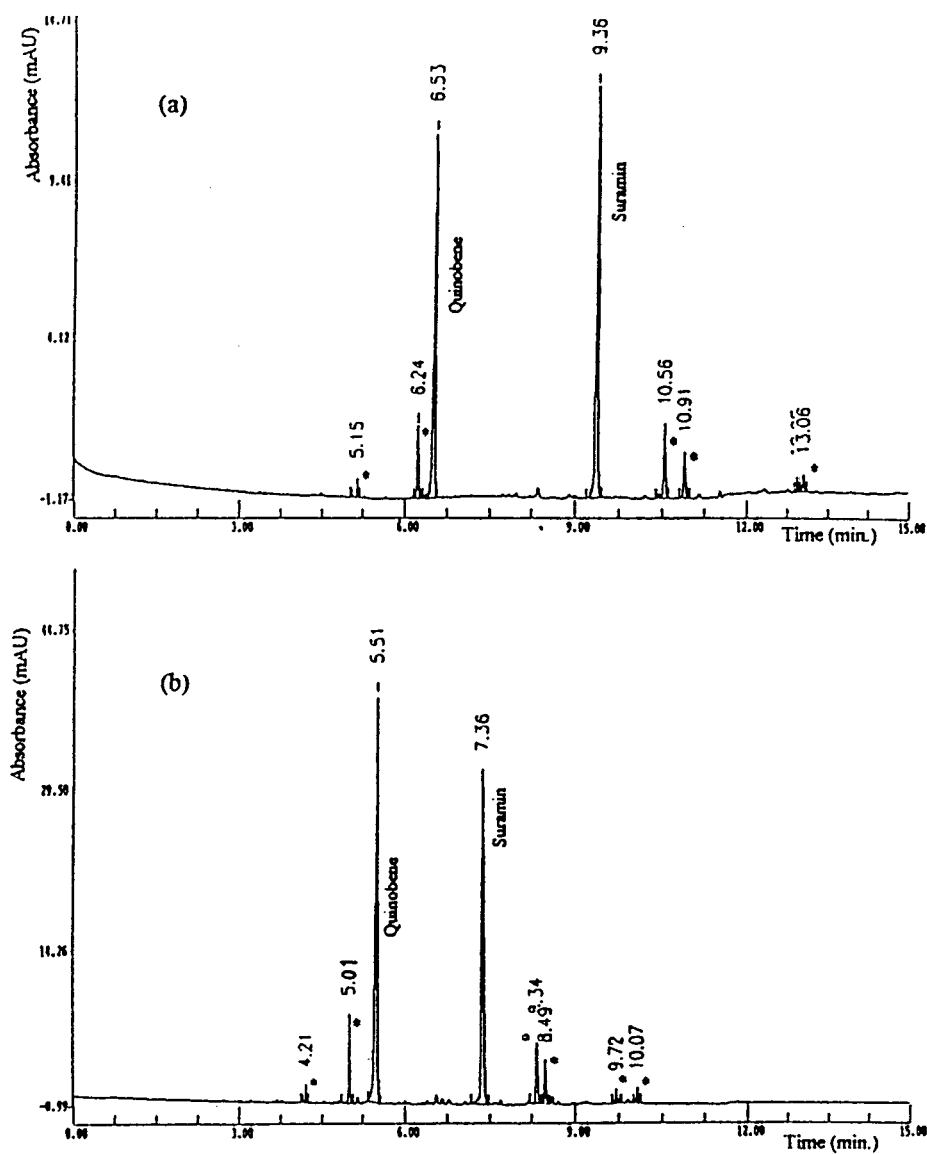
Fig. 4.

quantitative technique. In our previous paper [6] and here, we have discussed the quantitative limitations of CE and strategies to overcome them. In this paper, we demonstrated that by proper choice of an internal standard and the mobility of the analytes, an accurate and rugged CE assay with precision equal to that of HPLC can be routinely achieved. With these and other demonstrations, the authors hope that CE assays will eventually be accepted as a routine assay, complementary to HPLC assay, by the pharmaceutical establishment.
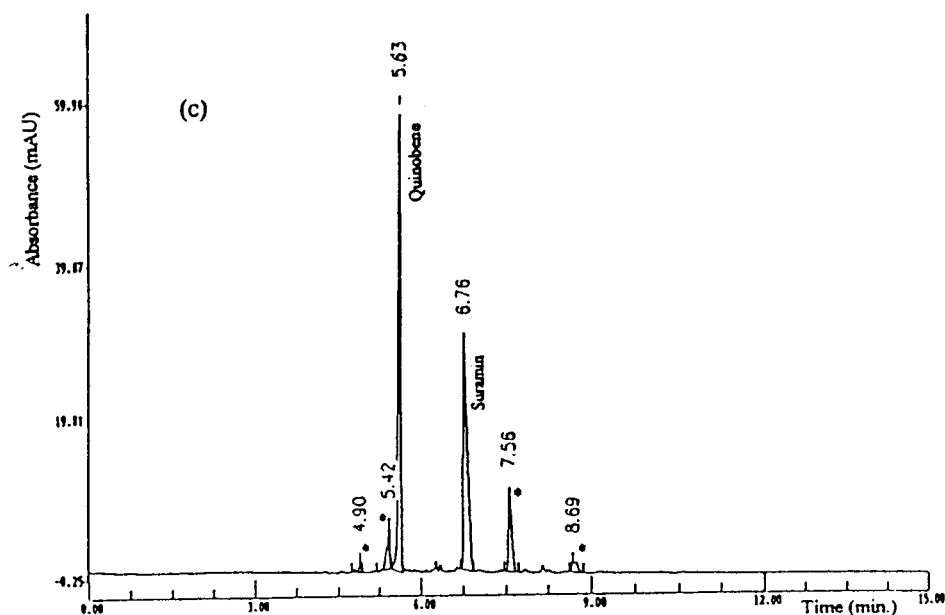
Fig. 4. Electropherograms of a mixture of thermally decomposed suramin and quinobene in (a) 16% PEG electrolyte, (b) 4% PEG electrolyte, and (c) 1% PEG electrolyte; other conditions: 24 cm × 50 μm capillary, run voltage 15 kV, pressure injection, $2.67 \cdot 10^9$ Pa s (30 p.s.i. s), and detection at 254 nm. Asterisks denote decomposition peaks of suramin.

References

[1] D.N. Heiger, High Performance Capillary Electrophoresis–An Introduction, Hewlett-Packard, Waldbronn, Germany, 1992, p. 6.

[2] R.P. Oda and J.P. Landers, in J.P. Landers (Editor), Hand Book of Capillary Electrophoresis, CRC Press, Boca Raton, FL, 1993, p. 12.

[3] N.J. Dovichi, in P. Camileri (Editor), Capillary Electrophoresis, Theory and Practice, CRC Press, Boca Raton, FL, 1993, p. 29.

[4] S. Hjerten and K. Kubo, Electrophoresis, 14 (1993) 390.

[5] J.K. Towns and F.E. Regnier, Anal. Chem., 64 (1992) 2473.

[6] K. Hettiarachchi and A.P. Cheung, J. Pharm. Biomed. Anal., 11 (1993) 1251.

[7] M. Gilges, M.H. Kleemiss and G. Schomburg, Anal. Chem., 66 (1994) 2038.

[8] S. Hjerten, Ark Kemi, 13 (1958) 151.

[9] S. Hjerten, J. Chromatogr., 347 (1985) 191.

[10] A.S. Cohen and B.L. Karger, J. Chromatogr., 397 (1987) 409.

[11] D. Schmalzing, C.A. Piggee, F. Foret, E. Carrilho and B.L. Karger, J. Chromatogr. A, 652 (1993) 149.

[12] R.V. La Rocca, C.A. Stein, R. Danesi and C.E. Myers, J. Steroid Biochem. Mol. Biol., 37 (1990) 893.

[13] C.E. Myers, C. Stein, R. La Rocca, M. Cooper, J. Cassidy and N. McAtee, Proc. Am. Soc. Clin. Oncol., 256 (1989) 66.

[14] E. De Clercq, Cancer Lett., 8 (1979) 9.

[15] H. Mitsuya, M. Popovic, R. Yarchoan, S. Matsushita, R.C. Gallo and S. Broder, Science, 226 (1984) 172.

[16] S. Broder, R. Yarchoan, J.M. Collins, H.C. Lane, P.D. Markham, R.W. Klecker, R.R. Redfield, H. Mitsuya, D.F. Hoth, E. Gelmann, L. Resnick, C.E. Myers and A.S. Fauci, Lancet, 2 (1985) 627.

[17] J.M. Collins, R.W. Klecker, R. Yarchoan, H.C. Lane, A.S. Fauci, R.R. Redfield, S. Broder and C.E. Myers, J. Clin. Pharmacol., 26 (1989) 22.

[18] R.W. Klecker and J.M. Collins, J. Liq. Chromatogr., 8 (1985) 1685.

[19] T.J. Stolzer, G. LaFollette, J. Gambertoglio, F. Aweeka and E.T. Lin, J. Liq. Chromatogr., 10 (1987) 3451.

[20] J.G. Supko and L. Malspeis, J. Liq. Chromatogr., 13 (1990) 727.

[21] W.P. Tong, H.I. Scher, D.P. Petrylak, A. Dnistrian, T. Curley and J. Vasquez, J. Liq. Chromatogr., 13 (1990) 2269.

[22] U.R. Tjaden, H.J.E.M. Reeuwijk, J. Van Der Greef,

G. Pattyn, E.A. De Bruijn and A.T. Van Oosterom, J. Chromatogr., 525 (1990) 141.

[23] E.A. De Bruijn, G. Pattyn, L. Denis, C. Mahler, A.T. Van Oosterom and E. Desmedt, J. Liq. Chromatogr., 14 (1991) 3719.

[24] T. Fornstedt, J. Chromatogr., 612 (1993) 137.

[25] L.L. Garcia and Z.K. Shihabi, J. Liq. Chromatogr., 16 (1993) 1279.

[26] L.L. Garcia and Z.K. Shihabi, J. Liq. Chromatogr., 16 (1993) 2049.

[27] T. Tran, K. Hettiarachchi and A.P. Cheung, unpublished data.

[28] B.R. Thomas, X.G. Fang, X. Chen, R.J. Tyrrell and S. Ghodbane, J. Chromatogr. B, 657 (1994) 383.

[29] W. Nashabeh, K.F. Greve, D. Kirby, F. Foret, B.L. Karger, D.H. Reifsnyder and S.E. Builder, Anal. Chem., 66 (1994) 2148.

[30] J.B. Nair and C.G. Izzo, J. Chromatogr., 640 (1993) 445.

[31] H. Nishi, T. Fukuyama, M. Matsuo and S. Terabe, J. Pharm. Sci., 79 (1990) 519.

[32] P.D. Grossman, J.C. Colburn, H.H. Lauer, R.G. Nielsen, R.M. Riggin, G.S. Sittampalam and E.C. Rickard, Anal. Chem., 61 (1989) 1186.

[33] T.E. Peterson and D. Trowbridge, J. Chromatogr., 603 (1992) 298.

[34] H. Soini, M.-L. Riekkola and M.V. Novotny, J. Chromatogr., 608 (1992) 265.

[35] K.D. Altria and M.T. Kersey, LC·GC, 13 (1995) 40.

[36] R.R. Chadwick, J.C. Hsieh, K.S. Resham and R.B. Nelson, J. Chromatogr. A, 671 (1994) 403.

Enantiomeric purity determination of propranolol by cyclodextrin-modified capillary electrophoresis

M. Fillet, I. Bechet, P. Chiap, Ph. Hubert, J. Crommen*

Laboratory of Drug Analysis, Institute of Pharmacy, University of Liège, rue Fusch, 5, B-4000 Liège, Belgium

Abstract

A capillary electrophoretic method for the enantiomeric purity determination of either enantiomer of propranolol was developed using cyclodextrins as chiral additives and uncoated fused-silica capillaries thermostated at 15°C. The effect of the type and concentration of cyclodextrin added to a triethanolamine–phosphate buffer (pH 3.0) on chiral resolution and migration times was studied. The propranolol enantiomers could be separated with all cyclodextrins tested (β-cyclodextrin and seven of its derivatives), except dimethyl-β-cyclodextrin. A particularly high resolution value of 4.4 was obtained for propranolol enantiomers with a buffer containing 10 mM carboxymethyl-β-cyclodextrin. This buffer was selected for testing the enantiomeric purity of propranolol, making it possible to reach detection limits of less than 0.1% for the minor enantiomer. The R enantiomer of propranolol (second migrating) could be quantified at the 0.5% level with good precision (intra-day R.S.D. = 1.7%) in samples of the S enantiomer (first migrating), while the limit of quantification of the latter, when present as an impurity in the R enantiomer, was 0.1%. The method also gave good results in terms of linearity and accuracy.

1. Introduction

Most often the enantiomers of chiral drugs have different pharmacological and toxicological properties and therefore the quantitative enantiomeric composition of these drugs should be determined [1–3]. The separation and determination of enantiomers are required for enantiomeric purity testing, chiral stability testing of pharmaceutical formulations (absence of racemization of drug enantiomers) and in pharmacokinetic and clinical studies.

Capillary electrophoresis (CE) using cyclodextrins as chiral selectors has proved to be very useful in chiral analysis, owing to its high separation efficiency and enantioselectivity [4–6]. However, only few papers have considered so far quantitative aspects of chiral CE [7–9].

Propranolol (cf., Fig. 1) is a β-adrenergic blocking agent, i.e., a competitive inhibitor of the effects of catecholamines at β-adrenergic receptor sites. It is widely used in therapeutics for its antihypertensive, antiangorous and antiarrhythmic properties. Pharmacological studies
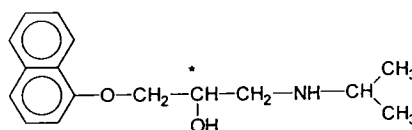
Fig. 1. Structure of propranolol.

* Corresponding author.

have shown that the *S*-(−) enantiomer of pro-pranolol is about 100 times more active than the *R*-(+) enantiomer [10].

Native and derivatized cyclodextrins [11–17] have often been used in free solution capillary zone electrophoresis (CZE) for the enantiosepa-ration of propranolol. The resolution of propran-olol enantiomers could be obtained by adding β-cyclodextrin or one of its derivatives to phos-phate buffers of low pH (2.4–3.1) [11–16]. With carboxymethyl-β-cyclodextrin, ionizable at high-er pH, chiral resolution for propranolol was improved by increasing the buffer pH up to 5.8 [14]. Propranolol was also enantioseparated by CZE by use of a running buffer containing hydroxypropyl-β-cyclodextrin, an uncharged de-rivative, and a hydrophilic polymeric additive at pH 7.0 [17].

In addition to cyclodextrins, cellulase was found to be a good chiral selector for the CZE enantiomeric separation of β-blockers, including propranolol [18]. Micellar electrokinetic capillary chromatography (MEKC) was also recently ap-plied to the resolution of propranolol enantio-mers, using either sodium dodecyl sulfate with cyclodextrins [19] or a chiral surfactant, such as N-dodecoxycarbonylvaline [20].

In this work, a CZE method for the enantio-meric purity determination of propranolol was developed. β-Cyclodextrin and seven of its de-rivatives were tested as chiral additives. The effect of the type and concentration of cyclodex-trin on the resolution and migration behaviour of propranolol enantiomers was studied, using a triethanolamine phosphate buffer (pH 3.0) and uncoated fused-silica capillaries thermostated at 15°C. Optimum conditions with respect to chiral resolution were selected for testing the enantio-meric purity of propranolol. This enantioselec-tive CE method has been validated and the results of this validation are given.

2. Experimental

2.1. Apparatus

All experiments were performed on a Model [3D]CE system (Hewlett-Packard, Palo Alto, CA,

USA) equipped with a diode-array detector, an automatic injector, an autosampler and a tem-perature control system (15–60°C,±0.1°C). An HP Vectra 486/66XM computer was used for instrument control and data handling. The pH of the buffers was adjusted by means of a Delta 345 pH meter (Mettler, Halstead, UK).

2.2. Chemicals and reagents

Phosphoric acid (85%) and triethanolamine were of analytical-reagent grade from Merck (Darmstadt, Germany). Water was of Milli-Q quality (Millipore, Bedford, MA, USA). β-Cyclodextrin (βCD) and heptakis(2,3,6-tri-O-methyl)-β-cyclodextrin (TMCD) were purchased from Sigma (St. Louis, MO, USA), heptakis (2,6-di-O-methyl)-β-cyclodextrin (DMCD) and hydroxypropyl-β-cyclodextrin (HPCD) from Janssen Chimica (Geel, Belgium) and carboxymethyl-β-cyclodextrin (CMCD), carbo-xyethyl-β-cyclodextrin (CECD), succinyl-β-cyclodextrin (SCD) and methyl-β-cyclodextrin (MCD) from Cyclolab (Budapest, Hungary). Propranolol hydrochloride racemate was kindly supplied by SMB (Brussels, Belgium). (*R*)-(+) and (*S*)-(−)-propranolol hydrochlorides were purchased from Sigma. All compounds were used without further purification.

2.3. Electrophoretic technique

Separations were carried out with uncoated fused-silica capillaries (48.5 cm × 50 μm I.D., 40 cm to the detector). Before use, the capillary was washed successively with basic solutions (i.e., 1 *M* NaOH followed by 0.1 *M* NaOH), water and separation buffer. The latter consisted of 0.1 *M* phosphoric acid adjusted to pH 3 with tri-ethanolamine. At the beginning of each working day, the capillary was washed with separation buffer for 10 min, and after each sample injec-tion the capillary was washed with water for 2 min and with buffer for 3 min.

The applied voltage was 25 kV and UV detec-tion was performed at 210 nm. Injections were made using the hydrodynamic mode (injection pressure 5 kPa) for 2 s (resolution studies) or 30 s (enantiomeric purity testing). The capillary was

thermostated at 15°C. The standard solutions were prepared by dissolving salts of racemic propranolol at a concentration of 50 μg/ml and salts of pure enantiomers at a concentration of 25 μg/ml.

The resolution (R_s) was calculated according to the standard expression based on peak width at half-height [21].

3. Results and discussion

3.1. Buffer composition

All enantiomeric separations reported were performed with buffers made of 100 mM phosphoric acid adjusted to pH 3.0 with triethanolamine and containing β-cyclodextrin or one of its derivatives [15]. Under these conditions, analyte interactions with the capillary wall were minimized and the electroosmotic flow was reversed, with a low, fairly constant mobility value of $-4 \cdot 10^{-5}$ cm^2 V^{-1} s^{-1}, which gave rise to highly reproducible migration times. The use of triethanolamine, a co-ion of low mobility, also resulted in good peak symmetry for cationic analytes such as propranolol, low currents (40–60 μA) and high efficiency (ca. 100 000 theoretical plates per capillary in the low concentration range). At the pH used, propranolol was fully

ionized whilst all cyclodextrins tested were principally in uncharged form.

3.2. Influence of the type and concentration of cyclodextrin

β-Cyclodextrin (βCD) and seven of its derivatives, methyl-β-cyclodextrin (MCD), heptakis-(2,6-di-O-methyl)-β-cyclodextrin (DMCD), heptakis (2,3,6-tri-O-methyl)-β-cyclodextrin (TMCD), hydroxypropyl-β-cyclodextrin (HPCD), carboxymethyl-β-cyclodextrin (CMCD), carboxyethyl-β-cyclodextrin (CECD) and succinyl-β-cyclodextrin (SCD), were tested as chiral selectors for the enantiomeric separation of propranolol, injected as racemate.

Table 1 shows the influence of the nature and the concentration of the eight cyclodextrins on the enantioseparation of propranolol. A dash indicates that no resolution was observed between the enantiomers ($R_s < 0.5$) and a resolution value lower than 0.7 means that the enantiomers were partially resolved but not sufficiently to permit a precise determination of R_s.

Table 1 clearly shows that large differences in chiral resolution are generally obtained with the different cyclodextrins at a given concentration. The propranolol enantiomers can be completely resolved with all β-cyclodextrin derivatives ex-

Table 1
Effect of cyclodextrin type and concentration on resolution of propranolol enantiomers

CD	Cyclodextrin concentration (mM)							
	1	2	5	10	15	20	30	50
DMCD	$-$[a]	$-$	$-$	$-$	$-$	$-$	$-$	$-$
HPCD	0.8	1.5	2.2	2.4	2.3	2.0	1.8	1.4
TMCD	$-$	$-$	0.7	1.3	1.6	1.8	2.0	2.1
βCD	$-$	<0.7	1.0	1.1	1.0	/[b]	/	/
CMCD	1.0	1.6	3.0	4.4	/	/	/	/
CECD	<0.7	1.0	1.4	1.4	1.6	1.5	1.3	/
MCD	0.9	1.4	1.9	1.5	1.4	1.2	0.9	/
SCD	<0.7	0.7	1.3	1.4	1.5	1.5	1.2	/

Buffer, 100 mM phosphoric acid adjusted to pH 3 with triethanolamine containing β-cyclodextrin or one of its derivatives. Injection mode, hydrodynamic, 5 kPa, 2 s. Other conditions as described under Experimental.
[a] $-$ No detectable resolution.
[b] /, Not determined (migration times longer than 50 min.).

cept DMCD, which gives no resolution in the concentration range studied. With the native β-CD, only partial resolution was obtained.

Table 2 shows the influence of the type and concentration of cyclodextrin on the migration times of propranolol. When chiral resolution is obtained, the migration times, given in Table 2, are those of the first enantiomer of propranolol. An increase in migration time with increasing cyclodextrin concentration was observed in all cases, even when the increase in buffer viscosity was taken into account, indicating that the propranolol enantiomers have a more or less pronounced tendency to interact with all cyclodextrins, including DMCD.

As can be seen from Table 1, for each cyclodextrin there is an optimum concentration at which chiral resolution reaches a maximum value [12,15]. Three of the β-cyclodextrin derivatives (TMCD, HPCD and CMCD) were found to be particularly suitable, since they gave resolution values higher than 2. A maximum resolution value of 4.4 was obtained for propranolol enantiomers with a buffer containing 10 mM CMCD. A typical electropherogram obtained under these conditions is presented in Fig. 2. The buffer giving the highest resolution was selected for testing the enantiomeric purity of propranolol.

3.3. Validation of the method developed for the enantiomeric purity testing of propranolol

Several performance criteria were studied, including selectivity, linearity of detector response, limits of detection and quantification for the minor enantiomer, accuracy and reproducibility of peak area measurements.

Selectivity

The homogeneity of the peaks of propranolol enantiomers (absence of interferences from the sample matrix) was tested by use of the diode-array detector. Each enantiomer was then injected alone and no trace of the other enantiomer was detectable, which demonstrated the enantiomeric purity of the propranolol enantiomers tested. The first migrating peak was identified as the S enantiomer of propranolol (the more active enantiomer) and the second migrating peak as the R enantiomer (the less active).

Linearity

Two calibration graphs were constructed in order to demonstrate the linearity of the detector response (cf., Table 3): the first in the range 0.1–10% of the S enantiomer and the second in the range 0.5–10% of the R enantiomer in

Table 2
Effect of cyclodextrin type and concentration on migration times of propranolol enantiomers

CD	Cyclodextrin concentration (mM)							
	1	2	5	10	20	30	50	
DMCD	9.6	10.7	13.1	16.0	18.2	19.5	22.0	29.9
HPCD	11.1	12.5	15.4	19.0	21.4	23.2	26.1	31.2
TMCD	9.1	9.4	9.9	10.5	11.4	12.4	14.3	17.7
βCD	9.9	10.6	12.9	15.5	17.3	/[a]	/	/
CMCD	10.9	13.1	17.3	21.3	/	/	/	/
CECD	9.9	12.5	15.6	19.1	25.7	28.9	34.2	/
MCD	10.9	11.6	14.7	18.3	18.7	19.8	22.2	/
SCD	9.1	9.9	11.8	14.4	16.6	18.1	21.9	/

Buffer, 100 mM phosphoric acid adjusted to pH 3 with triethanolamine containing β-cyclodextrin or one of its derivatives. Injection mode, hydrodynamic, 5 kPa, 2 s. Other conditions as described under Experimental.
[a] Not determined (migration times longer than 50 min).

Migration times
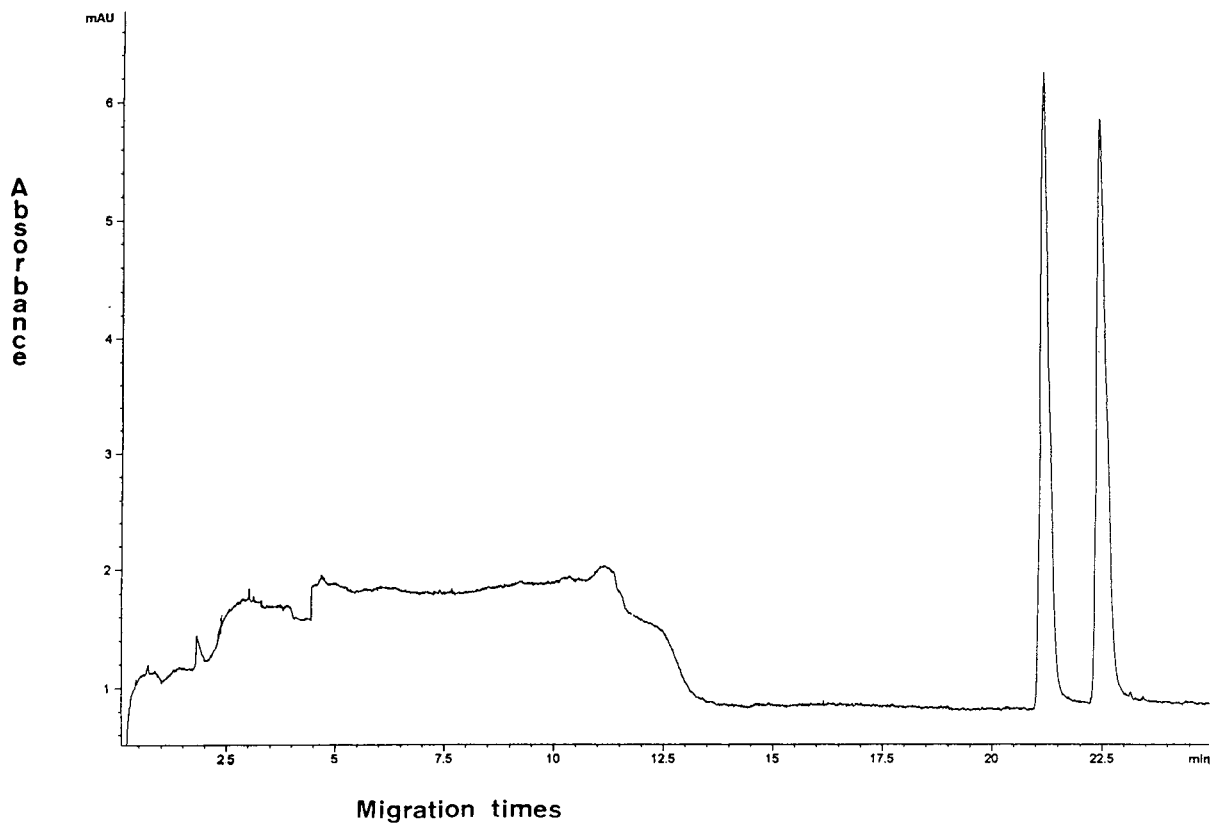
Fig. 2. CE separation of propranolol enantiomers. Buffer: 10 mM carboxymethyl-β-cyclodextrin in 100 mM phosphoric acid adjusted to pH 3 with triethanolamine. Hydrodynamic injection: 5 kPa, 2 s. Samples: 50 μg/ml solution of racemic propranolol in diluted buffer. Other conditions as under Experimental.

samples of their stereoisomer, each calibration point ($n = 5$) being injected in triplicate. Linear regression analysis, plotting the analyte peak area (y) versus the percentage of impurity (x), gave the following equations:

S enantiomer: $y = 9.25x + 0.44$ (± 0.86)

R enantiomer: $y = 7.61x - 0.05$ (± 0.39)

The adequate linearity of the calibration graphs is demonstrated by the determination coefficients ($r^2 > 0.999$) obtained for the regression lines.

Limits of detection and quantification

Limits of detection (LOD) and quantification (LOQ), corresponding to signal-to-noise ratios of 3 and 10, respectively, were calculated from linear regression analysis made by plotting the analyte peak height versus the percentage of impurity.

LODs of 0.03% and 0.06% and LOQs of 0.10% and 0.22% were obtained for the S and R enantiomers, respectively (cf., Table 3). These limits are particularly low for the S enantiomer, which migrates first. Typical electropherograms of propranolol enantiomers containing low levels

Table 3
Linearity, limits of detection and quantification

Parameter	S enantiomer	R enantiomer
Calibration range (%)	0.1–10	0.5–10
Calibration points	5	5
Slope ± S.D.	9.25 ± 0.06	7.62 ± 0.03
Intercept ± S.D.	0.44 ± 0.30	−0.05 ± 0.14
S.D. of residuals	0.86	0.39
Coefficient of determination (r^2)	0.9995	0.9998
Comparison of the intercept to zero (Student's test):		
t calculated	1.46	0.36
t from the table	2.16	2.16
Existence of a significant slope (Fisher's test):		
F_1 calculated	25604	77678
F_1 from the table	4.67	4.67
Limit of detection (%)	0.03	0.06
Limit of quantification (%)	0.10	0.22

Table 4
Reproducibility of peak areas

Spiking level of the minor enantiomer (%)	n	R.S.D. (%)	
		S enantiomer	R enantiomer
Intra-day precision			
10	6	0.5	1.5
1	6	2.8	1.9
0.5	6	ND[a]	1.7
0.1	6	3.4	–[b]
Inter-day precision			
10	3	0.9	1.8
1	3	3.2	5.2
0.5	3	ND[a]	8.5
0.1	3	20.4	–[b]

[a] Not determined.
[b] Below to the limit of quantification.

of their stereoisomers are presented in Fig. 3. Limits of detection and quantification for the R enantiomer could probably be improved by the injection of smaller volumes of more concentrated samples.

Accuracy

The accuracy of the method at the 0.1% and 0.5% levels for the S and R enantiomers, respectively, in samples of their stereoisomers were

also determined in terms of recovery. The following results were obtained: S enantiomer, 96.77 ± 8.13%; and R enantiomer, 97.77 ± 3.74%. As the theoretical value of 100% was included in the confidence interval, the test procedure could be considered accurate over the range studied.

Reproducibility

The relative standard deviations (R.S.D.s) for peak area measurements are given in Table 4.
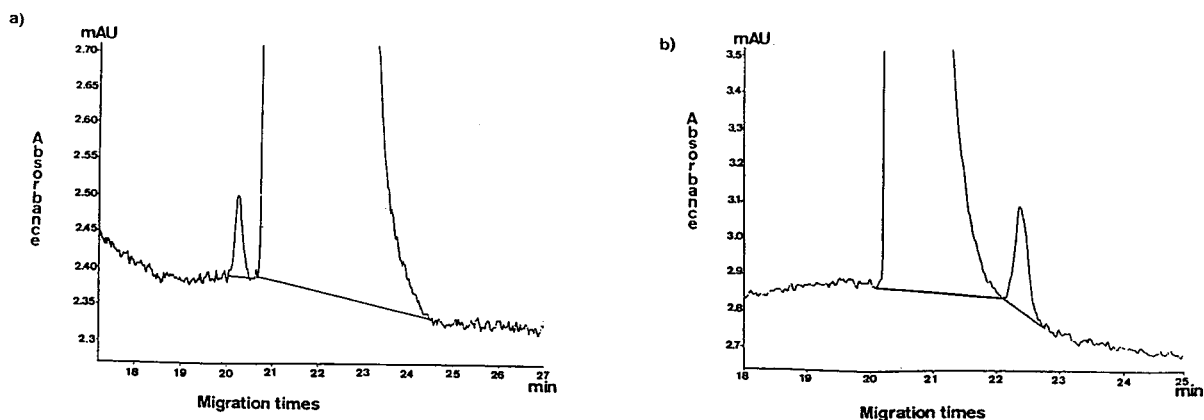
Fig. 3. Typical electropherograms of propranolol enantiomers containing low levels of their stereoisomers. (a) 0.1% of S enantiomer in R enantiomer; (b) 0.5% of R enantiomer in S enantiomer. Hydrodynamic injection: 5 kPa, 30 s. Samples: 25 μg/ml solutions of propranolol enantiomers in diluted buffer. Other conditions as in Fig. 2.

The intra-day precision was evaluated at three percentages for each enantiomer. The inter-day precision was studied on four different days. The intra-day R.S.D.s are 1.7% for 0.5% of the *R* enantiomer and 3.4% for 0.1% of the *S* enantiomer in samples of their stereoisomers. The inter-day R.S.D.s at the LOQ are relatively high but still acceptable for such low levels of the minor enantiomer.

Stability of sample solution

Solutions of both enantiomers were stored for 3 months at 22°C and analysed again by the chirally selective CE method. No racemization of the enantiomers had occurred, indicating a sample solution shelf-life of at least 3 months.

Acknowledgement

References

[1] K. Williams and E. Lee, Drugs, 30 (1985) 333.
[2] D.E. Drayer, Clin. Pharmacol. Ther., 40 (1986) 125.
[3] D.E. Drayer, Ther. Drug Monitor., 10 (1988) 1.
[4] H. Nishi, Y. Kokusenya, T. Miyamoto and T. Sato, J. Chromatogr. A, 659 (1994) 449.
[5] T.E. Peterson, J. Chromatogr., 630 (1993) 353.
[6] W. Schutzner and S. Fanali, Electrophoresis, 13 (1992) 687.
[7] K.D. Altria, A.R. Walsh and N.W. Smith, J. Chromatogr., 645 (1993) 193.
[8] K.D. Altria, D.M. Goodall and M.M. Rogan, Electrophoresis, 15 (1994) 824.
[9] A. Guttman and N. Cooke, J. Chromatogr. A, 685 (1994) 155.
[10] T.J. Ward, Anal. Chem., 66 (1994) 633A.
[11] S. Fanali, J. Chromatogr., 545 (1991) 437.
[12] S.A.C. Wren and R.C. Rowe, J. Chromatogr., 603 (1992) 235.
[13] T.E. Peterson, J. Chromatogr., 630 (1993) 353.
[14] T. Schmitt and H. Engelhardt, Chromatographia, 37 (1993) 475.
[15] I. Bechet, P. Paques, M. Fillet, P. Hubert and J. Crommen, Electrophoresis, 15 (1994) 818.
[16] Z. Aturki and S. Fanali, J. Chromatogr. A, 680 (1994) 137.
[17] A. Guttman and N. Cooke, J. Chromatogr. A, 680 (1994) 157.
[18] L. Valtcheva, J. Mohammad, G. Petterson and S. Hjerten, J. Chromatogr., 638 (1993) 263.
[19] H. Siren, J.H. Jumppanen, K. Manninen and M.-L. Riekkola, Electrophoresis, 15 (1994) 779.
[20] J.R. Mazzeo, E.R. Grover, M.E. Swartz and J.S. Petersen, J. Chromatogr. A, 680 (1994) 125.
[21] The European Pharmacopoeia, Maisonneuve, Sainte-Ruffine, 2nd ed., 1987, Part I.V.6.20.4.

Ion-pair chromatography and micellar electrokinetic capillary chromatography in analyzing beta-adrenergic blocking agents from human biological fluids

P. Lukkari, H. Sirén*

Laboratory of Analytical Chemistry, Department of Chemistry, University of Helsinki, P.O. Box 55, FIN-00014 University of Helsinki, Helsinki, Finland

Abstract

Ion-pair chromatography (IPC) and micellar electrokinetic capillary chromatography (MECC) were used for the separation and determination of parent β-blockers from human biological fluids. In both these techniques, N-cetyl-N,N,N-trimethylammonium bromide (CTAB) was used as a buffer additive. In IPC, CTAB was an ion-pair former, and in MECC it was a micelle-forming surfactant. The effectiveness of the IPC method using methanol-gradient elution and that of MECC were compared for drug-spiked serum and urine samples. Detection was performed with a diode-array detector in the IPC method and with a 214-nm filter in the MECC technique. In both methods a phosphate buffer (pH 7.0) was used. In MECC the buffer solution contained 10 mM CTAB, while in IPC the CTAB concentration was decreased from 7 to 4 mM during the separation when a methanol gradient was used. The study showed that the IPC technique performed better for bioanalyses than the high-performance MECC technique, since in MECC UV detection presented a problem because of the low sample concentration. However, in MECC sample preparation was less time-consuming, using hydrolyzation and protein precipitation and, unlike the IPC technique, it did not require any liquid–liquid extraction step.

1. Introduction

Reversed-phase high-performance liquid chromatographic (RP-HPLC) separations and identifications of β-blockers after isolation from biological matrices have been developed in many laboratories as methods alternative to the derivatization of the drugs and their analysis by gas chromatography (GC). Time-consuming pretreatment steps of the biological fluids are needed for GC separations. However, the main advantage of the latter over other separation techniques is the simultaneous analysis of several

β-blockers, which may be difficult with RP-HPLC [1]. Drawbacks in RP-HPLC include the resolution efficiency and intensity problems at UV wavelengths, which have been surmounted in ion-pair chromatographic (IPC) separations [2].

Recently, many techniques for faster and easier sample pretreatment and analysis of β-blockers with HPLC have been developed [3,4]. On-line and off-line GC techniques [5–7] have also proved to be very practical, especially when automation of the procedure is not required or when only a few samples have to be analyzed. Among the latest analysis techniques for the components discussed here are the capillary

---

* Corresponding author.

electrophoretic (CE) methods developed by Lukkari et al. [8–11]. These methods can easily be automated. Another advantage is that, especially in urine matrix, no further clean-up steps other than filtration are needed. However, the CE techniques are not transferable to clinical bioanalyses without extra concentration steps due to the small sample amount in the capillaries, which reduces the response in UV detection.

Some HPLC studies have reported the simultaneous separation of more than two parent β-blockers [12]. The authors have mainly demonstrated the selectivity of the method used. In bioanalysis, a considerable amount of work has been done using RP-HPLC to screen one β-blocker. A different β-blocker was used as an internal standard [13]: it was assumed that the two β-blockers are unlikely to appear simultaneously in the same sample. However, in MECC all β-blockers available on the Finnish market can easily be analyzed within one electrophoretic run [8,9]. In MECC the separation of the analytes is based on the equilibrium partitioning between the micelles and the surrounding solution. This is possible when the electrolyte solution contains surfactant above the critical micelle-formation concentration (CMC), which is dependent on the concentrations of all the additives in the electrolyte used. Therefore, e.g. MECC with a cationic surfactant (CTAB) is highly effective for the analysis of drugs and their metabolites in body fluids [8–11,14,15]. Furthermore, when the analytes are ionized, their electrophoretic mobilities also affect the separations. In MECC the micelles form their own zone, which is the main difference between MECC and IPC. In IPC the ion-pair former (reversed-phase) is partly adsorbed onto a nonpolar stationary phase in the chromatographic column, is partly free in the eluent and partly forms uncharged ion-pairs with the analytes by Coulombic forces.

With the IPC method described in this paper, we studied the simultaneous separation of six parent β-blockers (acebutolol, alprenolol, atenolol, metoprolol, oxprenolol and propranolol) and their mixture spiked in serum and in urine. The method was based on reversed-phase ion-pair (RP-IP) formation. The ion-pair former was CTAB (N-cetyl-N,N,N-trimethylammonium bromide), the concentration of which varied during the gradient elution. With the MECC method described in this paper, we studied the simultaneous separation of ten parent β-blockers (acebutolol, alprenolol, atenolol, labetalol, metoprolol, nadolol, oxprenolol, pindolol, propranolol and timolol), spiked in serum and in urine, with an inside uncoated silica capillary using phosphate buffer (pH 7.0) containing CTAB as the surfactant. In both IPC and MECC, the only pretreatment for urine samples was filtration. The serum samples were hydrolyzed and proteins precipitated, after which the supernatant was solid-phase extracted (SPE). The studies demonstrate the suitability of IPC and MECC for the separation of β-blockers from biological matrices: IPC with diode-array detection (DAD) can be used for pretreated samples, but MECC with UV detection can reliably be used only when the analytes are concentrated before introducing them into the system.

2. Experimental

Capacity factors (k') were not calculated because in MECC the values are biased by uncertainties in the true ionic electrophoretic mobility [16]. In addition, it was difficult to find a reliable and detectable marker for the micelle mobility, i.e. one which is totally partitioned into the micelle under the MECC conditions used. In both IPC and MECC the resolution values (Eq. 1) and the effective theoretical plates per meter (Eq. 2),

$$R = \frac{t_{r,2} - t_{r,1}}{w_{1/2,1} + w_{1/2,2}} \tag{1}$$

$$N = 5.545 \left(\frac{t'_r}{w_{1/2}}\right)^2 \tag{2}$$

were calculated by the general half-width ($w_{1/2}$) method to compare these two methods more

accurately. The t_0-values were determined by methanol in IPC and MECC.

2.1. Instrumentation

The liquid chromatograph was a Hewlett-Packard Model 1090 instrument equipped with an HP 1040A diode-array detector and an HP85B single-channel personal computer. An HP 9121 disc drive unit, a DPU multichannel integrator, an HP 3392A integrator and an HP 7470A plotter were used for data storage and reporting (Hewlett-Packard, Avondale, PA, USA). The column system used was an HP C_{18} guard column (10×4.6 mm I.D., 5 μm) connected to a C8P-50 separation column (Asahipak, Japan, 150×4.6 mm I.D., 5 μm). Detection was performed at wavelengths 220, 230, 260 and 280 nm. The sample loop volume was 20 μl. The experiments were carried out at ambient temperature (23–25°C). Methanol-gradient elution was used in modifying the phosphate buffer (pH 7.0) containing 10 mM CTAB.

MECC was performed in 680×0.050 mm I.D. and 560×0.050 mm I.D. fused-silica capillary tubes (Polymicro Technologies, White Associates, Pittsburgh, PA, USA) with 600 mm and 480 mm, respectively, as the effective lengths for separation. A Waters Quanta 4000 capillary electrophoresis system (Millipore Corporation, Waters Chromatography Division, Milford, MA, USA) was employed. A wavelength of 214 nm was used for detection. All experiments were carried out at ambient temperature (ca. 25°C). Samples were injected hydrostatically for 30 s, and the running voltage was −26 kV. The current during the separations was 97 μA. The data (peak height) were collected with an HP 3392A integrator.

The pHs of the buffers used were adjusted with a Jenway 3030 pH meter connected to a Jenway electrode (Jenway, Felsted, UK) containing 4 M KCl and saturated calomel. Calibration of the electrode system was made with potassium hydrogen phthalate (0.05 M, pH 4.00) and sodium tetraborate (0.01 M, pH 9.81) solutions.

The urine samples were filtered through Sar-

torius Minisart NML sterile filter units (0.45 μm; Sartorius, Göttingen, Germany) or Millex filters (0.5 μm; Nihon Millipore, Kogyo K.K. Yonezawa, Japan).

All eluents in IPC and electrolyte solutions in MECC were filtered through Millipore filters (0.45 μm; Millipore, Molsheim, France) and degassed before use by ultrasonication.

2.2. Materials

The β-blocking agents used in these experiments were acebutolol hydrochloride, alprenolol hydrochloride, atenolol, labetalol hydrochloride, ($\pm$)-metoprolol ($+$)-tartrate, nadolol, oxprenolol hydrochloride, pindolol, S-($-$)-propranolol hydrochloride and timolol maleate, all from Sigma (Sigma Chemical, St. Louis, MO, USA). 2,6-Dimethylphenol (internal standard) in MECC, biphenylamine (internal standard) in IPC, sodium dihydrogenphosphate monohydrate, disodium hydrogenphosphate dihydrate and N-cetyl-N,N,N-trimethylammonium bromide (CTAB) were from Merck (E. Merck, Darmstadt, Germany). Other reagents used in the method development were of analytical grade. All the reagents were used without further purification. Distilled water was ion-exchanged through a Water-I system from Gelman Sciences (Ann Arbor, MI, USA).

2.3. Preparation of standards

Standard stock solutions were prepared separately for each drug (1 mg/ml for IPC and 4 mg/ml for MECC) in methanol and in a mixture of methanol and water. Calibration reference solutions for biological fluids were prepared by spiking the urine blank or serum blank with each standard stock solution.

2.4. Sample preparation

For IPC the samples were prepared by adding 500 μl of each stock solution to 900 μl of serum (taken from human volunteers into Venoject tubes, Leuven, Belgium, VT-050 PZX, silicone initial coating, sizes 5 and 10 ml) or 900 μl of

drug-free urine (pooled). The urine samples were filtered before injection, but the serum samples were hydrolyzed with β-glucuronidase (EC 3.2.1.31) type H-1 from *Helix Pomatia* (416 800 units/g) enzyme at 60°C for 1 h before further clean-up steps [2,9]. After that, proteins were precipitated by adding methanol, centrifuged at 2000 g and the supernatant was cleaned up [2] with Supelclean LC-18 SPE tubes (3 ml; Supelco, Bellefonte, USA) before filtration and introduction onto the HPLC system.

For MECC a human urine pool taken from volunteers who were coffee or tea drinkers, but not drug users, was diluted with water (1:2, v:v). The mixture was spiked with a stock solution containing a known amount of each β-blocker. The urine samples were filtered using 0.5-μm pore-size membranes and then analyzed by MECC. The serum samples were hydrolyzed with type H-1 enzyme as in the IPC samples in a sonification bath for 30 min. After this the samples were cleaned up with Supelclean LC-18 SPE tubes (3 ml) (Supelco).

2.5. Preparation of buffers

The buffers (pH 7.0) were made up of 0.1 M and 0.08 M sodium dihydrogen phosphate and 0.1 M and 0.08 M disodium hydrogen phosphate solutions. After mixing the two phosphate solutions to give pH of 7.0, 10 mM CTAB was added.

2.6. Instrumental procedures

In IPC, the preconditioning and the conditioning before each run were done by 0.1 M phosphate buffer containing 7.0 mM CTAB for 10 min. The drugs were eluted with methanol gradient in phosphate buffer. The methanol content was maintained at 30% for 4 min and was then increased to 45% at a rate of 5%/2 min, to 50% at 5%/2 min and finally to 60% at 10%/2 min. The CTAB concentration was decreased as follows: 7.0, 5.5, 5.0 and 4.0 mM during the four steps, respectively.

In MECC the conditioning procedure was much simpler than in IPC. The capillary was

only purged for 2 min with the phosphate buffer solution before each injection.

3. Results and discussion

In the IPC system an analytical method was developed to separate six β-blockers and the internal standard (biphenylamine, ISTD), all of which were spiked into biological fluids (serum and urine) in a single run after sample pretreatment before injection. The separated β-blockers in order of elution were: 1. atenolol, 2. acebutolol, 3. metoprolol, 4. oxprenolol, 5. alprenolol and 6. propranolol (Figs. 1 and 2). By using MECC, ten β-blockers were separated from urine, and their elution order was as follows: 1. acebutolol, 2. nadolol, 3. timolol, 4. atenolol, 5. metoprolol, 6. 2,6-dinitrophenol (ISTD), 7. oxprenolol, 8. pindolol, 9. alprenolol, 10. labetalol and 11. propranolol (Figs. 3 and 4). However, the MECC analyses of serum samples were performed without ISTD, because neither of the compounds (2,6-dinitrophenol, biphenylamine) was suitable for MECC. Because
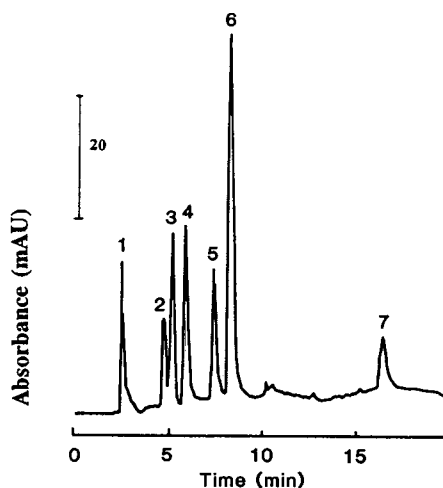

Fig. 1. Ion-pair chromatogram of human serum spiked with 670 ng of 1 = atenolol, 2 = acebutolol, 3 = metoprolol, 4 = oxprenolol, 5 = alprenolol, 6 = propranolol. Peak number 7 is the ion-pair former, CTAB. Separation conditions as described in the Experimental section. Detection at wavelength 280 nm.
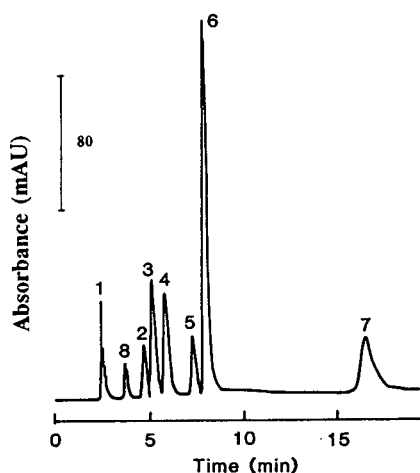
Fig. 2. Ion-pair chromatogram of human urine spiked with 250 ng of 1 = atenolol, 2 = acebutolol, 3 = metoprolol, 4 = oxprenolol, 5 = alprenolol, 6 = propranolol. Peak numbers 7 and 8 are the ion-pair former CTAB and caffeine, respectively. Separation conditions as described in the Experimental section. Detection at 260 nm.

Fig. 4. Electropherogram of human urine spiked with 75 μg/ml (except timolol and 2,6-dimethylphenol 150 μg/ml) of 1 = acebutolol, 2 = nadolol, 3 = timolol, 4 = atenolol, 5 = metoprolol, 6 = 2,6-dimethylphenol (internal standard), 7 = oxprenolol, 8 = pindolol, 9 = alprenolol, 10 = labetalol, 11 = propranolol. Migration conditions as described in the Experimental section. Capillary 68 cm × 50 μm I.D.

the 2,6-dinitrophenol peak was split in serum samples, it was not suitable as an ISTD. Biphenylamine did not absorb intensively enough at 214 nm.

From Table 1 it can be seen that the resolution of the separated β-blockers in the IPC system is more effective when the drugs are isolated from serum than from urine. The reason for this is that some endogenic compounds (e.g. uric acid,
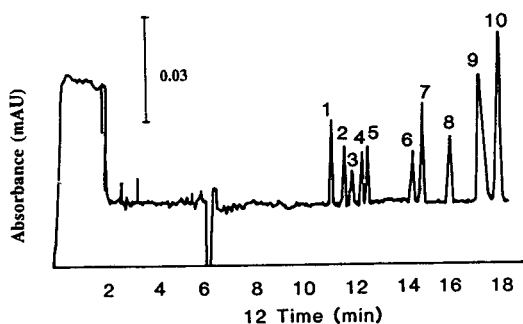
Fig. 3. Electropherogram of human serum spiked with 400 μg/ml of 1 = acebutolol, 2 = nadolol, 3 = timolol, 4 = atenolol, 5 = metoprolol, 6 = oxprenolol, 7 = pindolol, 8 = alprenolol, 9 = labetalol, 10 = propranolol. Migration conditions as described in the Experimental section. Capillary 56 cm × 50 μm I.D.

Table 1
The IPC method. The resolution (R) and the number of effective theoretical plates (N) with standard deviations for β-blockers spiked in serum and urine

Compound/ matrices	R	N $(1/m) \times 100$
1 a[a]	6.2 ± 0.3	24 ± 2
b[a]	3.1 ± 0.1	49 ± 1
2 a	0.7 ± 0.2	47 ± 6
b	0.5 ± 0.1	69 ± 10
3 a	7.0 ± 0.7	52 ± 7
b	3.6 ± 0.4	62 ± 6
4 a	7.7 ± 0.4	67 ± 10
b	3.5 ± 0.3	67 ± 8
5 a	6.8 ± 0.9	289 ± 16
b	3.4 ± 0.4	378 ± 41
6 a	4.8 ± 0.6	448 ± 33
b	2.6 ± 0.4	409 ± 47
ISTD a		700 ± 75
ISTD b		654 ± 54

[a] a is serum and b is urine. Number of replicates is 6 for both a and b.
Wavelength, 260 nm. Column, Asahipak C8P-50. Compounds: 1 = atenolol, 2 = acebutolol, 3 = metoprolol, 4 = oxprenolol, 5 = alprenolol and 6 = propranolol.

glucose conjugates) and exogenic compounds (e.g. caffeine and its metabolites) in urine may interfere with the screening of β-blockers, especially when the drugs are present at low concentrations (e.g. below 0.1 μg/ml); thus IPC (see R-values in Table 1) is less reliable in urine than in serum, where the concentrations of the interfering compounds are lower. In MECC the reverse applies, with the difference in separation efficiencies in the two matrices being much smaller (Table 2). However, in the MECC system the resolution of the fifth compound (metoprolol) from oxprenolol is better in serum than in urine, because serum samples were analyzed without an internal standard [as the internal standard (2,6-dimethyl phenol) migrates

poorly]. In contrast to resolution values, in the IPC system the effective theoretical plate numbers are higher in urine than in serum samples. Exceptions were oxprenolol and propranolol (Table 1). From Table 2 the same phenomenon is seen in the MECC system. The only exception is labetalol, which gives N-values larger in serum than in urine matrix due to the improved recovery after the clean-up steps. According to Table 2, the hydrolyzation and the solid-phase extraction caused greater variation in the N-values calculated with labetalol than in those calculated with the other β-blockers. Furthermore, labetalol showed an exceptional behaviour for a β-blocker in our MECC studies with organic buffer modifiers [11].

By employing gradient elution in the IPC system, the interaction of other normally used β-blockers such as sotalol, nadolol, timolol, pindolol and labetalol could also be studied. The results showed that sotalol interfered with the analysis of atenolol (substantial co-elution). Nadolol was eluted together with caffeine, timolol with acebutolol, pindolol with oxprenolol and labetalol with ISTD. These compounds were then excluded from the IPC studies. In the MECC methods described here, neither of these parent compounds nor caffeine interfered with each other during the analyses, because the endogenic compounds and caffeine migrated before t_0. Though the resolution values in IPC are larger than in MECC, all of these ten β-blockers could be separated in a single MECC run. Comparison between N-values obtained by IPC and MECC methods shows that in MECC early migrating β-blockers have approximately ten times more theoretical plates than in IPC. However, in IPC and in MECC slower-eluting compounds have equal N-values because of the gradient step in IPC. The Asahipak column used in this study has also been reported to give high effective plate numbers [17].

Table 2
The MECC method. The resolution (R) and the number of effective theoretical plates (N) with standard deviations for β-blockers spiked in serum and urine

Compound/ matrices	R	N (1/m) × 100
1 a[a]	1.83 ± 0.18	196 ± 43.3
b[a]	2.50 ± 0.02	263 ± 7.60
2 a	1.10 ± 0.10	178 ± 41.0
b	1.22 ± 0.06	216 ± 2.65
3 a	1.32 ± 0.11	217 ± 50.1
b	2.00 ± 0.08	304 ± 66.0
4 a	0.96 ± 0.10	260 ± 47.6
b	1.26 ± 0.04	295 ± 4.11
5 a	5.84 ± 0.41	326 ± 58.6
b	3.76 ± 0.24	417 ± 18.2
6 a ISTD	–	–
b	2.49 ± 0.18	172 ± 6.79
7 a	1.08 ± 0.12	324 ± 46.8
b	1.35 ± 0.02	388 ± 15.8
8 a	3.16 ± 0.32	408 ± 43.8
b	4.27 ± 0.12	446 ± 3.29
9 a	2.95 ± 0.58	366 ± 61.7
b	2.56 ± 0.17	531 ± 27.1
10 a	1.02 ± 0.22	285 ± 19.0
b	1.94 ± 0.06	147 ± 6.73
11 a		322 ± 82.8
b		542 ± 8.35

[a] a is extract from human serum and b is filtrate of human urine. Number of replicates for a is 6 and for b, 5.
Wavelength, 214 nm. Compounds: 1 = acebutolol, 2 = nadolol, 3 = timolol, 4 = atenolol, 5 = metoprolol, 6 = 2,6-dinitrophenol (ISTD), 7 = oxprenolol, 8 = pindolol, 9 = alprenolol, 10 = labetalol and 11 = propranolol.

4. Conclusions

In capillary zone electrophoresis (CZE), the number of plates for drug analytes is typically at

least 1.5 orders of magnitude greater than in isocratic HPLC [18]. In this study with MECC, we had approximately one order of magnitude more effective plates than in IPC for the β-blockers studied. In many applications the CZE or MECC system with higher resolution can be competitive with HPLC even after a great deal of efficiency is lost. This is particularly true in terms of instrumentation: CZE is simpler and easier to apply, and the basic instrument can be very inexpensive. In addition, there is a great difference in the cost of analyses, e.g. the volumes of solvents, buffers and samples. Furthermore, the clean-up steps of column materials after each IPC run in HPLC are time-consuming.

The resolution of the ten β-blockers was not good enough for simultaneous routine screening of the compounds in a single IPC run. However, using the MECC in this study, the ten β-blockers can be completely separated in a single run.

The main advantage of IPC over MECC noted in this study is that the detection by diode-array detector can be done at the desired wavelength, which also makes it possible to eliminate the absorbance of the background. Furthermore, IPC is more sensitive than MECC in analyzing β-blockers under the conditions described: in IPC the detection limits varied from 100 to 670 ng/ml in serum [2], and in MECC from 10 to 20 μg/ml in urea [8] and 1 to 50 μg/ml in serum [9]. Of the two methods, only IPC can be used for clinical bioanalyses of β-blockers, when parent compounds must be determined. The detector response in MECC is too low when unconcentrated samples are analyzed. However, when the real samples are concentrated about eightfold, the native β-blockers in biological matrices may be detected with the UV technique.

The effectiveness of MECC can be seen in Tables 1 and 2. All ten drug compounds can be separated from each other in a single run in MECC, and the pretreatment steps of the biological samples (serum) are easier and simpler than those in IPC measurements. The diminutive sample preparation requirements present an attractive advantage. In addition, being able to

omit the extraction step results in greater accuracy. The main drawbacks with CZE involve peak identification and occasional difficulties with biological matrices. These disadvantages were surmounted by using MECC.

Acknowledgement

References

[1] H. Maurer and K. Pfleger, J. Chromatogr., 382 (1986) 147.
[2] H. Sirén, M. Saarinen, S. Hainari, P. Lukkari and M.-L. Riekkola, J. Chromatogr., 632 (1993) 215.
[3] W.H. Pirkle, J. Chromatogr., 558 (1991) 1.
[4] M.T. Saarinen, H. Sirén and M.-L. Riekkola, J. Chromatogr. A, 664 (1995) 341.
[5] C.L. Davies, J. Chromatogr., 531 (1990) 131.
[6] T. Hyötyläinen, M. Saarinen and M.-L. Riekkola, in P. Sandra and G. Devos (Editors), Proceedings of the 6th International Symposium on Capillary Chromatography, Riva del Garda, Italy, 1994, p. 1386.
[7] K. Hartonen and M.-L. Riekkola, in P. Sandra and G. Devos (Editors), Proceedings of the 6th International Symposium on Capillary Chromatography, Riva del Garda, Italy, 1994, pp. 1729–1739.
[8] P. Lukkari, H. Sirén, M. Pantsar and M.-L. Riekkola, J. Chromatogr., 632 (1993) 143.
[9] P. Lukkari, T. Nyman and M.-L. Riekkola, J. Chromatogr. A, 674 (1994) 241.
[10] P. Lukkari, H. Vuorela and M.-L. Riekkola, J. Chromatogr. A, 652 (1993) 451.
[11] P. Lukkari, H. Vuorela and M.-L. Riekkola, J. Chromatogr. A, 655 (1993) 317.
[12] K.V. Buhsing and A. Garbe, J. Chromatogr., 382 (1986) 215.
[13] M. Ahnoff, M. Ervik, P.-O. Lagerström, B.-A. Persson and J. Vessman, J. Chromatogr., 340 (1985) 73.
[14] P. Lukkari, J. Jumppanen, K. Jinno, H. Elo and M.-L. Riekkola, J. Pharm. Biomed. Anal., 10 (1992) 561.
[15] P. Lukkari, Ph.D. Thesis, Helsinki, Finland, 1994.
[16] S. Terabe, K. Otsuka, K. Ichiakva, A. Tsuchiya and T. Ando, Anal. Chem., 56 (1984) 111.
[17] H. Sirén, Ph.D. Thesis, Helsinki, Finland, 1991.
[18] L. Bao and P.K. Dasgupta, Anal. Chem., 64 (1992) 991.

Chiral separation of amphetamines by high-performance capillary electrophoresis

Emmanuel Varesio, Jean-Luc Veuthey*

Laboratory of Pharmaceutical Analytical Chemistry, University of Geneva, Boulevard d'Yvoy 20, 1211 Geneva 4, Switzerland

Abstract

The chiral separation of amphetamines is of great importance in clinical and forensic analysis, because it is well known that enantiomers do not have identical pharmacological activity; for example, *d*-amphetamine is 3–4 times more effective in central nervous system stimulation than the *l*-isomer, whereas the latter is slightly more potent in its cardiovascular action. This paper describes the method development for the chiral separation of a mixture of amphetamine analogues by cyclodextrin-modified capillary zone electrophoresis. The use of different cyclodextrin types as chiral selectors and the influence of experimental parameters such as the temperature, the voltage applied, the buffer concentration and the capillary length are investigated. The ability to determine the enantiomers in urine samples is also discussed.

1. Introduction

Amphetamine and its analogues are substances which have a potent central nervous system (CNS) stimulating effect. Some amphetamines have been accepted for their medical usage for years, whereas others have never been medically accepted and are purely drugs of abuse [1]. The amphetamine analogues most commonly consumed illegally in Europe are amphetamine (A) itself, methamphetamine (MA), methylenedioxyamphetamine (MDA), methylenedioxymethamphetamine (MDMA or Ecstasy) and more recently methylenedioxyethylamphetamine (MDE or Eve). All of these compounds possess a chiral centre and it is well known that the *d*- and *l*-enantiomers have different pharmacological activities. For example, *d*-methamphetamine is a more effective CNS

stimulant than its *l*-enantiomer [2]. Hence it is necessary to develop an analytical procedure which can separate the enantiomers in biological matrices such as urine, serum, plasma or whole blood. Further, enantiomer separation can be useful for forensic analyses in order to identify the synthetic pathways of clandestine amphetamine samples [3].

The enantiomeric separation of amphetamine analogues can be carried out by numerous techniques. However, chromatographic methods such as gas chromatography (GC) [4–7] and high-performance liquid chromatography (HPLC) [8–12], in direct or indirect mode, are the most convenient. In the case of biological matrices, amphetamine concentrations have to be detected in the range 0.01–10 μg/ml [1] and often a prederivatization step is necessary in order to reach these limits of detection with both techniques. In the last few years, high-performance capillary electrophoresis (CE) has become

---

* Corresponding author.

a complementary analytical tool to the classical GC and HPLC techniques for the separation of drugs in biological matrices; the advantages of CE include small injection volumes, high separation efficiency, high resolution, low consumption of polluting solvents and rapid and inexpensive analyses.

Many recent publications have reviewed the applications of CE in enantiomeric separations [13–22] and numerous possibilities are available for the separation of drugs such as amphetamine analogues. As for chromatography, it is possible to separate enantiomers directly or after a pre-derivatization step. In the separation of amphetamine analogues, Lurie [23] used 2,3,4,6-tetra-O-acetyl-β-D-glucopyranosyl isothiocyanate (GITC) as a derivatization reagent and separated the diastereomers by micellar electrokinetic chromatography (MEKC). The chiral separation of amphetamine, methamphetamine, ephedrine, pseudoephedrine, norephedrine and norpseudoephedrine is carried out with UV detection. However, most applications are conducted by CE with β-cyclodextrin as chiral selector in the buffer mobile phase. Different β-cyclodextrin derivatives have been used with success in order to separate ephedrine and analogous compounds [24–31]. Nevertheless, few publications have dealt with the analysis of biological matrices and, to our knowledge, no enantiomeric separation of MDA, MDMA and MDE has been reported. This paper describes the enantiomeric separation of these compounds by capillary electrophoresis with (2-hydroxy)propyl-β-cyclodextrin as a chiral selector. Different parameters were optimized and the method was successfully applied to urine samples.

2. Experimental

2.1. Instrumentation

The experiments were carried out on a HP^{3D}CE system (Hewlett-Packard, Waldbronn, Germany). This system consists of a capillary electrophoresis unit equipped with a diode-array detector, an autosampler and a high-velocity air-cooled capillary cartridge. The HP^{3D}CE ChemStation software was used for instrument control, data acquisition and data analysis. Hewlett-Packard capillaries of 50 μm I.D. (375 μm O.D.) and 64.5 cm total length (56 cm from inlet to the detector window) were used for all experiments unless stated otherwise. These capillaries were made of fused silica and equipped with an extended path-length detection window of 150 μm I.D. ("bubble cells"). New capillaries were flushed for 3 min with 1 M NaOH, then for 5 min with 0.1 M NaOH and finally for 10 min with water. Between each run, the capillaries were flushed for 5 min with phosphate buffer. When analysing biological samples, the capillaries were first flushed for 2 min with 0.1 M phosphoric acid and then for 5 min with phosphate buffer.

2.2. Chemicals

All the cyclodextrins were purchased from Cyclolab (Budapest, Hungary), except α- and β-cyclodextrin, which were from Sigma (St. Louis, MO, USA). Amphetamine, 3,4-methylenedioxyamphetamine (MDA) and 3,4-methylenedioxymethamphetamine (MDMA) were purchased as racemic mixtures from Sigma and the optically pure enantiomers (99%) of amphetamine and methamphetamine and racemic 3,4-methylenedioxyethylamphetamine (MDE) were purchased as standard solutions in methanol from Alltech (Deerfield, IL, USA). Phenylethylamine from Fluka (Buchs, Switzerland) was used as an internal standard. Individual stock solutions (100 μg/ml) of each racemic amphetamine were prepared in 0.1 M hydrochloric acid and were kept at 4°C. All the other reagents and solvents were of analytical-reagent grade and obtained from Fluka, except for methanol, which was supplied by SDS (Peypin, France). Ultrapure water was provided by a Milli-Q RG unit from Millipore (Bedford, MA, USA).

2.3. Electrophoretic conditions

Samples (5 nl) were injected by pressure (50 mbar for 4 s) and electrophoresis was performed

at a constant voltage of 25 kV (388 V/cm) after a 1-min ramp step. This ramp of voltage is used to ensure there is no loss of sample on injection, which could lead to some problems in quantification [32]. All runs were carried out at 15°C unless stated otherwise. Detection was performed using a diode-array detector scanning the wavelengths from 190 to 600 nm; the electropherograms were monitored at 200 nm with a band width of 10 nm and a reference signal at 350 nm (band width of 80 nm).

2.4. Buffer preparation

For 100 ml of 200 mM phosphate buffer (buffer A), we dissolved 1.153 g of 85% phosphoric acid and 1.212 g of 99% anhydrous NaH_2PO_4 in water in a 100-ml volumetric flask. The pH was adjusted to 2.5 with 1 M NaOH and the mixture was diluted to 100 ml with water. The buffer solution was filtered through a 0.45-μm nylon syringe filter.

In order to obtain a 20 mM (2-hydroxy)-propyl-β-cyclodextrin buffer solution, we dissolved 0.300 g of chiral selector in 10 ml of phosphate buffer. After the addition of the chiral selector, the buffer was filtered through a 0.2-μm nylon syringe filter prior to use.

The phosphate buffer used for solid-phase extraction experiments was 100 mM phosphate buffer prepared by dissolving 1.212 g of 99% anhydrous NaH_2PO_4 in water in a 100-ml volumetric flask. The pH was adjusted to 6.0 with 1 M sodium hydroxide and the mixture was diluted to 100 ml with water.

2.5. Preparation of urine samples

One part of a urine sample (blank) was spiked with 1 μg/ml each of racemic amphetamines (amphetamine, methamphetamine, MDA, MDMA, MDE and phenylethylamine as an internal standard), and was either pretreated using one of the following procedures, or not pretreated and directly injected. The same procedures were applied to the unspiked urine sample.

Ultrafiltration

We used a MicroSpin 24S centrifuge from Sorvall Instruments (DuPont, Wilmington, DE, USA) and MicroCon 10 filters units with a molecular mass cut-off 10 000 from Amicon (Beverly, MA, USA). For centrifugation, 500 μl of urine sample were transferred into the ultrafiltration device and were centrifuged at ca. 12 500 g for 20 min, then the filtrate was injected.

Solid-phase extraction (SPE)

Bond Elut Certify cartridges (Varian, San Fernando, CA, USA) were used on a Visiprep SPE vacuum manifold unit from Supelco (Bellefonte, PA, USA). The extraction procedure was carried out according to Gan et al. [33]. A 2-ml volume of urine was transferred into 15-ml plastic conical-bottomed tubes, to which were added 2 ml of 0.1 M phosphate buffer (pH 6.0). The tubes were vortexed mixed for 15 s. Initially, the Bond Elut Certify cartridges were conditioned with 2 ml of methanol and 2 ml of 0.1 M phosphate buffer (pH 6.0). Volumes of 2 ml of urine samples were introduced and slowly drawn through the columns under low vacuum. The columns were then rinsed with 1 ml of 1 M acetic acid, then dried under vacuum for 5 min. The columns were rinsed with 6 ml of methanol, and then dried again under vacuum for 2 min. The analytes were eluted with 5 ml of 2% ammonia solution in ethyl acetate (freshly prepared). The eluate was evaporated to dryness under a slow stream of nitrogen at room temperature. Two drops of acetic acid were added to the eluate to prevent losses of the volatile amphetamines during the evaporation step [34]. Finally, 1 ml of 0.1 M hydrochloric acid was added to solubilize the analytes before injection.

Liquid–liquid extraction

We followed the procedure described by Kinberger [35]. To 500 μl of urine were added 100 μl of 1 M sodium hydroxide. After vortex mixing for 30 s, 1 ml of diethyl ether was added and the tube was vortex mixed again for 1 min. After centrifugation (5 min at ca. 12 500 g), the organic layer was transferred into another tube, then 50 μl of 0.1 M hydrochloric acid were
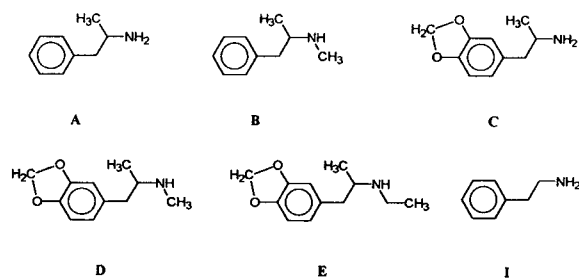
Fig. 1. Structures of the amphetamines tested. (A) Amphetamine; (B) methamphetamine; (C) 3,4-methylenedioxyamphetamine (MDA); (D) 3,4-methylenedioxymethamphetamine (MDMA, Adam or Ecstasy); (E) 3,4-methylenedioxyethylamphetamine (MDE or Eve); (I) phenylethylamine (internal standard).

added and the tube was vortex mixed for 1 min and centrifuged for 2 min. The diethyl ether layer was aspirated off and discarded. The acidic phase was injected without any further treatment.

3. Results and discussion

All the method development steps were carried out on a racemic amphetamine sample in order to determine the influence of some experimental factors on the resolution of the separation. Once the method had been optimized, we analysed a mixture of five racemic amphetamines (Fig. 1) with an internal standard for further quantification. Unless stated otherwise, all the samples used in this study were injected three times each.

3.1. Choice of the chiral selector and its concentration

In capillary zone electrophoresis (CZE), many types of chiral selectors, such as cyclodextrins, crown ethers, oligosaccharides and macrocyclic antibiotics, may be applied for enantiomeric separations. However, cyclodextrins (CDs) are by far the most commonly used. CDs are cyclic, non-reducing oligosaccharides with a truncated cylindrical molecular shape. They are produced from the decomposition of starch by the bacterial enzyme cyclodextrin glycosyltransferase. Many cyclodextrin derivatives have been developed in order to increase their solubility in water and to modify their cavity shape [36–38].

As mentioned by Terabe et al. [20], the enantiorecognition mechanism is based on the formation of an inclusion complex between the chiral selector and the analyte. The enantiomeric separation by cyclodextrin-modified CZE is based on the difference in the stability constants of a pair of enantiomers with the chiral selector.

In our study, we tested different kinds of α- and β-CDs as the γ-CDs are not suitable for the size of the tested amphetamines because their cavities are too large. As shown in Table 1, no resolution of the enantiomers occurs when using α-CDs. This is explained by the fact that, in

Table 1
Resolution obtained with different kinds of chiral selectors

Chiral selector	MT[a] (min)		Resolution
	l-Form	*d*-Form	
20 mM α-CD	11.9	11.9	0.0
17 mM (2-hydroxy)propyl-α-CD	12.3	12.3	0.0
20 mM dimethyl-β-CD	20.9	21.1	0.8
20 mM methyl-β-CD	16.8	17.0	0.9
22 mM β-CD in 1 M urea	19.6	19.9	2.1
20 mM (2-hydroxy)propyl-β-CD	15.7	16.0	2.2

Buffer A with a chiral selector. Other conditions: injection at 200 mbar s (pressure); $E = 388$ V/cm (1-min voltage ramp); $T = 15°C$; detection wavelength = 200 nm; bandwidth = 10 nm. Sample: *d,l*-amphetamine (15 μg/ml) in 0.1 M HCl.
[a] Migration time.

contrast to γ-CDs, the size of the cavity is too small for the inclusion of the amphetamine.

However, we obtained good resolution values with the β-CDs. This resolution seems to be dependent on the polarity and on the steric hindrance of the substituents. Good resolution was achieved with the native β-CD and also with (2-hydroxy)propyl-β-CD. It is important to note that urea has to be added to the native β-CD in order to increase its solubility in the buffer solution. Without urea or some other co-solvents such as acids or bases, the solubility of the β-CD is limited to 16 mM [39–41]. We chose to work further with (2-hydroxy)propyl-β-CD because it offers many advantages over native β-CD: a slightly better resolution, a shorter analysis time and a more stable baseline with UV detection at 200 nm. We also varied the concentration of the chiral selector from 10 to 40 mM in the phosphate buffer (Fig. 2). The resolution is improved with an increase in the chiral selector concentration, but at the expense of the analysis time. We chose a concentration of 20 mM of (2-hydroxy)propyl-β-CD in the buffer because the resolution was sufficient with a shorter analysis time. We also chose this concentration for economic reasons, because CD derivatives are fairly expensive.

3.2. Effect of temperature

The temperature of the capillary has to be very carefully controlled as it can modify the viscosity of the buffer used for the separation and thus influence the electroosmotic flow velocity. This could lead to variations in the migration times (MT), and therefore to unsatisfactory run-to-run or day-to-day reproducibility.

On increasing the temperature, higher diffusion occurs which enhances the band broadening of the peaks and decreases the efficiency. As can be seen in Fig. 3, the resolution between the enantiomers decreases with increase in temperature. We chose 15°C, which is the lowest temperature for the instrument when working at ambient temperature (25°C).

Wren and Rowe [29,42] proposed a mathematical model to explain the chiral separation of
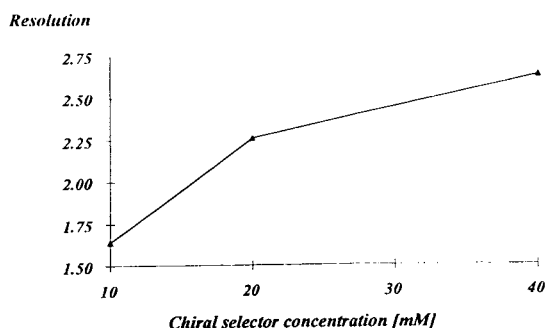

Fig. 2. Effect of chiral selector concentration on resolution. Buffer A with (2-hydroxy)propyl-β-CD as a chiral selector. Sample: d,l-amphetamine (15 μg/ml) in 0.1 M HCl. For other experimental conditions, see Table 1.

a pair of enantiomers in capillary zone electrophoresis. In their model, the resolution between two enantiomers depends on several parameters, including the equilibrium constants of the inclusion complexes [42,43]. Varying the temperature affects the thermodynamics of complex formation and therefore modifies the resolution between enantiomers.

3.3. Effect of applied voltage

The applied voltage influences mainly the electroosmotic flow velocity, the Joule heating and also the peak efficiency. We found that on increasing the voltage, the migration time de-
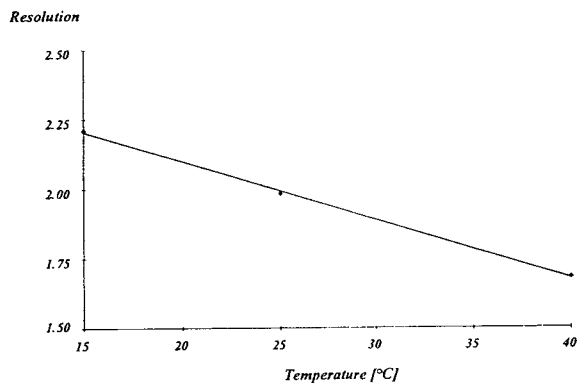

Fig. 3. Effect of temperature on resolution. Buffer A with 20 mM (2-hydroxy)propyl-β-CD. Sample: d,l-amphetamine (30 μg/ml) in 0.1 M HCl. For other experimental conditions, see Table 1.

Resolution

Resolution

Electrical field [V/cm]

Buffer concentration [mM]

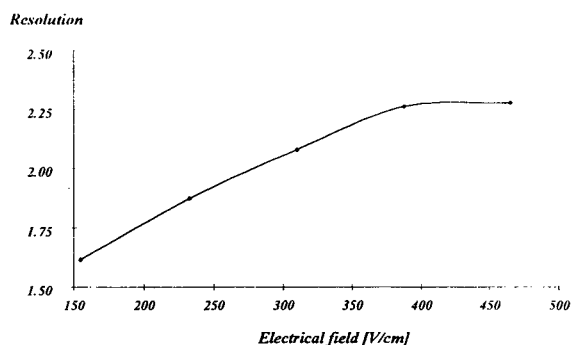72.0 cm / 80.5 cm (total length)

56.0 cm / 64.5 cm (total length)

Fig. 4. Effect of applied voltage on resolution. Buffer A with 20 mM (2-hydroxy)propyl-β-CD. Sample: d,l-amphetamine (30 μg/ml) in 0.1 M HCl. For other experimental conditions, see Table 1.

Fig. 5. Effects of buffer concentration and capillary length on resolution. Buffer A at different concentrations with 20 mM (2-hydroxy)propyl-β-CD. Sample: d,l-amphetamine (30 μg/ml) in 0.1 M HCl. For other experimental conditions, see Table 1.

creases and the resolution increases (Fig. 4). We chose to work at 25 kV (388 V/cm), as the gain in resolution at 30 kV (465 V/cm) is too low in comparison with the amount of heat generated by the Joule effect. We also noticed that at 25 kV (388 V/cm) we were no longer in the linear range of Ohm's law. Working at a high voltage leads to higher efficiencies and a faster analysis time as long as there are no bubbles in the capillary to cause disturbances in the analysis.

3.4. Effect of buffer concentration and capillary length

When working at a high buffer concentration, which means at high ionic strength, the zeta potential of the double layer is decreased, and this results in a decrease in the electroosmotic flow [44–46]. A buffer of high ionic strength gives significantly higher efficiencies and enhances the resolution, since the analytes remain longer in the capillary (Fig. 5). Buffers of high ionic strength also prevent analyte–analyte or analyte–wall adsorption in the capillary, and thus lead to better quantification and reproducibility [45]. A major drawback to working at high buffer concentrations is the generation of a high current through the capillary, owing to an enhanced conductivity of the buffer. This phenomenon therefore limits the usable buffer concentration, since a higher temperature could cause disturbances in the separation, as seen before.
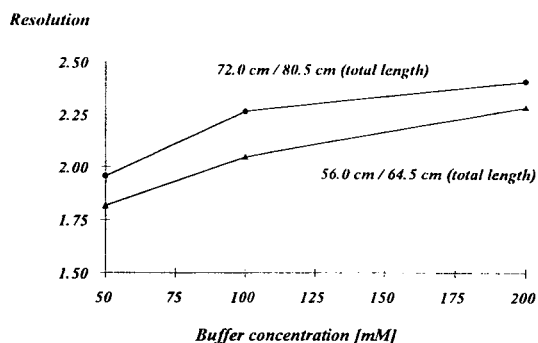
We also noted that the resolution is better with an 80.5-cm capillary (total length) than a 64.5-cm capillary, but leads to a longer analysis time. By using the shorter capillary, we were able to analyse five racemic amphetamines in less than 30 min.

3.5. Injection volume

As mentioned by Shihabi and Garcia [47], a rule of thumb restricts the sample volume to less than 1% of the total capillary volume in order to avoid overloading of the capillary and distortion of the peaks. We varied the injection volume of a racemic amphetamine sample in order to optimize this parameter. We injected 2.4–35.7 nl, which represents 0.2–2.8% of the total capillary volume (1.27 μl). As shown in Fig. 6, the relationship between the injection volume and the height of the peaks is linear for the whole range tested. Nevertheless, we chose to use a sample volume of 14.3 nl (600 mbar s), because the resolution between the peaks decreases with larger sample volumes injected.

3.6. Electrophoretic analysis

Once the method had been optimized, we injected a mixture of five racemic amphetamines (amphetamine, methamphetamine, MDA, MDMA and MDE) (Fig. 7). We achieved their
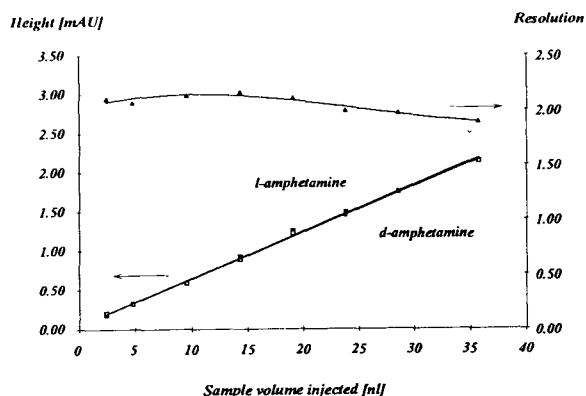
Fig. 6. Linearity of the injection volume. Buffer A with 20 mM (2-hydroxy)propyl-β-CD. Sample: d,l-amphetamine (1 μg/ml) in 0.1 M HCl. For other experimental conditions, see Table 1.

enantiomeric separation in less than 30 min and always with baseline resolution. We then tested the repeatability of the method (12 injections intra-day) with a standard mixture containing 1 μg/ml of each racemic amphetamine and 1 μg/ml of the internal standard (phenylethylamine) (Table 2). For the migration times we obtained R.S.D. values between 0.3 and 0.4%. However, for the peak areas the R.S.D. values were between 4.3 and 9.1%, as shown in Table 2. These poor values are due to the low concentration of the amphetamine sample, as men-
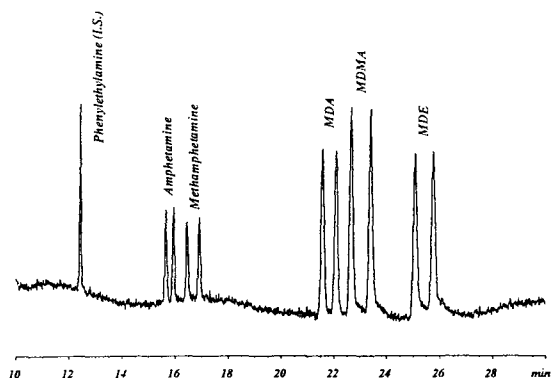
tioned by Silverman and Shaw [49]. It should be mentioned that the peak areas of the enantiomers were corrected by their respective migration times in order to take into account the difference in mobilities between the analytes [48].

Preliminary results showed good linearity of the method in the concentration range 500–10 000 ng/ml with standard aqueous samples ($r >$ 0.999 for all enantiomers tested). Nevertheless, the linearity, the repeatability and the limits of detection and quantification of the method will be determined further directly for the determination of the amphetamines in real urine samples and illicit tablets.

3.7. Application of the method to urine samples

We tested four modes of pretreatment for the urine samples before the capillary electrophoretic analysis. A blank urine sample was spiked with 1 μg/ml of each racemic amphetamine (amphetamine, methamphetamine, MDA, MDMA, MDE) and with 1 μg/ml of phenylethylamine as internal standard. A fraction of this sample was injected directly without any pretreatment, a fraction was purified by ultrafiltration and the two last fractions were purified by liquid–liquid extraction (LLE) and by solid-phase extraction (SPE). The same blank urine sample, but this time unspiked, was treated as described above.

All the analyses were carried out under the conditions described in Fig. 7 and each sample was injected three times. As shown in Fig. 7, all the amphetamines (racemic mixtures) and the phenylethylamine were resolved in less than 30 min for a standard aqueous solution. Without any pretreatment, the unspiked and the spiked samples gave a complex electropherogram (results not shown). Neither quantitative nor qualitative results were obtained even if it was possible to assign some amphetamines. The samples purified by ultrafiltration also gave very complex electropherograms which cannot be used for analytical purposes. In view of these results, it appears that, in order to purify the sample

Fig. 7. Separation of a sample containing the five racemic amphetamines (1 μg/ml). Buffer A with 20 mM (2-hydroxy)-propyl-β-CD each. Other conditions: injection at 600 mbar s (pressure); $E = 388$ V/cm (1-min voltage ramp); $T = 15°C$; detection wavelength = 200 nm; bandwidth = 10 nm.

Table 2
Repeatability of the method

Compound	MT[a] (min)	R.S.D. (MT) (%)	Area[b]/MT (mAU)	R.S.D. (area/MT) (%)	Relative area[c]	R.S.D. (rel. area) (%)
Internal standard	12.43	0.3	0.735	5.5	–	–
l-Amphetamine	15.71	0.4	0.369	6.8	0.50	6.2
d-Amphetamine	16.00	0.4	0.385	7.0	0.52	7.0
l-MA	16.53	0.3	0.326	7.6	0.45	9.1
d-MA	17.00	0.4	0.309	5.5	0.42	6.8
MDA-1	21.80	0.4	0.762	2.8	1.04	4.3
MDA-2	22.34	0.4	0.763	2.9	1.04	4.6
MDMA-1	22.94	0.4	0.950	5.3	1.30	6.1
MDMA-2	23.70	0.4	0.900	4.9	1.23	4.9
MDE-1	25.46	0.4	0.722	4.8	0.98	4.7
MDE-2	26.17	0.4	0.696	4.5	0.95	4.7

For experimental conditions, see Fig. 7. Sample: mixture of five racemic amphetamines (1 μg/ml each) in 0.1 *M* HCl.
[a] Migration time.
[b] The corrected areas (area divided by migration time) are preferably used for the calculations rather than the simple areas, as has been shown by Altria [48].
[c] The relative area is the corrected area of one enantiomer divided by the corrected area of the internal standard.

before the analysis, an extraction step is necessary.

As shown in Figs. 8A and 9A, the SPE procedure gives a cleaner extract than LLE for the same blank urine sample. With the former

method, no or few interference peaks appear in the time window expected for the amphetamines. Figs. 8B and 9B also show the electropherograms of the spiked urine samples after the SPE and LLE pretreatments and indicate that,
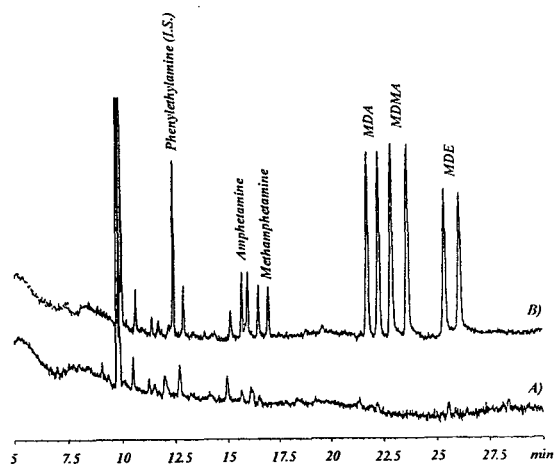

Fig. 8. Separation of a sample containing the five racemic amphetamines after SPE pretreatment. (A) Blank urine sample (unspiked); (B) spiked urine sample (1 μg/ml of each racemic amphetamine and 1 μg/ml of internal standard). For experimental conditions, see Fig. 7. Sensitivity: 2 mAUFS.
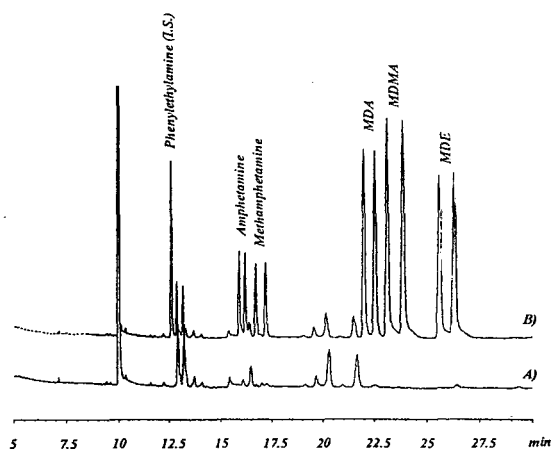

Fig. 9. Separation of a sample containing the five racemic amphetamines after LLE pretreatment. (A) Blank urine sample (unspiked); (B) spiked urine sample (1 μg/ml of each racemic amphetamines and 1 μg/ml of internal standard). For experimental conditions, see Fig. 7. Sensitivity: 20 mAUFS.

with the SPE procedure, qualitative and quantitative analyses can be easily carried out. The LLE procedure can also be used, but with more interfering peaks which might induce some errors during quantitative analysis; nevertheless, this procedure is faster than SPE.

These preliminary results show that, before undertaking a capillary electrophoretic analysis of urine samples, an extraction procedure is necessary. Work is in progress in order to determine statistically the recoveries of the SPE and LLE procedures for all the enantiomers and to validate the entire analytical method.

4. Conclusions

Because of its high efficiency, high-performance capillary electrophoresis has been shown to be a useful additional tool to the analytical techniques available for the resolution of enantiomers. We have demonstrated that five racemic amphetamines can be separated in less than 30 min with a very good resolution.

After having optimized certain parameters, we concluded that the most significant one is the nature of the chiral selector. The mechanisms of enantiorecognition with the substituted CDs are not yet well defined, and their study is under investigation in order to determine what kind of selector has to be used for the separation of a class of pharmaceuticals. Some experimental work is in progress for complete validation of the method for the determination of amphetamines in biological fluids such as urine, serum and saliva.

Acknowledgements

References

[1] J. Osterloh and B.L. Lee, in R.C. Baselt (Editor), Amphetamines, Abused Drugs Monograph Series, 1988, p. 1.
[2] M.R. Baylor and D.J. Crouch, Am. Assoc. Clin. Chem., 14 (1993) 103.
[3] H.F. Skinner, Forensic Sci. Int., 48 (1990) 123.
[4] H.L. Jin and T.E. Beesley, Chromatographia, 38 (1994) 595.
[5] W.A. König, Carbohydr. Res., 192 (1989) 51.
[6] W.A. König, S. Lutz, G. Wenz and E. Von der Bey, J. High. Resolut. Chromatogr., 11 (1988) 506.
[7] J.T. Cody, J. Chromatogr., 580 (1992) 77.
[8] F.X. Zhou and I.S. Krull, Chromatographia, 35 (1993) 153.
[9] C. Vogt, T. Jira and T. Beyrich, Pharmazie, 45 (1990) 691.
[10] D.M. Desai and J. Gal, J. Chromatogr., 629 (1993) 215.
[11] F.T. Noggle, Jr., J. DeRuiter and C.R. Clark, J. Chromatogr. Sci., 28 (1990) 529.
[12] A.M. Rizzi, R. Hirz, S. Cladrowa-Runge and H. Jonsson, Chromatographia, 39 (1994) 131.
[13] J. Snopek, I. Jelinek and E. Smolkova-Keulemansova, J. Chromatogr., 609 (1992) 1.
[14] R. Kuhn and S. Hoffstetter-Kuhn, Chromatographia, 34 (1992) 505.
[15] I.E. Valko, H.A.H. Billiet, H.A.L. Corstjens and J. Frank, LC · GC Int., 6 (1993) 420.
[16] K. Otsuka and S. Terabe, Trends Anal. Chem., 12 (1993) 125.
[17] F. Lelièvre, P. Gareil and M. Caude, Analusis, 22 (1994) 413.
[18] T.J. Ward, Anal. Chem., 66 (1994) 633A.
[19] M.V. Novotny, H. Soini and M. Stefansson, Anal. Chem., 66 (1994) 646A.
[20] S. Terabe, K. Otsuka and H. Nishi, J. Chromatogr. A, 666 (1994) 295.
[21] T.L. Bereuter, LC · GC Int., 7 (1994) 78.
[22] M.M. Rogan, K.D. Altria and D.M. Goodall, Chirality, 6 (1994) 25.
[23] I.S. Lurie, J. Chromatogr., 605 (1992) 269.
[24] M.W.F. Nielen, Anal. Chem., 65 (1993) 885.
[25] M. Heuermann and G. Blaschke, J. Chromatogr., 648 (1993) 267.
[26] S. Fanali, J. Chromatogr., 474 (1989) 441.
[27] T. Schmitt and H. Engelhardt, J. High. Resolut. Chromatogr., 16 (1993) 525.
[28] C. Quang and M.G. Khaledi, Anal. Chem., 65 (1993) 3354.
[29] S.A.C. Wren, J. Chromatogr., 636 (1993) 57.
[30] T. Schmitt and H. Engelhardt, Chromatographia, 37 (1993) 475.
[31] I.S. Lurie, R.F.X. Klein, T.A. Dal Cason, M.J. LeBelle, R. Brenneisen and R. Weinberger, Anal. Chem., 66 (1994) 4019.

[32] J.H. Knox and K.A. McCormack, Chromatographia, 38 (1994) 279.

[33] B.K. Gan, D. Baugh, R.H. Liu and A.S. Walia, J. Forensic Sci., 36 (1991) 1331.

[34] X. Chen, J. Wijsbeek, J. Van Veen, J.P. Franke and R.A. De Zeeuw, J. Chromatogr., 529 (1990) 161.

[35] B. Kinberger, J. Chromatogr., 213 (1981) 166.

[36] M. Jung, S. Mayer and V. Schurig, LC · GC, 12 (1994) 458.

[37] J. Snopek, I. Jelinek and E. Smolkova-Keulemansova, J. Chromatogr., 452 (1988) 571.

[38] J. Snopek, H. Soini, M.V. Novotny, E. Smolkova-Keulemansova and I. Jelinek, J. Chromatogr., 559 (1991) 215.

[39] D.Y. Pharr, Z.S. Fu, T.K. Smith and W.L. Hinze, Anal. Chem., 61 (1989) 275.

[40] Cyclodextrin News, 7 (1993) 331.

[41] Cyclodextrin News, 7 (1993) 349.

[42] S.A.C. Wren and R.C. Rowe, J. Chromatogr., 603 (1992) 235.

[43] S.A.C. Wren, R.C. Rowe and R.S. Payne, Electrophoresis, 15 (1994) 774.

[44] R. Kuhn and S. Hoffstetter-Kuhn, Capillary Electrophoresis: Principles and Practice, Springer, Berlin, 1993.

[45] S. Naylor, L.M. Benson and A.J. Tomlinson, J. Capillary Electrophoresis, 1 (1994) 181.

[46] S.F.Y. Li, Capillary Electrophoresis—Principles, Practice and Applications, Elsevier, Amsterdam, 1992.

[47] Z.K. Shihabi and L.L. Garcia, in J.P. Landers (Editor), Handbook of Capillary Electrophoresis, CRC Press, Boca Raton, FL, 1994, Ch. 20, p. 537.

[48] K.D. Altria, Chromatographia, 35 (1993) 177.

[49] C. Silverman and C. Shaw, in J.P. Landers (Editor), Handbook of Capillary Electrophoresis, CRC Press, Boca Raton, FL, 1994, Ch. 10, p. 233.

Ultra-fast chiral separation of basic drugs by capillary electrophoresis

Anthony Aumatell[a], András Guttman[b],*

[a]Beckman Instruments Australia, 24 College Street, Gladesville, NSW 2111, Australia
[b]Beckman Instruments, 2500 Harbor Blvd. C-12-D, Fullerton, CA 92634-3100, USA

Abstract

Chiral separation-methods development is usually very time-consuming, due to the diversity in chemical structures of pharmaceutical drug substances as well as the suitable separation conditions and the problem to choose the appropriate chiral selector. This paper shows an ultra-fast, capillary electrophoresis based screening procedure which was developed for chiral separation of several basic pharmaceuticals using dimethyl-β-cyclodextrin as chiral selector. Complete enantiomeric separations of basic drugs (metaproterenol and isoproterenol) were achieved as fast as in 40–50 s, with an R.S.D. for the absolute migration time reproducibility of less than 0.75%. The peak efficiency of the separations was usually over one million theoretical plates per meter, which correspond to an efficiency generation rate above 30 000 plates/m s.

1. Introduction

A large number of pharmaceutical drugs contain one or more chiral centers and may exist in two or more enantiomeric forms [1]. In most instances, only one of the enantiomeric forms is active therapeutically [2] while the other enantiomer is either much less active, inactive, or sometimes even toxic. The drug regulatory agencies in many countries have expressed an interest in investigations of the stereoisomeric composition of the drugs and their associated therapeutic and toxicological consequences. In general, only highly biologically active enantiomers are used in the production of drugs [1,3]. Hence, there is a real necessity to develop rapid and sensitive chiral separation methods required in the investigation of drug enantiomers composition.

Chiral gas and liquid chromatography were the first tools employed in the analytical separation of enantiomers [4]. In the last several years, capillary electrophoresis (CE) has become a powerful technique as an alternative to chiral chromatography methods, because it is fast, inexpensive, and usually does not require the labor-intensive pre- or post-column derivatization steps [5]. This very efficient separation method can easily be adapted to an additional, fast chiral separation and enantiomeric purity validation method in the modern pharmaceutical industry [6]. The separation principle of CE is based on the different electrophoretic mobilities of solutes, which, in turn, depend on their charge densities [7]. Similar to high-performance liquid chromatography (HPLC), secondary equilibria also can be employed in CE separations by means of the use of special additives in the running buffer, such as inclusion com-

* Corresponding author.

plexation agents like cyclodextrins (CDs). CD inclusion complexes can be used for the optical resolution of enantiomers by capillary electrophoresis, based on the differences in electrophoretic mobility of the complexes arising from different complex-formation constants with the analyte [8]. It has been demonstrated that several factors impact peak resolution in chiral CE separations. Rawjee and Vigh [9] showed that basic chiral compounds can be involved in three different types of cyclodextrin-mediated capillary electrophoresis separations. The separation is desionoselective when only the non-dissociated enantiomer complexes selectively with the cyclodextrin. The separation is ionoselective when only the dissociated enantiomer complexes selectively, and the separation is duoselective when both the non-dissociated and dissociated enantiomer complex selectively with the chiral selector. Thus, separation methods development of basic compounds should be primarily based on the pH of the running buffer, besides the vital separation parameters of cyclodextrin type and cyclodextrin concentration. Once the initial separation conditions have been achieved (pH, CD type, CD concentration [10]), further enhancements can be made by adjusting the applied electric field strength, temperature, and capillary length in order to decrease analysis time.

There have been reports on the use of CDs to separate enantiomers of basic pharmaceutical drug compounds [11–24] by CE. In these chiral methods, low-pH buffers with various concentrations of modified β-CDs [11–13,16–18,25–28] were used, including dimethyl-β-cyclodextrin (DM-β-CD) which has been demonstrated to resolve optically the largest number of chiral compounds [13,18,25–28] in CE.

2. Experimental

In all these studies, the P/ACE system 5500 capillary electrophoresis apparatus (Beckman Instruments, Fullerton, CA, USA) was used in normal (anode on the injection side) polarity mode. The separations were monitored on-column at 200 nm. The temperature of the cartridge

holding the capillary column was thermostatted at $15 \pm 0.1°C$ by the liquid cooling system of the P/ACE instrument. The electropherograms were acquired and stored on an IBM 486/66 MHz computer and were evaluated with the System Gold software package (Beckman Instruments).

In all the capillary electrophoresis experiments the eCAP chiral methods development kit was used (Beckman Instruments), with a 7 and 20 cm effective length (27 cm total length) low electroosmotic flow (EOF $< 1.5 \cdot 10^{-5}$ cm^2/V s) neutrally coated capillary column (50 μm I.D. and 375 μm O.D.). The kit also contains all the necessary buffers and chiral selectors needed for separation-methods development, including DM-β-CD (substitution rate: 14) which was chosen during the experiments as chiral selector. Before each analysis, the capillary was rinsed at 138 kPa with 0.1 M HCl for 0.5 min, deionized water for 2 min, and the running buffer for 2 min. This procedure was also used when a new capillary was employed.

The racemates of metaproterenol and isoproterenol (Sigma, St. Louis, MO, USA) were dissolved in deionized water in 0.01 mg/ml concentration. The samples were injected electrokinetically (2 s, 10 kV) into the capillary and were stored at $-20°C$ or freshly used. All the buffer solutions were filtered through a 0.20-μm pore size filter (Schleicher and Schuell, Keene, NH, USA) and carefully vacuum degassed before use.

3. Results and discussion

The water solubility of β-CD can be increased and its enantioselectivity can be altered by chemically modifying the CD with alkyl substituents [13,29–33], which also changes the size and flexibility of the CD cavity [31]. The orientation of bulky and/or charged substituents on the CD cavity can decrease the enantioselectivity by causing steric hindrance and/or coulombic repulsion, preventing guest–host inclusion complex formation [30,34]. DM-β-CD used in this work is an alkyl-modified β-CD and available in various forms with different molar proportion of methyl-

group substitution on the β-CD. The physical characteristics of DM-β-CD appear to make it an attractive chiral additive for CE in two respects: it is highly water soluble, in fact well in excess of the parent β-CD, and each grade is a complex cocktail of related substances varying in both the position and the number of methyl groups attached [35].

Usually, DM-β-CD is a complex mixture, where one of these CDs might form host–guest complexes with certain racemates that approaches the optimum for separation by CE whereas another might be more suitable in the CE separation of another racemate. This may explain the wider range of structural types resolved by CE with DM-β-CD compared to β-CD. We investigated the use of DM-β-CD with the average substitution rate of 14, in the CE separation of some chiral basic drugs.

Initial chiral separation conditions, such as pH and CD type were suggested to be pH 2.5 and DM-β-CD, respectively, based on the methods-development protocol and flow chart published in previous work [36]. Therefore, low-pH phosphate buffers (pH 2.5) were prepared with low (10 mM) and high (50 mM) DM-β-CD concentrations. Enantiomeric separations were attempted using normal polarity separation mode (anode at the injection side) with a low electroosmotic flow (EOF) neutrally coated capillary column. Since chiral separations were achieved for both compounds with both of the concentrations of the CD type chosen (DM-β-CD) in the low-pH running buffer, we concluded that separations obtained were iono- or duoselective types. Thus, further optimization steps were made to increase enantiomeric resolution by varying the concentration of the chiral selector between the preliminary low and high concentrations of 10 and 50 mM. It is important to note that, based on our previous results [10], the applied voltage and the separation temperature were maintained at the maximum level of 30 kV and minimum value of 15°C, respectively, during the CD concentration optimization. As Fig. 1 shows, using the above separation conditions of pH 2.5 buffer, 30 kV, and 15°C, the chiral selector concentration of 30 mM DM-β-
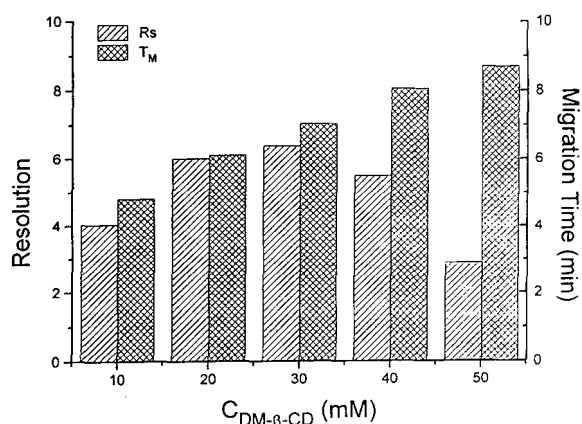

Fig. 1. Effect of the chiral selector concentration on the resolution (R_s) between the R- and S-enantiomers and the migration time (T_M) of the S-enantiomer of metaproterenol. Conditions: 27-cm neutrally coated capillary (20 cm effective length), low-pH buffer (25 mM phosphate, pH 2.5), detection: UV at 200 nm, $E = 1111$ V/cm (normal polarity), temperature: 15°C, injection: 2 s, pressure.

CD was found to be optimal for the separation of the chiral pharmaceuticals metaproterenol and isoproterenol using a 20-cm effective length neutrally coated capillary column. Fig. 1 also exhibits the increase in migration time of the solute when the chiral selector concentration is increased. The use of the neutral coated, low-EOF capillary ensured the predicted migration direction of the basic solutes with the low-pH running buffer, i.e. the use of normal polarity (anode at the injection side). In other words, when EOF is present, at a given pH, the vectorial sum of the solute's electrophoretic mobility and the EOF defines the resultant mobility of the solute. This can cause confusion in the prediction of the migration direction if the EOF and the mobility of the solute are unknown. When no or minimal EOF is present, the migration direction of a basic solute can be easily defined if the pK of the solute and the running buffer pH are known. Fig. 2 shows the separation of metaproterenol under the above-found optimal conditions. The resolution achieved in this separation was $R_s = 6.38$ for the two enantiomers (migration times of 6.58 and 7.04 min, Fig. 2). The peak efficiency, i.e. the theoretical plates
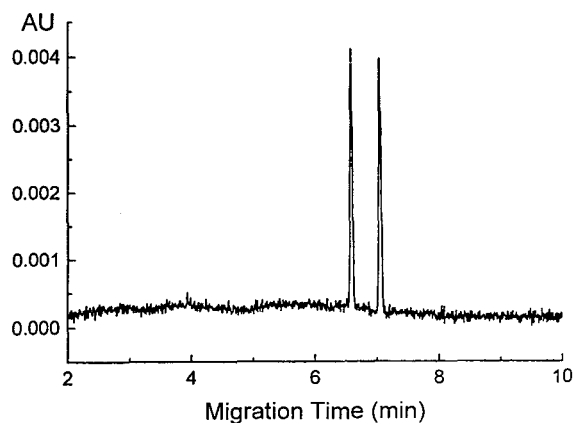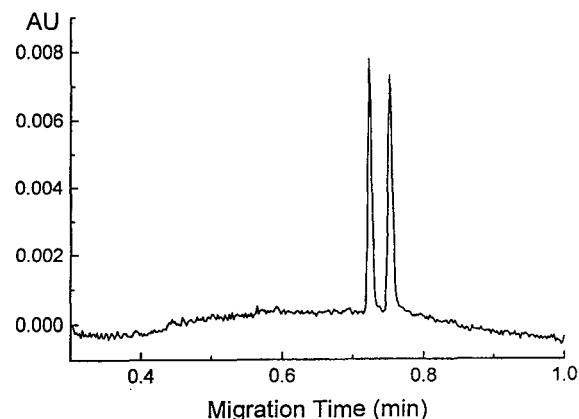
Fig. 2. Separation of the R- and S-enantiomers of meta-proterenol. Conditions: 27-cm neutrally coated capillary (20 cm effective length), low-pH buffer (25 mM phosphate, pH 2.5) containing 30 mM DM-β-CD, detection: UV at 200 nm, $E = 1111$ V/cm (normal polarity), temperature: 15°C, injection: 2 s, pressure.

obtained for the two enantiomers, were 720 000/m and 696 500/m, respectively.

In order to decrease the analysis time, the separation capillary length was reduced from 20 to 7 cm. As Fig. 3 shows, baseline separation of the two enantiomers of metaproterenol was

achieved in 45 s when using the shorter column, maintaining the same applied voltage of 30 kV and temperature of 15°C. The resolution attained was still greater than 2 ($R_s > 2.11$), which is enough for low enantiomeric contamination assessment [37]. The peak efficiencies of this separation were found to be $1.36 \cdot 10^6$ and $0.88 \cdot 10^6$ plates/m for the two enantiomers, respectively. These numbers correspond to an average efficiency generation rate of 30 000 plates/m s.

Fig. 4 shows the ultra-fast separation of another structurally alike basic drug, the isoproterenol enantiomers, using a 7-cm effective length capillary. Similar to the case of metaproterenol, the same concentration (30 mM) of chiral selector DM-β-CD was found to be optimal for the separation of the optical isomers of isoproterenol. Here, complete baseline separation of the two enantiomers was achieved in less than 40 s. The theoretical plate numbers achieved are similar to those in Fig. 3, and both are above 1 million plates per meter.

The migration-time stability of the enantiomers resolved was satisfactory, reflected by migration time %R.S.D. ranging from 0.3–0.8 for inter- and 0.6–0.7 for intra-day reproducibility (Table 1). The asymmetry factors of the
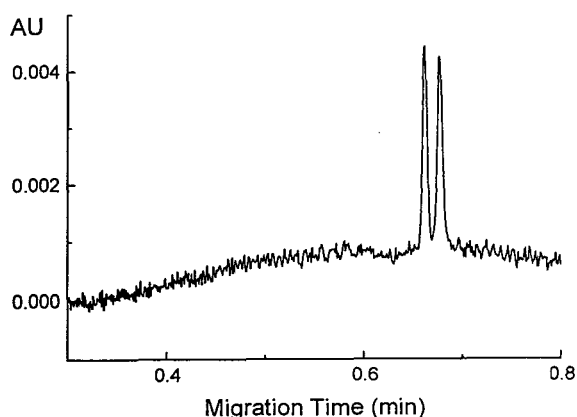

Fig. 3. Ultra-fast separation of the R- and S-enantiomers of metaproterenol. Conditions: 27-cm neutrally coated capillary (7 cm effective length), low-pH buffer (25 mM phosphate, pH 2.5) containing 30 mM DM-β-CD, detection: UV at 200 nm, $E = 1111$ V/cm (normal polarity), temperature: 15°C, injection: 2 s, 10 kV.

Fig. 4. Ultra-fast separation of the R- and S-enantiomers of isoproterenol. Conditions: 27-cm neutrally coated capillary (7 cm effective length), low-pH buffer (25 mM phosphate, pH 2.5) containing 30 mM DM-β-CD, detection: UV at 200 nm, $E = 1111$ V/cm (normal polarity), temperature: 15°C, injection: 2 s, 10 kV.

Table 1
Migration time reproducibility data

Compound		R	S	
Metaproterenol	Mean T_M	0.656	0.671	Day 1
	S.D.	0.0036	0.0037	
	%R.S.D.	0.56	0.49	
	n	10	10	
Isoproterenol	Mean T_M	0.725	0.754	
	S.D.	0.002	0.002	
	%R.S.D.	0.28	0.27	
	n	3	3	
Metaproterenol	Mean T_M	0.653	0.668	Day 2
	S.D.	0.0047	0.0049	
	%R.S.D.	0.73	0.75	
	n	19	19	
Metaproterenol	Mean T_M	0.655	0.667	Day-to-day
	%R.S.D.	0.65	0.62	
	n	29	29	

peaks in the enantiomeric separations were in the range 1.15–1.6, and can be improved by better mobility matching between the buffer coions and the solute ions, if necessary [38].

4. Conclusion

The rapid analysis time, characteristic of capillary electrophoresis, allowed the development of an easy to use and ultra-fast chiral separation method for basic drugs. Based on the size and the shape of the test compounds metaproterenol and isoproterenol, the chiral selector employed during this method development was chosen to be dimethyl-β-cyclodextrin. In the separation of basic solutes, the use of a low-pH phosphate buffer was the recommended choice with the use of a low-EOF, neutrally coated capillary. Once the appropriate separation pH was defined, and initial enantiomeric separation was achieved, further separation optimization steps were accomplished by varying the CD concentration, while the applied electric field strength and separation temperature were maintained the applicable maximum and minimum level, respectively. Under the optimized conditions of 30 mM DM-β-CD in the pH 2.5 phosphate buffer, 30 kV applied voltage, and 15°C temperature, with the use of a 7-cm neutrally coated capillary, ultra-fast (less than one minute) chiral separations were attained with extremely high efficiency (over 1 million plates/m) for the basic solutes of metaproterenol and isoproterenol. Employing this ultra-high-speed analysis technique, we are currently using this method for fast enantio-separation screening of another 35 basic chiral compounds of pharmaceutical interest, which will be reported later.

Acknowledgements

References

[1] M.J. Cope, Anal. Proc., 30 (1993) 498.
[2] FDA Policy Statement for the Development of New Stereoisomeric Drugs, Washington, DC, May 1992.

[3] M.J. Cope, Anal. Proc., 29 (1992) 180.

[4] D.W. Armstrong, in S. Ahuja (Editor), Chiral Separations by Liquid Chromatography, ACS, Washington, DC, 1991.

[5] R. Vespalec and P. Bocek, Electrophoresis, 15 (1994) 755.

[6] K.D. Altria, A.D. Walsh and N.W. Smith, J. Chromatogr, 645 (1993) 193.

[7] J.W. Jorgenson and K.D. Lukas, Anal. Chem., 53 (1981) 1298.

[8] R. Kuhn and S. Hoffstetter-Kuhn, Chromatographia, 34 (1992) 505.

[9] Y.Y. Rawjee and Gy. Vigh, Anal. Chem., 66 (1994) 416.

[10] A. Guttman and N.J. Cooke, J. Chromatogr. A, 680 (1994) 157.

[11] M. Heuermann and G. Blaschke, J. Chromatogr., 648 (1993) 267.

[12] R.J. Tait, P. Tan, D.O. Thompson, V.J. Stella and J.F. Stobaugh, Presented at the 5th International Symposium on High Performance Capillary Electrophoresis, Orlando, FL, January 1993, Paper W214.

[13] S. Fanali, J. Chromatogr., 545 (1991) 437.

[14] K.D. Altria, D.M. Goodall and M.M. Rogan, Chromatographia, 34 (1992) 19.

[15] C. Quang and M. G. Khaledi, Anal. Chem., 65 (1993) 3354.

[16] T.E. Peterson, J. Chromatogr., 630 (1993) 353.

[17] S.A.C. Wren and R.C. Rowe, J. Chromatogr., 636 (1993) 57.

[18] H. Soini, M.L. Rickkola and M.V. Novotny, J. Chromatogr., 608 (1992) 265

[19] V.L. Herring and J.A. Johnson, J. Chromatogr., 612 (1993) 215.

[20] S.A.C. Wren and R.C. Rowe, J. Chromatogr., 635 (1993) 113.

[21] S. Li and D.K. Lloyd, Anal. Chem., 65 (1993) 3684.

[22] S.A.C. Wren and R. C. Rowe, J. Chromatogr., 609 (1992) 363.

[23] L. Valtcheva, J. Mohammad, G. Pettersson and S. Hjerten, J. Chromatogr., 638 (1993) 263.

[24] S. Fanali, L. Ossicini, F. Foret and P. Bocek, J. Microcol. Separ., 1 (1989) 190.

[25] S. Fanali, J. Chromatogr., 474 (1989) 441.

[26] M.E. Swartz, J. Liq. Chromatogr., 14 (1991) 923.

[27] S. Fanali and P. Bocek, Electrophoresis, 11 (1990) 757.

[28] M.W.F. Nielen, Anal. Chem., 65 (1993) 885.

[29] A. Aumatell and R.J. Wells, J. Chromatogr. Sci., 31 (1993) 502.

[30] R.J. Tait, D.J. Skanchy, D.P. Thompson, N.C. Chetwyn, D.A. Dunshee, R.A. Rajewski, V.J.S. Higuchi and J.F. Stobaugh, J. Pharm. Biomed. Anal., 10 (1992) 615.

[31] M.J. Sepaniak, R.O. Cole and B.K. Clark, J. Liq. Chromatogr., 15 (1992) 1023.

[32] R. Kuhn and S. Hoffstetter-Kuhn, Chromatographia, 34 (1992) 505.

[33] A. Guttman, A. Paulus, S. Cohen, N. Grinberg and B.L. Karger, J. Chromatogr., 448 (1988) 41.

[34] I. Cruzado, Y.Y. Rawjee, A. Shitangkoon, Gy. Vigh, Presented at the 5th International Symposium on High Performance Capillary Electrophoresis, Orlando, FL, January 1993, Paper W203.

[35] J. Szejtli, Cyclodextrins and their Inclusion Complexes, Akademiai Kiado, Budapest, Hungary, 1982.

[36] A. Guttman, C. Jurado, S. Brunet and N. Cooke, Presented at 7th International Symposium on High Performance Capillary Electrophoresis, Würzburg, Germany, January 1995, Paper 204.

[37] A. Guttman and N. Cooke, J. Chromatogr. A, 685 (1944) 155.

[38] Y.Y. Rawjee, R. L. Williams and Gy. Vigh, Anal. Chem., 66 (1994) 3777.

Development and validation of a bioanalytical method for the quantification of diltiazem and desacetyldiltiazem in plasma by capillary zone electrophoresis

Carsten Coors[a,*], Hans-Georg Schulz[b], Frank Stache[b]

[a]3M Medica, Analytical Development, D-46325 Borken, Germany
[b]Fachhochschule Münster, Abteilung Steinfurt, Fachbereich Chemieingenieurwesen, D-48565 Steinfurt, Germany

Abstract

A CZE method for the quantification of diltiazem and desacetydiltiazem in plasma was developed and validated. Separation was accomplished at pH 2.5 in a 0.044 M phosphate buffer. Sample preparation was performed by liquid–liquid extraction and no interferences with plasma compounds were detected. The calibration graph is linear over the range 5–250 ng/ml with verapamil as internal standard. The precision and accuracy are better than 13% at 5 ng/ml, and better than 10% between 10 and 250 ng/ml. The long-term reliability of the CZE system was checked over a 3-month period. The CZE method is a useful alternative to the already established HPLC method.

1. Introduction

Diltiazem (DTZ) (Fig. 1) is a calcium channel blocker used in the treatment of angina pectoris, hypertension and supraventricular tachyarrythmias [1]. Several high-performance liquid chromatographic (HPLC) methods have been developed for the determination of diltiazem and the major metabolite desacetyldiltiazem (M1) [1,2] in plasma. The methods described usually involve an extraction step for sample clean-up and concentration.

The main analytical tools for monitoring drugs in body fluids in pharmacokinetic studies are HPLC, GC and immunoassays. Each of these techniques, however, has certain restrictions. The use of capillary zone electrophoresis (CZE)

* Corresponding author.

or micellar electrokinetic chromatography (MEKC) in that field is not very common, and only a few reports have appeared [3]. One reason for this may be the lower concentration sensitivity of CE systems in comparison with HPLC [4]. Different attempts have been made to enhance the sensitivity in CZE by improving the detection techniques and employing sample pretreatment prior to the CZE separation [5].

The separation and determination of DTZ and its metabolites by MEKC was investigated by Nishi et al. [6–8]. To our knowledge, no quantitative bioanalytical methods using CZE or MEKC have been published. In this paper, we describe the method development and validation of a bioanalytical method and demonstrate the suitability of CZE as an alternative to HPLC for pharmacokinetic studies with drug concentrations in the low ng/ml range.
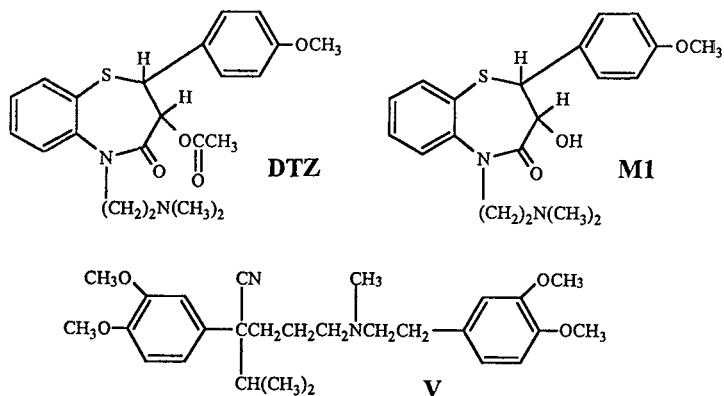
Fig. 1. Structures of diltiazem (DTZ), desacetyldiltiazem (M1) and verapamil (V).

2. Experimental

2.1. Instrumental

CZE system

CZE experiments were carried out on an HP^{3D} CE– system (Hewlett-Packard, Waldbronn, Germany) equipped with a diode-array detector. Capillaries with 50 μm I.D. and 365 μm O.D., standard detection window and bubble cell (extended light path) were obtained from Hewlett-Packard. All capillaries had a total length of 64.5 cm and an effective length of 56 cm. Data processing was done on a Hewlett-Packard Vectra 486/66 XM computer using the HP^{3D} CE – software for instrument control, signal integration and spectral analysis. Statistical calculations were performed with Microsoft EXCEL 5.0 software.

HPLC system

The chromatographic system consisted of a Spectra-Physics (San Jose, CA, USA) SP 8810 double-piston pump, an SP 8780 autosampler (injection volume 50 μl), an SP 8490 UV detector (set to 238 nm) and an SP 4270 integrator. Chromatographic experiments were performed on a Spherisorb ODS 2 (10 μm) column (250 × 4 mm I.D.) (Promochem, Wesel, Germany). The mobile phase was acetonitrile–0.01 M ammo-

nium phosphate buffer (aqueous solution of 1.15 g/l $NH_4H_2PO_4$ plus 0.6 ml of triethylamine, adjusted to pH 3.7 with phosphoric acid) (60:40).

2.2. Materials

Water was deionized with a Milli-Q Reagent Grade Water System (Millipore, Molsheim, France). Phosphoric acid extra pure (85%), sodium dihydrogenphosphate dihydrate extra pure and tert.-butyl methyl ether for residue analysis were purchased from Merck (Darmstadt, Germany). Methanol (HPLC grade), acetonitrile and triethylamine (analytical-reagent grade) were obtained from J.T. Baker (Deventer, Netherlands). During method development, the following 20 mM buffer solutions for HPCE from Fluka (Buchs, Switzerland) were used: sodium citrate buffers of pH 3.0, 4.5 and 6.0 and sodium phosphate buffers of pH 6.5 and 7.5. Sodium dihydrogenphosphate buffer solutions in the pH range 2.0–2.5 and with concentrations between 0.020 and 0.088 M were freshly prepared for the separation experiments by dissolving $NaH_2PO_4 \cdot 2H_2O$ in deionized water and adjusting the pH with phosphoric acid (85%).

Diltiazem hydrochloride and verapamil hydrochloride were supplied by Welding (Hamburg, Germany). Desacetyldiltiazem was synthesized

by ester hydrolysis from diltiazem and purified and characterized according to the literature.

2.3. Procedures

Capillary washing was executed with 1 and 0.1 M sodium hydroxide solutions for HPCE (Fluka) and with buffer solution. New capillaries were preconditioned by rinsing for 10 min with 1 M NaOH, 5 min with 0.1 M NaOH and 5 min with buffer solution. Before each analysis, the capillary was purged for 1.5 min with 0.1 M NaOH and 3 min with buffer.

Electrokinetic injection was tested for aqueous solutions of diltiazem hydrochloride and desacetyldiltiazem in the voltage range 0.75–10 kV and time range 1–10 s. Solutions containing 0.017 M phosphoric acid were checked with injection voltages ranging from 2.6 to 30 kV. The injection time was 10, 15 or 20 s.

Hydrodynamic injection was performed by applying a pressure of 50 mbar to the sample. The injection time was varied between 20 and 150 s. After hydrodynamic sample injection, buffer solution was injected for 20 s at 50 mbar.

2.4. Standard solutions

DTZ and M1

Stock standard solutions of the appropriate amount of diltiazem hydrochloride, corresponding to 1 mg/ml diltiazem free base and 1 mg/ml desacetyldiltiazem free base, were prepared in water and methanol, respectively. Aliquots were subsequently diluted with water to obtain 10 and 1 µg/ml working standard solutions.

Internal standard

A 1 mg/ml aqueous solution of verapamil hydrochloride was prepared and further diluted with water to give working standard solutions of 2.5 µg/ml for the CZE method and 0.5 µg/ml for the HPLC method. A 250-µl aliquot (625 ng for the CZE method and 125 ng for the HPLC method) was added to each 1-ml aliquot of plasma standard or specimen.

2.5. Extraction procedure

To a 100 × 13 mm glass tube, fitted with a glass stopper, were added 1 ml of plasma, 250 µl of internal standard solution and 5 ml of tert.-butyl methyl ether as extraction solvent. The tubes were shaken for 10 min on a Reax2 overhead mixer (Heidolph, Kelheim, Germany) and then centrifuged at 1800 g for 10 min. A 4-ml aliquot of the organic phase was transferred into a glass tube and back-extracted with 40 µl (CZE method) or 150 µl (HPLC method) of 0.017 M phosphoric acid by shaking for 3 min on an overhead mixer. After centrifugation at 2800 g for 10 min, the organic phase was discarded and the phosphoric acid solution was transferred into a vial and an aliquot of ca. 45 nl (CZE method) or 50 µl (HPLC method) was injected.

2.6. Calibration

Calibration graphs were constructed by transferring aliquots of the respective 1 µg/ml standard solutions to blank plasma to give final concentrations of 5, 10, 25, 50, 100 and 250 ng/ml. These calibration standards were extracted as described above. The concentrations of DTZ and M1 in samples were determined by using linear regression (1/concentration weighted) of peak area ratios.

3. Results and discussion

As a starting point for CE method development, we used our already existing HPLC method used previously for the pharmacokinetic characterization of a diltiazem retard formulation. This HPLC method includes two liquid–liquid extraction steps and uses the calcium channel blocker verapamil (V) as internal standard (I.S.). This HPLC method is mainly based on the system described by Dubé et al. [9].

Nishi et al. [6–8] reported the separation of DTZ and metabolites by MEKC; no separation was achieved in CZE systems in the pH range 7–9.

To obtain a reliable CZE method for the

quantification of DTZ and M1 in plasma, over-coming the lack of concentration sensitivity of CE, the bioanalytical method was optimized with respect to the separation and quantification of DTZ, M1 and internal standard verapamil (V); short- and long-term testing of the reproducibility and reliability of the CZE system and method; sample preparation of concentration of the analytes and removal of the interfering plasma compounds; and validation of the CZE method.

3.1. Separation and quantification

Experiments with DTZ, M1 and IS in aqueous solutions

To establish the optimum conditions for separation and quantification, we used an aqueous solution of 10 μg/ml each of DTZ, M1 and internal standard verapamil. We investigated separation buffers between pH 2.0 and 9.0. Decreasing the buffer pH below 4.5 resulted in complete separation of DTZ and M1. The best results were obtained at pH 2.5 with a 0.044 M phosphate buffer.

We studied the effects of different modes of run control, different injection modes and different procedures for capillary washing and their influence on the relative standard deviation (R.S.D.) ($n = 6$) of the peak-area values of DTZ and M1. Our results can be summarized as follows: (1) there was no significant difference between power, current and voltage control; (2) hydrodynamic injection is more reliable than electrokinetic injection; and (3) washing with 0.1 M NaOH and buffer before each run was necessary.

With this preliminary method, we started the next optimization cycle. We sought the best compromise between increased sample loading and better signal-to-noise ratio without losing too much resolution and plate number. Performance data were determined for injection times between 20 and 70 s. The best signal-to-noise ratio was achieved at an injection time of about 45 s. The resolution between M1 and DTZ and the number of theoretical plates were maximum at 20 s and minimum at 70 s; the resolution ranged between 4.2 and 0.7 and plate numbers

between 207 000 and 15 000. As the best compromise, we selected hydrodynamic injection at 50 mbar for 40 s. The results for DTZ, M1 and IS in aqueous solution are shown in Fig. 2.

Long-term reliability of the CE system

In addition to the optimization procedure, we were interested in the long-term reliability of the CE system. Therefore, we also used an aqueous 10 μg/ml mixture, which was injected six times per sequence. Engelhardt et al. [4] reported that in general the R.S.D. for an external standard method usually ranges between 2 and 3%.

In our long-term testing, over 600 injections were preformed over a period of 3 months. The R.S.D. of each sequence ($n = 6$) for the peak-area values was calculated. The R.S.D.s were in the range 0.5–5%, most being in the range 1–
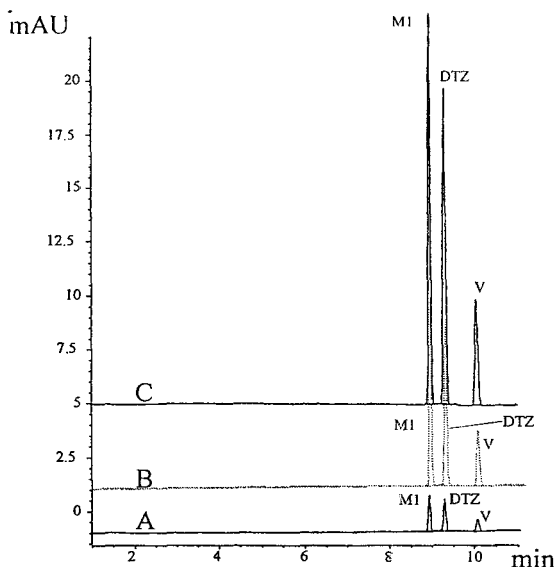

Fig. 2. Electropherograms of three solutions containing desacetyldiltiazem (M1), diltiazem (DTZ) and verapamil (V) in 0.017 M phosphoric acid. Each compound has a concentration of (A) 1, (B) 5 and (C) 10 μg/ml. Buffer, 6.9 g/l NaH$_2$PO$_4$·2H$_2$O (pH 2.5); capillary, fused silica, 64.5 cm (56 cm to detector) $\times$ 50 μm I.D, no extended light path; voltage, 30 kV; detection, 238 nm; temperature, 25°C; injection, hydrodynamic, 50 mbar sample for 40 s followed by 50 mbar buffer for 20 s.

3% (see Fig. 3). No improvement was achieved with migration time-corrected area values.

When using the internal standard method (area for M1 divided by area for internal standard), the R.S.D. of the area ratio was nearly always below 1.5% (Fig. 3). This gives good confidence in the reliability of the CE system,

which is essential for working with limited amounts of plasma in pharmacokinetic studies.

3.2. Sample preparation
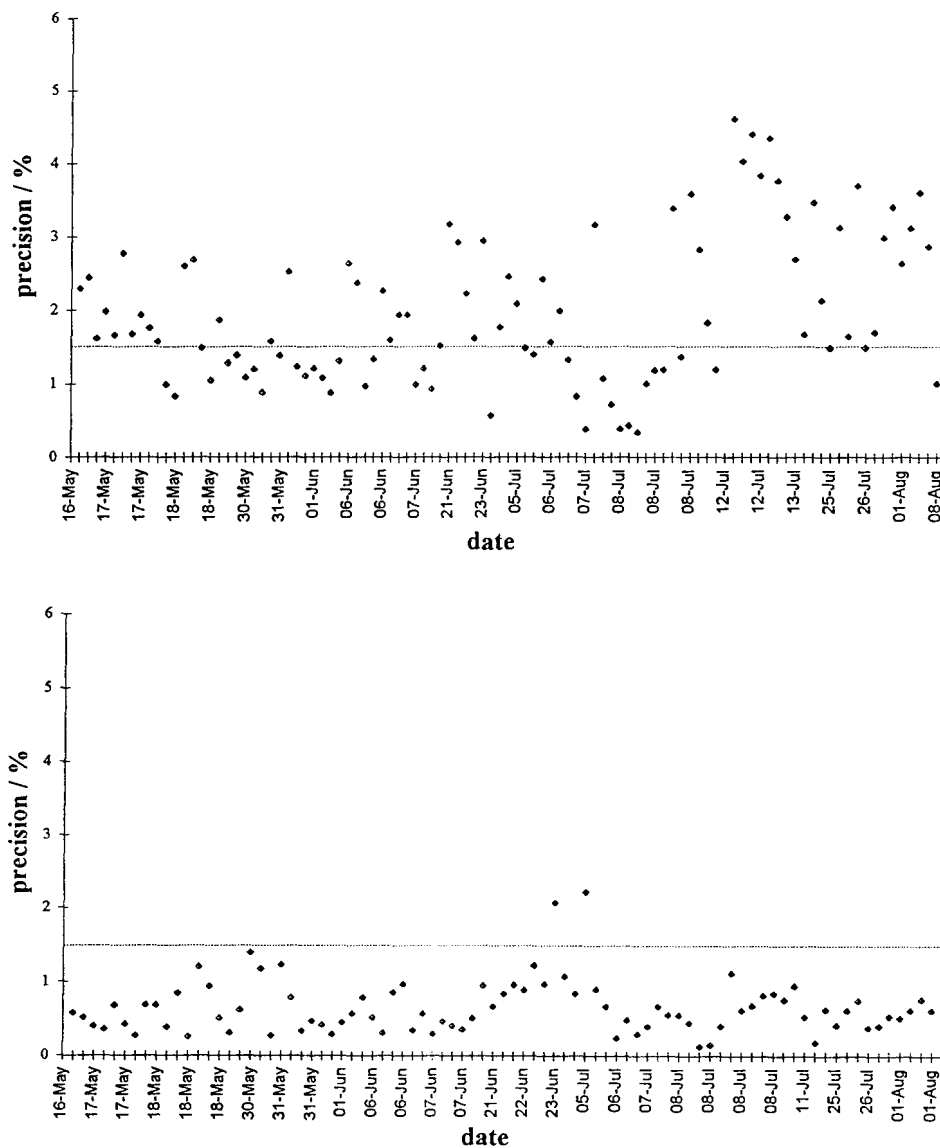
The problem of establishing a CZE or MEKC method for the determination of DTZ and M1 in

Fig. 3. Temporal variation of the precision of area data for desacetyldiltiazem (top) and area ratio data (bottom). For each sequence of six injections the R.S.D. was calculated.
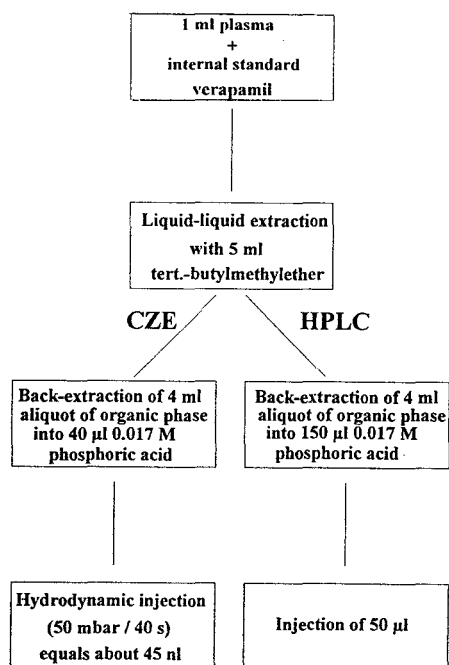
Fig. 4. Sample preparation of CZE and HPLC methods.

concentration sensitivity is usually more important.

We focused our attempts on determining down to 5 ng/ml levels of DTZ and M1 in plasma by optimizing the sample preparation. Sample preparation can be performed by a variety of methods, mainly liquid–liquid extraction (LLE), liquid–solid extraction (LSE) and protein precipitation [10]. For DTZ and M1 we obtained the best results for the HPLC assay with LLE with tert.-butyl methyl ether. We modified the LLE by back-extraction into 40 μl of 0.017 M H_3PO_4, as described in Fig. 4.

The possibility of concentrating an analyte into a small volume of liquid is an advantage of LLE, because LSE without subsequent solvent evaporation does not usually allow concentration into a few microlitres of solvent. Thus, the sample preparation utilizes the extreme high mass sensitivity and overcomes the low concentration sensitivity of CE detection systems.

3.3. Validation results of CZE and HPLC methods

The bioanalytical CZE method was validated with respect to linearity of the detector response, method precision and accuracy, quantitation and detection limit, selectivity and recovery (see also Ref. [11]). Validation data for the CZE method are given in Table 1, example electropherograms in Fig. 5 and for the corresponding HPLC method in Table 2 and in Fig. 6.

The calibration equations and the calibration graphs for DTZ and M1 were linear over the

plasma is sensitivity. Using an aqueous solution of DTZ and M1, the detection limit (signal-to-noise ratio ca. 3:1) is more than fifteen times higher for the CZE system (ca. 50 ng/ml) than for the HPLC system (ca. 3 ng/ml) (for conditions see Figs. 2 and 6). Calculating the absolute sample loading, based on injection volumes of 45 nl and 100 μl, respectively, the CZE system (2.3 pg) is more sensitive than the HPLC system (300 pg). For a bioanalytical method, the

Table 1
Validation data for determination of diltiazem and desacetyldiltiazem in plasma with internal standard verapamil by CZE

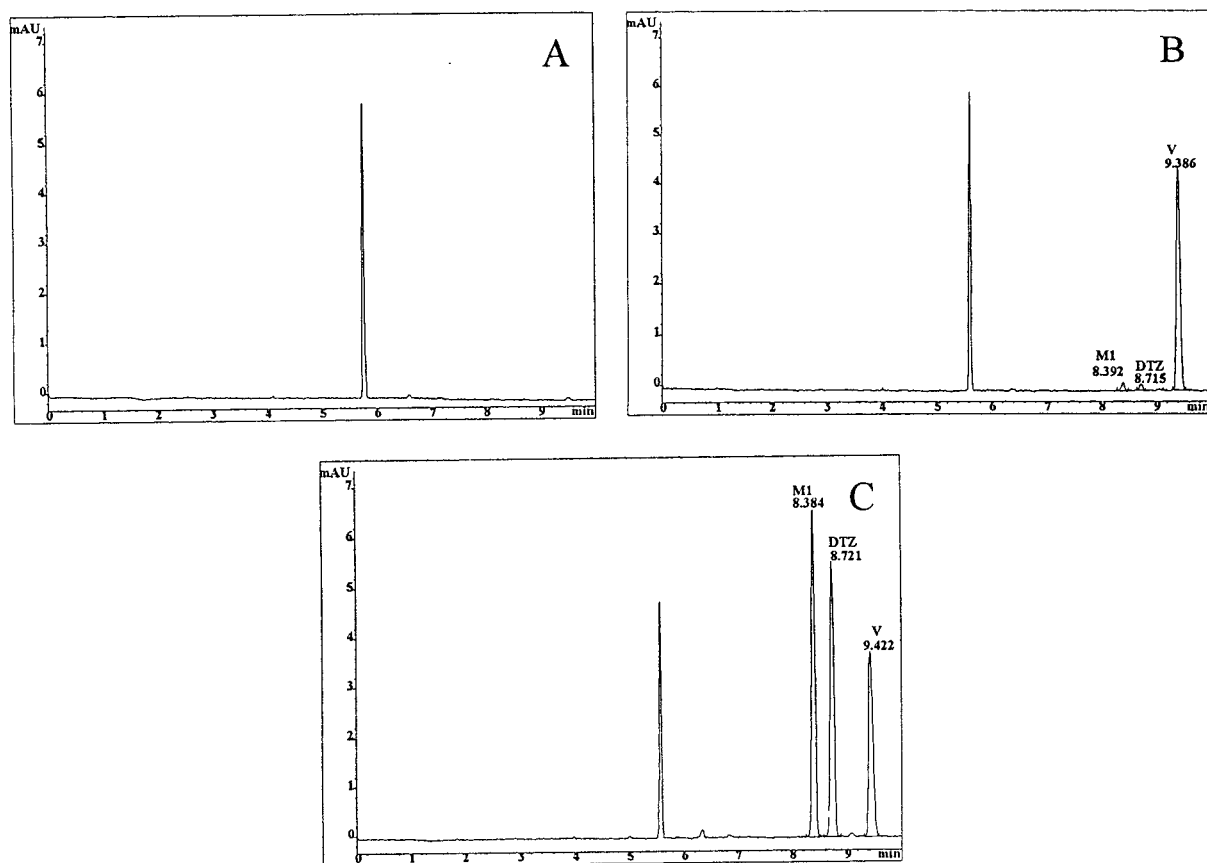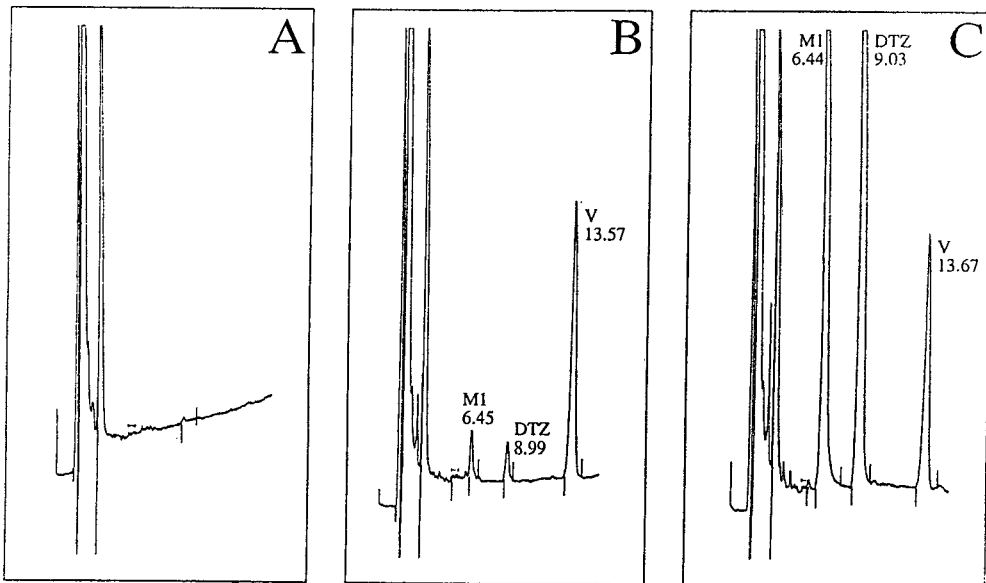| Parameter	Desacetyldiltiazem				Diltiazem			
Nominal value (ng/ml)	5	10	50	250	5	10	50	250
Number of values	7	7	7	7	7	7	7	7
Average (ng/ml)	4.87	10.1	50.7	252.9	4.77	10.4	47.2	250.8
Accuracy (%)	−2.5	+1.4	+1.4	+1.2	−4.7	+3.7	−5.5	+0.3
Precision (%)	11.2	4.6	2.1	4.0	12.7	7.4	2.6	3.6
Correlation coefficient (r)			0.9994				0.9991	

Fig. 5. Electropherograms of the extracts of three plasma samples. (A) Blank plasma without internal standard; (B) plasma sample containing 5 ng/ml desacetyldiltiazem (M1) and diltiazem (DTZ) plus internal standard verapamil (V); (C) plasma with 250 ng/ml M1 and DTZ, and with internal standard.

Table 2
Validation data for determination of diltiazem and desacetyldiltiazem in plasma with internal standard verapamil by HPLC

Parameter	Desacetyldiltiazem			Diltiazem		
Nominal value (ng/ml)	5	50	250	5	50	250
Number of values	10	7	7	10	7	7
Average (ng/ml)	5.2	50.5	242.8	5.1	50.4	243.9
Accuracy (%)	+4.0	+1.0	−2.9	+2.0	+0.8	−2.4
Precision (%)	12.5	2.2	3.8	10.4	3.4	4.0
Correlation coefficient (r)		0.9999			0.9999	

Fig. 6. Chromatograms of the extracts of three plasma samples. (A) Blank plasma without internal standard; (B) plasma sample containing 5 ng/ml desacetyldiltiazem (M1) and diltiazem (DTZ) plus internal standard verapamil (V); (C) plasma with 250 ng/ml M1 and DTZ, and with internal standard. Flow-rate, 1.0 ml/min; injection, 50 μl; column, Spherisorb ODS 2, 10 μm (250 × 4 mm I.D.); mobile phase, acetonitrile–0.01 M ammonium phosphate buffer (pH 3.7) (60:40); detection, 238 nm. Numbers on peaks are retention times (min).

range 5–250 ng/ml for both the HPLC and CZE methods with correlation coefficients greater than 0.999. The calibration equations were as follows:

M1 (CZE method):
  $y = 5.4089 \cdot 10^{-3}x + 4.2581 \cdot 10^{-3}$
M1 (HPLC method):
  $y = 2.19914 \cdot 10^{-2}x - 1.96434 \cdot 10^{-2}$
DTZ (CZE method):
  $y = 5.0490 \cdot 10^{-3}x + 5.0335 \cdot 10^{-3}$
DTZ (HPLC method):
  $y = 1.96033 \cdot 10^{-2}x + 3.813 \cdot 10^{-4}$

where y = area ratio value and x = concentration (ng/ml).

The detection limit (signal-to-noise ratio ≈ 3) was about 1.5 ng/ml for DTZ and M1 for the HPLC method and about 2 ng/ml for the CZE method. No interferences from plasma components were detected. Precision and accuracy were assessed by repeated sample preparation and analyses of plasma controls containing various concentrations of DTZ and metabolite. The precision and accuracy for plasma concentration below 10 ng/ml are less than 13% and for the range 10–250 ng/ml are less than 10% (Tables 1 and 2). The recovery for DTZ and M1 was about 70%.

3.4. Comparison

Although there is the advantage of better reproducibility for HPLC in comparison with CE using aqueous solutions, this has no impact on the precision and accuracy of the bioanalytical method. Also, the linearity, selectivity and long-term reliability of the two methods are the same. In terms of detection limit HPLC has a slight advantage over CZE, but this can be compensated by a further decrease in the back-extraction volume, which was checked down to 20 μl. An advantage for CZE is that there is a sufficient sample volume for several repeated analyses and less solvent consumption, and further only water-based buffers are used.

4. Conclusion

The HPCE assay described provides a selective and reliable method for the quantification of diltiazem and desacetyldiltiazem in plasma. By decreasing the back-extraction volume, the disadvantage of CE concerning the lower concentration sensitivity in comparison with HPLC could be eliminated. A quantitation limit of 5 ng/ml for diltiazem and desacetyldiltiazem in plasma could be achieved with good precision over the linear range 5–250 ng/ml. This method is a useful alternative to our already established HPLC method.

Acknowledgements

References

[1] D.J. Mazzo, C.L. Obetz and J. Shuster, Analytical Profiles of Drug Substances and Excipients, Vol. 23, Academic Press, San Diego, 1994, p. 53.

[2] R.N. Gupta, CRC Handbook of Chromatography: Drugs, Vol. IV, CRC Press, Boca Raton, Fl, 1989, p. 218.

[3] W. Thormann, in N.A. Guzman (Editor), Capillary Electrophoresis Technology, Marcel Dekker, New York, 1993, Ch. 24, p. 693.

[4] H. Engelhardt, W. Beck, J. Kohr and T. Schmitt, Angew. Chem., 105 (1993) 659.

[5] C.A. Monnig and R.T. Kennedy, Anal. Chem., 66 (1994) 280R.

[6] H. Nishi, T. Fukuyama, M. Matsuo and S. Terabe, J. Chromatogr., 513 (1990) 279.

[7] H. Nishi, T. Fukuyama, M. Matsuo and S. Terabe, J. Chromatogr., 515 (1990) 233.

[8] H. Nishi, T. Fukuyama, M. Matsuo and S. Terabe, J. Microcolumn Sep., 1 (1989) 234.

[9] L.M. Dubé, N. Mousseau and I.J. McGilveray, J. Chromatogr., 430 (1988) 103.

[10] R.D. McDowall, J. Chromatogr., 492 (1989) 3.

[11] V.P. Shah, K.K. Midha, S. Dighe, I.J. McGilveray, J.P. Skelly, A. Yacobi, T. Layloff, C.T. Viswanathan, C.E. Cook, R.D. McDowall, K.A. Pittman and S. Spector, Pharm. Res., 9 (1992) 588.

Enantioseparation of mianserine analogues using capillary electrophoresis with neutral and charged cyclodextrin buffer modifiers
13C NMR study of the chiral recognition mechanism [☆]

Bezhan Chankvetadze[1], Gabriele Endresz, Dieter Bergenthal, Gottfried Blaschke*

Institute of Pharmaceutical Chemistry, University of Münster, Hittorfstr. 58–62, 48149 Münster, Germany

Abstract

The enantiomers of the antidepressant drug $(\pm)$-1,2,3,4,10,14b-hexahydro-2-methyldibenzo[c,f]pyrazino[1,2-a]azepine (mianserine, Tolvin) [$(\pm)$-MN] and its 11 structural analogues were resolved with capillary electrophoresis (CE) using native β-cyclodextrin (β-CD) and three charged CD-derivatives as chiral buffer modifiers.

The effect of the nature and position of substituents of the chiral solute on the resolution is discussed. Sulfonated β-CD derivatives such as sulfobutyl (SBE-β-CD) and sulfoethyl (SEE-β-CD) ethers of β-CD permit adequate enantioseparations at rather lower concentrations as chiral selectors in comparison with carboxymethyl-β-CD (CM-β-CD) and especially with native β-CD. In a previous paper, we ascribed the high chiral resolving power of SBE-β-CD to the counter-current mobility of this chiral selector. Another important advantage of SBE–β-CD, its more stereoselective binding to the chiral selectand, is proved here on the basis of 13C NMR studies. This last technique seems to be useful for estimation of the stoichiometry of the host–guest complexes as well as for determination of the apparent binding constants. A number of well-resolved 13C NMR signals which belong to the CD complexes with the $(+)$- or $(-)$-enantiomer of the chiral solute enable racemic samples to be used for the study of the enantioselective binding parameters. Additionally, these CD derivatives can be recommended as useful water-soluble chiral shift reagents for the enantiomeric excess determination by 13C NMR technique.

1. Introduction

Enantioseparation via capillary electrophoresis (CE) is a relatively new and very rapidly developing technique [1,2]. The most popular non-charged (native α-, β-, and γ-cyclodextrin, CD,

hydroxypropyl-, and methylated-β-CD) derivatives in the early stage of the development of this technique [3–6] are being gradually substituted with increasing frequency by more versatile, charged CD-derivatives [6–18]. In 1989 Terabe reported the application of the positively charged ethylene diamine derivative of β-CD for the resolution of dansylated amino acid enantiomers [7]. At the present time, anionic CD-derivatives are more commonly used as chiral selectors in CE [6,9–18] than cationic ones [7,8]. Among anionic derivatives, besides carboxylated

---

* Corresponding author.
[☆] Dedicated to Professor Dr. H. Möhrle on the occasion of his 65th birthday.
[1] Permanent address: Department of Chemistry, Tbilisi State University, Chavchavadze ave 1, 380028, Tbilisi, Republic of Georgia.

cyclodextrins [6,10,11], sulfonated derivatives show very interesting chiral recognition properties [12–18].

The very first application of the sulfobutyl ether (SBE-β-CD), one of the members of this series, did not demonstrate any remarkable advantages. In contrast, undesirable effects, such as large variation in the run-to-run migration times and no elution, were observed [9]. The same derivative in our studies showed a very high enantiomer resolving ability and permitted baseline separations of a number of racemates in the concentration range 20–100 μM in the run buffer [12,17]. The direct measurement of the electrophoretic mobility of the chiral selector [19] allowed us to ascribe the high effectiveness of SBE-β-CD to the counter-current mobility of this chiral selector, which was comparable to the migration of the chiral analytes [12]. Other authors also observed chiral separations using SBE-β-CD or its sulfopropyl analogue in relatively low concentration (1 mM), and ascribed that effect to the self-mobility of the chiral selector [13–16].

Basically, enantioseparations in CE are achieved as a result of (i) different binding constants of the enantiomers to the chiral selector and (ii) differences in the mobilities of the bound and free analytes. An oppositely charged selector and selectand pair is advantageous for achieving the greatest difference between the mobilities of the bound and free analytes and is consequently superior for enantiomer resolution, as already emphasized in our previous study [12]. The former of these two effects, the stereoselectivity of binding of a racemic solute to the chiral selector, is the subject of the present study. The role of the nature and position of substituents on the chiral solutes in their chiral resolution and correlations between the data of ^{13}C NMR spectrometry and CE are also reported.

2. Experimental

2.1. Equipment

Two CE systems: (a) a Grom system 100 (Herrenberg, Germany), equipped with a Linear

Instruments (Reno, NV, USA) UVIS 200 detector and a HP 3396 A integrator (Hewlett-Packard, Avondale, PA, USA) and (b) a P/ACE 2050 (Beckmann Instruments, Fullerton, CA, USA) were used with an untreated fused-silica capillary (Grom) of (a) 61 cm and (b) 47 cm total length × 50 μm I.D. The samples were introduced (a) hydrostatically (10 cm) during 5 s and (b) with low pressure for 2 s at the anodic end of the capillary. The detection of the solutes was carried out at (a) 210 nm and (b) 214 nm. The electric field was 400 V/cm, the temperature 21 ± 1°C. The anode and cathode buffers had the same pH and molarity as the run buffer and contained no chiral selectors.

The selectivity of the enantioseparation was characterized with α_{rel}, which is the ratio of the effective mobilities of enantiomers and is an average value of two measurements. The resolution of enantiomers was calculated according to the following equation:

$$R_s = \frac{2(t_2 - t_1)}{w_1 + w_2} \qquad (1)$$

where t_2 and t_1 are the migration times and w_1 and w_2 the baseline peak width of the first and second eluted enantiomers, respectively. Baseline resolutions of enantiomers were achieved in almost all cases where $\alpha_{rel} \geqslant 1.02$.

2.2. Chemicals and reagents

The racemic (±)-MN and its analogues (Fig. 1) were gifts from Dr. F.A. van der Vlugt (Organon, Netherlands). The optically pure R-(−)- and S-(+)-MN were prepared in our laboratory by enantioselective preparative liquid chromatography using cellulose triacetate as chiral packing material and a methanol–ethanol mix-
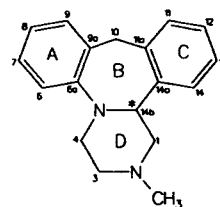

Fig. 1. Structures of (±)-MN and its analogues.

ture (1:1, v/v) as mobile phase. SBE-β-CD (substitution degree ca. 3.14, $M_r = 1684$) was a gift from Prof. J.F. Stobaugh and Prof. V.J. Stella (Center for Drug Delivery Research, The University of Kansas, Lawrence, KS, USA). β-CD, CM-β-CD (substitution degree ca. 2.1, indicated by the manufacturer), and the sulfoethyl ether, SEE-β-CD (substitution degree ca. 2.8, indicated by the manufacturer) were from Wacker Chemie (Munich, Germany).

Analytical grade KH_2PO_4, Na_2HPO_4, H_3PO_4, and NaOH were purchased from Merck (Darmstadt, Germany).

2.3. Buffer and sample preparation

Stock solutions of 50 mM KH_2PO_4 and 50 mM Na_2HPO_4 were prepared in double distilled, deionized water. The pH was adjusted with 1.5 M H_3PO_4 or 0.5 M NaOH. The run buffers were prepared accordingly after the addition of appropriate amounts of the chiral selectors. All solutions were filtered and degassed by sonication before use.

Stock solutions of 1 mg/ml of the racemic compounds were prepared, stored at 4°C, and diluted to 60 μg/ml before use.

2.4. NMR

^{1}H and ^{13}C NMR, homonuclear correlated spectroscopy (HOMCOR), heteronuclear chemical shift correlation (HETCOR), attached proton test (APT), and distortionless enhancement by polarization transfer (DEPT) spectral analysis were carried out with a Varian Gemini 200 NMR-spectrometer at 200 MHz (^{1}H) and 50 MHz (^{13}C). [2]H$_2$O was used as a solvent, and a solution of tetramethylsilane (TMS) in tetrachloromethane served as external standard. The peak assignment of ($\pm$)-MN in ^{1}H NMR and ^{13}C NMR spectra was performed using HOMCOR, HETCOR, APT, and DEPT spectra of ($\pm$)-MN and of some analogues. CD signals in ^{1}H NMR and ^{13}C NMR spectra were assigned using literature data [20,21] for β-CD. Stoichiometry of the selectand–selector complexes was determined by the continuous variation method [22,23] using

the chemical shift of C(6) carbon atom of the ($\pm$)-MN molecule. The total concentration of the interacting species was kept constant at 17 mM, and the molar fraction of the guest was varied in the range 0.2–0.8.

3. Results and discussion

3.1. Effect of the nature and position of the substituents on ($\pm$)-MN molecule on chiral recognition

The results of the enantioseparations of ($\pm$)-MN and its analogues are summarized in Table 1. The quite different effectiveness of each chiral selector given in Table 1 did not allow us to use them in the same or similar concentrations.

Aromatic A and C moieties of the ($\pm$)-MN molecule are most probably involved in a host–guest complex, and therefore, substituents in both aromatic moieties A and C should play a critical part in chiral recognition. Geometric considerations on the basis of the crystal structure study of ($\pm$)-MN [24] and cavity size of β-CD suggest a multimodal complex formation between ($\pm$)-MN and its analogues on the one hand and CDs on the other. For example, the ($\pm$)-MN molecule (or analogues) could be complexed with the chiral selector via aromatic rings A or C. Alternatively, both A and C can simultaneously partially enter the cavity of CD. All above-mentioned complexes are characterized with a 1:1 stoichiometry. A sandwich-like ($\pm$)-MN–CD complex with 1:2 stoichiometry is also expected when the ($\pm$)-MN molecule is complexed via rings A and C simultaneously with two different CD molecules. A number of effects were found depending on the nature and position of the substituents.

Position 7
A methyl substituent in position 7 has a minor influence on the separations, whereas a chloro substituent changes the chiral recognition significantly. The enantioseparation of ($\pm$)-7-Cl-MN was markedly better than that of ($\pm$)-MN when the sulfonated SBE-β-CD and SEE-β-CD

Table 1
Enantioseparations of the (±)-MN and its analogues

Mianserine and analogues with various substituents		20 mM β-CD		5 mM CM–β-CD		0.1 mM SBE–β-CD		0.1 mM SEE–β-CD	
		α_{rel}	R_s	α_{rel}	R_s	α_{rel}	R_s	α_{rel}	R_s
(±)-MN		1.08	2.04	1.24	2.98	1.06	0.89	1.04	0.91
7	–CH₃	1.06	1.70	1.27	4.27	1.06	1.18	1.08	1.53
	–Cl	1.04	1.20	1.15	4.08	1.16	1.84	1.23	2.78
8	–CH₃	1.05	1.45	1.24	3.93	1.19	2.68	1.12	1.67
	–OCH₃	1.04	1.40	1.25	6.36	1.16	2.25	1.13	2.25
	–Cl	1.03	0.81	1.15	4.72	1.21	2.04	1.23	1.36
	–F	1.07	1.88	1.24	4.59	1.09	1.30	1.05	0.90
9	–CH₃	1.06	1.60	1.22	3.63	1.18	2.00	no separation 1.02[a]	1.13[a]
10	cis-OH	1.02	0.94	1.05	1.45	no separation 1.02[a]	2.81[a]	no separation 1.02[a]	3.33[a]
	trans-OH	1.10	2.57	1.17	3.97	1.02	0.60	1.02	0.74
12	–Cl	1.01	0.20	1.10	2.10	1.08	0.79	1.01	0.15
13	–CH₃	1.08	2.07	1.23	4.02	1.08	1.20	1.04	0.99

[a] 0.5 mM chiral selector.
Conditions: Beckmann P/ACE; 50 mM phosphate buffer, pH 3.0.

were used as chiral selectors. In contrast, the enantioselectivity is substantially worse for (±)-7-Cl-MN in comparison with (±)-MN in the case of β-CD and CM-β-CD as chiral selectors.

Position 8

The effect of the nature of substituents on chiral recognition was studied in more detail for the position 8.

The native β-CD and CM-β-CD behave similarly. The enantioselectivity of the separation for the (±)-MN derivatives decreases in the order H ⩾ F > CH₃ ⩾ OCH₃ > Cl for native β-CD and H ≈ F ≈ CH₃ ≈ OCH₃ > Cl for CM-β-CD. Both sulfonated derivatives are almost similar again in this case. The dependence of enantioselectivity on a substituent can be given as follows: Cl ⩾ CH₃ > OCH₃ > F > H for SBE-β-CD and Cl ≫ OCH₃ ⩾ CH₃ > F ≈ H for SEE-β-CD. An absence of correlation between the electron withdrawing ability of substituents on the (±)-MN molecule and their chiral recognition indicates that electron interactions do not play an important role in this case. Rather, the geometric dimension of the substituents should be the more

important factor for chiral recognition. Nearly the reverse order of the selectivity dependence on substituents was observed for pairs of the native β-CD and CM-β-CD on the one hand and for SBE-β-CD and SEE-β-CD on the other. This indicates that the structure of the diastereomeric complexes formed in the first two cases is different from that in the latter two selectors.

Position 10

The CH₂ group which bridges both phenyl rings in position 10 seems to be the key position for stereoselective complex binding. Thus, the chiral recognition ability of all CD derivatives under study is markedly lower for (±)-cis-10-hydroxy-MN than for (±)-MN. The same substituent in the trans-C(10) position also decreases the chiral recognition ability of the sulfonated CDs, but does not alter markedly that of the native and carboxymethyl derivate of β-CD.

Methyl substituents in various positions

The selectivity of the enantioseparation does not strongly depend on the position of the methyl substituent for β-CD and CM-β-CD,

whereas this dependence is very substantial for SBE-β-CD. In particular, the introduction of a methyl substituent in position 7 in ring A or its equivalent position 13 in ring C does not affect the selectivity of the enantioseparation, whereas the selectivity increases drastically by the introduction of the same substituent in position 8 or 9.

As already mentioned above, the dependence of selectivity on the nature and position of substituents is almost similar for the two sulfonated derivatives of β-CD. A substantial difference between these two derivatives was established when the methyl group is substituted in position 8 and, moreover, an even more drastic difference when the same group is substituted in position 9. These two chiral selectors possess the same ionic end group, but they have different lengths of the alkyl spacer and different degrees of substitution. Which one of these two factors is responsible for the considerable variation in chiral recognition abilities in this particular case is the subject of further studies.

Rings A and C

In order to estimate the role of rings A and C of ($\pm$)-MN in the complex with CDs, it was interesting to study the effect of the introduction of bulky substituents like chloro groups in the most likely complex positions such as 7, 8, 9, 12, or 13. Both sulfonated CDs, SBE-β-CD and SEE-β-CD, separate the enantiomers of 7- or 8-chloro-substituted ($\pm$)-MN derivatives better than the native ($\pm$)-MN. The reverse effect is observed again for β-CD and CM-β-CD, which separate the ($\pm$)-MN enantiomers with a substantially higher selectivity than any of its monochloro-substituted analogues. As for the Cl-substituent in equivalent positions of rings A and C, it seems worth mentioning that all CD derivatives in this study separate 8-Cl-substituted ($\pm$)-MN with a substantially higher enantioselectivity than 12-Cl-substituted ($\pm$)-MN.

3.2. pH dependence of the enantioseparation

One of the important advantages of the sulfonated CD derivatives in contrast to the native ones is the presence of a negative charge in the whole pH region acceptable in CE. As a result, SBE-β-CD as a chiral selector shows an optimum stereoselectivity for basic compounds in acidic buffer [12,17]. In contrast to Ref. [14], basic buffers are not necessary for separations. On the other hand, the stereoselectivity for basic compounds decreases drastically in basic medium (Fig. 2). The most likely explanation of this fact is that with increasing pH the electroosmotic flow (EOF) also increases, which is unfavourable for enantioseparation [12,15–17].

The compounds depicted in Fig. 2 are deprotonated at a pH above ca. 7.0–7.5 and behave as neutral compounds. Under these conditions, they can also be separated but with a higher concentration of chiral additives (ca. 0.5 mM).

The decrease in the electrostatic selectand–selector attraction could be another reason for the reduction of enantioselectivity in basic medium. This effect seems to be of much less importance because all anionic CD-derivatives studied are able to enantioselectively recognize not only positively charged and neutral, but also negatively charged chiral analytes [18].

3.3. ^{13}C NMR study of the chiral recognition mechanism

As already mentioned above, our aim was to test whether or not any remarkable differences exist in the binding pattern and stereoselectivity of the various CD derivatives towards the en-
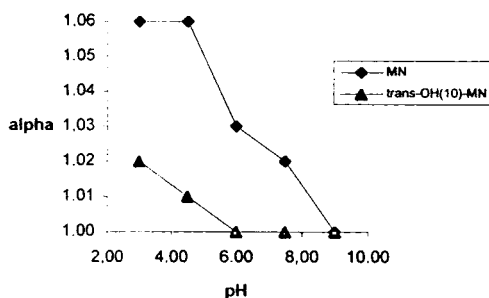

Fig. 2. pH dependence of the enantioselectivity of the separation. Conditions: Beckmann P/ACE, 50 mM phosphate buffer, 0.1 mM SBE-β-CD.

antiomers of (±)-MN. On the basis of the migration time measurements in CE, Stobaugh and co-workers [15] considered it unlikely that a large increase in binding constant for SBE-β-CD for (±)-ephedrine, as compared with those for other CDs, is responsible for the comparable separation of the (±)-ephedrine enantiomers using SBE-β-CD in 10–13 times smaller concentrations than native β-CD and (2,6-dimethyl)-β-CD. Here it seems worth mentioning that since the binding of the racemic solute with a chiral selector is a prerequisite for enantio-separation, no directly proportional dependence may necessarily exist between the binding strength and the stereoselectivity. A number of examples are known in high-performance liquid chromatography (HPLC) [25,26] and CE [27] in this respect. A factor of rather more importance in this case is certainly the difference between binding strengths of the enantiomers, although stronger binding does not always mean a higher binding-strength difference between the enantiomers.

The complexation-induced chemical shifts of selected CD protons (up-field) as well as of some protons of the (±)-MN molecule (down-field) were observed in our experiments using ^{1}H NMR spectroscopy. However, in 200 MHz spectra of (±)-MN–CD complexes, the quantitative assessment of the concentration dependence of the chemical shifts, either of CDs or (±)-MN protons, was impossible due to the overlapping of the selector and selectand signals. No ^{1}H NMR signal splitting was observed for any of the (±)-MN proton signals upon addition of any CD derivative in this study in the range of a host/guest ratio of 0.5–2.5. Therefore, the calculation of the stoichiometry of the selectand–selector complexes formed was based on ^{13}C NMR data. This technique is more and more used for the measurement of enantiomeric excess [28]. Although ^{13}C NMR experiments are more time-consuming, they have some advantages, such as less broadening of the spectral lines, broader spectral width and, as a result, better resolution and easier assignment of signals.

Since CDs are widely used as chiral shift reagents in ^{1}H NMR spectroscopy [29,30], only

few data involving ^{13}C NMR have been published. The use of complexation-induced ^{13}C NMR chemical shifts for measurement of binding constants of the nonchiral [31] or optically pure but nonracemic [32] compounds has been also reported.

^{13}C NMR spectra of (±)-mianserine and SBE-β-CD

The ^{13}C NMR spectra of (±)-MN and equimolar mixtures (8.5 mM each) of SBE-β-CD/(±)-MN, SBE-β-CD/(−)-MN, and SBE-β-CD/(+)-MN are given in Fig. 3. As shown in these spectra, a number of ^{13}C NMR signals of (±)-MN are split as a result of nonequivalence of complexation-induced chemical shifts of (+)- and (−)-MN with SBE-β-CD. No splitting of signals was observed in ^{13}C NMR spectra of
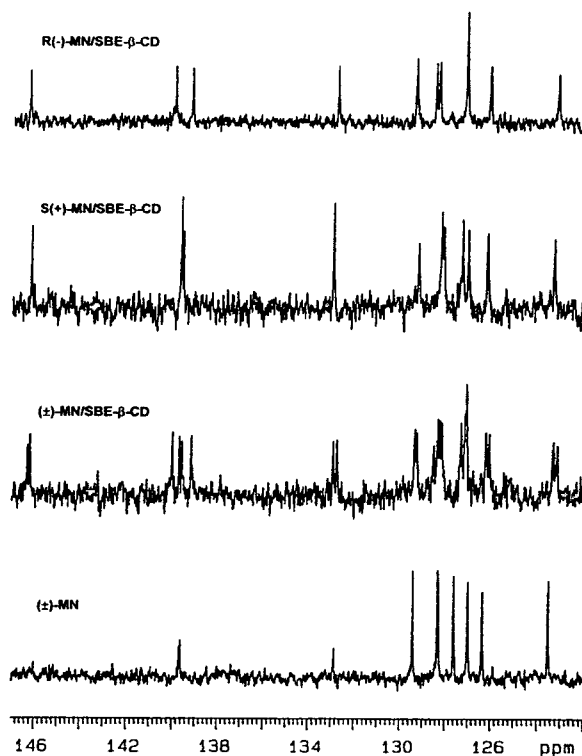
Fig. 3. ^{13}C NMR spectra of (±)-MN and equimolar mixtures (8.5 mM each) of (±)-MN/SBE-β-CD, S-(+)-MN/SBE-β-CD and R-(−)-MN/SBE-β-CD in [2]H$_2$O.

SBE-β-CD complexes with either (+)- or (−)-MN. This result means that the exchange between complexed and free substance is fast on the NMR time scale, and signal splitting occurs only as a result of enantiomeric composition. Among the aliphatic carbon signals of the (±)-MN molecule, only the carbon signal in position 10 is clearly split, whereas most signals in the aromatic region are duplicated. The split ^{13}C-signal of the aliphatic carbon (position 10) is shifted up-field, whereas both up-field [C(6), C(8), C(9)] as well as down-field shifts [C(6^a)] were observed for the aromatic region.

It is also noteworthy that ^{13}C-signals for *R*-(−)-MN are shifted more than those for *S*-(+)-MN, which is in good agreement with the migration behavior of this species in CE (migration order *S*-(+)-MN in front of *R*-(−)-MN, see Fig. 5c).

Stoichiometry of the (±)-MN complexes with CDs

Another important advantage of the use of ^{13}C NMR in this case is the clear splitting of a number of (±)-MN signals. This enables the use of the racemic mianserine for a study of enantiospecific binding parameters and the stoichiometry of the selector–selectand complexes. The study of the competitive binding of enantiomers to the chiral selector is also made possible.

For a more detailed characterization of the above-mentioned (±)-MN–CD complexes, an attempt was made to determine the stoichiometry of the complexes of (±)-MN with these chiral selectors. This was done by plotting the product of complexation-induced chemical shifts of C(6) carbon atom by molar fraction of (±)-MN versus molar fraction of (±)-MN in solutions of (±)-MN/CD mixtures. According to the theory of the Job plot, this dependence should reach a maximum for stoichiometric selectand–selector mixtures.

The Job plots of the (±)-MN complexes with various CDs given in Fig. 4 show that 1:1 guest–host complexes predominate in all cases. Thus, a different stoichiometry of the selector–selectand complexes does not seem to be the reason for the variation in chiral recognition ability of the
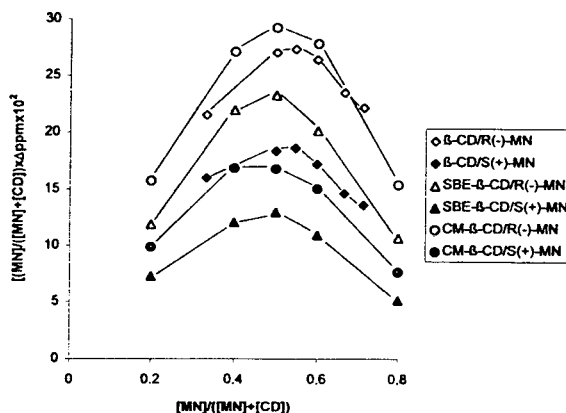
Fig. 4. Job plots for (±)-MN complexes with various CDs.

chiral selectors under study. Different stoichiometries of naproxen [32] as well as of binaphthyl derivatives [33] with various CDs have been reported recently.

The complexation-induced chemical shift differences of (±)-MN with various CDs

The complexation-induced chemical shift differences between enantiotopic signals were found to be strongly dependent on the type of chiral selector, which means qualitatively that in addition to mobility, these CD derivatives differ also in terms of the enantiospecific binding. As an illustrative example of the correlation between ^{13}C NMR spectra and CE results, the electropherograms of the enantioseparation of racemic (±)-MN using various CD chiral selectors, each in a comparable concentration of 0.06 m*M*, are depicted parallel to the fragments of the ^{13}C NMR spectra of the equimolar mixtures of the same species in Fig. 5. A correlation between the separation selectivity and complexation-induced chemical shift differences is obvious. It should be noted that only the difference in binding enantioselectivity with (±)-MN is responsible for the marked variation in efficiencies of CM-β-CD and SBE-β-CD, as no substantial difference exists between the mobilities of these two chiral selectors under the same conditions [18]. Thus, one can conclude that the
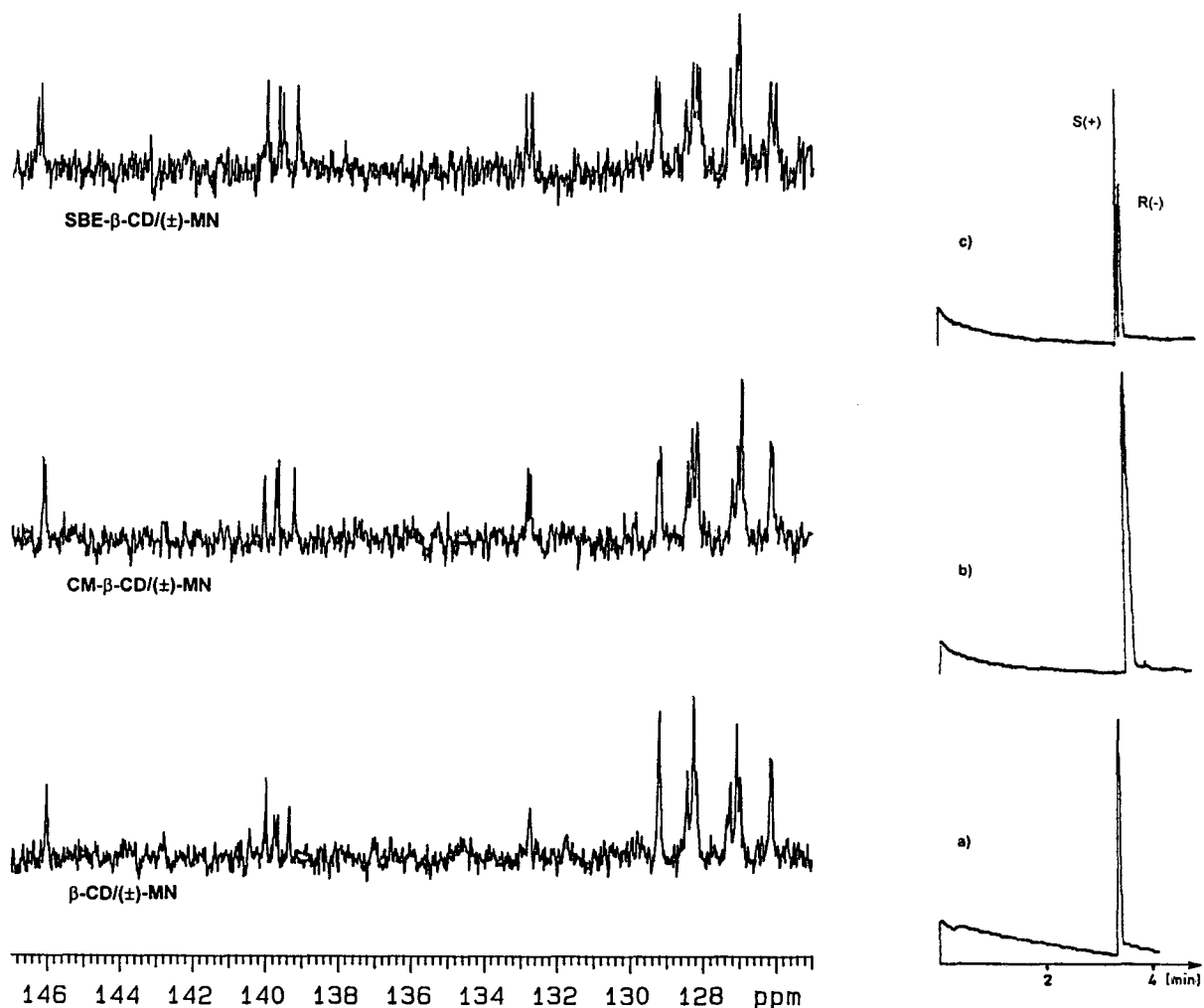
Fig. 5. Correlation between selectivity of the enantioseparation (α) and complexation-induced chemical shift differences of the enantiotopic signals of the (±)-MN molecule. CE conditions: GROM, 50 mM phosphate buffer, pH 6.0: (a) 0.06 mM β-CD, (b) 0.06 mM CM-β-CD and (c) 0.06 mM SBE-β-CD. ^{13}C NMR spectra were taken in equimolar (8.5 mM each) solutions of CDs and (±)-MN in ^{2}H$_2$O. TMS was used as the external standard.

counter-current mobility of anionic CD-derivatives is one of their important advantages [12–17]. Further, the higher stereoselectivity of binding of the racemic compounds in comparison with native and other nonionic CD-derivatives, proved on the basis of direct ^{13}C NMR measurements, can also contribute to the higher separation efficiency of charged CD-derivatives.

References

[1] S. Terabe, K. Otsuka and H. Nishi, J. Chromatogr. A, 666 (1994) 295.

[2] H. Engelhardt, W. Beck and Th. Schmitt, Kapillarelektrophorese, Methoden und Möglichkeiten, Vierfweg, 1994, p. 134.

[3] S. Fanali, J. Chromatogr., 474 (1989) 441.

[4] S. Fanali and P. Bocek, Electrophoresis, 11 (1990) 757.

[5] M. Heuermann and G. Blaschke, J. Chromatogr., 648 (1993) 505.

[6] Th. Schmitt and H. Engelhardt, J. High Resolut. Chromatogr. Chromatogr. Commun., 16 (1993) 525.

[7] S. Terabe, Trends Anal. Chem., 8 (1989) 129.

[8] A. Nardi, A. Eliseev, P. Bocek and S. Fanali, J. Chromatogr., 638 (1993) 247.

[9] B. Pahlen and J.F. Stobaugh, Fourth International Symposium on Pharmaceutical and Biomedical Analysis, April 18–21, 1993, Baltimore, MD, USA, Poster TP-E-12.

[10] N.W. Smith, J. Chromatogr. A, 652 (1993) 259.

[11] Th. Schmitt and H. Engelhardt, Chromatographia, 37 (1993) 475.

[12] B. Chankvetadze, G. Endresz and G. Blaschke, Electrophoresis, 15 (1994) 804.

[13] S. Mayer and V. Schurig, Electrophoresis, 15 (1994) 835.

[14] C. Dette, S. Ebel and S. Terabe, Electrophoresis, 15 (1994) 799.

[15] R.J. Tait, D.O. Thompson, V.J. Stella and J.F. Stobaugh, Anal. Chem., 66 (1994) 4013.

[16] I.S. Lurie, R. Klein, T.A. Dal Cason, M.J. LeBelle, R. Brenneisen and R.E. Weinberger, Anal. Chem., 66 (1994) 4019.

[17] B. Chankvetadze, G. Endresz and G. Blaschke, J. Chromatogr. A, 700 (1995) 43.

[18] B. Chankvetadze, G. Endresz and G. Blaschke, J. Chromatogr. A, 704 (1995) 234.

[19] B. Chankvetadze, G. Endresz and G. Blaschke, unpublished results.

[20] P.V. Dermarco and A.W. Thakkar, J. Chem. Soc. Chem. Commun., (1970) 2.

[21] J.A. Ripmeester and A. Majid, in O. Huber and J. Szejitli (Editors), Proceedings of the fourth International Symposium on Cyclodextrins, 1988, Kluwer Academic Publisher, Dordrecht, p. 165.

[22] P. Job, Ann. Chem., 9 (1928) 113.

[23] M. Cotta Ramusino and S. Pichini, Carbohydr. Res., 259 (1994) 13.

[24] C. van Rij and D. Feil, Tetrahedron, 29 (1973) 1891.

[25] D.T. Witte, J.P. Franke, F.J. Bruggeman, D. Dijksta and R.A. De Jeeuw, Chirality, 4 (1992) 389.

[26] B. Chankvetadze, E. Yashima and Y. Okamoto, J. Chromatogr. A, 670 (1994) 39.

[27] K.-H. Gahm and A.M. Stalcup, Anal. Chem., 67 (1995) 19.

[28] J.W. Jaroszewski and A. Olsson, J. Pharm. Biomed. Anal., 12 (1994) 295.

[29] D.D. MacNicol and D.S. Rycroft, Tetrahedron Lett., (1977) 2173.

[30] A.F. Casy, Trends Anal. Chem., 12 (1993) 185.

[31] J.P. Behr and J.M. Lehn, J. Am. Chem. Soc., 98 (1976) 1743.

[32] G. Bettinetti, F. Melani, P. Mura, R. Monnanni and F. Giordano, J. Pharm. Sci., 80 (1991) 1162.

[33] K. Kano, Y. Tamiya, C. Otsuki, T. Shimomura, T. Ohno, O. Hayashida and Y. Murakami, Supramol. Chem., 2 (1993) 137.

Application and optimization of capillary zone electrophoresis in vitamin analysis

Jörg Schiewe*, Yahya Mrestani, Reinhard Neubert

Institute of Pharmaceutical Technology and Biopharmaceutics, Martin Luther University, Weinbergweg 15, D-06120 Halle/Saale, Germany

Abstract

The application of capillary zone electrophoresis to the determination of ascorbic acid and biotin in vitamin mixtures (pharmaceutical formulations and also native citrus juice and fruit beverage) was investigated. A method was developed for determining them together with thiamine, nicotinamide and nicotinic acid in a single run. For ascorbic acid, addition of L-cysteine as antioxidant was necessary to obtain reliable results. The performance of the method was tested according to sensitivity, detection limit and standard deviation.

1. Introduction

The determination of vitamins in pharmaceutical formulations is very important with regard to the standardization and to the monitoring of the stability of such formulations. In recent years, mainly HPLC techniques have been used for this purpose. Nowadays interest is focused on the use of capillary zone electrophoresis (CZE), micellar electrokinetic chromatography (MEKC) and isotachophoresis (ITP) for the determination of pharmaceuticals and drugs due to their high efficiency [1]. Although the chemical structure of specific vitamins is very different, these methods are very useful also in determining water-soluble vitamins. Recently, several papers have demonstrated the application of high-performance electrophoretic techniques for the determination of vitamins of the B group and niacin [2–6] and also for vitamin C [6–8]. The determination of biotin

(vitamin H) by means of CZE has not yet been reported.

The application of CZE for the determination of ascorbic acid and biotin was of special interest to us. The speciation and the determination of the stability of these substances in vitamin mixtures (pharmaceutical formulations and native samples) was the aim of the present studies. Therefore, it was necessary to develop a method for determining several vitamins in a single run. The performance of the developed CZE method for the determination of ascorbic acid and biotin in beverages and pharmaceutical preparations was tested with regard to sensitivity, detection limit and standard deviation.

2. Experimental

2.1. Apparatus

A Hewlett-Packard (Waldbronn, Germany) ^{3D}CE system fitted with a 600 mm (515 mm to

* Corresponding author.

the detector) × 0.05 mm I.D. (extended light path) fused-silica capillary and an on-column diode-array detector (190–600 nm) was used in all measurements.

2.2. Chemicals

Thiamine hydrochloride, pyridoxine, nicotin-amide, riboflavin-5'-phosphate, nicotinic acid (all BioChemika grade) and L-ascorbic acid, L-cysteine, D-(+) biotin (all analytical-reagent grade) were obtained from Fluka (Buchs, Switzerland). Phosphate buffers of pH 5, 6, 7 and 8, all 20 mM, were prepared using analytical-reagent grade potassium dihydrogenphosphate and sodium hydrogenphosphate dihydrate (Fluka). Doubly distilled water was used throughout.

2.3. Sample and buffer preparation

The standard vitamins were dissolved in water so as to have concentrations in the range 1–500 μg/ml. In the case of vitamin C, a 10 mM concentration of L-cysteine was added for stabilization. The vitamin preparations were dissolved in water. Fruit juices were diluted in water if necessary. The solid preparation containing biotin was dissolved in water and filtered. All samples and the buffers were filtered through a 0.2-μm syringe filter and injected immediately. Buffers were degassed by ultrasound for at least 10 min before use.

2.4. Analysis conditions

The capillary was preconditioned for 10 min with 1.0 M NaOH before the first run and then for 2 min with 0.1 M NaOH and for 3 min with run buffer prior to each following run. The standard separation conditions were voltage (detection end) −30 kV, pressure injection 200 mbar s, capillary temperature 25°C and 20 mM phosphate run buffer of pH 8.0.

3. Results and discussion

3.1. Set-up of the method

For the optimization of the separation conditions, the pH must be chosen first so as to have the analytes in their respective ionic forms. Fig. 1 shows the net ionic charge of the five vitamins thiamine, nicotinamide, biotin, ascorbic acid and nicotinic acid calculated from the pK_a values given in the literature.

Consequently, a pH >4.5 should be maintained to form anions from the acids. Nicotinamide in these media occurs as a neutral compound and cannot be separated and determined in real samples. Nevertheless, we used nicotinamide as a neutral marker in determining the ionic mobility of the other vitamins.

The pH also influences the magnitude of the electroosmotic flow that is directed towards the negative end of a fused-silica capillary. For the simultaneous determination of cations and anions in free zone electrophoresis in a reasonable analysis time, it was necessary to force an electroosmotic flow (EOF) towards the detector (negative end) whose magnitude exceeds the migration velocity of the analyte anions. Therefore, we selected a phosphate buffer of pH 8.0 where the separation run time does not exceed
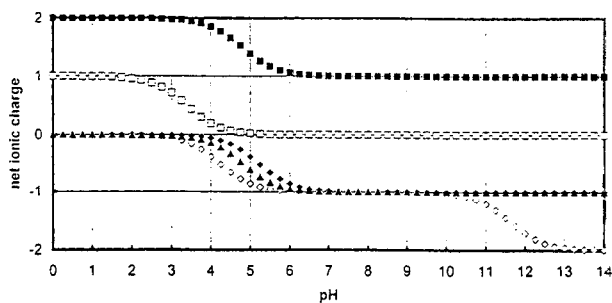
Fig. 1. Net ionic charges (sum of the products of molar fraction and charge of the co-existing ionic forms) of (■) thiamine (pK_a = 4.80 [10]), (□) nicotinamide (pK_a = 3.42 [11]), (◆) biotin (pK_a = 5.20 [12]), (◇) ascorbic acid (pK_{a_1} = 4.17; pK_{a_2} = 11.57 [9]) and (▲) nicotinic acid (pK_a = 4.76 [13]).

10 min, and an optimum separation could be achieved.

Another serious problem in determining vitamins is the chemical stability of the substances. Especially in the case of ascorbic acid, which is easily oxidized, reliable results cannot be expected without the use of stabilizing buffer additives. Fig. 2 shows the stability of ascorbic acid with and without the addition of L-cysteine in phosphate buffers of pH 5.0 and 8.0, respectively.

Cysteine has a more negative redox potential than ascorbic acid and so it acts as an antioxidant. A 50-fold excess of cysteine was added to the standard vitamin C solutions. Therefore, the $t(90\%)$ level (the moment at which 90% of ascorbic acid is still present in solution) of ascorbic acid decay could be extended to 155 min. In contrast to ascorbic acid, biotin was stable in 20 mM phosphate buffer (pH 5–8) for at least 96 h.

3.2. Analytical parameters

Table 1 summarizes the estimated analytical parameters (qualitative and quantitative) of the free zone electrophoretic separation of the
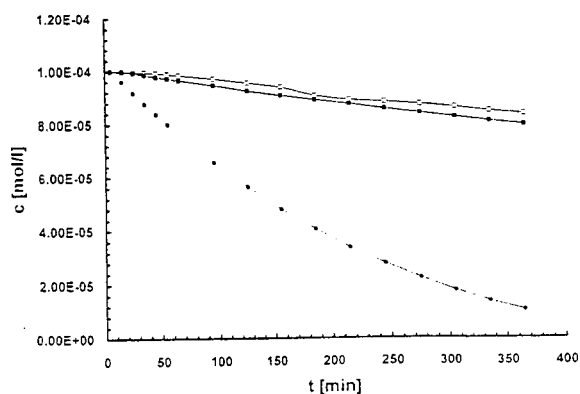
Fig. 2. Stability of a 10^{-4} mol/l ascorbic acid solution in 20 mM phosphate buffer. ● = pH 8.0 without, ■ = pH 8.0 with and □ = pH 5.0 with addition of 0.005 mol/l cysteine over a period of 6 h. Data from UV spectra.

water-soluble vitamins thiamine, nicotinamide, D-(+)-biotin, L-ascorbic acid and nicotinic acid.

Each analyte could be specified by its ionic mobility and its characteristic UV spectrum. The highest absorption for most of the vitamins was found at 200 nm, except for ascorbic acid, where the maximum absorption occurred at 266 nm. The detection limits were at the low ppm level (1–4 μg/ml) and good precision could be achieved.

3.3. Applications
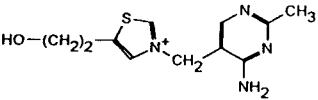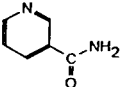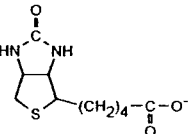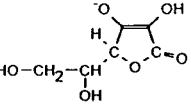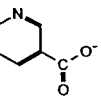
We applied the free zone electrophoretic method to the determination of ascorbic acid in pharmaceutical formulations, native citrus juices and fruit beverages. We always found only one peak for L-ascorbic acid. Isoascorbic acid was not detected. Fig. 3 shows the electropherogram of a multi-vitamin preparation, Multi Sanosvit Fe (Roland Arzneimittel, Hamburg, Germany). Quantification was effected by calibration from standard vitamin solutions. The peak areas were corrected for the retention time. The confidence intervals were calculated from the standard deviation of the linear regression with $P = 0.95$, $f = 7$.

We could identify two of the additional peaks as pyridoxine and riboflavin phosphate by comparing the migration times and the UV spectra with those of standard substances. Table 2 demonstrates the agreement of the results obtained with those declared by the producer.

The result for thiamine is in good accordance with the content given by the producer. However, we found that the content of nicotinamide was too high. Nicotinamide was present as a neutral compound, so it could not be separated from other neutral sample ingredients. For ascorbic acid we found only about 65% of the given content. This is due to its low chemical stability towards oxygen.

From the electropherograms of tangerine juice and commercially available orange nectar, we were able to identify and determine ascorbic acid. We found values in the range 508–516 μg/ml (± 5 μg/ml) vitamin C for freshly pressed

Table 1
Analytical parameters for the five vitamins

Analyte	Formula	Qualitative parameters		Quantitative parameters		
		Ionic mobility $(cm^2/V \cdot s)$	UV spectrum, λ_{max} (nm)	Sensitivity $[AU \cdot s \cdot l/g]$	R.S.D. (%)	Detection limit $(\mu g/ml)$
Thiamine		$16.0 \cdot 10^{-5}$ $\pm\ 0.6 \cdot 10^{-5}$	232 269	0.43 ± 0.01 (200 nm)	2.9 ($n = 8$)	2.7
Nicotinamide		0	215 262	0.99 ± 0.03 (200 nm)	3.4 ($n = 8$)	1.6
Biotin		$-16.7 \cdot 10^{-5}$ $\pm\ 0.4 \cdot 10^{-5}$	–	0.376 ± 0.003 (200 nm)	2.2 ($n = 8$)	3.4
Ascorbic acid		$-20.8 \cdot 10^{-5}$ $\pm\ 0.3 \cdot 10^{-5}$	266	1.26 ± 0.03 (266 nm)	2.5 ($n = 8$)	1.2
Nicotinic acid		$-24.1 \cdot 10^{-5}$ $\pm\ 0.6 \cdot 10^{-5}$	215 262	1.9 ± 0.1 (200 nm)	3.5 ($n = 6$)	0.9

tangerine juice and 143–164 $\mu g/ml$ ($\pm 2\ \mu g/ml$) vitamin C for orange nectar (Kirberg, Germany).

The content of biotin in native samples is very low (ppb range), hence we could not determine it by CZE. In a pharmaceutical preparation, Gabunat (Wölfer, Bovenau, Germany), for the treatment of biotin deficiency phenomena (brittle and cracked nails or hair), we determined the content of biotin. The result agreed well with the given content of 5 mg of biotin per capsule (see Fig. 4).

4. Conclusions

Using the advantages of HPCE such as high separation efficiency, short analysis time and ease of instrumentation and sample preconditioning, we were able to employ this method for determining water-soluble vitamins. The method was applied to the determination of ascorbic acid and biotin in pharmaceuticals and beverages. During the analysis ascorbic acid could be stabilized by adding L-cysteine to the samples. This made it possible to extend the analysis time so as
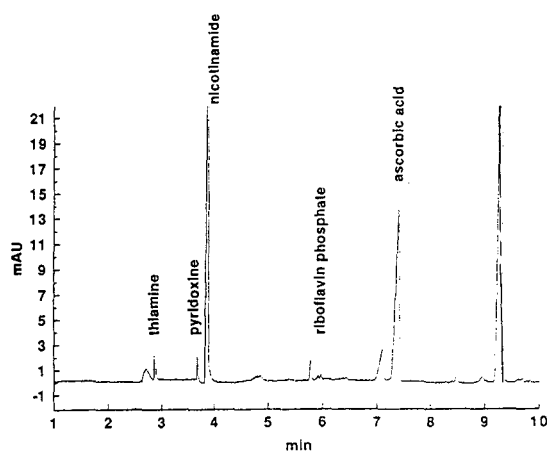
Fig. 3. Electropherogram of Multi Sanosvit Fe. Standard separation conditions, detector signal at 200 nm.

Fig. 4. Electropherogram of Gabunat. Standard separation conditions, detector signal at 200 nm. Result: 4.63 ± 0.04 and 4.79 ± 0.04 mg of biotin (duplicate analysis).

to perform calibration and sample analysis automatically. The detection limits of CZE were in the low ppm range. Therefore, biotin could not be detected in native samples. The method offered good precision.

Table 2
Analytical results for Multi Sanosvit Fe

Vitamin	Content in 5 ml of juice (mg)	Result related to 5 ml of juice (mg)
Thiamine hydrochloride	1.0	0.8
		1.1
Riboflavin phosphate	1.0	Detected
Pyridoxine hydrochloride	0.5	Detected
Ascorbic acid	50.0	31.9
		30.7
Nicotinamide	5.0	7.6
		7.4

The density of the formulation was determined only once at room temperature and amounted to 1.237 g/ml. Therefore, no confidence interval could be given for the results.

References

[1] J. Sadecka, J. Polonsky and Shitani, Pharmazie, 49 (1994) 631.
[2] U. Jegele, J. Chromatogr. A, 652 (1993) 495.
[3] R. Huopalahti and J. Sunell, J. Chromatogr., 636 (1993) 133.
[4] H. Nishi, N. Tsumagari, T. Kakimoto and T. Terabe, J. Chromatogr., 465 (1989) 331.
[5] S. Bonkerd, M.R. Detaevernier and Y. Michotte, J. Chromatogr. A, 670 (1993) 209.
[6] S. Fujiwara, S. Iwase and S. Honda, J. Chromatogr., 447 (1988) 133.
[7] M. Chiari, M. Nesi, G. Carrea and P.G. Righetti, J. Chromatogr., 645 (1993) 197.
[8] E.V. Koh, M.G. Bissell and R.K. Ito, J. Chromatogr., 633 (1993) 245.
[9] Beilsteins Handbuch der Organischen Chemie, 4. Auflage, 3. und 4. Ergänzungswerk, Bd. 27, Teil 3, Springer, Berlin, 1983, p. 1765.
[10] Beilstein Handbook of Organic Chemistry, 4th ed., 5th Supplementary Series, Vol. 22, Part 2, Springer, Berlin, 1990, p. 81.
[11] Beilsteins Handbuch der Organischen Chemie, 4. Aufl., 3. und 4. Ergänzungswerk, Bd. 27, Teil 11, Springer, Berlin, 1984, p. 7980.
[12] H.J. Roth, K. Eger and R. Troschütz, Pharmazeutische Chemie II, Arzneistoffanalyse, Reaktivität—Stabilität—Analytik, Geory Thieme, Stuttgart, 3. Auflage, 1990.
[13] Beilstein Handbook of Organic Chemistry, 4th ed., 5th Supplementary Series, Vol. 22, Part 2, Springer, Berlin, 1990, p. 58.

Analysis of the components of *Lycopus europaeus* L. in body fluids during metabolism studies
Comparison of capillary electrophoresis and high-performance liquid chromatography

H. Wojciechowski[a,*], H.G. Gumbinger[b], U. Vahlensieck[b], H. Winterhoff[b],
A. Nahrstedt[c], F.H. Kemper[a]

[a]*Umweltprobenbank für Human-Organproben, Westfälische Wilhelms-Universität, Domagkstr. 11, D-48149 Münster, Germany*
[b]*Institut für Pharmakologie und Toxikologie, Westfälische Wilhems-Universität, Domagkstr. 12, D-48149 Münster, Germany*
[c]*Institut für Pharmazeutische Biologie und Phytochemie, Westfälische Wilhelms-Universität, Hittorfstr. 56, D-48149 Münster,
Germany*

Abstract

During pharmacokinetic studies with extracts obtained from medicinally used plants, analysis in body fluids is mainly performed by HPLC, an established separation method. In this paper high-performance capillary electrophoresis (HPCE) is investigated for its ability to separate such complex extracts. Crude extracts of *Lycopus europaeus* L. (Lamiaceae) are traditionally used against mild forms of hyperthyroidism. The metabolism of a 70% ethanolic extract with respect to some of its individual main components (rosmarinic and caffeic acid, luteolin-7-glucoside) and a mixture of the pure compounds were investigated using isolated perfused rat liver. After solid-phase extraction metabolites were determined using HPCE and HPLC separation techniques. A buffer solution composed of 0.05 mol l^{-1} Na$_2$HPO$_4$ at pH 7.0 with 30% acetonitrile was found to be the most suitable electrolyte for HPCE separation. The best mobile phase for isocratic HPLC was 0.03% TFA–acetonitrile (82:18, v/v). Data obtained with HPCE are in good accordance with those from HPLC; HPCE, however, is clearly more rapid and simple to perform.

1. Introduction

Plant extracts from *Lycopus europaeus* L. (Lamiaceae, "Wolfstrapp") are traditionally used in mild forms of hyperthyroidism. In animal experiments crude extracts show antithyreotropic and antigonadotropic effects [1–4]. Phenolic substances of the extract, e.g. rosmarinic and caffeic acid, are responsible for the biological

effects [1–7]. The activity of the single phenolic constituents proved to be much smaller than that shown by the crude plant extracts. Therefore differences in metabolism between crude extracts and single compounds could account for such differences. To check this assumption the metabolism of an ethanolic extract of *Lycopus europaeus* L. was compared to that of three main components (rosmarinic and caffeic acid, luteolin-7-glucoside) and a mixture of these. For these investigations isolated perfused rat liver

* Corresponding author.

was used as the model system [10,11]. Analysis of the obtained samples (perfusates) is usually performed by HPLC [8,9]. In this paper CE is investigated for its ability to separate such complex samples during metabolism studies.

2. Experimental

2.1. Apparatus and conditions

All CE analyses were carried out on a Waters Quanta 4000 capillary electrophoresis system (Waters, Eschborn, Germany) equipped with a UV detector set at 280 nm and an untreated fused-silica capillary (CS, Chromatographie-Service, Langerwehe, Germany) of 60 cm (total capillary length) $\times$ 75 μm I.D. and 360 μm O.D. The detection window was placed at 52 cm. Samples were introduced by hydrodynamic injection for 10, 12 or 20 s at the anodic end of the capillary. Running conditions were as follows: run time, 10 min; applied voltage, 25 kV (constant voltage, positive power supply); current, 273 μA; ambient temperature, 24–25°C. The electrolyte was a buffer consisting of 0.05 mol l^{-1} Na$_2$HPO$_4$ and 30% acetonitrile, adjusted to pH 7.0 with 1 M hydrochloric acid. The electrolyte was filtered through a 0.45-μm filter before use.

The HPLC system consisted of a pump (Waters M 45, Waters, Eschborn, Germany), a detector (Pye Unicam LC 3 UV, Cambridge, UK) set at 280 nm, an injector (Rheodyne 7161 + 7125) and an integrator (Pye Unicam CDP1, Cambridge, UK). A 10-μl injection volume and a column combination of a pre-column (LiChrosorb RP 18, 10 μm, 5 cm $\times$ 4 mm, Merck, Darmstadt, Germany) and an analytical column (LiChrosorb RP 18, 10 μm, 25 cm $\times$ 4 mm, Merck, Darmstadt, Germany) were used for all HPLC analyses. The mobile phase for isocratic HPLC separation was 0.03% TFA–acetonitrile (82:18, v/v) with a flow-rate of 1.2 ml min^{-1}.

Solid-phase extraction (SPE) was carried out on an Adsorbex SPU 19835 apparatus (Merck) with Bakerbond SPE Phenyl columns (3 ml size,

Baker, Groß-Gerau, Germany). The column was conditioned using 3 ml methanol and 3 ml water. Sample preparation: 1 ml sample was acidified with 100 μl 1 M HCl. Sample application: 1–6 ml of acidified sample. Column washing: 1 $\times$ 3 ml water. Analyte elution: 2 $\times$ 3 ml methanol, evaporate to dryness, redissolved in 100–200 μl acidified methanol–water (1:1, v/v).

2.2. Model of the liver perfusion

According to the method described in Ref. [11] the isolated liver is connected to the perfusion apparatus described in Ref. [10]. For a single liver perfusion a period of 90 to 110 min is necessary. Samples (fractions 1–11) were taken at 10 min intervals. After an equilibration time of 10 min, the test substances were added to the perfusion medium (flow-rate 20 ml min^{-1}) over a 30-min interval (10–40 min). During each run an additional sample of perfusion medium was taken for chromatographic analysis shortly before liver passage (VL) usually at 30 min in order to determine the real concentration of the test compounds. This is necessary as loss of substance occurs within the system. The difference between the concentration before (determined from VL) and after liver passage (determined from F1–F11) is used to calculate the metabolic rate of the substances after the following scheme [12]:

–Before liver passage: VL $\cdot$ 20 $\cdot$ 30 = x (μg) = 100%.

–After liver passage: (F1–F11) $\cdot$ 20 $\cdot$ 10 = y (μg).

–Metabolic rate (%): $100 - \dfrac{100 \cdot y}{x}$.

2.3. Materials

Perfusion medium for the in vitro model

As perfusion medium a modified Krebs–Henseleit solution was used: NaCl 0.119 mol l^{-1}, KCl 4.74 $\cdot$ 10^{-3} mol l^{-1}, NaHCO$_3$ 2.5 $\cdot$ 10^{-2} mol l^{-1}, KH$_2$PO$_4$ 1.16 $\cdot$ 10^{-3} mol l^{-1}, MgSO$_4$ 1.16 $\cdot$ 10^{-3} mol l^{-1}, CaCl$_2$ 2.0 $\cdot$ 10^{-3} mol l^{-1}, MOPS (3-N-morpholinopropanesulfonic acid)

$3.0 \cdot 10^{-3}$ mol l^{-1}, glucose $1.15 \cdot 10^{-2}$ mol l^{-1}, bovine serum albumin (BSA) 0.5% and sodium taurocholate $2 \cdot 10^{-5}$ mol l^{-1}. BSA was of chemical grade and purchased from UCB (Brussels, Belgium). All other chemicals used for the perfusion medium were of analytical grade and purchased from Merck or Sigma (Munich, Germany).

Acetonitrile for CE and HPLC was of ultragradient quality and obtained from Baker. Na$_2$HPO$_4$ and methanol for the buffer solution were obtained from Merck. Natural substances (caffeic and rosmarinic acid, luteolin, luteolin-7-glucoside and protocatechualdehyde) were purchased from Roth (Karlsruhe, Germany).

Preparation of the test substances

An amount of 200 ml of the 70% ethanolic extract of *Lycopus europaeus* L. (obtained from Finzelberg, Kleinostheim, Germany) was evaporated until the amount of ethanol was less than 1% (data obtained from headspace GC). The residue was redissolved in 50 ml perfusion medium and filtered through an 8-μm filter. Caffeic acid ($5.5 \cdot 10^{-4}$ mol l^{-1}) was dissolved in 100–200 μl hot water and diluted with physiological buffer. Luteolin-7-glucoside is only poorly soluble in the perfusion medium. A complete solution can be obtained by dissolving $1.1 \cdot 10^{-4}$ mol l^{-1} luteolin-7-glucoside in 30–50 μl 2 M NaOH with ultrasound treatment. This solution was filled up with buffer to 50 ml. Rosmarinic acid is readily soluble in the buffer.

2.4. HPLC of perfusates

HPLC of standard mixtures of the three main components

For HPLC analysis of the perfusates from liver perfusion, samples were deproteinized with 3% trichloroacetic acid and centrifuged at 4000 g, the supernatant was used for HPLC. Metabolites in the perfusates were determined after solid-phase extraction on phenyl columns.

Recovery

A mixture of three main components of *Lycopus europaeus* L. (for structures see Fig. 1) was dissolved in physiological buffer, acidified with 100 μl 1 M HCl per ml, injected directly onto the HPLC system and detected at 280 nm. The peak areas were taken to 100%. The sam-

luteolin-7-glucoside (1)   luteolin (2)
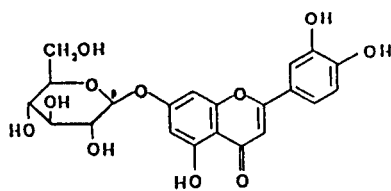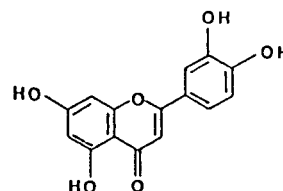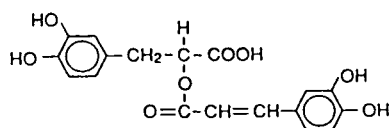
rosmarinic acid (3)   protocatechualdehyde (4)   caffeic acid (5)
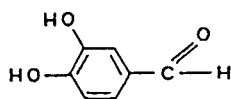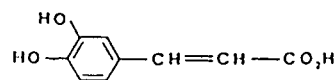
Fig. 1. Structures of five substances from the ethanolic extract of *Lycopus europaeus* L.

Table 1
Recovery rates for three main components after SPE

Component	Concentration (mol l^{-1})	Recovery rate (%)
Luteolin-7-glucoside	$2.45 \cdot 10^{-3}$	82 ± 6.6
Caffeic acid	$7.20 \cdot 10^{-4}$	95 ± 8.8
Rosmarinic acid	$2.78 \cdot 10^{-3}$	94 ± 7.3

The concentration of the substances corresponds to the concentration found in the crude extract.

ples were acidified and concentrated via solid-phase extraction (SPE, $n = 5$).

3. Results and discussion

3.1. Recovery

For recovery experiments a comparison was made between the direct injection of the three main components into the HPLC system followed by injection of samples which had been purified by solid-phase extraction (SPE). Table 1 shows recovery rates between 82 and 95% when the three compounds were used in a concentration as obtained for the crude plant extract. Table 2 shows that a variation between ca. 75 up to 105% of the recovery exists dependent on the amount of each individual compound over a range from 0.01 to 1 mg ml^{-1}.

Recovery ($\pm$ R.S.D.) over a concentration range from 0.01–1 mg ml^{-1} ($n = 3$) varies as shown in Table 2.

3.2. Efficiency

Fig. 2 shows the CE and HPLC separations of the crude extract; the separation of a mixture of the five components of *L. europaeus* is depicted in Fig. 3. All five components can be detected within 6 min following CE analysis, whereas only four components can be found after 30 min using HPLC isocratic elution. CE analysis leads to better peak shape and efficiency and, moreover, a better resolution between peak 4 and 5 is obtained. In Table 3 efficiency, expressed in terms of number of theoretical plates (N), is compared for CE and HPLC analysis for the crude extract. Table 3 clearly shows that CE provides a higher separation efficiency in comparison to HPLC.

3.3. Linearity

To determine the linearity for both techniques plots of peak area versus concentration over the range 0–1060 μg ml^{-1} were made for a mixture of the three main components of *L. europaeus*. CE and HPLC regression equations of the curves and correlation coefficients as presented in Table 4 are in good accordance.

3.4. LOD (limit of detection)

In Table 5 the limits of detection for CE and HPLC analysis for the three main components are compared using the signal-to-noise ratio (2:1) at 280 nm. Data are based on three replicate injections with 20 s HD injection for CE and 10 μl injection for HPLC. HPLC proved

Table 2
Recovery rates (%) for three components after SPE over a range from 1.0–0.01 mg ml^{-1}

Substance	Concentration (mg ml^{-1})				
	1.0	0.25	0.1	0.025	0.010
Luteolin-7-glucoside	82 ± 6.2	87 ± 5.0	87 ± 4.2	105 ± 5.7	107 ± 8.7
Caffeic acid	103 ± 1.2	87 ± 5.9	88 ± 6.6	87 ± 8.3	106 ± 8.7
Rosmarinic acid	92 ± 4.4	83 ± 4.0	76 ± 1.0	87 ± 7.8	91 ± 8.6
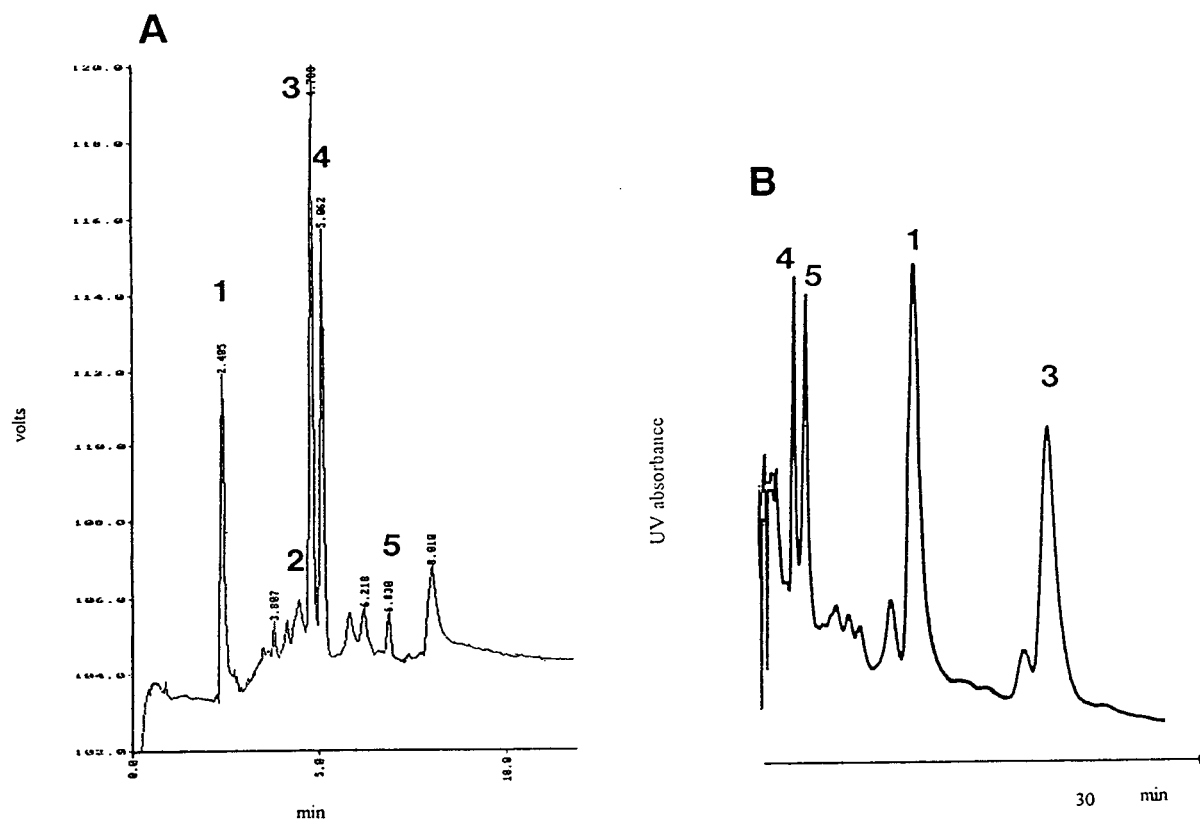
Fig. 2. Separation of the crude extract with both techniques. Peaks: 1 = luteolin-7-glucoside, 2 = luteolin, 3 = rosmarinic acid, 4 = protocatechualdehyde, 5 = caffeic acid. (A) CE analysis. Conditions: sample, original 70% ethanolic extract dissolved with water (1:1, v/v), filtered through 0.45-μm before use; buffer, 0.05 mol l^{-1} Na$_2$HPO$_4$, pH 7.0, with 30% acetonitrile; capillary, 60 cm (52 cm to detector) × 75 μm I.D.; voltage, 25 kV; current, 273 μA; temperature, 24–25°C; detector, UV 280 nm; injection, 12 s hydrodynamic. (B) HPLC analysis. Conditions: sample, see above; column combination: LiChrosorb RP 18, 10 μm, 5 cm × 4 mm and LiChrosorb RP 18, 10 μm, 25 cm × 4 mm; eluent, 0.03% trifluoroacetic acid–acetonitrile (82:18, v/v); flow-rate, 1.2 ml min^{-1}; temperature, 25°C; detector, UV 280 nm; injection, 10 μl.

to be more sensitive for luteolin-7-glucoside and caffeic acid. This is explained by the small size of the detector flow cell used with CE.

3.5. Precision

To control the reproducibility of peak areas for both techniques, ten injections of a mixture of caffeic acid (7.2 · 10^{-4} mol l^{-1}), rosmarinic acid (2.8 · 10^{-3} mol l^{-1}) and luteolin-7-glucoside (2.45 · 10^{-3} mol l^{-1}) were made. All substances were dissolved in buffer and concentrated via SPE before use. The relative standard deviation

(R.S.D.) in peak area is shown in Table 6. Differences in R.S.D. between both methods can be explained by the different injection volumes used (CE e.g. 80 nl, HPLC e.g. 10 μl).

3.6. Metabolism studies

Metabolic rates

Metabolism studies were carried out using the model of the isolated perfused rat liver [10,11] as described in the Experimental section. After an equilibration time (10 min), the test substances (crude extract, individual components, mixture
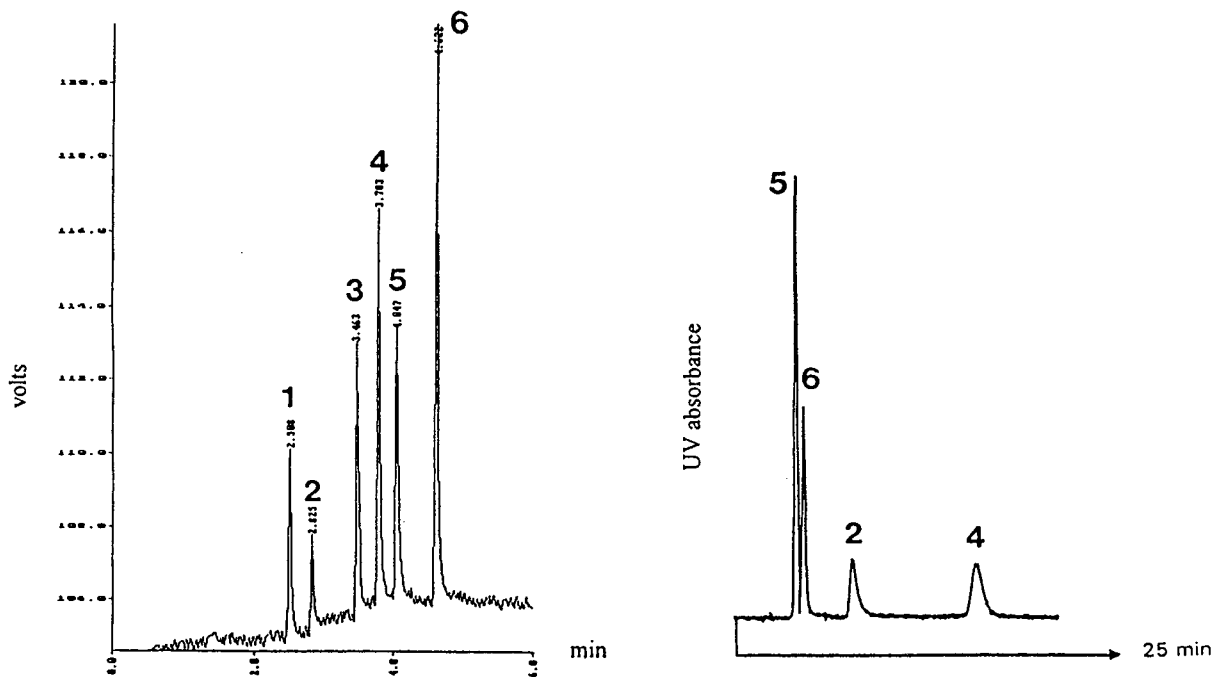
Fig. 3. Separation of a standard mixture with both techniques. Peaks: 1 = methanol, 2 = luteolin-7-glucoside, 3 = luteolin, 4 = rosmarinic acid, 5 = protocatechualdehyde, 6 = caffeic acid. (Left) CE analysis. Injection, 20 s hydrodynamic; for conditions see Fig. 2. (Right) HPLC analysis. For conditions see Fig. 2.

Table 3
Efficiency for both techniques

Substance	N (CE)	N (HPLC)
Luteolin-7-glucoside	$3.0 \cdot 10^3$	$1.3 \cdot 10^2$
Luteolin	$1.6 \cdot 10^2$	n.d.
Caffeic acid	$2.3 \cdot 10^4$	$8.7 \cdot 10^1$
Rosmarinic acid	$2.9 \cdot 10^4$	$2.9 \cdot 10^2$
Protocatechualdehyde	$8.9 \cdot 10^4$	$4.2 \cdot 10^1$

Table 4
Linearity for both techniques

	CE	HPLC
Luteolin-7-glucoside	$y = -0.041x + 0.049$ ($r = 0.9993$)	$y = -0.669x + 0.284$ ($r = 0.9994$)
Caffeic acid	$y = -0.552x + 0.321$ ($r = 0.9998$)	$y = 1.697x + 0.195$ ($r = 0.9985$)
Rosmarinic acid	$y = -0.575x + 0.108$ ($r = 0.9987$)	$y = 0.490x + 0.103$ ($r = 0.9993$)

Table 5
Limit of detection

Substance	Concentration detection limit (mol l^{-1})	
	CE	HPLC
Luteolin-7-glucoside	$5.6 \cdot 10^{-5}$	$2.2 \cdot 10^{-5}$
Caffeic acid	$5.5 \cdot 10^{-5}$	$5.5 \cdot 10^{-6}$
Rosmarinic acid	$2.8 \cdot 10^{-5}$	$2.8 \cdot 10^{-5}$

Table 6
Standard deviation of peak areas obtained by CE and HPLC

	CE	HPLC
Luteolin-7-glucoside	5.6%	3.9%
Caffeic acid	8.1%	4.1%
Rosmarinic acid	9.8%	4.0%

of the components) were added between 10 and 40 min to the flowing medium over a period of 30 min. The perfusion medium during liver perfusion was collected in 10 min intervals (= fractions F1–F11). For determining metabolism rates the difference between the concentration before (VL, measured once at 30 min) and after liver passage (sum of fractions) was calculated (see Experimental).

Standard mixtures and individual components were administered at the same concentration as in the crude extract. Using the analytical procedure developed above, first results ($n = 3$) were obtained with the three main components.

The results of liver perfusion of the three main components from the crude extract are shown in Fig. 4. Concentrations of the components in the different fractions were measured with both CE and HPLC, after purification of the samples by
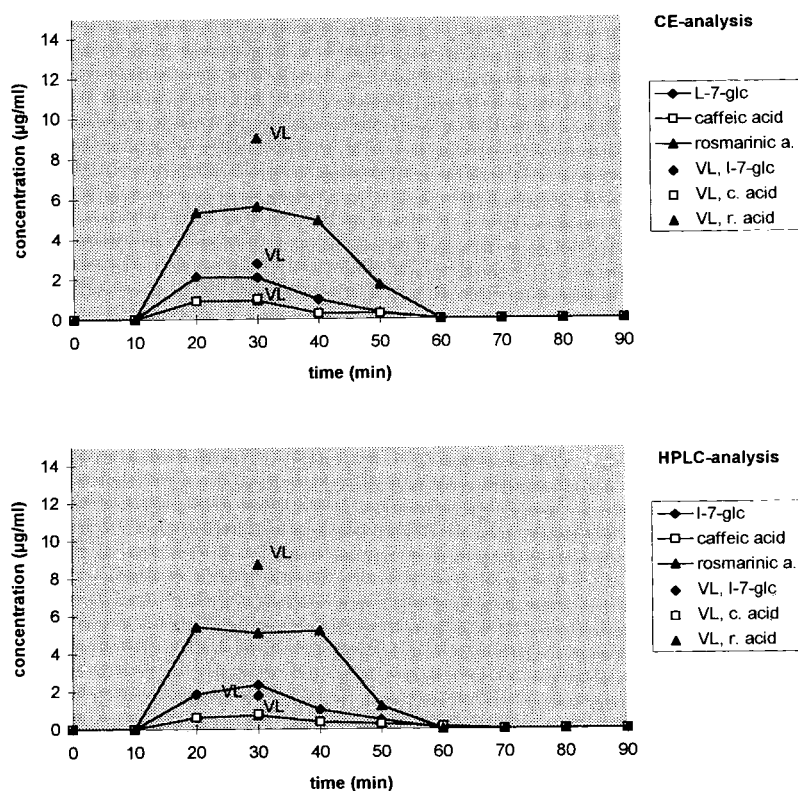
Fig. 4. Concentration of three components of the crude extract in perfusion medium before (VL) and after liver passage as determined by CE analysis (top) and HPLC analysis (bottom); addition of $2.2 \cdot 10^{-3}$ mol l^{-1} of luteolin-7-glucoside (l-7-glc), $2.78 \cdot 10^{-3}$ mol l^{-1} rosmarinic acid (r. acid) and $5.5 \cdot 10^{-4}$ mol l^{-1} caffeic acid (c. acid) per min over 30 min.

SPE. When the three substances are applied in a mixture, similar curves can be obtained; but the decline in concentration of luteolin-7-glucoside is more pronounced now (see Fig. 5).

After application of each of the three components individually the curves presented in Figs. 6a–c were observed. Each figure shows the analysis with both separation techniques.

Differences in the degree of metabolization between the applied preparations are clearly visible. Metabolic rates calculated from Figs. 4–6 are shown in Fig. 7 for CE and in Fig. 8 for HPLC. The results obtained by both methods are in principle comparable. Rosmarinic acid shows a larger deviation as this is the most sensitive compound against oxidative influences. Interestingly, the metabolic rates differ between

the different forms of preparation. Although luteolin-7-glucoside is preferentially metabolized, the rate of its metabolism differs greatly, from 30–35% when administered in the crude extract, over 55–60% when applied as an individual compound, to 65–70% when given in the standard mixture of the three pure compounds. Caffeic acid is clearly better metabolized when given alone; rosmarinic acid, on the other hand, seems to be better metabolized from the crude extract or from the standard mixture. Although these data are preliminary, they indicate that metabolic rates of individual compounds are influenced by accompanying substances; this points to interactions in the metabolism of secondary constituents when applied in crude plant extracts versus application as a pure
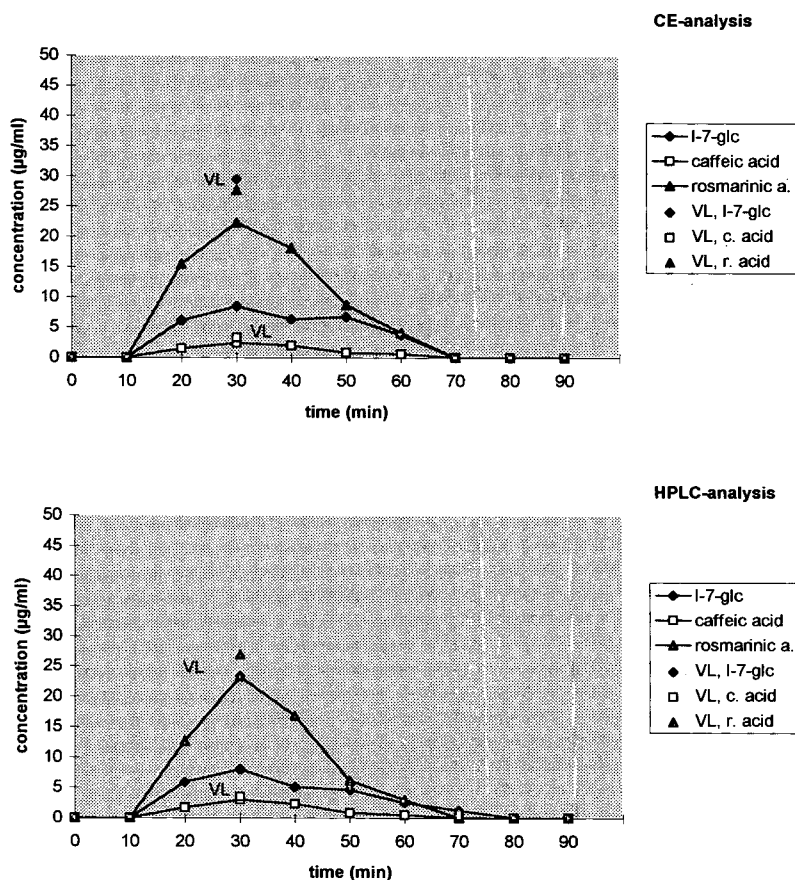
Fig. 5. Concentration of three components applied as a mixture before and after liver passage. Concentrations are the same as in the crude extract (Fig. 4). (top) CE analysis, (bottom) HPLC analysis.
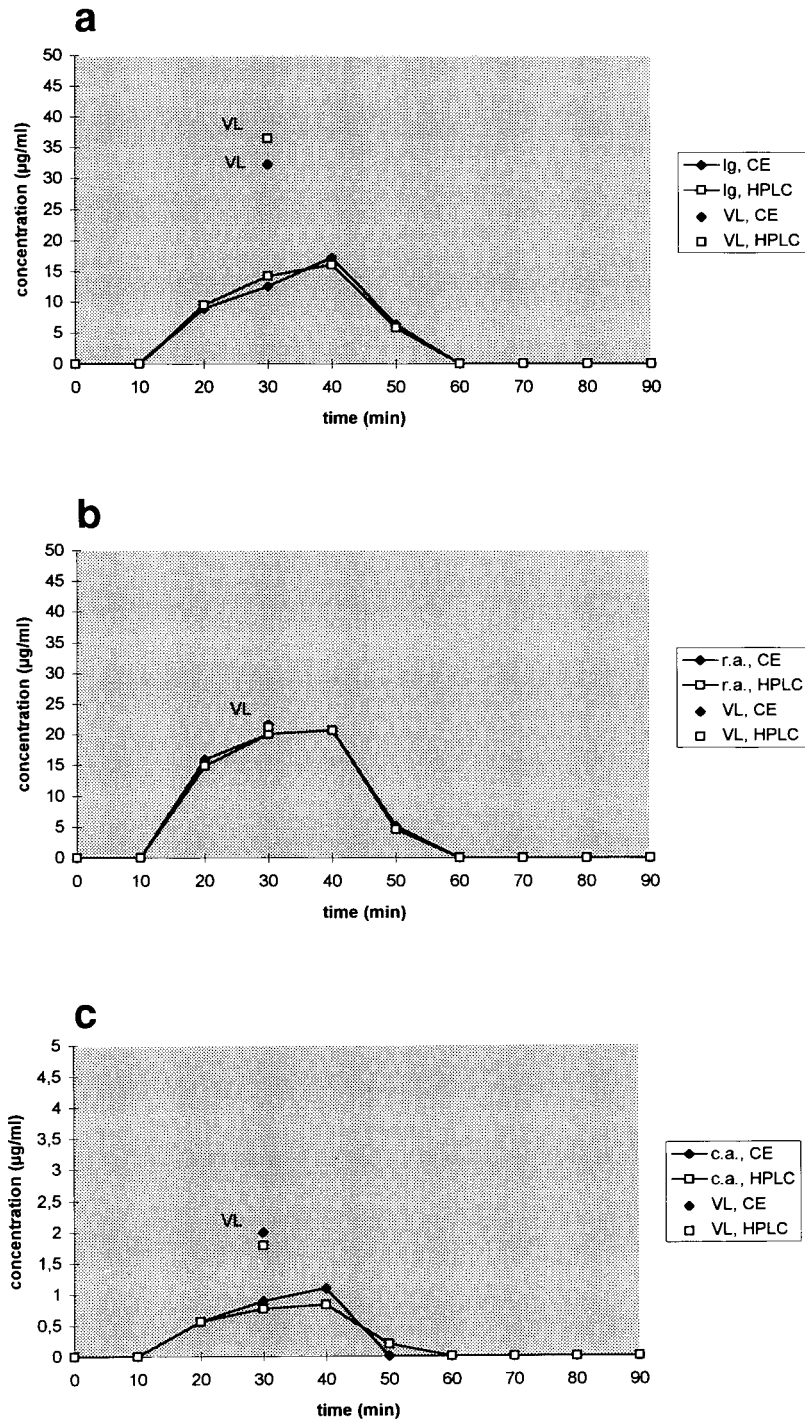
Fig. 6. Concentrations of the components before and after liver passage after individual application of $2.2 \cdot 10^{-3}$ mol l^{-1} luteolin-7-glucoside (a), $2.78 \cdot 10^{-3}$ mol l^{-1} rosmarinic acid (b) and $5.5 \cdot 10^{-4}$ mol l^{-1} caffeic acid (c) per min over 30 min.
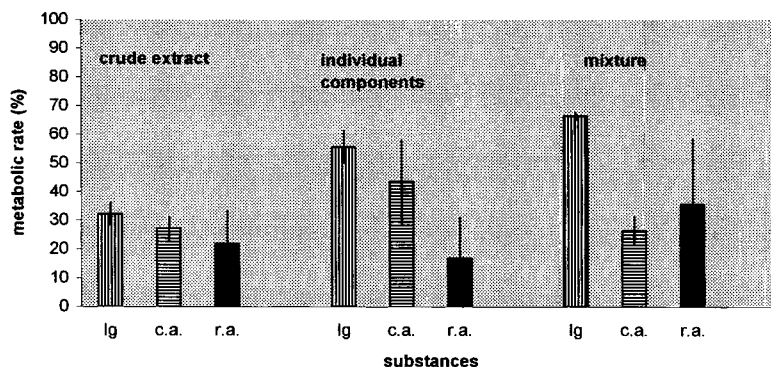
Fig. 7. Comparison of metabolic rates (determination by CE; $n = 3$).
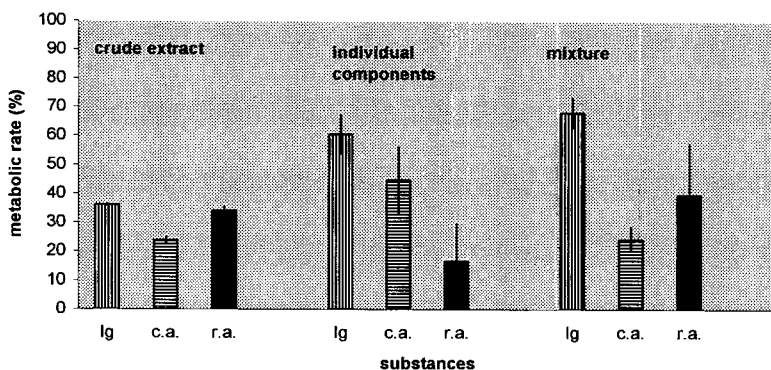
Fig. 8. Comparison of metabolic rates (determination by HPLC; $n = 3$).

compound. These data, of course, need further substantiation.

In conclusion, CE determination of the compounds in question exceeds HPLC in that it is quicker, less expensive and provides a better resolution. Crude plant extracts as well as crude liver perfusates can be well separated after a short purification. CE is a usable tool to elucidate the metabolism of secondary plant constituents.

References

[1] H. Winterhoff, H.G. Gumbinger and H. Sourgens, Planta Med., 54 (1988) 101–106.

[3] H. Winterhoff, H.G. Gumbinger, U. Vahlensieck, F.H. Kemper, H. Schmitz and B. Behnke, Arzneim. Forsch./ Drug Res., 44 (1994) 41–45.

[4] F.H. Kemper, H. Winterhoff, H. Sourgens and K.D. Niehaus, Planta Med., 33 (1978) 311.

[5] G. Madaus, Fr.E. Koch and G. Albus, Z. Gesamte Exp. Med., 109 (1941) 411–424.

[6] B. Wylde, A. Sosa, F. Winternitz, H. Winterhoff and F.H. Kemper, Planta Med., 39 (1980) III-62.

[7] H.G. Gumbinger and H. Winterhoff, Z. Phytother., 8 (1987) 172–174.

[8] H.G. Gumbinger, U. Vahlensieck and H. Winterhoff, Planta Med., 59 (1993) 485–578.

[9] D. Strack and H.G. Gumbinger, Personal communication.

[10] C. Egen-Schwind, R. Eckard and F.H. Kemper, Planta Med., 58 (1992) 301–388.

[11] T. Sugano, K. Suda, N. Shimada and N. Oshino, J. Biochem., 83 (1978) 995–1007.

[12] H. Wojciechowski, unpublished results.

ELSEVIER

Application of β-cyclodextrin for the analysis of the main alkaloids from *Chelidonium majus* by capillary electrophoresis

Hermann Stuppner*, Markus Ganzera

Institute of Pharmacognosy, University of Innsbruck, A-6020 Innsbruck, Austria

Abstract

Capillary zone electrophoresis (CZE) with multi-wavelength detection was used for the separation of the main alkaloids from *Chelidonium majus*. Optimum separation was achieved with a fused-silica capillary tube (70 cm × 50 μm I.D.) and a running electrolyte at pH 5.5 prepared from 40 mM citric acid and 80 mM Na_2HPO_4 solutions. Addition of β-cyclodextrin (12.5 mmol/l) to the buffer system was found to be essential for the separation. The applied voltage was 25 kV and the capillary temperature was kept constant at 25°C.

1. Introduction

Chelidonium majus L. (Papaveraceae) is a herbaceous perennial plant indigenous to Europe and Asia. The aerial parts are ingredients of many herbal preparations used mainly for the treatment of gall, stomach and intestinal ailments [1]. The main constituents of *C. majus* have been shown to be berberine, chelidonine, coptisine, homochelidonine, protopine and stylopine, along with minor constituents such as allocryptopine, chelerythrine and sanguinarine [1] (Fig. 1). Some of these alkaloids exhibit interesting pharmacological and biological activities [1]. So far, analyses for these compounds have been accomplished using TLC and HPLC [2–5]. In this study, a capillary zone electrophoresis (CZE) method for the rapid separation and determination of the main alkaloids in *C. majus* extracts was developed. The influence of pH, the ionic strength of the buffer, the applied

voltage, temperature and the cyclodextrin concentration on the separation is discussed.

2. Experimental

2.1. Materials

Methanol, Na_2HPO_4 and citric acid were purchased from Merck (Darmstadt, Germany), β-cyclodextrin from Serva (Heidelberg, Germany), berberine, protopine, chelidonine and sanguinarine from Sigma (Deisenhofen, Germany) and allocryptopine from Professor J. Slavik (Brno, Czech Republic). Stylopine and coptisine were isolated from plant material. Plant material of *C. majus* (aerial parts) was purchased from Leopold Bichler (Innsbruck, Austria); commercial preparation A, Choleodoron drops, from Weleda (Vienna, Austria); and commercial preparation B, Cholagogum-N Nattermann drops, from Nattermann (Cologne, Germany). Voucher specimens have been de-

* Corresponding author.
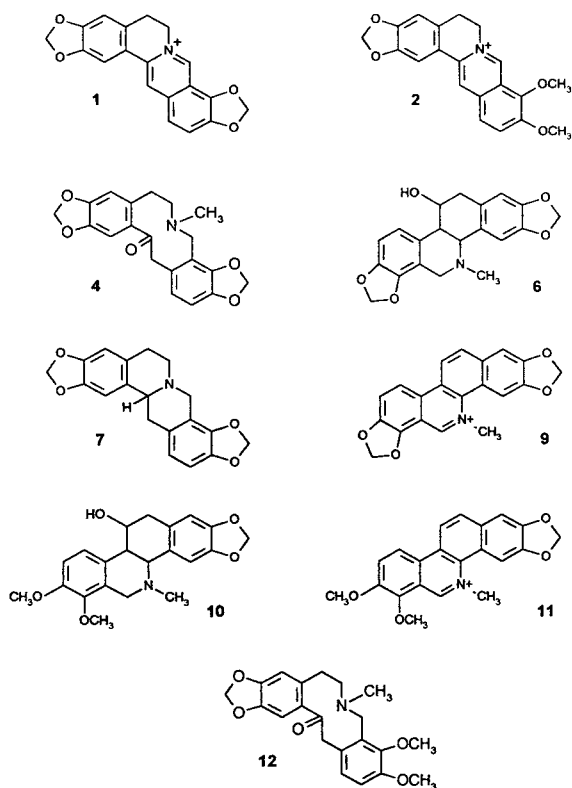
Fig. 1. Structures of coptisine (1), berberine (2), protopine (4), chelidonine (6), stylopine (7), sanguinarine (9), homo-chelidonine (10), chelerythrine (11) and allocryptopine (12).

posited at the Institute of Pharmacognosy, University of Innsbruck (Austria).

2.2. Sample preparation

Powdered aerial parts (5.307 g) of *C. majus* were extracted with a Soxhlet apparatus using methanol as solvent. For qualitative and quantitative analyses, the extract obtained was evaporated to dryness (1.500 g) and the residue was dissolved in 50 ml of methanol. For qualitative analyses prior to injection, the methanolic solution was purified through a BondElut C_{18} cartridge using methanol as solvent. A 5-ml volume of the commercial products A and B were evaporated to dryness, the residues were dissolved in 1 ml of H_2SO_4 (2%), the solutions were extracted with 1 ml of dichloromethane

(four times) and the aqueous phase again evaporated to dryness. The residue (41.2 mg) of preparation A was dissolved in 1 ml of methanol and that of preparation B in 4 ml of methanol, the solutions were filtered and evaporated to dryness (10.7 mg residue) and the residue was dissolved in 1.00 ml of methanol.

2.3. Calibration

Calibration graphs were obtained from standard solutions containing the alkaloids berberine (2), protopine (4) and chelidonine (6) at concentrations between 0.0375 and 1.500 mg/ml (solvent, methanol).

2.4. Analytical method

The experiments were performed with a Spectra Phoresis 1000 system (Thermo Separation Products, Fremont, CA, USA) equipped with a high-speed scanning UV–Vis detector, an automatic injector, a temperature-controlled column cartridge with a fused-silica capillary (70 cm × 50
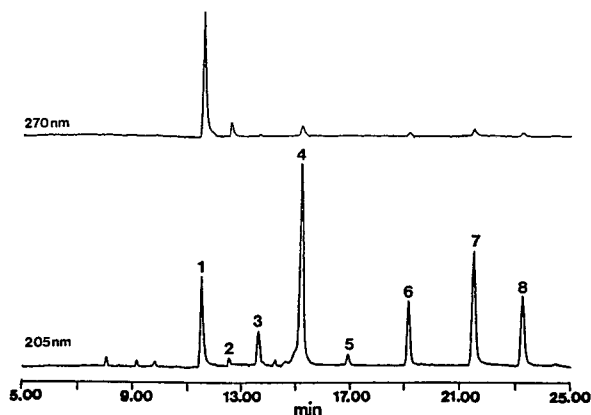
Fig. 2. Electropherograms of a methanolic extract of the aerial parts of *C. majus*. Peaks represent coptisine (1), berberine (2), protopine (4), chelidonine (6) and stylopine (7). Running electrolyte, citric acid–Na_2HPO_4 buffer prepared from 40 m*M* citric acid and 80 m*M* Na_2HPO_4 solutions (pH 5.5) and β-cyclodextrin (12.5 mmol/l); column, fused silica (70 cm × 50 μm I.D.), injection, vacuum mode, 2 s; voltage, 25 kV; detection, UV at 205 and 270 nm; temperature, 25°C.
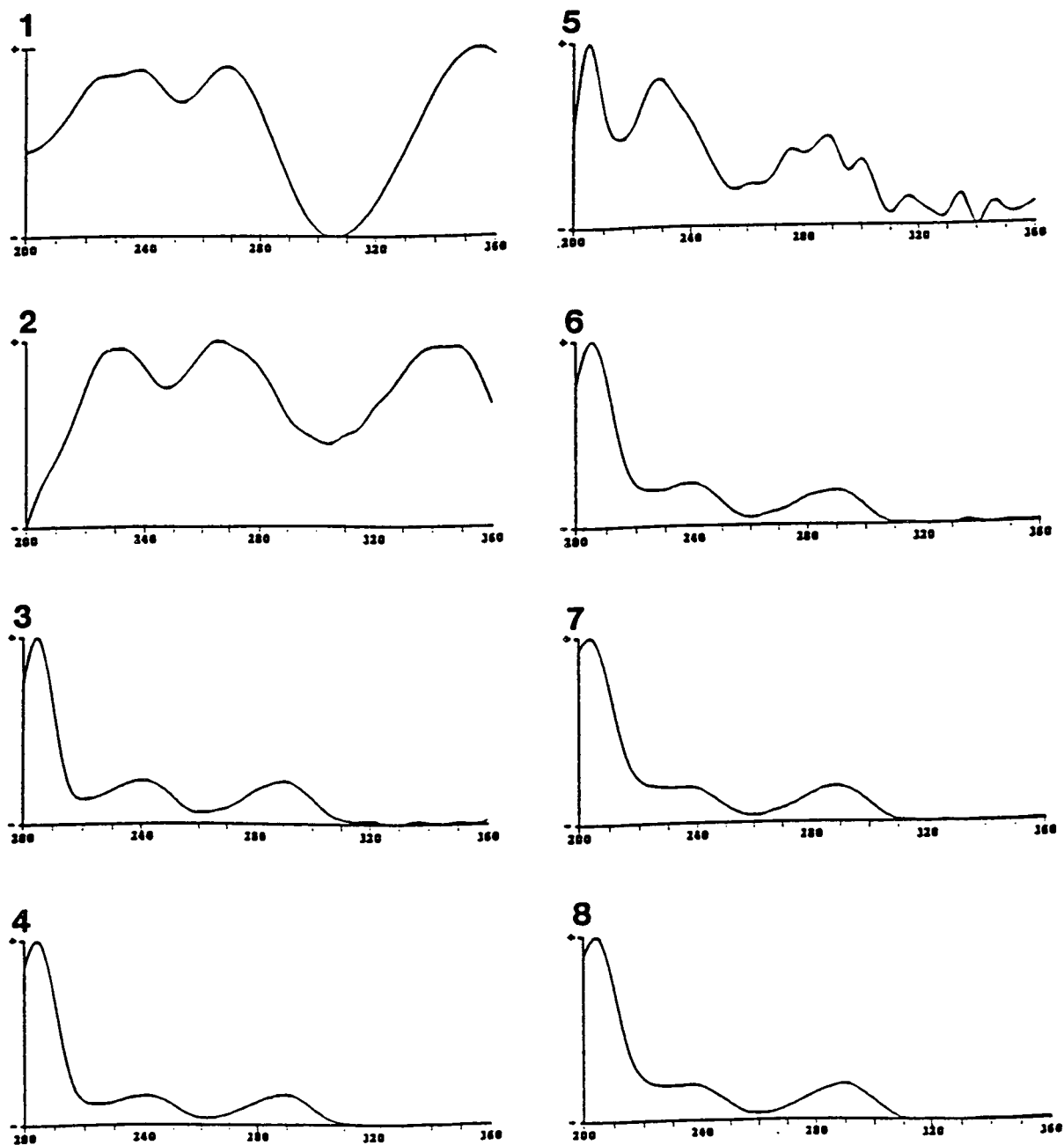
Fig. 3. UV spectra of the alkaloids **1–8** recorded on-line by the high-speed scanning detector.

μm I.D.), an autosampler and a printer. The detection wavelengths were 205 and 270 nm. All experiments were carried out at 25°C at a con-

stant voltage of 25 kV. Temperatures between 10 and 40°C were used to study the effect of temperature on the resolution. When studying

the effect of the electric field on the resolution, voltages between 15 and 30 kV were used. Injections were made using the vacuum mode for 2 s each. The electrolyte solutions (3.9–124.2 mmol/l) were prepared from aqueous solutions of citric acid (40 mmol/l) and Na_2HPO_4 (80 mmol/l). The pH of each buffer solution was checked with a pH meter. The effect of β-cyclodextrin on the resolution of adjacent alkaloids was studied by adding 0–15 mmol/l to the running electrolyte. All sample and buffer solutions were filtered through 0.45-μm filters (Sartorius, Göttingen, Germany). Between runs, the capillary was washed with 0.1 M NaOH for 3 min, followed by equilibration with running buffer (3 min).

3. Results and discussion

Electropherograms of a methanolic extract of the aerial parts of C. majus are shown in Fig. 2. Peaks 1, 2, 4, 6 and 7 were identified as coptisine, berberine, protopine, chelidonine and stylopine, respectively, following comparison of the migration times and UV absorption spectra (Fig. 3) with those of authentic standards. Peaks 3, 5 and 8 could not be identified. However, all compounds on TLC gave a positive reaction with Dragendorff reagent, indicating the presence of alkaloids [6]. Chelerythrine and sanguinarine were present only in trace amounts and therefore not detectable in the electropherograms of the extracts. Baseline separation of these compounds could be achieved by using a fused-silica capillary tube with a citric acid–phosphate buffer (pH 5.5, prepared from 40 mM citric acid and 80 mM Na_2HPO_4 solutions) as running electrolyte containing β-cyclodextrin (12.5 mmol/l). The applied voltage was 25 kV and the capillary was thermostated at 25°C. UV detection was performed at 205 and 270 nm.

Allocryptopine, a minor Chelidonium alkaloid, co-eluted with protopine. In the chosen electrolyte system the alkaloids are positively charged and migrate to the cathode. Optimi-

zation of the parameters was carried out by investigating the influence of electrolyte composition, pH, electric field, ionic strength, temperature and β-cyclodextrin concentration on the separation efficiency.

The parameter with the greatest influence on the separation of the C. majus alkaloids 1–8 was found to be the β-cyclodextrin concentration in the electrophoretic buffer system (Fig. 4). Without β-cyclodextrin, three of seven alkaloid pairs remained unseparated. Excellent resolution of adjacent alkaloid pairs ($R_s > 4$) was obtained by adding 12.5 mmol/l of β-cyclodextrin to the buffer system. Above this concentration β-cyclodextrin was no longer soluble in the electrolyte buffer. Below a cyclodextrin concentration of 7.5 mmol/l, alkaloids 5 and 6 change their order of elution. Enhancement of the selectivity by the use of cyclodextrins is usually
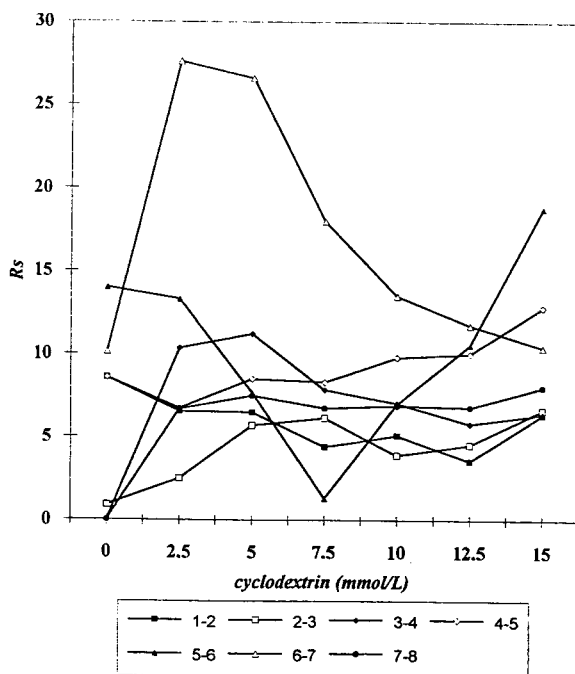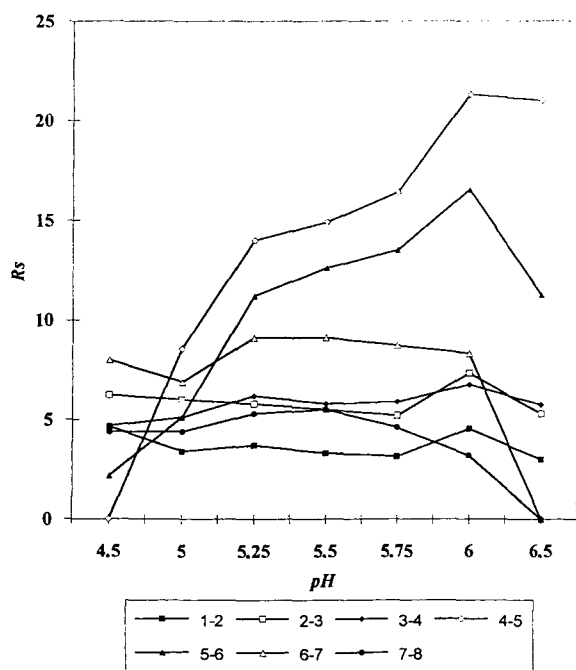

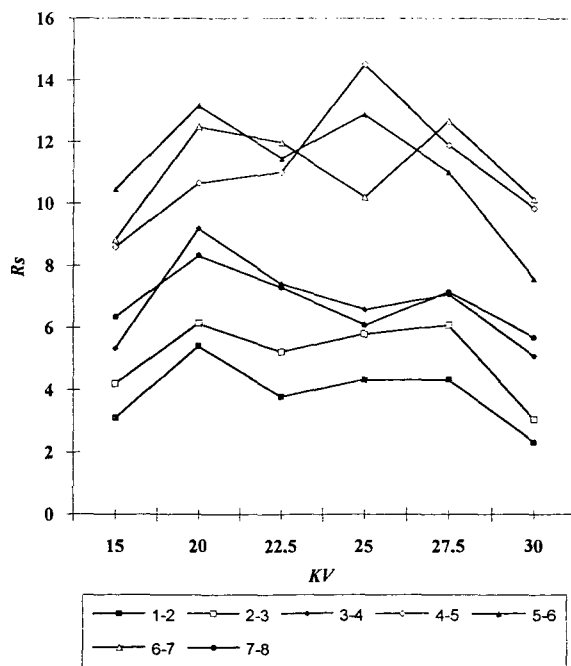Fig. 4. Effect of β-cyclodextrin (0–15 mmol/l) on resolution (R_s) of the alkaloid pairs 1–2, 2–3, 3–4, 4–5, 5–6, 6–7 and 7–8. Other conditions as in Fig. 2.
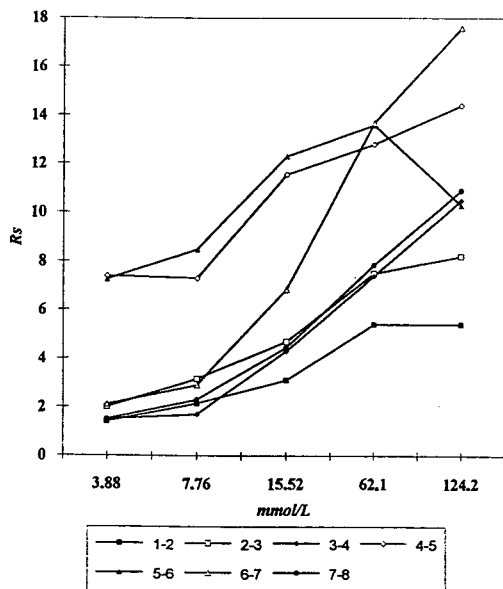
attributable to their ability to include selectively a wide variety of guest molecules in their hydrophobic cavity [7]. It can be assumed that differences in the stability of the inclusion complexes for structurally related solutes provide the mechanism to improve the separation of the *C. majus* alkaloids.

The pH of the electrolyte is known to have a strong influence on the mobilities of alkaloids, depending on the pK_a values of these weak bases [7]. Sufficient ionization of the alkaloids can only be achieved in an acidic medium. Resolutions (R_s) of adjacent alkaloid pairs at five pH values of the citric acid–phosphate buffer in the range 4.5–6.5 are shown in Fig. 5. An acceptable resolution (R_s) for all adjacent pairs of alkaloids was observed at pH 5.5. At pH 4.5 the alkaloid pair **4–5** remained unseparated. The pairs **6–7** and **7–8** were also unseparable at pH 6.5.

Fig. 6. Effect of voltage (15–30 kV) on resolution (R_s) of the alkaloid pairs **1–2**, **2–3**, **3–4**, **4–5**, **5–6**, **6–7** and **7–8**. Other conditions as in Fig. 2.

Fig. 5. Effect of pH (4.5–6.5) on resolution (R_s) of the alkaloid pairs **1–2**, **2–3**, **3–4**, **4–5**, **5–6**, **6–7** and **7–8**. Other conditions as in Fig. 2.

The electric field strength and temperature are of minor importance for obtaining complete separation (Figs. 6 and 7). Within the temperature range 15–30°C and at applied voltages of 15–30 kV the resolution of adjacent alkaloid pairs was without exception higher than 2.

Good resolution of adjacent pairs of alkaloids was obtained with an ionic strength of the running electrolyte of 62.1 mmol/l (Fig. 8). Lowering the citric acid–Na_2HPO_4 buffer (pH 5.5) concentration caused a decrease in resolution of all alkaloid pairs. A higher concentration of the buffer system resulted in a worse separation of the compound pair **5–6**.

Determination of the major alkaloids in the crude methanolic extracts of the aerial parts of *C. majus* and two pharmaceutical preparations (A and B) was performed by using the external standard method. Calibration was carried out
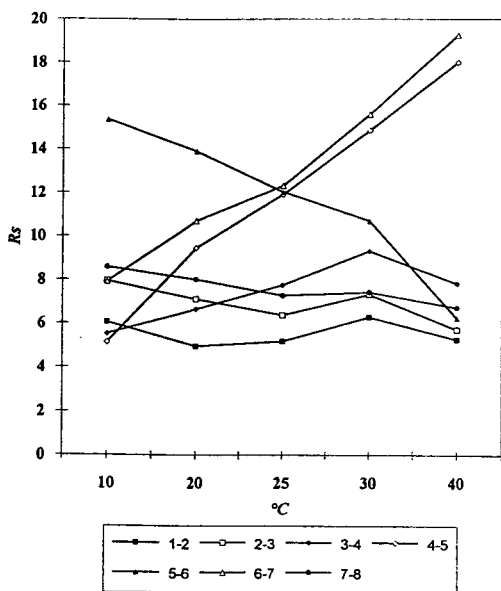
Fig. 7. Effect of capillary thermostating temperature (10–40°C) on resolution (R_s) of the alkaloid pairs **1–2**, **2–3**, **3–4**, **4–5**, **5–6**, **6–7** and **7–8**. Other conditions as in Fig. 2.

Table 1
Regression equations and correlation coefficients for berberine (**2**), protopine (**4**) and chelidonine (**6**)

Compound	Regression equation	r^2
2	$y = 25.73 + 575.46x$	0.997
4	$y = 137.43 + 3356.34x$	0.997
6	$y = 21.82 + 3298.63x$	0.997

with compounds **2**, **4** and **6**. The graphs obtained were linear in the range 37.5–1500 μg/ml (Table 1). The detection limit was approximately 10 μg/ml. Coptisine (**1**) was determined using the calibration graph for berberine (**2**), which according to the literature [4] has a similar response factor. Compounds **3**, **5**, **7** (stylopine) and **8** were determined by using the calibration graph for protopine (**4**). The results are given in Table 2. The relative standard deviations for the quantitative analyses of the methanolic extract (six experiments) and the commercial preparations A and B were between 1.2 and 9.3% for all compounds studied. For analyses of the commercial preparations a clean-up procedure was necessary.

In conclusion, the developed CZE method can be used successfully for the qualitative and quantitative determination of alkaloids from *C. majus*. Further, it can be applied to fingerprint analyses of methanolic extracts of *Berberis vulgaris* L., *Hydrastis canadensis* L. and *Jatheorhiza palmata* (LAM) Miers (Fig. 9), plants which have a similar alkaloid pattern to *C. majus*. Further investigations are in progress concerning peak identification and optimization of the CZE separation of the major alkaloids of these plants.

Fig. 8. Effect of buffer concentration on resolution (R_s) of the alkaloid pairs **1–2**, **2–3**, **3–4**, **4–5**, **5–6**, **6–7** and **7–8**. Ionic strength: citric acid–Na_2HPO_4 buffer, 3.9–124.2 mmol/l. Other conditions as in Fig. 2.

Acknowledgement

Table 2
Determination of alkaloids **1–8**

Compound	Concentration (g per 100 g)		
	Sample 1	Sample 2	Sample 3
1	0.717 (2.52)	0.046 (3.52)	0.048 (2.50)
2	0.075 (9.27)	–	–
3	0.039 (7.74)	0.019 (11.9)	0.048 (2.50)
4	0.219 (3.77)	0.047 (3.95)	0.176 (4.91)
5	–	–	–
6	0.049 (2.24)	0.063 (4.54)	0.501 (1.19)
7	0.092 (4.23)	–	–
8	0.045 (3.30)	–	–
Total	1.24	0.18	0.73

Data are means of six replicates; relative standard deviations (%) are given in parentheses. Sample 1, methanolic extract of the aerial parts of *C. majus*; samples 2 and 3, phytopharmaceutical preparations A and B, respectively.
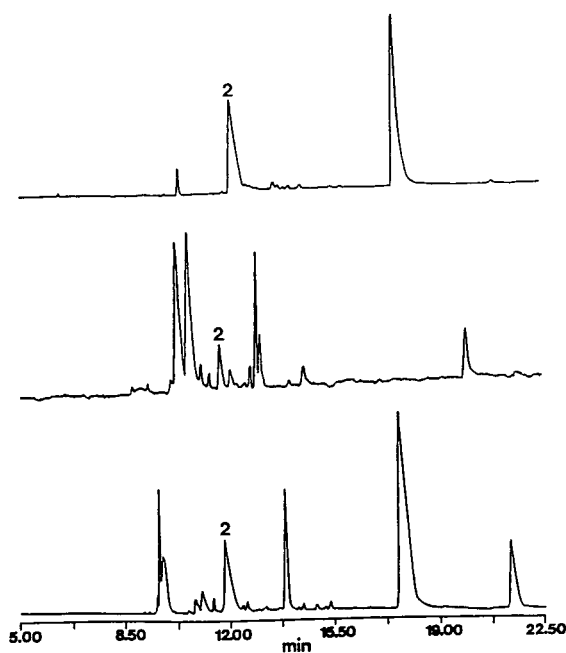
Fig. 9. Electropherograms of methanolic extracts of the aerial parts of (top) *Hydrastis canadensis*, (middle) *Jatheorhiza palmata* and (bottom) *Berberis vulgaris*. UV detection at 205 nm; other conditions as in Fig. 2. Peak 2 = berberine.

References

[1] K. Hoffmann-Bohm, E. Stahl-Biskup and P. Gorecki, in R. Hänsel, K. Keller, H. Rimpler and G. Schneider (Editors), Hagers Handbuch der Pharmazeutischen Praxis, Vol. 4, Springer, Berlin, 5th ed., 1992, p. 835.
[2] W.E. Freytag and W. Stapf, Planta Med., 40 (1980) 278.
[3] W.E. Freytag and W. Stapf, Dtsch. Apoth.-Ztg., 21 (1986) 1113.
[4] W.E. Freytag and W. Stapf, Pharm. Ztg., 138 (1993) 126.
[5] G. Fulde and M. Wichtl, Dtsch. Apoth.-Ztg., 134 (1994) 17.
[6] H. Wagner, S. Bladt and E.M. Zgainski, Drogenanalyse, Springer, Berlin, 1983, p. 57.
[7] S.F.Y. Li, Capillary Electrophoresis, Elsevier, London, 1992, pp. 202 and 259.

Concentration and separation of hypoglycemic drugs using solid-phase extraction–capillary electrophoresis

M.A. Strausbauch[a], S.J. Xu[b], J.E. Ferguson[b], M.E. Nunez[b], D. Machacek[b], G.M. Lawson[b], Peter J. Wettstein[a], James P. Landers[b],*

[a]*Departments of Surgery and Immunology, Mayo Clinic/Mayo Foundation, Rochester, MN 55905, USA*
[b]*Clinical Capillary Electrophoresis Facility, Department of Laboratory Medicine and Pathology, Mayo Clinic/Mayo Foundation, Rochester, MN 55905, USA*

Abstract

Solid-phase extraction–capillary electrophoresis (SPE–CE) is a technique whereby very dilute analytes may be selectively extracted from a sample matrix and concentrated on-line for analysis. This study describes the first phase in the development of a method exploiting this technique for the direct analysis of hypoglycemic drugs in urine. Effective separation and detection of six sulfonylurea drug standards at concentrations below the detection limit of conventional capillary electrophoretic techniques is shown to be attainable. Since surfactant interfered with the on-line concentration process, non-MEKC (micellar electrokinetic chromatography) separation conditions were defined. Using 250 mM borate/5 mM phosphate at pH 8.4, all drugs in a mixture at 285 ng/ml were effectively extracted, concentrated from an injected volume of 2.5 μl, non-selectively desorbed with an organic-based elution buffer and electrophoretically resolved. Sample loading was found to be linear in the 0.12–1.9 μl range and drugs in a volume of up to 190 μl could be concentrated and detected with a sensitivity of $\approx$5 ng/ml. Not only was resolution of the desorbed material uncompromised by the presence of the SPE-tip, but separation of glipizide and glyburide was observed despite the fact that these drugs were unresolved under the same separation conditions by standard capillary zone electrophoresis (CZE). From these results, it is clear that SPE–CE not only increases the sensitivity for detection but that selectivity may be altered due to chromatographic processes occurring on the solid-phase resin.

1. Introduction

Capillary electrophoresis (CE) has been shown to be useful for a diverse array of molecules including ions [1], sugars [2,3], peptides [4,5], oligonucleotides [6] and proteins [7,8]. Of particular relevance to the present study, the free solution capillary zero electrophoresis (CZE) and micellar electrokinetic chromatography (MEKC) modes have proven to be extremely useful for the analysis of a variety of drugs [9–15]. This has revealed the potential for CE in the clinical laboratory [16] and, in particular, for the analysis of drugs in body fluids [17].

Sulfonylurea drugs such as glipizide (Gp), glyburide (Gb), chlorpropamide (Cp), acetohexamide (Ah), tolbutamide (Tb) and tolazamide (Ta) have been utilized extensively for the treatment of hyperglycemia. "Factitious" or "drug-

---

* Corresponding author.

induced" hypoglycemia has been reported as a result of the surreptitious use of sulfonylurea drugs. Problems associated with their surreptitious abuse arise from the differential diagnosis of drug-induced hypoglycemia, which is difficult to distinguish from insulinoma (pancreatic tumor)-induced hypoglycemia [18] and has actually led to unnecessary exploratory surgery and even partial removal of the pancreas (subtotal pancreatectomy) [19]. At the present time, there are relatively few effective analytical methodologies for detecting sulfonylurea drugs in biological fluids. Although semi-quantitative HPLC methodology has been described [20] for detecting chlorpropamide in plasma at a concentration of 10 μg/ml, these levels are dramatically higher than the urinary levels expected with sulphonylurea drugs (100–500 ng/ml). GC–MS has proven to be problematic as a result of the non-volatility and difficulty in derivatizing the sulfonylurea drugs, while LC–MS is not commonly used. It is for these reasons that a capillary electrophoretic method for these compounds has been pursued [21]. MEKC was shown to provide rapid analysis for both second and third generation sulfonylurea drugs in less than 8 min. However, the extensive off-line extraction procedure required for partial purification of the urine prior to CE analysis makes it cumbersome and costly. Hence, it was clear that an on-line preconcentration of the drugs from urine would improve the cost-effectiveness of this assay.

On-line sensitivity enhancement with CE is attainable through a number of approaches including stacking [22] and isotachophoresis [23]. However, despite their effectiveness with many analyte systems, these preconcentration methods are often either unsuitable or lack the simplicity of a packed-inlet concentrator method such as that provided with SPE–CE. It is noteworthy that the preconcentration strategy employed with SPE–CE methodology is not novel. Guzman [24], Guzman et al. [25] and Fuchs and Merion [26] have described devices similar in construction and implementation to the SPE concentrator tip. Debets et al. [27] also employed a concentration "micro precolumn" (reversed-phase C_8) which was switched on- and off-line to

a CZE capillary. This device allowed for the extraction and concentration of analytes from extremely large sample volumes, but required a liquid pump for sample loading and off-line switching to perform the CZE separation, all of which added to the complexity of the apparatus. Benson et al. [28] and Schwartz and Merion [14] have demonstrated the usefulness of a solid-phase (C_{18}) packed inlet capillaries for the analysis of drugs. Interestingly, Beattie et al. [29] independently developed a solid-phase concentrator virtually identical in construction and implementation to the SPE–CE concentrator tip described in this study. Beattie's results correlate well with our own observations in that concentrators constructed in this manner are robust, reusable and can reproducibly provide analyte concentration/separation that does not markedly deteriorate with normal use.

The SPE–CE concentrator described in the present study remains on-line and, with a short rinse to regenerate the reversed-phase, can be used for multiple consecutive analyses. Since there is no requirement for exotic instrumentation for detection and interpretation of results [30] or modification of the commercial P/ACE (Beckman Instruments) unit, the SPE–CE experiments can be performed under an automated, programmed sequence and allow for unattended operation and a high degree of reproducibility. These characteristics are perfectly suited to application of this technology for clinical method development.

In this study, we describe the results of the first phase of this study for implementing solid-phase extraction–capillary electrophoresis (SPE–CE) for the on-line analysis of sulfonylurea drugs. The ultimate goal of this approach, phase two, is to identify hypoglycemic drugs directly in urine without the requirement for a labor-intensive off-line solid-phase extraction procedure. This is difficult due to the micro-scalar nature of the concentrator but will most likely be achieved by exploiting the fine instrumental control capabilities of modern CE instrumentation for sample clean-up and selective elution. The results of the phase-one studies show the potential of SPE–CE for the analysis of hypoglycemic drugs at dilute

concentrations (ng/ml) below the detection limit of standard CZE. The performance of the SPE-tip is evaluated in terms of the loading capacity, sensitivity and linearity for concentrating and electrophoresing these particular drugs at low concentrations.

2. Experimental

2.1. Materials

Acetonitrile (ACN; HPLC-UV spectral grade) and hydrochloric acid (HCl) were purchased from Fisher Scientific (Pittsburgh, PA, USA). Phosphate buffer (50 mM, pH 2.5) was purchased from Scientific Resources (Eatontown, NJ, USA). C_{18} material was removed from a SPE™ column purchased from JT Baker (Phillipsburg, NJ, USA). Glass fiber was removed from the bed support of a common disposable "spin column". Polyethylene tubing, IntraMedic #7405, was purchased from Clay Adams (Parsippany, NJ, USA). Poros resin (R20), was provided courtesy of PerSeptive Biosystems (Framingham, MA, USA).

2.2. CE instrumentation

HPCE separation was carried out on a Beckman P/ACE System 5510 equipped with a monochromatic UV detector. An IBM 486 Value-Point computer utilizing System Gold software (V.8.1) was used for instrument control and data collection. All peak information (migration time and integrated peak areas) was obtained through the System Gold software.

2.3. SPE–CE capillary construction

The SPE capillary is a hybrid design consisting of two parts, a replaceable concentrator tip and a separation capillary. The concentrator tip for this study contains a 50–200 nl bed of reversed-phased (C_{18}) material that is dry-packed into a polyethylene sleeve between two frits (glass fibers, gently tamped into place) so that two short sections of capillary can be slid into the sleeve to retain the entire assembly and provide a tight seal without adhesives. The device is relatively resistant to blockage by the use of solid phase of a large sized mesh and the glass fiber frits forming the bed supports. The high flow-rate and minimal restriction allow the assembly to remain on-line with the separation capillary throughout the analysis and may remain on-line for multiple analysis if desired. Breakage of the tip or capillary joint and exposure to incompatible buffers are the most common events requiring assembly of a new unit. The complete assembly of the SPE–CE concentrator tip is usually accomplished in minutes with an uncoated separation capillary. The concentrator tip is mated to the inlet of the separation capillary (preinstalled in a P/ACE cartridge) by removing a short section of the inlet leg and replacing it with the SPE–CE concentrator tip. This is accomplished by joining the two sections with a second polyethylene sleeve which should be renewed every time an inlet section is replaced. The capillary tip used for the standard CZE separations is the same section of separation capillary that was originally removed to accommodate the SPE–CE concentrator tip. In this way the same separation capillary can be used both for SPE–CE or standard CZE separations dependent on the type of tip attached to the inlet.

2.4. CZE and SPE–CE separation methods

The capillary was rinsed with three column volumes of elution buffer, and then re-equilibrated with ten column volumes of separation buffer prior to sample injection. The CZE separations as well as sample concentration and release were as described in the figure legends. The CZE and SPE–CE capillaries were rinsed with elution buffer (0.5 min) as a post-separation treatment for regeneration of the solid phase. For SPE–CE analyses, standard drug mixtures were prepared by diluting stock solutions in 100% methanol into water.

2.5. Evaluation of SPE-tip performance

Lifetime

A newly assembled SPE-capillary with a 0.5 mm × 370 μm packed bed of C_{18} reversed-phase and a 47 cm × 75 μm I.D. (40 cm to detector) separation capillary was used to test the performance of the tip for no fewer than 30 consecutive separations. The reversed-phase material was regenerated with a short (0.5 min at $1.38 \cdot 10^5$ Pa) rinse using ACN–separation buffer (80:20) for regeneration of the phase between analysis.

Sample loading capacity

Total sample capacity of the 0.5 mm × 370 μm SPE concentrator was determined by doubling the injection time over a range of 0.5–32.0 min with an applied injection pressure of $3.4 \cdot 10^3$ Pa. The concentration of the Gp and internal standard (I.S.) used for these experiments was 2 μg/ml. Integrated peak areas were obtained using the System Gold software.

Detection sensitivity

A mixture containing glipizide and the internal standard was used as a means of determining the detection sensitivity of SPE–CE using a standard SPE-tip and UV detection at 200 nm. A simple two-component mixture was used for this study and contained Gp and I.S. at 2 μg/ml (0.2 min at $1.38 \cdot 10^5$ Pa; 1.9 μl), 200 ng/ml (2.0 min at $1.38 \cdot 10^5$ Pa; 19 μl) and 20 ng/ml (20 min at $1.38 \cdot 10^5$ Pa; 190 μl).

3. Results and discussion

The sulfonylurea drugs of interest in this study are generally considered to be weak acids with pK_a values in the 5.0–6.4 range [31,32] and, therefore, are expected to behave as non-polar, weakly charged analytes. Since CZE of these analytes was initially unsuccessful, an MEKC method has been developed [21] for their effective CE separation when extracted from urine containing the drugs at concentrations in the 100–500 ng/ml range (Fig. 1A). The goal of the
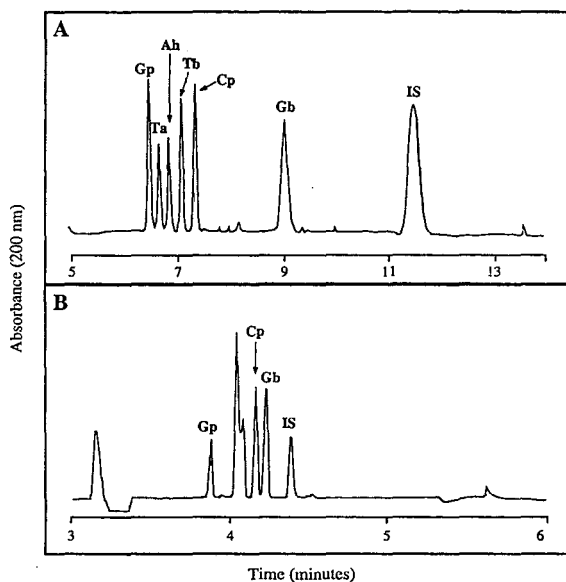
Fig. 1. MEKC separation of six sulfonylurea drugs and the internal standard. Separation was carried out in 5 mM borate–5 mM phosphate containing sodium cholate (25 kV) following a 2 s hydrodynamic injection. (A) Standard drugs (143 μg/ml), 75 mM cholate. (B) Standard drugs (143 μg/ml), 10 mM cholate. Separation was carried out in a 47 cm × 50 μm capillary thermostatted at 24°C at 25 kV.

present study was to extrapolate these separation conditions for use with the SPE–CE system that had been shown to be effective for the direct analysis of ng/ml levels of peptides [33]. It was thought that, with the SPE–CE approach, it may be possible to circumvent part of the labor-intensive off-line extraction procedure currently required for detection with the MEKC-based system. However, it was identified early in the study that the presence of surfactant (75 mM sodium cholate) in the separation buffer, a critical component for effecting the resolution of these drugs, interfered with the solid-phase extraction process. Attempts to identify a lower surfactant concentration that would not interfere with the solid-phase extraction process but still allow for resolution of the mixture components were nonproductive. Fig. 1B shows the ineffective separation that was obtained when the cholate concentration in the buffer was reduced.

Therefore, it was clear that surfactant-free conditions (i.e., non-MEKC) would be required.

Under the initial non-MEKC conditions tested, glipizide and glyburide could not be resolved. Glyburide has been shown to have a pK_a in the range 6.15–6.4 [34] while that for glipizide is 5.94 [35]. This is consistent with the observation that, at higher pH (8.50), Gb and Gp co-migrate slower than the EOF indicating that they are similarly charged and net negative. In theory, Gp and Gb should be separable at a pH between their pK_as where they would be differentially charged. Electrophoresing in 100 mM phosphate buffer varying from pH 6.3 to pH 6.0 showed that Gb and Gp were only separable at a pH of 6.0 (data not shown), at which point Gb co-migrates with the EOF (indicating that it had become uncharged). While these conditions were found to resolve Gb and Gp, the separation was extremely sensitive to slight changes in buffer pH. As a result, extensive electrophoresis (multiple runs in the same separation buffer) led to run-to-run reproducibility problems. Furthermore, having Gb co-migrate with the EOF was of limited use from the perspective of clinical assay development, since it would not be resolved from any of the uncharged (or neutral) compounds present in the sample. As a result, other conditions were sought for separation of Gb and Gp.

Through the testing of a number of buffer systems, it was eventually determined that Gp and Gb could be partially resolved at a pH higher than the pK_a range of these two drugs. Fig. 2A shows that 100 mM phosphate buffer, pH 7.07, containing 20% methanol allowed for the separation of Gp and Gb as well as five of the six other components in the mixture. Both the presence of methanol and the concentration of phosphate used in the buffer were found to be essential for this separation: use of a similar buffer containing 50 mM phosphate led to inadequate resolution. Unfortunately, Ta and I.S. were not resolved under these conditions and this was overcome by slightly altering the pH (in the presence of 20% methanol) (Fig. 2B). The analysis time (20 min) associated with separation of the mixture under these conditions was con-
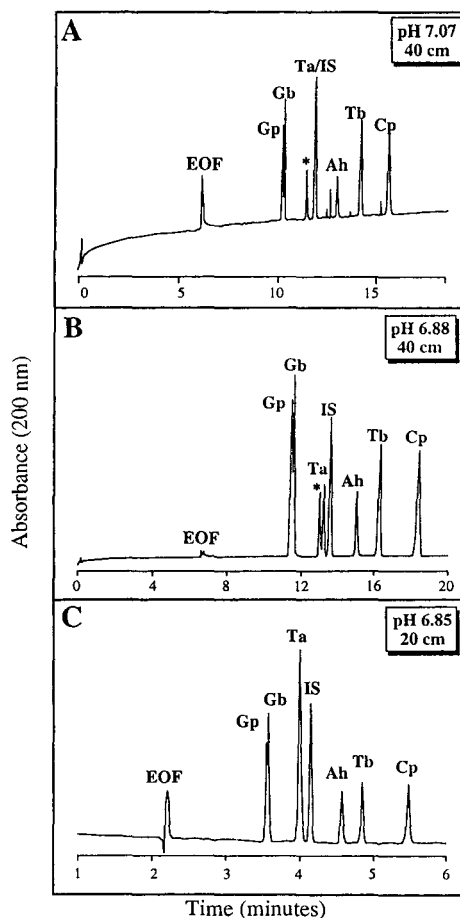
Fig. 2. CZE (non-MEKC) separation of sulfonylurea drugs and the internal standard. Separation was carried out in 100 mM phosphate–20% methanol at the designated pH (15 kV, 184 μA) following a 2 s hydrodynamic injection of the standard mixture (143 μg/ml) into a 47 cm × 50 μm (A and B) or 27 cm (C) capillary thermostatted at 24°C. Asterisk indicates a degradation product of Ah.

sidered to be undesirable. The analysis time was decreased by shortening the effective length of the capillary from 40 cm to 20 cm which allowed for baseline resolution of Ta, I.S., Ah, Tb and Cp, and partial resolution of Gb and Gp (Fig. 2C). The accompanying analysis time of less than 6 min was competitive with that attainable using the MEKC-based analysis [21]. These conditions were considered to be adequate and were used in the initial attempts to implement SPE–CE for

the concentration and separation of these analytes.

Solid-phase extraction–capillary electrophoresis (SPE–CE) was initiated with the construction of a SPE-tip from common laboratory materials as shown in Fig. 3. Initial attempts to extrapolate the non-MEKC conditions defined in Fig. 2 to SPE–CE were found to be only partially successful. Following injection of a mixture containing all seven compounds into the SPE-capillary, only Gb and Gp (which were unresolved) and I.S. appeared to be retained by the SPE-tip and desorbed with an elution buffer injection prior to electrophoresis (Fig. 4). It became clear that, when the SPE-tip and hybrid capillary were rinsed with the separation buffer containing 20% methanol prior to electrophoresis, Cp, Ta, Ah, and Tb were selectively desorbed from the solid phase and, therefore, were not detectable. It also became clear that the separation buffer should have two important characteristics: it should (1) not induce premature desorption of the analytes from the SPE-tip prior to elution buffer injection and (2) provide
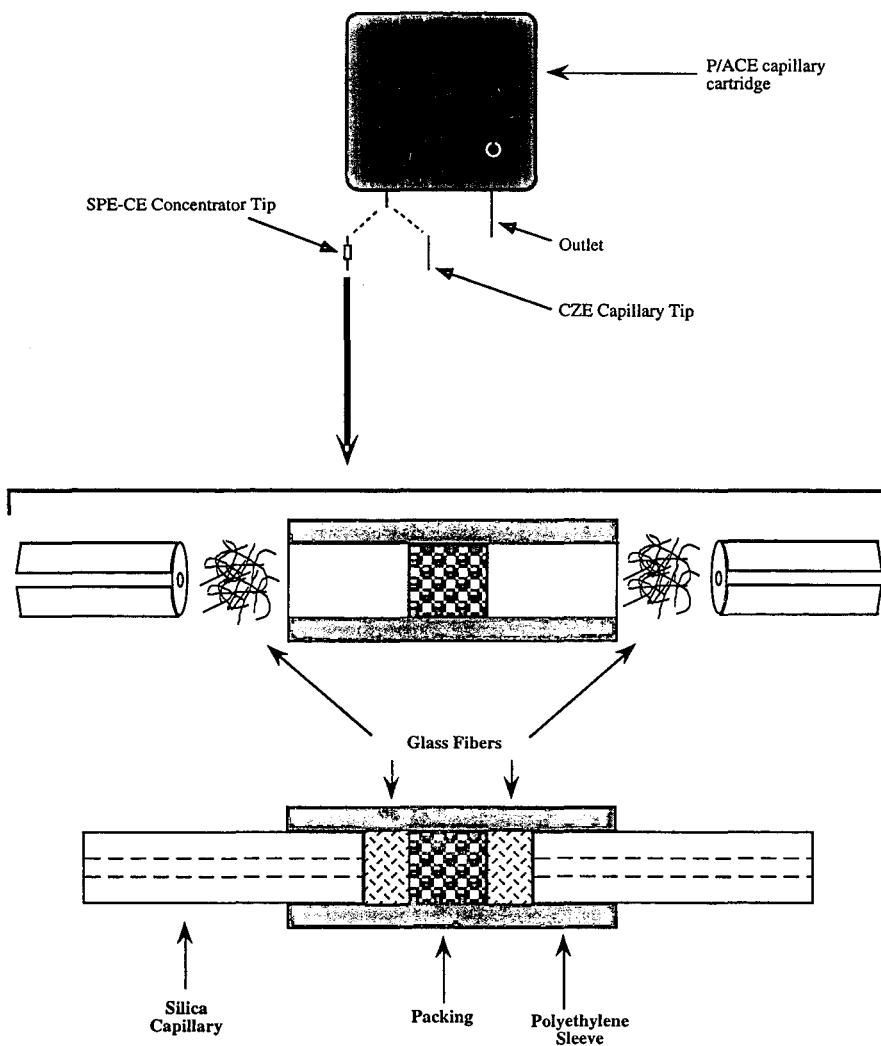
Fig. 3. Diagrammatic representation of the solid-phase extraction tip construction and placement.
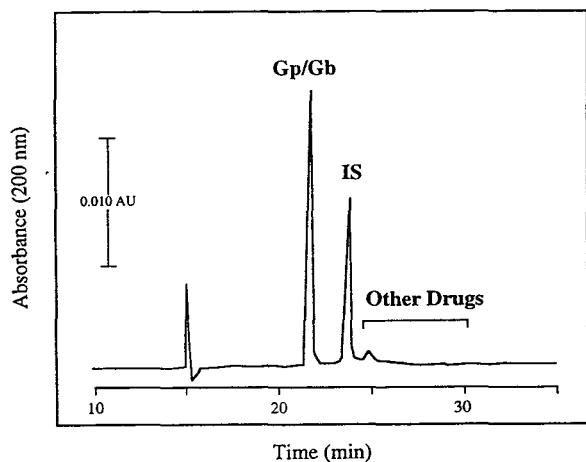
Fig. 4. Concentration and separation of hypoglycemic drugs on an SPE-tip containing a 0.5 mm × 370 μm C_{18} packing. A standard mixture was prepared containing the seven compounds at 143 μg/ml. The solution was loaded onto the SPE-tip by pressure for 0.2 min at $1.38 \cdot 10^5$ Pa. Elution buffer was 20% 50 mM phosphate, pH 2.5–80% ACN and was injected for 0.20 min at $3.45 \cdot 10^3$ Pa followed by a second injection of separation buffer for 0.5 min at $3.45 \cdot 10^5$ Pa. Separation was then carried out at 10 kV in 50 mM phosphate buffer–20% methanol pH 7.1 in a 47 cm × 75 μm capillary maintained at 20°C.

Fig. 5. Standard CZE of the sulfonylurea drugs in 250 mM borate–5 mM phosphate buffer, pH 8.4. A standard drug mixture was prepared by mixing equal volumes of each drug from 1 mg/ml stock solutions in methanol. This solution was diluted in water to the final concentrations shown in the figure. The solution was injected onto the capillary by pressure for 2 s at $3.45 \cdot 10^3$ Pa. Separation was then carried out at 20 kV while the capillary specified in the figure was maintained at 20°C.

adequate separation of the analytes of interest. After testing several buffer systems, an aqueous 250 mM borate–5 mM phosphate buffer, pH 8.4, was chosen despite the fact that Gp and Gb were not resolved. Fig. 5A shows a standard CZE separation of the drug mixture under these conditions in a 37 cm × 50 μm capillary. Since SPE–CE has been found to be more effective in longer capillaries with larger internal diameters [33], analysis of the same sample was carried out in a 67 cm × 75 μm capillary fitted with a CZE-tip (i.e., no SPE-tip) (Fig. 5B). These separations serve as reference for comparison between the CZE and SPE–CE methods and establish the integrity of the separation capillary without the SPE-tip attached. Seven baseline-resolved peaks were evident, with Gb and Gp co-migrating as a single peak and a degradation product of Ah providing the seventh response as indicated by the asterisk in the figures. When the sample was diluted 500-fold in water (final concentration of 285 ng/ml) and a replicate CZE

analysis performed, the electropherogram presented in Fig. 5C was observed. At this dilution, the concentration of the drugs in the sample closely approximated the concentration that would be present in an unconcentrated urine specimen. This highlights the unsuitable nature of standard CZE for the direct analysis of the drugs without some form of off-line concentration. The 67 cm × 75 μm capillary was then fitted with the SPE-concentrator tip and the 500-fold diluted sample introduced into the inlet of the capillary in a large volume ($\approx$2.5 μl by a timed

pressure injection). This represented a sample volume equal to the total inlet-to-detector volume (2.5 μl). The capillary and attached SPE-tip were then rinsed with several capillary volumes of the separation buffer while the drugs remained immobilized on the solid phase. Elution of the drug mixture from the solid phase was accomplished with a timed injection of elution buffer which varied in either composition or volume and electrophoresed (Fig. 6). As the injection time was decreased from 1 min to 0.5 min using 20% separation buffer–80% acetonitrile as elution buffer, the resolution increased markedly (Fig. 6A,B). Generally, the best separations (approaching the performance of standard CZE) were obtained by injecting the minimal volume of elution buffer (0.33 min; 60 nl) required to release the most hydrophobic of the analytes, i.e. Gb, Gp, and I.S. The elution volume was found to be critical to the efficiency of the separation since too little elution buffer resulted in selective retention of some of the analytes on the solid phase and excessive elution volumes precluded electrophoretic resolution of the analytes [36]. Inclusion of a low pH component in the elution buffer dramatically improved the peak shape and response (Fig. 6C). Comparing Fig. 5C to Fig. 6C highlights the power of direct extraction and concentration of the drug mixture on a solid phase resin that is in-line with the separation capillary.

The enhanced separation efficiency associated with the inclusion of a low pH buffer in the elution buffer is interesting. This may be due, in part, to the suppression of turbulence at the interface of the elution and separation buffers, a phenomenon previously reported by Chien and Burgi [37] that is believed to be caused by the mismatch of local EOF velocities in the discontinuous buffer system. In theory, this effect may cause a mixing and laminar backflow at the interface of the buffers and seriously degrade resolution and peak shape. Alternatively, pH stacking may be occurring due to the pH step gradient produced by the low pH elution buffer injection. Further study of this effect and its potential impact on SPE–CE separations is un-
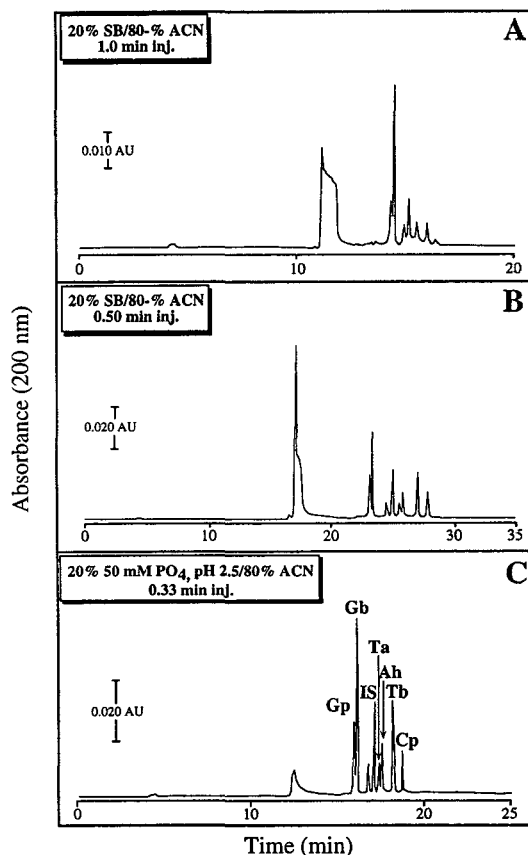
Fig. 6. The effect of elution buffer composition and volume on the desorption of analytes from the SPE tip. Sulfonylurea drugs (285 ng/ml in water) were loaded onto the SPE-tip for 0.2 min at $1.38 \cdot 10^5$ Pa and the packing washed for 1 min with separation buffer (SB; 250 mM borate–5 mM phosphate). The drugs were then desorbed by injection of an elution buffer as indicated in the figure. A $3.45 \cdot 10^3$ Pa injection of separation buffer preceded electrophoresis at 15 kV, 70 μA in a 67 cm × 75 μm capillary at 20°C.

derway. It is important to note that enhanced separation of Gp and Gb was also accomplished without the addition of MeOH to the separation buffer. This may provide evidence that, despite the small bed volume in the SPE-tip (≈50 nl), some chromatography occurs during the desorption of the drugs from the solid phase. These chromatographic effects can have positive effects or negative effects [33] on the separation. In this

particular case, the chromatographic component appears to have been beneficial to the separation.

Reproducibility and SPE-tip lifetime for this particular application was determined using a fresh SPE-capillary containing a 0.5 mm × 370 μm packed bed of C_{18} reversed phase and a 47 cm × 75 μm (40 cm to detector) separation capillary. The flow-rate of the capillary was calculated by injection of an aqueous buffer at the inlet of the capillary (using $1.38 \cdot 10^5$ Pa) and measuring the time required for the buffer to reach the detector. The following was observed in this particular case: time to detector, 0.19 min at $1.38 \cdot 10^5$ Pa; inlet to detector volume, 1.77 μl plus an estimated void volume of ≈ 50 nl in the concentrator tip; calculated flow-rate, 9.56 μl/min. This estimated flow-rate correlated well with the observed rate of sample consumption and was used as a general indicator of the physical integrity of the SPE–CE capillary. The flow-rate of the capillary was found to decrease slightly ($\approx 10\%$ based on rinse buffer inlet to detector times) during the first few separations and then remained stable. These separations were considered to be a "break-in" period for the SPE-tip. To shorten the analysis time, the separation buffer concentration was decreased to 125 mM borate/2.5 mM phosphate, pH 8.4, which still provided adequate resolution for the two-drug mixture. The SPE-tip performed well for a minimum of 30 consecutive analyses with regeneration of the reversed phase being accomplished with a short (0.5 min at $1.38 \cdot 10^5$ Pa) rinse using 80% ACN–20% buffer. At the completion of this set of experiments, the SPE-tip was intentionally-overloaded with sample – 5 min at $1.38 \cdot 10^5$ Pa with 2 μg/ml; total 48 μl or 96 ng – which prematurely destroyed functionality. In other experiments, an SPE-tip was found to easily perform up to 50–100 consecutive analyses under conditions where sample overloading was avoided. Run-to-run migration time was found to be relatively reproducible although minor shifts in the migration time became evident over several consecutive separations. This shift is negligible from run to run but obvious when comparing analyses separated by several runs. This is illustrated in Fig. 7 which shows the sixth and fifteenth separation of the same sample, and the slight shift in migration time associated with consecutive use. The shift is likely the result of the inability to rinse the capillary with 0.1 M NaOH which is avoided to prevent destroying the solid phase.

To determine the sensitivity (detection limit) associated with this particular application of the SPE–CE technology, a simple two-component mixture containing Gp and I.S. was employed to (1) ensure that, at low levels, resolution was
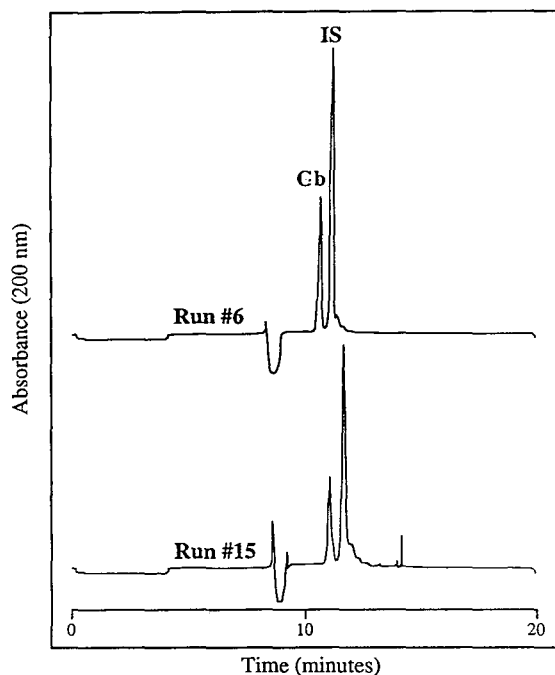
Fig. 7. Reproducibility associated with consecutive use of an SPE tip. Concentration and separation of sulfonylurea drug Gp and I.S. at 2 μg/ml on an SPE capillary containing a 0.5 mm × 370 μm C_{18} packing. Sample buffer solution was loaded onto the SPE tip by low pressure $3.45 \cdot 10^3$ Pa, followed by a separation buffer rinse. The separation buffer was 20% 50 mM phosphate (pH 2.5)–80% ACN and was injected for 0.30 min at $3.45 \cdot 10^3$ Pa followed by a second injection of separation buffer for 0.5 min at $3.45 \cdot 10^3$ Pa. Separations were then carried out at 15 kV in 125 mM borate–2.5 mM phosphate pH 8.0 buffer in a 47 cm × 75 μm capillary maintained at 28°C.

unaffected in comparison with the standard CZE electrophoretic separation and (2) determine whether samples serially diluted 10-fold (2 μg/ml, 200 ng/ml and 20 ng/ml) could be applied directly onto the SPE concentrator. The data in Fig. 8 demonstrates that detection of both Gp and I.S. as low as 20 ng/ml was easily attainable, but that extraction efficiency drops dramatically

(apparently exponentially) with dilution beyond this point. It is noteworthy that the extraction efficiency is markedly different for Gp and I.S. and that further dilution of the sample resulted in complete loss of I.S. detectability. This is not surprising since differences in the inherent affinities of analytes for reversed phases is the basis for chromatographic separations. Provided that resolution is not affected, increasing the packed-bed volume should increase the sensitivity of the technique for the Gb as demonstrated in Fig. 9 where 190 μl of sample has been concentrated and detected. Note that the data in this figure was generated using the same 47 cm × 75 μm separation capillary utilized in the other experiments but with an SPE-tip that had a reversed-phase volume that was four times that used in the experiments evaluating lifetime and

Fig. 8. Extraction efficiency vs. sample concentration. Concentration and separation of Gp and I.S. after sample loading of 2.0, 0.2 and 0.02 μg/ml at 0.05, 0.5 and 5.0 min injection times on an SPE capillary containing a 0.5 mm × 370 μm C_{18} packing. Sample buffer solution was loaded onto the SPE tip by low pressure ($3.45 \cdot 10^3$ Pa) followed by a separation buffer rinse. The elution buffer was 20% 50 mM phosphate, pH 2.5–80% ACN and was injected for 0.30 min at $3.45 \cdot 10^3$ Pa followed by a second injection of separation buffer for 0.5 min at $3.45 \cdot 10^3$ Pa. Separations were then carried out at 15 kV in 125 mM borate–2.5 mM phosphate pH 8.0 buffer in a 47 cm × 75 μm capillary maintained at 28°C.

Fig. 9. Detection of Gb at 5.0 ng/ml using SPE–CE. Concentration and separation of sample blank and Gb on an SPE capillary containing a 1.0 mm × 370 μm C_{18} packing. Sample was loaded onto the SPE tip by high pressure ($1.38 \cdot 10^5$ Pa) for 20 min (equivalent to injection of 190 μl) followed by a separation buffer rinse. Elution buffer was 20% 50 mM phosphate, pH 2.5–80% ACN and was injected for 0.30 min at $3.45 \cdot 10^3$ Pa followed by a second injection of separation buffer for 0.5 min at $3.45 \cdot 10^3$ Pa. Separation was then carried out at 15 kV in 125 mM borate–2.5 mM phosphate pH 8.0 buffer in a 47 cm × 75 μm capillary maintained at 28°C.

loading capacity. The larger volume of packing allowed for an increase in sensitivity but, if excessive, resolution may be lost as a result of the increased elution volume required to release the bound analytes.

The sample loading capacity was determined using a single concentration of Gp and I.S. (2 μg/ml) and by doubling the injection time over a range of 0.5–32.0 min using an applied injection pressure of $3.4 \cdot 10^3$ Pa. The peak area was found to increase linearly with injection time over the range of 0.5–8.0 min with a calculated correlation coefficient (r^2) of 0.999 for both Gp and I.S. (Fig. 10). With injections of 16.0 and 32.0 min, the resultant recovery of Gp and I.S. was no longer linear, presumably due to the fact that the capacity of the solid phase was approached ($\approx$15 ng of each drug loaded with an injection of 32 min at $3.4 \cdot 10^3$ Pa). When an extremely large volume of sample was injected (5.0 min at $1.38 \cdot 10^5$ Pa = 47.8 μl), the capacity of the concentrator tip was exceeded and the exchange of I.S. for Gp on the solid phase was observed as evidenced by the corresponding decrease in I.S. peak area as the peak area of Gp continued to increase.

As a means of evaluating other phases with different physical characteristics, an SPE-tip was constructed with a Poros R2 resin provided by PerSeptive Biosystems. This solid-phase packing was unique in that it is extremely stable over a wide pH range (pH 1–14). Concentration and separation on a Poros R2 SPE-tip showed that, while the binding affinity of the drugs to this resin was apparently lower than that with the C_{18} silica, the SPE-tip was not affected by the use of high pH buffers or conventional reconditioning techniques (i.e., 0.1 *M* NaOH buffers) that typically necessitated the renewal of the silica-based SPE tips (data not shown). The Poros material also allows for high flow-rates and low restriction due to the favorable physical characteristics of this support, and thus, is a favorable solid phase for use in SPE–CE methods. Unfortunately, the additional chromatographic component observed with the silica-based packings could not be reproduced with the Poros solid phase. This may be an indication of the different selectivities that can be expected with different packings. While this solid phase may not be perfectly suited to this particular application (these analytes), it may be better suited to other more hydrophobic analytes.

4. Conclusions

The results of this study indicate that SPE–CE appears to be effective for the analysis of the hypoglycemic drugs in the low ng/ml range. The ability to inject and concentrate up to 190 μl of sample on a system that is typically restricted to a maximum injection of 25 nl, translates to an increase in sensitivity of approximately 3–4 orders of magnitude. This sensitivity should, in theory, allow for the development of a method for the direct detection of hypoglycemic drugs in urine at 100–500 ng/ml. Sample loading was linear until the capacity of the solid support is approached and the SPE-tip was shown to be robust in that it is capable of multiple consecutive analyses with minimal regeneration. The ability to automate the sample, elution and buffer injections as well as the electrophoretic process are critical for effective application of this technology to clinical assay development. The potential for elimination of off-line extraction procedures presently required prior to analysis by CE or other standard techniques is enticing. Solid supports with different adsorption/desorption selectivities may be utilized to produce customized methods for individual analyses. Therefore, the use of a diverse array of solid-phase packing materials will impart a tremendous flexibility and range to this CE technique.
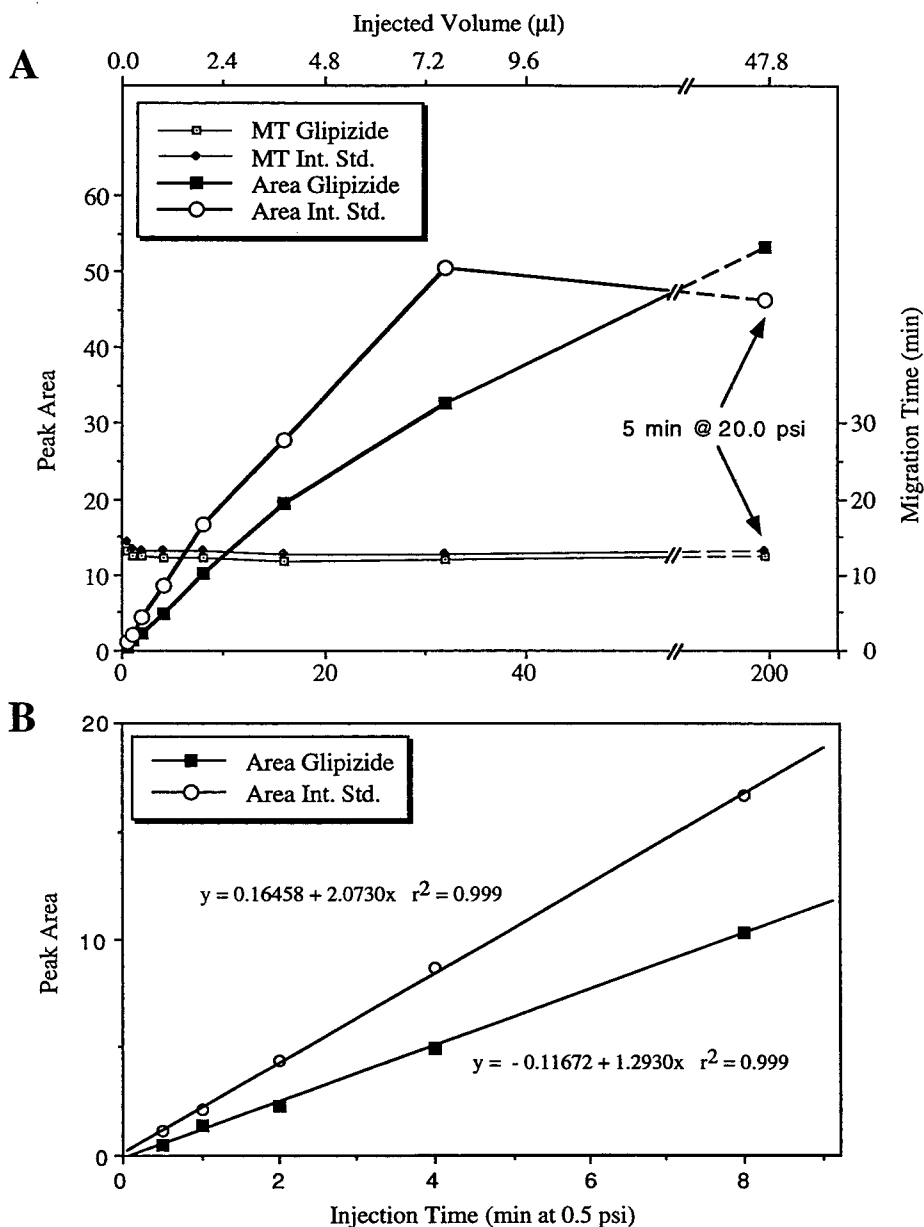
Fig. 10. Extraction efficiency vs. injection time. (A) Linearity of extraction efficiency vs. injection time: Concentration and separation of sulfonylurea drug Gp and I.S. at 2 μg/ml on an SPE capillary containing a 0.5 mm × 370 μm C$_{18}$ packing. Sample buffer solution was loaded onto the SPE tip by low pressure (3.45 · 10^3 Pa), except where noted in figure, followed by a separation buffer rinse. Elution buffer was 20% 50 mM separation buffer–80% ACN and was injected for 0.30 min at 3.45 · 10^3 Pa followed by a second injection of separation buffer for 0.5 min at 3.45 · 10^3 Pa. Separations were then carried out at 15 kV in 125 mM borate–2.5 mM phosphate pH 8 buffer in a 47 cm × 75 μm capillary maintained at 28°C. (B) Correlation of peak area vs. injection time with injections over a range of 0.5–8.0 min.

References

[1] W.R. Jones, P. Jandik and R. Pfeifer, American Laboratory 40–46 (1991).

[2] S.L. Carney and D.J. Osborne, Anal. Biochem., 195 (1991) 132–140.

[3] J. Liu, O. Shirota and M. Novotny, Anal. Chem., 63 (1991) 413–417.

[4] P.D. Grossman, J.C. Colburn, H.H. Lauer, R.G. Nielsen, R.M. Riggin, G.S. Sittampalam and E.C. Rickard, Anal. Chem., 61 (1989) 1186–1194.

[5] R.P. Oda, B.J. Madden, J.C. Morris, T.C. Spelsberg and J.P. Landers, J. Chromatogr. A, 680 (1994) 341–351.

[6] K.J. Ulfelder, H.E. Schwartz, J.M. Hall and F.J. Sunzeri, Anal. Biochem., 200 (1992) 260–267.

[7] M. Bushey and J. Jorgenson, J. Chromatogr., 480 (1989) 301–310.

[8] N. Cohen and E. Grushka, J. Cap. Electrophoresis, 215 (1994) 112–115.

[9] S. Terabe, K. Otsuka, K. Ishikawa, A. Tsuchiya and T. Ando, Anal. Chem., 56 (1984) 111–113.

[10] I.M. Johansson, R. Pavelka and J.D. Henion, J. Chromatogr., 559 (1991) 515–528.

[11] L.L. Garcia and Z.K. Shihabi, J. Liq. Chromatogr., 16 (1993) 2049–2057.

[12] J. Morita and J.-J. Sawada, J. Liq. Chromatogr., 641 (1993) 375–381.

[13] P. Gariel, J.P. Grammond and F.J. Guyon, J. Chromatogr., 615 (1993) 317–325.

[14] M.E. Schwartz and M. Merion, J. Chromatogr., 632 (1993) 209–213.

[15] P. Wernly and W. Thormann, Anal. Chem., 64 (1992) 2155–2159.

[16] J.P. Landers, Clin. Chem., 41 (1995) 495–509.

[17] W. Thorman, S. Molteni, J. Caslavska and A. Schumtz, Electrophoresis, 15 (1994) 3–12.

[18] D.A. Alquist, R.L. Nelson and C.W. Callaway, Ann. Intern. Med., 93 (1980) 281–282.

[19] R.M. Jordan, H. Kammer and M.R. Riddle, Arch. Intern. Med., 137 (1977) 390–393.

[20] G.M. Shenfield, J.S. Boutagy and C. Webb, Ther. Drug Monit., 2 (1990) 393–397.

[21] M.E. Nunez, J.E. Ferguson, D. Machacek, G. Lawson and J.P. Landers, Anal. Chem., in press.

[22] P. Gebauer, W. Thorman and P. Bocek, J. Chromatogr., 608 (1992) 47–57.

[23] F. Foret, V. Stustacek and B. Bocek, J. Microcol. Sep., 2 (1990) 229–233.

[23] W.J. Adams, G.S. Skinner, P.A. Bombardt, M. Courtney and J.E. Brewer, Anal. Chem., 54 (1982) 1287–1291.

[24] N.A. Guzman, US patent #5,202,010, 1993.

[25] N.A. Guzman, M.A. Trebilcok and J.P. Advis, J. Liq. Chromatogr., 14 (1991) 997–1015.

[26] Fuchs and M. Merion, US patent #5,246,577, 1993.

[27] A.J.J. Debets, M. Mzereeuw, W.H. Voogt, D.J. Van Iperen, H. Lingeman, K.-P. Hupe and U.A.Th. Brinkman, J. Chromatogr., 608 (1992) 151–158.

[28] L.M. Benson, A.J. Tomlinson and S. Naylor, J. High Resolut. Chromatogr., 17 (1994) 671–673.

[29] J.H. Beattie, R. Self and M.P. Richards, Electrophoresis, 16 (1995) 322–328.

[30] A.J. Tomlinson, L.M. Benson and S. Naylor, J. High Resolut. Chromatogr., 17 (1994) 729–731.

[31] T. Rydberg, E. Wåhlin-Boll and A. Melander, J. Chromatogr., 564 (1991) 223–233.

[32] E. Wåhlin-Boll and A. Melander, J. Chromatogr., 164 (1979) 541–546.

[33] M. Strausbauch, P.J. Wettstein and J.P. Landers, Electrophoresis, 16 (1995) 541–548.

[34] M. Uihlein and N. Sistovaris, J. Chromatogr., 227 (1982) 93–101.

[35] M.J. Crooks and K.F. Brown, Biochem. Pharmacol., 24 (1975) 298–299.

[36] M. Strausbauch et al., Anal. Chem., submitted.

[37] R.L. Chien and D.S. Burgi, Anal. Chem., 64 (1992) 1046–1050.

Child cerebrospinal fluid analysis by capillary electrophoresis and laser-induced fluorescence detection

G. Nouadje[a,b], H. Rubie[c], E. Chatelut[d], P. Canal[d], M. Nertz[a], Ph. Puig[b], F. Couderc[e,*]

[a]ZETA Technology, Parc Technologique du Canal, 31520 Ramonville, Toulouse, France
[b]Laboratoire de Chimie Analytique et Bromatologie, Université des Sciences Pharmaceutiques, 31062 Toulouse Cedex, France
[c]Service de Pédiatrie Oncologique, Centre Hospitalier Régional de Purpan, 31300 Toulouse Cedex, France
[d]Laboratoire de Pharmacocinétique, Centre Claudius Regaud, Rue Saint Pierre, 31300 Toulouse Cedex, France
[e]Laboratoire de Biologie Moléculaire Eucaryote du CNRS, 118 Route de Narbonne, 31062 Toulouse Cedex, France

Abstract

Capillary electrophoresis with laser-induced fluorescence detection (CE–LIF) was used to analyze a 50-μl sample of cerebrospinal fluid from leukaemic children treated with high doses of methotrexate. Free amino acids and primary amines are labelled with fluorescein isothiocyanate prior to analysis. Electropherograms containing more than 50 peaks were obtained in less than 22 min. Twenty-one peaks were identified, and 19 were quantitated. Observed differences in individual amino acid levels are compared with healthy reference values. The results indicate that CE–LIF is useful as a selective, rapid and sensitive tool for the determination of free amino acids and amines in clinical biology studies.

1. Introduction

Cerebrospinal fluid is secreted in the brain and is in a steady state with the fluid surrounding brain cells. It plays a critical role in providing a constant chemical environment for neurons and glia and is the body fluid most likely to reflect a disturbance of the amino acids metabolic pathway. Free amino acids levels in cerebrospinal fluids have been studied [1–3], and their implication in several diseases such as central nervous system disorders or metabolic diseases has been shown [3,4]. Moreover, the way of collecting samples, time of lumbar puncture and position of

* Corresponding author.

the patient may have some influence on the level of amino acids [5].

Analyses by gas chromatography [2], high-performance liquid chromatography (HPLC) [6], ion-exchange chromatography [7], isotachophoresis [8] and capillary electrophoresis [9] have been used to identify and quantify free amino acids in the brain with conventional detection modes. Capillary electrophoresis (CE) offers some advantageous characteristics for the analysis of biological samples [10,11]: very small injection volumes (very small quantities of samples are consumed, leaving a greater sample for other analyses), high separation efficiency, and easy use of a highly sensitive detection mode such as laser-induced fluorescence detection (LIF). LIF is used more and more for CE

analysis, as an 'on-column' detector. Because of the very low injection volumes, the amount of product to be detected is too small for UV absorbance detection. Moreover, selectivity due to labelling reactions and appropriate laser wavelength excitation allows one to record only well-defined molecules, e.g., amines and amino acids.

A large number of studies have been published on the labelling of amines and amino acids, and different reagents have been used: fluorescein isothiocyanate (FITC) [12], naphthalenedialdehyde (NDA) [13] and 3-(4-carboxybenzoyl)-2-quinolinecarboxaldehyde (CBQCA) [14]. The detection limit of each labelling dye is identical, around 10^{-11}–10^{-12} M.

Studies on the composition of free amino acids in the brain using CE–LIF have been reported. Glutamic and aspartic acids in mouse brain microdialysis samples have been identified [12]. More recently, Bergquist et al. [14] have carried out quantitative analyses of ten CBQCA-labelled amino acids in cerebrospinal fluid from patients with psychiatric or neurological diseases.

In this paper, we present CE–LIF in a quantitative study of FITC-labelled amino acids and amines in cerebrospinal fluid samples from acute lymphoblastic leukaemic children treated with high doses of methotrexate [15]. These samples were collected between one and three days after drug administration.

2. Experimental

2.1. Instrumentation and separation conditions

A modular injector and high-voltage power supply SpectraPHORESIS 100 (TSP, Freemont, CA, USA) equipped with a modular CE–LIF detector (Zeta Technology, Toulouse-Ramonville, France) and a 488-nm wavelength laser (Model 54225A, ILT, Salt Lake City, UT, USA) were used. Data collection, processing and analysis were performed using a Boreal software package (JMBS Developpements, Grenoble, France). Data were collected at a sampling rate of 10 Hz. A 75 cm × 50 μm I.D., fused-silica capillary (Polymicro Technology, Phoenix, AZ,

USA) had an effective length of 42 cm. All chemicals were purchased from Aldrich (St. Quentin Falavier, France)

The separation buffer consisted of 100 mM of sodium dodecyl sulfate (SDS) and 100 mM boric acid, adjusted to pH 9.3 by the addition of sodium hydroxide. The capillary was rinsed with 0.1 M NaOH for 3 min, with water for 2 min, and then with separation buffer for 3 min. Samples were injected by hydrodynamic injection for 2 s (15 nl).

The separation voltage was +20 kV, resulting in an electrophoretic current of 42 μA.

2.2. Derivatization procedure

A 2.1 · 10^{-4} M solution of FITC isomer I in acetone was prepared by dissolving 2.5 mg of FITC in 30 ml of acetone. Then 2 mg of each amino acid was dissolved in 2 ml of 0.2 M carbonate buffer at pH 9.0. Of each amino acid solution, 1 ml was allowed to react with 1 ml of FITC solution for 2 h in the dark. At the same time, 1 ml of a 2.1 · 10^{-4} M solution of the FITC in acetone was mixed with 1 ml of 0.2 M carbonate buffer to obtain a blank, and was kept in darkness for 2 h.

A 50-μl sample of each cerebrospinal fluid was mixed with 50 μl of 2.1 · 10^{-4} M FITC solution and left to react for 2 h in darkness. Each solution obtained was diluted either 1000 times or 100 times prior to injection.

2.3. Identification and quantitation

Peaks were identified by spiking cerebrospinal fluid samples with known quantities of standard solutions of amino acids. Amino acids were quantified using linear calibration curves based on peak height. Each calibration curve contained data points at a minimum of six different concentrations, and each curve spanned the range of concentrations found in the cerebrospinal fluid sample diluted 100 or 1000 times. Linearity was assessed using standard least-squares analysis of the logarithm of peak height versus logarithm of concentration plots. Co-injection of known quantities of fluorescein thiocarbamyl (FTC)

glutamic acid, aspartic acid, ornithine, glycine and taurine showed that experimental errors on quantitation (without internal standard) remain below 1.2%.

2.4. Cerebrospinal fluid

Cerebrospinal fluid (CSF) came from children with acute lymphoblastic leukemia (6–14 years old), who were treated with high amounts of methotrexate. This is a cytotoxic drug used to eliminate leukaemic cells [15]. Table 1 shows the details of the patients.

A high dose of methotrexate (HDMTx) was given in a 24-h infusion (5 g/m^2) with 500 mg/m^2 given in 1 h and 4500 mg/m^2 given in the 23 subsequent hours. During the HDMTx infusion, alkaline hydration (3 l/m^2) was administered in order to maintain urinary pH above 7. Adjuvant drugs: 6-mercaptopurine (6MP; 25 mg/m^2) was given orally every morning after fasting; cytosine arabinoside (CA; 1 g/m^2) was given during 1-h infusion after the beginning of the methotrexate infusion.

Samples were collected to quantitate methotrexate in cerebrospinal fluid, and we carried out quantitative studies of amines and amino acids on unused samples. Lumbar punctures were performed in the L3-4 or L4-5 interspace in the morning with the patient in a recumbent position. Samples were collected between one and three days after drug administration. The first 3 ml of cerebrospinal fluid was collected in plastic

tubes and gently mixed to avoid a gradient effect. This amount of each sample was used for different analyses, i.e., methotrexate quantitation, and only 50 μl of these samples was used to perform CE–LIF experiments. The albumin ratio [cerebrospinal fluid albumin (in mg/l) divided by serum albumin (g/l)] was the measure of blood barrier function, in order to exclude samples from patients with pathologically increased levels of serum in their cerebrospinal fluid [16].

3. Results and discussion

Fig. 1 shows the electropherogram of the standard FTC-amino acids and amines levels under experimental conditions. FTC-amines and -amino acids have a quantity of 15 amol ($1 \cdot 10^{-9}$ M solutions injected).

The fluorescent intensity measured for all amino acids and amines was linearly correlated with the sample concentration injected over a range of 10^{-8}–$5 \cdot 10^{-10}$ M. The linearity was determined from repeated injection at six different concentrations of each amine and amino

Table 1
Characteristics of the patients

Patients	J	M	C
Age (years)	11	14	6
Sex	M	F	F
Diagnostic	ALL	ALL	ALL
Plasmatic proteins concentration	63	65	67
CSF proteins concentration	0.38	0.41	0.3
Associated drugs	6MP	6MP and CA	6MP

ALL = Acute lymphoblastic leukemia, 6MP = 6-mercaptopurine, CA = cytosine arabinoside.
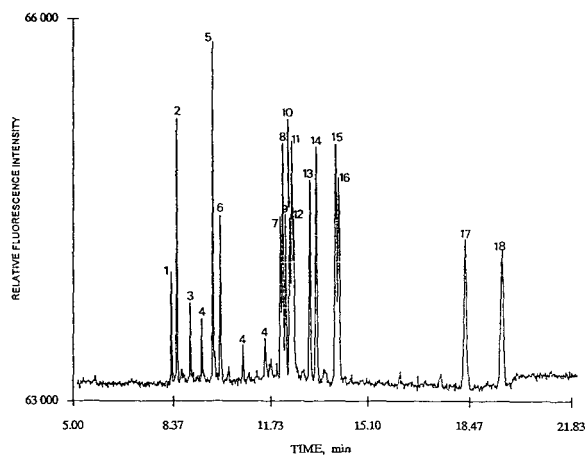
Fig. 1. Electropherogram of 17 FTC-standards (10^{-9} M). Electrophoretic conditions: buffer, boric acid 100 mM, SDS 100 mM, pH = 9.3. Analysis: +20 kV, 42 μA, hydrodynamic injection 2 s. Peaks: 1 = Lys, 2 = Arg, 3 = ornithine, 4 = blank, 5 = ammonia, 6 = tyramine, 7 = Leu, 8 = Gln, 9 = Tyr, 10 = Val, 11 = Thr, 12 = Phe, 13 = Ser, 14 = Ala, 15 = taurine, 16 = Gly, 17 = Glu, 18 = Asp.

acid. The following equation was used to evaluate the linearity of the method:

$$\log Y = \log A + r \log C$$

where $\log C$ is the log of concentration, $\log A$ is a constant, $\log Y$ refers to the log of relative fluorescence intensity, and r is the slope of the curve. The regression equations of these curves and their correlation coefficients are shown in Table 2. The linearity was achieved without an internal standard, which probably would have increased the correlation coefficients.

By running five replicates of the standard (10^{-9} M), each FTC-amino acid or -amine showed high reproducibility in terms of peak heights or elution times, giving standard deviations of standard products between 1.7 and 4.2%. The detection limit for each amino acid was less than 1.3 amol ($2 \cdot 10^{-10}$ M). The separation of amino acids was completed within 22 min. Fig. 2 shows the electropherograms of cerebrospinal fluid from leukaemic children treated with methotrexate.

Table 3 shows the mean CSF levels of free amino acids (taken from the literature [1]) in agreement with data obtained previously by ion-

Fig. 2. Separation of FTC-amino acids and -amines from the acute lymphoblastic leukemic patient J. Conditions and peaks are identical to those in Fig. 1, with 19 = citruline and 20 = Asn.

exchange chromatography, HPLC and GC [5–7]. Table 4 indicates the results we have found for three children.

Table 2
Logarithm of amino acid or amine concentration (x) versus fluorescence intensity (y) ($n = 6$)

Amino acid or amine	Regression equation	r^2
Lys	$y = 10.955 + 0.96496x$	0.999
Arg	$y = 11.012 + 0.92160x$	0.993
Ornithine	$y = 10.454 + 0.90610x$	1.000
Tyramine	$y = 11.420 + 0.98768x$	0.983
Leu	$y = 11.303 + 0.99481x$	0.996
Gln	$y = 12.022 + 1.0509x$	0.995
Tyr	$y = 11.501 + 0.99318x$	1.000
Val	$y = 11.488 + 1.0240x$	0.999
Thr	$y = 11.443 + 0.9960x$	0.996
Phe	$y = 11.673 + 1.0267x$	0.994
Ser	$y = 11.277 + 1.0127x$	0.995
Ala	$y = 11.705 + 1.0595x$	0.994
Taurine	$y = 11.667 + 1.0150x$	0.998
Ammonia	$y = 11.022 + 0.9216x$	0.984
Gly	$y = 11.571 + 1.0470x$	0.992
Asp	$y = 12.515 + 1.1557x$	0.995
Glu	$y = 11.571 + 1.0670x$	0.985

Table 3
Levels of free amino acids and amines in cerebrospinal fluids from [1]

Amino acid or amine	CSF, mean values ($\mu M/1$)	Range ($\mu M/1$)
Ammonia[a]	30.9	14.2–40.5
Ala[b]	30.3	18–44
Arg[b]	20.9	7–30
Asp[b]	2.6	0.3–6
Gln[b]	535	355–885
Glu[b]	9.8	1–48
Gly[b]	6.9	3–11
Leu[b]	13.8	7–23
Lys[b]	25.5	15–37
Ornithine[b]	4.9	3–7
Phe[b]	9.8	5–15
Ser[b]	28.5	20–41
Taurine[b]	7.2	4–11
Thr[b]	32.8	18–45
Tyramine[c]	<0.1	<0.1
Tyr[b]	8.7	5–17
Val[b]	18.5	7–31

[a] Ref. [24].
[b] Ref. [1].
[c] Ref. [21].

Table 4
Levels of free amino acids and amines in cerebrospinal fluids from 1000 × dilution of the three leukemic children derivatized samples

Amino acid or amine	CSF levels, (μM) mean, S.D. ($n = 3$)		
	Patient J	Patient M	Patient C
Ammonia	140.0 ± 23.3	131.1 ± 25.2	142.3 ± 22.0
Ala	45.1 ± 0.2	45.9 ± 0.2	40.0 ± 0.2
Asn	DNQ	DNQ	DNQ
Asp[a]	0.54 ± 0.09	0.85 ± 0.08	0.73 ± 0.09
Arg	34.2 ± 0.1	19.7 ± 2	18.3 ± 2
Citruline	DNQ	DNQ	DNQ
Gln	371.2 ± 15.6	347.3 ± 16.4	350.0 ± 14.2
Glu[a]	0.43 ± 0.07	1.05 ± 0.10	1.23 ± 0.15
Gly	13.5 ± 0.2	14.8 ± 0.1	13.1 ± 0.2
Leu	23.0 ± 0.2	21.3 ± 0.2	UD
Lys	14.8 ± 0.1	8.9 ± 0.1	6.2 ± 0.1
Ornithine	25.9 ± 0.1	UD	3.5 ± 0.1
Phe	6.7 ± 0.1	4.7 ± 0.1	5.7 ± 0.1
Ser	45.0 ± 0.6	37.1 ± 0.5	49.7 ± 0.3
Taurine	78.3 ± 1.2	106 ± 3.5	73 ± 2.5
Thr	85.1 ± 1.3	59.3 ± 1.5	91.2 ± 1.9
Tyr	19.8 ± 0.3	56.3 ± 0.5	34.3 ± 0.2
Tyramine	23.0 ± 1.4	5.6 ± 0.2	3.4 ± 0.1
Val	23.8 ± 0.7	22.4 ± 0.7	35.4 ± 0.9

[a] Quantitated with 100 × dilution.
UD = undetermined, DNQ = detected but unquantitated.

In this study, most amines and amino acids are approximately within the range of normal values, but the levels of ammonia, taurine, threonine and tyrosine were increased in each leukaemic child. Ornithine was increased in patient J, tyrosine in patients M and C. Lysine was decreased in patients M and C. Little information is available on amines and amino acids in human fluids of leukaemic patients [17,18], and to our knowledge no attempts has been made to study the role of cerebrospinal fluid amino acids in this disorder. The abnormal concentrations of ammonia and taurine in the brain are often correlated to liver disorders [19], which may be induced by high doses of methotrexate [20]. Indeed, the plasma transaminase levels of these children increased in the days following chemotherapy. Tyramine has not been quantitated before in cerebrospinal fluid, but usually cathecolamines are in the 0.1 μM range [21]. The relatively high concentration of tyramine could be correlated to the high level of tyrosine because the usual biological source of tyramine is the decarboxylation of tyrosine [22]. High levels of threonine, taurine and tyrosine were described in the plasma of acute leukaemic patients [23]. No conclusions can be drawn for ornithine and lysine since the levels do not evolve in the same way for each patient. Although ammonia levels are very high, the mean level of amino acids in the cerebrospinal fluid remains constant in our patients (mean of 760 ± 50 μM), in accordance with normal mean concentrations (755 μM); no aminoaciduria is observed, as was reported for patients treated with other chemotherapy [23,24].

4. Conclusion

MEKC with laser-induced fluorescence has been used to analyze amino acids and some amines in cerebrospinal fluids in a single run. This technique allows us to use a small amount of CSF. Precolumn derivatization with FITC does not require product purification prior to analysis, and allows the detection of very small quantities of amines (in the attomole range). Studies on cerebrospinal fluids of acute lymphoblastic leukaemic children treated with high amounts of methotrexate have been made, and differences between normal children and those with leukemia have been shown, indicating that differences in CSF composition of amino acids in this kind of disease and its medical treatment can be observed by CE–LIF.

References

[1] M.A. Gelot, Ann. Biol. Clin., 45 (1987) 15.
[2] J. Desgres, D. Boisson and P. Padieu, J. Chromatogr., 162 (1979) 133.
[3] G. Huether, Amino Acids Avaiability and Brain Function in Health Desease, NATO Advance Science Institute Series, Series H Cell Biology, Vol. 20, Springer Verlag, Berlin, 1988.
[4] T.L. Perry, C. Krieger, S. Hansen and A. Eisen, Ann. Neurol., 28 (1990) 12.
[5] J. Kornhuber, M.E. Kornhuber, G.M. Hartmann and A.W. Kornhuber, Neurochem. Int., 12 (1988) 25.
[6] D.A. Spink, J.W. Swann, O.C. Snead, R.A. Waniewski and D.L. Martin, Anal. Biochem., 158 (1986) 79.
[7] L. Hagebfeld, L. Bjerkenstedt, G. Edman, G. Sedvall and F.A. Wiesel, J. Neurochem., 42 (1984) 833.
[8] A. Hiraoka, I. Miura, I. Tominaga and M. Hattori, Clin. Biochem., 22 (1989) 293.
[9] S. Tellez, N. Forges, A. Roussin and L. Hernandez, J. Chromatogr., 608 (1992) 189.
[10] F.T.A. Chen, C.M. Liu, Y.Z. Hsieh and J.C. Stenberg, Clin. Chem., 37 (1991) 14.
[11] N.A. Guzman, C.L. Gonzalvez, L. Hernandez, C.M. Berk, M.A. Trebilcock and J.P. Advis, in N.A. Guzman (Editor), Capillary Electrophoresis Technology, Marcel Dekker, New York, 1993, Ch. 22.
[12] L. Hernandez, J. Escalona and N. Joshi, J. Chromatogr., 559 (1991) 183.
[13] M. Janson and J. Roaraade, Anal. Chem., 65 (1993) 2766.
[14] J. Bergquist, S.D. Gilman, A.G. Ewing and R. Ekman, Anal. Chem., 66 (1994) 3512.
[15] W.A. Bleyer, Cancer, 41 (1978) 36–51.
[16] K.J. Lin and G. Tibbling, Scand. J. Clin. Lab. Invest., 37 (1977) 391.
[17] J. Shreiber, W. Lohmann, F. Berthold and F. Lampert, Fresenius' Z. Anal. Chem., 325 (1986) 476.
[18] L.A. Lavi, J.S. Holcenberg, D.E. Cole and J. Jolivet, J. Chromatogr., 377 (1986) 155.
[19] T. Jonung, B. Jeppsson, P. Herlin, A. Nobin, B. Hultberg and U. Aslund, Int. Congr. Ser. Excerpta Med., 761 (1988) 177.
[20] Dictionnaire Vidal, OVP Paris, France, 1987, p. 959.
[21] H. Kishikawa, Okayama Igakkai Zasshi, 87 (1975) 451.
[22] A.A. Boulton, Adv. Biochem. Psychopharm., 15 (1993) 57.
[23] R.R. Brown, Science, 157 (1967) 432.
[24] C. Wiseman, R.F. McGregor and K.B. McCredie, Cancer, 38 (1976) 219.

ELSEVIER

Trace analysis of fluorescein-derivatized phenoxy acid herbicides by micellar electrokinetic chromatography with laser-induced fluorescence detection

Martin Jung[1], William C. Brumley*

U.S. Environmental Protection Agency, Environmental Monitoring Systems Laboratory, P.O. Box 93478, Las Vegas, NV 89193-3478, USA

Abstract

Micellar electrokinetic chromatography (MEKC) with laser-induced fluorescence (LIF) detection was used for the trace analysis of phenoxy acid herbicides. Capillary electrophoresis (CE) with LIF detection, which has not previously been used for pesticide analysis, overcomes the poor sensitivity of on-column UV detection. A novel derivatization procedure was developed which is suitable for nanogram amounts of organic acids. In this procedure, the acids are activated by hydroxybenzotriazol (HOBT) and diisopropylcarbodiimide (DIC) and reacted with 5-(aminoacetamido)fluorescein in dimethylformamide at ambient temperature. The fluorescent derivatives of all relevant phenoxy acid herbicides were separated in a single run by MEKC. A 488 nm Ar laser line was used for excitation. The reproducibility and reliability of the method were evaluated. The detection limit was 2 fg for a 4-nl injection, but for practical reasons, a minimum of 1 ng per compound should be subjected to the derivatization. The applicability of the described method to the extract of an aqueous sample was demonstrated.

1. Introduction

High-performance capillary electrophoresis (HPCE or CE) is a powerful, fast, and inexpensive analytical technique, yet in principle simple. In the past decade, numerous applications have been demonstrated in pharmaceutical and biochemical analysis [1–3]. There are, however, hardly more than a dozen reports on the use of CE for the analysis of pesticides [4–20]. This is principally due to the insufficient sensitivity of standard CE techniques with on-column UV detection. Consequently, most of these reports

[4–13,15–19] deal with analytical concentrations in the ppm range in standard solutions or real extracts. Environmental trace analysis at sub-ppb levels (i.e., at concentrations in the ppb range after extraction), can become feasible only if sample preconcentration techniques or improved detection systems are used. The principal possibilities, as recently summarized by Nielen [14], include on-line isotachophoretic preconcentration, field-amplified injection techniques, or improved detection techniques such as laser-induced fluorescence (LIF) detection. Using CE with field-amplified injection after solid-phase extraction (SPE), Nielen [14] was able to determine phenoxy acid herbicides in 40-ml water samples at sub-ppb levels. Recently, Kaniansky et al. [20] achieved ultratrace determination of

---

the herbicides paraquat and diquat in water by using CE with isotachophoretic sample pretreatment. Cai and El Rassi [6] accomplished a 10- to 35-fold preconcentration of triazine herbicides by using on-line coupling with capillaries having surface-bonded octadecyl functions. However, all these preconcentration techniques are hardly suitable for automated analysis with commercially available equipment and software.

Phenoxy acids, such as 2,4-D, constitute an important class of herbicides and are used worldwide in agriculture. A common method for their trace analysis in water samples is GC with electron-capture detection (ECD) after liquid–liquid extraction and derivatization with diazomethane [21]. Detection limits are in the upper ppt or low ppb range, but the hazards associated with diazomethane are a major disadvantage for this method. Butz et al. [22] recently described the analysis of 34 acidic pollutants, including all phenoxy acid herbicides, at low ppt levels in water. They used GC–MS with single-ion monitoring (SIM) after solid-phase extraction of the pollutants and derivatization with pentafluorobenzyl bromide. HPLC with UV detection can also be used, but detection limits for water samples are only in the ppb range, and the limited resolution provided by HPLC does not allow the analysis of a large number of herbicides in one run [23]. Sensitivity for HPLC can be improved by using LIF detection after derivatization of the phenoxy acids with 9-anthryldiazomethane (ADAM) [24]. Thus, detection limits in the upper ppt range could be achieved for spiked water samples. CE has also been applied to the analysis of phenoxy acids [9,12–14,16]. However, as discussed above, sensitivity is poor, and thus far only Nielen [14] has accomplished their trace analysis at sub-ppb levels in water samples.

A major goal of the analytical chemistry research program at the U.S. EPA (Las Vegas) is to ensure that novel analytical techniques become incorporated into the tools available for routine monitoring of pesticides and other pollutants in the environment. CE with LIF detection has not previously been used for pesticide analysis. It is a relatively simple, though highly sensi-

tive technique. Of course, the need for fluorescent labelling of the analytes prior to analysis is an inherent disadvantage. In this paper we report on a novel procedure that allows the derivatization and subsequent analysis of nanogram amounts of all relevant phenoxy acid herbicides in a single run by micellar elektrokinetic chromatography (MEKC or MECC). The emphasis of this work was on developing conditions for derivatization and separation rather than on solid-phase extraction of real samples.

2. Experimental

2.1. Chemicals

Phenoxy acid standards were obtained from Aldrich (Milwaukee, WI, USA) or Chem Service (West Chester, PA, USA). 5-(Amino-acetamido)fluorescein was obtained from Molecular Probes (Eugene, OR, USA). Other chemicals were purchased from Aldrich (Milwaukee, WI, USA) or Sigma (St. Louis, MO, USA). High purity solvents were used throughout (Baxter, McGaw Park, IL, USA). Deionized water was used (Barnstead/Thermolyne, Dubuque, IA, USA) for all aqueous solutions.

2.2. Instrumentation

All CE experiments used a P/ACE Model 5000 instrument (Beckman, Fullerton, CA, USA). It was equipped with a commercial Beckman LIF detector. In this setup, the exciting light (488 nm) was provided by an argon laser source (3 mW), and a 520-nm band pass emission filter was used. The Beckman System Gold software was used for system control, data collection, and processing.

2.3. Capillary electrophoresis

A 47 cm (40 cm to detector) × 50 μm I.D. fused-silica capillary (Beckman) was installed in a temperature-controlled (25°C) cartridge spe-

cially designed for the LIF detector. The voltage was 30 kV, and the current was ca. 60 μA with the running buffer described below. Injections were by pressure (35 mbar) for 5 s. The capillary was conditioned every morning before starting a sequence of runs by rinsing in the high-pressure mode for 5 min with 0.1 M sodium hydroxide, 5 min with water, and 5 min with the running buffer. Pre-run rinsing was performed for 4 min with the running buffer. After every run it was rinsed for 8–15 min (ca. 1/3 of the run time) with 0.1 M sodium hydroxide and for 4 min with water. When not in use, the capillary was kept filled with 0.01 M sodium hydroxide.

A 50 mM phosphate buffer (pH 7.0) was prepared by mixing appropriate amounts of 50 mM solutions of monobasic and dibasic sodium phosphate. Running buffer (100 ml) was prepared by dissolving 1.327 g of sodium dodecyl sulfate (SDS), 10.030 g of urea, and 22.2 ml of methanol in ca. 60 ml of 50 mM phosphate buffer (pH 7.0). After complete dissolution, more phosphate buffer was added to give a total volume of 100 ml. The resulting solution was ca. 39 mM in phosphate, 46 mM in SDS, 1670 mM in urea, and contained 22.2% (v/v) methanol. The buffer was filled into 5-ml minivials and stored in a freezer for up to a week. For optimal reproducibility of migration times and selectivity, the inlet buffer vial was replaced after every CE run.

2.4. Derivatization of phenoxy acids

The following individual solutions were prepared in dimethylformamide (DMF): 40 mM diisopropylethylamine (DIPEA), 20 mM hydroxybenzotriazol (HOBT) monohydrate, 750 mM diisopropylcarbodiimide (DIC), and 0.5 mM 5-(aminoacetamido)fluorescein. The solutions of HOBT and DIC were freshly prepared directly before use. The DIPEA solution was stable at room temperature, and the solution of the fluorescein reagent was stored for up to several weeks in a freezer. To a stock solution of the phenoxy acids in 250 μl DMF in a 5-ml minivial, 25 μl of each of the following reagent

solutions were added: DIPEA, HOBT, DIC, and the fluorescein reagent. An electric 250-μl pipet (Rainin, Woburn, MA, USA) was used for this operation. After allowing the mixture to stand at ambient temperature overnight (18 h, or only 3 h if MCPB and 2,4-DB are not present; see Fig. 1), a 25-μl portion was taken and diluted with 150 μl of phosphate buffer (pH 7.0). A 40-μl portion of this solution was injected to the CE from a microvial. Because of slow deterioration, the analysis was performed within approx. 12 h. Excess reaction mixture was stored in a freezer for up to several days. Caution: all glassware must be rinsed with 50 % acetic acid to destroy remaining highly toxic carbodiimide, and excess DIC reagent must be destroyed in the same manner.

2.5. Extraction of phenoxy acids from water

Distilled water (250 ml) was spiked with 1 nmol/l of every phenoxy acid, fortified with 1.5 ml of methanol and adjusted to pH 5.5 with monobasic and dibasic phosphate. As specified in the manufacturer's instructions, a C_{18} membrane disk (Empore 3M, distributed by Varian, Harbor City, CA, USA) was washed and conditioned with methanol. The sample was passed through the disk at a flow-rate of approx. 0.2 l/min to remove non-acidic contaminants. After washing the disk with 100 ml of water (adjusted to pH 5.5 and containing 0.5% (v/v) methanol), the purified eluate was acidified to pH 1.5 with 10 ml of 10 M hydrochloric acid and again subjected to solid-phase extraction with a clean disk. After passing the sample through, the disk was dried by applying a vacuum for 1 h. The herbicides were then eluted with two 8-ml portions of methanol. A boiling chip was added to the combined eluate, which was then taken to dryness using an oil bath at 110°C. The residue was dried in an oven at 110°C for 20 min. The derivatization was carried out as described in section 2.4, except that 40 mM HOBT, 900 mM DIC, and 2.5 mM fluorescein reagent solutions were used, and that the reaction time was only 2 h.

3. Results and discussion

3.1. Choice of the derivatizing reagent

Commonly used fluorescent labelling reagents for organic acids are bromomethyl coumarin derivatives and 9-anthryl- or 1-pyrenyl-diazomethane (ADAM and PDAM) [25,26]. PDAM was recently used for the determination of short-chain dicarboxylic acids in blood serum in the μmol/l concentration range by CE with LIF detection [27]. Compared with those reagents, derivatization with a suitable fluorescein reagent offers several advantages:

- sensitivity is higher because fluorescein derivatives are among the most intensely fluorescent molecules;
- the excitation wavelength exactly matches the 488 nm light provided by an argon laser that is used in at least one commercially available CE system with LIF detection;
- the use of long-wavelength excitation light reduces problems with light scattering and thus enhances sensitivity;
- the carboxy group on fluorescein may make it easier to separate the derivatives as anions with CE techniques.

No analytical derivatization procedure for low-molecular-mass organic acids with a fluorescein reagent has been described in the literature. In initial experiments we attempted the esterification of phenoxy acids with 5-bromomethyl fluorescein. However, this procedure proved to be more complex than the well-established analogous reaction with 4-bromomethyl-7-methoxy-coumarin in acetone with potassium carbonate as a base [28,29]. The derivatization was only partly successful for microgram amounts of phenoxy acids in DMF after deprotonation with a very small amount of the hindered base 1,8-diazobicyclo[5.4.0]undec-7-ene (DBU). Nevertheless, the reagent tended to decompose and this approach was finally abandoned.

A more suitable derivatization procedure for the phenoxy acids pictured in Fig. 1a was found in the formation of an amide linkage by employing a fluorescein reagent with a reactive amino group. Several fluorescein reagents with amino functions have been used for the derivatization of certain reactive carboxy groups in proteins and other biomolecules, employing either carbodiimide-mediated or enzyme-catalyzed coupling reactions [25]. The carboxy function found in fluorescein itself is not reactive to carbodiimides [25]. This is also verified in this work because the reagent does not readily react with itself, even after overnight contact at large excess (cf. below). Thus far, amine-substituted fluorescein reagents have only been used in biochemical applications, and no generally applicable analytical derivatization procedure has been reported for the labelling of small organic acids with these reagents.

We did not use the readily available aminofluoresceins (fluorescein amines) as fluorescent labelling reagents for phenoxy acids because aromatic amino groups are not reactive enough with carboxylic acids such as those of proteins [25]. The phenoxy acid substrates are resistant to amide formation and are unreactive without an activating agent (cf. below). Shipchandler et al. [30] reported on the usefulness of 4'-(aminomethyl)fluorescein as a reagent in immunodiagnostic techniques. However, that reagent is chiral and exists as a mixture of two rotamers [30], and as a consequence the derivatization of chiral phenoxy acids would lead to a mixture of diastereomers. Therefore, we chose another commercially available reagent, 5-(aminoacetamido)fluorescein (fluorescein glycine amide, Fig. 1b), previously used for the derivatization of milligram amounts of the undecapeptide O-acetyl-cyclosporin A [31]. The reagent's excitation wavelength at 489 nm best matches the argon laser line at 488 nm.

3.2. Optimization of derivatization conditions

We adopted a method commonly used in peptide synthesis [32,33], i.e., a one-step procedure consisting of the activation of the analytes with HOBT [33] and carbodiimide and reaction with the amine, using DIPEA as a base and DMF as the solvent. DIC [34] was found more suitable than dicyclohexylcarbodiimide (DCC)
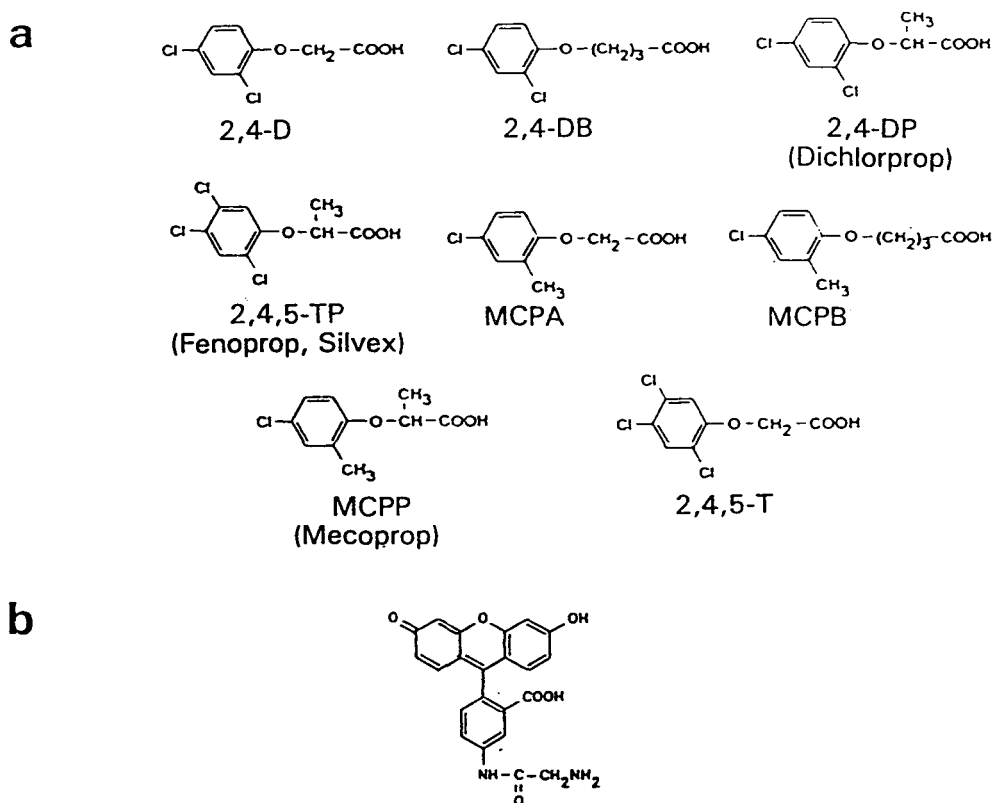
Fig. 1. Structures of (a) the phenoxy acid herbicides and (b) the derivatizing reagent 5-(aminoacetamido)fluorescein (fluorescein glycine amide).

because no precipitate formed upon dilution of the reaction mixtures with an aqueous buffer. In initial experiments we used a slight excess of the phenoxy acid to test the completeness of the procedure by MEKC with LIF detection. When the concentrations were lowered to analytically useful levels, the reaction became considerably slower. Part of the labelling reagent, which was now used in a large excess, was lost to side reactions. By carefully optimizing the concentrations of all reagents, we maximized the rate of reaction, while suppressing decomposition reactions of the labelling reagent to a reasonably small extent. The reaction was unsuccessful without any HOBT present, although only a small amount was needed. The concentration of DIPEA did not seem to influence rates and extent of main and side reactions. Our con-

ditions may be compared to those of Mechref and El Rassi [35] who first derivatized acidic carbohydrates with aminoaromatic sulfonic acids for sensitive detection in CE.

The optimized derivatization conditions are described in the Experimental section. Under these conditions, the reaction is complete for most analytes after 3 h at ambient temperature. Only the butyric acid derivatives, MCPB and 2,4-DB (Fig. 1a), react more slowly (ca. 1/8), as can be seen by following the reaction kinetics using MEKC with LIF detection. For MCPB and 2,4-DB, the derivatization is complete only after one night (18 h) at room temperature. Heating to 60°C was not found useful since it enhances side reactions. The reaction can be considered complete for all analytes when MEKC analysis yields the same peak areas for the MCPB and

2,4-DB derivatives as it does for the other acid derivatives. After 18 h, only approx. 30% of the reagent are lost to side reactions.

3.3. Optimization of analytical conditions

After optimization of the running buffer, the separation of all investigated phenoxy acid adducts, as well as the excess reagent and its decomposition products, could be achieved by MEKC in a single run. Although they are not herbicides, 3,4-D and 2,3-D were also studied since these compounds could serve as internal standards or herbicide surrogates. Typical chromatograms for all the phenoxy acids are shown in Fig. 2. For the selected capillary dimensions, a separation efficiency corresponding to 170 000–230 000 theoretical plates was observed.

Capillary zone electrophoresis (CZE) was not successful, and both methanol and urea were necessary as buffer additives to provide the required selectivity. Comparable results were not obtained when a phosphate buffer at pH 7.5 or borate buffer at pH 8.4 was used instead of the phosphate buffer at pH 7.0. As often observed in CE, the separation was best when the pH of the running buffer is close to the pK_a of the analytes, which is 6.5. A lower pH cannot be chosen because only the anions of the fluorescein derivatives are fluorescent [25]. The peak of 3,4-D often tended to be broadened. Surprisingly, the electric field strength also affected the selectivity to a certain extent; the separation of 2,3-D and MCPP deteriorated upon changing the voltage from 30 to 25 kV when the capillary length was kept the same.

It should be noted that, as a consequence of the large excess of the reagent, even minor decomposition products can give additional peaks, which can easily be larger than those of the phenoxy acid derivatives. Fortunately these peaks are concentrated in the first part of the chromatogram and therefore do not interfere. A very small peak appeared after 2,4-DB and another one after 2,4-DP. These small peaks were fully separated from the phenoxy acid peaks and were also found in a blank derivatization run (i.e., without any phenoxy acids

present) (Fig. 2g). Prior to analysis, a 25-μl portion of the reaction mixture was diluted with 150 μl phosphate buffer (pH 7.0). Considerable peak broadening resulted if less than 150 μl of buffer were added. The concentration of the buffer used for dilution had no obvious influence on analysis. A borate buffer at pH 8.4 could not be used for dilution of the sample because peak splitting was then observed for 2,4,5-T and 2,4,5-TP when methanol concentrations below 22% (v/v) in the running electrolyte were employed.

3.4. Reliability and reproducibility

To evaluate the described procedure, six individually prepared mixtures, each containing 100 pmol of every investigated phenoxy acid, were derivatized and analyzed in consecutive runs. The results are listed in Table 1. Relatively stable migration times could be obtained when the column was thoroughly rinsed with sodium hydroxide after every run, as described in the Experimental section. The replacement of the running buffer after every run further enhanced reproducibility. The day-to-day reproducibility is affected by any changes of the capillary surface that affect the electroosmotic flow (EOF). Therefore, it is better to rely on relative migration times, whose reproducibility was found to be much better. As far as the peak areas are concerned, the reproducibilities were good, except for MCPB and 2,4-DB. We attribute the somewhat larger standard deviation for those herbicides to their much slower rate of derivatization. They may not always be quantitatively derivatized, sometimes only to ca. 95%. A complete derivatization of MCPB and 2,4-DB in real extracts may become impossible in cases where the extracts contain substances that accelerate the decomposition of the derivatizing reagent.

3.5. Limit of detection

For the derivatization and injection conditions described in the Experimental section, the injection volume according to Hagen–Poiseuille's law is approx. 4 nl for a 175 mbar s injection [18].
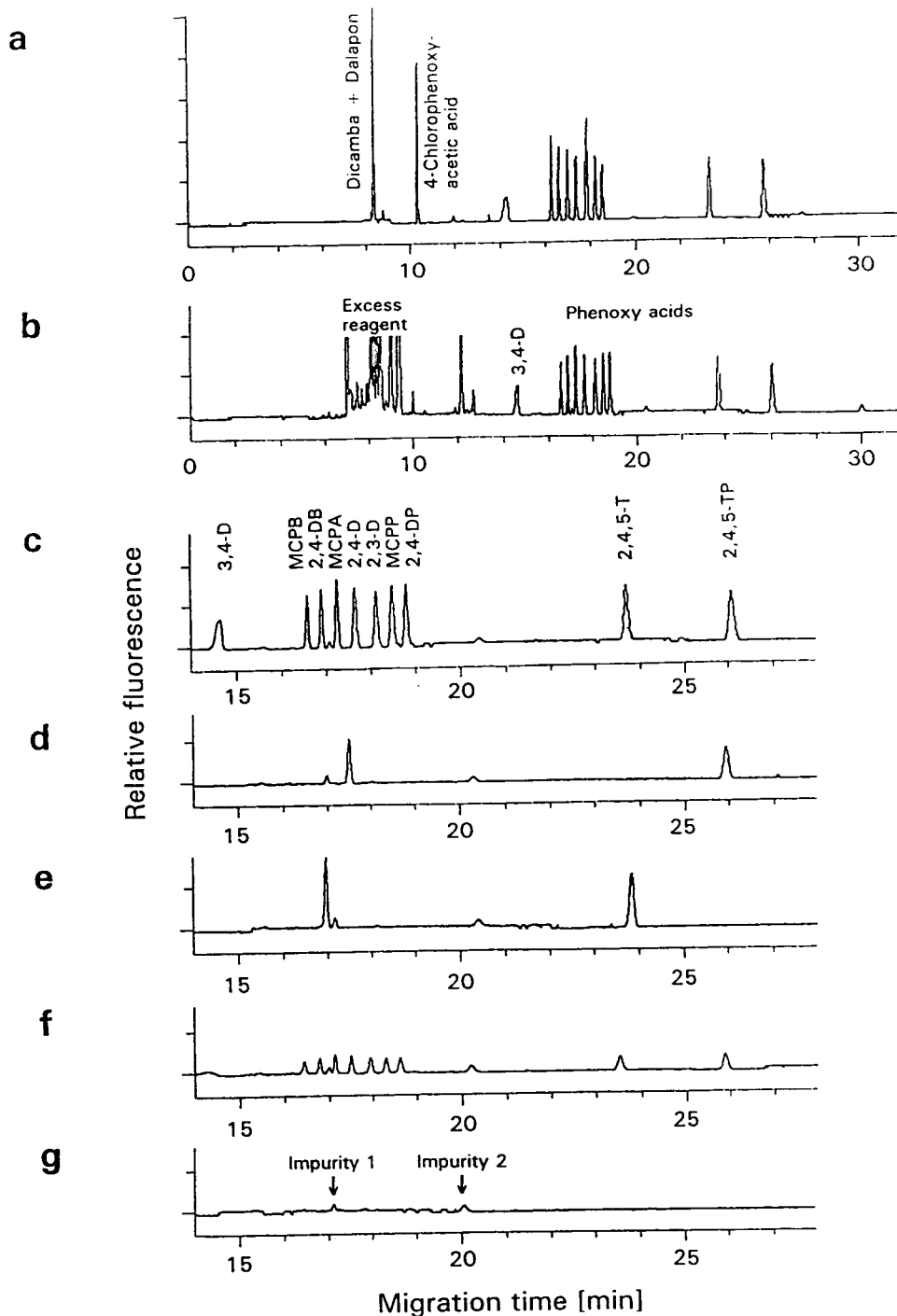
Fig. 2. Chromatograms from trace analysis of phenoxy acid herbicides by MEKC with LIF detection after derivatization of stock solutions as described in the Experimental section. Analytical conditions: voltage, 30 kV; capillary, 47 cm (40 cm to detector) × 50 μm I.D.; buffer, 39 mM phosphate pH 7.0, 46 mM sodium dodecyl sulfate, 1670 mM urea, 22.2% (v/v) methanol. (a) Artificial mixture of acid derivatives prepared at a semi-preparative scale; (b) derivatization of a mixture containing 100 pmol (approx. 20 ng) per phenoxy acid; (c) enlargement of the relevant part of chromatogram b; (d) derivatization of 2,4-D and 2,4,5-TP, 100 pmol each; (e) derivatization of 2,4-DB and 2,4,5-T, 100 pmol each; (f) derivatization of a mixture containing 20 pmol per phenoxy acid; (g) blank derivatization without phenoxy acids.

Table 1
Reliability and reproducibility data for the derivatization[a] of phenoxy acids with fluorescein glycine amide and analysis of the derivatives by MEKC[b]

Analytes	Relative standard deviation (%) of absolute migration times ($n = 6$)	Mean relative migration times (2,3-D = 1)	R.S.D. (%) of relative migration times ($n = 6$)	Mean corrected[c] relative peak areas (2,3-D = 100)	R.S.D. (%) of relative peak areas ($n = 6$)
3,4-D	1.9	0.784	1.1	140	1.9
MCPB	2.4	0.894	0.3	87	10.6
2,4-DB	2.5	0.917	0.2	95	9.7
MCPA	2.7	0.945	0.1	114	2.0
2,4-D	2.6	0.970	0.1	110	1.5
2,3-D	2.7	1	–[d]	100	–[d]
MCPP	3.0	1.021	0.1	109	2.9
2,4-DP	2.9	1.043	0.2	104	3.8
2,4,5-T	3.6	1.359	0.9	89	1.6
2,4,5-TP	3.9	1.519	1.3	86	3.2

[a] The derivatization was carried out six times using individually prepared mixtures, each containing 100 pmol per phenoxy acid.
[b] Analytical conditions as in Fig. 2; cf. Experimental section.
[c] With on-column detection, the peak areas directly depend on the migration times. To obtain comparable values, the data acquisition software automatically corrects the measured peak areas accordingly.
[d] Not applicable.

For stock solutions of phenoxy acids, the detection limit per injection is 2 fg for a signal-to-noise ratio of 8. However, handling and derivatization for practical reasons require a minimum of approx. 1 ng. For extracts of real samples, higher detection limits have to be expected, depending on the sample.

3.6. Extraction from water samples

The extraction of water samples spiked with phenoxy acids was performed by solid-phase extraction using C_{18} membrane disks under similar conditions as described previously [16,22]. Before extraction at pH 1.5, the sample was purified by means of another extraction step at pH 5.7, thus removing non-acidic organic compounds. However, we found that there were still side reactions occuring during our derivatization procedure, resulting in enhanced decomposition of the derivatizing reagent and in additional peaks in the chromatogram. For water samples spiked at 1 nmol/l (approx. 0.2 ppb) per phenoxy acid, recoveries in the 60–80% range

were obtained for most analytes. The recovery of 2,4,5-TP was poor (approx. 30%). An example is shown in Fig. 3. MCPB and 2,4-DB are barely visible since the reaction time for derivatization was only 2 h. After longer reaction times, the background noise level resulting from side reactions was found to be higher. Further work towards optimization and development of suitable conditions for sample preparation and extraction is in progress.

4. Conclusion

MEKC with LIF detection is applicable to the determination of nanogram levels of phenoxy acid herbicides. The described procedure can be performed with commercial equipment, using an autosampler for automated analysis. The high efficiency of CE allows the separation of the fluorescein derivatives of all target phenoxy acids in a single run while still not crowding the chromatogram. However, the derivatization procedure is not as robust as some well-established
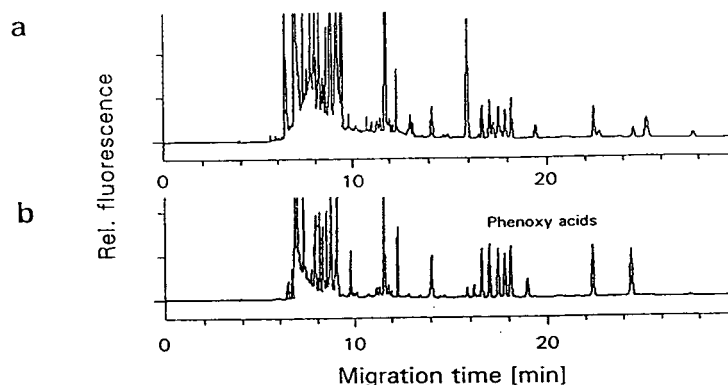
Fig. 3. (a) Trace analysis of phenoxy acid herbicides in an extract of a 250-ml water sample spiked to give 1 nmol/l per acid; (b) reference: direct derivatization of corresponding amounts of phenoxy acids from a stock solution. Peak assignment and other conditions as given in Fig. 2.

procedures. Extracts of real samples may contain compounds that enhance the decomposition of the derivatizing reagent, thus necessitating a modification of the procedure. It is expected that analytical conditions similar to those developed in this work can be applied not only to phenoxy acids, but also to other classes of compounds after derivatization with a suitable fluorescein reagent.

Notice

The U.S. Environmental Protection Agency (EPA), through its Office of Research and Development (ORD), partially funded and collaborated in the research described here. It has been subjected to Agency's peer review and has been approved as an EPA publication. Mention of trade names or commercial products does not constitute endorsement or recommendation for use.

Acknowledgements

References

[1] W.G. Kuhr, Anal. Chem., 62 (1990) 403R–414R.
[2] W.G. Kuhr and C.A. Monnig, Anal. Chem., 64 (1992) 389R–407R.
[3] C.A. Monnig and R.T. Kennedy, Anal. Chem., 66 (1994) 280R–314R.
[4] F. Frantisek, V. Sustacek and P. Bocek, Electrophoresis, 11 (1990) 95–97.
[5] S. Wakida, S. Takeda, M. Yamane, A. Kawahara and K. Higashi, Anal. Sci., 7 (1991) 1109–1110.
[6] J. Cai and Z. El Rassi, J. Liq. Chromatogr., 15 (1992) 1179–1192.
[7] J. Cai and Z. El Rassi, J. Liq. Chromatogr., 15 (1992) 1193–1200.
[8] J. Cai and Z. El Rassi, J. Chromatogr., 608 (1992) 31–45.
[9] Q. Wu, H.A. Claessens and C.A. Kramers, Chromatographia, 34 (1992) 25–30.
[10] C. Desiderio and S. Fanali, Electrophoresis, 13 (1992) 698–700.
[11] G. Dinelli, A. Vicari and P. Catizone, J. Agric. Food Chem., 41 (1993) 742–746.
[12] M. Aguilar, A. Farran and V. Marti, Sci. Total Environ., 132 (1993) 133–140.
[13] M.W.F. Nielen, J. Chromatogr., 637 (1993) 81–90.
[14] M.W.F. Nielen, Trends Anal. Chem., 12 (1993) 345.
[15] D. Crosby and Z. El Rassi, J. Liq. Chromatogr., 16 (1993) 2161–2187.
[16] W.C. Brumley and C.M. Brownrigg, J. Chromatogr., 646 (1993) 377–389.
[17] J.T. Smith, W. Nashabeh and Z. El Rassi, Anal. Chem., 66 (1994) 1119–1133.
[18] J.T. Smith and Z. El Rassi, J. Microcol. Sep., 6 (1994) 127–138.
[19] M.C. Carneiro, L. Puignou and M.T. Galceran, J. Chromatogr. A, 669 (1994) 217–224.

[20] D. Kaniansky, F. Ivanyi and F.I. Onuska, Anal. Chem., 66 (1994) 1817–1824.

[21] Test Methods for Evaluating Solid Waste (SW-846), U.S. Environmental Protection Agency, Washington, DC, Revision 2, November 1992, Methods 8150B-8151.

[22] S. Butz, Th. Heberer and H.-J. Stan, J. Chromatogr. A, 677 (1994) 63–74.

[23] I.S. Kim, F.I. Sasinos, R.D. Stephens, J. Wang and M.A. Brown, Anal. Chem., 63 (1991) 819–823.

[24] T. Suzuki and S. Watanabe, J. Chromatogr., 541 (1991) 359–364.

[25] R.D. Haugland, Handbook of Fluorescent Probes, Molecular Probes, Eugene, OR, USA, 1992, pp. 42–53, 134, and references cited therein.

[26] D.R. Knapp, Handbook of Analytical Derivatization Reactions, Wiley Interscience, New York, 1979.

[27] J. Schneede, J.H. Mortensen, G. Kvalheim and P.M. Ueland, J. Chromatogr. A, 669 (1994) 185–193.

[28] W. Dünges, Chromatographia, 9 (1976) 624–626; Anal. Chem., 49 (1977) 442–445.

[29] S. Lam and E. Grushka, J. Chromatogr., 158 (1978) 207–214.

[30] M.T. Shipchandler, J.R. Fino, L.D. Klein and C.L. Kirkemo, Anal. Biochem., 162 (1987) 89–101.

[31] P.A. Paprica, A. Margaritis and N.O. Petersen, Bioconjugate Chem., 3 (1992) 32–36.

[32] J.C. Sheehan and G.P. Hess, J. Am. Chem. Soc., 77 (1955) 1067–1068.

[33] W. König and R. Geiger, Chem. Ber., 103 (1970) 788–798 (in German).

[34] Technical Information Bulletin No. AL-168, Aldrich, Milwaukee, WI, USA, 1988.

[35] Y. Mechref and Z. El Rassi, Electrophoresis, 15 (1994) 627–634.

ELSEVIER

Determination of polycyclic aromatic hydrocarbons in soil samples by micellar electrokinetic capillary chromatography with photodiode-array detection

Oliver Brüggemann, Ruth Freitag[*]

Institut für Technische Chemie, Universität Hannover, Callinstr. 3, D-30167 Hannover, Germany

Abstract

The reliable quantification even of trace amounts of polycyclic aromatic hydrocarbons (PAHs) is of great concern in environmental and also in medical analysis. PAHs are typically small, uncharged, hydrophobic molecules which do not dissolve well in water. Several methods were investigated and compared for the determination of such substances by capillary electrophoresis, including systems where the analytes are provided with a charge (tetraalkylammonium ions) via solvophobic interaction and systems based on micellar electrokinetic capillary electrophoresis (MECC) using sodium dodecyl sulphate (SDS) and cetyltrimethylammonium bromide as micelle-forming agents. Diode-array detection permitted the positive identification of the separated pure substances via their prerecorded UV–Vis spectra. By using an aqueous–organic electrophoresis buffer [8.5 mM borate, 85 mM SDS, 50% (v/v) acetonitrile, pH 9.9], a mixture of seven standard PAHs could be separated and quantified within 10 min. The detection limit was 10 pg. The calibration graph was linear over five orders of magnitude. Compared with the chromatographic analysis used so far, the MECC method is faster, has a higher mass sensitivity and requires a smaller sample volume. The method was used to quantify the PAH content of soil samples (heath sand) deliberately contaminated with a mixture of standard PAHs and with machine oil. Two PAHs (anthracene and chrysene) could be determined in samples collected during a biological soil decontamination process.

1. Introduction

Polycyclic aromatic hydrocarbons (PAHs) contain at least two aromatic rings in their basic structure. Nowadays they are released in large amounts into the environment when oil, coal, wood and related energy sources are converted. Adhering to dust particles, they are then ubiquitously distributed and as hydrophobic substances are enriched in the soil or on entering the food chain, in the fatty tissue of humans and animals. Although less toxic than, e.g., benzene, a number of PAHs have been established as carcinogenic and mutagenic. These potential hazards call for reliable and sensitive PAH determinations in soil and water samples and also in blood and tissue specimens.

Although the total number of PAHs is large, certain of them have been named by governmental agencies such as the US Environmental Protection Agency (EPA) (sixteen PAHs) as indicators of PAH contamination in general. A requirement for soil decontamination will be

---

* Corresponding author.

based on the analysis of these sixteen EPA PAHs.

Currently, the determination of these substances is dominated by chromatographic methods such as reversed-phase HPLC [1–8]. Capillary electrophoresis (CE) has become a serious competitor to HPLC in various analytical fields. PAHs, however, appear to be singularly unsuited to CE analysis. In CE the analytes are separated based on differences in their migration velocity in an electrical field. Aqueous buffers are used. Typical PAHs such as anthracene, phenanthrene, fluoranthene and benz[a]anthracene are neutral, non-ionizable molecules, of similar hydrophobicity, which do not dissolve well in water in large amounts. The smallness of the required sample, however, together with the high separation power and mass sensitivity, which are inheritant to CE methods, would extend the scope of PAH analysis, e.g., to single cells, airborne water droplets or the determination of PAH metabolites produced by humans or PAH-degrading bacteria.

Only a few approaches to the determination of PAHs by CE have been reported. In one type the analytes are supplied with a charge by forced complex formation with tetraalkylammonium ions and then separated by conventional capillary zone electrophoresis [9,10]. Aqueous–organic (acetonitrile–water) media with various water contents are used as electrophoresis buffers in this approach. More common is separation by micellar electrokinetic capillary chromatography (MECC), often in the presence of sodium dodecyl sulphate (SDS) as a micelle-forming agent and a second migration modifier such as γ-cyclodextrin or methanol [11–15]. Investigations have so far been restricted to the analysis of standard solutions [16]. By using conventional UV detection, a detection limit in the femtomole range is usually attainable, and by using the native UV and fluorescence properties of the PAH for detection, even subattamole levels may be reached [10].

Both UV and fluorescence detection are unspecific. Substances are identified mainly by their migration times. Although this is highly informative in the case of reference or standard samples, it is often not sufficient in the case of real environmental or pharmaceutical samples. Here components of the sample matrix may influence the migration of the analyte to an extent where reliable identification is no longer possible by migration time alone. In addition, often not only the original PAHs are of interest, but also their metabolites, which also constitute highly active carcinogens. Since the metabolic pathways are at present not fully known, little information is available on the exact nature of these derivatives. Specific information on the analytes may be obtained by a coupled technique such as CE–MS, but also by using diode-array detector, which in comparison is a fairly simple and inexpensive alternative. With diode-array detection the entire UV–Vis spectrum of each analyte becomes available and thus enables assumptions to be made concerning the molecular structure.

In this paper, a method is described for the CE determination of PAHs in soil samples with the use of diode-array detection for the on-column identification of the individual substances.

2. Experimental

2.1. Chemicals

Sodium dodecyl sulphate (SDS) was obtained from Serva (Heidelberg, Germany), cetyltrimethylammonium bromide (CTAB) from Lancaster (Morecambe, UK) and boric acid from Merck (Darmstadt, Germany).

2.2. Standards

The PAH standard used contained seven PAHs (anthracene, benzo[a]pyrene, chrysene, fluoranthene, fluorene, phenanthrene and pyrene) at a concentration of 1 mg/ml each. The solvent was acetonitrile.

A mixture of machine oils was obtained from a garage in Hannover, Germany.

2.3. Capillary electrophoresis

CE was performed on a Hewlett-Packard 3D-CE instrument. For data collection, data analysis, spectral identification and system control, HP 3D-CE (Rev. A. 01.02.) software was used. Detection was by measurement of UV–Vis absorbance with a photodiode-array detector (total range, 190–690 nm; range used, 190–350 nm). Capillaries were obtained from Hewlett-Packard (Böblingen, Germany) or CS-Chromatographie Service (Langerwehe, Germany). Unless indicated otherwise, 8.5 mM borate buffer (pH 9.9) containing 85 mM SDS and 50% (v/v) acetonitrile was used as the electrophoresis buffer. The capillary dimensions were 28 cm (from inlet to the detector) × 50 μm I.D., a voltage of 30 kV was applied and the capillaries were thermostated at 20°C. Pressure injection (30 mbar, 5 s) was used. After each analysis, the capillaries were regenerated with consecutive washes with 0.1 M NaOH (1 min) and electrophoresis buffer (2 min).

The buffer in the outlet vial was exchanged after each run to improve the reproducibility. After each injection the capillary was briefly dipped in a second buffer vial to remove all traces of sample from the outer capillary wall.

2.4. Contamination of soil samples

A 10 g amount of sand (heath) was wetted with 0.5 ml of a solution containing the seven standard PAHs each at a concentration of 1 mg/ml.

A 30 g amount of sand (heath) was contaminated with 1 ml of spent machine oil. Extraction was carried out after 2 h.

2.5. Extraction of soil samples

In the standard procedure, 0.5 g of soil was extracted with 6 ml cyclohexane with vigorous shaking (15 min), washed with an additional 4 ml of cyclohexane, evaporated to dryness and the residue dissolved in 0.5 ml of acetonitrile.

After contamination with machine oil, 10 ml of cyclohexane were used for extraction of 10 g soil (10 ml for washing). The dried residue was dissolved in 2.5 ml of acetonitrile.

2.6. Biological soil decontamination

Samples from a biological soil decontamination process were kindly provided by D. Brinkmann (Institut für Technische Chemie, University of Hannover, Germany). In this process, the water content of the PAH-containing soils is increased to a point where the resulting slurries can be handled in an airlift or rotating drum reactor [17,18]. The soil decontamination is then performed with a mixed culture of aerobic bacteria capable of PAH digestion. At this point it is not clear whether the PAHs are completely converted into CO_2 and H_2O or whether more complex (and putatively still harmful) metabolites are produced. PAH-determination is carried out by reversed-phase chromatography (column dimensions, 100 mm × 4.6 mm I.D.; stationary phase, adsorbosphere C_{18} (Alltech), particle diameter 3 μm; mobile phase, acetonitrile–water (86.4:13.6); flow-rate, 1.26 ml/min; detection wavelength, 254 nm).

3. Results and discussion

The separation of electrically neutral molecules of similar size and hydrophobicity by CE is difficult. Unless the analytes can somehow be converted into charged species, MECC may often constitute the only way to effect such an analysis.

Since charged molecules can often be separated in free solution whereas MECC requires complex electrolysis buffers, first we tried the solvophobic method introduced by Walbroehl and Jorgenson [9] for PAH separation. In this method, the hydrophobic analytes are forced to form complexes with tetraalkylammonium ions. However, neither the commonly used tetrahexyl-
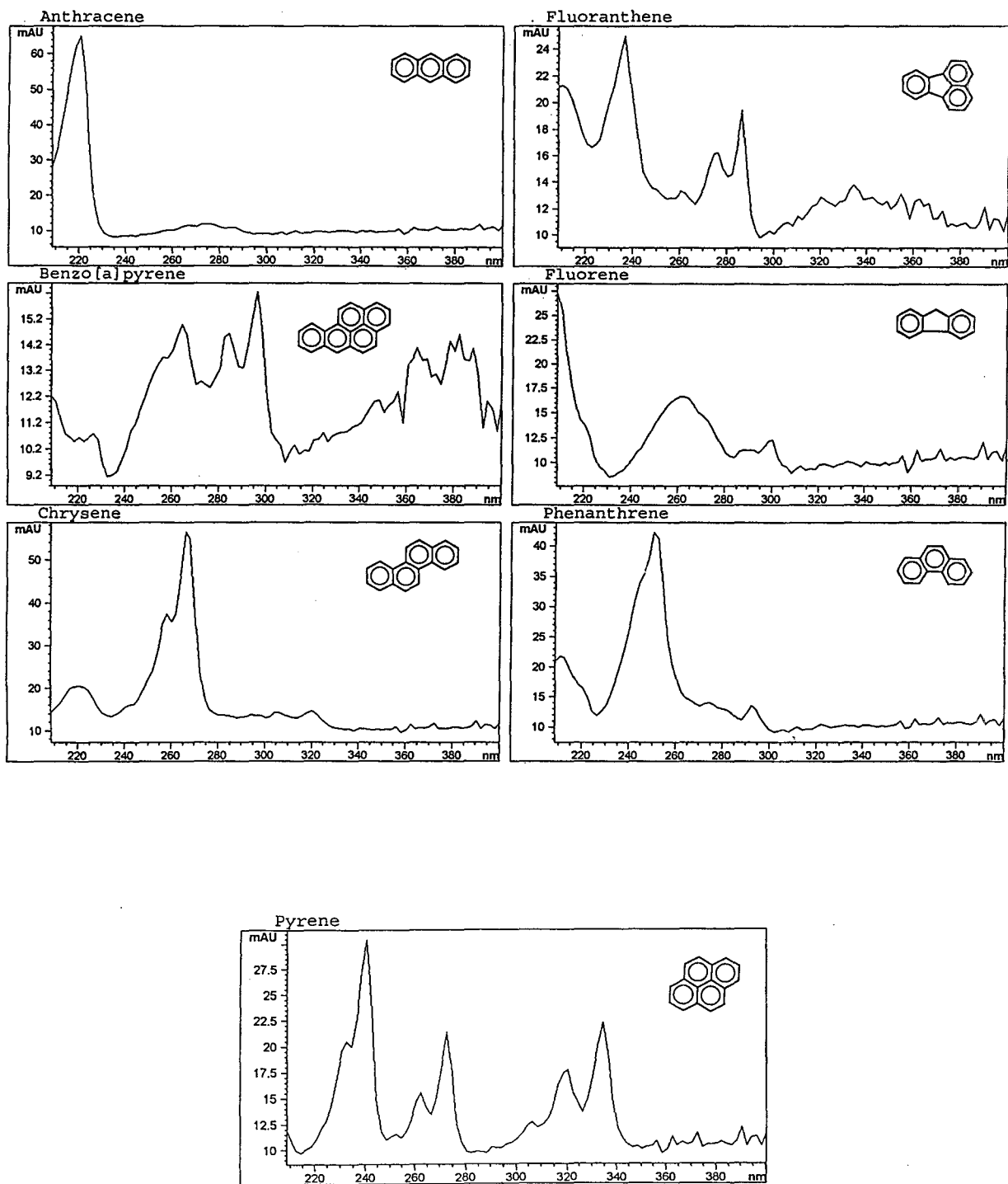
Fig. 1. UV–Vis spectra of the standard PAHs.

ammonium ion nor the use of tetraheptylammonium, tetraoctylammonium, tetradodecylammonium, tetraacetylammonium, N-(2-ethylhexyl)trimethylammonium or N-octyltrimethylammonium ions resulted in an applicable method. Acetonitrile–water mixtures of various compositions were investigated and the effect of different modifier concentrations was evaluated, but to no avail. In addition, the bromides used here were difficult to dissolve in the aqueous–organic buffers.

MECC is the classical CE method for the analysis of neutral hydrophobic molecules. The surface charge of the micelles draws them at a characteristic speed towards the corresponding electrode, in the case of SDS this being the anode, i.e., under standard conditions opposite to the electroendosmotic flow (EOF) and away from the detector. Largely governed by their hydrophobicity, the analytes will partition between the hydrophobic interior of the micelles and the bulk of the electrophoresis buffer, where the migration of neutral molecules will in uncoated capillaries be determined by the EOF. As in reversed-phase chromatography, which is governed by similar interactions, the attractiveness of the bulk buffer phase may be enhanced by the addition of an organic modifier such as acetonitrile.

Since the differences in hydrophobicity of the PAHs are not very pronounced, the addition to the electrophoresis buffer of a second substance, such as γ-cyclodextrin, has been suggested, which also interacts actively with the analytes
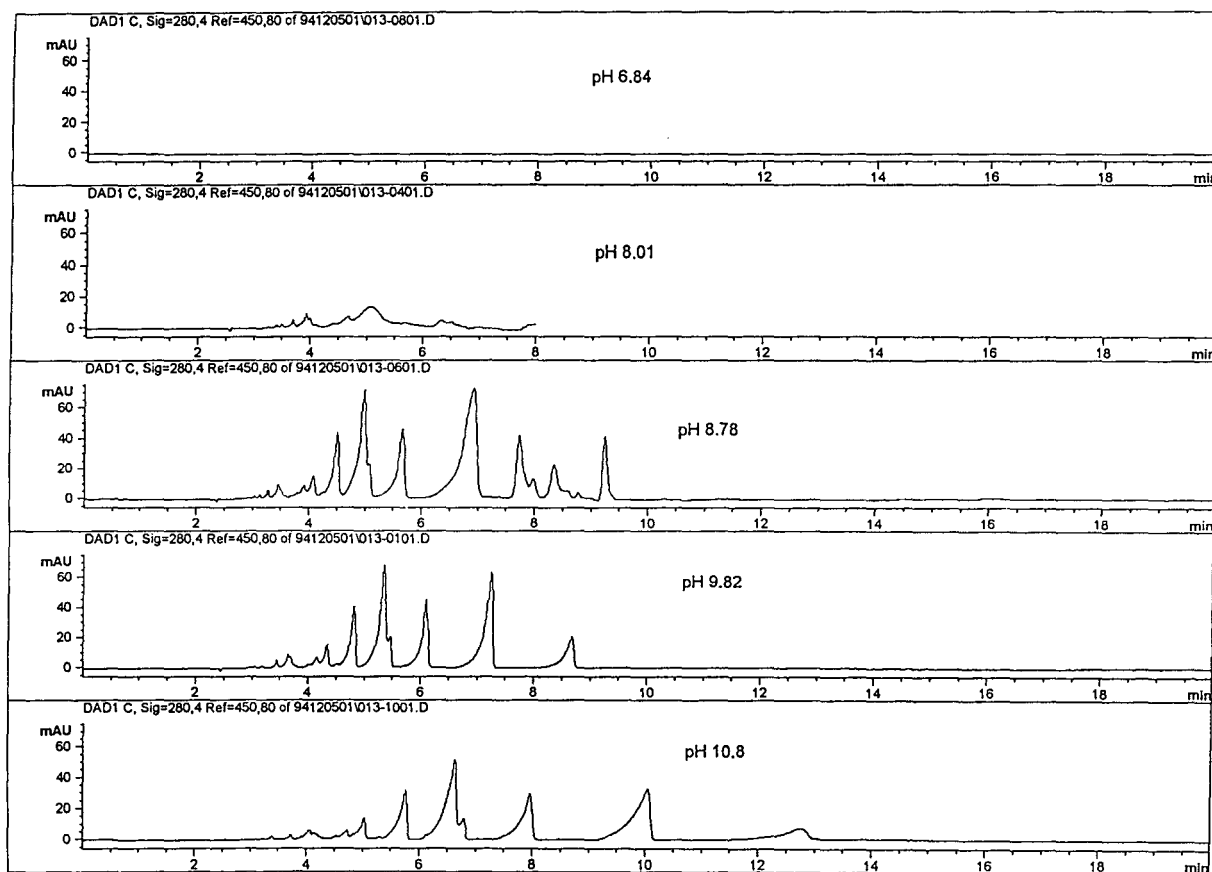
Fig. 2. Influence of buffer pH on the PAH separation.

[14,15]. However, this renders the fine tuning of the analytical conditions difficult and we found the modification of the bulk buffer by addition of acetonitrile to be more suited to our purposes.

3.1. Method development

Capillary dimensions

For method development, a PAH standard mixture was used that contained anthracene, fluorene, phenanthrene, fluoranthene, pyrene, chrysene and benzo[a]pyrene in acetonitrile at a concentration of 1 mg/ml each. The UV–Vis spectra of these standard PAHs were compiled into a spectral bank (Fig. 1). Unless indicated otherwise, the capillaries had an I.D. of 50 μm and an effective length (inlet to detector) of 28

cm. A larger I.D. resulted in a lower detection limit owing to the increase in the optical path length. However, as high voltages of up to 30 kV were used, the ensuing radial temperature gradient was detrimental to the resolution in the case of, e.g., a 100 μm capillary. Hewlett-Packard offers the use of bubble cell capillaries to circumvent this problem, but we did not find these capillaries useful in our case. An effective capillary length of 28 cm represents a compromise between the resolution and the duration of an analysis.

Influence of the buffer pH

The influence of the pH of the electrophoresis buffer on the separation is depicted in Fig. 2. At
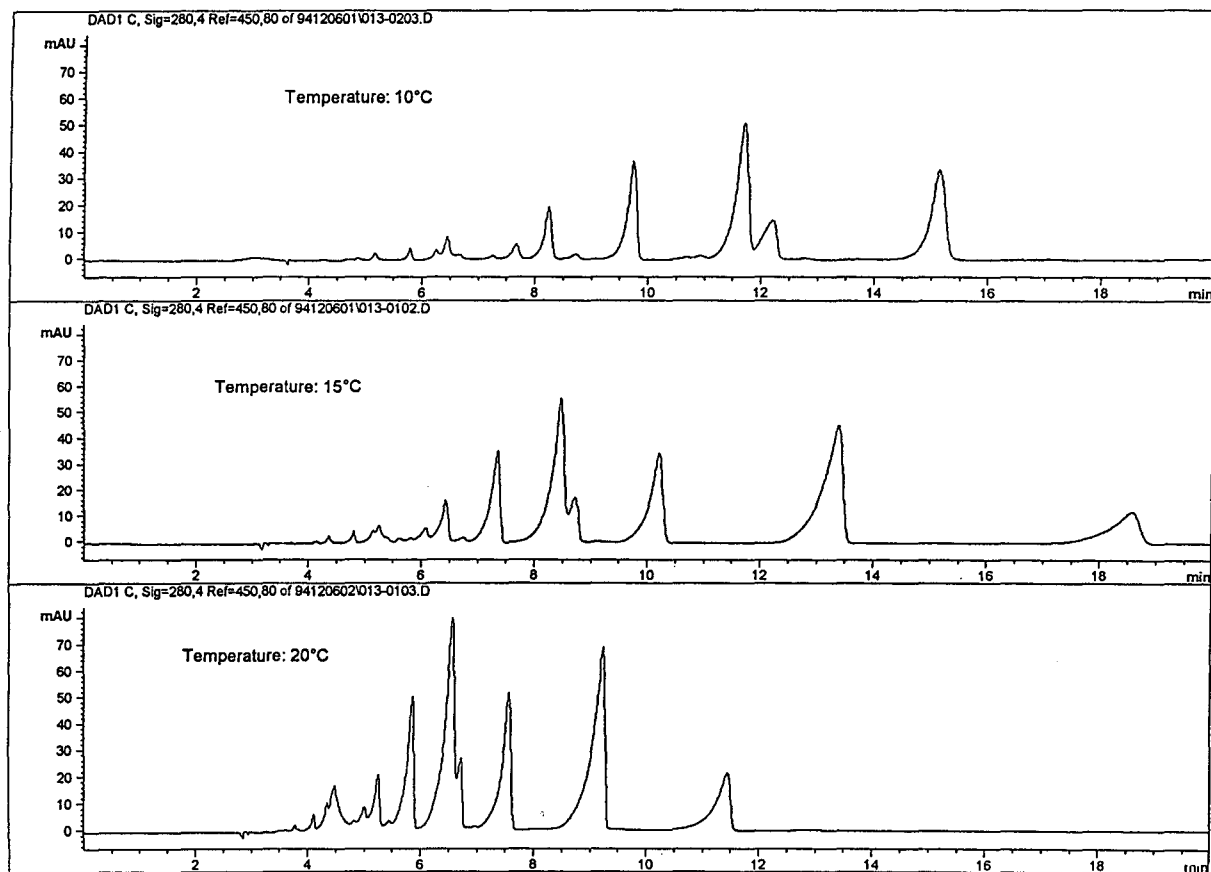
Fig. 3. Influence of temperature on the PAH separation.
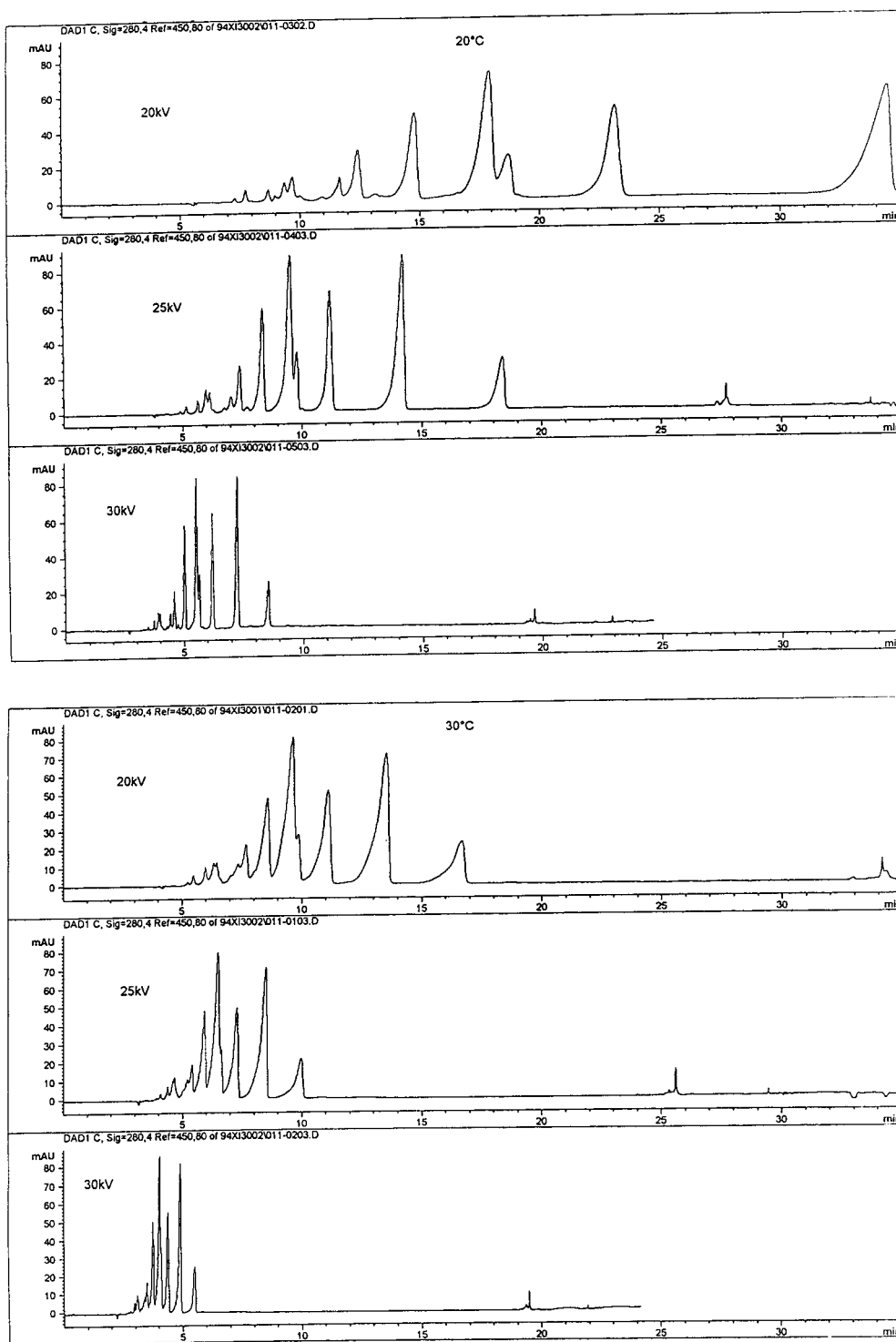
Fig. 4. Influence of applied voltage on the PAH separation.

a pH of 6.5 no signals are detected. Presumably the EOF is not strong enough in this case to counteract the movement of the micellar phase towards the capillary inlet. If a pH of more than 8.0 is applied, the analytes begin to pass the detector, but the separation is not satisfactory. If the pH is increased further, the separation improves to some extent, while the migration time increases with increasing pH. A buffer pH of 9.9 was adopted for standard applications, since it combined good resolution with a comparatively short analysis time. A borate-based buffer was chosen, since this yielded the lowest background absorption in the wavelength range investigated. Compared with a phosphate buffer of similar

ionic strength, the electric current and thus the Joule heat produced were lower for a given voltage. With regard to the detrimental effect of heat in general, a low buffer concentration of 8.5 mM was used. This, however, calls for an exchange of the buffer in the capillary vials after each NaOH wash, or else its pH and concomitantly the electrophoretic character of the CE system are altered.

Influence of temperature and applied voltage

Temperature and applied voltage also influence the duration and to some extent the resolution of a given separation. The migration time will increase with decreasing temperature (Fig.
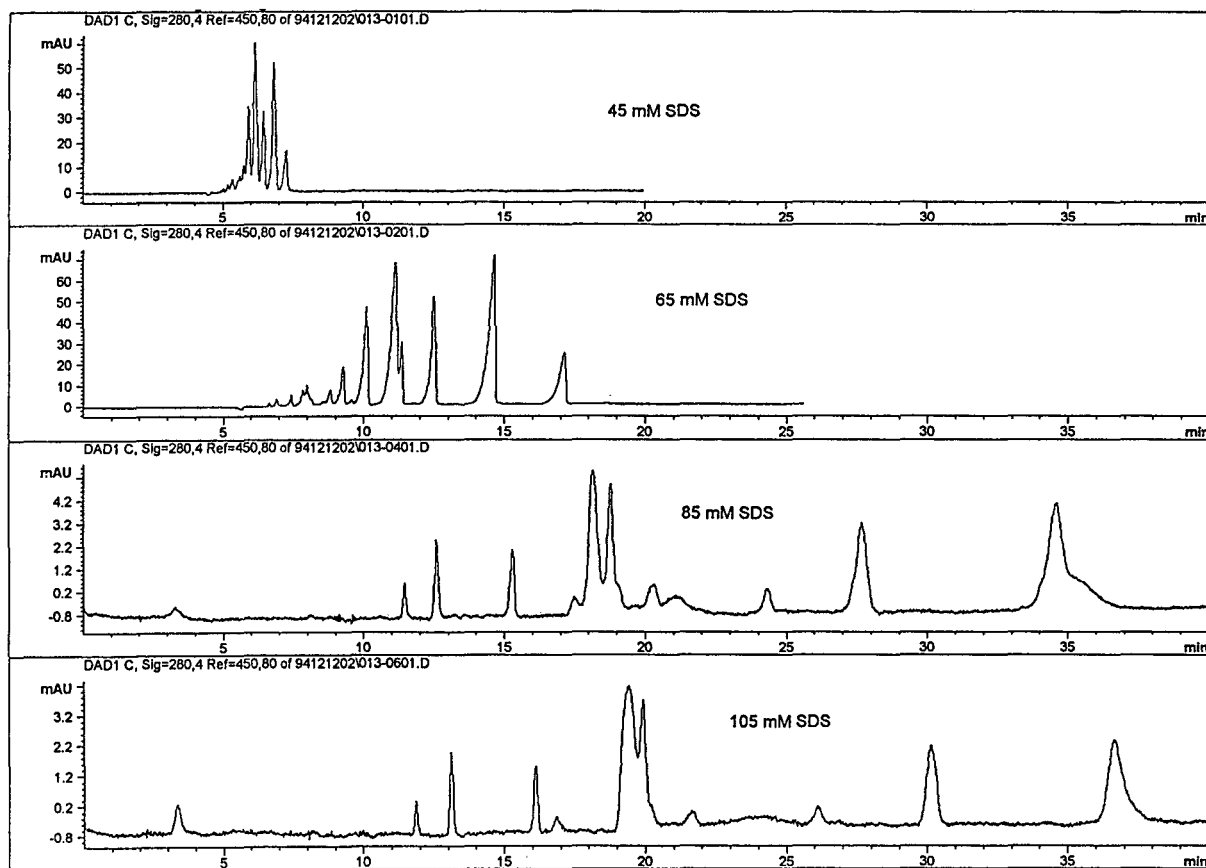
Fig. 5. Influence of SDS concentration on the PAH separation.

3), since the viscosity of the buffer will also increase in that case. Increasing the applied voltage from 20 to 25 and 30 kV for a given temperature reduces the migration time in all cases (Fig. 4). However, at 30°C no baseline separation was found even in those cases, e.g., at 25 kV, where the separation took longer than a similar separation performed at 20°C and 30 kV. A voltage of 30 kV was therefore adopted for standard PAH determinations, while the capillary was thermostated at 20°C. Under these conditions, good resolution of the PAH standard mixture was achieved, with the exception of fluoranthene and pyrene. These two PAHs can, however, still be identified via their UV–Vis

spectra and be quantified from the peak height. This is not possible with the reversed-phase chromatographic method used as the reference method for PAH determination.

Influence of micelle and modifier concentration

The influence of the SDS concentration of the PAH separation was investigated using a 40 cm capillary and the above-defined standard conditions. As other workers, we observed an increase in migration time on increasing the SDS concentration, i.e., from 45 to 65, 85 and 105 mM [14]. SDS concentrations below the critical micelle concentration were not investigated. The observed increase is caused by the increase in
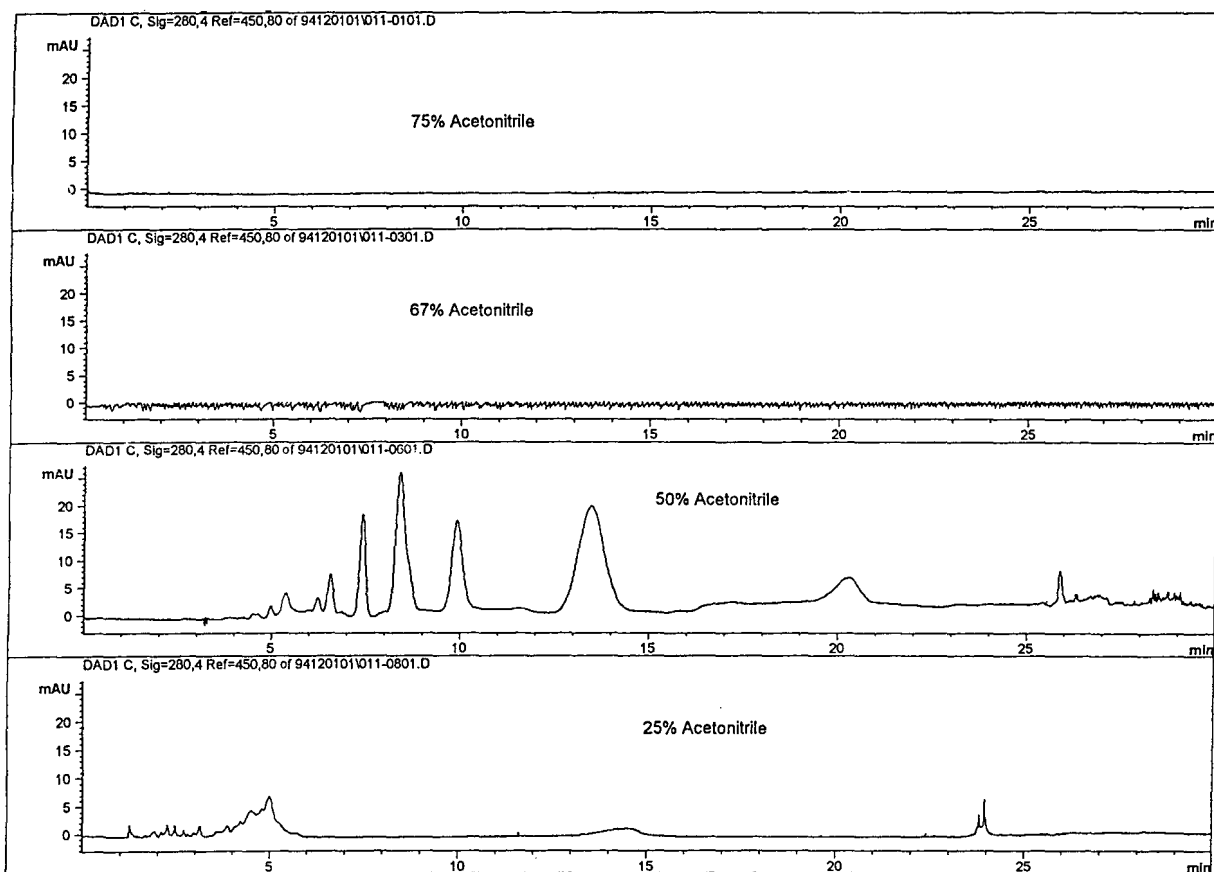
Fig. 6. Influence of acetonitrile concentration on the PAH separation.

micelle concentration. The resolution in terms of a fluoranthene–pyrene separation was best with an SDS concentration of 85 mM (Fig. 5).

Similar reasoning led to the addition of 50% acetonitrile to the electrophoresis buffer (Fig. 6). At too low an acetonitrile concentration the solubility of the analytes is low and at too high a concentration micelle formation appears to suffer interference.

3.2. CTAB as micelle forming agent

A similar development led to an alternative method in which CTAB rather than SDS was employed as a micelle-forming agent. The 50 mM borate buffer (pH 9.5) used contained 100 mM CTAB and 25% acetonitrile. The capillaries had an optimum length of 58 cm and an I.D. of 75 μm. The capillaries were thermostated at 25°C and a voltage of 20 kV was applied. However, with this method the resolution, especially of fluoranthene and pyrene, was inferior to that in the SDS method (Fig. 7).

3.3. Applications

A detection limit of 10 ng/μl, i.e., 10 pg, was established for the developed method. The calibration graph is linear over five orders of magnitude (Fig. 8). An analysis requires less than 10
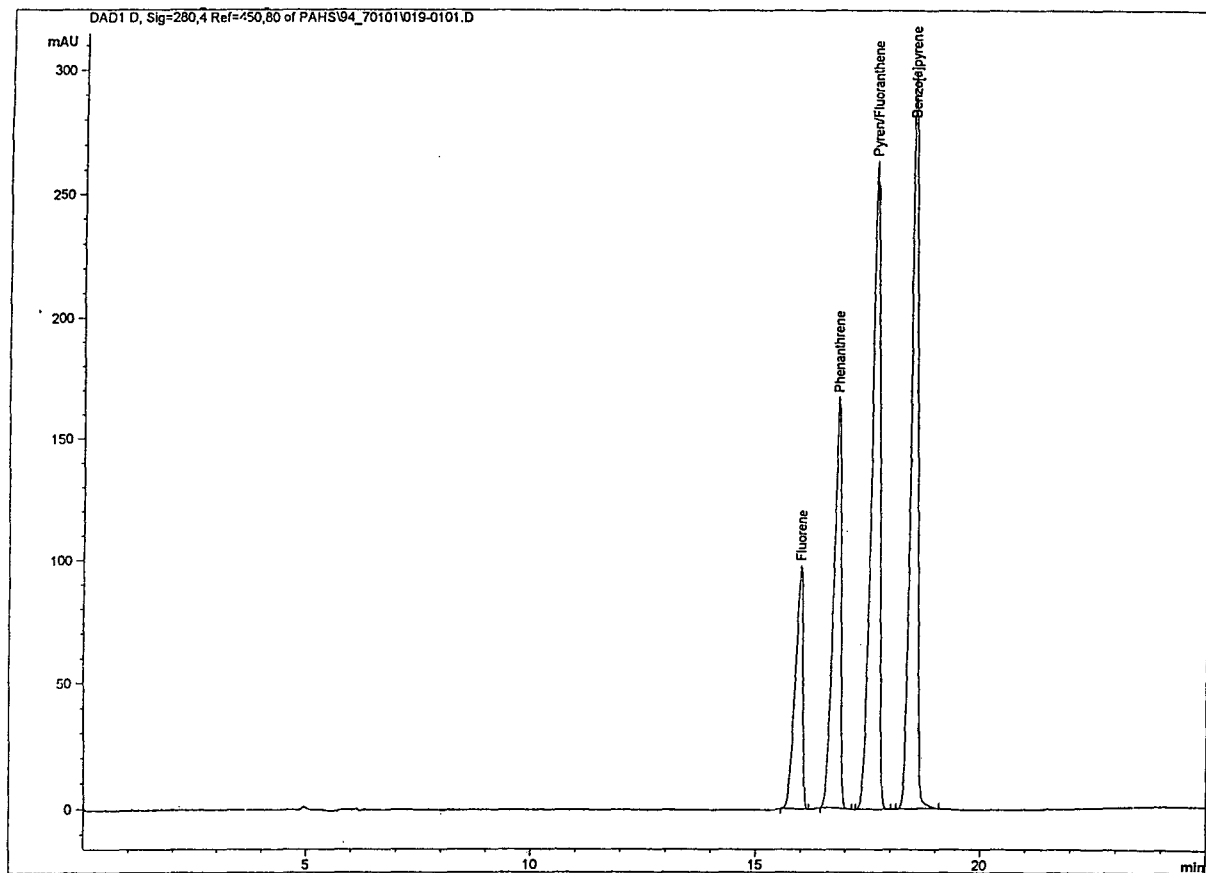
Fig. 7. Separation of a five PAH standard mixture by the CTAB method.
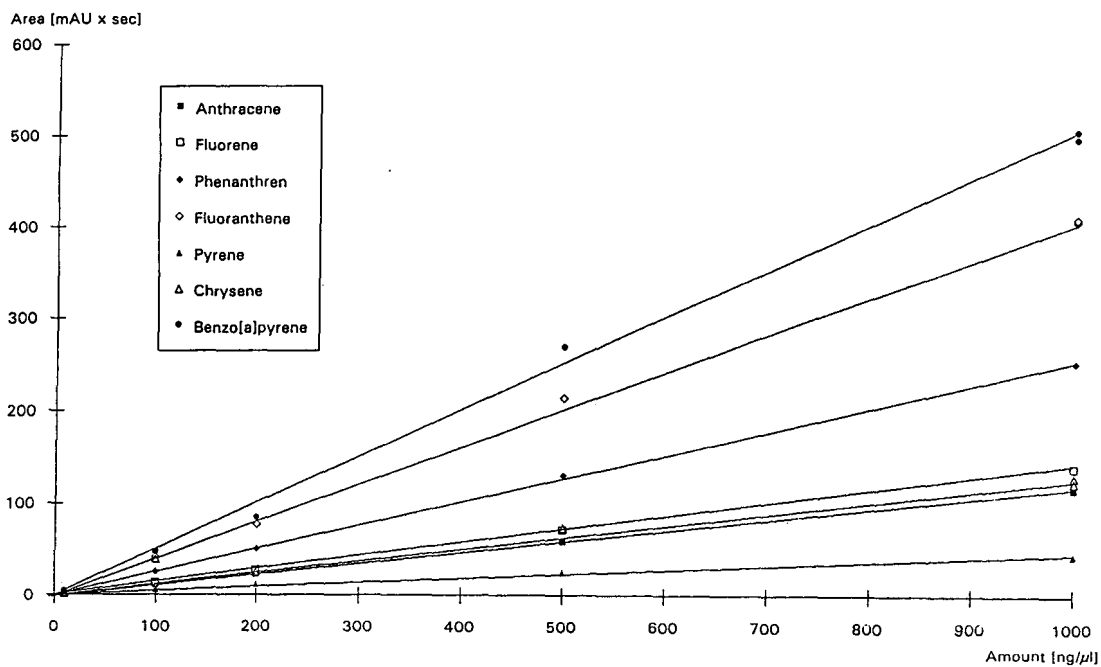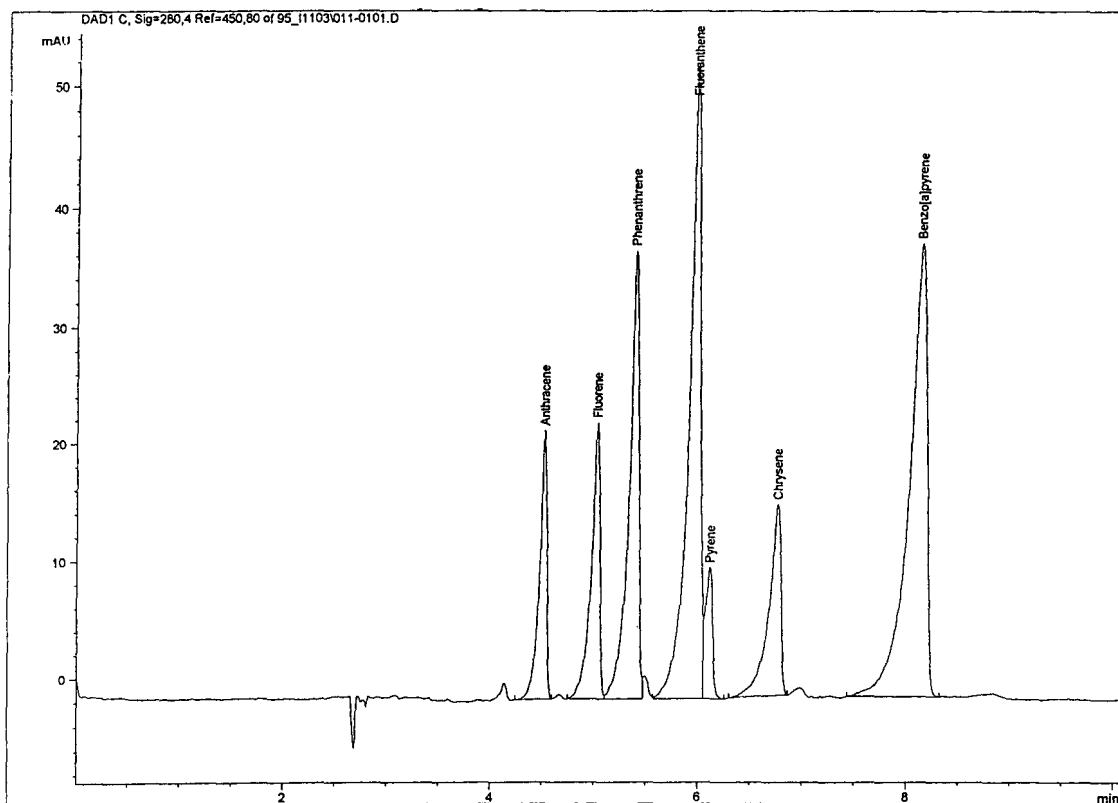
Fig. 8. Calibration graph for the standard PAHs (SDS method).
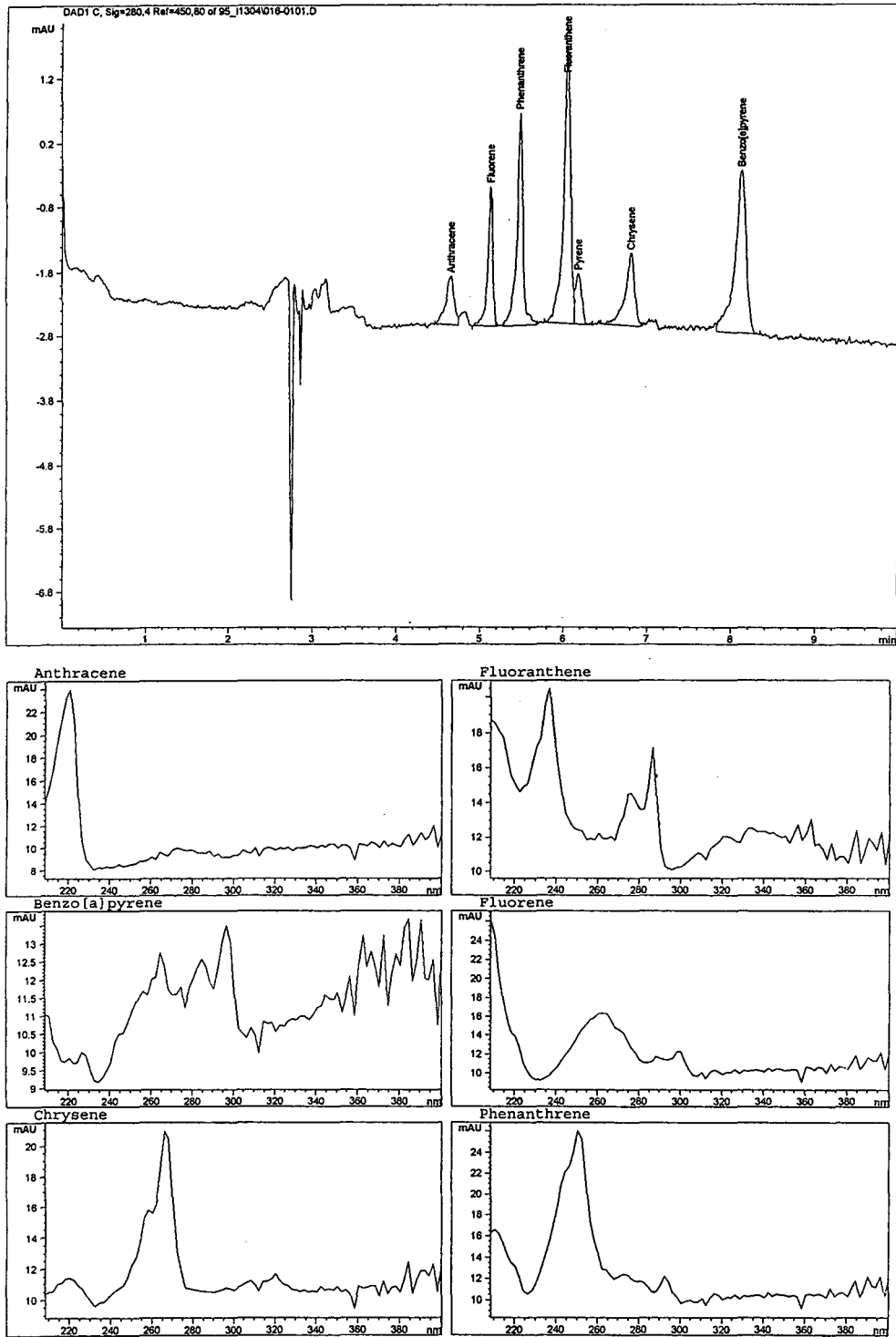
Fig. 9.
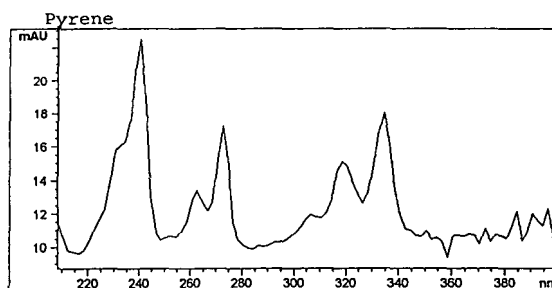
Fig. 9. Analysis of a soil sample contaminated with a PAH mixture. The spectra assigned to the peaks are also given.

min. The analytes are well separated and can be positively identified by comparison with their stored reference UV–Vis spectra. To increase the reproducibility of an analysis, the use of an internal standard, most conveniently the acetonitrile peak, is recommended. In comparison, 40 min are required for an analysis using the conventional RP-HPLC method. There the detection limit is 0.5 ng and no separation of fluoranthene and pyrene is possible.

Analysis of a soil sample contaminated by a PAH mixture

Ultimately, the developed method is to be used to monitor the success of the decontamination of PAH-polluted soils by PAH-degrading bacteria. To simulate such an analysis, a "soil sample", i.e., 10 g of sand (heath), was "contaminated" with 0.5 ml of a solution containing seven PAHs each at a concentration of 1 mg/ml. The standard extraction procedure that had
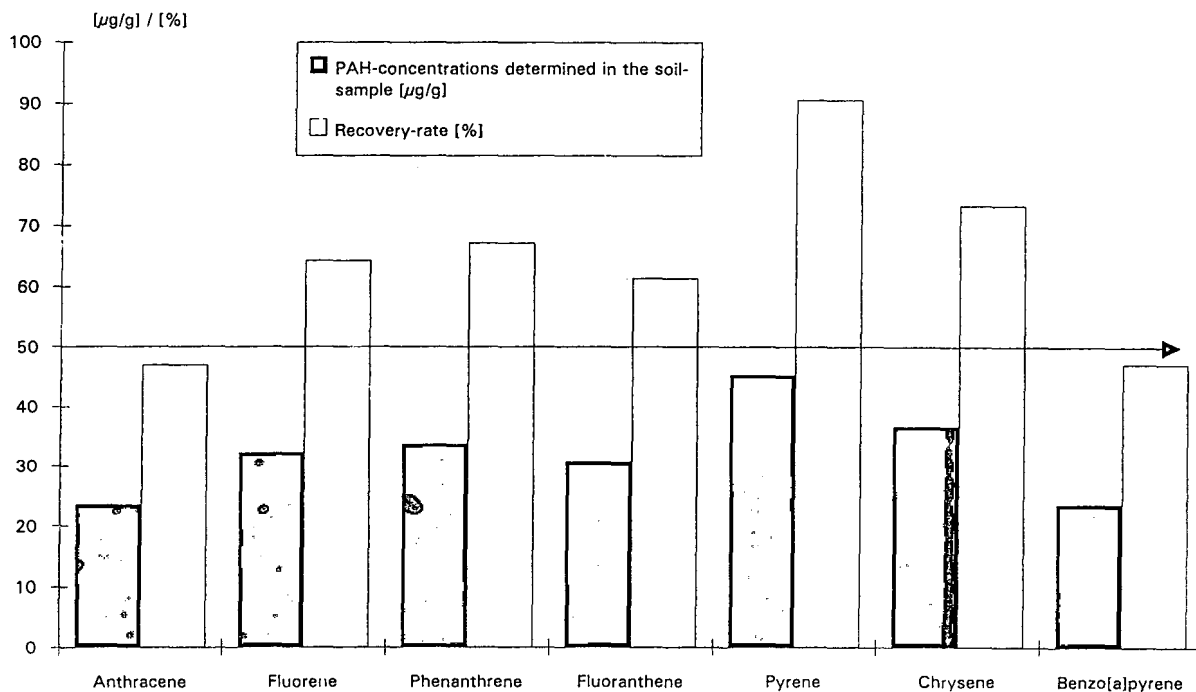
Fig. 10. Quantification of the various PAHs identified in the soil sample compared with the original amount.

originally been developed for the RPC analysis was used to prepare the sample for analysis. The results are depicted in Fig. 9. All substances are identified by their spectra. The quantification is unsatisfactory, as only 45–90% of the original amount is recovered (Fig. 10). Further efforts need to be directed towards the optimization of the extraction procedure.

Analysis of a soil sample contaminated by machine oil

Soil contamination was also simulated with spent machine oil. A 30 g amount of sand (heath) was contaminated with 1 ml of spent machine oil. After 2 h, extraction (by a modified

procedure) and MECC analysis were carried out. The MECC analysis yielded reproducible results, an example being given in Fig. 11. However, no PAH identification was possible. Presumably, either no pure substances were separated or the PAHs considered so far were not present in this sample.

Analysis of samples collected during a biological soil decontamination process

In the samples collected during a biological soil decontamination process, chrysene and anthracene could be identified and determined (Fig. 12).
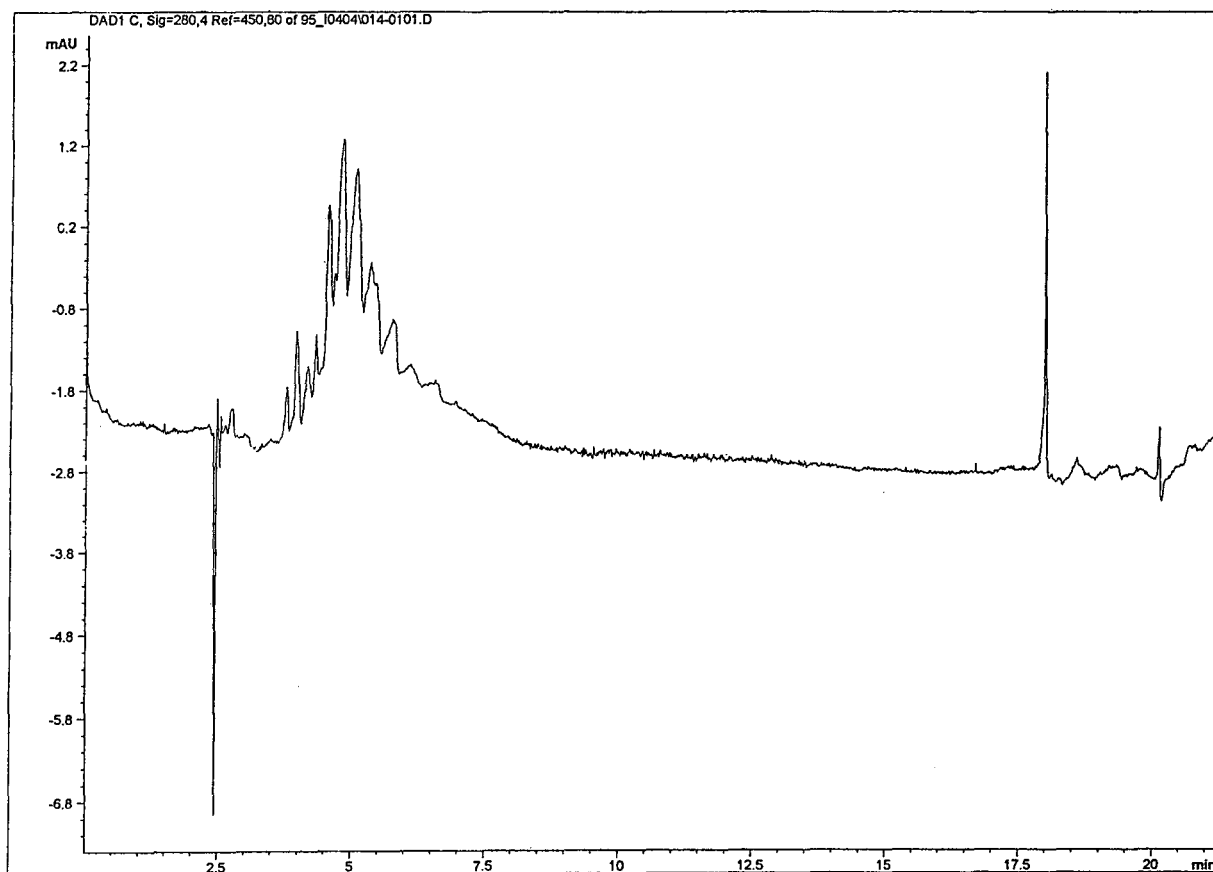
Fig. 11. Analysis of a soil sample contaminated with machine oil.
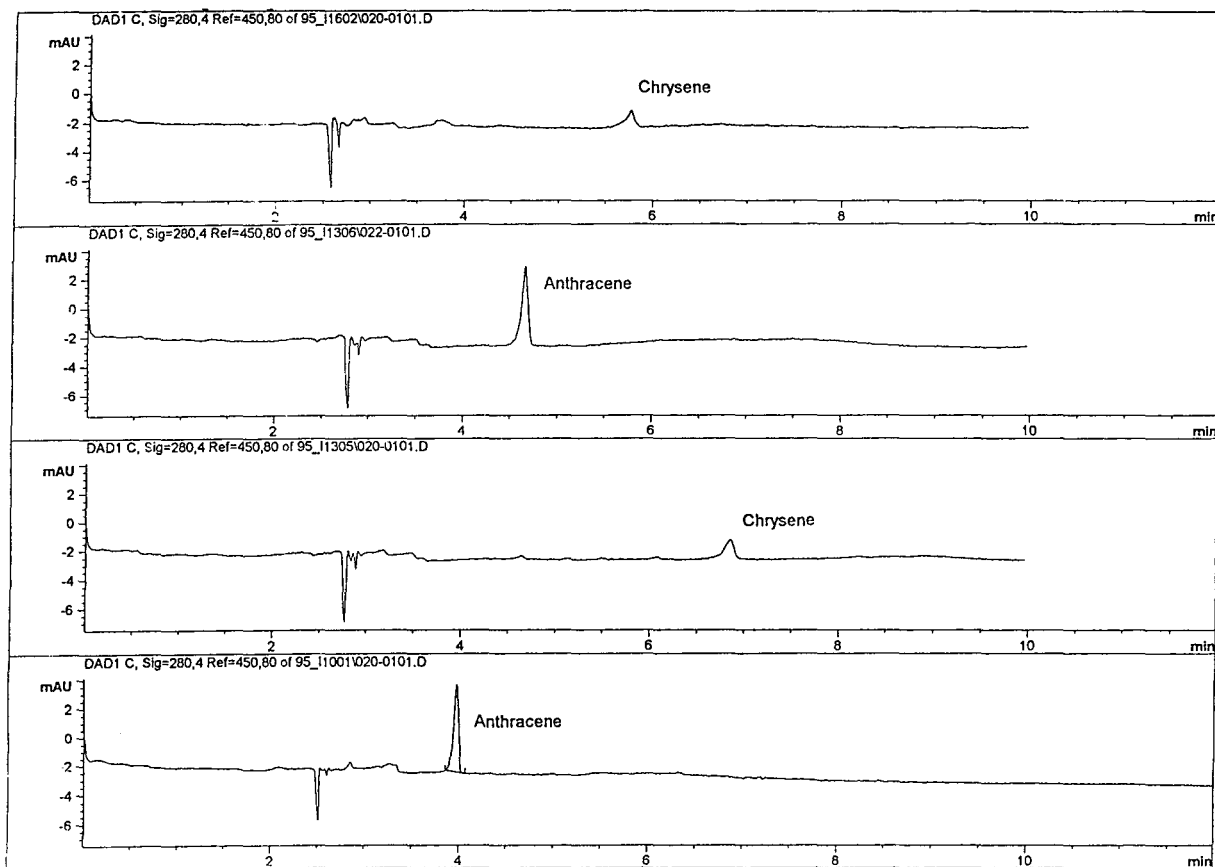
Fig. 12. Analysis of soil samples collected during a biological soil decontamination procedure.

Acknowledgements

References

[1] T. Vo-Dinh (Editor), Chemical Analysis of Polycyclic Aromatic Compounds, Wiley, New York, 1989.
[2] J. Bundt and R. Stegmann, GIT Spezial Chromatogr., 2 (1993) 64.
[3] K. Krengel-Rothensee, Bioengineering, 1 (1993) 13.
[4] M. Battista, A. di Corcia and M. Marchetti, J. Chromatogr., 454 (1988) 233.
[5] US EPA, Determination of Polycyclic Aromatic Hydrocarbons in Drinking Water by HPLC with Liquid–Solid Extraction, Method 550, EPA Environmental Monitoring Systems Laboratory, Office of Research and Development, Cincinnati, OH, 1990.
[6] US EPA, Determination of Polycyclic Aromatic Hydrocarbons in Drinking Water by HPLC with Liquid–Solid Extraction, Method 550.1, EPA Environmental Monitoring Systems Laboratory, Office of Research and Development, Cincinnati, OH, 1990.
[7] US EPA, Determination of Polycyclic Aromatic Hydrocarbons in Municipal and Industrial Discharges, Method 610, EPA Environmental Monitoring Systems Laboratory, Office of Research and Development, Cincinnati, OH, 1982.

[8] US EPA, Determination of Polycyclic Aromatic Hydrocarbons in Ground Water and Wastes, Method 8310, EPA Environmental Monitoring Systems Laboratory, Office of Research and Development, Cincinnati, OH, 1986.

[9] Y. Walbroehl and J.W. Jorgenson, Anal. Chem., 58 (1986) 479.

[10] S. Nie, R. Dadoo and R.N. Zare, Anal. Chem., 65 (1993) 3571.

[11] S. Terabe, Y. Miyashita, O. Shibata, E.R. Barnhart, L.R. Alexander, D.G. Patterson, B.L. Karger, K. Hosoya and N. Tanaka, J. Chromatogr., 516 (1990) 23.

[12] S. Terabe, Y. Miyashita, Y. Ishihama and O. Shibata, J. Chromatogr., 636 (1993) 47.

[13] R.O. Cole, M.J. Sepaniak, W.L. Hinze, J. Gorse and K. Oldiges, J. Chromatogr., 557 (1991) 113.

[14] Y.F. Yik, C.P. Ong, S.B. Khoo, H.K. Lee and S.F.Y. Li, Environ. Monit. Assess., 19 (1991) 73.

[15] Y.F. Yik, C.P. Ong, S.B. Khoo, H.K. Lee and S.F.Y. Li J. Chromatogr., 589 (1992) 333.

[16] P. Schmitt and A. Kettrup, GIT, 12 (1994) 1312.

[17] J. Parthen, Ph.D. Thesis, University of Hannover, 1992.

[18] D. Brinkmann, Ph.D. Thesis, University of Hannover, 1995.

Separation of desulphoglucosinolates by micellar electrokinetic capillary chromatography based on a bile salt

Charlotte Bjergegaard[a], Søren Michaelsen[b], Peter Møller[a], Hilmer Sørensen[a],[*]

[a]*Chemistry Department, Royal Veterinary and Agricultural University, 40-Thorvaldsensvej, DK-1871 Frederiksberg C, Denmark*
[b]*Novo Nordisk A/S, Enzyme Research, Microbial Metabolism, Novo Allé, DK-2880 Bagsværd, Denmark*

Abstract

Micellar electrokinetic capillary chromatography (MECC) has been developed as a promising method for the determination of 40 desulphoglucosinolates. A sodium cholate based MECC method was found to be efficient for the qualitative and quantitative analysis of desulphoglucosinolates produced in an on-column, enzymatic step from the corresponding intact glucosinolates. Separation conditions and sensitivity of the method have been optimised with respect to different parameters, including capillary types, where the 75-μm I.D. capillary increased the sensitivity 2.5 times over that of a 50-μm capillary. With use of a high-sensitivity optical cell assembly (Z-cell), the sensitivity was further increased ten times, resulting in detection of picogram amounts, or concentration levels corresponding to 10^{-6} M. Repeatability with a 75-μm capillary was good, with the relative standard deviation varying between 0.2% and 0.9% for relative migration times and for relative normalised areas between 1.0% and 3.0%. Linearity of the optimised method gave correlation coefficients between 0.99 and 0.9999 for the 50-μm capillary and 0.99 and 0.9997 for the 75-μm capillary. Separation efficiency expressed as number of theoretical plates (N/m) was in the range of 250 000–300 000 for the 50-μm capillary and 210 000–250 000 for the Z-cell. Limitations and possibilities of the MECC method here presented are discussed with respect to analyses of glucosinolates occurring in a wide range of cruciferous seed, vegetative plant parts including cabbage varieties, feed and food.

1. Introduction

Glucosinolates constitute a well-defined group of more than a hundred naturally occurring compounds which has attracted special attention due to their importance in relation to quality of food and feed [1,2]. The effect of glucosinolates, and especially their degradation products, may be of positive or negative character, e.g., anti-nutritive, toxic and off-flavour effects [3–5], as well as anticarcinogenic properties [6,7], and functions in herbivore host-plant recognition [8].

The various physiological effects, which can be related to glucosinolates and products thereof [2,9], result in the need for fast, inexpensive and reliable quantitative methods of analysis.

Qualitative and quantitative determination of glucosinolates has until recently been performed by the use of gas chromatography (GC) and high-performance liquid chromatography (HPLC) [1,10–12], and during the last few years, HPLC of desulphoglucosinolates has been the reference method of the EU [13]. Capillary electrophoresis (CE) for the analysis of intact and desulphoglucosinolates was introduced four years ago [14,15]. The method, based on micel-

---

* Corresponding author.

lar electrokinetic capillary chromatography (MECC) with cetyltrimethylammonium bromide (CTAB) as surfactant, proved to be superior to both GC and HPLC for intact glucosinolates with respect to separation capacity as well as cost. The separation of the desulphoglucosinolates, obtained after on-column enzymatic desulphation of crude glucosinolate extract [1,12,13], was, however, suboptimal compared with the separation of the intact glucosinolates and various transformation products of glucosinolates [16,17]. Determination of glucosinolates is in several cases hampered by interfering compounds, which may occur in some vegetative plant parts, food and feed. Methods based on desulphoglucosinolates are in such cases a powerful supplement to ones based on intact glucosinolates, as has also been concluded for methods based on HPLC [1,12]. The limitations of desulphoglucosinolate techniques are related to on-column desulphation [1,12], and this comprises thus both HPLC [1,13] and HPCE–MECC [16]. Determinations based on desulphoglucosinolates have, however, due to their isolation, some advantages in analytical specificity compared with the determination of the intact glucosinolates, and there is thus a need for this more specific technique based on a more efficient MECC separation system for the compounds than obtainable with both HPLC [13] and the MECC system based on CTAB [14,15].

The present study introduces the use of a cholate-based micellar system for the analysis of desulphoglucosinolates. The developed MECC system was evaluated with respect to qualitative performance of the method, including discussion of factors of importance for sensitivity, and in this connection introduction of a special Z-cell detection system. Results for repeatability, linearity and separation efficiency of the method of analysis are also presented.

2. Experimental

2.1. Apparatus

The apparatus used was an ABI Model 270 A-HT capillary electrophoresis system (Applied Biosystems, Foster City, CA, USA) with a 1000 mm × 0.05 mm or 0.075 mm I.D. fused-silica capillary. Detection was performed by on-column measurements of UV absorption (230 nm) at a position 760 mm from the injection end of the capillary. For investigations on improvements of the sensitivity, a high-sensitivity optical cell assembly was used, comprising a fused-silica capillary (1000 mm × 0.075 mm I.D.) with an optical cell (Z-cell) placed 780 mm from the injection end. The path length for the optical cell is specified at 3 mm. Data processing was carried out by use of an IBM-compatible 486 DX, 50 MHz personal computer with Turbochrom 3.3 (PE Nelson, Perkin-Elmer, Beaconsfield, UK).

2.2. Samples and reagents

Glucosinolates (potassium salts) from the collection in this laboratory were used [1,8,12]. The compounds were extracted from various plants and isolated and purified as desulphoglucosinolates, as described elsewhere [1,18]. Identification and determination of glucosinolate purity were based on paper chromatography, high-voltage electrophoresis, UV and NMR spectroscopy, and HPLC [1,11].

The names and structures of the desulphoglucosinolates used in this study are presented in Figs. 1 and 2 and Table 1, together with numbers used in the other figures and tables.

Boric acid and sodium cholate were from Sigma (St. Louis, MO, USA). All chemicals were of analytical reagent grade.

2.3. Procedure

The different test mixtures of the desulphoglucosinolates were prepared by mixing the isolated and purified single compounds.

The separation buffer was prepared with 250 mM sodium cholate and 200 mM boric acid, and the pH was adjusted to 8.5. Filtration of buffers was performed through a 0.20-μm membrane filter prior to use.

Washing of the capillary was performed with 1.0 M NaOH for 2 min and with separation buffer for 5 min before each analysis. Buffers

General structure:

No.	Structure of R group
1	CH₂=CH–CH₂–
2	CH₂=CH–CH₂–CH₂–
3	CH₂=CH–CH₂–CH₂–CH₂–
4	CH₂=CH–C(OH)H–CH₂–
5	CH₂=CH–CH(H)(OH)–CH₂–
6	CH₂=CH–CH₂–C(OH)H–CH₂–
8	CH₃–S–CH₂–CH₂–CH₂–CH₂–
10	CH₃–SO–CH₂–CH₂–CH₂–
11	CH₃–SO–CH₂–CH₂–CH₂–CH₂–
12	CH₃–SO–CH₂–CH₂–CH₂–CH₂–CH₂–
13	CH₃–SO–CH=CH–CH₂–CH₂–
14	CH₃–SO₂–CH₂–CH₂–CH₂–
15	CH₃–SO₂–CH₂–CH₂–CH₂–CH₂–
28	CH₃–
29	CH₃–C(CH₃)(OH)–CH₂–
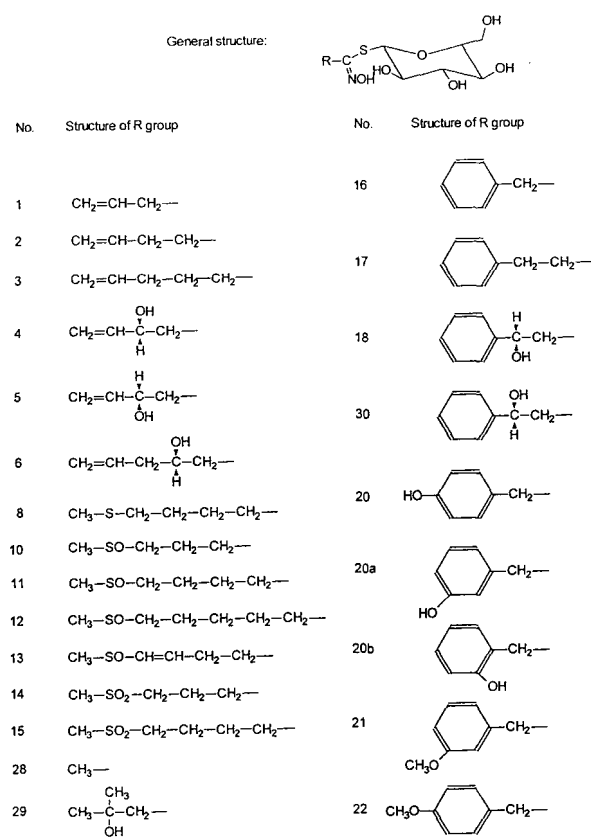
Fig. 1. Numbers and structures of aliphatic and aromatic desulphoglucosinolates used in the MECC analyses. Trivial names of the individual desulphoglucosinolates are indicated in Table 1.

were changed by auto buffer vial change on the ABI 270A-HT instrument after five analyses.

The separation parameters for the sodium cholate system were: a voltage of 15 kV and a temperature of 60°C. Detection was performed at 230 nm. Injection by vacuum was performed from the positive end of the capillary for 1 s.

2.4. Calculations

Calculations of relative migration times (RMT) (relative to an internal standard, trigonellinamide), normalised areas (NA), relative normalised areas (RNA) and resolution (R_s) were performed as described elsewhere [15,16]. RMT was calculated relative to trigonellinamide, whereas RNA was calculated relative to sinigrin

(1) in test mixture A and relative to glucolimnanthin (21) in test mixture B. The types of compounds included in the test mixtures and in the samples analysed are shown in connection with Tables 1–5 and Figs. 1–5. The numbers of theoretical plates (N) were calculated by the Foley–Dorsey approximation, assuming an exponentially modified Gaussian distribution as the skewed peak model. The equation for N is:

$$N = \frac{41.7(MT/W_{0.1})^2}{B/A + 1.25}$$

where MT is the migration time for the peak, $W_{0.1}$ is the peak width at 10% of peak height, and B/A is an empirical asymmetry ratio.

The linearity of the method was determined from linear regression analysis based on least-squares estimates. Repeatability was estimated from the means and relative standard deviations (R.S.D.).

3. Results and discussion

Analysis of desulphoglucosinolates may be complicated by the procedure used for isolation and purification, resulting in incomplete recovery of certain compounds from the column system [1,12]. This is a problem when the glucosinolates have acidic or readily oxidisable groups in the side chain, and those with an acylated thioglucose part create special problems with their transformation into desulphoglucosinolates [1]. However, techniques based on desulphoglucosinolates will lead to a more specific analysis, an advantage if the glucosinolates occur in vegetative plant parts, food and feed with appreciable amounts of interfering compounds, justifying the development of a specific method for these compounds.

The structural variations in the desulphoglucosinolates considered reside in their side chains. Desulphoglucosinolates are compounds without charge if their side chains are without protolytical active groups [1], and separation in a MECC system should therefore mainly be based on hydrophobic interaction between the micellar phase and preferably with possibilities of sepa-
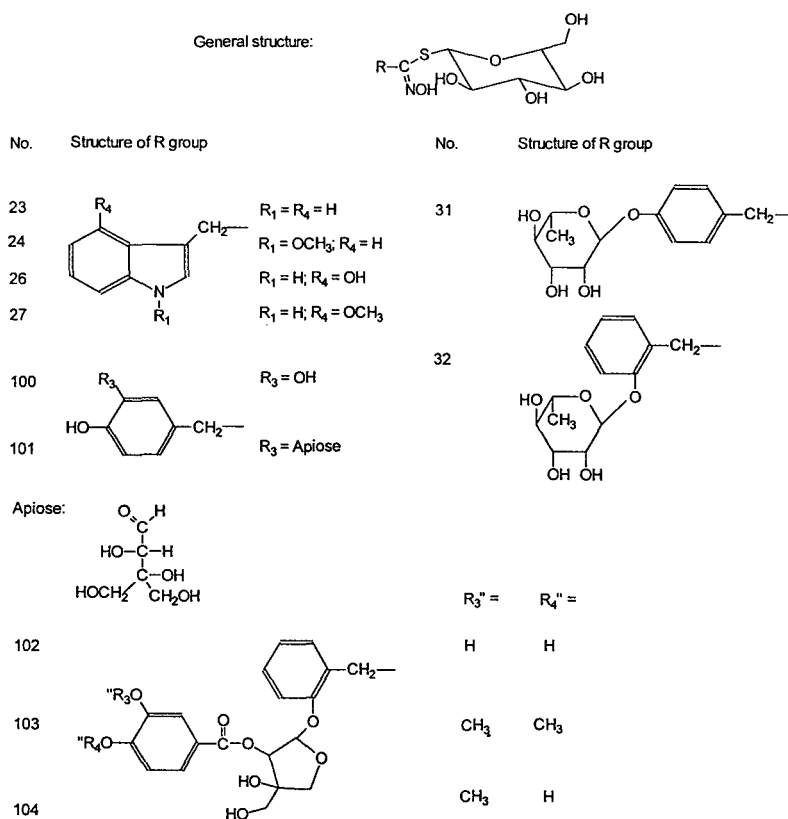
Fig. 2. Numbers and structures of indolyldesulphoglucosinolates and glycosylated desulphoglucosinolates used in the MECC analyses. Trivial names of the individual desulphoglucosinolates are indicated in Table 1.

ration of stereoisomeric glucosinolates. The MECC system introduced here, using the negatively charged cholate as the surfactant, should theoretically provide a good system for the separation of the uncharged desulphoglucosinolates. Cholate creates a kind of 'inverse micelles', having a negatively charged core and a hydrophobic uncharged surface, which is a micellar structure giving priority to separation based on hydrophobic interaction [16].

3.1. Migration order

The migration order of a wide spectrum of desulphoglucosinolates was determined, in order to demonstrate the significance of the small differences in structure necessary for acceptable

separation of the compounds (Fig. 3). It appears that the behaviour of desulphoglucosinolates in the cholate system are based mainly on differences in hydrophobicity, as clearly demonstrated by the migration order of the homologous series such as 1–2–3, 10–11–12, and 16–17. Generally, the aliphatic desulphoglucosinolates appeared early in the electropherogram, followed by the aromatic compounds, and with the indolyl-derivatised desulphoglucosinolates and desulphoglucosinolates having more than one aromatic group in the side chain migrating with the lowest velocity (Fig. 4). The importance of the steric hindrance for the interaction of desulphoglucosinolates with the micelles was seen by the separation of the epimers 18 and 30. Also, the structural isomers, such as 20–20b, 21–22 and

Table 1
Trivial names of desulphoglucosinolates used in the MECC cholate analyses

Number	Trivial name[a]	Number	Trivial name[a]
1	Sinigrin	21	Glucolimnanthin
2	Gluconapin	22	Glucoaubrietin
3	Glucobrassicanapin	23	Glucobrassicin
4	Progoitrin	24	Neoglucobrassicin
5	Epiprogoitrin	26	4-Hydroxyglucobrassicin
6	Napoleiferin	27	4-Methoxyglucobrassicin
8	Glucoerucin	28	Methylglucosinolate
10	Glucoiberin	29	2-Hydroxy-2-methyl-propylglucosinolate
11	Glucoraphanin	30	Glucosibarin
12	Glucoalyssin	31	p-Rhamnopyranosyloxybenzylglucosinolate
13	Glucoraphenin	32	o-Rhamnopyranosyloxybenzylglucosinolate
14	Glucocheirolin	100	3,4-Dihydroxybenzylglucosinolate
15	Glucoerysolin	101	3-Apiosyloxy-4-hydroxybenzylglucosinolate
16	Glucotropaeolin	102	3-[2″-(3,4-Dihydroxybenzoyl)apiosyloxy]-4-
17	Gluconasturtiin		hydroxybenzylglucosinolate
18	Glucobarbarin	103	3-[2″-(3,4-Dimethoxybenzoyl)apiosyloxy]-4-
20	Sinalbin		hydroxybenzylglucosinolate
20a	Glucolepigramin	104	3-[2″-(3-Methoxy-4-hydroxybenzoyl) apiosyloxy]-4-
20b	o-Hydroxybenzylglucosinolate		hydroxybenzylglucosinolate

The trivial names are as for the corresponding intact glucosinolates. Numbers as in Figs. 1 and 2. Separation conditions as described in the Experimental section.
[a] The semisystematic names were given for **20b**, **28**, **29**, **31**, **32** and **100–104**.

27–24 were well separated, demonstrating the high separation capacity of the MECC system (vide infra). Glycosylated desulphoglucosinolates would generally be expected to appear earlier in the electropherogram than the corresponding non-glycosylated compounds due to the lower hydrophobicity caused by the sugar moiety. As seen for, e.g., **20b–32** and **100–101** (Fig. 5), this was, however, not the case. An increased size of the glycosylated compounds, counteracting the change in hydrophobicity, may be the explanation for this observation, and derivatives of these glycosides have increased affinity to the micelles and thereby increased MT, as seen for the compounds **102–104**.

```
First    4  10  11  12  29/13/14/11  1/6  2  100  30  18

         20/20b/21/3/8  16  22/32  26/101  23  17  27/102  104/24   103  Last
```

Fig. 3. Migration order of desulphoglucosinolates analysed in the MECC cholate system. Numbers as in Fig. 1. Separation conditions as described in the Experimental section.

3.2. Repeatability

Two test mixtures A and B, described in the Experimental section, were used for determination of the repeatability of MT, RMT, NA and RNA using traditional 50-μm and 75-μm I.D. capillaries. As revealed from the results (Table 2), the method performed satisfying, with R.S.D. values generally below 1% for RMT, except for test mixture B (50-μm capillary). Some adjustments of the method are, however, still needed in order to obtain reproducible peak areas, although use of RNA instead of NA in test mixture A improved the results partly. No systematic effect of the capillary diameter on R.S.D. values could be observed.

3.3. Linearity

Correlation coefficients (r^2) from linear regression analysis by the least-squares method of NA and various concentrations of desulphog-

Fig. 4. Electropherogram of desulphoglucosinolates isolated from Savoy cabbage. Numbers as in Fig. 1. The peak labelled i.st. is the internal standard (trigonellinamide). Separation conditions as described in the Experimental section.

ent study should thus only be considered a reference compound in the calculation of RMT. Preliminary studies of the relative response factors indicate the same course of values as found in HPLC, using UV (230 nm) as the detection system [12,13,19].

3.4. Sensitivity

Introduction of the high-sensitivity optical cell assembly has opened up the possibility of improved sensitivity without changing the UV detection system used in the present method. Results from the registration of NA for test mixture A obtained with the high-sensitivity optical cell assembly (capillary 75 μm I.D., path length 3 mm), a standard 75-μm capillary and a standard 50-μm capillary are presented in Table 4. A ten-fold increment in response was obtained compared with results with the corresponding 75-μm standard capillary, whereas the NA values were increased by a factor of about 2.5 upon changing the internal diameter of the standard capillaries from 50 to 75 μm.

3.5. Separation efficiency

The resolution and number of theoretical plates per meter of capillary were calculated for the mixture used in the sensitivity test (vide supra). As shown in Table 5, R_s ranged from 2.2–6.1, whereas N/m generally exceeded 200 000, with the highest values obtained for the 50-μm capillary. Although not in the same range as obtained for the intact glucosinolates [15] (R_s: 10.1–35.8; N/m: 296 000–566 000), this may be considered as satisfactory, especially compared with typically no more than 20 000 N/m in HPLC analyses of both intact and desulphoglucosinolates. Surprisingly, the high-sensitivity optical cell assembly showed better separation efficiency than the standard 75-μm capillary, and this, combined with the high sensitivity of the system, makes it an evident choice for, e.g., low-concentration samples.

lucosinolates analysed in the MECC cholate system (test mixtures A and B) are given in Table 3. Correlation coefficients were in general high, ranging from 0.9876 to 0.9999 for the 50-μm capillary and from 0.9866 to 0.9997 for the 75-μm capillary, respectively. The good linearity is, together with acceptable repeatability of NA/RNA values, a precondition for quantitative analyses, which also provides the use of an internal standard, and knowledge of the relative response factors for the actual system, as is the case for HPLC [1,12,13]. The internal standard chosen should optimally be related in structure to desulphoglucosinolates, and a good choice would be a well-defined desulphoglucosinolate absent from the sample of interest. Trigonellinamide used in the pres-

Fig. 5. Electropherogram of desulphoglucosinolates isolated from (a) *Hesperis matronalis* and (b) *Reseda lutea*. Numbers as in Fig. 1. Separation conditions as described in the Experimental section.

Table 2
Relative standard deviation (%) of migration times (MT), relative migration times (RMT), normalised peak area (NA) and relative normalised peak area (RNA), as an expression of repeatability of the MECC cholate method for determination of desulphoglucosinolates ($n = 5$–11)

Test mixture	Number	Relative standard deviation (%)							
		50-μm Capillary				75-μm Capillary			
		MT	RMT[a]	NA	RNA[b]	MT	RMT[a]	NA	RNA[b]
A	**1**	0.87	0.63	4.27	–	3.90	0.80	9.07	–
	2	0.87	0.73	3.86	2.40	3.80	0.75	9.44	1.04
	18	0.95	0.78	5.51	4.27	3.82	0.80	10.13	2.95
	20	0.98	0.82	6.49	5.30	3.91	0.94	10.01	1.50
	16	1.16	0.98	5.10	3.65	3.87	0.88	9.81	1.56
B	**10**	–	–	–	–	0.22	0.22	–	–
	13	2.72	1.57	3.28	5.53	0.21	0.21	5.10	8.90
	14	2.78	1.61	4.73	6.89	0.21	0.21	6.34	2.68
	21	3.71	2.59	6.30	–	0.30	0.31	7.89	–
	17	4.26	3.18	6.93	5.13	0.42	0.42	5.83	2.52

Numbers as in Fig. 1. Separation conditions as described in the Experimental section.
[a] Relative to the internal standard trigonellinamide.
[b] Relative to sinigrin (**1**) in standard A and relative to glucolimnanthin (**21**) in standard B.

Table 3
Results from linearity studies of desulphoglucosinolates analysed in the MECC cholate system ($n = 6$–8)

Test mixture	Number	50-μm Capillary		75-μm Capillary	
		Concentration range (mM)	r^2	Concentration range (mM)	r^2
A	1	0.1338–4.28	0.9998	0.0334–4.28	0.9996
	2	0.1066–3.41	0.9998	0.0266–3.41	0.9995
	18	0.1119–3.58	0.9999	0.0280–3.58	0.9994
	20	0.1553–4.97	0.9999	0.0388–4.97	0.9993
	16	0.1119–3.58	0.9997	0.0280–3.58	0.9994
B	10	–	–	0.0950–3.04	0.9866
	13	0.2113–3.38	0.9876	0.2113–3.38	0.9982
	14	0.0853–2.73	0.9889	0.0853–2.73	0.9995
	21	0.1441–4.61	0.9890	0.1441–4.61	0.9988
	17	0.1016–3.25	0.9896	0.1016–3.25	0.9997

Numbers as in Fig. 1. Separation conditions as described in the Experimental section.

Table 4
Results from sensitivity studies of desulphoglucosinolates analysed in the MECC cholate system

Capillary type	NA of number				
	1	2	18	20	16
50 μm	147.3	114.8	115.9	309.2	132.9
75 μm	325.5	255.1	256.6	724.6	301.3
75 μm[a]	3466.0	2701.6	2746.0	6721.9	3091.5

Numbers as in Fig. 1. Separation conditions as described in the Experimental section.
[a] High-sensitivity optical cell assembly (Z-cell).

4. Conclusions

In conclusion, MECC based on cholate proved to be a very effective system for separating a wide range of structurally different desulphoglucosinolates. The migration order of the investigated compounds could easily be explained by the structure-property variation among the

Table 5
Separation efficiency (R_s and N/m) obtained for test mixture A analysed in the MECC cholate system

Capillary type	N/m of number					R_s of numbers			
	1	2	18	20	16	1–2	2–18	18–20	20–16
50 μm	267 843	251 464	259 904	274 482	266 189	5.6	6.1	2.8	4.0
75 μm	216 979	188 445	200 201	209 167	185 463	4.9	5.1	2.0	3.7
75 μm[a]	218 971	211 959	241 549	218 967	214 513	5.0	–	2.2	3.5

Numbers as in Fig. 1. Separation conditions as described in the Experimental section.
[a] High-sensitivity optical cell assembly (Z-cell).

analytes, including hydrophobicity and size of the R-group, but stereoisomers were separated as well. Differences in mass/charge ratio and ion-pairing with the micelles, as in the case of the intact glucosinolates, were, on the other hand, without importance, as the desulphoglucosinolates are uncharged compounds, which explains the advantage of the cholate micelles compared with the system used for the negatively charged intact glucosinolates.

The separation capacity of the MECC system was high, with N/m around 200 000–300 000, and R_s ranging from 2.2 to 6.1. The repeatability and linearity of the method were in general satisfactory; however, some improvements are still needed for acceptable quantitative determination of the actual compounds. The experience using the high-sensitivity optical cell assembly was very good, improving the sensitivity of the system considerably without losing any separation efficiency. It thus provides an evident alternative to the standard unbowed capillary for low-concentration samples, as may be the case with some plant extracts.

Acknowledgements

References

[1] H. Sørensen, in F. Shahidi (Editor), Rapeseed/Canola: Production, Chemistry, Nutrition and Processing Technology, Van Nostrand Reinhold, New York, 1990, Ch. 9, p. 149.

[2] C. Bjergegaard, P.W. Li, S. Michaelsen, P. Møller, J. Otte and H. Sørensen, Bioactive Subst. Food Plant Orig., 1 (1994) 1.

[3] N. Bille, B.O. Eggum, I. Jacobsen, O. Olsen and H. Sørensen, Z. Tierphysiol. Tierernähr. Futtermittelkd., 49 (1983) 195.

[4] R. McDanell, A.E.M. McLean, A.B. Hanley, R.K. Heaney and G.R. Fenwick, Food Chem. Toxicol., 26 (1988) 59.

[5] B. Bjerg, B.O. Eggum, I. Jacobsen, J. Otte and H. Sørensen, Z. Tierphysiol. Tierernähr. Futtermittelkd., 61 (1989) 227.

[6] S. Loft, J. Otte, H.E. Poulsen and H. Sørensen, Food Chem. Toxicol., 30 (1992) 927.

[7] S.R.R. Musk and I.T. Johnson, Carcinogenesis, 14 (1993) 2079.

[8] L.M. Larsen, J.K. Nielsen and H. Sørensen, Entomol. Exp. Appl., 64 (1992) 49.

[9] S. Michaelsen, J. Otte, L.-O. Simonsen and H. Sørensen, Acta Agric. Scand., 44 (1994) 25.

[10] P. Helboe, O. Olsen and H. Sørensen, J. Chromatogr., 197 (1980) 199.

[11] O. Olsen and H. Sørensen, J. Am. Oil Chem. Soc., 58 (1981) 857.

[12] B. Bjerg and H. Sørensen, in J.P. Wathelet (Editor), World Crops: Production, Utilization, Description: Glucosinolates in Rapeseeds: Analytical Aspects, Vol. 13, Martinus Nijhoff, Dordrecht, 1987, p. 59.

[13] J. European Communities (1990) No. L 170, 03.07.27-34.

[14] C. Bjergegaard, S. Michaelsen, P. Møller and H. Sørensen, GCIRC-Congress, Saskatoon, Canada, III (1991) 822.

[15] S. Michaelsen, P. Møller and H. Sørensen, J. Chromatogr., 608 (1992) 363.

[16] S. Michaelsen and H. Sørensen, Pol. J. Food Nutrition Sci., 3/44, No. 1 (1994) 5.

[17] C. Feldl, P. Møller, J. Otte and H. Sørensen, Anal. Biochem., 217 (1994) 62.

[18] B. Bjerg and H. Sørensen, in J.P. Wathelet (Editor), World Crops: Production, Utilization, Description: Glucosinolates in Rapeseeds: Analytical Aspects, Vol. 13, Martinus Nijhoff, Dordrecht, 1987, p. 125.

[19] P. Møller, O. Olsen, A. Plöger, K.W. Rasmussen and H. Sørensen, in H. Sørensen (Editor), Advances in the Production and Utilization of Cruciferous Crops, Vol. 11, Martinus Nijhoff/Dr. W. Junk Publ., Dordrecht, 1985, p. 111.

Ball-lens laser-induced fluorescence detector as an easy-to-use highly sensitive detector for capillary electrophoresis Application to the identification of biogenic amines in dairy products

G. Nouadje[a,b] M. Nertz[a], Ph. Verdeguer[a], F. Couderc[c,*]

[a]ZETA Technology, Parc Technologique du Canal, 31520 Ramonville-Toulouse, France
[b]Laboratoire de Chimie Analytique et Bromatologie, Université des Sciences Pharmaceutiques, 31062 Toulouse Cedex, France
[c]Laboratoire de Biologie Moléculaire Eucaryote du CNRS, 118 Route de Narbonne, 31062 Toulouse Cedex, France

Abstract

A ball-lens laser-induced fluorescence detector based on the conventional collinear arrangement is described for use with capillary electrophoresis. It allows better mechanical tolerances for capillary adjustment in front of the laser beam. Its sensitivity is equal to that of the conventional collinear arrangement. Micellar electrokinetic chromatographic determination of biogenic amines in dairy products is described as an application of this detector.

1. Introduction

Since Gassman et al. [1] introduced laser-induced fluorescence detection (LIFD) for capillary electrophoresis (CE) instead of the xenon lamp fluorescence proposed by Jorgensson and Lukacs [2], LIFD has gradually become the most sensitive technique for analyte detection in narrow-bore capillaries. The large number of papers that have been published testify to the usefulness of this kind of detection [1,3–8].

The two most popular on-column LIF systems are based on two different optical arrangements: (1) an orthogonal arrangement detection as described by Jorgensson and co-workers [2,9] and Zare and co-workers [1,10] and (2) a collinear arrangement as described by Hernandez and co-workers [5,11,12]. A third on-column

arrangement, with axial beam illumination [13], has been described, but its use today is limited.

Wu and Dovichi [14] used a sheath flow cuvette detector as an "end-column" detector. The sheath flow cuvette and an on-column collinear arrangement seems to allow the same sensitivity limits of around ten fluorescent molecules detected [3,15,16]. In most work on LIF an on-column detector is used because of its ease of use.

The sensitivity level of orthogonal and collinear on-column arrangements has been discussed earlier [11] and is slightly better for the collinear arrangement. Hernandez and co-workers [5,11,12] have summarized the advantages of using the coaxial arrangement, viz., capillary adjustment easy to realize with an XYZ displacement device, minimum Raman noise level and the possibility of using objectives with a very high numerical aperture.

* Corresponding author.

The principal difficulty with collinear CE–LIFD is adjusting the capillary window in front of the light beam. For instance, the *XYZ* mechanical tolerances of adjustment of the capillary in front of the objective may be less that 2.5 μm (*XYZ* axes are defined in Fig. 1).
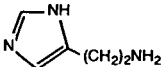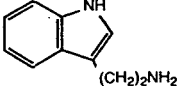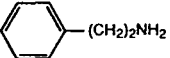
We report here a new optical device, containing a ball-lens, which allows one to make this adjustment with a higher mechanical tolerance of ca. 40 μm. The sensitivity results are almost identical with those obtained with Hernandez and co-workers' optical arrangement, but no further adjustment is necessary after removing the capillary. The optimum laser power and the photomultiplier tube (PMT) voltage were studied. A linear range from 10^{-8} to 10^{-12} *M* was observed with two standard fluorescent dyes [fluorescein isothiocyanate (FITC) and Rhodamine 123]. This new optical device detector was used for the determination of biogenic amines in dairy products.

During the ripening of cheese, casein is slowly degraded by proteolitic enzymes. This mostly leads to a steady increase in the content of free amino acids, some of which can be subjected to subsequent breakdown reactions. Decarboxylation is such a reaction. It is catalysed by specific bacterial decarboxylases and gives rise to the formation of carbon dioxide and amines. These amines are designated as biogenic because they are formed by the action of living organisms. The most important biogenic amines that can be found in cheese are listed in Table 1 together with their precursors [17].

Whereas in most hard paste cheeses the content of biogenic amines is low [17], some soft cheeses have fairly high levels [18]. The consumption of large amounts of these amines can bring about symptoms of intoxication such as headache, nausea, hypo- or hypertension, cardiac palpitation and possibly shock [19]. As a result, biogenic amines are indicators of food quality. Therefore, it is important to determine certain biogenic amines, in the presence of amino acids in different food matrices.

Different methods have been used to separate and detect these amines, but the separations may be time consuming, might give poor chromato-

Table 1
Biogenic amines and their precursor

Biogenic amine	Formula	Amino acid precursor
Tyramine	(CH$_2$)$_2$NH$_2$ / HO-ring	Tyrosine
Putrescine	$H_2N(CH_2)_4NH_2$	Ornithine
Histamine	NH / N ring (CH$_2$)$_2$NH$_2$	Histidine
Cadaverine	$H_2N(CH_2)_5NH_2$	Lysine
Tryptamine	NH ring (CH$_2$)$_2$NH$_2$	Tryptophan
Phenylethylamine	(CH$_2$)$_2$NH$_2$	Phenylalanine

graphic or electrophoretic resolutions and have poor sensitivity levels. Thin-layer chromatography [20–22] and thin-layer electrophoresis [21–23] with different detection reactions have been used. Gas chromatography of volatile biogenic derivatives has also been described [24,25]. More recently, ion-exchange chromatography [21,26,27], isotachophoresis [28,29] and reversed-phase-high-performance liquid chromatography (HPLC) [30–34] have given the most sensitive results. Most amines or non-aromatic amino acids show neither natural UV absorption nor fluorescence, and different chemical precolumn derivatization reagents have been tested for the analysis of amines, e.g., ninhydrin in amino acid analysers with postcolumn derivatization [35], 5-dimethylaminonaphthalene-1-sulfonylchloride, *o*-phthaldeialdehyde and 9-fluorenylmethyl chloroformate [32,33,36]. The best sensitivity is estimated as ca. $0.5 \cdot 10^{-6}$ mol of biogenic amine [36].

In this work, we evaluated the sensitivity performance of our "easy-to-use" LIF detection

system for the determination of fluorescein thiocarbamyl (FTC) biogenic amines and FTC-amino acids in fresh and 1-month-old French soft cheese (Camembert).

2. Experimental

2.1. Instrumentation

For the ball-lens experiments, a capillary electrophoresis manual sampler and a high voltage power supply from a Spectra-Phoresis 100 (TSP, Freemont, CA. USA) were used. The instrumental design of the LIF detector is illustrated in Fig. 1. Laser radiation of 488 nm from a low-power argon ion laser (7 mW) (ILT, Salt Lake City, UT, USA) (1) passes through a laboratory-made optical fibre device (2), then the laser light is reflected by a 45°, 488 nm dichroic mirror (3) (Andover, Salem, NH, USA) and focused by an achromatic 5×0.2 lens (focal length 11 mm) (Zeiss, Le Pecq, France) (4) and a capillary ball-lens cell from a TSP capillary electrophoresis detector (5), where the sapphire ball-lens is placed in direct contact with the detection window of a fused-silica capillary of dimensions 50–75 μm I.D. (Polymicro Technologies, Phoenix, AZ, USA) (6). The capillary holder is mounted on an XYZ micropositioner table (Melles Griot, Irvine, CA, USA). The detection window (4 mm length) is formed by burning off the polyimide coating with an electri-

cal coiled resistance. Light emitted from the capillary is collected by the ball-lens and the achromatic lens and passed through the dichroic mirror, a laboratory-made spatial filter (7), a notch filter centred on wavelength 488 nm (Andover) (8) and a high-pass filter (Oriel, Straford, CT, USA) (9). The fluorescence signal is then detected by a PMT (Type 928, Hamamatsu, Bridgewater, NJ, USA), the high voltage supply (10) of which may be adjusted. The signal is collected at a 10-Hz sampling rate with a Boreal data acquisition system (JMBS-Developpements, Grenoble, France) running on an IBM PC.

For classical collinear arrangement experiments, an IRIS 2000 [Europhor Instruments (now Zeta Technology), Toulouse, France] was used.

2.2. Optimization of optical arrangement

Studies on optical optimizations were carried out by flushing a 10^{-8} M rhodamine 123 solution in the capillary and recording the fluorescence intensity for each position of the capillary ball-lens cell.

For pinhole diameter experiments, the optical arrangement was adjusted to its optimum fluorescence intensity XYZ positions. The fluorescence of the 10^{-8} M rhodamine 123 solution and water flushed in the capillary was recorded for each diameter. Between rhodamine and water measurements, the capillary was washed consecutively for 3 min with 0.1 M NaOH solution and for 3 min with water. The signal-to-water ratio is defined as the ratio of the fluorescence intensity of the 10^{-8} M rhodamine 123 solution to that of water.

2.3. Chemicals and reagents

All chemicals and reagents were purchased from Aldrich (St. Quentin Fallavier, France), and used without purification.

2.4. Procedure for FITC derivatization

Rhodamine 123 and FITC were diluted with water (HPLC grade) to give concentrations from
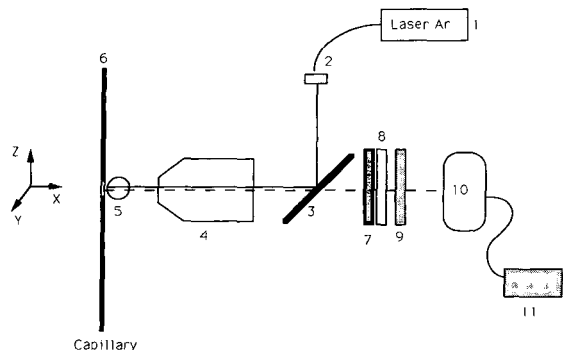
Fig. 1. Schematic diagram of ball-lens laser-induced fluorescence detector.

10^{-8} to 10^{-13} M were obtained. These dyes have a maximum absorption near 488 nm.

Biogenic amines and amino acids were diluted with water–methanol (90:10, v/v) to give concentrations from $5 \cdot 10^{-7}$ to $5 \cdot 10^{-11}$ M. Derivatization with FITC was performed as described in Ref. [11].

2.5. Preparation of cheese sample

Fresh and 1-month-old Camembert (French soft cheese), pasteurized and unpasteurized, were chopped up and homogenized with 0.1 M HCl in the proportions: 0.1 M HCl = 4:3 (w/w). A 0.23-g amount of the paste was suspended in 5 ml of 0.1 M HCl. After centrifugation, the supernatant solution was filtered. The residue was extracted twice with 5 ml of 0.1 M HCl and filtered. After neutralization of the resulting combined extract with 0.2 M sodium carbonate solution, derivatization of amino acids and biogenic amines with FITC was carried out as described elsewhere [11]. The derivatized samples were diluted 100 000-fold and analysed by CE–LIF.

2.6. Separation conditions

All separations were carried out using an 80-cm long fused-silica capillary (50 cm effective length). For Rhodamine 123 and FITC studies, a 75 mm I.D. capillary and 50 mM sodium tetraborate borate buffer (pH 8.3) were used with 15 s, 16 kV electrokinetic injection and a separation potential of 16 kV. The separation buffer for FTC-amino acids and biogenic amines consisted of 100 mM SDS–100 mM boric acid. The pH was adjusted to 9.2 by addition of sodium hydroxidy solution. A 50 mm I.D. capillary was used with 2 s hydrodynamic injection (17.5 nl) and a separation potential of 24 kV. In both cases the capillary was rinsed for 3 min with 0.1 M NaOH, 3 min with distilled water and 3 min with buffer.

2.7. Analysis

Peaks were identified by spiking diluted cheese samples with standard solutions of amino acids and biogenic amines. Biogenic amines were determined using linear calibration graphs based on peak height. Each calibration graph contained data points at a minimum of six different concentrations, and each graph spanned the range of concentrations found in diluted cheese samples. Linearity was assessed using standard least-squares analysis of the logarithm of peak height vs. logarithm of concentration plots. Detection limits were estimated at twice the peak-to-peak noise by extrapolation from plots of peak height vs. concentration.

3. Results and discussion

3.1. Detector optimization

Difficulties met with the classical collinear arrangement for adjusting with extreme precision the capillary in front of the capillary window led ut to seek a new procedure to eliminate such small mechanical tolerances. Hlousek [37] proposed for spectrophotometric analysis in fused-silica capillaries the use of a small ball-lens, to obviate the importance of mechanical tolerances and to allow easier mounting and replacement of the capillary.

Fig. 2A and B show the intensity of the fluorescence signal vs. XY position of the ball-lens in front of the laser beam for the two optical arrangements. We can see (Fig. 2A) that the Y position is critical for the two systems, but the mechanical tolerance is much greater for the new system (ca. 180 mm compared with 8 mm for a signal reduced by 50%). The ball-lens mounted on the capillary allows the mechanical tolerances to be increased by a factor of 22. The ball-lens acts as a very short focal length lens to convert the slowly converging light [low numerical aperture (NA) of microscope objective; here $NA = 0.2$] to a rapidly converging cone of light (high numerical aperture, here $NA = 0.88$) that will impage the source into the area of interest in the sample cell. Fig. 2B shows the X positioning, provided that X is lower than the microscope objective focal length and that the laser spot illuminating the ball lens has a smaller area than the circular area of the ball-lens. Studies on the
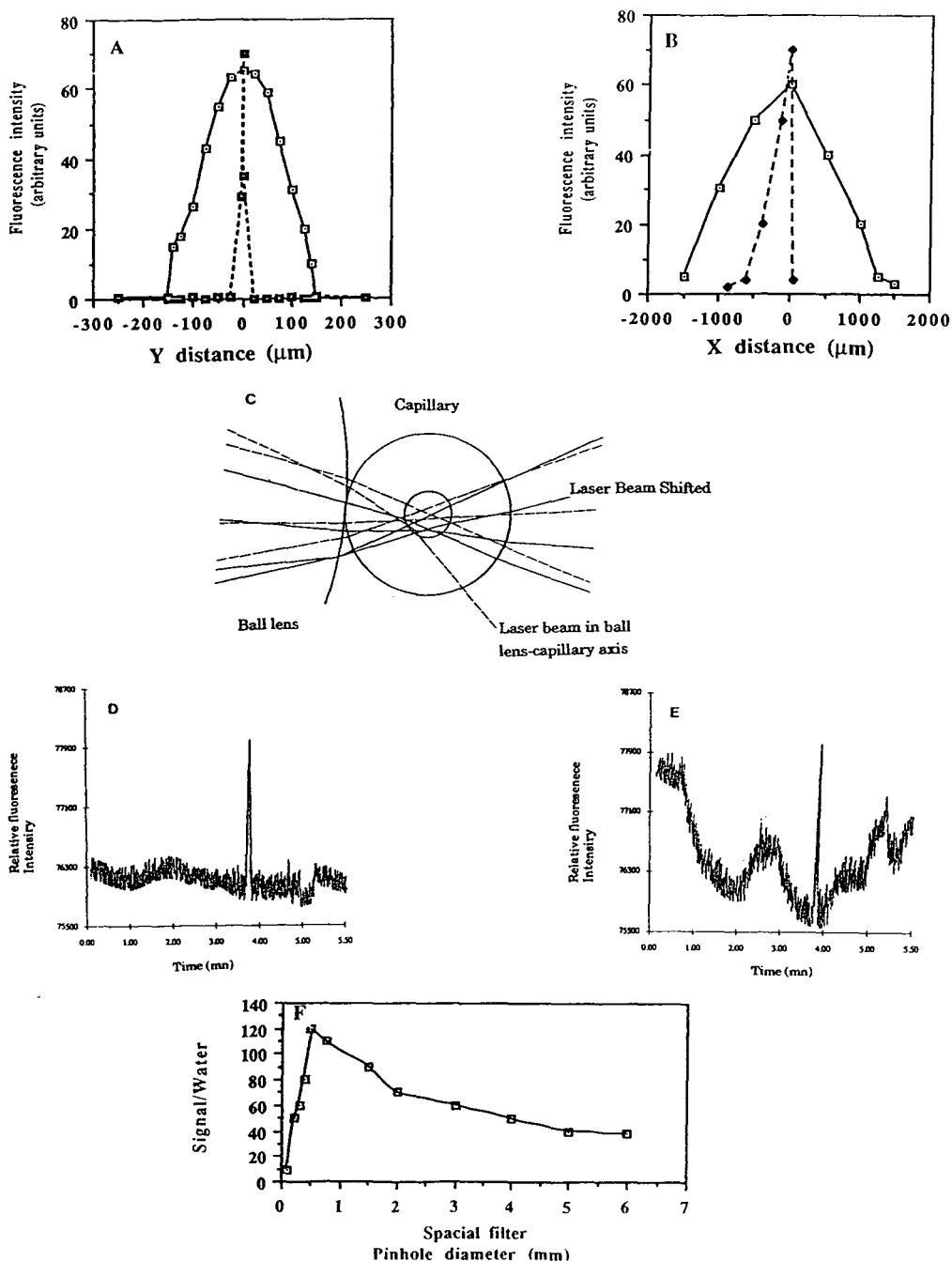
Fig. 2. Influence of X and Y positions of ball-lens–capillary cell relative to the laser beam. The zero point is defined as the optimum for relative fluorescence intensity of a 10^{-8} M Rhodamine 123 solution. Solid line, ball-lens detector; dashed line, conventional collinear detector. (A) Influence of Y position; (B) influence of X position, point $0 = 10\,200$ μm for ball-lens detector, 160 μm for classical collinear arrangement detector; (C) schematic ray diagram of a ball-lens showing ray traces through the ball-lens and the capillary cell; (D) analysis of $1.5 \cdot 10^{-12}$ M Rhodamine 123 solution after optimization of LIF detector; (E) analysis $1.5 \cdot 10^{-12}$ M Rhodamine 123 solution after removing the capillary ball-lens cell from the detector and putting it in the detector again without any new adjustment; (F) influence of pinhole diameter.

Z distance indicated that the laser spot has to be collimated on the ball-lens circular area. These results confirm that a high NA allow small variations of the laser beam position with regard to the ball-lens and capillary to be compensated (Fig. 2C) [37].

Because the adjustment of the capillary is critical for the conventional collinear arrangement, removing the capillary implies adjusting its position in front of the microscope objective. Using the ball-lens optical arrangement we show that this post-removal adjustment is not so critical. The sensitivity level is the same and the laser beam is collimated on the ball-lens and capillary as when the ball-lens cell and capillary are removed and replaced in front of the laser beam. A $1.5 \cdot 10^{-12}$ M solution of Rhodamine 123 gave the same signal-to-noise ratio in both cases (S/N = 21) (Fig. 2D and E).

The influence of the spatial filter pinhole diameter was also studied. Fig. 2F shows that the optimum diameter for such a filter is 500 μm. This means that when the diameter is becoming smaller, reflections of the laser beam on the microscope objective, the ball-lens and capillary are less important: the signal-to-water ratio increases. When the hole has a diameter of less than 500 μm, the fluorescence signal is much too reduced and it becomes of the same order as dark noise; the signal-to-water ratio decreases.

3.2. Detector performance

Scott [38] stated that if a response, R, arises as a function of concentration, C, then the function $R = AC^B$ where A and B are constants, will describe the response curve. Therefore, the equation $\log R = \log A + B \log C$ should describe a straight line with a slope B. Scott arbitrarily proposed that for a "linear" dependence of response on concentration, B should lie in the range 0.98–1.02. Values outside this range imply degrees of non-linearity. Standard curves for "non-linear" responses can be used provided that B is uniform over the analytical concentration range and that R can be accurately determined.

For the classical collinear arrangement [39],

we found a linear dynamic range close to four orders of magnitude for Rhodamine 123 between 10^{-8} and 10^{-12} M and a slope B of 1.01. For the ball-lens detector a slope of 0.96 ($r^2 = 0.998$) for FITC and 1.05 for Rhodamine 123 ($r^2 = 0.999$) was obtained. As reported elsewhere, the LIF detector might be non-linear with Scott's definition for some fluorophores [40] but give a linear dynamic range of at least 5 (10^{-8}–$3.5 \cdot 10^{-13}$ M) and 4 (10^{-8}–$5 \cdot 10^{-12}$ M) orders of magnitude for Rhodamine 123 and FITC, respectively.

3.3. Fluorescein thiocarbamyl (FTC)-amino acids and FTC-biogenic amines in soft cheese samples

Amino acids are commonly studied with LIF–CE [41–43]. Because most amines show neither natural UV nor fluorescence, chemical derivatization is necessary for detecting derivatives of amines prior to CE separation. As reported by Nouadje et al. [44], contrary to UV detection, LIF allows the selective detection of labelled compounds, independently of micellanous non-fluorescent compounds.

Standard mixture of histamine, tyramine, putrescine, β-phenylethylamine cadaverine and tryptamine mixtures were analysed. All six biogenic amines are separated with baseline resolution in less than 15 mn. Separation efficiencies obtained range from 60.000 theorical plates for tryptamine (tr = 13,48 mn) up to 200.000 theorical plates for histamine (tr = 9.65 mn). Detection limits for the six biogenic amines range from 0.5 10^{-10} M for B phenylamine up to $1,5 \cdot 10^{-10}$ M for tryptamine.

3.4. Analysis of cheese samples

Analyses of dansylated samples with CE–UV detection give very complex electropherograms (data not shown), which cannot be used to identify amino acids and to quantify biogenic amines. Cheeses are very complex mixtures which contain many compounds that absorb in the UV wavelength range.

The selectivity of fluorescent primary amine labelling with FITC allows one to detect only

ammonia, primary amines, amino acids and proteins. The use of FTC-amino acids and FTC-amines reduces the interference with fluorescence of other natural compounds which are generally excited in the UV range [44]. Moreover, high dilution prevents the detection of such naturally fluorescent molecules, which have low concentrations, and which have very low fluorescent quantum yields at 488 nm.

The two electropherograms of fresh and matured pasteurized 1-month-old cheese in Fig. 3A

and B demonstrate the use of LIF detection. For cadaverine and putrescine we did not take into account the two labelling site due to the presence of diamino group. The two labelled molecules are eluted with a longer elution time. We did not use an internal standard because the extraction procedure is achieved without multiple steps, in a very short time, and moreover the reproducibility of 2-s hydrodynamic injections of a mixture of 10^{-9} M FITC and Rhodamine 123 showed a relative standard deviation of 8.9% ($n = 6$).

Table 2 shows the amounts of biogenic amines detected in 100 000-fold diluted samples. Ammonium ions, arginine, lysine, phenylalanine, alanine, aspartic acid, glycine and tyrosine were identified in fresh and matured cheese, but the concentrations are about ten times higher in matured than in fresh cheese. Amino acids come from β-casein degradation during ripening [45,46]. We found relatively high cadaverine and putrescine concentrations in matured and fresh cheese, as described Ten Brink et al. [18] in fermented foods.

Histamine, histidine and tyramine were not detected, but we identify a large amount of tyrosine. We may explain the absence of histamine and histidine by the rapid transformation of histidine into histamine and degradation of the latter during prolonged ripening [47]. No explanation was found for the absence of tyramine, which is normally found in soft cheese [22]. No significant differences were found between pasteurized and unpasteurized cheese.

Fig. 3. LIF electropherograms of 100 000-fold diluted samples of (A) fresh and (B) 1-month-old pasteurized cheese. Hydrodynamic injection time 2 s, 80 cm length capillary, 100 mM SDS, 100 mM boric acid buffer (pH 9.2), 24 kV separation. Peaks: 1 = Lys; 2 = Arg; 3 = ornithine; 4 = ammonia; 5 = putrescine; 6 = blank; 7 = β-phenylethylamine; 8 = cadaverine; 9 = Tyr; 10 = Phe; 11 = Ser; 12 = Ala; 13 = Gly; 14 = Asp.

4. Conclusion

Our "easy-to-use" LIF detector offers very good sensitivity and can be used many times without adjusting the capillary position in front of the laser beam. The ball-lens cell leads to very high sensitivity and decreases the importance of mechanical tolerances. Moreover, compared with other optical collinear arrangements which use a poor UV transmission, high-magnification objective, our optical device includes a small magnification objective and a ball-lens, both of which allow either visible or UV wavelengths to

Table 2
Determination of biogenic amines in fresh and 1-month-old pasteurized or unpasteurized cheese

Sample	Concentration (10^{-9} M)					
	Histamine	Tyramine	Tryptamine	Putresceine	Cadaverine	β-Phenylethylamine
Unpasteurized fresh cheese	UD[a]	UD	UD	0.80 ±0.05	3.10 ±0.12	0.50 ±0.02
Unpasteruised 1-month-old cheese	UD	UD	UD	1.80 ±0.08	34.95 ±1.37	1.40 ±0.05
Pasteurized fresh cheese	UD	UD	UD	3.10 ±0.12	5.62 ±0.21	0.44 ±0.02
Pasteurised 1-month-old cheese	UD	UD	UD	<0.08	28.05 ±0.95	2.65 ±0.05

[a] Undectected.

be transmitted very well. UV-transmitting, high-magnification objectives are very expensive, prices varying between US $5500 and 20 000.

The linear range of external standard calibrations of close to five orders of magnitude allows easy quantification and we have determined the concentrations of certain biogenic amines in soft cheese at the sub-attomole level.

Acknowledgements

References

[1] E. Gassman, J.E. Kuo and R. Zare, Science, 230 (1985) 813.

[2] J.W. Jorgensson and K.D. Lukacs, Anal. Chem., 3 (1981) 1298.

[3] J.Y. Zhao, D.Y. Chen and N.J. Dovichi, J. Chromatogr., 608 (1992) 117.

[4] N.A. Guzman, J. Trebilcock and M.A. Advis, Anal. Chim. Acta, 249 (1991) 247.

[5] L. Hernandez and N. Joshi, Spectra 2000, 153 (1990) 40.

[6] W.G. Kuhr and E.S. Yeung, Anal. Chem., 60 (1988) 2642.

[7] S. Carson, A.S. Cohen, A. Belenkii, M.C. Ruiz-Martinez, J. Berka and B.L. Karger, Anal. Chem., 65 (1993) 3219.

[8] J.W. Jorgensson and K.D. Lukacs, Science, 222 (1983) 266.

[9] E.J. Guthrie and J.W. Jorgensson, J. Chromatogr., 352 (1986) 337.

[10] R.N. Zare and E. Gassmann, US Pat., 675 300 (1987).

[11] L. Hernandez, J. Escalona, N. Joshi and N. Guzman, J. Chromatogr., 559 (1991) 183.

[12] L. Hernandez, N. Joshi, E. Murzi, Ph. Verdeguer, J.C. Mifsud and N. Guzman, J. Chromatogr. A, 652 (1993) 399.

[13] J.A. Taylor and E.S. Yeung, Anal. Chem., 64 (1992) 1741.

[14] S. Wu and N. Dovichi, J. Chromatogr., 480 (1989) 141.

[15] D.Y. Chen and N.J. Dovichi, J. Chromatogr. A, 657 (1994) 265.

[16] D.Y. Chen, K. Adelhelm, X. Li Cheng and N.J. Dovichi, Analyst, 119 (1994) 349.

[17] J.H.M.L. Joosten and J. Stadhouders, Neth. Milk Dairy J., 41 (1987) 247.

[18] B. Ten Brink, C. Damink, H.M.L.J. Joosten and J.H.J. Huis in't Hed, Int. J. Food Microbiol., 11 (1990) 73.

[19] G.J. Silverman and F.V. Kosikowski, J. Dairy Sci., 39 (1956) 1134.

[20] S.P. Srivastava and V.K. Dua, Anal. Chem., 48 (1976) 367.

[21] S. Seiler, J. Chromatogr., 146 (1977) 221.

[22] H.M. Garat, J.C. Basilico and A.C. Simonetta, Rec. Fac. Ing., 47 (1985) 7.

[23] H. Bayzer, J. Chromatogr., 24 (1966) 372.

[24] H. Bruecker and M. Hausch, Milchwissenschaft, 45 (1990) 421.

[25] A. Baudichau, D. Bruyer, R. Ontiveros and W. Shermer, J. Sci. Food Agric., 38 (1987) 1.

[26] A. Martelli, M. Arlorio and M.L. Torun, Riv. Sci. Aliment., 22 (1993) 261.

[27] P. Jandera and J. Churacek, J. Chromatogr., 98 (1974) 1.

[28] T. Tsuda, M. Yamada and Y. Nakazawa, Milchwissenschaft, 48 (1993) 74.

[29] H. Klein and W. Stoya, Lebensmittelchem. Lebensmittelqual., 4 (1991) 125.

[30] C. Tricard, J.M. Cazabeil; M.H. Salagoity, Analusis 19 (1991) M53.

[31] H.M.L.J. Joosten and C. Olieman, J. Chromatogr., 356 (1986) 311.

[32] J. Kirschbaum, B. Luckas and W.D. Beinert, J. Chromatogr. A, 661 (1994) 193.

[33] E. Menstani, C. Sarzanini, O. Abollino and V. Porta, Chromatographia, 31 (1991) 41.

[34] K. Takeba, T. Maryama, T. Matsumoto and H. Nakazawa, J. Chromatogr., 504 (1990) 441.

[35] P. Vandekerckhove and H.K. Hendrickx, J. Chromatogr., 82 (1973) 379.

[36] M. Roth, Anal. Chem., 43 (1971) 880.

[37] L. Hlousek, US Pat. 5 037 199 (1991).

[38] R.P.W. Scott, J. Chromatogr. Libr., 2 (1977) Ch. 2.

[39] F. Couderc, C. Toulas and R. Kerr, Rev. Instrum. Biol. Med., 14 (1992) 140.

[40] T.L. Lee and E.S. Yeung, J. Chromatogr., 595 (1992) 319.

[41] K.C. Waldron, S. Wu, C.W. Earle, H.R. Harke and N.J. Dovichi, Electrophoresis, 11 (1990) 777.

[42] J.Y. Zhao, D.Y. Chen and N.J. Dovichi, J. Chromatogr., 608 (1992) 117.

[43] T. Ueda, F. Kitamura, R. Mittchell, T. Metcalf, T. Kuwana and A. Nakamoto, Anal. Chem., 63 (1991) 2979.

[44] G. Nouadje, F. Couderc, Ph. Puig and L. Hernandez, J. Capillary Electrophoresis, in press.

[45] S. Takafuji, Dev. Food Sci., 32 (1993) 191.

[46] J.W. Lee, S.W. Lee, J.H. Jeong and R. Yang, Han'guk Sikp'um Kwahakhoechi, 22 (1990) 337.

[47] M. Vallestrico, A. Azzi and I.M. De Clemente, Ind. Aliment., 28 (1989) 1084.

ELSEVIER

Determination of polyamines in serum by high-performance capillary zone electrophoresis with indirect ultraviolet detection

Ge Zhou[a], Qingnan Yu[a], Yinfa Ma[b], Jun Xue[c], Yan Zhang[c], Bingcheng Lin[c],*

[a]Dalian No. 3 Municipal Hospital, Dalian, China
[b]Northeast Missouri State University, Kirksville, MO, USA
[c]Dalian Institute of Chemical Physics, Chinese Academy of Sciences, Dalian, China

Abstract

A method for determining polyamines in serum by capillary zone electrophoresis (CZE) with indirect ultraviolet detection was established. The concentrations of polyamines in the sera of six healthy adults were determined and the results were in accordance with those obtained previously by high-performance liquid chromatography (HPLC). However, the CZE method is superior to HPLC in that it has high sensitivity, small sample consumption and easy sample pretreatment.

1. Introduction

Polyamines, mainly putrescine, spermidine and spermine, exist in all living organs and play important roles in cell growth and differentiation. Since Russell [1] reported in 1971 that polyamine concentrations in the urine of some tumour patients were higher than normal, the relationship between polyamines and tumour status has aroused the interest of many researchers and many cases of different tumours with variations in polyamine concentrations have been reported [2,3], and appropriate evaluation of the relationship between polyamine levels and some diseases, including tumours, is still progressing. The main methods for polyamine detection have been high-performance liquid chro-

matography (HPLC) and thin-layer chromatography. However, both methods require that polyamines be derivatized or labelled before detection since they have no chromophore and cannot be detected with an ultraviolet detector. This makes the methods tedious and time consuming.

Capillary zone electrophoresis (CZE) has proved to be a powerful technique in separating charged biomolecules with high resolution [4,5], and indirect detection has become a simple and sensitive method for CZE [6,7]. CZE involving indirect detecting has not been reported in serum polyamine detection. Polyamines in serum can reflect most directly the body polyamine level. In this work, CZE with indirect detection was employed for detecting polyamines in serum and proved to have several advantages, such as high sensitivity, small sample consumption and easy sample pretreatment.

* Corresponding author.

2. Experimental

2.1. Equipment

A Bio-Focus 3000 and HPE-100 capillary electrophoresis system (Bio-Rad Labs., Richmond, CA, USA), UV detection and electrokinetic injection were used.

2.2. Pretreatment of capillary column

Capillary columns (Hebei Yongnian Photoconductive Fibre Factory, Hebei, China) of 50 mm I.D. were cleaned with 0.1 M HCl and 0.1 M NaOH in sequence and then coated with polyacrylamide. Coated columns with effective lengths of 35.2–40.2 cm were used

2.3. Reagents

Quinine sulfate monohydrate was purchased from Fisher Scientific (Fairlawn, NJ, USA). Putrescine (PU) and spermine (SPM) were purchased from Sigma (St. Louis, MO, USA) and spermidine (SPD) from Serva (Heidelberg, Germany).

2.4. Preparation of background electrolyte [8]

Quinine sulfate (392 mg) was dissolved in a mixture of 20 ml of 95% ethanol and 70 ml of deionized water, the pH was adjusted to 3.0 with 0.1 M HCl and the volume was then brought to 100 ml.

2.5. Pretreatment of serum

A 1-ml volume of acetone was added to 100 ml of serum and the denatured proteins were removed by centrifugation at 30 000 g for 10 min. The deproteinized serum was obtained after volatilizing acetone from the supernatant. SPD and SPM in serum were determined by adding SPD and SPM standards to the original deproteinized serum. As the PU peak was covered by the first unknown peak in the electropherogram of serum, the identification of PU was subject to interference. After diluting the serum

tenfold, the diluted unknown substance and PU were satisfactorily separated. Hence the position of PU was determined in the electropherogram of the tenfold dilution of the original deproteinized serum. A volume of 72–75 ml of deproteinized serum was obtained after pretreatment of 100 ml of serum and the concentrations of SPD and SPM in the serum were converted into concentrations in 100 ml after obtaining the concentrations in the original 72–75 ml of deproteinized serum.

3. Results and discussion

3.1. Determination of polyamine standards

The electropherogram of the three polyamine standards is shown in Fig. 1. The relative peak positions of the three polyamine standards were in accordance with the expected result based on the consideration of the Z/M values, which are PU 0.0227, SPD 0.0206 and SPM 0.0197. Because of the absorption of quinine sulfate at 236 nm, the three polyamine peaks actually appeared upside down. For convenience of observation, the electropherograms in this paper have been reversed to that the sample peaks appear as if they were absorption peaks.

With injection conditions of 5 kV, 3 s and a separation voltage of 9 kV, the regressional equations for the polyamines were $y = 9.325 + 0.1511x$ for PU, $y = 22.30 + 0.9654x$ for SPD
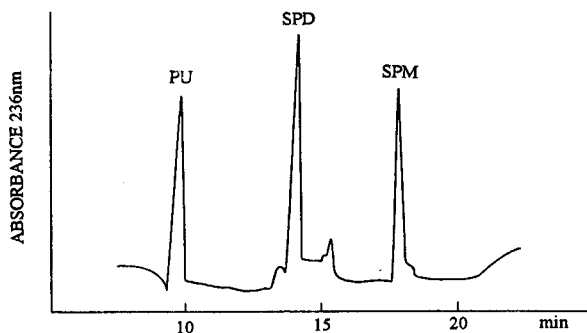
Fig. 1. Determination of polyamine standards by CZE with indirect UV detection. Load, 8 kV, 2 s; run, 8 kV; detection, 236 nm, 0.02 AU.

and $y = 79.94 + 2.830x$ for SPM, in which y is the peak height (mm) and x is the concentration (10^{-8} mol/l). The linear range of polyamine detection was investigated and a linear response over two orders of magnitude ($5 \cdot 10^{-8} - 5 \cdot 10^{-6}$ mol/l) for each polyamine was obtained. The detection limit for the three polyamines was $1 \cdot 10^{-12}$ mol/l.

3.2. Precision

A mixture of polyamine standards was analysed five times repeatedly and the results expressed as average peak height $\pm$ R.S.D. were 12.2 mm $\pm$ 4.1% for PU ($4.39 \cdot 10^{-7}$ mol/l), 46.1 mm $\pm$ 2.3% for SPD ($2.21 \cdot 10^{-7}$ mol/l) and 113.3 mm $\pm$ 5.7% for SPM ($1.35 \cdot 10^{-7}$ mol/l).

3.3. Relative recovery of polyamines

A 20-ml volume of polyamine standard mixture (PU $3.51 \cdot 10^{-7}$, SPD $1.76 \cdot 10^{-7}$ and SPM

$1.08 \cdot 10^{-7}$ mol/l) was added to 100 ml of serum and the sample was subjected to the entire pretreatment procedure as described above. The relative recovery was calculated using the following equation:

$$R_r = (C_{Srm+Std} - C_{Srm})/C_{Std}$$

where R_r = relative recovery, $C_{Srm+Std}$ = polyamine concentration in the serum sample with polyamine standards added, C_{Srm} = polyamine concentration in the serum and C_{Std} = concentration of polyamine standards. The PU concentration in serum was assumed to be zero. The average recoveries $\pm$ R.S.D. ($n = 5$) of the polyamines were PU 92.3 ± 10.2, SPD 94.3 ± 10.3 and SPM $99.7 \pm 12.5\%$.

3.4. Determination of polyamines in serum

The three polyamines in serum were identified
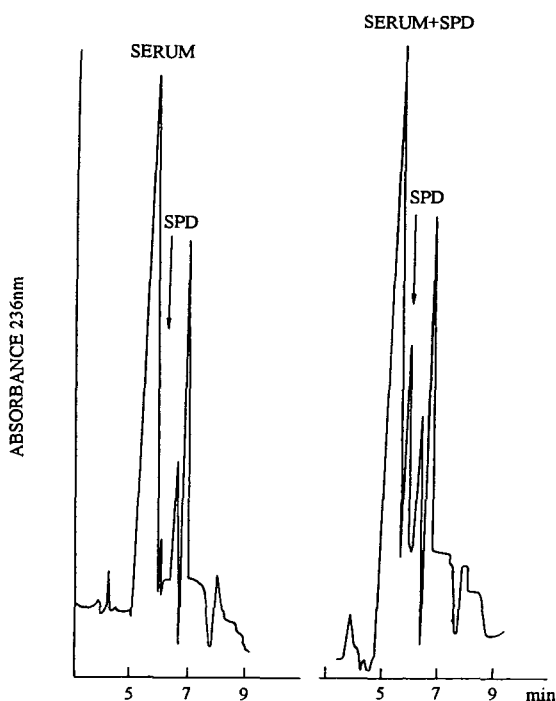
Fig. 2. Determination of spermidine in serum by CZE with indirect UV detection. Load, 5 kV, 3 s; run, 9 kV; detection, 236 nm, 0.005 AU.
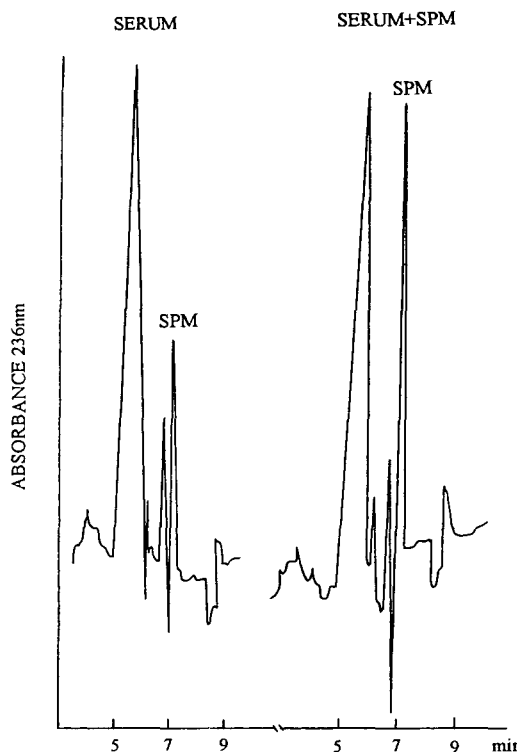
Fig. 3. Determination of spermidine in serum by CZE with indirect UV detection. Conditions as in Fig. 2.

Table 1
SPD and SPM concentrations (10^{-7} mol/l) in human sera

Polyamine	Sample						
	1	2	3	4	5	6	Average
SPD	1.11	1.01	1.15	1.22	1.21	1.22	1.15
SPM	2.12	1.39	1.61	1.58	1.09	1.06	1.48
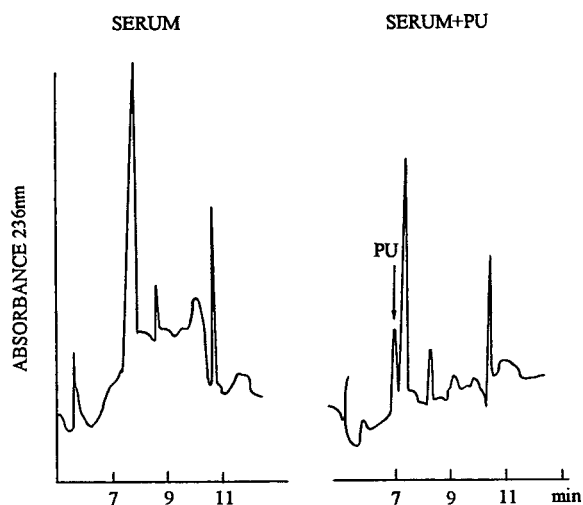
Fig. 4. Determination of putrescine in serum by CZE with indirect UV detection. Conditions as in Fig. 2.

by adding standards to serum as shown in Figs. 2–4. The relative positions of the three polyamines in the electropherograms were in accordance with those of the standard solution. SPD and SPM were detected in the original deproteinized serum. PU was not found in the serum, and after adding PU standard to the sample the PU peak and the unknown peak in the electropherogram overlapped. Subsequently PU standard was added to a tenfold dilution of the serum and the PU was well separated. Of the three polyamines, SPM was found to have the highest concentration in serum, then SPD, and PU was almost undetectable. The result was in accordance with previous reports on polyamine detection using other methods [2,4].

Blood erythrocytes have a great ability to absorb polyamines in blood plasma, especially PU and SPD. Although 80% of blood polyamines are in erythrocytes, there is still very little PU present in erythrocytes [9]. This might account for our not finding PU in serum. We only gave the position where PU should be located in the electropherogram if there were a sufficient concentration in the serum.

The concentrations of SPD and SPM in the sera of a group of healthy adults are shown in Table 1. The average concentrations of SPD and SPM were $1.15 \cdot 10^{-7}$ and $1.48 \cdot 10^{-7}$ mol/l, respectively, in agreement with reports of polyamine concentrations of many types of body cells within the submillimolar range. For example, Loser et al. [3] reported $2.86 \cdot 10^{-7}$ mol/l for SPD and $1.75 \cdot 10^{-7}$ mol/l for SPM in human serum, obtained using HPLC. Although only six subjects were included in our experiment, the average concentrations of serum polyamines were within the range of common acceptance.

4. Conclusion

A rapid, simple and sensitive method for determining polyamines in serum was developed. The sample consumption is small and the pretreatment is easy.

Acknowledgements

References

[1] D.H. Russell, Nature New Biol., 233 (1971) 144–149.
[2] J. Liao, R. Oyang, R. Pan, N. Shao, X. Chen and Z. Xuan, Cancer (Chin.) 9 (1990) 268–270.
[3] C. Loser, U.R. Folsch, C. Paprotny and W. Creutzfeldt, Cancer, 65 (1990) 958–966.
[4] N.N. Heiger, A.S. Cohen and B.L. Karger, J. Chromatogr., 516 (1990) 33–48.
[5] M.V. Novotny, K.A. Cobb and J. Lin, Electrophoresis, 11 (1990) 735–749.
[6] W.G. Kuhr and E.S. Yeung, Anal. Chem., 60 (1988) 2462–2468.
[7] W. Beck and H. Engelhardt, Chromatographia, 33 (1992) 313–316.
[8] R. Zhang, C.L. Cooper and Y. Ma, Anal. Chem., 65 (1993) 704–706.
[9] K.D. Cooper, Clin. Chim. Acta, 73 (1976) 71–76.

Capillary electrophoretic determination of degradation products of nitrilotriacetic acid used as a complexing agent in a desulphuration process

S. Schäffer[a], P. Gareil[a,*], L. Carpot[b], C. Dezael[c]

[a]Laboratoire d'Electrochimie et de Chimie Analytique (URA CNRS 216), Ecole Nationale Supérieure de Chimie de Paris, 75231 Paris cedex 05, France
[b]Institut Français du Pétrole, B.P. 3, 69390, Vernaison, France
[c]Institut Français du Pétrole, B.P. 311, 92506 Rueil-Malmaison cedex, France

Abstract

Capillary electrophoresis (CE) was assessed for the determination of the expected degradation products of nitrilotriacetic acid (NTA), viz., imiodiacetic acid (IDA), dimethyliminoacetic acid (DMIA), N-methylglycine (NMG), glycine (GLY), acetate, formate and ammonium, in solutions containing iron(III)–NTA complexes which were used for the desulphuration of industrial gases. Owing to the wide range of absolute mobilities and acidic constants of these analytes, the analytical requirements were best met with three different sets of operating conditions, all carried out with indirect absorbance detection. The more mobile ions (formate, acetate and NTA) were obtained without interference with other process-relevant anions using a buffer of pH 6 and an electroosmotic flow modifier under reversed polarity. Using normal polarity and no modifier, the less anionic species (GLY, NMG, DMIA) were determined at pH 9.5, while the major degradation product, IDA, was best determined at pH 7. Ammonium can be detected in the last two cases. The cumbersome presence of iron (III) ions was avoided by either precipitation (potassium hydroxide) or complexation (ethylenediaminetetraacetic acid). Special attention was paid to method validation. The analyses were fast (<6 min) and exhibited low relative standard deviations for migration times (<0.1%) and peak areas (<5%). The methods were applied to monitor the process of desulphuration. The results are well correlated with those obtained by ion chromatography (IC), but CE appeared simpler and more versatile and cost effective.

1. Introduction

A number of processes intended to eliminate gaseous hydrogen sulphide (H_2S) from industrial smokes are based on the washing of the gases with aqueous solutions containing an oxidizing agent capable of converting hydrogen sulphide into sulphur, but also amenable to subsequent regeneration through oxidation. In some of these processes, iron(III) was selected to meet these conditions. The chemical reactions involved are

$$H_2S + 2\ Fe^{3+} \rightarrow S + 2\ Fe^{2+} + 2H^+$$

$$2\ Fe^{2+} + 2H^+ + 1/2\ O_2 \rightarrow 2\ Fe^{3+} + H_2O$$
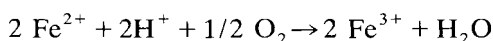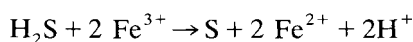
the balance of which is

* Corresponding author.

$$H_2S + 1/2 \ O_2 \rightarrow S + H_2O$$
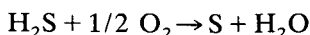
However, as written, this reaction scheme could only be implemented in acidic media, which would greatly restrict its interest for a desulphuration process. To delay the precipitation of both iron(III) hydroxide and iron(II) sulphide to neutral or even slightly basic media, a chelating agent of Fe(III) and Fe(II) should be added to the desulphuration bath. A still more appropriate additive should also slightly lower the redox potential of the Fe(III)–Fe(II) system, so as to make easier thermodynamically and kinetically the reoxidation of Fe(II) by air. This last point implies that the stability constant of the Fe(III) chelate should be higher than that of the Fe(II) chelate. Candidate additives are nitrilotriacetic acid (NTA), ethylenediaminetetraacetic acid (EDTA) and hydroxyethylenediaminetriacetic acid (HEDTA), the most cost effective being NTA. On the other hand, these chelating agents undergo slow degradation under the effect of the alternate formation of iron(III) and iron(II) chelates, leading to a series of known or unknown products, the chelating power of which is less and less pronounced. Eventually, NTA degradation limits the lifetime of the desulphuration solution, as it results in losses of Fe(III) by precipitation.

Addition of some organic or inorganic compounds has been shown to slow the degradation rate. The proper understanding of the degradation schemes and degradation kinetics and of the inhibitory effect of some additives and ultimately the effective monitoring of industrial units require the complete determination of the species involved in such solutions. The classical methods of analysis such as potentiometry, titrimetry, spectrophotometry, determination of nitrogen, sulphur and total organic carbon and chemical oxygen demand provide only partial information and are not suited for monitoring industrial units. Ion chromatographic (IC) techniques have been implemented for this task, but are not entirely satisfactory, insofar as they fail to allow the easy identification and determination of all the components involved. They also require the use of several expensive columns.

The purpose of this work was to assess capillary electrophoresis (CE) as an alternative method for desulphuration solution monitoring. The most attractive features of this technique are its separation selectivity, different from that of IC as a result of the different separation principles, its short analysis times, flexibility, ease of implementation, automation capability and low running costs. In this paper, we describe the CE methods that were developed to determine NTA and its degradation products in the presence of iron ions, hydrogen sulphide and the resulting oxidation products. A method allowing the rapid monitoring of total iron ions was also developed. Validation aspects were especially emphasized. Experiments were conducted at two different sites (referred to as laboratories A and B) by different authors of this paper and the consistency of the results was examined.

2. Experimental

2.1. Apparatus

CE was performed with a Quanta 4000 capillary electrophoresis system (Waters, Milford, MA, USA) equipped with either a positive or a negative high-voltage power supply. Fused-silica capillaries of effective length 58 or 60 cm and 50 or 75 μm I.D. were used. The window for on-column detection was created by burning off a small section (0.5 cm) of the polyimide coating. Both indirect and direct UV detection were performed with a mercury lamp and 254- or 185-nm optical filters. The samples were introduced into the capillary using the gravity injection device provided with the instrument with the capillary inlet raised 10 cm above the outlet for 10, 20 or 30 s. The separation voltage was set at 20 or 30 kV depending on the kind of separation. In some cases the direction of the electroosmotic flow was reversed using OFM BT Anion reagent (Waters). Data processing was performed with a Waters Model 820 data station.

All solutions, electrolytes and standards were prepared using 18 MΩ water generated by a

Milli-Q laboratory water–purification system (Millipore, Milford, MA, USA).

2.2. Standards

Nitrilotriacetic acid disodium salt (NTA), iminodiacetic acid (IDA), N,N-dimethylglycine (DMIA) and N-methylglycine (NMG) were obtained from Sigma (St. Louis, MO, USA), glycine (GLY) from Merck (Darmstadt, Germany) and ethylenediaminetetraacetic acid disodium salt dihydrate (EDTA) from Prolabo (Paris, France). In laboratory A a standard solution in water was prepared containing the analytes NTA, IDA, GLY, NMG, DMIA, formate, acetate, malonate, sulphate, carbonate, two important process-relevant but confidential components and a 1:2 metal–ligand complex of Fe^{3+}–EDTA. The concentration of each ion in this solution was 1 mmol/l. For all species of interest separate standard solutions each at a concentration of 1 mmol/l were also prepared.

In laboratory B, working standard solutions were prepared by diluting stock standard solutions of NTA (500 ppm), IDA (800 ppm) and GLY (1000 ppm) to various concentrations to cover the required linearity ranges. For peak identification, working standard solutions of sulphate, formate, acetate and two confidential ions were prepared from stock standard solutions of concentration 1000 ppm.

2.3. Sample preparation

The samples obtained from the desulphuration process contain the important components iron(III), at an expected concentration 0.05 mol/l, and NTA as complexing agent, at an expected concentration of 0.1 mol/l. The process also requires the utilization of a buffer (pH 7) and other additives. The accurate composition of the desulphuration mixture cannot be given in this paper on the grounds of confidentiality. The samples were recovered at run times in the process up to 384 h. They were all filtered through a 0.22-μm membrane either before or after dilution.

A difficulty arising from the presence of iron(III) ions in the desulphuration solutions was circumvented either by precipitation (laboratory B) or by complexation (laboratory A). Iron(III) was completely precipitated by addition of 1.2 ml of 1 mol/l potassium hydroxide solution per millilitre of undiluted sample. After precipitation the samples were diluted 1:100 and filtered through a 0.22-μm membrane. The second approach was total complexation of iron(III) in the solution by addition of 10 μl of 0.1 mol/l EDTA solution to 10 μl of filtered sample. Finally, the samples were diluted 1:100, 1:40 or 1:10, depending on the nature and concentration of the ion of interest.

2.4. Electrolytes

The carrier electrolyte for the determination of IDA was prepared from 8 mmol/l p-anisic acid and 33 mmol/l Bis-Tris [bis(2-hydroxyethyl)iminotris(hydroxymethyl)methane]. The pH obtained was 7.0. For the separation of GLY, NMG and DMIA a carrier electrolyte containing 10 mmol/l p-anisic acid and 63 mmol/l ammediol (2-amino-2-methyl-1,3-propanediol) at pH 9.5 was used. The determination of iron was carried out with an electrolyte prepared from 20 mmol/l boric acid and 0.1 mmol/l EDTA. The pH was adjusted to 9.2 with 1 mol/l NaOH.

For the separation of sulphate, oxalate, formate, NTA and IDA, a carrier electrolyte was made up with 20 mmol/l benzoic acid. The reversal of the electroosmotic flow was obtained by adding OFM BT Anion solution to the electrolyte (dilution factor 1:40). The pH was finally adjusted to 6 with LiOH. After preparation, all electrolytes were filtered (0.45 μm) and degassed in an ultrasonic bath for 20 min or with a vacuum pump for 5 min.

3. Results and discussion

Basically, the desulphuration solution contains the active species iron(III) and nitrilotriacetate, the accompanying ions being sulphate and sodium, but with ageing it is liable to include degradation products of NTA, viz, IDA, GLY,

NMG, DMIA, formate acetate and ammonium. By analogy with the mechanism described by Matsuda and Nagai [1], it can be assumed that the degradation of NTA into IDA and GLY follows an oxidation process; however, the experimental conditions in the desulphuration process are not identical with those mentioned in Ref. [1]. Fig. 1 shows the degradation scheme of NTA into IDA and GLY. NTA loses two electrons per molecule in the first step with formation of IDA. In the second step, glycine is produced from IDA [1]. Carr et al. [2] reported the oxidation of NTA to IDA, GLY and ammonium and the disproportionation of NTA into methyliminodiacetic acid (MIDA) and dimethyliminodiacetic acid (DMIA) and their further degradation to N-methylglycine (NMG), dimethylamine and methylamine (Fig. 2). As this disproportionation seems slower and less probable, the main degradation products of NTA are probably IDA, GLY and ammonium.

Fig. 2. Overall oxidation scheme of NTA according to Ref. [2].

3.1. Interference elimination of iron(III)

The cumbersome interferences produced by iron(III) ions present in the desulphuration solutions with the other process-relevant ions were avoided through two different methods of sample preparation: either a full complexation of iron(III) with EDTA (laboratory A) or total precipitation of iron(III) by the addition of potassium hydroxide (laboratory B). It has been observed that the Fe(III)–EDTA complex produces a narrow peak which does not hinder the determination of the species of interest.

3.2. Overall separation strategy

The large differences in absolute mobilities and acidic constants of all the analytes of interest made it difficult to find a single set of analytical conditions for the entire process monitoring that fulfilled the demands on resolution, speed and sensitivity. This problem was circumvented using different, more specifically optimized carrier electrolytes. The more mobile ions (sulphate, oxalate, formate, NTA, acetate, IDA) were best determined using a buffer of pH 6 and an electroosmotic flow modifier under reversed polarity. The separations of the less mobile ions [Fe(III)–EDTA complex, IDA, acetate] and of the amphoteric species (NMG, DMIA and

Fig. 1. Degradation scheme of NTA into IDA and GLY according to Ref. [1].

GLY) were preferably carried out without an electroosmotic flow modifier and under normal polarity with a buffer pH of ca. 7–8 for the former and ca. 9–10 for the latter.

3.3. Separation of the less mobile anionic process–relevant species

Several carrier electrolytes were tried in laboratory A to find the optimum analytical conditions for the determination of IDA. The use of carrier electrolyte containing 8 mmol/l p-anisic acid as UV-absorbing species and 33 mmol/l Bis-Tris as buffer (pH 7.0) turned out to be the method of choice. A very good separation of the Fe(III)–EDTA complex, IDA, free EDTA, acetate, a confidential anion, NTA and formate, in that order, was obtained by injecting a standard mixture containing all the species of interest. Oxalate and the other major anions of the desulphuration solution, having electrophoretic mobilities higher than the electroosmotic mobility, cannot be detected in this way, which is perceived here as an advantage. This is particularly the case for sulphate, the high concentration of which has no reason to vary during the process. The peak of formate is asymmetric, owing to the large difference in electrophoretic mobilities between the analyte and the UV-absorbing background ion. The less negatively charged species NMG, DMIA and GLY are not detectable under these conditions and will be considered later. The application of this method to a desulphuration solution sampled 24 h after the start of the process is shown in Fig. 3. All peaks were identified by injecting the components of the standard solution separately. Formate ion was not detected in the solutions sampled early during the process.

Before introducing the sample into the capillary, iron(III) was completely bound to EDTA as a result of strong complexation. From the stability constants found in the literature [3], it is inferred that the prevailing complex formed under these conditions is anionic, with a 1:2 stoichiometric metal-to-ligand ratio. On varying the amount of EDTA added to the samples, it was ascertained that iron(III) remained fully
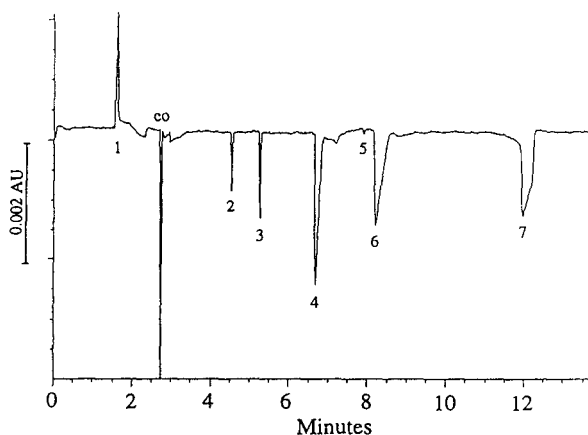
Fig. 3. Electropherogram of a desulphuration solution sampled after 24 h of process run time. Fused-silica capillary, 58 cm × 50 μm I.D. (effective length 50.5 cm); electrolyte, 8 mmol/l p-anisic acid–33 mmol/l Bis-Tris (pH 7.0); separation voltage, +30 kV; indirect UV detection at 254 nm; gravity injection for 10 s; sample filtered, diluted 1:100 with water and made up to 1 mmol/l EDTA. Peaks: 1 = sodium; eo = electroosmosis; 2 = Fe(III)–EDTA complex; 3 = IDA; 4 = EDTA; 5 = acetate; 6 = confidential; 7 = NTA.

complexed during the whole migration inside the capillary. The peaks of the complex and free form of EDTA in excess show no interference with IDA and other process-relevant components (Fig. 3). Apart from that, the deformation of the last peak corresponding to NTA does not seem to be fully explained by the mobility difference between NTA and anisate. As a consequence, this method was not retained for the determination of NTA.

Special attention was paid to method validation. To avoid any matrix discrepancy between the standard solutions used for calibration and the real solutions, the initial solution, in which no IDA had been detected, was spiked with four different concentrations of IDA. This method results in a similar matrix for the standard and the unknown solutions and hence in similar electrophoretic behaviours. Fig. 4 shows the calibration graph obtained with four different solutions of known concentration of IDA and how it was utilized for the determination of IDA in the desulphuration solutions. The plot of time-
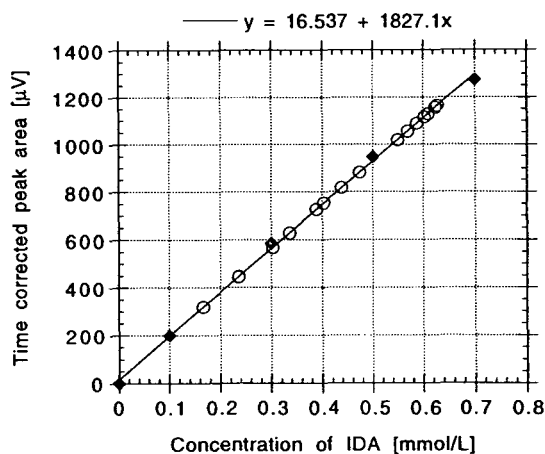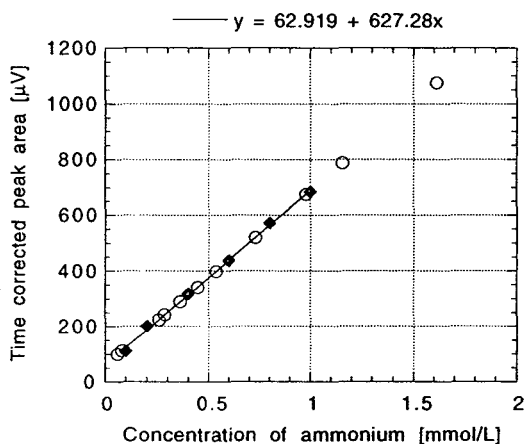
Fig. 4. Calibration graph of time-corrected peak areas as a function of the concentration of IDA added to the initial desulphuration solution. ◆ = Calibration points; ○ = points corresponding to the unknown samples of desulphuration positioned after their measured corrected peak areas. For operating conditions, see Fig. 3.

corrected peak areas versus concentration passes through the origin and is linear with a correlation coefficient of 0.9993.

As shown in Table 1, this method developed in laboratory A allows the determination of IDA with good relative standard deviations (R.S.D.) ($n = 3$) for migration times ($\leq 0.2\%$) and peak areas ($\leq 2\%$).

3.4. Separations of the more mobile anionic process relevant species

A different approach was investigated in laboratory B for monitoring the more mobile compounds involved in the desulphuration solutions, i.e., sulphate, oxalate, formate, NTA, IDA and two confidential ions. An electrolyte composed of lithium benzoate adjusted to pH 6.0, in which benzoate acts both as a chromophore for indirect absorbance detection and as a buffering species,

Table 1
Concentration of IDA as a function of sampling time during the desulphuration process, as determined by two different electrophoretic methods in laboratories A and B, and R.S.D. ($n = 3$) for migration times and peak areas

Process run time (h)	Laboratory A			Laboratory B	
	Concentration of IDA (mmol/l)	R.S.D. for migration times (%)	R.S.D. for peak areas (%)	Concentration of IDA (mmol/l)	R.S.D. for peak areas (%)
0	0.0	–	–	0.0	–
24	23.5	0.2	5.3	22.8	7.6
48	40.3	0.0	2.2	36.5	5.5
72	56.9	0.1	0.5	56.3	4.5
96	60.0	0.5	1.1	60.6	0.7
120	61.0	0.1	0.1	62.4	1.3
144	62.8	0.1	0.9	55.3	1.8
168	62.4	0.2	1.8	58.6	3.0
192	58.7	0.1	3.2	58.3	3.4
216	54.9	0.2	0.5	61.7	2.4
240	47.4	0.0	0.4	47.0	1.6
264	44.0	0.1	1.2	–	–
288	38.9	0.5	0.8	37.4	6.2
312	33.5	0.1	1.0	37.4	3.5
336	30.2	0.1	0.8	35.6	5.0
360	23.6	0.1	1.1	25.1	14.4
384	16.6	0.0	4.4	17.2	–

Electrolytes: laboratory A, anisate–Bis-Tris (pH 7.0); laboratory B, lithium benzoate–OFM BT Anion electroosmotic flow modifier (pH 6.0). See text for further explanations.

was developed. As some of these analytes are amenable to having their effective mobility greater than the electroosmotic mobility, it was highly desirable to reverse the natural cationic electroosmotic flow by adding OFM BT Anion reagent to the electrolyte. These conditions allowed a satisfactory separation of the afore-mentioned process-relevant ions. Fig. 5 shows the electropherogram of the desulphuration solu-tion sampled after 72 h of process run time. A key advantage of this method for kinetics moni-toring of the degradation products of the de-sulphuration solution is its speed. The degra-dation of NTA into IDA was followed quantita-tively through the determination of both NTA and IDA. The results obtained by this method are given in Table 1. The repeatability ($n = 3$) was mainly less than 5% for the corrected peak areas. In Fig. 6, the calibration graph obtained with seven different concentrations of NTA is plotted. The calculated linear correlation coeffi-cient was 0.9995, which represents excellent linearity. Fig. 7 enables one to compare the
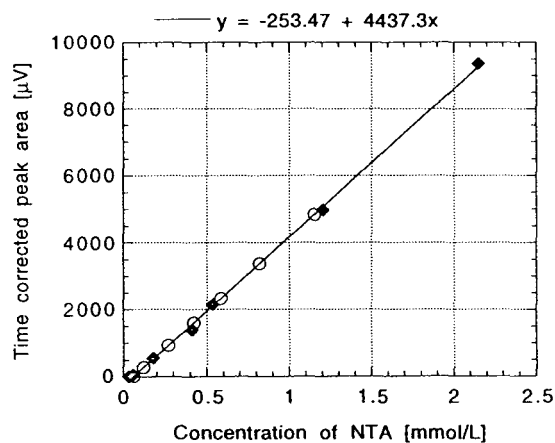
Fig. 6. Calibration graph of time-corrected peak areas as a function of the concentration of NTA. ◆ = Calibration points; ○ = points corresponding to the unknown samples of desulphuration positioned after their measured corrected peak areas. For operating conditions, see Fig. 5.

results obtained for IDA by the methods de-veloped in laboratories A and B and to obtain further insight into the level of confidence of the electrophoretic techniques. It clearly appears that both methods lead to identical results and they are both suitable for monitoring IDA in the desulphuration process.
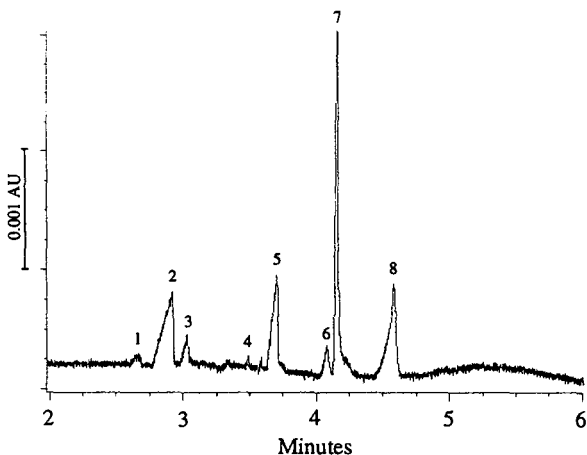
Fig. 5. Electropherogram of a desulphuration solution sam-pled after 72 h of process run time. Fused-silica capillary, 60 cm × 75 μm I.D. (effective length 52.5 cm); electrolyte, 20 mmol/l benzoic acid–OFM BT Anion (dilution factor 1:40), adjusted to pH 6.0 with LiOH; separation voltage, −20 kV; indirect UV detection at 254 nm; gravity injection for 30 s; iron removed by alkaline precipitation; sample diluted 1:100 with water and filtered. Peaks: 1 = confidential; 2 = sulphate; 3 = oxalate; 4 = formate; 5 = NTA; 6 = acetate; 7 = con-fidential; 8 = IDA.
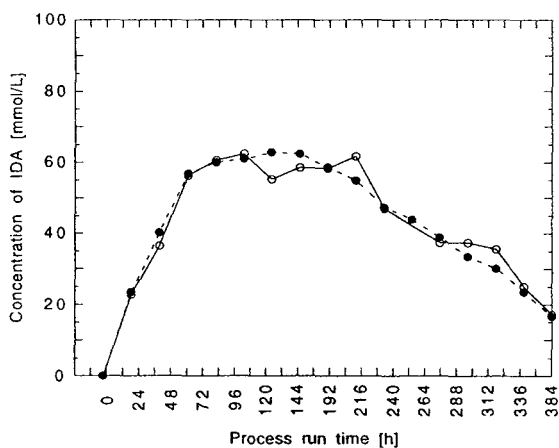
Fig. 7. Comparison of the results for IDA determinations in the desulphuration solutions obtained in laboratories A and B with two different methods. For operating conditions, see Table 1 and text.

3.5. Separations of the amphoteric process relevant species

According to Carr et al. [2], GLY, NMG and DMIA are theoretically possible amphoteric degradation products of NTA. The acid–base dissociation constants found in the literature [4] are 9.78 for GLY, 10.12 for NMG and 9.80 for DMIA. A more appropriate electrolyte with a higher pH value in the vicinity of the pK_1 values of the analyte was therefore sought in laboratory A. Using the anisate–Bis-Tris carrier electrolyte of pH 7.0, the three species were not resolved from the signal corresponding to the electroosmotic flow, the pH value being too close to their isoelectric points, located in the range 6.0–6.2. On injecting a standard mixture, the analytes were best separated with respect to one another, the signal of electroosmotic flow and the other process–relevant compounds dealt with above, with an anisate–ammediol electrolyte of

pH 9.5 (Fig. 8a). This electrolyte also results in an increase in the electroosmotic flow, which speeds up the separation and provides satisfactory conditions for indirect absorbance detection. Fig. 8b shows the electropherogram of a desulphuration solution sampled near the end of the process, 360 h after its start, exhibiting a peak assigned to GLY. In fact, GLY was detected in every solution sampled beyond 72 h, whereas DMIA and NMG were never found, in agreement with the assumption that the disproportionation of NTA which produces DMIA and NMG is less likely to occur [2].

The quantitative aspects of GLY determination under these conditions were then considered. In order to obtain known solutions of GLY in a matrix as close to the unknown desulphuration solutions as possible, the GLY solutions used for calibration were prepared by supplementing the initial desulphuration solution (in which GLY had not been detected) with four
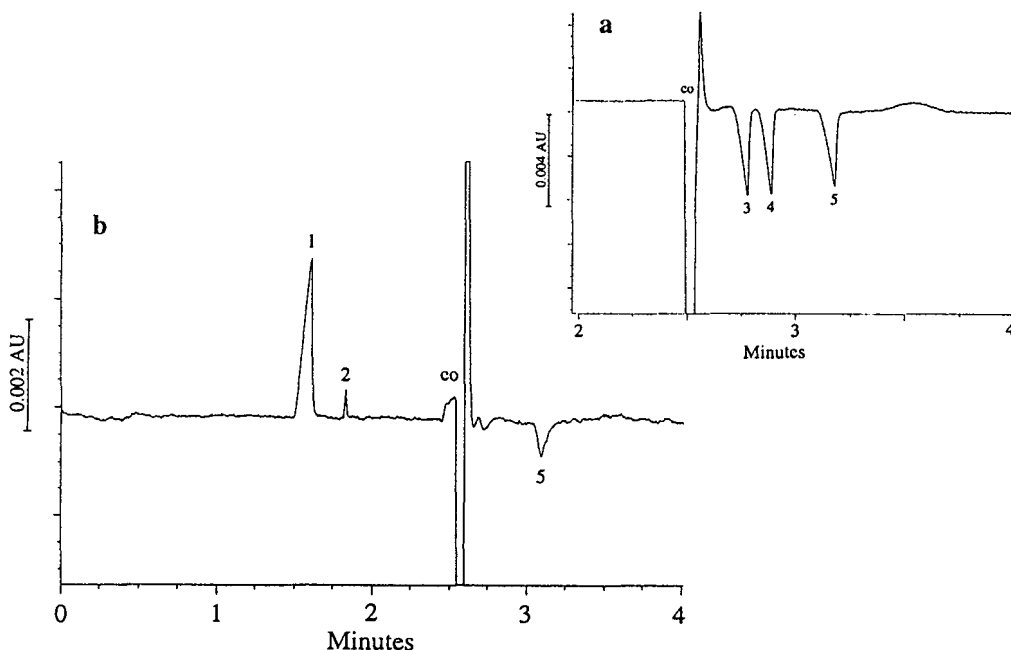
Fig. 8. Electropherograms of (a) a standard mixture of NMG, DMIA and GLY, 1 mmol/l each, and (b) a desulphuration solution sampled after 360 h of process run time. Fused-silica capillary, 58 cm × 50 μm I.D. (effective length 50.5 cm); electrolyte, 10 mmol/l p-anisic acid–63 mmol/l ammediol (pH 9.5); separation voltage, +30 kV; indirect UV detection at 254 nm; gravity injection for 20 s; desulphuration sample filtered, diluted 1:40 with water and made up to 2.5 mmol/l EDTA. Peaks: 1 = sodium; 2 = ammonium; eo = electroosmosis; 3 = NMG; 4 = DMIA; 5 = GLY.

different known concentrations of GLY. The method appeared to be well adapted to the determination of GLY, as can be seen from the calibration graph in Fig. 9. This graph is linear with a correlation coefficient of 0.9996.

Using this calibration step, GLY was next determined by laboratory A in all desulphuration process samples, as shown in Fig. 9. For this series, the relative standard deviations ($n = 3$) for migration times and corrected peak areas ranged between 0.0 and 0.2% and between 1.4 and 10%, respectively.

An alternative method for determining GLY was carried out by laboratory B with an electrolyte consisting of 5 mmol/1 borax (pH 9.2) and using direct UV detection at 185 nm. With a voltage of 22 kV, the separation was completed in 6 min. The detection sensitivity was lower than that obtained previously with the anisate–ammediol electrolyte but the surface repeatability was correct. Under these conditions, DMIA was not resolved from the neutral species but the method was nevertheless applied in laboratory B for the sake of comparison as it had been established previously that DMIA was absent from all process samples. Fig. 10 shows that the
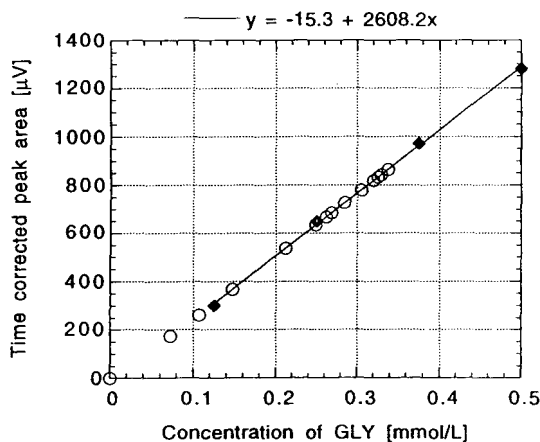
Fig. 10. Comparison of the results of GLY determinations in the desulphuration solutions obtained in laboratories A and B with two different methods. Electrolytes: laboratory A, anisate–ammediol (pH 9.5) (indirect UV detection); laboratory B, borate (pH 9.2) (direct UV detection). See text for further explanations.

values obtained with the two methods for the determination of GLY are comparable, except for the last ones, which could be explained by degradation of the sample before its processing.

3.6. Separations of the cationic process relevant species

One of the unique features of capillary electrophoresis under electroosmotic flow conditions is that it makes possible the simultaneous separation of cationic and anionic species. Further, it is known [5–8] that cationic species can still be detected with acceptable sensitivity in the indirect absorbance mode when an anionic chromophore is used. In effect, with electrolytes of pH 7.0 and 9.5, sodium, originating from both the buffer and additives present in the desulphuration solution and from EDTA used as the disodium salt added to the samples, was detected in all solutions. A second cation identified as ammonium was detected in the solutions sampled beyond 144 h of process run time. However, in this respect, a major benefit of the anisate–ammediol (pH 9.5) carrier electrolyte is that it precludes any interference in case of the

Fig. 9. Calibration graph of time-corrected peak areas as a function of the concentration of GLY added to the initial desulphuration solution. ◆ = Calibration points; ○ = points corresponding to the unknown samples of desulphuration positioned after the measured corrected peak areas. For operating conditions, see Fig. 8.

occurrence of potassium. This electrolyte was therefore chosen for the determination of ammonium, the final degradation product of NTA. The analysis can be completed within 2 min. The corresponding electropherogram for the determination of ammonium is presented in Fig. 8b.

As the sodium peak becomes triangular owing to electrophoretic dispersion when too high a concentration is injected, the concentration of EDTA disodium salt added to the samples was lowered to a 1:1 Fe(III)-to-ligand ratio. Under these modified conditions, return to the baseline was always preserved between the peaks of sodium and ammonium, which markedly improved the determination of ammonium. Fig. 11 shows the calibration graph obtained by spiking the initial desulphuration solution with six different concentrations of ammonium. It shows a very good linearity (linear correlation coefficient 0.9990). We next attempted to determine the ammonium concentration in the series of desulphuration samples. The corrected areas of the peaks corresponding to the unknown solutions are reported in Fig. 11. Repeatability was observed, as indicated by the R.S.D. ($n = 3$) of migration times (0.0–0.3%, according to the samples) and corrected peak areas (0.4–15%).

3.7. Monitoring of total iron concentration

As the lifetime of the desulphuration solution was obviously related to keeping iron(III) in the solution, thorough control of the process also required this species to be monitored. Using anisate–Bis-Tris electrolyte (pH 7.0), a narrow peak for the Fe(III)–EDTA complex was obtained with samples supplemented with EDTA in excess with respect to iron(III) (Fig. 3). However, no attempt was made to correlate this signal with iron(III) concentration. A more specific capillary electrophoresis method, using direct UV detection but still based on the fact that Fe(III)–NTA complexes are quantitatively replaced by Fe(III)–EDTA complexes on addition of excess EDTA to the samples, was developed. Dissociation of the complex during its migration inside the capillary into free EDTA and metal ion was totally eliminated by addition of 0.1 mmol/l of EDTA to the electrolyte. Finally, to take advantage of the absorbance of the Fe(III)–EDTA complex near 254 nm, a very transparent buffer, such as borate (pH 9.2), was selected. Fig. 12 shows the electropherogram of

Fig. 11. Calibration graph of time-corrected peak areas as a function of the concentration of ammonium added to the initial desulphuration solution. ◆ = Calibration points; ○ = points corresponding to the unknown samples of desulphuration positioned after the measured corrected peak areas. For operating conditions, see Fig. 8b.
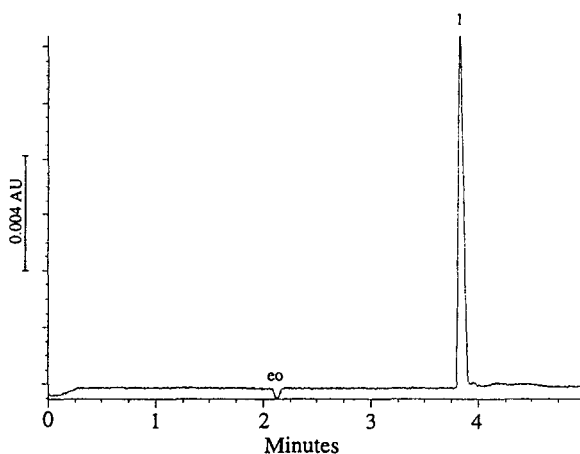
Fig. 12. Electropherogram of a desulphuration solution at zero process run time (initial solution). Fused-silica capillary, 58 cm × 50 μm I.D. (effective length 50.5 cm); electrolyte, 20 mmol/l borate (pH 9.2); separation voltage, +30 kV; direct UV detection at 254 nm; gravity injection for 20 s; sample filtered, diluted 1:10 with water and made up to 50 mmol/l EDTA. Peaks: eo = electroosmosis; 1 = Fe(III)–EDTA complex.

the initial desulphuration solution. A single and symmetrical peak was produced, allowing its easy quantification. It must also be emphasized that under these conditions, Fe(III) and Fe(II) merged into a single peak, presumably because of oxidation of Fe(II) to Fe(III) before or during the electrophoretic process. The method was applied to the determination of total iron in all the solutions sampled during the process. The four calibration points and the points corresponding to the corrected areas measured for the unknown samples are displayed in Fig. 13. The linear correlation coefficient for the calibration points was 0.9991. Finally, the analyses for iron were performed in less than 5 min with R.S.D. ($n = 3$) ranging from 0.0 to 0.2% for the migration times and from 0.1 to 0.9% for the corrected peak areas.

3.8. Overall monitoring of degradation of the desulphuration solution

To gain a deeper insight into the process of degradation of the desulphuration solution, the variations of the concentrations of NTA, IDA, GLY, ammonium and Fe(III) should be considered together. The first panel of Fig. 14 clearly
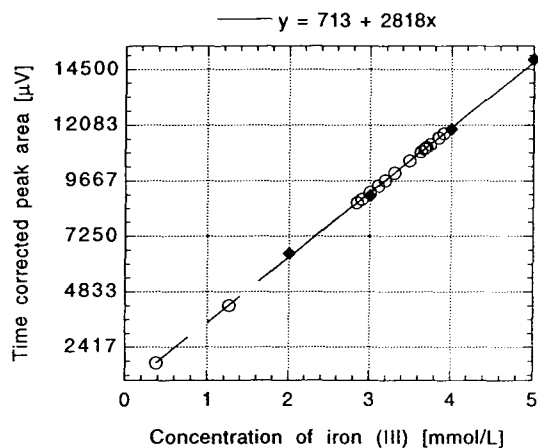
Fig. 13. Calibration graph of time-corrected peak areas as a function of the concentration of iron(III) in the standard solution. ◆ = Calibration points; ○ = points corresponding to the unknown samples of desulphuration positioned after the measured corrected peak areas. For operating conditions, see Fig. 12.
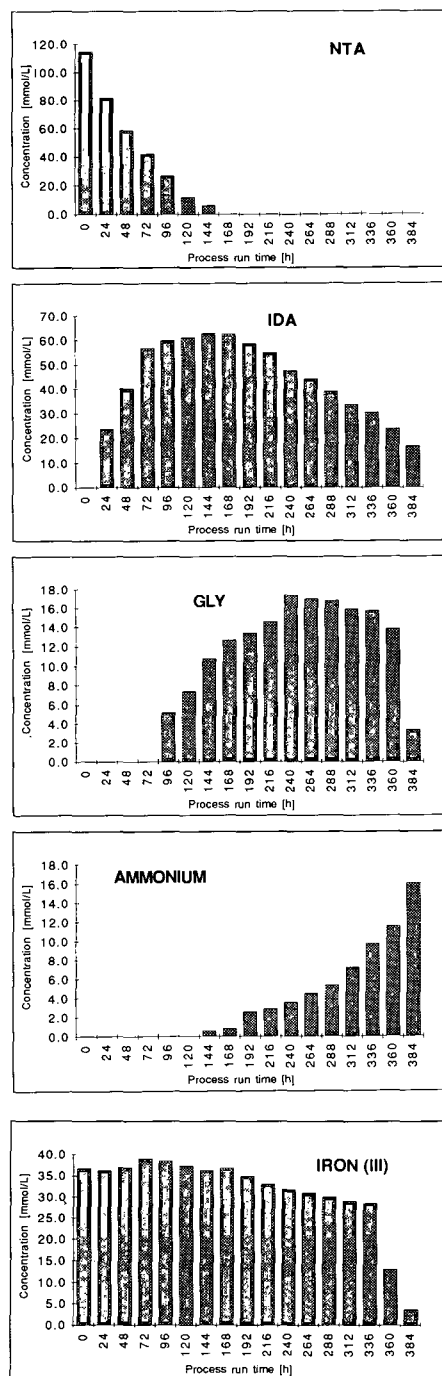
Fig. 14. General outline illustrating the simultaneous variation of the concentrations of NTA, IDA, GLY, ammonium and Fe(III) in the desulphuration solutions as a function of process run time. For further explanations, see text.

illustrates the rapid decomposition of NTA, which totally disappears within 150 h of desulphuration run time. The first step of the degradation leads to IDA, which was detected at a 23 mmol/l concentration level as early as 24 h after the run start. The concentration of IDA increases as long as it is fed by the degradation of NTA, then passes through a maximum as soon as NTA has disappeared and subsequently decreases (Fig. 14, second panel). The following steps of degradation produce GLY and ammonium successively. The degradation of IDA into GLY starts after 96 h of run time, just at the beginning of the period when the concentration of IDA almost reaches a plateau (Fig. 14, third panel). After passing through a maximum, the concentration of GLY decreases in turn at a time corresponding to a larger increase in the concentration of ammonium, appearing as a final degradation product (Fig. 14, fourth panel). Lastly, the results are still corroborated by the variation of Fe(III) concentration (Fig. 14, last panel), which first shows a slow decrease in the concentration of iron(III) as NTA is replaced by IDA and GLY in solution, and in accordance with the order of decreasing stability of the complexes Fe(III)–NTA, Fe(III)–IDA and Fe(III)–GLY [3], [9]. Beyond ca. 350 h of run time the concentration of iron(III) drops drastically, as there is no more complexing agent in the solution.

4. Conclusion

Capillary electrophoresis appears to be a simple, rapid, flexible and cost-effective technique for the quantitative assessment of the various species involved in this desulphuration process. Granted the large differences in absolute mobilities, dissociation constants and charge signs of all the analytes of interest, it was deemed preferable to tailor a few well adapted, distinct methods, rather than a single method, each of them leading to analysis times shorter than 5 min. Special attention was paid throughout this work to quantitative and method validation aspects as they have not often been reported in the past. Very satisfactory repeatabilities were obtained for migration times and peak areas under various electrolyte conditions and with both direct and indirect absorbance modes. As illustrated in Fig. 14, the coherence of the overall results testifies to the confidence that can be placed in these methods. The excellent agreement obtained for the determination of IDA and GLY by different methods and in two different laboratories is also worthy of note. Finally, for the desulphuration process that was the incentive for this study, this set of capillary electrophoresis methods is considered to be very appropriate for fine tuning of the composition of the solution and hence optimizing its lifetime, and subsequently for controlling a scaled-up industrial process.

References

[1] T. Matsuda and T. Nagai, Talanta, 30 (1986) 951.
[2] J.D. Carr, P.B. Kelter and A.T. Ericson, Environ. Sci. Technol., 15 (1981) 184.
[3] L.G. Sillen and A.E. Martell, Stability Constants of Metal-Ion Complexes, Chemical Society, London, 1964.
[4] D.D. Perrin, Dissociation Constants of Organic Bases in Aqueous Solution, London 1965.
[5] F. Foret, S. Fanali, L. Oscini and P. Bocek, J. Chromatogr., 470 (1989) 299–308.
[6] H. Poppe, Anal. Chem., 64 (1992) 1908–1919.
[7] J.L. Beckers, J. Chromatogr. A, 679 (1994) 153–165.
[8] J. Collet and P. Gareil, J. Chromatogr. A, 716 (1995) 115.
[9] D.D. Perrin, Stability Constants of Metal-Ion Complexes, Part B: Organic Ligands, Oxford, 1979.

Capillary electrophoretic analysis of the sodium salt of naphthalenesulfonic acid, formaldehyde polymer in waste water using a polyethylene glycol-coated capillary

Albert J. Nitowski[a,*], Areej A. Al-Mudamgha[b], Phyllis K. Chickering[a]

[a]Uniroyal Chemical Company, World Headquarters, 199 Benson Road, Middlebury, CT 06749, USA
[b]Beckman Instruments, Somerset, NJ 08875, USA

Abstract

Industrial surfactants such as the sodium salt of naphthalenesulfonic acid, formaldehyde polymer are widely used in manufacturing for process control. These water-soluble materials are eliminated with the waste water. This necessitates sensitive and accurate determinations of surfactant concentration in effluents as a prerequisite for effective pollution abatement. Monitoring the concentration of these surfactants by conventional spectrophotometric tests which are currently in use is non-differentiating and subject to gross interferences by many sources. Alternatively, determination of the above surfactant by HPLC methods has not been effective at resolving the various ionic species found. This work describes the selective separation of anionic species by the suppression of the EOF through the judicious choice of a commercially available coated column which increases selectivity by eliminating neutrals and cations through a bi-directional separation system. This is a significant enhancement over traditional approaches like HPLC which observe all UV-absorbing components and interferences. This selectivity is superior to that of the UV methods generating comparatively equivalent CE results when no interferences are present, and more accurate CE results when interferences are present.

1. Introduction

Emulsifiers have important widespread domestic and industrial applications. These materials are ultimately fated for treatment in waste water facilities. Accurate monitoring of these chemicals in pre-treated and post-treated effluents is essential for effective waste water processing. The specific determination of one complex anionic industrial emulsifier, the sodium salt of naphthalenesulfonic acid, formaldehyde polymer (NSA-FP) was previously performed by UV

* Corresponding author.

spectrophotometry [1]. The UV method was found to be non-specific for NSA-FP in the presence of other UV-absorbing chemicals which caused erroneously high results for NSA-FP. Other methods for the determination of anionic surfactants in effluents relied heavily on specific complexing of the anionic species with a fluorescent dye, rhodamine 6G, followed by fluorescence detection [2,3], or by reaction with methylene blue and colorimetric UV–Vis spectrophotometric detection [4–6]. These techniques can yield artificially high values because they lack the specificity required to monitor NSA-FP in the presence of other anionic surfactants and UV-

absorbing chemicals. Additionally, HPLC procedures have been complicated due to the ionic character of these compounds [7–10]. These procedures lack either specificity, sufficient analyte resolution, or sensitivity.

~ While CE offers a viable alternative for the separation of anionic species, certain limitations must be considered when designing a separation strategy. The high electroosmotic flow inherent with a fused-silica CE technique could hinder the analysis of complex anions in solution by creating bulk fluid movement toward the injector side of the capillary column when a negative potential is applied (anode at the detector). A positive potential must be avoided if the goal of the experiment is to attract the anionic species past the detector window, since the anode is on the injector side of the column and the electrophoretic mobility of the anions will be toward the anode. The best way to solve this paradox of polarity-dependent mobility and EOF is by suppressing the EOF. Other works have described this EOF suppression or reversal by addition of modifiers such as quaternary ammonium salts and alcohols [11–14]. In the present work, free solution capillary electrophoresis (FSCE) is employed using a commercially available PEG-100 coated capillary column and buffer. The separation of anionic components is based purely on electrophoretic mobility of the analytes since the EOF is greatly suppressed. Unwanted neutral species and cations migrate toward the injector side of the column because of minimal EOF and reversed polarity, respectively. Since the anions migrate with strong mobility toward the detector side of the column, a bi-directional system exists. This bi-directional system provides a simplified process for separating and detecting the analytes of interest over traditional techniques like HPLC.

The UV test measures the absorbance of the effluents at 230 nm and a NSA-FP standard calibration curve is used for quantitation. However, this test has an unacceptable bias when interfering chemicals are present. Sample preparation steps for the UV test require filtration and dilution. No separation of NSA-FP analytes from other UV-absorbing species is attempted. Direct measurement of sample absorption versus a NSA-FP standard is the criterion for a positive result. The purpose of this FSCE methodology is the industrial process utilization of CE to replace a non-specific UV test. This study will explore the advantages of using FSCE in a simple approach to determine $\mu g/ml$ levels of a commercial anionic surfactant. This paper presents a comparative study for the determination of NSA-FP in an industrial effluent system by CE and UV methods.

2. Experimental

2.1. CE experimental

The CE system used for this study was the Beckman P/ACE 5500 capillary electrophoresis instrument, equipped with a diode array detector (DAD) and System Gold software integration package (Beckman Instruments, Fullerton, CA, USA). A polyethylene glycol (PEG-100) coated capillary column 57 cm × 75 μm I.D. from Scientific Resources (SRI, Eatontown, NJ, USA) was employed to minimize the electroosmotic flow. The detector window was located 50 cm from the injection end of the capillary column. The CE electrical configuration was in reversed-polarity mode for anion detection (anode at the detector end) using a constant-current mode set at 30 μA (approximately 20 kV required).

New capillary columns were conditioned by rinsing with acetonitrile for 5 min, followed by a 5-min HPLC grade water rinse, and a 10-min rinse with the run buffer solution. A 3-min rinse of run buffer solution preceded and followed each sample and standard run.

The analysis run buffer solution was 40 mM sodium tetraborate, pH 9.0 (SRI, Eatontown, NJ, USA).

Pressure sampling was employed for 7 s using a pressure of 138 kPa to inject approximately 41 nl of sample or standard. This was followed by an injection of the sodium tetraborate electrolyte for 1 s at 138 kPa for a 6-nl buffer slug to eliminate diffusion of the sample into the injec-

tion run buffer vial. This sandwich technique significantly improved the precision of the test. The column was maintained at 18°C with the liquid cooling capability of the P/ACE system.

Detection for electropherograms was achieved at 228 nm with a 4-nm band width and was employed for all CE quantitative work. The DAD scanned in purity mode from 200 to 500 nm at a rate of 4 Hz, with the "scan on impurity" function activated. This function stores UV spectral data only when a component elutes with an adsorption within the scan range. This process was used to monitor for the presence of UV-absorbing materials not related to NSA-FP.

Samples were prepared by filtering a 1.0-ml sample aliquot with a 0.2-μm PTFE membrane (syringe type, Scientific Resources, Eatontown, NJ, USA). The filtrate was diluted to 4.4 ml by adding 1.0 ml of electrolyte solution, and 2.4 ml water. Quantitation was achieved with a five-point linear calibration curve of the emulsifier NSA-FP at a concentration range of 45 to 275 μg/ml. The calibration curve was generated by the response of NSA-FP at 228 nm (NSA-FP λ_{max}). The analysis time is 27 min.

2.2. UV–Vis experimental

The UV–Vis spectrophotometry testing was performed on a Beckman DU-70 UV–Vis spectrophotometer using a 1-cm cell path length at 230 nm. Samples were prepared by direct dilution with water at 1:200. Quantitation was achieved with a five-point linear calibration curve of the emulsifier NSA-FP at a concentration range of 0.7 to 5.5 μg/ml.

2.3. GC–MS experimental

Gas chromatography–mass spectrometry (GC–MS) support testing was performed on a Hewlett-Packard 5970B MSD GCMS system equipped with a 30 m × 0.25 mm I.D., 0.25 μm film thickness DB-5 MS capillary column (5% phenyl, 95% methyl, J&W Scientific, Houston, TX, USA). Samples were prepared by liquid–liquid extraction of 5 ml of sample with 0.5 ml of

dichloromethane. The dichloromethane phase was isolated, concentrated to 100 μl, and a 1-μl aliquot was injected onto the GC–MS system. The GC capillary injection port was in the splitless mode for one minute at 240°C, and the column temperature program was as follows: 35°C for one minute, ramp at 8°C per minute to 300°C, hold at 300°C for 15 min. Helium pressure was held constant at 21 kPa. The mass spectrometer was scanned from 40 u to 700 u at 1.0 scan per second. The electron multiplier detector was maintained at 2400 eV; data was acquired on a HP Chemstation personal computer.

2.4. Reagents

All standard solutions were prepared by diluting 4 μg/ml stock solution containing the analyte, sodium salt of naphthalene sulfonic acid–formaldehyde polymer (Henkel Corp., Ambler, PA, USA). The NSA-FP is obtained as a 45% aqueous solution. Samples were prepared with 40 mM sodium tetraborate, pH 9.0 (Scientific Resources) and de-ionized water filtered by a HPLC grade water filtration system (Millipore, Bedford, MA, USA). Other interference reference materials were obtained as follows: sodium dimethyldithiocarbamate (Uniroyal Chemical, Middlebury, CT, USA); 2,6-bis-(1,1-dimethylethyl)-4-methylphenol (BHT: Aldrich, Milwaukee, WI, USA).

3. Results and discussion

3.1. Interferences eliminated

Prior to developing any electrophoretic separation, to accurately determine NSA-FP in effluents in the presence of neutral and ionic species, an understanding of the characterization of the undesired materials present in the effluents is required. Qualitative GC–MS was used as a support technique to identify neutral species present in the effluents which would interfere with the spectrophotometric test and would have to be resolved or screened by the CE. Some of

Table 1
Identification of neutrals present in effluents which could interfere with the UV test

Peak	Identification
1	Toluene
2	Phenol
3	N,N-Dimethyl methanthioamide
4	1,3-Dichlorobenzene
5	1-Phenylethanone (acetophenone)
6	4-Methylphenol
7	Alkylated phenols
8	Tetramethyl thiourea
9	1-Benzazine (quinoline)
10	2,3-Benzopyrrole (indole)
11	2,6-Bis-(1,1-dimethylethyl)-4-methylphenol (BHT)
12	1-Naphthalenol and 2-naphthalenol
13	Nonylphenol isomers
14	Alkylated benzothiophene
15	1,1-Sulfonylbis[4-chlorobenzene]
16	2,2'-Methylenebis[6-(1,1-dimethylethyl)-4-ethylphenol]

the UV-absorbing materials identified through the use of GC–MS are observed in Table 1. A total-ion chromatogram of a dichloromethane extract of industrial effluent is shown in Fig. 1. The N,N-dimethyl methanthioamide and tetramethylthiourea are secondary to the process effluent; their existence is due to the normal degradation of sodium dimethyldithiocarbamate (Na-DMDTC), as an anionic industrial process aid [15], which was present in the industrial effluents used in this study. The DMDTC anion is a strong UV absorber with approximately 30% of the extinction coefficient of NSA-FP at 230 nm. The presence of DMDTC introduces bias to the spectrophotometric test, generating erroneously high results for NSA-FP. To illustrate this bias, both a neutral and anionic species were specifically added to effluent at three different
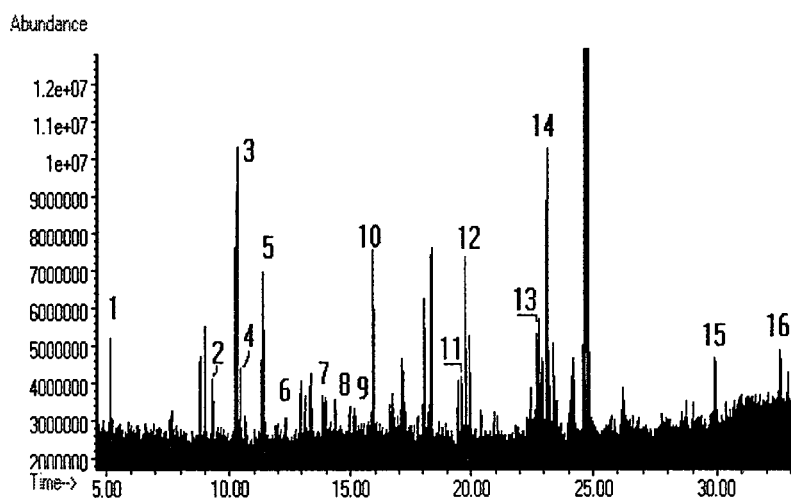
Fig. 1. GC–MS total-ion chromatogram of dichloromethane extract of industrial effluent. Components identified to be UV absorbers are identified in Table 1.

concentrations and analyzed by both UV and CE. The elimination of neutral species in the effluent is demonstrated by the addition of BHT (2,6-bis-[1,1-dimethylethyl]-4-methylphenol). A composite of six effluent samples was spiked with three levels of BHT. The composite was analyzed by CE and UV tests. The bias for NSA-FP values attributed to the spiked samples was significant for the UV test; negligible for the CE test. The DMDTC anion is readily separated and observed in the CE test. Thus, neutrals which bias the UV test are eliminated in the CE test, and anions which interfere with the UV test and are observed in the CE test are readily separated from the analyte of interest, NSA-FP. Table 2 shows both test results from spiking an effluent with an anion (Na-DMDTC) and a neutral species (BHT).

The elimination of neutral and cationic UV-interfering chemicals from the electrophoretic system by reversed polarity and minimal EOF accounts for the simple and accurate determination of the NSA-FP emulsifier by CE (Fig. 2). Neutral organics present in the waste water are not observed in the CE test since the EOF is extremely low due to the use of the polyethylene glycol coated capillary. Attempts to measure the EOF were not successful due to its extremely low value. A maximum EOF of 0.08 cm/min was calculated. Any EOF generated by the reversed
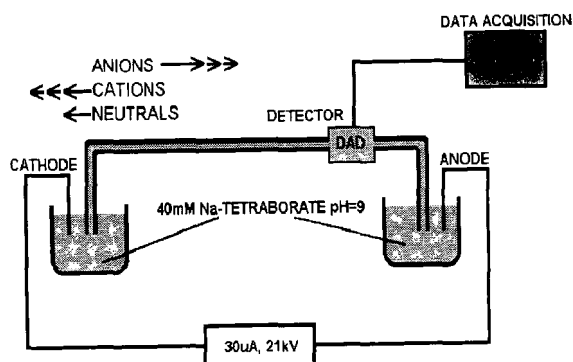
Fig. 2. Schematic diagram of the CE instrumentation used in this work. This configuration employs negative potential and a PEG-100 coated capillary column to eliminate EOF.

polarity mode is in the direction of the injector, causing neutrals to exit the capillary without passing the detector window. The reversed polarity is also responsible for the rapid migration of cations to the injector exit of the capillary column. Thus, only anionic species migrate through the coated capillary and are detected. Correlation of CE and UV results for the determination of NSA-FP in waste water effluents is generally good when no other UV-absorbing materials are present since both techniques monitor the NSA-FP when interferences are absent. The anionic materials present which were not related to NSA-FP were separated by the high resolving power of the FSCE. Fig. 3 shows the electrophoretic separation of DMDTC and NSA-FP.

The NSA-FP standard material is a complex, multiple component emulsifier. NSA-FP is a polymeric material with an average molecular mass of 2600 u. The generic structure for NSA-FP described in Fig. 4 is thought to contain an average of one sulfonic acid group (one negative charge) for each 220 u. Thus, the charge-to-mass ratio, which dictates the migration order of the analytes, tends to be constant for the bulk of the NSA-FP polymeric components. This constant-ratio theory is supported by the bulk of the NSA-FP components exhibiting the same electrophoretic mobility. Table 3 lists the electrophoretic mobilities of the NSA-FP and Na-DMDTC materials. The mobility values in Table

Table 2
Effects of spiking waste-water solution with Na-DMDTC and BHT

Amount added (μg/ml)	Found (μg/ml)	
	UV	CE
BHT		
0	0	0
1	1	0
10	4	0
100	38	3
Na-DMDTC		
0	0	0
402	99	6
1295	360	5
3687	1094	1
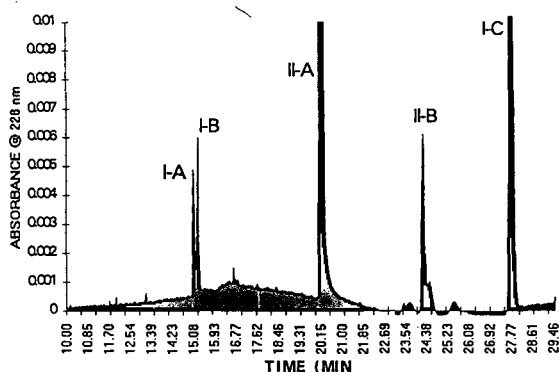
Fig. 3. Analysis of NSA-FP emulsifier in an industrial effluent with a Na-DMDTC spike resolved. Peak numbers refer to chemical structures in Fig. 4. Analytical conditions: capillary, fused-silica (PEG-100 coated 57 cm × 75 μm I.D.); electrolyte, 40 mM sodium tetraborate buffer (pH 9.0); constant current mode, 30 μA (approximately 21 kV applied); detection, UV absorbance at 228 nm.

3 are based on migration times and assume a zero electroosmotic flow. It should be noted that peaks I-A and I-B (Fig. 3) are indigenous to NSA-FP but exhibit different electrophoretic mobilities than the bulk of the NSA-FP con-
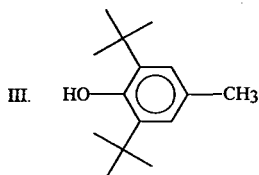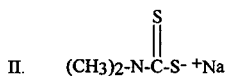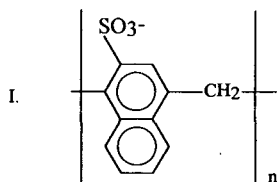
Fig. 4. List of the standards employed in this study: sodium salt of naphthalene sulfonic acid–formaldehyde polymer (I), sodium dimethyldithiocarbamate (II), and 2,6-bis-(1,1-dimethylethyl)-4-methylphenol (III).

stituents. The identity of peaks I-A and I-B is unknown; however, based on peak shapes, migration times, and pertinent chemistries it can be inferred than these two components are small-molecular-mass anions, perhaps inorganic sulfates. Peaks I-A and I-B are found in the standard NSA-FP, and are therefore not from the industrial effluent.

3.2. Determination of NSA-FP

Fig. 5 shows the results of quantifying NSA-FP in an industrial effluent stream over time. When other compounds which absorb at similar wavelengths are present in the effluent, the UV results for NSA-FP are higher than the CE results. The results of the 30-day effluent study show an 8 percent lower average value for NSA-FP for CE compared to UV.

A three-level calibration curve with duplicate injections of standard NSA-FP was done daily. The standard calibration curve for NSA-FP was based on the peak area of the major NSA-FP peak (peak I-C, Fig. 3). Standard concentrations ranged from 30 to 250 μg/ml. Correlation coefficients of 0.9999 are typical using a least squares linear regression method. This method is rectilinear over the concentration range of interest (50–7000 μg/ml) and is sensitive to 50 μg/ml.

3.3. Repeatability and reproducibility

The calculations for repeatability (intra-day precision) and reproducibility (inter-day precision) were based on the assay values of a six-sample effluent composite. The initial concentration was diluted to make three samples; concentrations corresponded to the low (140 μg/ml), medium (250 μg/ml), and high (850 μg/ml) points of the calibration curve. This was accomplished using five replicates of each sample analyzed each day for three days. The CE test solutions were injected in duplicate and peak areas were averaged. Table 4 displays these statistical calculations for repeatability and reproducibility in %R.S.D.

The three-day average values (NSA-FP) for

Table 3
Electrophoretic mobility of NSA-FP and Na-DMDTC

Species	μ_{ep} (cm^2 min^{-1} V^{-1}, $\times 10^3$)
Peak I-A (NSA-FP)	10.26
Peak I-B (NSA-FP)	10.08
Peak II-A (Na-DMDTC)	7.62
Peak II-B (Na-DMDTC degradent)	6.41
Peak I-C (NSA-FP, main component)	5.59
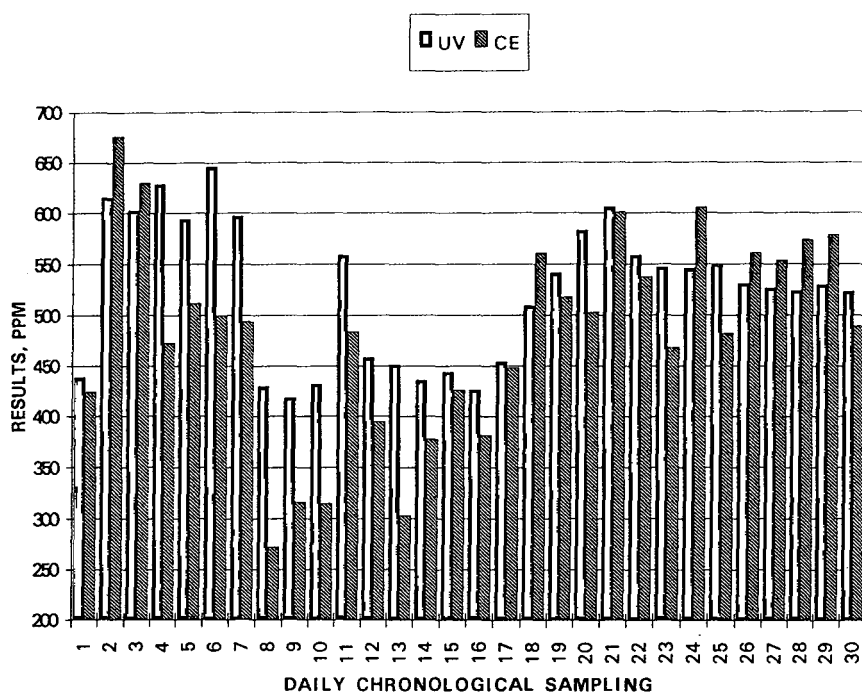
Fig. 5. Column chart displaying the comparison of CE vs. UV results for NSA-FP in industrial effluent samples collected over a 30-day period. CE values are significantly lower than UV values when other UV-absorbing chemicals are present. CE values were found to be an average of 8% lower than UV results for these samples.

Table 4
NSA-FP assay variability for CE and UV tests (in %R.S.D.)

Effluent dilution	Day 1		Day 2		Day 3		Inter-day	
	CE	UV	CE	UV	CE	UV	CE	UV
1:1	10.5	0.1	10.6	0.2	11.3	0.4	4.2	0.4
1:2	5.5	0.2	5.6	0.1	4.4	0.3	8.3	0.3
1:5	10.7	0.8	7.5	0.6	9.9	0.3	7.2	0.3

intra-day variability were found to be greater for CE than for the UV test by a factor of 22. The stability of the repeatability demonstrated by the UV test is partially attributed to the greater (1:200) dilution factor used in sample preparation, as opposed to 1:4.4 for the CE test. The UV test also demonstrated better reproducibility than the CE test by a factor of 20. The better precision of the UV test is offset by the better accuracy of the CE test. The values obtained for the three dilutions of the composite effluent were found to be 192, 104, and 42 μg/ml (or 22%, 41%, and 31%) greater for UV than CE for the 1:1, 1:2, and 1:5 dilutions, respectively. These higher values show the bias of the non-differentiating UV test.

4. Conclusions

Capillary electrophoresis using reversed polarity and coated column technology provides efficient, rapid, and accurate analysis of the surfactant, (sodium salt of) naphthalene sulfonic acid–formaldehyde polymer in waste water. Arduous sample preparations are not necessary, cations and neutral species do not interfere, and anionic chemicals are separated from the analyte. Results obtained by this method combine response from all polymeric analytes of interest while eliminating interfering chemicals. This method provides an increased level of confidence in the determination of NSA-FP in industrial effluents over existing spectrophotometric methodologies. The precision of the UV test is superior to that of the CE test for repeatability and reproducibility. Average relative standard deviations for both of these parameters were found to be 0.3% (UV) and 7.0% (CE). The CE test demonstrates greater accuracy than the UV test, estimated at 30% better based on comparative assays at three concentration levels for NSA-FP. The specificity of CE provides accurate data for the efficient control of pollution abatement procedures for municipal and industrial waste-water treatment facilities. The replacement of non-specific testing for the NSA-FP emulsifier in municipal and industrial effluents with capillary electrophoresis demonstrates the utility of the technique beyond the research laboratory environment.

References

[1] C. Puchalsky, Method CCL-1249 Uniroyal Chemical Co., 1989, Uniroyal Chemical Co., World Headquarters, Middlebury, CT 06749.
[2] J. Gao and F. Yu, J. Fenxi Huaxue, 19 (1991) 1395–1397.
[3] S. Rubio-Barroso, M. Gomez-Rodriguez and L. Polo-Diez, Microchem. J., 37 (1988) 93–98.
[4] P.A. Perov, L. Yu. Glukhova, I.I. Germasheva and A.P. Rudoi, Zavod. Lab., 55 (1989) 3–6.
[5] L. Wood and M. Keynes, British Standards Institute Report, BS6068 (1986) S.2.23: 1986.
[6] S.N. Shtykov and E.G. Sumina, Zh. Anal. Khim., 40 (1985) 907–910.
[7] K. Levsen, M. Emmrich and S. Behnert, J. Anal. Chem., 346 (1993) 732–737.
[8] A. Marcomini, A. Di Corcia, R. Samperi and S. Capri, J. Chromatogr., 644 (1993) 59–71.
[9] L. Nitschke and L. Huber, J. Anal. Chem., 345 (1993) 585–588.
[10] L. Nitschke, R. Mueller, G. Metzner and L. Huber, J. Anal. Chem., 342 (1992) 711–713.
[11] N.J. Benz and J.S. Fritz, J. Chromatogr. A, 671 (1994) 437–443.
[12] P. Jandik and W.R. Jones, J. Chromatogr., 546 (1991) 431.
[13] J. Romano, P. Jandik, W.R. Jones and P.E. Jackson, J. Chromatogr., 546 (1991) 411.
[14] W.R. Jones and P. Jandik, J. Chromatogr., 608 (1992) 385.
[15] R.R. Barnhart, Kirk-Othmer Encyclopedia of Chemical Technology, John Wiley and Sons, Vol. 20, 1982.

Capillary electrophoresis of inorganic anions and organic acids using suppressed conductivity detection Strategies for selectivity control

M. Harrold, J. Stillian, L. Bao, R. Rocklin, N. Avdalovic*

Dionex Corporation, 1228 Titan Way, Sunnyvale, CA 94086, USA

Abstract

The use of suppressed conductivity as a detection scheme for capillary electrophoresis (CE) is described. A comparison is made between several electrolytes for CE with suppressed conductivity detection (CESC) in terms of efficiency of separation and peak shape. The ability to modify electrophoretic mobility and selectivity as a function of temperature and electrolyte ionic strength is demonstrated. The separation of a variety of low-molecular-mass organic acids is optimized using the addition of metal ions to the separation electrolyte.

1. Introduction

The traditional method of ion analysis, ion chromatography, has benefited greatly from the wide range of selectivity available from different stationary phases. The availability of stationary phases with differing selectivity has provided the analyst a range of options for solving difficult analytical problems. Isotachophoresis has also been described as a separations method for the determination of inorganic ions but suffers from poor detection limits [1–3]. Capillary electrophoresis (CE) has been attracting interest in recent years as a promising tool for the analysis of inorganic anions and low-molecular-mass organic acids. Unlike chromatography, however, separations using CE do not rely on interaction with a stationary phase but rather on differences in electrophoretic mobility between analyte ions. The electrophoretic mobility of an ion is often

viewed as a stable property and thus CE would have difficulty separating ions with similar electrophoretic mobilities. Separation of some species can be accomplished by changing electrolyte pH. This strategy, however, is effective in changing selectivity only if the electrolyte pH is changed in the vicinity of the analyte's pK_a, thereby changing the analyte's charge to mass ratio. For inorganic anions, which often have a pK_a less than 2, changing the electrolyte pH to modify selectivity is not practical. At low pH, the electroosmotic flow (EOF) in a silica capillary is too low to carry inorganic anions toward the detector when operating in a source-vial-positive-polarity configuration. It is possible to reverse the polarity so that the anions are moving in the same direction as the EOF, but the current generated at an electrolyte pH of less than 2 would make operation difficult, if not impossible.

The separation of inorganic anions using capillary electrophoresis has been the subject of many

---

* Corresponding author.

publications during the past five years [4–12]. For detection of these analytes, many researchers have turned to indirect UV detection. The method of indirect UV is attractive because it is a universal detection scheme for non-UV-absorbing ions and it uses existing instrumentation. However, it suffers from a high background, and consequently, high noise [11]. In addition, the concentration detection limits, linear range, and dealing with matrix effects are inferior to chromatographic methods. For these reasons, other detection schemes have been devised for capillary electrophoresis of inorganic anions. Several publications describe the use of electrochemical detection for capillary electrophoresis, including amperometry [13–18], conductivity [19–23], and suppressed conductivity [24,25]. Sensitivity of electrochemical techniques is not dependent on detector cell size, as is the case with UV detection, so there is no loss of sensitivity as a result of scaling down in size. Conductivity detection is also nearly universal for detection of inorganic anions.

Optimization of conditions for determining anions with CESC has not been studied in detail. For example, the effects of electrolyte concentration, temperature, and chemical composition have not been described for CE using suppressed conductivity detection. Modification of relative electrophoretic mobilities for aminobenzoic acids with UV detection has been described as a function of temperature [26]. The effect of buffer concentration on electrophoretic mobility and migration time has been reported by several researchers [27–31]. Selectivity modification using chelating agents in the electrolyte has been used as a means of separating metal ions [32–34]. The addition of metal ions to the leading electrolyte in isotachophoresis (ITP) has been described for selectivity control during ITP separations of inorganic anions but with mixed results [1–3]. Complexation has not been extensively developed for modifying anion selectivity in capillary zone electrophoresis.

This article describes efforts toward optimizing selectivity for capillary zone electrophoresis with suppressed conductivity detection for determining inorganic anions and organic acids by adding metal ions to the electrolyte. Also described are the variations in electrophoretic mobility for common inorganic anions as a function of temperature, electrolyte ionic strength, and the addition of metal additives to the separation electrolyte.

2. Experimental

2.1. Apparatus

The apparatus used for CE with suppressed conductivity was a modified version of one described previously [24]. A schematic of the assembly is shown in Fig. 1. Unless otherwise indicated, all work was done on the apparatus shown in Fig. 1. The separation capillary was a 60-cm long, 75 μm I.D., 360 μm O.D. fused-silica capillary (Polymicro Technologies,
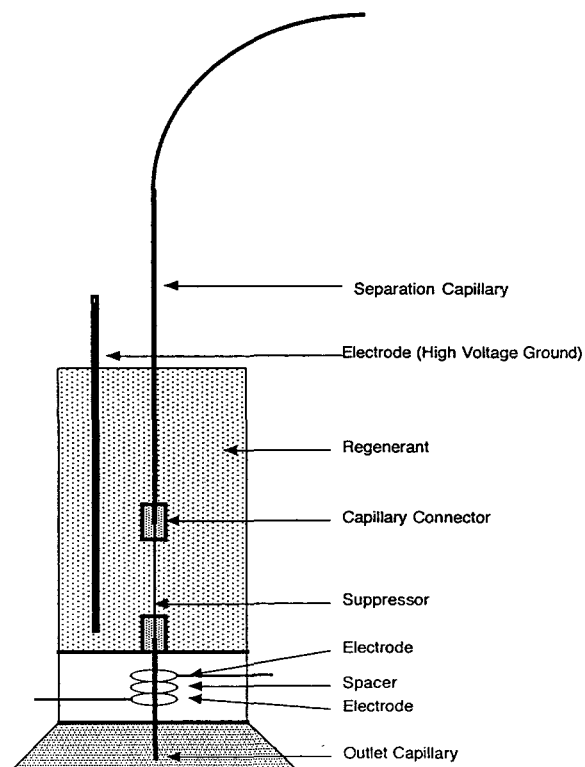
Fig. 1. Schematic of capillary–suppressor–conductivity cell assembly.

Phoenix, AZ, USA). All work was done on Dionex's CES-I with an ED40 electrochemical detector or CDM-II conductivity detector (Dionex, Sunnyvale, CA, USA). Data were collected and processed using a Dionex AI-450 chromatography workstation. Temperature control of the separation compartment was accomplished using a microprocessor controlled temperature controller, heater, and thermocouple (Omega Instruments, Stamford, CT, USA).

2.2. Reagents

High-purity sodium tetraborate, anhydrous (Aesar/Johnson-Matthey, Ward Hill, MA, USA), glycine (Sigma, St. Louis, MO, USA), taurine (Serva, Crescent Chemical, Hauppauge, NY, USA), and 4-cyanophenol (Aldrich, Milwaukee, WI, USA) were used as electrolytes for CE separations. Sulfuric acid regenerant concentrate, 500 mM, (Dionex) was used to prepare the working 5 mM regenerant. Sodium hydroxide (50%) (Fisher Scientific, Pittsburgh, PA, USA) was used to prepare titrant for pH adjustment of buffers. Anion standards were prepared using sodium salts from Fisher Scientific.

3. Results and discussion

3.1. Anion separations using CESC

The separation of anions using CE depends on the magnitude and direction of electroosmotic flow (EOF), and the electrophoretic mobility (μ_a) of the analyte ions. Both the electroosmotic flow and the electrophoretic mobility are vector quantities and are additive. In the case of anion analysis using an unmodified silica capillary, these two vectors are in opposite directions. The convention used for the sign of the vector is a positive number for migration toward the cathode, and a negative number for migration toward the anode. The magnitude of the electroosmotic flow is highly dependent on the buffer pH, ionic strength, and temperature of the separation.

At low buffer ionic strength (less than 5 mM) and high pH (greater than pH 9), the magnitude of the electroosmotic flow in a typical capillary is in the range of $85 \cdot 10^{-5}$ to $110 \cdot 10^{-5}$ cm^2/V·s. The electrophoretic mobilities (at infinite dilution) of common inorganic anions are shown in Table 1. Some inorganic anions can have mobilities as high as $-85 \cdot 10^{-5}$ cm^2/V·s, while lower-mobility inorganic anions and organic acids generally have mobilities less than $-60 \cdot 10^{-5}$ cm^2/V·s. Because the EOF and electrophoretic mobility are additive vectors, it is necessary for the magnitude of the EOF to exceed the analyte's electrophoretic mobility by at least $10 \cdot 10^{-5}$ cm^2/V·s so that the analyte's net migration velocity is toward the detector, as shown in Fig. 2. If an anion's net mobility is less than $10 \cdot 10^{-5}$ cm^2/V·s, the time required to detect the analyte will become excessively long.

Fig. 3 shows a separation under optimized conditions using 2 mM sodium tetraborate, pH

Table 1
Limiting ionic conductance and electrophoretic mobility at infinite dilution

Anion	Limiting ionic conductance[a] (cm^2/Ohm-equivalent)	Electrophoretic mobility (cm^2/V·s)
Fluoride	54.4	$-56.3 \cdot 10^{-5}$
Phosphate (HPO$_4^{2-}$)	57	$-59.1 \cdot 10^{-5}$
Nitrate	71.4	$-74.0 \cdot 10^{-5}$
Nitrite	71.8	$-74.4 \cdot 10^{-5}$
Sulfate	80.0	$-82.9 \cdot 10^{-5}$
Chloride	76.35	$-79.1 \cdot 10^{-5}$
Bromide	78.1	$-80.9 \cdot 10^{-5}$

[a] From Ref. [44].
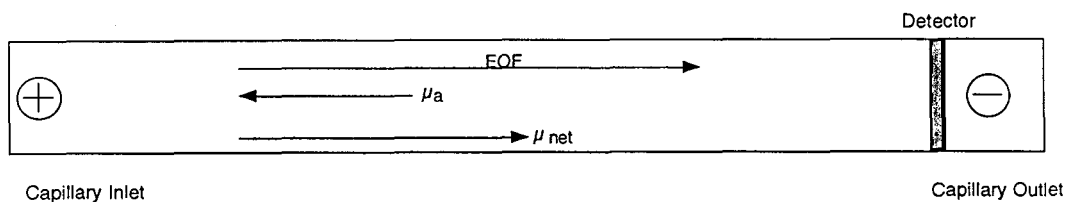
Fig. 2. Magnitude and direction of electroosmotic flow (EOF), electrophoretic mobility (μ_a), and net mobility [μ_{net} or μ_a (observed)]. Under the conditions used for separation of anions, the EOF is greater than and in the opposite direction of the electrophoretic mobility. This results in a net migration velocity of anions toward the cathode.

9.2, as an electrolyte. The EOF as measured by the water (neutral) dip is $97.3 \cdot 10^{-5}$ cm^2/V·s. The highest-mobility analyte, bromide, has an electrophoretic mobility of $-76.0 \cdot 10^{-5}$ cm^2/V·s and thus, a net mobility of $21.3 \cdot 10^{-5}$ cm^2/V·s toward the detector. This results in an overall migration time of 11.7 min for bromide. Note that when using this mode of separation, lower electrophoretic mobility analytes are detected first, whereas those with higher electrophoretic mobility are detected later.

3.2. Suppressible buffers for CESC

The use of suppressed conductivity detection imposes certain restrictions on the nature of the electrolyte that can be used. A variety of elec-

Fig. 3. Separation of anions using CESC. Electrolyte: 2.0 mM sodium tetraborate (ultrapure); capillary: 60 cm × 75 μm I.D. fused-silica; voltage: +24 kV, detector-end cathodic; hydrostatic injection: 40 mm/5 s; regenerant: 5 mM sulfuric acid; detection: suppressed conductivity; temperature: 30°C. Sample injected from water. Peaks (all at 1.0 ppm): 1 = water dip; 2 = fluoride; 3 = phosphate; 4 = nitrate; 5 = nitrite; 6 = sulfate; 7 = chloride; 8 = bromide.

trolytes are candidates for use with suppressed conductivity detection. While many electrolytes such as sodium carbonate, sodium borate, and sodium p-cyanophenate have been well characterized as eluents for ion chromatography [35], amino acid electrolytes such as taurine and glycine are less well known [36–38].

A suitable buffer for CESC has some unique constraints. The peak shape obtained for analytes in CE has been shown to depend on a close match of electrophoretic mobility of electrolyte ions and analyte ions [19]. Although no single electrolyte will match all analytes, the electrolyte should have an electrophoretic mobility similar to that of the analytes being separated to result in a good peak shape. In addition to these requirements, the use of suppressed conductivity detection for anions dictates that the electrolyte be convertible to a weakly conducting species when passed through a cation exchanger in the hydronium form. The mechanism of chemical suppression is well documented [39–41] and is analogous to chemical suppression in ion chromatography. These two constraints, the ability to be suppressed to a weakly conducting species and a suitable electrophoretic mobility, are the major considerations in picking an electrolyte for CESC.

For efficient separation of inorganic ions and organic acids, a suppressible electrolyte with electrophoretic mobility similar to the analytes is desired. The following compounds are potential candidates for CESC electrolytes: sodium tetraborate, sodium glycinate, sodium taurinate, sodium bisulfide, sodium phenate, sodium cyanide, sodium 4-cyanophenate and sodium carbonate. Although there are other suppressible electrolytes, primarily amino acids, only those listed above are expected to have sufficiently high
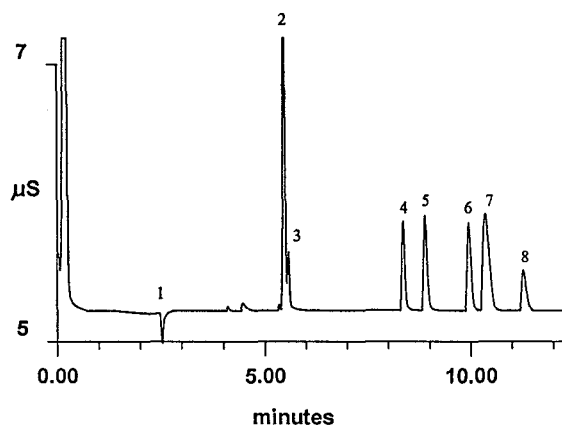
electrophoretic mobility. Due to the toxicity of sodium cyanide, sodium sulfide, sodium phenate, sodium 4-cyanophenate, and their suppression products, these electrolytes are considered inappropriate. Electropherograms using some of these electrolytes for CESC are shown in Fig. 4. The tailing of later migrating peaks in the electropherograms is indicative of a mismatch of electrophoretic mobilities between the electrolyte and analytes. The mismatch of electrophoretic mobility for the slow migrating electrolyte species is concurrent with an increase in efficiency for early migrating peaks. Therefore, while no single electrolyte will give a perfect peak shape for all analytes, an electrolyte suitable for the analytes of interest can be selected if we know relative electrophoretic mobilities. For the analysis of inorganic anions, borate and glycinate appear to be best suited.

3.3. Ionic strength effects on selectivity

The effect of electrolyte ionic strength on selectivity in CESC was examined using sodium tetraborate, pH 9.2, as an electrolyte. A seven-

anion test mixture was run repeatedly and the electrophoretic mobilities of the anions were calculated using the following formulas:

$$\mu_{EOF} = l_d l_t / t_w V \tag{1}$$

$$\mu_a(\text{observed}) = l_d l_t / t_a V \tag{2}$$

$$\mu_a(\text{actual}) = \mu_a(\text{observed}) - \mu_{EOF} \tag{3}$$

where μ_{EOF} is the electroosmotic flow, μ_a (observed) is the net electrophoretic mobility, and μ_a (actual) is the inherent electrophoretic mobility of the analyte ion. Further, l_d is the distance from the inlet to the detector, l_t is the total capillary length, t_w is the migration time of the water dip in seconds, t_a is the migration time of the analyte peak in seconds, and V is the separation voltage.

To examine the effect of ionic strength on selectivity, a series of electrolytes with different ionic strengths were run. The ionic strength of a dilute sodium tetraborate solution was calculated as simply twice the molar concentration. This simplification is appropriate at low millimolar concentrations of borate ion [42]. The range of total electrolyte ionic strength was from 2.0 to 10
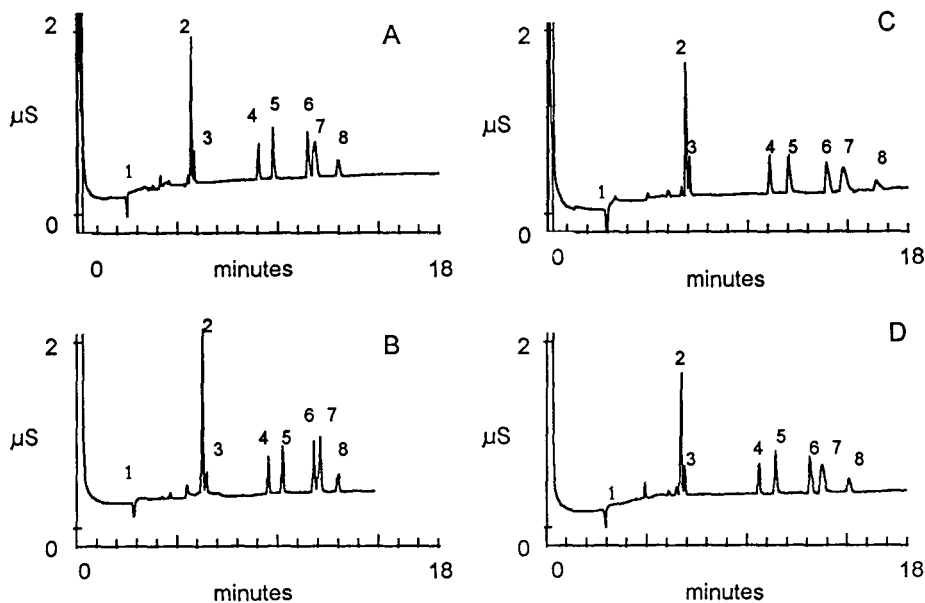
Fig. 4. Comparison of electrolytes for CESC. Conditions and peak identification same as Fig. 3, except for different electrolytes and voltages as follows: (A) 2.0 mM sodium tetraborate (pH 9.2), 24 kV; (B) 4.0 mM sodium glycinate (pH 10.5), 20 kV; (C) 4.0 mM sodium taurinate (pH 10.5), 20 kV; (D) 4.0 mM sodium p-cyanophenate (pH 10.5), 20 kV.

mM (1.0 to 5.0 mM Na$_2$B$_4$O$_7$). The resulting electropherograms are shown in Fig. 5. The front shoulder on the chloride peak observed at higher electrolyte ionic strength was previously reported to be the ^{37}Cl isotope [24].

Calculated electrophoretic mobility [μ_a (actual)] as a function of ionic strength is plotted in Fig. 6. As the ionic strength of the electrolyte increases there is a decrease in EOF. The decrease in EOF with increasing electrolyte ionic strength is well documented [27–31] and is attributed to a decrease in zeta potential due to compression of the electrical double-layer. The overall migration time also increases as the ionic strength is increased, but the overall migration time is the vector sum of the EOF and an ion's inherent electrophoretic mobility. The calculated electrophoretic mobilities of the analyte ions become slower with decreasing ionic strength and individual ions show differences in their response to changing ionic strength. At the highest ionic strength studied, the calculated electrophoretic mobilities of the analyte ions approach the values predicted by their limiting ionic conductance. Ionic strengths higher than 5 mM sodium tetraborate could not be studied because the low EOF at high ionic strength results in an excessively long run time. The observed behavior, a direct relationship between ionic strength and inherent mobility, is contrary to what is expected based on Kohlrausch's Law. Kohlrausch's Law predicts that the equivalent conductivity of an ion should have an inverse linear relationship with the square root of concentration [43]. The law also predicts a negative slope for a plot of equivalent conductivity versus concentration. Equivalent ionic conductance is directly related to electrophoretic mobility by the Faraday constant [43],
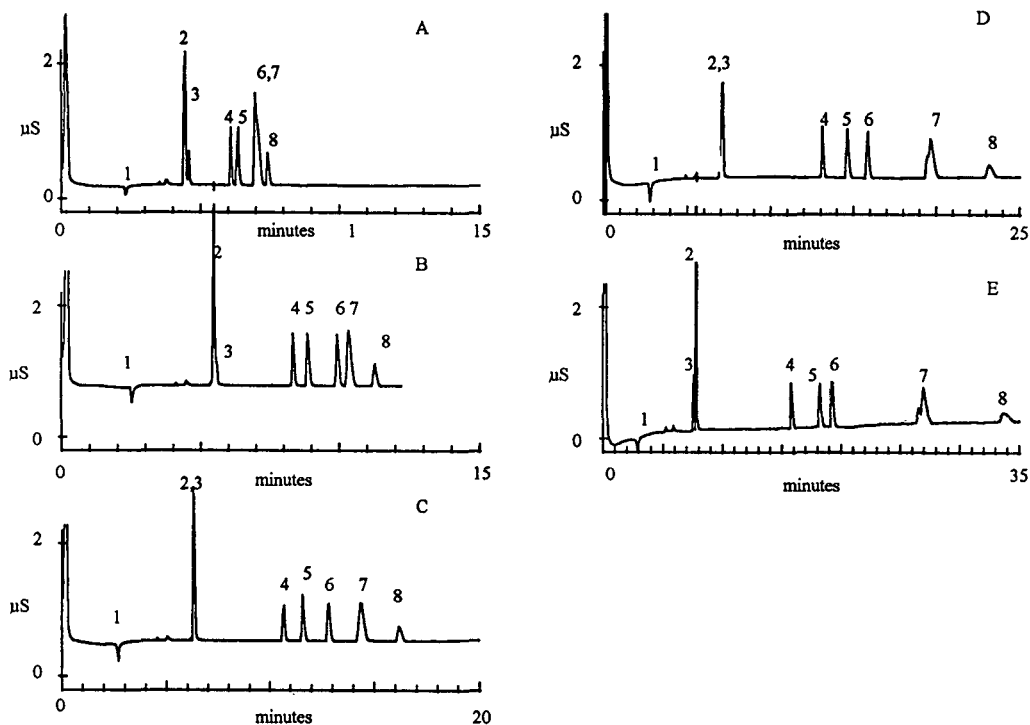
Fig. 5. Anion separation at different electrolyte ionic strengths. Conditions and peak identification same as Fig. 3, except for different electrolyte ionic strengths as follows: (A) 1.0 mM sodium tetraborate; (B) 2.0 mM sodium tetraborate; (C) 3.0 mM sodium tetraborate; (D) 4.0 mM sodium tetraborate; (E) 5.0 mM sodium tetraborate.
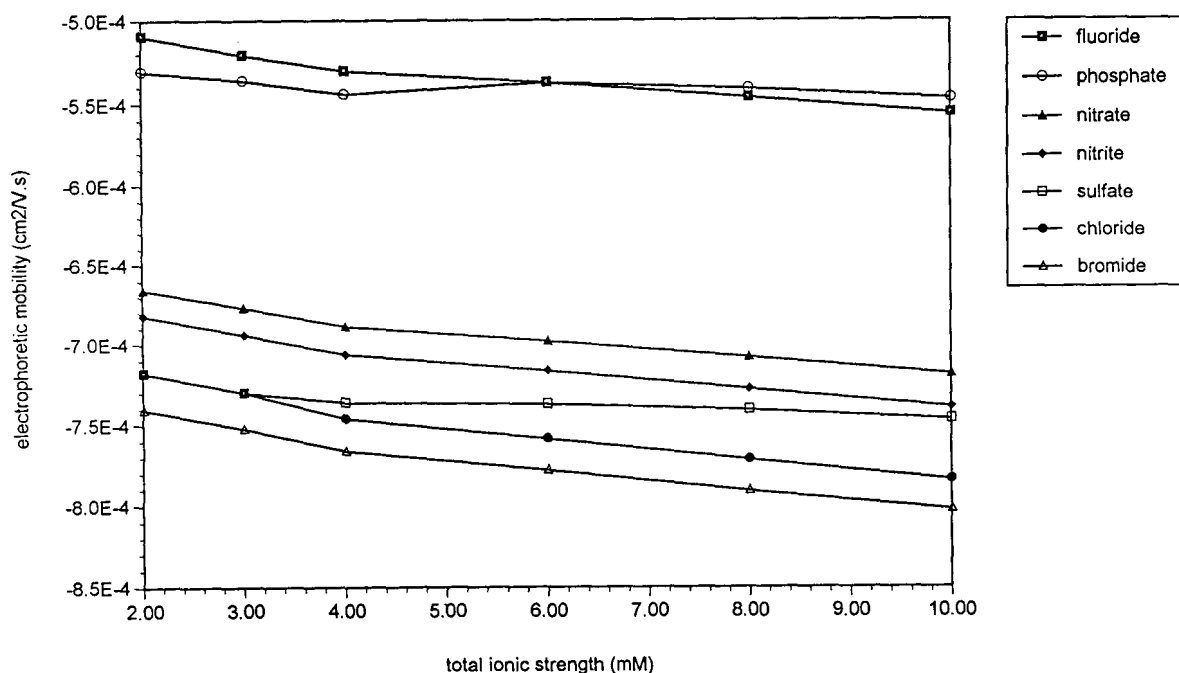
Fig. 6. Inherent electrophoretic mobility as a function of electrolyte ionic strength. Data plotted from electropherogram in Fig. 5. Electrophoretic mobilities were calculated using Eqs. 1, 2 and 3.

$$\mu = \lambda / F$$

where μ is the electrophoretic mobility in $cm^2/V \cdot s$, λ is the equivalent ionic conductance in cm^2/Ohm-equivalent, and F is the Faraday constant (96 489 C/mol).

Although Kohlrausch's Law applies to measurement of the equivalent conductivity of an ion in a solution of the same ions, it is expected to apply to the measurement of ions in a solution of a different electrolyte (as is the case in electrophoresis). It is also expected that as the ionic strength of the electrolyte decreases, the electrophoretic mobilities should approach the limiting values predicted from the equivalent ionic conductance at infinite dilution. The data in Fig. 6 show a different trend. At an electrolyte ionic strength of 10 mM, the electrophoretic mobilities of the anions are similar to those predicted from the equivalent ionic conductance at infinite dilution. As the ionic strength of the electrolyte decreases, the electrophoretic mobility of the anions appears to decrease to a value much less

than predicted at infinite dilution. The data show a trend contrary to Kohlrausch's Law; as the ionic strength of the electrolyte is decreased, the inherent electrophoretic mobility of the anions toward the anode becomes slower. It is possible that at the low ionic strength conditions used for this experiment, the mobilities of ions cannot be measured correctly. However, the phenomenon of changes in relative migration order (e.g., changes in selectivity) as a function of ionic strength is useful as a tool in optimizing electrophoretic separations.

As electrolyte ionic strength decreases, the inherent electrophoretic mobility of the anions toward the anode decreases while the EOF toward the cathode increases, resulting in an overall run time decrease. The important observation from the standpoint of selectivity manipulation is that the electrophoretic mobilities of the anions change at different rates in response to ionic strength changes. Most dramatic is the change in migration order of fluoride and phosphate ions as the ionic strength changes. At low

ionic strength, fluoride has a lower electrophoretic mobility [μ_a (actual)] than phosphate and a faster net migration through the capillary. Therefore, fluoride is detected before phosphate (Fig. 5A). As the ionic strength increases, the electrophoretic mobility of fluoride and phosphate converge (Fig. 5C). At higher ionic strength, the electrophoretic mobility of fluoride exceeds that of phosphate and thus, fluoride migrates after phosphate (Fig. 5E). Large changes in sulfate and chloride resolution are also observed. As the ionic strength of the electrolyte is increased, sulfate moves away from chloride and is detected near nitrite (Fig. 5E). The use of higher ionic strength may be useful in matrices with high concentrations of both sulfate and chloride.

Clearly, the electrolyte ionic strength is an important parameter in controlling observed electrophoretic mobility and, therefore, selectivity in the separation of inorganic anions. Through the proper choice of electrolyte ionic strength, selectivity and run time can be manipulated and optimized for a particular separation.

3.4. Temperature effects on selectivity

The effect of temperature on electrophoretic mobility was studied using a 2 mM Na$_2$B$_4$O$_7$ electrolyte. The temperature of the entire separation compartment was controlled using a forced air heating device. It is known that both the EOF and the electrophoretic mobility of an individual ion are a function of temperature. The dominant effect is thought to be a decrease in viscosity as temperature is increased. If a decrease in viscosity is the only effect, the overall effect of temperature should be negligible and would affect the overall analysis time, but not the relative migration velocities of the analyte ions. However, the electropherograms in Fig. 7 show changes in the relative migration order of the test analytes. A plot of electrophoretic mobility [μ_a (actual)], versus temperature at constant ionic strength is shown in Fig. 8.

As the temperature is increased, the EOF increases at 2% per degree Celsius as predicted from the change in viscosity with temperature. However, the overall run time decreases as the temperature is increased. This implies that the increase in EOF is greater for a given change in temperature than the change in analyte electrophoretic mobility for the same temperature change. If the magnitude of the change were the same for both the electrolyte and analyte, the two effects would cancel and the overall run time would be independent of temperature. Because the electroosmotic flow increases at a faster rate than the electrophoretic mobility of the analytes, the overall run time decreases as the temperature is increased.

The effect of increasing temperature is not simply limited to faster analysis times; the relative migration order of the analyte ions and, therefore, the selectivity of the system, changes as the temperature is increased. The resolution of fluoride and phosphate increases with increasing temperature because their electrophoretic mobilities change at different rates. Most interesting is the change in the migration order of sulfate, chloride, and bromide. Sulfate, which initially migrates before chloride and bromide, shows a relative increase in electrophoretic mobility as the temperature is increased. At the highest temperature studied (54.4°C), the electrophoretic mobility of sulfate has surpassed both chloride and bromide, and sulfate migrates last in the electropherogram. At this temperature, the analytes are detected in the order predicted by their limiting ionic conductance. At 54.4°C, the EOF is $147 \cdot 10^{-5}$ cm^2/V · s and the total run time is less than 7 min. Nielen [26] observed similar changes in the migration order of aminobenzoic acids and explained them on the basis of chemical equilibrium changes as a function of temperature. Strong acid inorganic anions are completely dissociated at the pH of the electrolyte (pH 9.2) and should not show a significant dependence on temperature. Yet the changes in relative migration order that we have observed appear to be a result of changes in electrophoretic mobility of anions in response to temperature. It is also apparent that the electrophoretic mobilities of different ions change at different rates in response to changes in separation temperature.

The changes in electrophoretic mobility as a
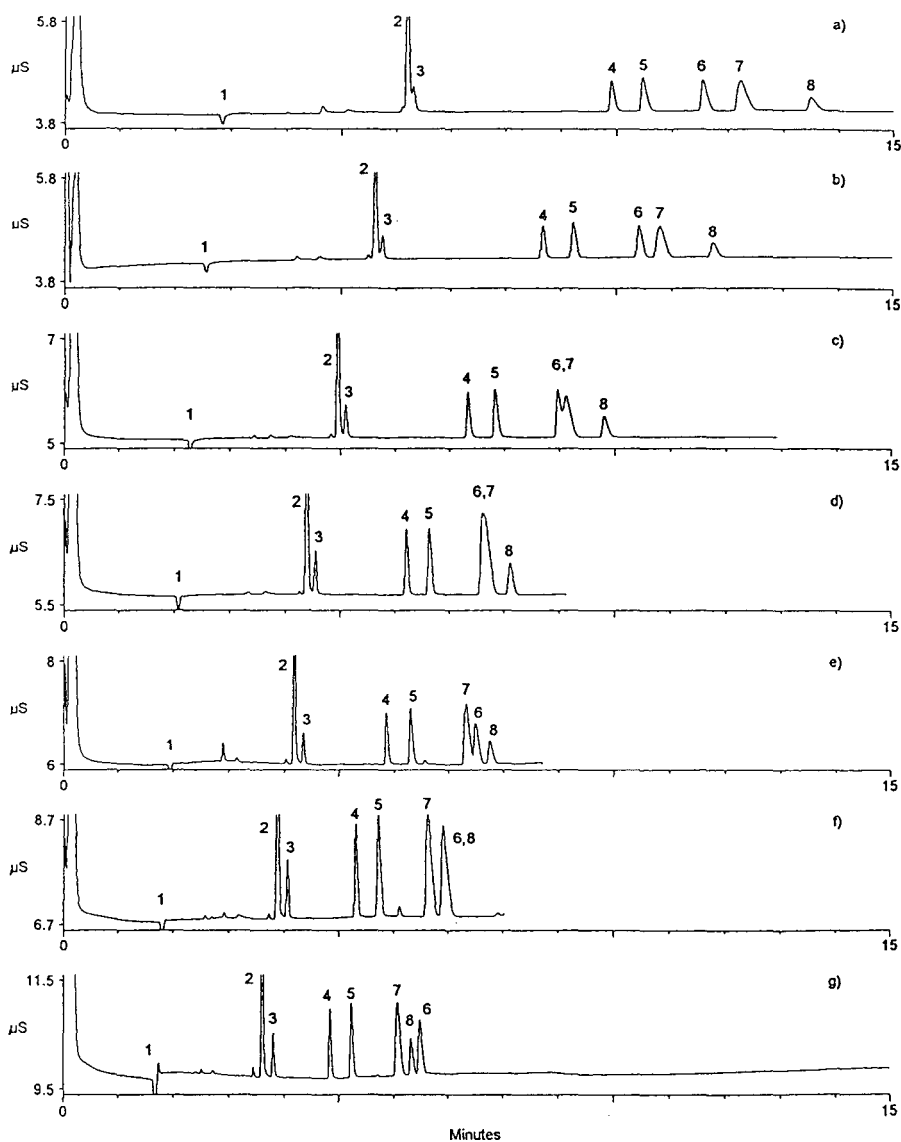
Fig. 7. Anion separations at different temperatures: (a) 21.1°C; (b) 26.7°C; (c) 32.2°C; (d) 37.8°C; (e) 43.3°C; (f) 48.9°C; (g) 54.4°C. Electrolyte: 2.0 mM sodium tetraborate (ultrapure); capillary: 60 cm × 75 μm I.D. fused-silica; voltage: + 24 kV, detector-end cathodic; hydrostatic injection: 40 mm/5 s; regenerant: 5 mM sulfuric acid; detection: suppressed conductivity. Sample injected from water. Peaks (all 1.0 ppm): 1 = water dip; 2 = fluoride; 3 = phosphate; 4 = nitrate; 5 = nitrite; 6 = sulfate; 7 = chloride; 8 = bromide.

function of temperature provide a means of affecting selectivity for ions in CE. This can be exploited as a means of modifying migration order and resolution of inorganic anions. Also, the observation that for a given change in tem-

perature the EOF increases faster than the electrophoretic mobility implies that overall run times can be shortened by running at elevated temperature. With a knowledge of the relationship between an anion's electrophoretic mobility
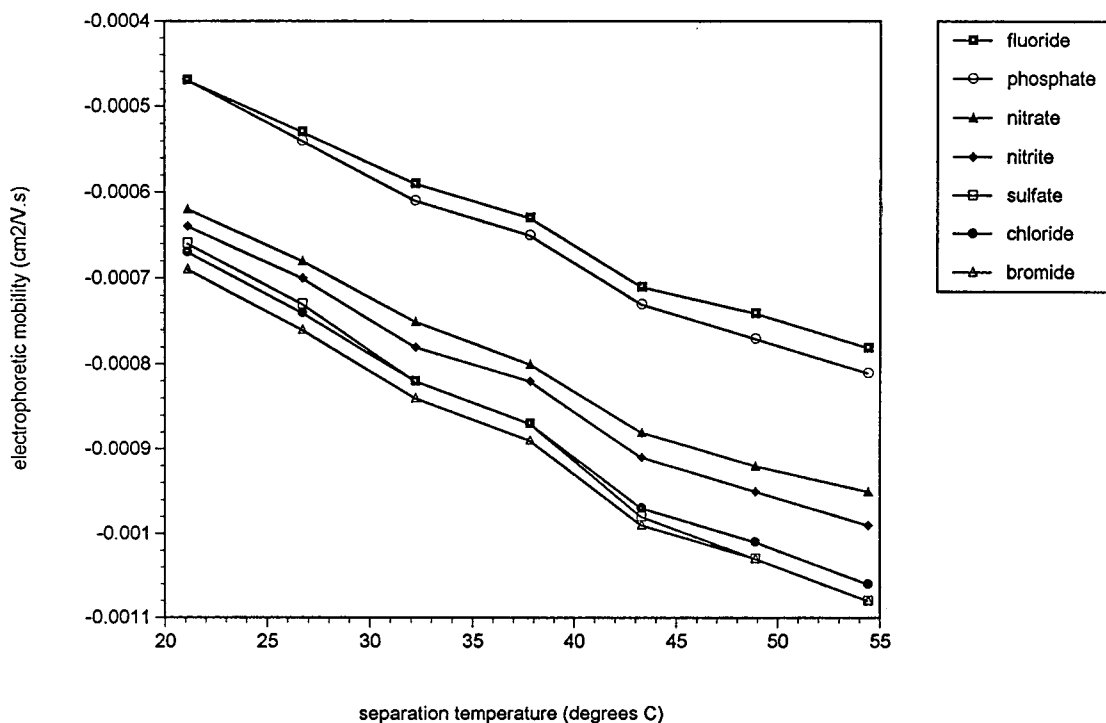
Fig. 8. Inherent electrophoretic mobility as a function of separation temperature. Data plotted from electropherogram in Fig. 7. Electrophoretic mobilities were calculated using Eqs. 1, 2 and 3.

and temperature, resolution of closely migrating analytes as well as overall run time can be optimized.

3.5. Effect of buffer additives on selectivity and resolution

The use of metal cations in the electrolyte has been reported for the purpose of mediating the mobility of selected inorganic anions using iso-tachophoresis. In one case, the authors used either calcium or magnesium to decrease the effective mobility of sulfate, and in another case cadmium to retard the mobility of chloride and sulfate. The result was unsuccessful due to the unacceptable change in mobility of other ions such as fluoride or to the loss of ions, probably due to precipitation, such as phosphate and fluoride, depending on the metal cation used. The use of metal cations in this work is intended

to change the selectivity of the system for inorganic anions versus organic acids.

The separation of a variety of organic acids has been accomplished using CESC. In fact, CESC may prove to be a superior method for the analysis of small organic acids because they are essentially separated as a class from strong acid anions. This class separation occurs because the electrophoretic mobilities of most organic acids are much lower than those of strong acid inorganic anions. This class separation can be enhanced by adding a micromolar concentration of metal ions to slow the EOF of the system. Since the electrophoretic mobility of the anions is in the opposite direction of the EOF, anions with faster mobilities will increase in migration time faster than anions with slower mobilities. The result is that essentially all of the inorganic anions in the sample are moved to a position later in the electropherogram, and the organic anions in the sample migrate first. There are,

however, certain pairs of organic acids whose electrophoretic mobilities in a particular electrolyte are too close for full resolution of the migrating bands. This problem is also addressed by the presence of micromolar concentrations of metal cations in the electrolyte, which can weakly complex some organic acids. Many organic acids are weak chelators and form complexes with metal ions in solution. The degree to which an organic acid complexes a metal is a function of the chemical environment, temperature, and the presence of competing chelators. The resulting complex has chemical properties different than the free organic acid and can include changes in charge, charge density, geometry, and relative hydrophobicity. Complexation of an organic acid with a metal cation generally decreases its charge and charge density, resulting in a slowing of the complexed acid relative to its free acid counterpart. The degree to which the analyte is slowed by complexation with the metal depends on the nature of the analyte and the stability of the analyte–metal complex. Generally, two co-migrating organic acids will not complex with a metal to the same degree and, therefore, their relative migration times are affected differently by the addition of a metal ion.

The addition of even a low concentration of di- or trivalent metal ions can significantly slow the EOF. This can be seen in Fig. 9, where the measured EOF is only $70 \cdot \times 10^{-5}$ cm^2/V·s with the addition of 0.02 mM barium borate, in comparison with $97 \cdot 10^{-5}$ cm^2/V·s with 2.0 mM sodium tetraborate electrolyte and no added metal. Under these conditions, many high-mobility inorganic anions will not be detected, but the resolution of the slower organic acids is greatly enhanced. The addition of micromolar concentrations of barium to the electrolyte has resulted in resolution of otherwise inseparable pairs of organic acids (Fig. 9). We have also
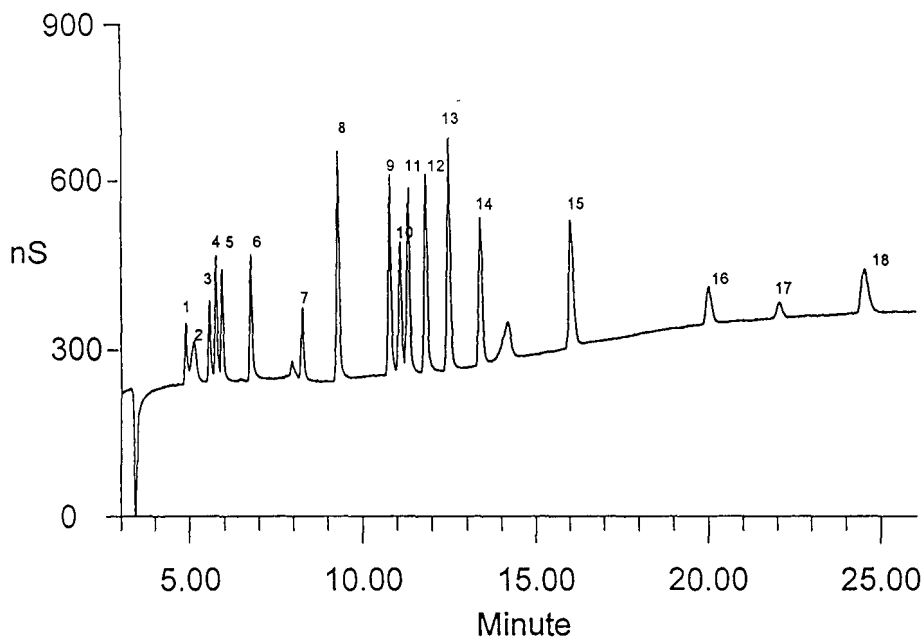
Fig. 9. Separation of organic acids with barium additive in electrolyte. Electrolyte: 2.0 mM sodium tetraborate (ultrapure), 0.02 mM barium borate; capillary: 60 cm × 75 μm I.D. fused-silica; voltage: + 24 kV, detector-end cathodic; hydrostatic injection: 3 mm/3 s; regenerant: 5 mM sulfuric acid; detection: suppressed conductivity. Sample injected from water. Peaks (all at 250 ppb unless noted): 1 = quinate; 2 = shikimate; 3 = benzoate; 4 = salicylate; 5 = lactate; 6 = acetate; 7 = mucate; 8 = saccharate; 9 = formate (125 ppb); 10 = succinate; 11 = malate; 12 = tartrate; 13 = fumarate; 14 = maleate; 15 = malonate; 16 = isocitrate; 17 = citrate; 18 = aconitate.

observed slightly different changes in selectivity for organic acids with the addition of calcium and magnesium cations to the electrolyte.

4. Conclusion

Capillary electrophoresis with suppressed conductivity detection (CESC) is a powerful and versatile technique for the analysis of inorganic anions and low-molecular-mass organic acids. A variety of electrolytes are compatible with this technique and high efficiency separations can be optimized for analytes of differing mobilities. The electrophoretic mobility of analyte ions, often viewed as a fixed property, can be changed though judicious choice of operating conditions. Ionic strength of the electrolyte has been shown to exhibit subtle control over electrophoretic mobility and can be used as a means of modifying selectivity. Likewise, separation temperature can have a dramatic effect on selectivity in CE and may prove to be a powerful tool in optimizing separations. Finally, the addition of weakly complexing metals to an electrolyte can modify the net electrophoretic mobility of organic acid analytes and resolve otherwise co-migrating pairs. Manipulation of these parameters allows the selectivity of CE separations to be optimized for particular application problems.

References

[1] P. Bocek, B. Kaplanova, M. Deml and J. Janak, Collec. Czech. Chem. Commun., 43 (1978) 441.
[2] D. Kaniansky and F.M. Everaets, J. Chromatogr., 148 (1978) 2707.
[3] J. Vacik and I. Muselasova, J. Chromatogr., 320 (1985) 199.
[4] F. Foret, S. fanali, L. Ossicini and P. Bocek, J. Chromatogr., 470 (1989) 299.
[5] B.J. Wildman, P.E. Jackson, W.R. Jones and P.G. Alden, J. Chromatogr., 546 (1991) 459.
[6] B. Kennedy, J. Chromatogr., 546 (1991) 423.
[7] A. Nardy, M. Cristalli, C. Desiderio, L. Ossicini, S.K. Shukla and S. Fanali, J. Microcol. Sep., 4 (1992) 9.
[8] P. Jandik and W.R. Jones, J. Chromatogr., 546 (1991) 431.
[9] W.R. Jones and P. Jandik, J. Chromatogr., 546 (1991) 445.
[10] M.P. Harrold, M.J. Wojtusik, J. Rivello and P. Henson, J. Chromatogr., 640 (1993) 463.
[11] Y. Ma and R. Zhang, J. Chromatogr., 625 (1992) 341.
[12] L. Kelly and R.J. Nelson, J. Liq. Chromatogr., 16 (1993) 2103.
[13] T.J. O'Shea, R.D. Greenhagen, S.M. Lunte, C.E. Lunte, M.R. Smith, D.M. Radzik and N. Watanabe, J. Chromatogr., 593 (1992) 305.
[14] R.A. Wallingford and A.G. Ewing, Anal. Chem., 59 (1987) 1762.
[15] R.A. Wallingford and A.G. Ewing, Anal. Chem., 61 (1989) 98.
[16] X. Huang and R.N. Zare, Anal. Chem., 62 (1990) 443.
[17] X. Huang, R.N. Zare, S. Sloss and A.G. Ewing, Anal. Chem., 63 (1991) 189.
[18] I.-C. Chen and C.-W. Wang, J. Chromatogr., 644 (1973) 208.
[19] F.E.P. Mikkers, F.M. Everaets and Th.P.E.M. Verheggen, J. Chromatogr., 169 (1979) 1, 11.
[20] F. Foret, M. Deml, V. Kahle and P. Bocek, Electrophoresis, 7 (1986) 430.
[21] X. Huang, J.A. Luckey, M.J. Gordon and R. Zare, Anal. Chem., 61 (1989) 776.
[22] X. Huang and R.N. Zare, Anal. Chem., 63 (1991) 2193.
[23] X. Huang, T.-K.J. Pang, M.J. Gordon and R.N. Zare, Anal. Chem., 59 (1987) 2747.
[24] N. Avdalovic, C.A. Pohl, R.D. Rocklin and J.R. Stillian, Anal. Chem., 65 (1993) 1470.
[25] P.K. Dasgupta and L. Bao, Anal. Chem., 65 (1993) 1003.
[26] M.W.F. Nielen, J. Chromatogr., 542 (1991) 173.
[27] H.J. Issaq, I.Z. Atamna, G.M. Muschik and G.M. Janini, Chromatographia, 32 (1991) 155.
[28] K.D. Altria and C.F. Simpson, Chromatographia, 24 (1987) 527.
[29] W. Nashabeh and Z.E. Rassi, J. Chromatogr., 514 (1990) 57.
[30] G.J.M. Bruin, J.P. Chang, R.H. Kuhlman, K. Zegers, J.C. Kraak and H. Poppe, J. Chromatogr., 471 (1989) 429.
[31] B.B. VanOrman, G.G. Liversidge, G.L. McIntire, T.M. Olefirowicz and A.G. Ewing, J. Microcol. Sep., 2 (1990) 176–180.
[32] D.F. Swaile and M.J. Sepaniak, Anal. Chem., 63 (1991) 179.

[33] F. Foret, S. Fanali, A. Nardi and P. Bocek, Electrophoresis, 11 (1990) 780.

[34] A. Weston, P.R. Brown, P. Jandik, W.R. Jones and A.L. Heckenberg, J. Chromatogr., 593 (1992) 289.

[35] H. Small, Ion Chromatography, Plenum Press, New York, NY, 1989, p. 160.

[36] O.A. Shpigun and Y.A. Zolotov, Fresenius Z. Anal. Chem., 335 (1989) 58.

[37] O.A. Shpigun, I.N. Voloshik and Yu.A. Zolotov, Anal. Sci., 1 (1985) 335.

[38] J.P. Ivey, J. Chromatogr., 287 (1984) 128.

[39] H. Small, T.S. Stevens and W.C. Bauman, Anal. Chem., 47 (1975) 1801.

[40] J. Stillian, LC Mag., 3 (1985) 802.

[41] S. Rabin, J. Stillian, V. Barreto, K. Friedman and M. Toofan, J. Chromatogr., 640 (1993) 97.

[42] F.A. Cotton and G. Wilkinson, Advanced Inorganic Chemistry, Wiley, New York, NY, 1980, p. 297.

[43] J.O'M. Bockris and A.K.N. Reddy, Modern Electrochemistry, Vol. 1, Plenum Press, New York, NY, 1970.

[44] J.A. Dean (Editor), Lange's Handbook of Chemistry, McGraw Hill, New York, 13th ed., 1985.

On-column chelation of metal ions in capillary zone electrophoresis

I. Haumann, K. Bächmann*

Fachbereich Chemie, Technische Hochschule Darmstadt, Petersenstr. 18, D-64287 Darmstadt, Germany

Abstract

A method for the chelation of metal ions is described in order to apply direct UV detection for the determination of these species in capillary zone electrophoresis. The chelating reaction was carried out on-column by mixing the zones of the reactants during the electrophoretic migration. The reaction, the stability of the products and the separation of the products from the chelating agent were investigated by the chelation of metal ions with EDTA. In comparison with a common indirect UV detection method the limit of detection was decreased by a factor of up to 10.

1. Introduction

The main features of the most common method for the determination of inorganic ions in capillary zone electrophoresis (CZE) include the use of indirect UV detection, additives such as weak complexing agents for supporting the separation and an electroosmotic flow modifier if necessary. This method is called inorganic capillary electrophoresis (ICE) or capillary ion electrophoresis (CIE). It is a powerful technique for the determination of both inorganic cations and anions, as shown by many applications published in recent years [1–9]. It is also possible to determine a large number of transition metals simultaneously with alkali and alkaline earth metal ions using ICE [7–9].

However, this method has also some limitations, since the electrolyte system must fulfil requirements for both an effective separation and for indirect detection. The indirect detection

is based on a charge displacement of the detectable background electrolyte caused by the analyte ions. Therefore, the change in the concentration of all ionic species such as additives in the electrolyte or matrix ions in the sample is sensed by the detector and may result in system peaks or disturbance of the baseline. During the separation of metal ions the effective positive charge may also be reduced by the equilibrium reaction between these ions and the anionic complexing agents, which decreases the charge displacement and results in an increase in the limits of detection. For this reason it is useful to develop methods for direct detection, especially for the determination of transition metal ions.

One possibility of applying the direct detection of metal ions in CZE is the formation of stable metal chelates, which can be measured using UV–Vis detection. There are different ways to perform the chelation. The precolumn reaction was used for the chelation of metal ions, while the products were separated by micellar electrokinetic capillary chromatography (MECC)

_____
* Corresponding author.

[10]. The precolumn reaction is also possible in cases where the products can be separated with zone electrophoresis [11–17]. The separation of the metal chelates by zone electrophoresis is often difficult, however, especially for equally charged metal ions that form chelates with the same stoichiometry. In this case there is only a small difference in the ratio of charge to radius, which results in nearly identical electrophoretic mobilities of the products. Another possibility is chelation after the separation of the metal ions by the use of a postcolumn reactor [18–24]. This method requires modification of the CE equipment and a significant difference in the absorptivities of the reagent and the product, because both appear in the detector at the same time.

This paper describes the development of an on-column chelation method with the example of the chelation of metal ions with EDTA. The chelating reaction, which occurs inside the capillary, is carried out by mixing the analyte zone and the reagent zone during the electrophoretic migration. The possibility of performing a chemical reaction during the contact time of zones in CZE is based on the technique of electrophoretically mediated microanalysis (EMMA), which has already been demonstrated by the enzymatic oxidation of ethanol [25].

2. Experimental

The CZE system was laboratory built and allows the injection of the sample and the electrolyte at both ends of the capillary. The equipment, which includes a UV detector (Dionex, Sunnyvale, CA, USA), has been described previously [26]. All solutions, electrolytes and standards were prepared using water purified with a Milli-Q system (Millipore, Eschborn, Germany). All other reagents were of analytical-reagent grade from Merck (Darmstadt, Germany). Stock solutions (10 mmol/l) of each cation were used to prepare the sample solutions. The fused-silica capillary (75 μm I.D.) was rinsed for 5 min with 0.1 mol/l sodium hydroxide solution, water and electrolyte at the beginning of each day and for 2 min with

electrolyte between all electrophoretic separations. The data were processed with an A/D board from ERC (Altegolfsheim, Germany) using the APEX chromatography software (Autochrom, Milford, MA, USA). The absorbance units are converted into microvolts by the A/D board. Therefore, the output of the data is in the voltage mode ($19 \cdot 10^3$ μV = 0.001 absorbance).

3. Results and discussion

Fig. 1 shows the principle of the mechanism of the on-column zone reaction in CZE. The first step is the injection of the sample and the chelating agent. Then an electrophoretic separation of the metal ions with either organic solvents or weak complexing agents such as lactic acid or hydroxyisobutyric acid is carried out (Fig.
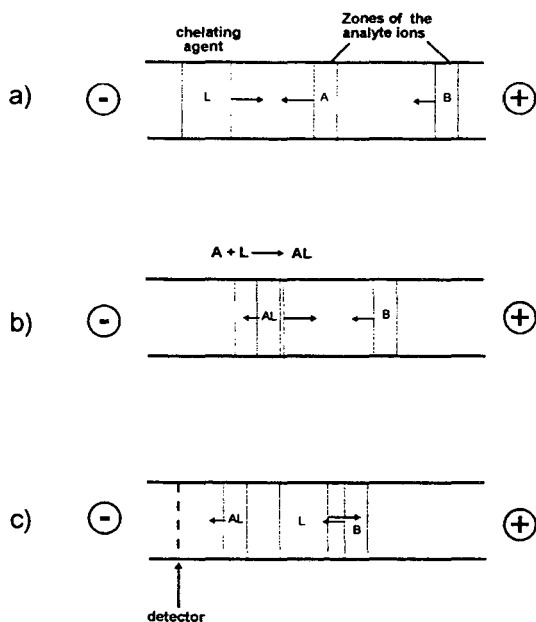
Fig. 1. Principle of on-column chelation. L = chelating agent; A and B = analyte ions. (a) Injection of the sample (A, B) and the reagent (L) and electrophoretic separation of the metal ions. (b) Mixing of the analyte zone and the reagent zone. (c) Separation of the products and the chelating agent followed by detection.

1a). After the separation, the analytes enter the reagent zone and the reaction takes place (Fig. 1b). Since the resulting products have different charges and therefore different electrophoretic mobilities compared with the chelating agent, they migrate out of the reaction zone towards the detector before the next analyte enter this area (Fig. 1c).

Some requirements have to be fulfilled for a successful on-column chelation. A fast reaction must occur during the contact time of the zones of the analyte and the chelating agent. After leaving the reaction zone, the resulting products must be stable enough to reach the detector. There should be significant differences in the electrophoretic mobilities of the metal chelates and the chelating reagent. Further, the products should be detectable.

For the development of the CZE on-column reaction, EDTA was used as a chelating agent. The chelation of metal ions with EDTA has been well investigated and used in chromatographic separations with UV detection [27–31]. EDTA forms stable anionic chelates with many metals and some of these, such as lead–, copper–, cobalt–, nickel–, iron– and bismuth–EDTA chelates, are detectable by UV detection. The optimum experimental conditions for parameters such as the mobility of the reactants and the products, the required length of the capillary for supporting the separation and the required direction and velocity of the electroosmotic flow, can be precalculated.

Fig. 2 shows the principle of the on-column reaction, which was developed especially for the chelation of the metal ions with EDTA. First the capillary is filled with electrolyte solution. The detector is placed near the anodic end of the capillary, where the sample is injected (Fig. 2a). Therefore, both hydrodynamic and electrokinetic injection are possible. The EDTA solution will be introduced at the cathodic end of the capillary. After the high voltage has been applied (Fig. 2b), the separation of the analyte ions starts and the first analyte migrates through the EDTA zone followed by the reaction. Then the EDTA anions and the metal–EDTA chelates, which are also anions but less negatively

charged, can be separated by electrophoresis (Fig. 2c).

Fig. 3 shows an electropherogram for the determination of four metal ions carried out with the on-column chelation technique. The electrolyte used was 10 mmol/l sodium acetate solution (pH 4.8) containing 2 mmol/l tartaric acid for supporting the separation of the metal ions. The concentration of the EDTA solution was 1 mmol/l. The electroosmotic flow is reversed by the addition of tetradecyltrimethylammonium bromide (TTAB). This allows the slow-moving metal–EDTA species of the trivalent cations also to reach the detector in a short time, whereas the peak broadening is still acceptable. EDTA, which is present in an excess concentration compared with the concentration of the analyte ions, is detectable at 242 nm and appears as the first peak in the electropherogram. Lead and nickel are separated before the reaction because the EDTA chelates of this species have the same electrophoretic mobility. Iron(III)–EDTA appears as the last peak because the mobility of this product differs most from the mobility of the EDTA anions.

In the following, investigations of some important aspects of on-column chelation in CZE are described, viz., the chelation of the analytes in the reaction zone, the stability of the chelates and the separation of the products from the chelating agent.

Fig. 4 shows the results of the investigations of the chelating process with the example of the reaction between EDTA and lead. The EDTA concentration was changed in a range between 10 μmol/l and 10 mmol/l whereas the lead concentration was constant at 100 μmol/l. Curve A shows the peak area of the EDTA peak at different concentrations. As can be seen from curve B, the area of the lead–EDTA peak is constant for EDTA concentrations between 10 mmol/l and 100 μmol/l. At lower EDTA concentrations, there is not enough chelating agent present and the lead–EDTA peak decreases. These results indicate that there is a quantitative and equimolar reaction during the contact time of the zones.

After the reaction, the metal chelates have to
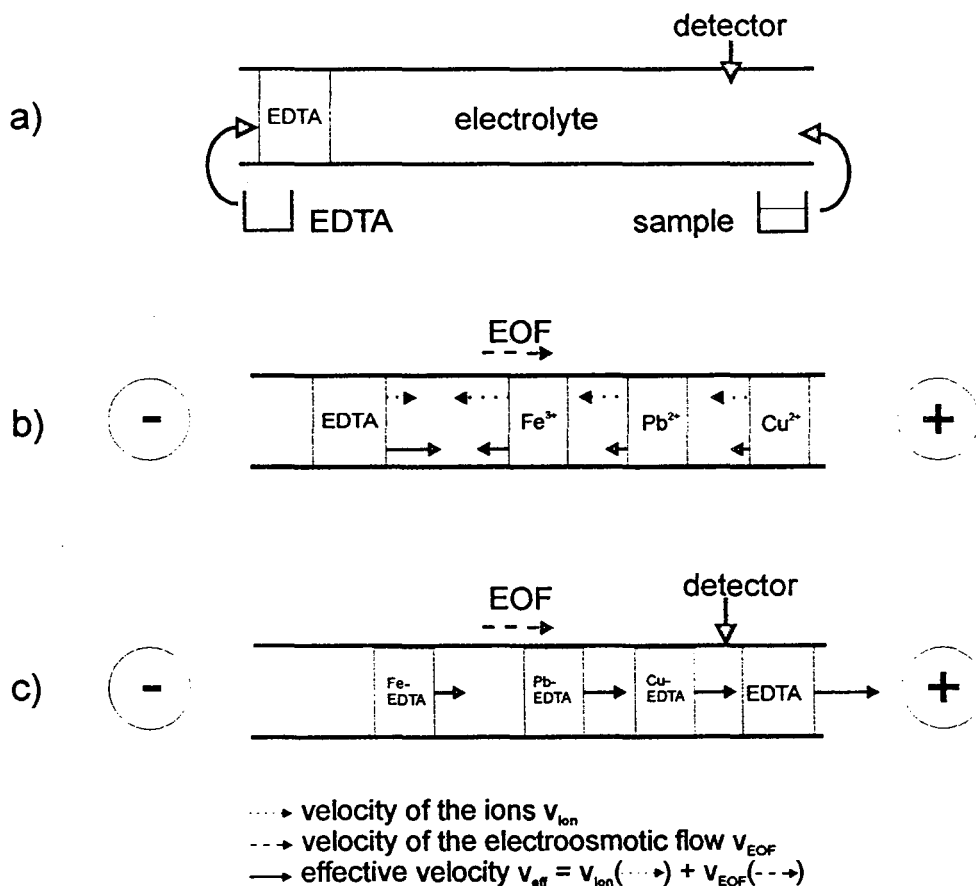
Fig. 2. Mechanism of the on-column reaction with EDTA as chelating agent. (a) Filling of the capillary with electrolyte and chelating agent and sample injection. (b) Electrophoretic separation of the metal ions. (c) Migration of the products towards the detector after the mixing of the zones and the reaction.

be stable in order to migrate through the electrolyte solution towards the detector. For the investigation of the stability of the products in the electrolyte system used, first the analyte ions and second the EDTA solution were introduced by hydrostatic injection at the cathodic end of the capillary. Therefore, the reaction occurs at the inlet side and the chelates are forced to migrate through nearly the whole capillary until they arrive at the detection window. Fig. 5 shows electropherograms of the EDTA chelates of copper, lead and iron. For these ions, separation before the reaction is not necessary, because the differences in the mobilities of these metal chelates are sufficient for an electrophoretic separation. The measurements were carried out by applying different high voltages. Therefore, the metal chelates migrate with different velocities and have different contact times with the electrolyte solution. Nevertheless, no decrease can be observed, in either peak height or peak area. Table 1 gives the values of peak height and peak area. Because of the different velocities of the analyte ions passing the detection window, the values of the peak areas are corrected by the migration time. Under these conditions, the stabilities of the metal chelates are sufficient for on-column zone chelation.

The chelation technique described here requires the separation of the metal chelates and
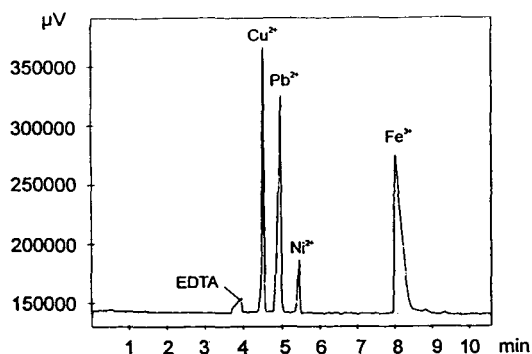
Fig. 3. Electropherogram of four metal ions after on-column chelation. Electrolyte: 10 mmol/l sodium acetate–2 mmol/l tartaric acid–0.2 mmol/l TTAB (pH = 4.8). Injection: (1) hydrostatic, 10 cm, 30 s, 1 mmol/l EDTA at the cathodic capillary inlet; (2) hydrostatic, 10 cm, 30 s, 50 μmol/l Pb, 75 μmol/l Cu, Ni and Fe at the anodic capillary inlet. Detection: UV at 242 nm. Separation voltage: 30 kV.

the chelating agent after the reaction. If EDTA is used as the chelating agent, the most important parameter for a successful separation of the reagents and the products is the pH of the electrolyte system. As some dissociation equilibria for EDTA in the pH range between 2 and 10 have to be considered, EDTA species of different charges exist at different pH values [32].

After the reaction with doubly negatively charged EDTA the chelates of the bivalent

Fig. 5. Investigation of the stability of the metal chelates during the migration in the electrolyte system. 1 = Cu–EDTA; 2 = Pb–EDTA; 3 = Fe–EDTA. Separation voltage: (a) 30; (b) 25; (c) 20; (d) 15 kV.

cations have the same charge as the EDTA anions and separation by zone electrophoresis is not possible. In this case, a higher pH is necessary for the separation. Fig. 6 shows the differences between the electrophoretic mobilities of EDTA and EDTA chelates of bi- and trivalent metal ions depending on the pH value. The mobilities are calculated from experimentally determined migration velocities. It can be seen that for bivalent cations a pH of 6 or higher is

Fig. 4. Investigation of the reaction during the contact time of the zones. ☐ = Peak area of 100 μmol/l Pb^{2+}; ▲ = area of the EDTA peak.

Table 1
Corrected peak areas of metal–EDTA chelates (Fig. 5) under different separation conditions

Separation voltage (kV)	Peak area (μV s)/migration time (s)		
	Cu–EDTA	Pb–EDTA	Fe–EDTA
30	21946	61306	19010
25	20273	60780	19590
20	20695	61454	19596
15	21254	60603	18586
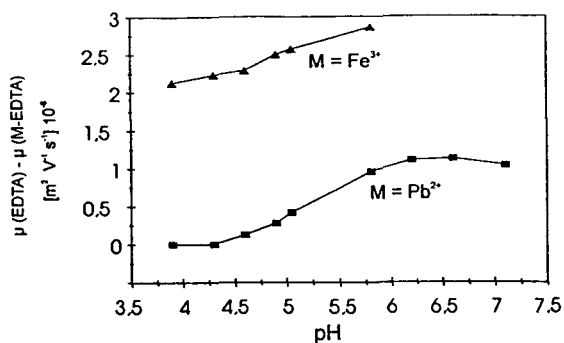
Fig. 6. Differences between the electrophoretic mobilities of EDTA and the metal–EDTA chelates depending on the pH of the electrolyte.

best for the separation. Because of hydroxide formation, some metals cannot be separated under these conditions. In this case the pH of the electrolyte has to be decreased and a less efficient separation has to be accepted.

The metal–EDTA species, which can be measured using UV detection, have absorption maxima at different wavelengths. Therefore, the limits of detection (LODs) of the different analyte ions depend on the wavelength used. In Table 2, the detection limits measured with the on-column chelating technique at 242 nm are compared with indirect detection which was carried out with a 4-aminopyridine electrolyte. The LOD was defined as three times the signal-

Table 2
Detection limits (μmol/l) measured with electrolyte systems for indirect and direct UV detection (signal-to-noise ratio = 3)

Metal	Indirect UV detection[a]	Direct UV detection[b]
Cu	10	1
Pb	10	0.5
Ni	8	3
Co	5	2
Fe	10	2

Injection: hydrostatic (10 cm, 15 s). Capillary: fused silica (70 cm × 75 μm I.D.).
[a] Electrolyte: 5 mmol/l 4-aminopyridine–2 mmol/l tartaric acid ($\lambda = 264$ nm).
[b] On-column chelation: 10 mmol/l sodium acetate–2 mmol/l tartaric acid (pH 4.8) ($\lambda = 242$ nm).

to-baseline noise ratio. The experimental conditions were the same. A 75 μm I.D. fused-silica capillary with a total length of 70 cm was used. The sample injection was hydrostatic by raising the capillary inlet side 10 cm for 15 s. With direct detection 3–10-fold lower detection limits can be achieved, depending on the position of the absorption maxima of the metal–EDTA ions and of their molar absorptivity at the wavelength used.

The calibration with hydrostatic injection is linear up to about three orders of magnitude above the detection limit. The correlation coefficients ranged from 0.991 for nickel to 0.999 for lead. The determination of high concentration levels of the analyte ions is limited by the amount of chelating agent that is available in the reaction zone and by the CZE separation of the metal ions, which must occur before the chelating reaction.

Using EDTA as the chelating agent, alkali metal ions up to a concentration of 50 mmol/l can be present in the sample without interferences, because the alkali metal ions migrate through the EDTA zone without a reaction. Fig. 7 shows the electropherogram for copper, lead, nickel and cobalt in the presence of 20 mmol/l sodium chloride.
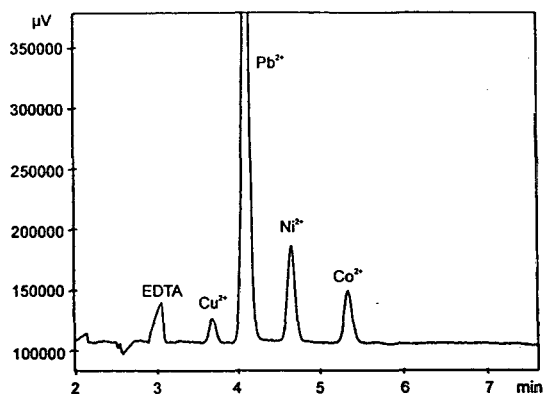
Fig. 7. Electropherogram of metal ions in sodium chloride solution. Sample: 20 μmol/l Cu–100 μmol/l Pb–50 μmol/l Ni–25 μmol/l Co–20 mmol/l NaCl. Electrolyte: 10 mmol/l sodium acetate–2 mmol/l tartaric acid–0.2 mmol/l TTAB (pH 4.8). Injection: hydrostatic (10 cm, 15 s). Separation voltage: 25 kV. Detection: UV at 242 nm.

4. Conclusion

The "on-column" reaction in CZE is an additional method complementing the commonly used pre- or postcolumn chelation of metal ions. It offers the possibility of carrying out chemical reactions of oppositely charged ions by mixing the zones of these species inside the capillary and during an electrophoretic separation. This may be useful, for example, if small sample volumes do not allow a precolumn reaction or if a postcolumn reaction disturbs the detection.

The possibility of mixing zones containing oppositely charged species is an advantage of the electrophoretic separation mechanism compared with a chromatographic separation, where the zones do not migrate in opposite directions.

The method allows the complexation or derivatization of analytes and therefore the direct detection in CZE determinations of UV-inactive species such as inorganic cations. This technique was developed with the example of the chelation of metal ions with EDTA because the equimolar reaction makes it easy to precalculate important parameters of the separation. The method may be improved by choosing other chelating agents to permit the determination of more metal ions. If the resulting products have a higher molar absorptivity than the metal–EDTA chelates, the detection will be more sensitive. This requires a knowledge of the chemistry of the reaction and parameters such as the stability and the charge of the reagents and the products in order to optimize the conditions for the reaction, separation and detection. Possibly it will be necessary to change the instrumental or the chemical conditions such as the sample injection, the position of the detector or the direction of the electroosmotic flow.

References

[1] W.R. Jones and P. Jandik, Am. Lab., June (1990) 51.
[2] P. Jandik and W.R. Jones, J. Chromatogr., 546 (1991) 431.
[3] J. Romano, P. Jandik, W.R. Jones and P.E. Jackson, J. Chromatogr., 546 (1991) 411.
[4] Y. Shi and J.S. Fritz, J. Chromatogr. A, 671 (1994) 429.
[5] A. Weston, R. Brown, A.L. Heckenberg, P. Jandik and W.R. Jones, J. Chromatogr., 602 (1992) 249.
[6] W. Beck and H. Engelhardt, Chromatographia, 33 (1992) 313.
[7] F. Foret, S. Fanali, A. Nardi and P. Bocek, Electrophoresis, 11 (1990) 780.
[8] A. Weston, P.R. Brown, P. Jandik, W.R. Jones and A.L. Heckenberg, J. Chromatogr., 593 (1992) 289.
[9] W. Beck and H. Engelhardt, Fresenius' J. Anal. Chem., 346 (1993) 618.
[10] T. Saitoh, H. Hoshino and T. Yotsuyanagi, J. Chromatogr., 469 (1989) 175.
[11] M. Aguilar, X. Huang and R.N. Zare, J. Chromatogr., 480 (1989) 427.
[12] W. Buchberger, O.P. Semenova and A.R. Timerbeav, J. High Resolut. Chromatogr., 16 (1993) 153.
[13] M. Aguilar, A. Farran and M. Martinez, J. Chromatogr., 635 (1993) 127.
[14] A. Timerbeav, O. Semenova and G. Bonn, Chromatographia, 31 (1993) 497.
[15] A. Timerbeav, W. Buchberger, O. Semenova and G. Bonn, J. Chromatogr., 630 (1992) 379.
[16] N. Iki, H. Hoshino and T. Yotsuyanagi, Chem. Lett., (1993) 701.
[17] D.F. Swaile and M.J. Sepaniak, Anal. Chem., 63 (1991) 179.
[18] T. Tsuda, Y. Kobayashi, Y. Hori, T. Matzumoto and O. Suzuki, J. Chromatogr., 465 (1988) 375.
[19] D.J. Rose, J. Chromatogr., 540 (1991) 343.
[20] D.R.J. Rose and J.W. Jorgenson, J. Chromatogr., 447 (1988) 117.
[21] B. Nickerson and J.W. Jorgenson, J. Chromatogr., 480 (1989) 157.
[22] M. Albin, R. Weinberger, E. Sapp and S. Moring, Anal. Chem., 63 (1991) 417.
[23] T. Tsuda, Y. Kobayashi, A. Hori and T. Matsumoto, J. Microcol. Sep., 2 (1990) 21.
[24] S.L. Pentoney, X. Huang, D. Burgi and R.N. Zare, Anal. Chem., 60 (1988) 2625.
[25] B.J. Harmon, D.H. Patterson and F.R. Regnier, Anal. Chem., 65 (1993) 2655.
[26] K. Bächmann, J. Boden and I. Haumann, J. Chromatogr., 626 (1992) 259.
[27] G. Sacchero, O. Abollino, V. Porta, C. Sarzanini and E. Mentasti, Chromatographia, 31 (1991) 539.
[28] W. Buchberger, P.R. Haddad and P.W. Alexander, J. Chromatogr., 558 (1991) 181.
[29] J.F. Jen and C.S. Chen, Anal. Chim. Acta, 270 (1992) 55.
[30] G.J. Nickless, J. Chromatogr., 313 (1985) 129.
[31] K. Hayakawa, T. Sawada, K. Shimbo and M. Miyazaki, Anal. Chem., 59 (1987) 2241.
[32] F. Umland, Theorie und Praktische Anwendung von Komplexbildnern, Akademische Verlagsgesellschaft, Frankfurt am Main, 1971.

Separation of transition metal cations by capillary electrophoresis
Optimization of complexing agent concentrations (lactic acid and 18-crown-6)

C. François, Ph. Morin*, M. Dreux

Laboratoire de Chimie Bioorganique et Analytique (LCBA), Université d'Orléans, URA CNRS 499, BP 6759, 45067 Orléans 02, France

Abstract

The simultaneous separation of alkali, alkaline earth and transition metal cations by capillary electrophoresis was achieved using an electrolyte containing imidazole as indirect UV co-ion and lactic acid and 18-crown-6 as complexing agents with indirect UV detection. The addition of lactic acid to the imidazole electrolyte allows the separation of transition metal cations, whereas 18-crown-6 allows one to resolve ammonium and potassium and also sodium and lead. An electrolyte containing 10 mM imidazole, 5 mM lactic acid and 0.5 mM 18-crown-6 at pH 4.5 and with the separation temperature fixed at 30°C allow the simultaneous separation of alkali, alkaline earth and transition metal cations by capillary electrophoresis. By increasing the hydrodynamic injection time to 15 s, a linear relationship between corrected peak area and cation concentration in the 0.1–1 ppm range was obtained for transition metal cations. Further, the separation of inorganic cations at a low concentration level (100 ng ml^{-1}) was achieved without any loss of resolution.

1. Introduction

Capillary electrophoresis (CE) is very useful for the separation of inorganic cations [1,2]. The analytical approach is based on the indirect detection mode because of the transparency of inorganic cations in the UV region and on separation using operating conditions such that the electroosmotic flow must be in the same direction as the electrophoretic mobility of the ions analysed in order to minimize their migration time. In order to use indirect photometric detection and to obtain symmetrical peaks, a UV-absorbing cationic compound having a similar electrophoretic mobility to that of the analyte cations must be selected as the main constituent of the electrolyte. Beck and Engelhardt [3] first proposed the imidazolium cation as a chromophore co-ion of the electrolyte for the separation of alkali and alkaline earth metal cations. We have previously studied the separation of ammonium, alkali and alkaline earth metal cations by capillary electrophoresis with an imidazole-

* Corresponding author.

based electrolyte to which 18-crown-6 was added [4]; Optimization of the 18-crown-6 concentration was achieved. The crown ether concentration appears to be a very convenient parameter to monitor the selectivity of cations (K^+/NH_4^+, Sr^{2+}/Ba^{2+}) during the analysis of complex matrix aqueous samples. Adding 2.5 mM 18-crown-6 to the 10 mM imidazole system (pH 4.5) generally gives the maximum resolution of ammonium and potassium cations; nevertheless, it is possible to shift the potassium peak in the electropherogram by adding up to 300 mM of 18-crown-6. The complexation constants of several cations with 18-crown-6 can be experimentally determined by capillary electrophoresis from electrophoretic mobilities versus $-\log[18\text{-}$crown-6] curves [4]. The high stability constants for potassium (log $K_s = 2.1$), barium (log $K_s = 3.6$) and strontium (log $K_s = 2.7$) explain their lower migration compared with those of ammonium and other cations.

Transition metal cations and alkali and alkaline earth metal cations have similar electrophoretic mobilities. The separation of all these cations requires the addition of a complexing agent to the electrolyte, in order to decrease their electrophoretic mobility by in-situ complexation. Table 1 reports some publications related to the separation of inorganic cations by capillary electrophoresis [5–13].

Shi and Fritz [5] compared different chromophores and complexing agents for the separation of alkali, alkaline earth, transition metal and lanthanide cations. Among selected UV-absorbing co-ions, phenylethylamine, benzylamine, p-toluidine and 4-methylbenzylamine were found to be the most satisfactory. They used α-hydroxyisobutyric (HIBA), phthalic, malonic, tartaric, lactic and succinic acids as complexing agents; among these, HIBA and phthalic acid gave higher selectivities. HIBA was previously used for the separation of several mono- and divalent cations [6], but good separations were subsequently obtained with phthalic acid [5]. It was found that even better separations of metal cations could be obtained with tartrate or lactate as complexing agent; an excellent separation of

alkali, alkaline earth and transition metal ions was achieved in less than 6 min using 8 mM 4-methylbenzylamine–15 mM lactate–5% methanol (pH 4.25).

In another study, the same group [7] resolved a metal cation mixture by capillary electrophoresis with 4-methylbenzylamine electrolyte containing lactic acid, 18-crown-6 and methanol; protonated 4-methylbenzylamine was used as a co-ion for indirect UV detection of the sample cations and for pH adjustment.

In order to obtain the separation of metal cations having similar electrophoretic mobilities, the equilibrium kinetics between the free metal cation and the complexed species must be very rapid to maintain a narrow analyte electrophoretic zone. If this equilibrium is too slow, the various chemical species of an analyte would migrate at different velocities and the electrophoretic zone of the analyte would become too broad. In a lactic acid-based electrolyte, no peak could be obtained for Al(III) cation owing to the slow kinetics of forming and dissociating the Al(III)–lactate complex. Thus, the non-complexing nicotinamide-based electrolyte allows the simultaneous separation of alkali, alkaline earth and Al(III) cations [7].

Lin et al. [8] studied the role of complexing agents (acetic, glycolic, lactic, α-hydroxyisobutyric, oxalic, malonic, tartaric and succinic acids) added to an imidazole-based electrolyte in the separation of alkali and alkaline earth metal cations. The best separations were achieved using malonic or succinic acid, but glycolic, lactic or HIBA acid also provide good separations. When the concentration of one analyte in the sample is particularly high (for instance, Na$^+$ matrix in a serum sample), the addition of oxalic or citric acid to the electrolyte will avoid the overlap of the large Na$^+$ peak with the minor peaks. In another study, Lee and Lin [9] used several background carriers (imidazole, pyridine, benzylamine) under acidic pH conditions during the separation of some metal cations and they selected glycolic acid rather than succinic acid as the complexing agent.

Recently, Yang et al. [10] reported the

Table 1
Selected examples of inorganic cation separations by capillary electrophoresis

Cations	Detection	Electrolyte	Separation time (min)	Ref.
K^+, Ba^{2+}, Ca^{2+}, Na^+, Mg^{2+}, Li^+, Pb^{2+}, Ni^{2+}, Cd^{2+}, lanthanides	Indirect UV, 214 nm	2 mM Phthalic acid–UV Cat 1– 20% MeOH (pH 3.3)	12	[5]
		2.5 mM Tartaric acid– 6 mM p-toluidine–20% MeOH (pH 4.8)	9	
		8 mM 4-Methylbenzylamine– 15 mM lactic acid– 5% MeOH (pH 4.25)	6	
Alkali, alkaline earth, lanthanides, transition metals	Indirect UV, 214 nm	10 mM Waters UV Cat-1– 4 mM HIBA (pH 4.4)	2	[6]
Metal cations and ammonium	Indirect UV, 214 or 254 nm	7.5 mM 4-Methylbenzylamine– 11 mM lactic acid–2.6 mM 18-crown-6 8% MeOH (pH 4.3)	7	[7]
		8 mM Nicotinamide–0.95 mM 18-crown-6 –12% MeOH (pH3.2)	14	
K^+, Ba^{2+}, Ca^{2+}, Na^+, Mg^{2+}, Li^+	Indirect UV, 215 nm	5 mM Imidazole– 2.1 mM acetic acid (pH 6)	2	[8]
		5 mM Imidazole– 4.55 mM glycolic acid (pH 4)	2	
		5 mM Imidazole– 5 mM lactic acid (pH 4)	2	
		5 mM Imidazole– 6.4 mM HIBA (pH 4)	4	
		5 mM Imidazole– 1.9 mM oxalic acid (pH 4)	2	
		5 mM Imidazole– 3 mM succinic acid (pH 4.5)	2	
		5 mM Imidazole– 4 mM malonic acid (pH 4)	2	
		5 mM Imidazole– 3.6 mM malic acid (pH 3.7)	2	
		5 mM Imidazole– 1.9 mM tartaric acid (pH 4)	2	
Li^+, Na^+, K^+, Cs^+, Mg^{2+}, Sr^{2+}, Ca^{2+}, Ba^{2+}, Mn^{2+}, Fe^{2+}, Co^{2+}, Ni^{2+}, Cu^{2+}, Zn^{2+}, Cd^{2+}, Ag^+, Al^{3+}, Pb^{2+}	Indirect UV, 210 nm 254 nm 210 nm 210 nm	10 mM Imidazole– 13 mM glycolic acid (pH 4)	15	[9]
		10 mM Pyridine– 12 mM glycolic acid (pH 4)	18	
		10 mM Benzylamine– 16 mM glycolic acid (pH 4)	15	
		5 mM Imidazole– 6.75 mM HIBA (pH 4)	12	
NH_4^+, K^+, Na^+, Li^+, Mg^{2+}, Ca^{2+}, Sr^{2+}, Mn^{2+}, Ni^{2+}, Zn^{2+}, Cu^{2+}	Indirect UV	5 mM Imidazole–0.53 mM–18-crown-6– 6.5 mM HIBA– 20% MeOH (pH 4.5)	10	[10]
Alkali, alkaline earth, transition metal, lanthanides	Indirect UV, 214 nm	6 mM N,N-Dimethylbenzylamine– 4.2 mM HIBA (pH 5)	11	[11]
K^+, Ba^{2+}, Sr^{2+}, Ca^{2+}, Na^+, Mg^{2+}, Li^+, NH_4^+, Cs^+	Indirect UV, 254 nm	5 mM Benzimidazole– 40 mM 18-crown-6– tartrate (pH 5.2)	4	[12]
K^+, Ba^{2+}, Sr^{2+}, Ca^{2+}, Na^+, Mg^{2+}, Li^+, NH_4^+	Indirect UV, 215 nm	4 mM Copper(II) sulfate–4 mM formic acid– 4 mM 18-crown-6 (pH 3)	5	[13]

simultaneous separation of ammonium and al-
kali, alkaline earth and transition metal cations
in a background electrolyte system composed of
imidazole, HIBA, 18-crown-6 and methanol.
Finally, other workers employed 18-crown-6 or
HIBA as complexing agents added to an elec-
trolyte containing N,N-dimethylbenzylamine
[11], benzimidazole [12] or copper(II) sulfate
[13] as chromophore agent for the separation of
inorganic cations.

In this work, we studied the influence of
several physico-chemical parameters (imidazole,
lactic acid and 18-crown-6 concentrations) on the
separation of ammonium, alkali, alkaline earth
and transition metal cations by capillary electro-
phoresis.

2. Experimental

2.1. Apparatus

Separations were carried out on a P/ACE 2210
apparatus (Beckman, Fullerton, CA, USA)
equipped with a UV detector with wavelength
filters (190, 200, 214, 254, 260 and 280 nm).
Fused-silica capillaries (Beckman) of dimensions
75 μm I.D., 375 μm O.D. and 57 cm long (50
cm to the detector) were used. The part where
the separation takes place was kept at a constant
temperature by immersion in a cooling liquid
circulating in the cartridge with a detection
aperture of 100×800 μm. The solutes were
injected at the anode end of the capillary in the
hydrodynamic mode by nitrogen superpressure
$3.45 \cdot 10^7$ Pa (0.5 p.s.i.). Indirect UV detection at
214 nm was performed by a light beam focused
directly on the capillary with the detection win-
dow set 7 cm from the end of the capillary. An
IWT computer and System Gold software ver-
sion 7.11 (Beckman) were used for instrument
control and for data collecting and processing.
The detector time constant was 0.1 s and the
data acquisition rate was 20 Hz.

The pH of each solution was verified on a
Beckman pH meter (Model ϕ 10).

2.2. Chemicals

Imidazole (99% purity) was obtained from
Sigma (St. Louis, MO, USA) and 18-crown-6
(99%) and lactic acid (85%) from Aldrich (Mil-
waukee, WI, USA). The water used in the
preparation of electrolytes and that necessary for
dilutions was of HPLC quality (Fisons, Milan,
Italy). The electrophoretic electrolyte pH was
adjusted to the desired pH by adding a 1 M
acetic acid stock solution (Carlo Erba, Milan,
Italy). Each buffer and rinsing solution was
filtered before use through a membrane filter
having a diameter of 25 mm and a porosity of 0.2
μm (Whatman, Maidstone, UK).

3. Results and discussion

The electrolyte used for the separation of
inorganic cations (alkali, alkaline earth and
transition metal) must contain an organic cation
which has an electrophoretic mobility close to
that of the analytes in order to obtain symmetri-
cal and efficient electrophoretic peaks, and also
which possesses an intense chromophore group
in the UV region. Imidazole is a nitrogen
heterocyclic compound ($pK_{a_1} = 6.9$ and $pK_{a_2} =$
14.5) whose UV absorption spectrum has a
maximum set at 211 nm ($\varepsilon = 3300$ l mol^{-1} cm^{-1}
at pH 4.5). The electrophoretic mobility of the
imidazolium cation ($45.8 \cdot 10^{-5}$ cm^2 V^{-1} s^{-1}) was
determined in 10 mM sodium acetate electrolyte
at pH 4.5; this UV-absorbing co-ion has an
electrolyte mobility close to those of Mg^{2+} and
Na$^+$ (46.3 and 48.10^{-5} cm^2 V^{-1} s^{-1}, respective-
ly), which were measured in 10 mM imidazole
electrolyte (pH 4.5) [4].

3.1. Effect of imidazole concentration

In recent paper [4], a study of the influence of
the imidazole electrolyte concentration at pH 4.5
on selectivity in the range 1–15 mM was re-
ported. The values of the resolution between
K$^+$/Ca^{2+}, Ca^{2+}/Na$^+$, Na$^+$/Mg^{2+} and Mg^{2+}/Li$^+$
are reported in Table 2. In the imidazole con-

Table 2
Influence of imidazole concentration on resolution of alkali and alkaline earth metal cation mixture

Imidazole concentration (mM)	Resolution (R_s)			
	K^+/Ca^{2+}	Ca^{2+}/Na^+	Na^+/Mg^{2+}	Mg^{2+}/Li^+
1	6.42	5.34	0.66	5.02
2	6.53	3.62	0.15	6.55
5	14.34	6	1.07	10.92
7	15.65	5.71	1.91	10.64
10	21.95	5.47	3.38	13.21
12	23.76	5.2	4.16	13.98
15	28.02	4.55	5.44	14.92

Fused-silica capillary dimensions, 57 cm (50 cm to detector) × 75 μm I.D., 100 μm × 800 μm aperture; electrolyte, imidazole (pH 4.5); indirect UV detection, 214 nm; applied voltage, 15 kV; temperature, 25°C; hydrodynamic injection, 2 s; cation concentration, 5 ppm.

centration range 1–5 mM, the resolution between sodium and magnesium cations is always too low ($0.66 < R_s < 1.07$). An increase in imidazole concentration from 7 to 12 mM improves the separation between strontium and calcium cations and also between nickel and zinc cations (Fig. 1), but the resolution between these two last transition metal cations always remains <1. Some transition metal cations [manganese, iron(II), cobalt, lead] co-migrated under such non-complexing conditions. Consequently, the addition of a complexing agent (lactic acid) to the electrolyte (pH 4.5) is necessary to resolve these cations.

3.2. Effect of lactic acid concentration

The concentration of lactic acid added to the electrolyte (10 mM imidazole, pH 4.5) would change the degree of complexation of the transition metal cations. By increasing the lactic acid concentration from 1 to 12 mM in the running electrolyte, we observed a decrease in the electrophoretic mobilities of some metal cations [nickel, zinc, cobalt, iron(II), copper]; for example, a 33% electrophoretic mobility loss was observed for copper cation. Under such conditions, the electrophoretic mobilities of other

cations (cadmium, manganese) remain constant (Fig. 2).

An increase in lactic acid concentration would change the migration order of cobalt, nickel, zinc, cadmium and lithium cations. Thus, nickel and zinc migrated between cadmium and cobalt cations in the lactic acid concentration range 1–3 mM, then migrated between cadmium and lithium for lactic acid concentrations <7 mM and finally migrated after lithium for lactic acid concentrations >7 mM. According to the nature of the sample matrix, we can shift the nickel and zinc peaks relative to the other cation peaks by adjusting the lactic acid concentration.

In our work, the best resolution was obtained by selecting 5 mM rather than 10 mM as the lactic acid concentration (Fig. 3).

Finally, if the addition of lactic acid to the imidazole electrolyte improves the separation of transition metal cations, another complexing agent (18-crown-6) must be added to this electrolyte to resolve not only ammonium and potassium cations, but also sodium and lead cations.

3.3. Effect of 18-crown-6 concentration

As is well known, the separation of K^+/NH_4^+ or Sr^{2+}/Ba^{2+} is favoured by complex formation
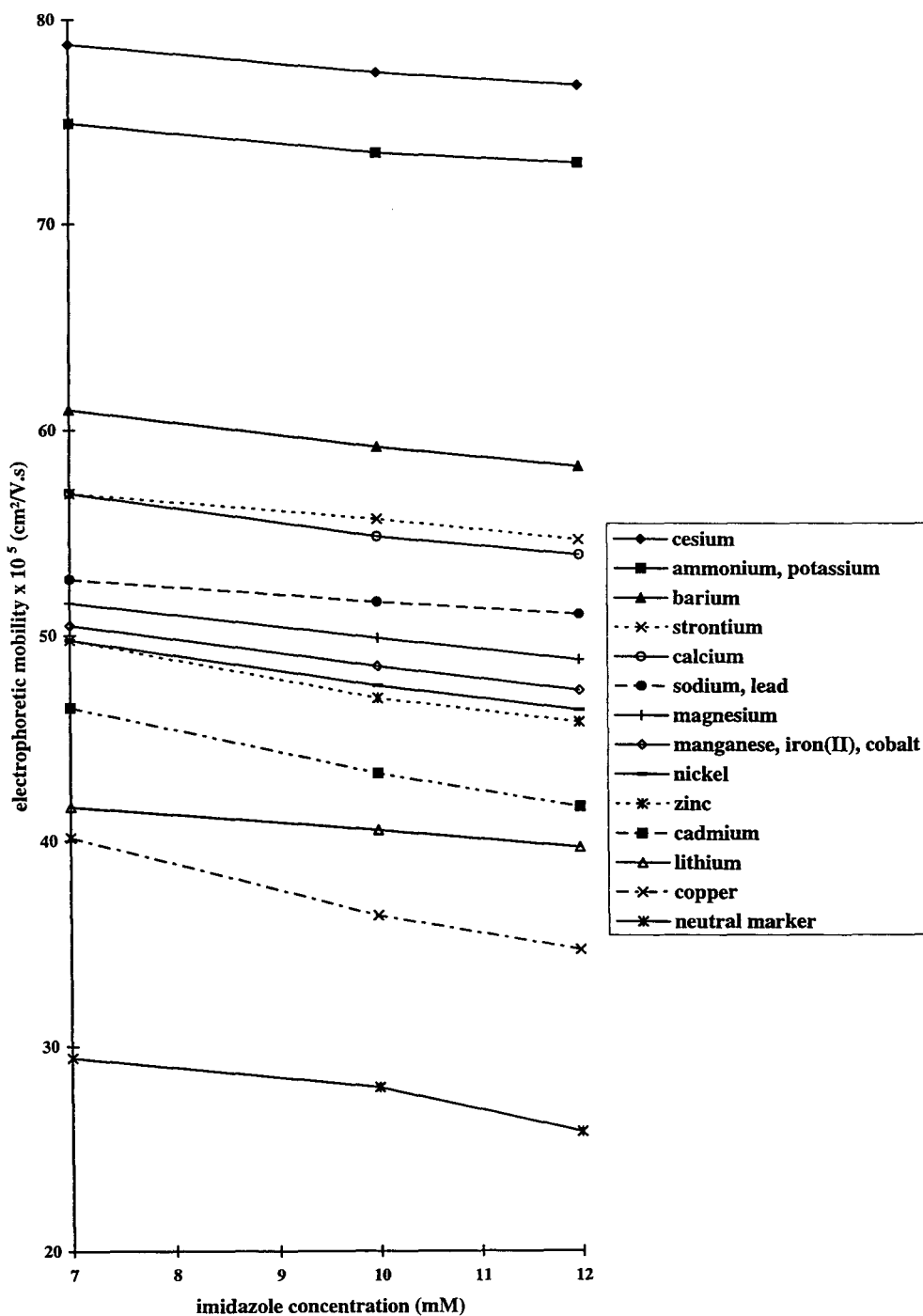
Fig. 1. Influence of imidazole concentration on the electrophoretic mobility of 17 inorganic cations. Fused-silica capillary dimensions, 57 cm (50 cm to detector) × 75 μm I.D., 100 μm × 800 μm aperture; electrolyte, imidazole (pH 4.5); indirect UV detection, 214 nm; applied voltage, 20 kV; temperature, 30°C; hydrodynamic injection, 2 s; cation concentration, 5 ppm except for caesium and lead (10 ppm) and barium and copper (20 ppm).
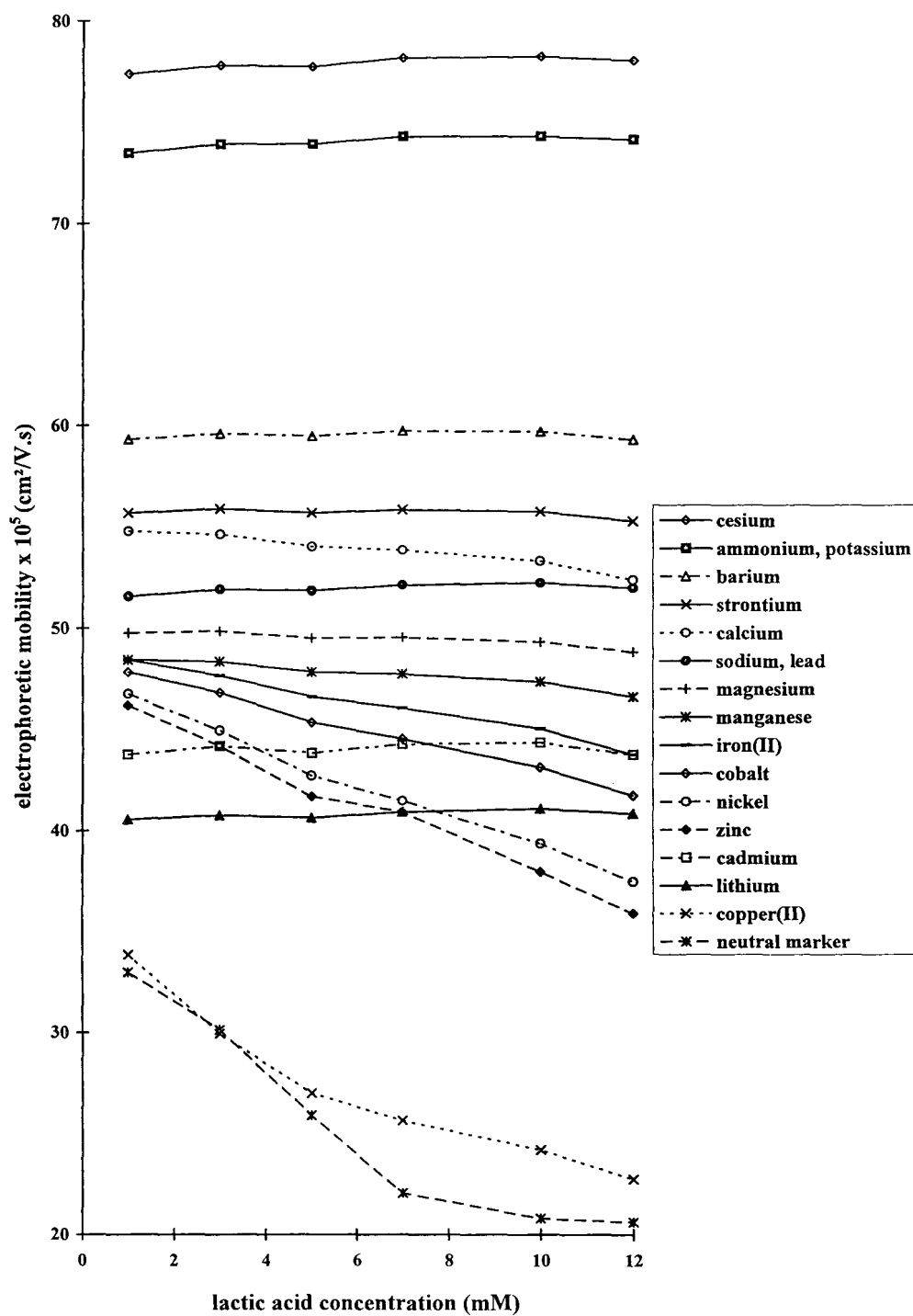
Fig. 2. Influence of lactic acid concentration on the electrophoretic mobility of 17 inorganic cations. Experimental conditions as in Fig. 1 except electrolyte composition, 10 m*M* imidazole–lactic acid (pH 4.5).
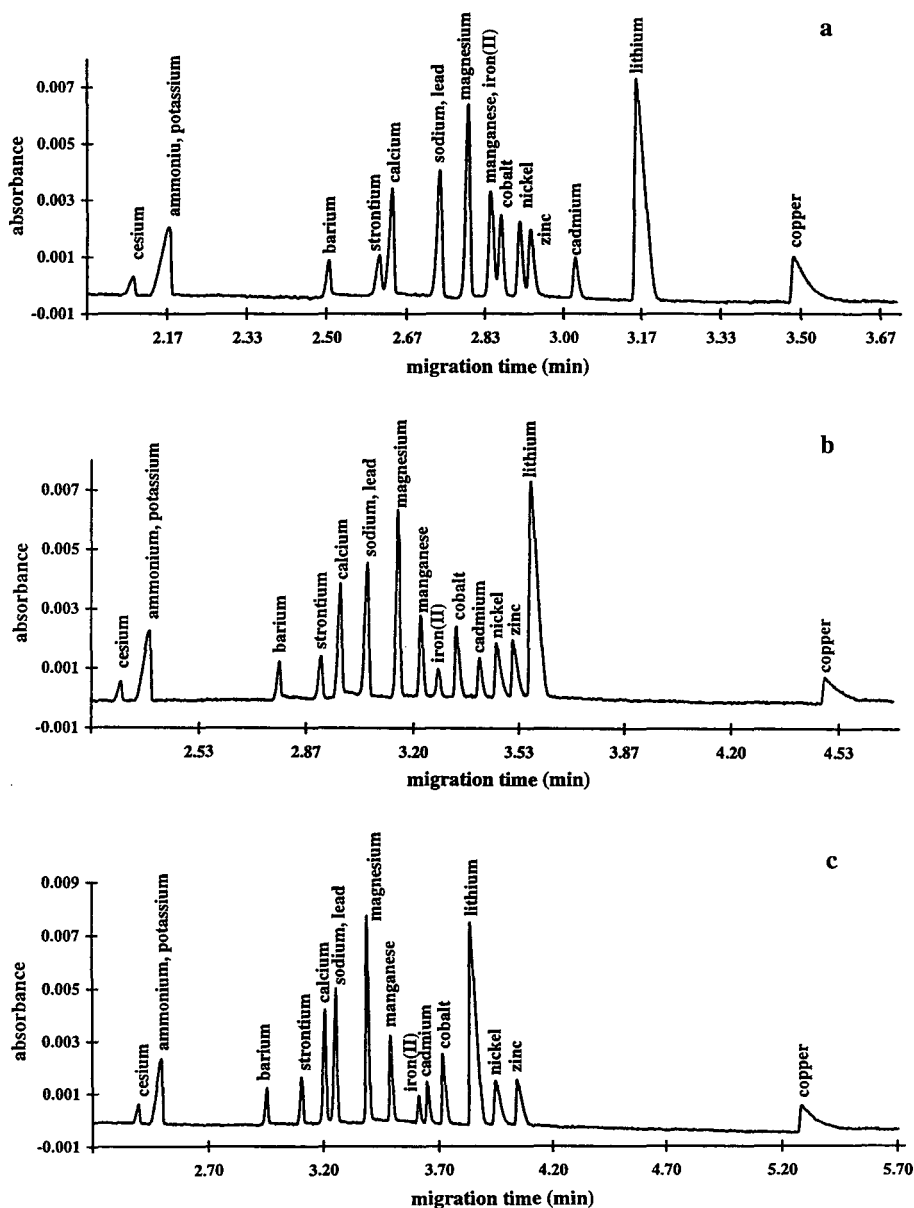
Fig. 3. Influence of lactic acid concentration on the separation of iron(II), cobalt and cadmium cations. Experimental conditions as in Fig. 2, except lactic acid concentration: (a) 1 mM; (b) 5 mM; (c) 10 mM.

with 18-crown-6 [4]. We studied the influence of the 18-crown-6 concentration in the range 0.5–1.5 mM on the selectivity by keeping the same imidazole and lactic acid concentrations (10 and 5 mM, respectively, at pH 4.5).

The addition of 18-crown-6 to the imidazole-based electrolyte containing lactic acid affects the migration of almost all cations except K$^+$ and NH$_4^+$. Thus, a low concentration of 18-crown-6 (0.5 mM) added to the imidazole electrolyte induces a migration time increase of 8%, 24% and 47% for Sr^{2+}, Ba^{2+} and Pb^{2+}, respectively

(Figs. 3b and 4a) due to the complexation of these cations with 18-crown-6.

Finally, increasing the 18-crown-6 concentra-

tion from 0.5 to 1.5 mM induces a modification of migration order (Fig. 4); thus, strontium cation migrates faster than sodium cation at 0.5
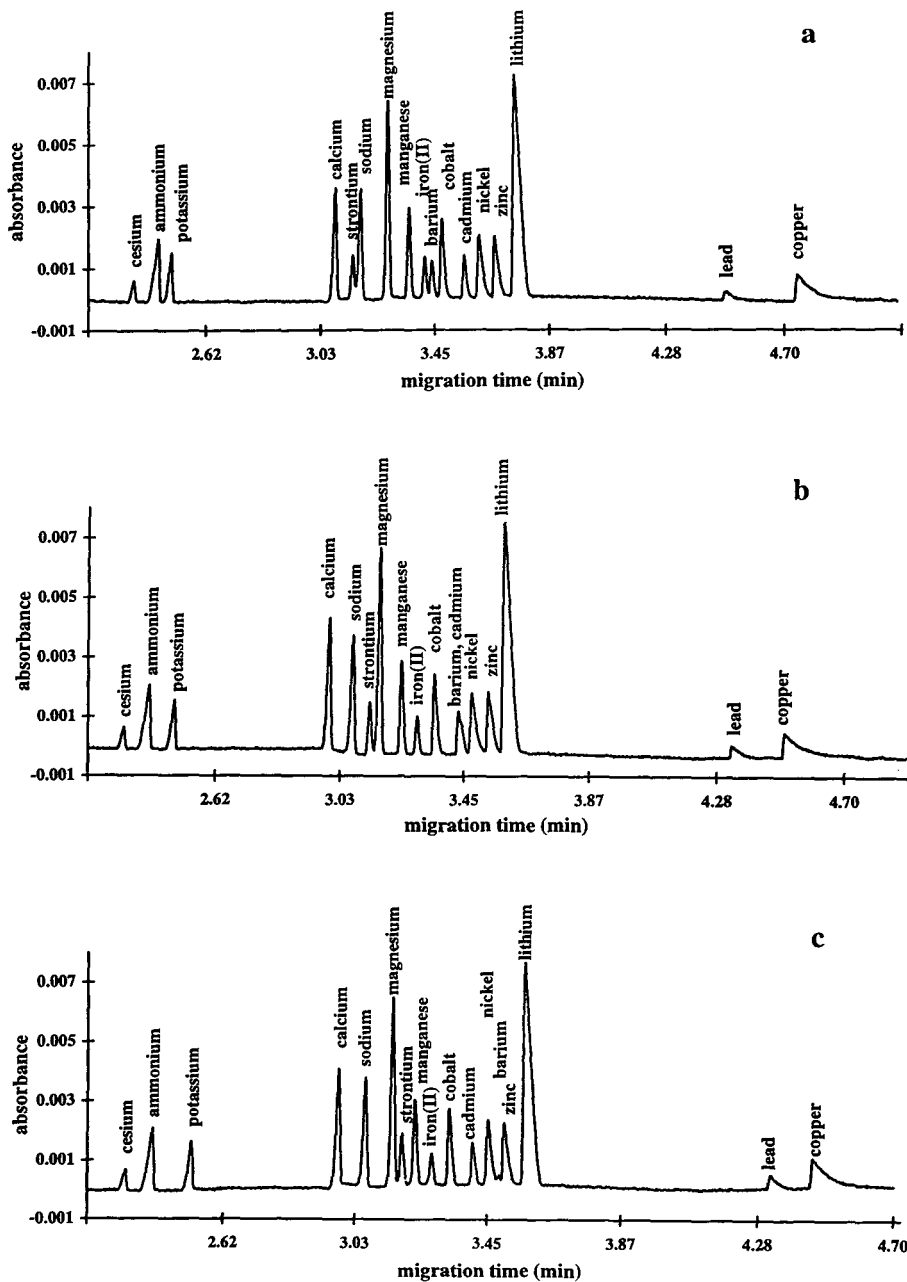
Fig. 4. Effect of 18-crown-6 concentration on the separation of strontium, barium and lead cations. Experimental conditions as in Fig. 3 except electrolyte, 10 mM imidazole–5 mM lactic acid (pH 4.5), and 18-crown-6 concentration: (a) 0.5 mM; (b) 1 mM; (c) 1.5 mM.
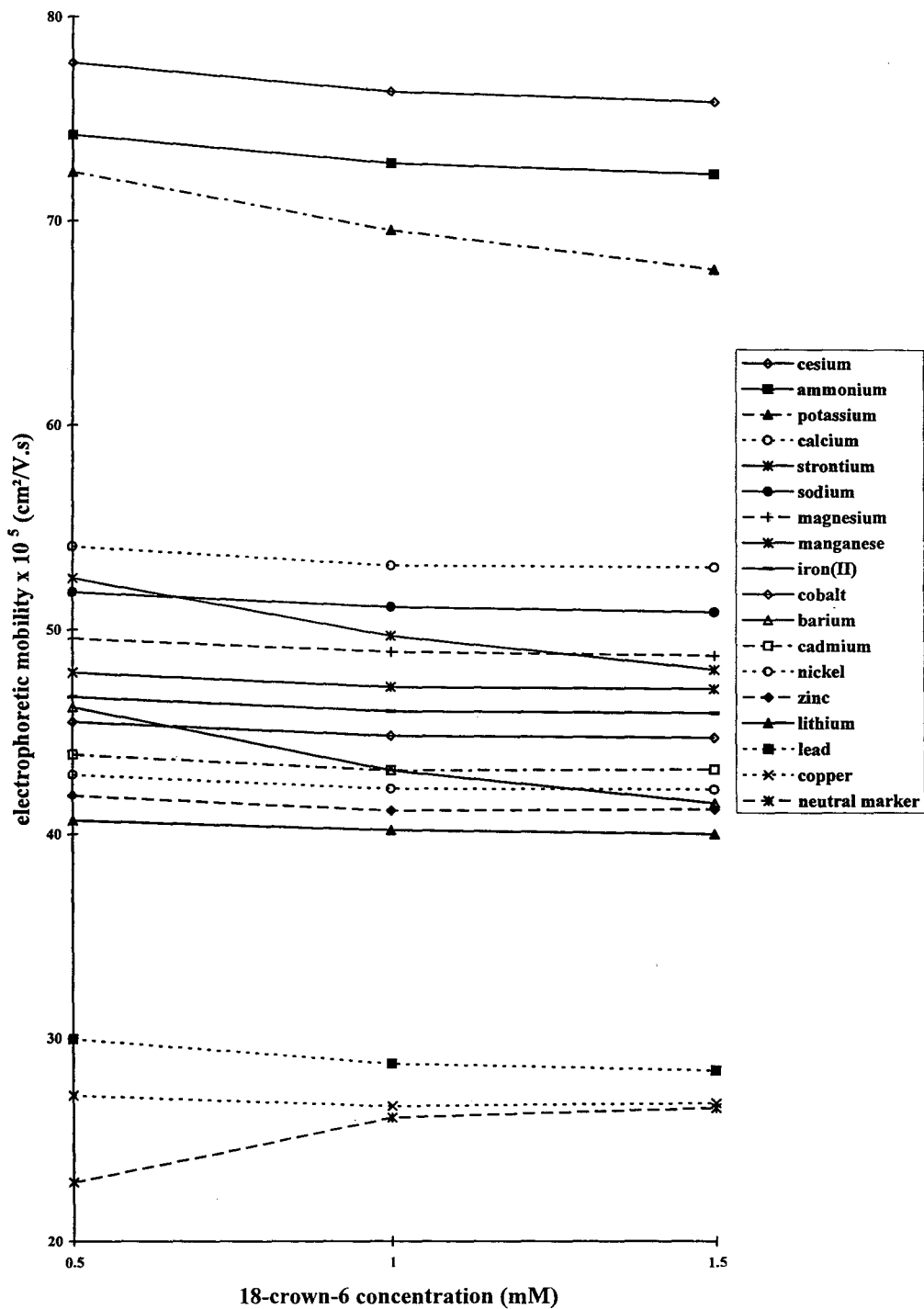
Fig. 5. Influence of 18-crown-6 concentration on the electrophoretic mobility of 17 inorganic cations. Experimental conditions as in Fig. 4.
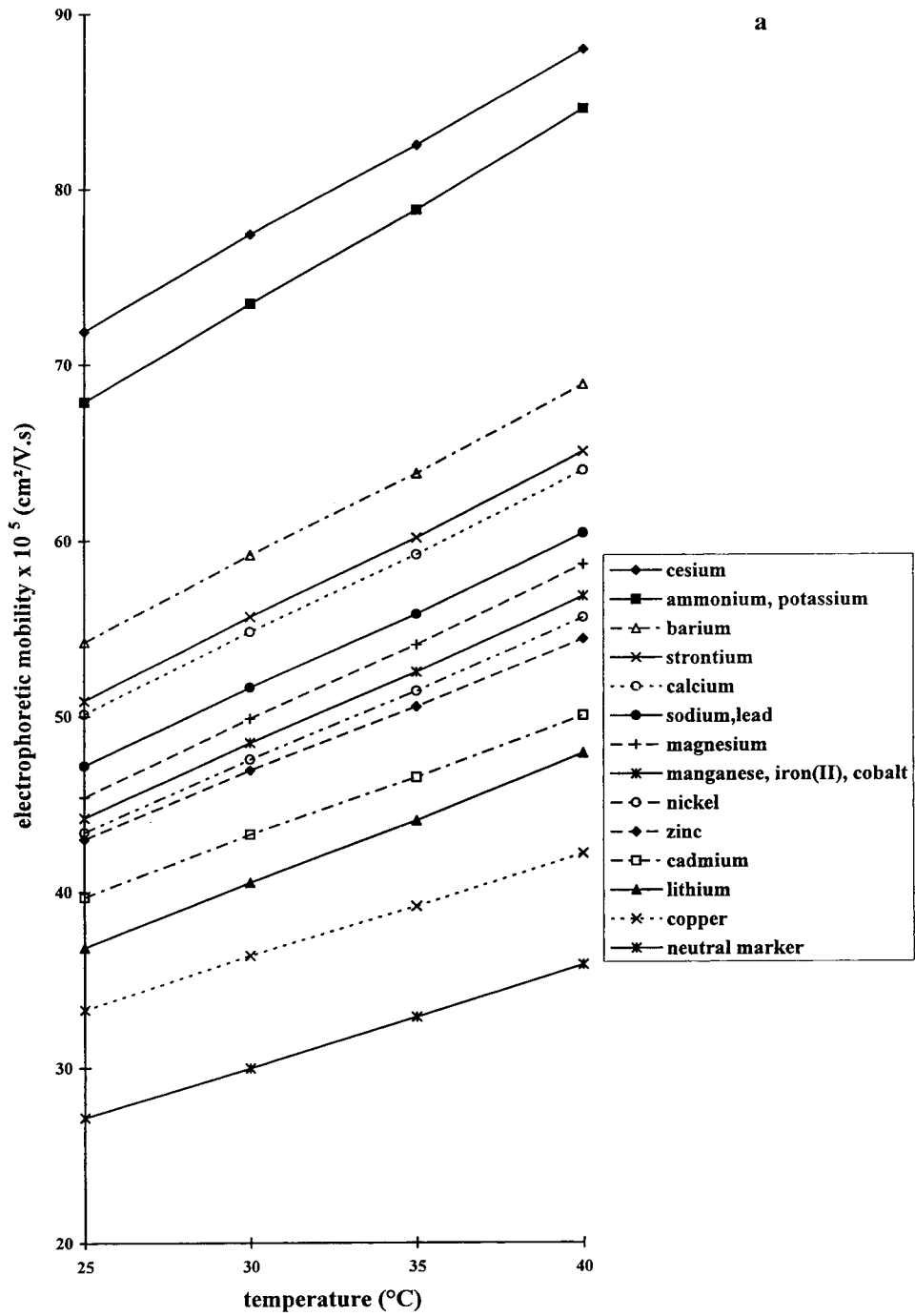
Fig. 6. (*Continued on p. 404*)
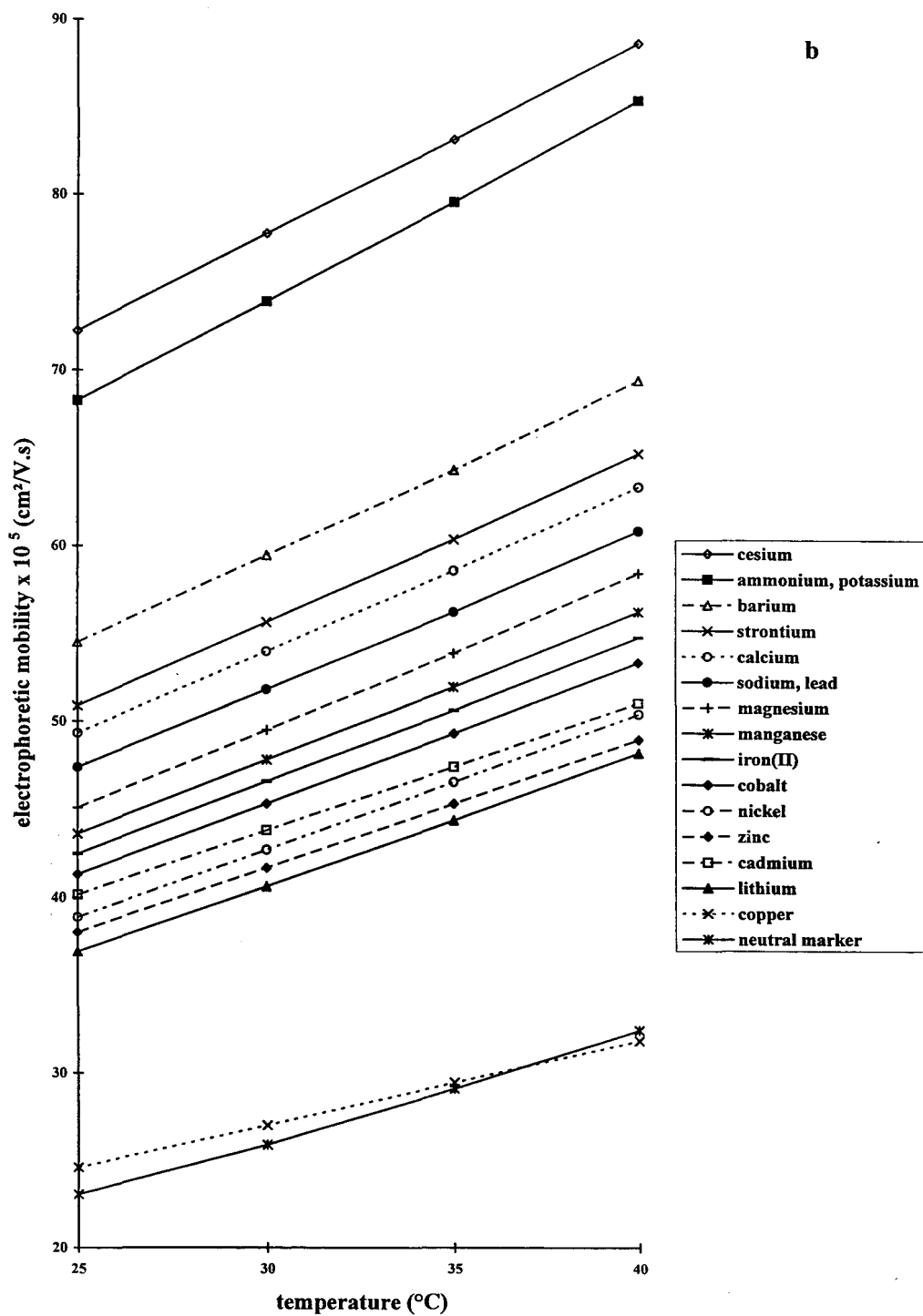
Fig. 6.
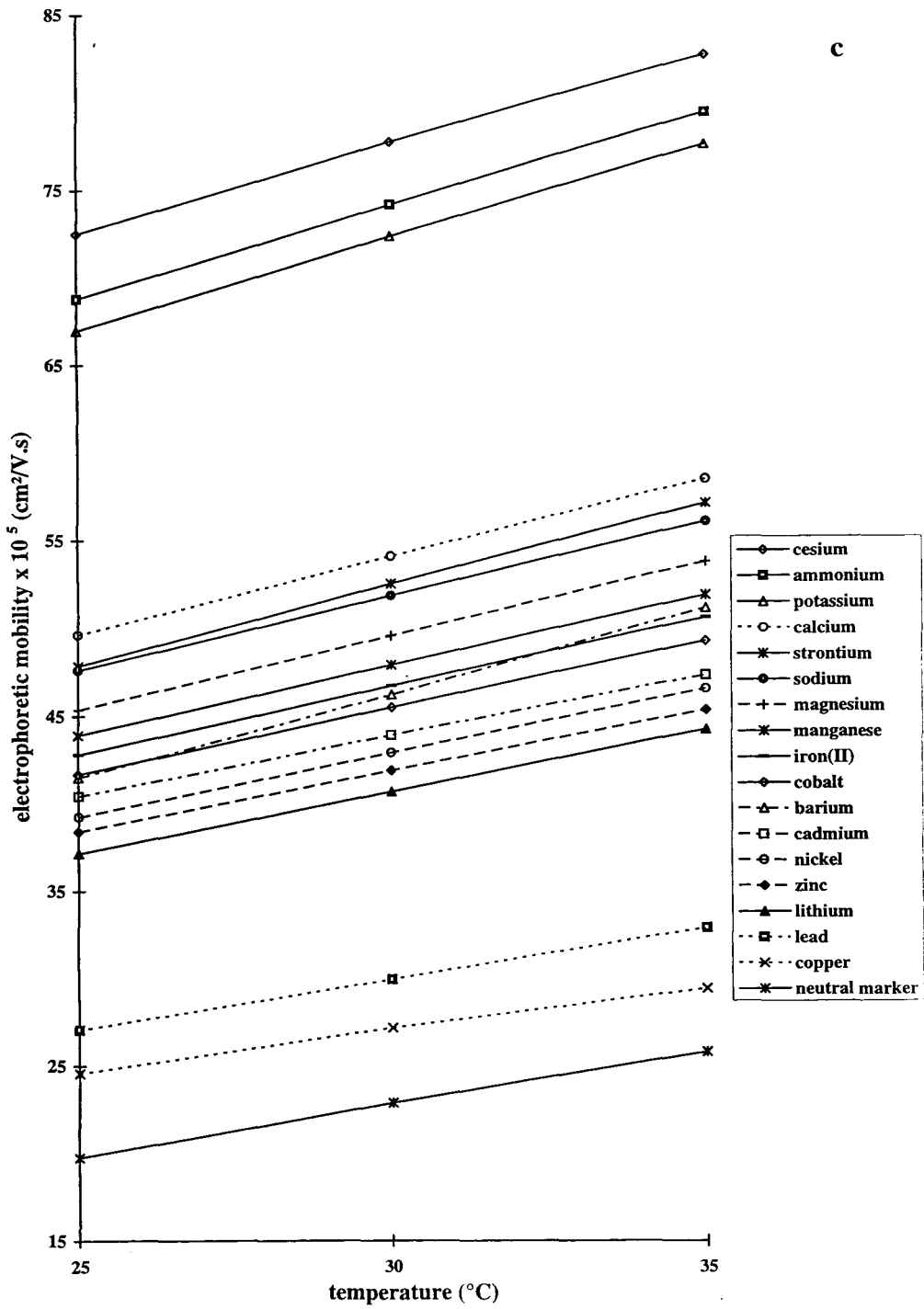
Fig. 6. Dependence of cation electrophoretic mobility on separation temperature. Fused-silica capillary dimensions, 57 cm (50 cm to detector) × 75 μm I.D., 100 μm × 800 μm aperture; indirect UV detection, 214 nm; applied voltage, 20 kV; hydrodynamic injection, 2 s; cation concentration, 5 ppm except for caesium and lead (10 ppm) and barium and copper (20 ppm). (a) 10 mM imidazole (pH 4.5); (b) 10 mM imidazole–5 mM lactic acid (pH 4.5); (c) 10 mM imidazole–5 mM lactic acid–0.5 mM 18-crown-6 (pH 4.5).

mM 18-crown-6 and faster than manganese cation at 1.5 mM 18-crown-6. Also, the electrophoretic mobility of the barium cation decreases when the 18-crown-6 concentration increases, but co-migrates with cadmium at 1 mM 18-crown-6 (Fig. 5). The 18-crown-6 concentration variation affects only the electrophoretic mobility of these two cations.

3.4. Effect of temperature

The effect of temperature on the separation was studied for three different electrolytes (10 mM imidazole, 5 mM lactic acid–10 mM imidazole and 0.5 mM 18-crown-6–5 mM lactic acid–10 mM imidazole). Temperature variations affect physical parameters such as electrolyte viscosity, analyte diffusion coefficient, and consequently, the electroosmotic flow and electrophoretic mobility of the analytes.

Fig. 6 shows the variation of electrophoretic mobility versus separation temperature in the range 25–40°C. For the different electrolytes, when the temperature increases from 25 to 40°C, the cation migration times decrease and so their electrophoretic mobilities increase.

The influence of separation temperature on resolution depends on the electrolyte composition. With the 10 mM imidazole electrolyte, a significant resolution improvement (142%) between nickel and zinc peaks was observed when the temperature was increased from 25 to 40°C. In contrast, no temperature variation improves the separation between manganese, iron(II) and cobalt cations. Using the electrolyte containing 10 mM imiadzole and 5 mM lactic acid, no
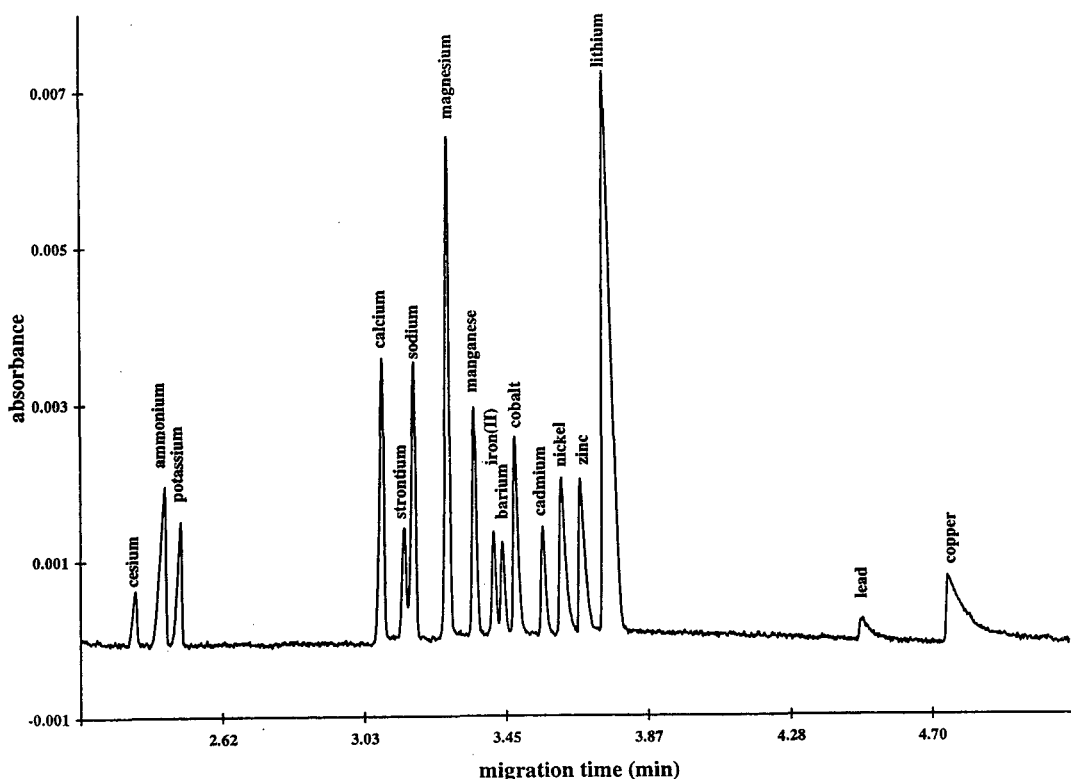
Fig. 7. Separation of a 17 inorganic cation mixture under optimized conditions. Experimental conditions as in Fig. 6c except temperature, 30°C.

significant modification of the resolution was observed with increase in temperature. Finally, using the electrolyte containing imidazole and the two complexing agents (lactic acid and 18-crown-6), the temperature is an important parameter for optimizing the separation of those cations. Thus, the resolution between strontium and sodium cations increases with increase in temperature from 25°C ($R_s = 0$) to 30°C ($R_s = 1.23$). Moreover, we can shift the barium peak relative to the other peak by increasing the temperature; for instance, barium cation mi-
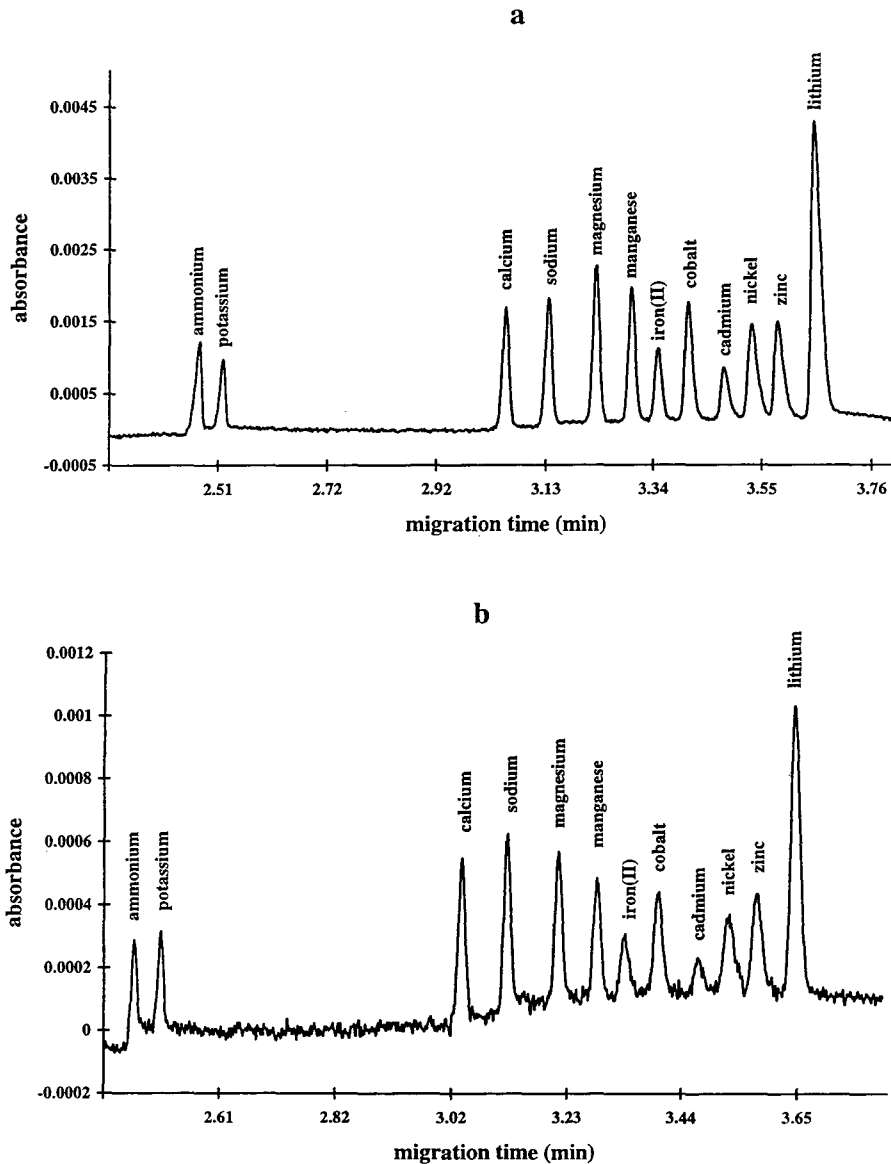
Fig. 8. Separation of standard mixture of 11 inorganic cations at sub-ppm concentrations by capillary electrophoresis. Experimental conditions as in Fig. 7 except cation concentrations: (a) ammonium, alkali and alkaline earth 0.5 ppm and transition metal 1 ppm; (b) ammonium, alkali and alkaline earth 50 ppb and transition metal 100 ppb.

Table 3
Parameters of linear calibration plots for several transition metal cations in the 0.1–1 ppm range

Cation	Slope (1/ppm)	Intercept	Correlation coefficient
Manganese	1.097	0.0038	0.99984
Iron(II)	1.947	0.016	0.99964
Cobalt	1.165	0.02	0.99970
Cadmium	2.237	0.0681	0.99752
Nickel	1.206	0.014	0.99925
Zinc	1.252	0.0101	0.99847

Experimental conditions as in Fig. 7.

grates slower than cobalt cation at 25°C whereas this cation migrates faster than cobalt and iron(II) cations at 35°C. Consequently, we selected 30°C as the optimum separation temperature owing to a better resolution between barium and iron(II) cations at 30°C than 35°C (resolution 1.10, 1.01, respectively). Fig. 7 shows the separation of alkali, alkaline earth and transition metal cations under such optimized conditions.

3.5. Quantitative aspects

Calibration graphs were determined for several transition metal cations [manganese, iron(II), cobalt, cadmium, nickel and zinc] using a hydrodynamic injection time of 15 s. These experiments were carried out using a 10 mM imidazole-based electrolyte containing the two complexing agents 5 mM lactic acid and 0.5 mM 18-crown-6. For all cations, the correlation coefficients were greater than 0.997 (Table 3). With this injection time (15 s), the separation of a sub-ppm inorganic cation mixture may be achieved without any resolution loss (Fig. 8).

4. Conclusion

The separation of ammonium, alkali, alkaline earth and transition metal cations was achieved by capillary electrophoresis with an imidazole-based electrolyte, to which two different complexing agents were added. Selectivity modifica-

tion was obtained by varying the concentration of each complexing agent, particularly during the analysis of complex matrix samples.

Whereas the separation of alkali and alkaline earth metal cations was successfully achieved with an imidazole electrolyte (10 mM, pH 4.5), the addition of 5 mM lactic acid to this imidazole electrolyte is required to resolve manganese, iron(II), cobalt, cadmium, nickel and zinc cations. Further, the addition of 0.5 mM 18-crown-6 to this imidazole–lactic acid electrolyte is necessary to resolve sodium and lead cations and also ammonium and potassium cations. Finally, the separation temperature appears also to be a very convenient parameter for monitoring the selectivity of these cations.

Acknowledgements

References

[1] Ph. Morin, C. François and M. Dreux, Analusis, 22 (1994) 178.
[2] Ph. Morin, C. François and M. Dreux, J. Liq. Chromatogr., 17 (1994) 3869.
[3] W. Beck and H. Engelhardt, Chromatographia, 33 (1992) 313.
[4] C. François, Ph. Morin and M. Dreux, J. Chromatogr. A, 706 (1995) 535.
[5] Y. Shi and J.S. Fritz, J. Chromatogr., 640 (1993) 473.
[6] A. Weston, P.R. Brown, P. Jandik, W. Jones and A.L. Henckenberg, J. Chromatogr., 593 (1992) 289.
[7] Y. Shi and J.S. Fritz, J. Chromatogr. A, 671 (1994) 429.
[8] T.I. Lin, Y.H. Lee and Y.C. Chen, J. Chromatogr. A, 654 (1993) 167.
[9] Y.H. Lee and T.I. Lin, J. Chromatogr. A, 675 (1994) 227.
[10] Q. Yang, J. Smeyers-Verbeke, W. Wu, M.S. Khots and D.L. Massart, J. Chromatogr. A, 688 (1994) 339.
[11] M. Chen and R.M. Cassidy, J. Chromatogr., 640 (1994) 425.
[12] E. Simunicova, D. Kaniansky and K. Loksikova, J. Chromatogr. A, 665 (1994) 203.
[13] J.M. Riviello and M.P. Harrold, J. Chromatogr. A, 652 (1993) 385.

Determination of thiocyanate, iodide, nitrate and nitrite in biological samples by micellar electrokinetic capillary chromatography

C. Bjergegaard, P. Møller, H. Sørensen*

Chemistry Department, Royal Veterinary and Agricultural University, 40 Thorvaldsensvej, DK-1871 Frederiksberg C, Denmark

Abstract

Micellar electrokinetic capillary chromatography (MECC) has been developed as an efficient method for the determination of the thiocyanate ion, iodide, nitrite and nitrate. The use of various alkyltrimethylammonium ions was found advantageous for MECC compared to negatively charged surfactants, as this resulted in low migration times for the anions and thereby fast analysis. Moreover, the MECC system, using positively charged surfactants (dodecyltrimethylammonium bromide, DTAB), was effective in separating the anions of interest from interfering organic anions present in extracts from biological samples such as milk and blood. Detection of the anions was performed by direct UV. The performance of the developed method was satisfying; however, a low number of theoretical plates for the thiocyanate ion indicated the need for some improvements in this respect. The sensitivity of the method increased with a factor two by using a 75 μm I.D. capillary instead of the 50 μm I.D. capillary, whereas use of a high-sensitivity optical cell assembly increased the sensitivity an additional nine times. Repeatability with the 50-μm capillary was satisfying with respect to migration time, relative migration time and normalised peak area (except for the thiocyanate ion) of the anions, with relative standard deviations varying between 0.24 and 0.29%, 0.07 and 0.16%, and 1.75 and 2.37%, respectively, whereas some improvements are still needed for the normalised and relative normalised peak areas for the thiocyanate ion (13.50 and 13.91%). Apart from the thiocyanate ion ($r^2 = 0.9748$), linearity studies gave correlation coefficients between 0.9962 and 0.9975 for the normalised peak areas.

1. Introduction

The thiocyanate ion is formed as a degradation product of indol-3-ylmethylglucosinolates and other glucosinolates which give a carbonium ion and the thiocyanate ion in non-enzymatic and enzyme-catalysed reactions [1]. When absorbed from digesta to the blood, the thiocyanate ion can be transferred to the milk [2–5] or transformed by liver enzymes. It may also competi-

tively inhibit the transfer of iodide to the thyroid hormones in the thyroid gland [6–10]. The thiocyanate ion and iodide are thus considered to be important in relation to studies of the quality of vegetables, e.g. antinutritional effects of glucosinolates [1] as well as processing effects on oilseed rape [11,12] and on cruciferous vegetables rich in indol-3-ylmethylglucosinolates [13]. For various other reasons nitrate and nitrite are considered to be important in relation to the quality of food and feed. It will therefore be of value to have a simple analytical method for the

* Corresponding author.

simultaneous determination of the thiocyanate ion, iodide, nitrate and nitrite in biological samples such as glucosinolate-containing vegetables [14], food, feed, blood and milk. An analytical technique which in addition can be used for other types of degradation products from glucosinolates would be preferable [1,15].

Recently, a most interesting method for the separation and detection of anions by high-performance capillary electrophoresis (HPCE) has been described [16]. This method and other pioneering work performed on various anions [17,18] use, however, a system with indirect photometric detection which is less efficient for the analysis of glucosinolates and its degradation products. This is also the case with a recently described HPCE method for the determination of nitrate and nitrite in plasma [19]. Micellar electrokinetic capillary chromatography (MECC) using alkyltrimethylammonium bromides as surfactants has formerly been developed for the determination of various types of natural products including glucosinolates [20] and different types of indolylic compounds from glucosinolate degradation [15]. This system was tested and found satisfying for the simultaneous determination of the thiocyanate ion, iodide, nitrate and nitrite, using detection by direct UV at 235 nm. In the present work, we describe the performance of this system with respect to separation efficiency, repeatability and linearity of the optimised MECC method as well as sensitivity, using a special Z-shaped high-sensitivity optical cell assembly. Determination of the anions in biological samples was also demonstrated.

2. Experimental

2.1. Apparatus

The apparatus used was an ABI Model 270 A-HT capillary electrophoresis system (Applied Biosystems, Foster City, CA, USA) with a 760 × 0.05 mm I.D. fused-silica capillary, unless stated otherwise. Detection was performed by on-column measurement of the UV absorption at a position 530 mm from the injection end of the

capillary. The performance of a high-sensitivity optical cell assembly (Applied Biosystems), consisting of a fused-silica capillary (1000 × 0.075 mm I.D.) with an optical cell (Z-cell) placed 780 mm from the injection end, was tested. The path length of the optical cell is specified to 3 mm. Data processing was carried out by use of an IBM-compatible 486 DX, 50 MHz personal computer with Turbochrom 3.3 (PE Nelson, Perkin-Elmer, Beaconsfield, UK).

2.2. Samples and reagents

Sodium nitrite, sodium nitrate, potassium iodide, potassium thiocyanate, dodecyltrimethylammonium bromide (DTAB) and cetyltrimethylammonium bromide (CTAB) were purchased from Sigma (St. Louis, MO, USA). All chemicals were of analytical-reagent grade.

2.3. Procedure

The separation buffer consisted of 50 mM surfactant, 18 mM sodium tetraborate, 30 mM disodium hydrogenphosphate and 10% 2-propanol. The pH was adjusted to 7.0 with 1 M hydrochloric acid. Buffers were filtrated through a 0.20-μm membrane filter prior to use. Washing of the capillary was performed with 1.0 M NaOH for 2 min and with buffer for 5 min before each analysis. Buffers were changed by auto buffer-vial change after varying numbers of analyses. The separation parameters used were: voltage of 20 kV and temperature of 60°C. Detection was performed at 235 nm. Injection by vacuum was performed from the negative end of the capillary for 1 s.

2.4. Calculations

Relative migration times (RMT), normalised peak areas (NA), relative normalised peak areas (RNA) and resolution (R_s) were calculated as described elsewhere [21]. Calculations of RMT and RNA were performed relative to nitrite. The number of theoretical plates (N) was calculated by the Foley–Dorsey approximation (PE Nelson, Perkin-Elmer, Beaconsfield, UK), assuming an

exponentially modified Gaussian distribution as the skewed peak model. The equation for N is

$$N = \frac{41.7(MT/w_{0.1})^2}{B/A + 1.25}$$

where MT is the migration time for the peak, $w_{0.1}$ is the peak width at 10% of peak height, and B/A is an empirical asymmetry ratio.

The linearity of the method was determined from linear regression analysis based on least-squares estimates. Repeatabilities were estimated from the means and relative standard deviations (R.S.D.)

3. Results and discussion

The separation of anions in the positive micellar system tested is based on simple differences in mass/charge ratio combined with variations in ionic interaction between the analytes and the micelles. This MECC system was found to give a more efficient separation of the inorganic anions from various organic anions and impurities in biological samples [20] than free-zone capillary electrophoresis. It was also found to be preferable to systems based on negative micellar systems such as sodium dodecylsulfate (SDS) and cholate [20]. The MECC system was optimised with respect to buffer composition, temperature and voltage by the procedure described for other anions [20,21]. The migration order obtained for anions in a test mixture using the optimised MECC-DTAB system is illustrated in Fig. 1, showing nitrite as the fastest migrating compound followed by nitrate, iodide and finally the thiocyanate ion. The total time of analysis can be held below 15 min, including wash of the capillary, which makes the developed method suitable for screening of large numbers of samples. Both DTAB and CTAB could be used as surfactants; however, generally DTAB was chosen, as it gave the best results for the degradation products of the indolylglucosinolates [15], and because the thiocyanate ion was better separated from the solvent peak.

The performance of the method varied with
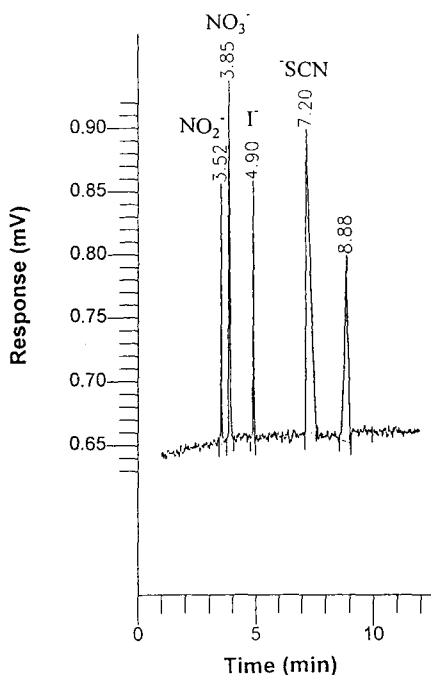
Fig. 1. Migration order of anions in the test mixture analysed in the MECC-DTAB system. Separation conditions were as described in the Experimental section.

the compound of interest, nitrite and iodide having the highest separation efficiency (100 000 and 125 000 N/m, respectively). The thiocyanate ion, giving problems because of its asymmetric peak shape (vide infra), gave a very low N/m. The resolutions for nitrite–nitrate, nitrate–iodide and iodide–thiocyanate ion were found to be 4.3, 12.6 and 9.2, respectively.

3.1. Linearity and detection limits

Linear regression analysis by the least-squares method was performed for the test mixture (100%; $[NO_2^-] = 18.12$ mM, $[NO_3^-] = 139.7$ mM, $[I^-] = 1.19$ mM, $[^-SCN] = 76.54$ mM), using stepwise dilution (down to 0.5%, $n = 18$). The correlation coefficients (r^2) obtained with NA as function of concentration were in general high, being 0.9964 for nitrite, 0.9975 for nitrate and 0.9962 for iodide. The thiocyanate ion showed

an unsatisfactory low correlation coefficient (r^2 = 0.9308) when concentrations higher than 38 mM were used, wich can probably be explained by the asymmetric peak shape for the thiocyanate ion at high concentrations ($>30\%$ = 22.96 mM). Calculation of the correlation coefficient for the dilution series 0.5–30% improved the r^2 value to 0.9748.

The detection limits (signal-to-noise ratio of 2:1) were determined from the results from the linearity study, using the standard conditions of a 1-s sample injection into a 760-mm long capillary with an internal diameter of 50 μm. Under the stated conditions, nitrite, nitrate and iodide could be detected at 0.27, 0.9 and 0.02 mM levels, respectively, whereas the detection limit for the thiocyanate ion was about 0.15 mM (further dilution of the 0.5% test mixture). With an injection volume calculated to be 4.28 nl [22,23], this corresponds to detection limits for nitrite, nitrate and the thiocyanate ion of ca. 1.2, 3.9 and 0.6 pmol, respectively, whereas the detection limit for iodide was about a factor 1000 lower (0.9 fmol). The detection limits in weight amounts were 80 pg, 327 pg, 143 fg and 58 pg for nitrite, nitrate, iodide and the thiocyanate ion, respectively. It was possible to improve the detection limits considerably by use of a high-sensitivity optical cell assembly (Z-cell). The sensitivity, based on NA found for the various anions, was thus increased by a factor of 18, changing the 50-μm capillary to the 75-μm capillary with a Z-cell. Compared to the 50-μm capillary, an ordinary 75-μm capillary improved sensitivity about 2-fold; however, this increase in response is due to an increased injection volume and does not affect the molar concentration detection limit. Theoretically, the increase in path length, obtained using the high-sensitivity optical cell assembly, should change the NA values found by a factor of 40 compared to the NA values found for the 75-μm capillary. This was, however, not the case. The reason for this is explainable from the concave/convex shape of the detection windows and for the Z-cell with a circular part included. However, the changed detection system had no negative effects on the resolution of the ions.

3.2. Repeatability

Repeatability of the MECC method for anions was tested, changing the buffer at the inlet side between each analysis and at the outlet side after five analyses. In general, repeatability of the migration time (absolute as well as relative) was very satisfactory, whereas NA and RNA varied between consecutive analyses, leading to high relative standard deviations (Table 1). This was especially pronounced for the thiocyanate ion, which showed a tendency for asymmetric peaks even for the diluted test mixture (30%; [$^-$SCN] = 22.96 mM) used in the repeatability study. Further optimisation of the MECC method with respect to peak profile for the thiocyanate ion should be performed prior to approaching quantitative analysis of this anion.

3.3. Anions in biological samples

The detection of anions in biological samples is rendered difficult by the high concentrations of interfering compounds present, and some degree of isolation/purification is generally required. We used a fast and simple ion-exchange technique for isolating the anions in blood and milk. A 400-μl volume of a sample (200 μl plasma/milk and 200 μl 100% test mixture) was transferred to a 1-ml pipette tip with 0.5 ml Sephadex A-25 (AcO$^-$), and washed four times with 1 ml water. Here 4 × 4 ml of 2 M NH$_4$OH was used as

Table 1
Repeatability of the MECC method for determination of nitrite, nitrate, iodide and the thiocyante ion

Anion	Relative standard deviation (%)[a]			
	MT	RMT[b]	NA	RNA[b]
Nitrite	0.24	–	2.37	–
Nitrate	0.29	0.14	1.75	3.27
Iodide	0.26	0.07	2.18	2.85
Thiocyanate ion	0.26	0.16	13.50	13.91

[a] n = 9.
[b] Relative to nitrite.
Separation conditions were as described in the Experimental section.
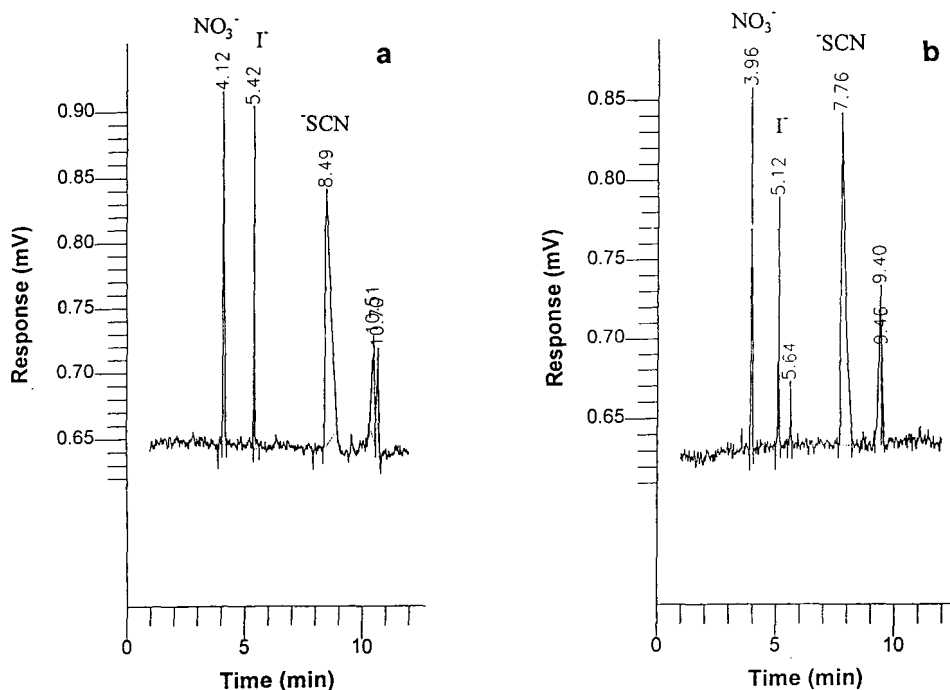
Fig. 2. Examples of detection of anions in (a) blood plasma and (b) milk. The samples were prepared as described in the Results and discussion section. Separation conditions were as described in the Experimental section.

eluent, and the 16 ml obtained was evaporated to dryness, redissolved in 600 μl water, and then analysed by MECC. An example of the determination of anions in blood and milk is given in Fig. 2. As seen, the purification method used was successful, eliminating most of the interfering compounds.

4. Conclusion

MECC based on DTAB has been developed for the determination of nitrite, nitrate, iodide and the thiocyanate ion. The four anions separated well within 10 min, with good repeatability as well as linearity of the method. Analysis of the anions in biological samples such as blood and milk was rendered possible with a very simple ion-exchange procedure, separating the compounds of interest from interfering substances such as proteins, etc. Moreover, the high-sensitivity optical cell assembly increased

the sensitivity of the method considerably, resulting in improved detection of anions at low concentration levels.

Acknowledgements

References

[1] C. Bjergegaard, P.W. Li, S. Michaelsen, P. Møller, J. Otte and H. Sørensen, Bioactive Subst. Food Plant Orig., 1 (1994) 1.
[2] A. Papas, J.R. Ingalls and P. Causfield, Can. J. Anim. Sci., 58 (1978) 671.
[3] A. Papas, J.R. Ingalls and L.D. Campbell, J. Nutr., 109 (1979) 1129.

[4] B. Laarveld, R.P. Brockman and D.A. Christensen, Can. J. Anim. Sci., 61 (1981) 625.

[5] M. Emanuelson, K.-Å. Ahlin and H. Wiktorsson, Livestock Prod., 33 (1993) 199.

[6] B. Laarveld, R.P. Brockman and D.A. Christensen, Can. J. Anim. Sci., 61 (1981) 131.

[7] B. Laarveld, R.P. Brockman and D.A. Christensen, Can. J. Anim. Sci., 61 (1981) 141.

[8] K. Ahlin, M. Emanuelson and H. Wiktorsson, Acta Vet. Scand., 35 (1994) 37.

[9] F. Schöne, G. Jahreis, G. Richter and R. Lange, J. Sci. Food Agric., 61 (1993) 245.

[10] W. Wemheuer, Reprod. Dom. Anim. 28 (1993) 385.

[11] S. Michaelsen, K. Mortensen and H. Sørensen, GCIRC Congress, Saskatoon, Canada, 1991, VI, 1890.

[12] V. Danielsen, B.O. Eggum, S.K. Jensen and H. Sørensen, Anim. Feed Sci. Tech., 46 (1994) 239.

[13] S. Loft, J. Otte, H.E. Poulsen and H. Sørensen, Food Chem. Toxicol., 30 (1992) 927.

[14] H. Sørensen, in F. Shahidi (Editor), Rapeseed/Canola: Production, Chemistry, Nutrition and Processing Technology, Van Nostrand Reinhold, New York, 1990, Ch. 9, p. 149.

[15] C. Feldl, P. Møller, J. Otte and H. Sørensen, Anal. Biochem., 217 (1994) 62.

[16] M.P. Harrold, M.J. Wojtusik, J. Riviello and P. Henson, J. Chromatogr., 640 (1993) 463.

[17] P. Jandik and W.R. Jones, J. Chromatogr., 546 (1991) 431.

[18] W.R. Jones and P. Jandik, J. Chromatogr., 546 (1991) 445.

[19] A.M. Leone, P.L. Francis, P. Rhodes and S. Moncada, Biochem. Biophys. Res. Commun., 200 (1994) 951.

[20] S. Michaelsen and H. Sørensen, Pol. J. Food Nutr. Sci., 3/44 (1994) 5.

[21] S. Michaelsen, P. Møller and H. Sørensen, J. Chromatogr., 608 (1992) 363.

[22] J. Harbaugh, M. Collette and H.E. Schwartz, Beckman Technical Information Bulletin, TIBC-103, Beckman, Palo Alto, CA, 1990.

[23] A. Vinther, Ph.D. Thesis, Novo Nordisk and Technical University of Denmark, Copenhagen, 1991, Ch. 5, p. 5.28.

Method development and validation for the determination of mineral elements in food and botanical materials by capillary electrophoresis

Q. Yang, C. Hartmann, J. Smeyers-Verbeke, D.L. Massart*

Pharmaceutical Institute, Vrije Universiteit Brussel, Laarbeeklaan 103, B-1090 Brussels, Belgium

Abstract

A capillary electrophoresis (CE) procedure was developed and validated for the determination of K^+, Na^+, Ca^{2+}, Mg^{2+} and Mn^{2+} in solid natural products. Closed-vessel microwave acid digestion [HNO_3–H_2O_2 (2:0.5)] was used for the sample preparation. Digests of these samples were diluted with deionized water and the resulting solutions injected for CE. The excess of nitric acid in the samples was found to influence the analytical performance, so its effect was investigated in detail. Direct calibration with aqueous standard solutions was applicable for the analysis of all sample types. To evaluate the bias of the proposed procedure, reference materials were analysed. The results agreed well with the certified or recommended values. The precision of the procedure was evaluated with a two-level nested analysis of variance. This allows one to estimate separately the variance due to three factors (the CE measurement, the sample preparation and time) that are expected to contribute to the variability of the measurement results. For all the elements determined, the CE system repeatability (R.S.D.) was smaller than 4%, method repeatability smaller than 6% and the within-laboratory reproducibility smaller than 9%. The limit of detection (LOD) and limit of quantification (LOQ) in solution are below 600 $\mu g/l$, except for K^+, for which the LOQ is about 2 mg/l.

1. Introduction

Currently, metallic elements in natural products and biological materials are mostly determined using atomic absorption spectrometry (AAS) or inductively coupled plasma combined with atomic emission spectrometry (ICP-AES) or mass spectrometry (ICP-MS), as well as ion chromatography (IC). However, capillary electrophoresis (CE) seems to be an alternative multi-element technique. With this technique, inorganic ions are electrophoretically separated in a capillary and monitored on-column by direct

or indirect UV detection. In case of indirect detection, a UV-absorbing substance is incorporated into the electrolyte buffer, providing a constant background absorbance. The zones of the ions are detected because they lead to a decrease in optical absorbance on passing through the detection window. The electrophoretic separation selectivity can be manipulated by complexation, changes in buffer pH [1], solvation of organic solvents [2,3] and addition of a surfactant to the electrolyte buffer [4]. For the separation of inorganic cations, we established a background electrolyte system composed of imidazole (as the absorbing probe), 2-hydroxy-isobutyric acid (HIBA) and 18-crown-6 (as com-

---

* Corresponding author.

plexing agents) and methanol, and described the mobility of the inorganic cations as a function of the important system parameters using an empirical [2] and a theoretical model [3], respectively. By applying the models, a selectivity optimization was carried out, resulting in a good separation of thirteen inorganic cations including ammonium and alkali, alkaline earth and transition metals. Separation of ions in tea infusion was conducted to examine the practical usefulness of the optimized CE method [2]. The experimental conditions derived earlier were applied here to evaluate the performance of the technique in the analysis of more complex samples.

There is growing interest in applying CE for the determination of metallic elements in real samples. Beck and Engelhardt [5] determined alkali and alkaline earth metals in mineral water and the results agreed with those obtained by using HPLC. A similar CE method [1] was applied to determine the elements in parenteral electrolyte solutions and beverages, and compared with flame atomic spectrometry (FAS). Most of the results obtained from both methods were in good agreement, except for Ca^{2+} in the parenteral solutions, showing slightly lower results than for FAS. This is probably due to the binding of the analyte ions to some sample components, such as proteins and amino acids [1,6]. It was suggested that a sample pretreatment was necessary [1]. Recently, Shi et al. [7] reported the determination of metallic elements in ocular lenses of animals and results comparable to those given by FAS were obtained. Oehrle et al. [8] determined metallic elements in waste water.

Solid materials have to be decomposed before performing CE. Wet acid digestion is commonly used to dissolve products such as foodstuffs and plants. The acid digestion is often carried out in a closed-vessel system and assisted by microwave heating, which ensures rapid sample preparation with minimized contamination and reduced loss of analytes [9,10]. Microwave-assisted digestion has been widely studied in the past and successful procedures are well documented. Recently, applying closed-vessel microwave-assisted diges-

tion, Morawski et al. [11] determined Na^+, K^+, Mg^{2+} and Ca^{2+} in certain food products with CE. Most of the results were comparable to those given by AAS and ion chromatography. The results for K^+ were higher than expected, however. According to the authors, this was due to the co-migration of K^+ and NH_4^+. Kajiwara et al. [12] reported the determination of Ca^{2+} and Mg^{2+} in wheat flour, where EDTA extraction of these divalent elements was performed.

In our previous work on AAS [10], a rapid closed-vessel microwave-assisted acid digestion procedure was developed. A wide range of foodstuffs were decomposed using a digestion mixture of HNO_3 and H_2O_2. The sample preparation procedure was validated for the determination of trace aluminium, lead and cadmium by graphite furnace atomic absorption spectrometry. Here, we applied the same procedure to decompose food and botanical reference materials and various tea samples. The resulting solutions were diluted with Milli-Q-purified water and injected hydrostatically for the determination of K^+, Na^+, Ca^{2+}, Mg^{2+} and Mn^{2+} with CE. It should be noted that the closed-vessel digestion results in an excess of acids in the sample solutions and therefore causes a high ionic strength, which can consequently affect the separation efficiency [13]. The effect of nitric acid was therefore investigated with synthetic solutions to understand better its influence on the analytical performance.

2. Experimental

2.1. Instrumentation

The capillary electrophoresis instrument was a Waters Quanta 4000 capillary electrophoresis system with a 20-sample carousel and a zinc lamp detector (214 nm). Accusep fused-silica capillaries (60 cm × 75 μm I.D.) were used in all analyses. A positive voltage of 20 kV was applied. The detector time constant was 0.3 s. Samples were introduced by hydrostatic injection from a 10-cm height for 20 s. The electrophero-

grams were recorded and treated with a Waters Model 810 data workstation equipped with a W51-Watch-Dog interface. Temperature control was carried out as described previously [1].

The digestions were performed on a programmable Milestone 1200 microwave digestion system with a maximum power supply of 1200 W and equipped with the ACM-100 automatic capping module. Teflon HPV 80 high-pressure vessels (80 ml) with safety shields which could withstand up to 120 bar of pressure and a temperature of 300°C were used.

2.2. Capillary preparation and cleaning

At the beginning of every working week, the capillary was washed successively with 0.1 M KOH, 0.1 M HCl, Milli-Q deionized water and background electrolyte, each for 5 min. Between each injection, the capillary was washed for 1 min with 0.1 M KOH and Milli-Q water and for 3 min with the electrolyte buffer. At the end of the day, the capillary was rinsed with Milli-Q water for 5 min and left filled with water.

2.3. Reagents and standards

Water used for the preparation of all solutions was obtained from a Milli-Q water purification system (Millipore, Bedford, MA, USA) and contained no detectable analyte cations.

Titrisol concentrates of 1000 μg/ml of Na^+, K^+, Mg^{2+}, Ca^{2+} and Mn^{2+} (Merck, Darmstadt, Germany) were used in this experiment. Standard solutions containing different concentrations of the above elements were prepared by mixing the appropriate amounts of the above concentrates.

Imidazole (99%, w/w) was of analytical-reagent grade (Merck). Methanol was of chromatographic grade (Merck). 2-Hydroxy-isobutyric acid and 18-crown-6 were 99% pure reagents (Aldrich-Chemie, Steinheim, Germany). HNO_3 (65%, w/w) of high purity (Suprapur; Merck) was used for sample preparation. Hydrogen peroxide (30%, w/w) was of analytical-reagent grade (Merck). HCl (1 M) used for the buffer pH adjustment was obtained from

Merck. 2-(Diethylamino)ethanol (99%, w/w) (zur Synthese; Merck) was used to neutralize samples.

2.4. Preparation of background electrolyte

First three stock solutions containing 500.0 mM imidazole, 130.6 mM HIBA and 50.0 mM 18-crown-6 were prepared. A CE background electrolyte buffer was then prepared by pipetting 5, 25 and 5.5 ml, respectively, of the above stock solutions and 100 ml methanol into a 500-ml plastic volumetric flask and diluting to volume with Milli-Q water. The pH of the buffer was adjusted to 4.5 ± 0.4 with 1 M HCl. The electrolyte solution was stored in a refrigerator. Just before use it was filtered through a 0.45-μm syringe filter (Millipore, Molsheim, France).

2.5. Standard reference materials, tea samples and their decomposition

NIST standard reference materials Bovine Liver (SRM 1577), Total Diet (SRM 1548), Oyster Tissue (SRM 1566a), Pine Needles (SRM 1575) and Citrus Leaves (SRM 1572) and IAEA reference material Fish Tissue (MA-B-3/TM) were used for the evaluation of the bias. From each type of reference sample, three portions of ca. 0.4 g were weighed. To each of the portions, 2 ml of HNO_3, 0.5 ml of H_2O_2 and 1 ml of Milli-Q water were added. Four samples were digested simultaneously using 180, 360 and 600 W power, each for 3 min, followed by 0 W for 3 min. The first three steps were then repeated. Finally, the system was operated for another 2 min at 0 W to remove possible acid vapour in the compartment of the oven. All of the digests were first diluted to 10 ml with Milli-Q water. The resulting solutions therefore contained at most 20% (v/v) nitric acid, which corresponds to 0.44 M (the consumption of nitric acid during digestion is not taken into account). The solutions were further diluted 25-, 50-, 125- or 250-fold to ensure that the element concentrations in the individual samples fell within the calibration range (0.5–10 μg/ml). Quantitative analysis was

performed with digests that had been diluted at least 50-fold.

Tea samples were bought at tea shops in China and Belgium. Two samples of ca. 0.4 g were digested and diluted. The digestion and dilution were described above.

Corresponding digestion blanks were also prepared according to the above procedure. The details about the contamination control and labware cleaning for the sample preparation can be found in Ref. [10].

3. Results and discussion

3.1. Use of the time-corrected peak area for calculation

Absolute peak areas for the standard solutions were observed to increase with time during the experiments. It is known that the peak area is inversely related to the migration velocity of the ions [1]. The slower an analyte zone moves, the larger is the absolute peak area. The velocity of the ion is influenced by many parameters, such as the temperature inside the capillary and capillary surface properties. The capillary surface influences the migration velocity, probably mainly through the change in electroosmotic flow (EOF). The EOF (V_{eof}) change causes variations in the effective migration velocity (V_{eff}) since $V_{eff} = V_{eof} + V_{ep} = (\mu_{eof} + \mu_{ep})E$, where μ_{eof} and μ_{ep} represent the electroosmotic mobility and electrophoretic mobility, respectively; E is the electrical field applied across the capillary. The ratio of the absolute peak area to migration time corrects for the change in migration caused by the variation in effective mobility of the analyte cations [14]. Therefore, the corrected area ($A_{corr.}$) was used in all calculations and computed as follows:

$$A_{corr.} = A / T_m$$

where A is the absolute peak area of an analyte cation zone and T_m is the migration time of the analyte cation.

3.2. Effect of nitric acid in samples on analytical performance

CE separation was found to be impossible if the sample solutions containing 20% (v/v) nitric acid (see Section 2.5) were injected directly. This is due to too high an ionic strength of the sample solutions, which lowers the separation efficiency [1,13]. The high ionic strength is caused by the excess of acid present after the sample digestion. In addition, the analytical performance can also be influenced by the high pH of these samples. Because of this, we first tried to neutralize the samples by titration with an organic base (2-diethylaminoethanol). However, this did not improve the results. Further, we investigated the effect of nitric acid using synthetic solutions containing 5 mg/l each of K^+, Na^+, Ca^{2+}, Mg^{2-} and Mn^{2+} and 4, 8, 16 or 40 mM nitric acid. This corresponds to diluting a 20% (v/v) solution of nitric acid 100-, 50-, 25- and 10-fold, respectively. For comparison, a solution containing 5 mg/l of each of the five cations but without nitric acid was also run. It was found that the nitric acid decreased the peak heights, except for K^+, for which the peak height was observed to increase. This is due to the fact that nitric acid significantly decreases the mobilities of K^+ (see Fig. 1A) and consequently the mobility of K^+ is closer to that of the imidazole co-ion. As a result, the electromigration dispersion is reduced and the plate height increased. It is also seen from Fig. 1A that μ_{eof} decreases as the nitric acid concentration increases. At 16 mM nitric acid the electroosmosis flow marker (water peak) was no longer observed. This suggests that nitric acid affects the capillary surface.

As can be seen in Fig. 2, the separation of the five cations becomes worse with increasing nitric acid concentration, and finally is lost when the nitric acid concentration reaches 40 mM. However it follows from Fig. 1B that in the range 0–8 mM nitric acid the time-corrected peak areas are constant for Na^+, Ca^{2+} and Mg^{2+} while they show a slight decrease for K^+ and Mn^{2+}. They change in the presence of higher concentrations of nitric acid owing to insufficient separation causing inaccurate integration of peak areas.
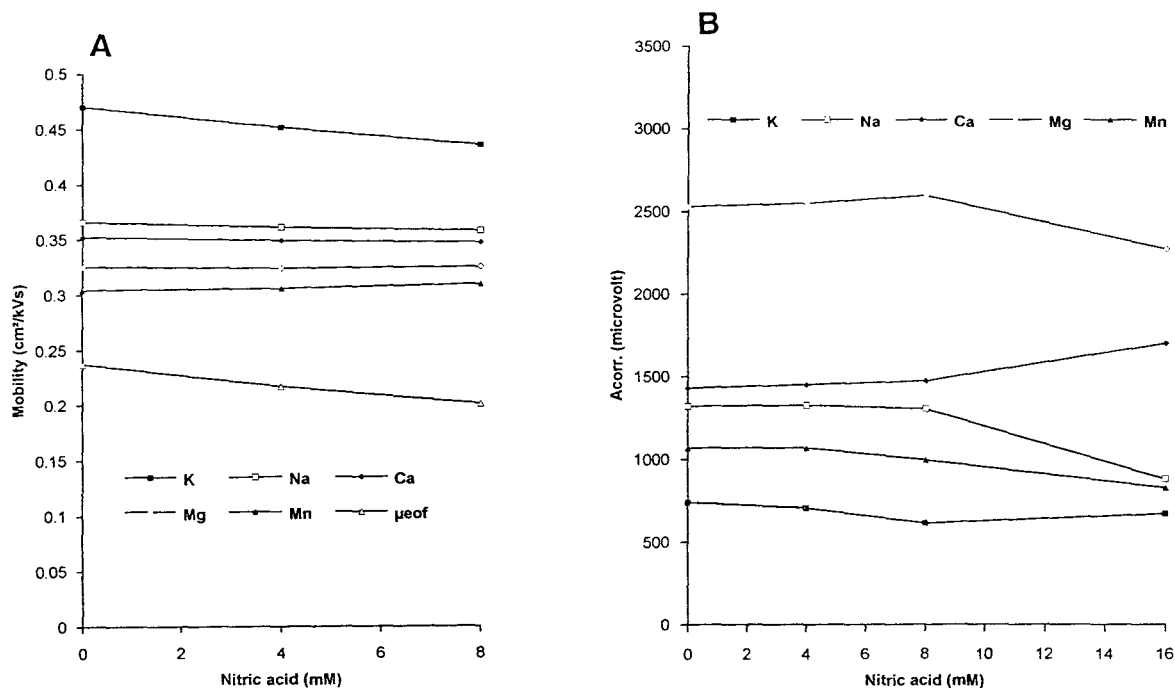
Fig. 1. (A) Change in mobilities of K^+, Na^+, Ca^{2+}, Mg^{2+} and Mn^{2+} with increasing nitric acid concentration in samples. (B) Change in time-corrected peak areas with increasing nitric acid concentration in the measurement solution.

Therefore, direct determination using the corrected peak area as the response parameter appears to be possible in the presence of up to about 8 mM nitric acid in the samples.

The effect of sulphuric acid in the sample on the separation of some alkali and alkaline earth metal ions in CE was investigated by Riviello and Harrold [15]. Small amounts of sulphuric acid decreased the migration time for all analytes. As the acid concentration approached 25 mM, the migration times of these ions began to plateau, except for K^+ and NH_4^+, for which the migration times increased significantly. The authors concluded that as high as 25 mM sulphuric acid in the sample did not significantly degrade the separation.

3.3. Method validation

Test for linearity of the calibration line

Six independent series of standard solutions containing 0.5, 1, 2, 4, 6, 8 and 10 μg/ml of

Na^+, K^+, Mg^{2+}, Ca^{2+} and Mn^{2+} were prepared. One injection was performed for each standard solution. The calibration lines were calculated using the time-corrected peak areas. It was found for Na^+, Ca^{2+}, Mg^{2+} and Mn^{2+} that the variances of the peak response increased with increase in the concentration of the analytes, in other words, the measurements are heteroscedastic. Therefore, weighted regression was applied for these cations [16]. The weights used are the reciprocal of the variances at each concentration level. Analysis of variance (ANOVA) for lack-of-fit to the ordinary or weighted regression lines [16,17] was performed to check the linearity of the calibration lines. In no case was lack of fit observed, which means that a straight-line model is adequate. The calibration lines are linear up to 10 mg/l.

Detection of matrix effects

The method of standard additions was used to detect matrix effects. It was performed on the
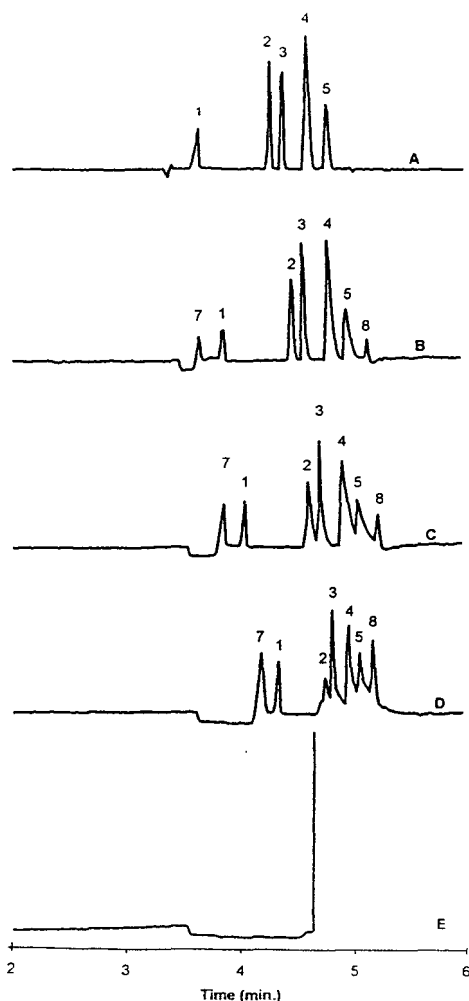
Fig. 2. Effect of nitric acid in the measurement solutions on the separation of K$^+$, Na$^+$, Ca^{2+}, Mg^{2+} and Mn^{2+} (5 mg/l): (A) 0, (B) 4, (C) 8, (D) 16 and (E) 40 mM nitric acid. Peaks: 1 = K$^+$; 2 = Na$^+$; 3 = Ca^{2+}; 4 = Mg^{2+}; 5 = Mn^{2+}; 7 = H$^+$ and NH$_4^+$; 8 = unidentified.

total diet, bovine liver reference material and two tea samples. The standard addition lines were obtained from 50-fold dilution of their digests (see Section 2.5). Fig. 3 shows some electropherograms of the digested samples. Matrix effects were evaluated by comparing the slopes of the standard addition line and an aqueous calibration line. Their ratios range from 0.96 to 1.06 for K$^+$, Na$^+$, Ca^{2+}, Mg^{2+} and Mn^{2+}, indicating the absence of important ma-

trix effects that result in a relative systematic error. Moreover, a comparison of the slopes of the standard addition line and the calibration line for K$^+$ by means of a t-test [18] showed the difference not to be statistically significant (α = 5%). Consequently, direct calibration with aqueous solutions can be used for the sample analysis.

Limit of detection (LOD) and limit of quantification (LOQ)

The LOD was evaluated from eight independent digestion blanks, which were spiked to produce a peak height, for each of the analyte cations, close to three times the baseline noise. It was estimated by taking three times the standard deviation of the peak areas obtained from these solutions and calculating the corresponding concentrations from the calibration lines. The LODs are 400 μg/l for K$^+$, 130 μg/l for Na$^+$, 170 μg/l for Ca^{2+}, 50 μg/l for Mg^{2+} and 220 μg/l for Mn^{2+}. By taking into account the dilution used (500 ml) and the dry sample mass (0.4 g), the LODs in the samples were obtained. They are 500 μg/g for K$^+$, 170 μg/g for Na$^+$, 220 μg/g for Ca^{2+}, 70 μg/g for Mg^{2+} and 280 μg/g for Mn^{2+}.

The LOQ is defined as the level at or above which the measurement precision is satisfactory for quantitative analysis. It was estimated by taking ten times [19] the standard deviation of the peak areas obtained form the eight blanks and subsequently calculating the corresponding concentrations from the calibration lines. The LOQs in solution are 2 mg/l for K$^+$, 410 μg/l for Na$^+$ and 580 μg/l for Ca^{2+}, 270 μg/l for Mg^{2+} and 560 μg/l for Mn^{2+}. These correspond to the following LOQs in the dry products: 2.5 mg/g for K$^+$, 520 μg/g for Na$^+$, 730 μg/g for Ca^{2+}, 340 μg/g for Mg^{2+} and 700 μg/g for Mn^{2+}.

Analysis of reference materials

Fig. 3 shows as an example the electropherograms of a total diet and an oyster tissue digest. Baseline separation of Na$^+$, Ca^{2+}, Mg^{2+}, Mn^{2+} and Zn^{2+} is achieved, regardless of the difference in relative concentration of the metals in

the individual sample types. The peak that always appears before the K^+ peak is due to H^+, and to NH_4^+ when this ion is present in the sample or generated during the digestion. The unidentified peak coming later (peak No. 8) may be an artefact caused by the presence of nitric acid in the samples. As can be seen from Fig. 2, this peak becomes larger as the concentration of nitric acid increases.

The concentration of K^+, Na^+, Ca^{2+} and Mn^{2+} in the reference samples are given in Table 1. They were obtained from three independent digests, for each of which duplicate injections were performed. The standard deviation was estimated from the range of the three digestion means [20]. The results obtained with CE agree well with the certified values. It is concluded that the proposed method is sufficiently accurate. The relative standard deviation obtained for all the samples is less than 10%. It should be mentioned that although Na^+ was found in citrus leaves and pine needles digests, the concentrations of Na^+ in these samples was not determined because the concentration in the measurement solution is below the LOQ (520 $\mu g/g$ for the dilution up to 500 ml and 260 $\mu g/g$ for the dilution up to 250 ml). Of the reference materials analysed, only citrus leaves digest contains detectable Mn^{2+}.

Precision

The proposed procedure contains two main steps, the sample preparation and the CE measurement. The latter determines the system repeatability while both the sample preparation and the CE measurement contribute to the repeatability of the whole analytical procedure. For an estimation of the within-laboratory reproducibility, the between-day variation has also to be taken into account, which means that measurements on different days have to be performed. A two-level nested analysis of variance [21,22] was carried out to separately estimate the variance due to the CE measurement (s_{CE}^2), the sample preparation (s_{sample}^2) and time (s_{time}^2). The first variance component corresponds to the system repeatability variance. The sum of the first two variance components corresponds to the repeatability variance of the whole analytical procedure and the sum of all three variance components corresponds to the within-laboratory reproducibility variance. Commercial software, Statgraphics Plus [23], was used for performing the nested analysis of variance.

The precision was determined for the oyster tissue reference material and for a tea sample. The experiments were performed according to a fully nested design. Each day, during 7 days, two

Table 1
Comparison of CE results[a] and certified or recommended values

Reference material	Value	K (%)	Na (%)	Ca (%)	Mg (%)	Mn ($\mu g/g$)
Total diet	CE	0.596 ± 0.046	0.592 ± 0.005	0.174 ± 0.006	0.0555 ± 0.0041	
(NIST SRM 1548)	Certified value	0.606 ± 0.028	0.625 ± 0.026	0.174 ± 0.007	0.0556 ± 0.0027	5.2 ± 0.4
Oyster tissue	CE	0.762 ± 0.016	0.398 ± 0.015	0.188 ± 0.006	0.109 ± 0.005	
(NIST SRM 1566a)	Certified value	0.790 ± 0.047	0.417 ± 0.013	0.196 ± 0.019	0.118 ± 0.017	12.3 ± 1.5
Fish tissue	CE	8.795 ± 0.346	1.905 ± 0.379	3.455 ± 0.070	1.227 ± 0.114	
(IAEA MA-B-3/TM)	Recommended value	9.00–10.0	2.00–2.31	3.18–3.60	1.04–1.20	2.22–3.03
Bovine liver	CE	1.096 ± 0.073	0.226 ± 0.006	0.0131 ± 0.0004	0.0589 ± 0.0036	
(NIST SRM 1577)	Certified value	0.97 ± 0.06	0.243 ± 0.013	0.0124 ± 0.0006	0.0604 ± 0.0009	10.3 ± 1.0
Pine needles	CE	0.346 ± 0.017		0.391 ± 0.012	0.108 ± 0.002	
(NIST SRM 1575)	Certified value	0.37 ± 0.02		0.41 ± 0.02		705.2 ± 24.7
Citrus leaves	CE	1.762 ± 0.026		3.123 ± 0.021	0.561 ± 0.005	675 ± 15
(NIST SRM 1572)	Certified value	1.82 ± 0.06	0.0160 ± 0.0020	3.15 ± 0.10	0.58 ± 0.03	23 ± 2

Experimental conditions: hydrostatic injection from 10 cm for 20 s; applied voltage, +20 kV; $I = \pm 5.4$ μA; background electrolyte, 5 mM imidazole–6.5 mM HIBA–0.55 mM 18-crown-6–20% (v/v) methanol (pH 4.5).
[a] The CE results were obtained from the analysis of three independent digests within one day. Each digest was injected twice. The S.D. was estimated as the range of the three digestion means divided by 1.91 [20].

independent samples were digested and for each digest duplicate injections were performed. The concentration of K^+, Na^+, Ca^{2+}, Mg^{2+} and Mn^{2+} were calculated from the calibration lines measured on the same day. Table 2 shows the design and the results. The relative system repeatability standard deviations due only to the CE measurement are <3% for the oyster tissue

and <4% for the tea sample. The relative method repeatability standard deviations are <6% for the oyster tissue and <4% for the tea. The relative within-laboratory reproducibility standard deviations are <9% for the oyster tissue and <5% for the tea. Therefore, it is concluded that the precision of the proposed procedure is acceptable.

Table 2
Precision obtained by a two-level nested analysis of variance

Nested design[a]			CE results (%, w/w)							
			Oyster tissue				Tea			
Day	Sample	Injection	K	Na	Ca	Mg	K	Ca	Mg	Mn
1	1	1	0.813	0.391	0.185	0.132	1.816	0.479	0.212	0.105
1	1	2	0.755	0.390	0.187	0.136	1.754	0.448	0.221	0.108
1	2	1	0.794	0.396	0.192	0.131	1.824	0.437	0.206	0.103
1	2	2	0.818	0.401	0.196	0.128	1.865	0.418	0.211	0.103
2	1	1	0.781	0.395	0.187	0.129	1.615	0.462	0.225	0.114
2	1	2	0.822	0.401	0.184	0.124	1.618	0.465	0.221	0.118
2	2	1	0.777	0.422	0.185	0.125	1.597	0.458	0.233	0.107
2	2	2	0.761	0.428	0.190	0.130	1.591	0.449	0.238	0.107
3	1	1	0.813	0.411	0.177	0.115	1.785	0.429	0.209	0.106
3	1	2	0.807	0.413	0.176	0.117	1.809	0.427	0.209	0.113
3	2	1	0.834	0.439	0.188	0.112	1.727	0.435	0.199	0.107
3	2	2	0.824	0.436	0.181	0.114	1.731	0.435	0.202	0.114
4	1	1	0.746	0.397	0.164	0.115	1.755	0.451	0.206	0.104
4	1	2	0.770	0.402	0.160	0.114	1.723	0.448	0.205	0.113
4	2	1	0.806	0.423	0.173	0.117	1.719	0.439	0.206	0.110
4	2	2	0.767	0.429	0.167	0.113	1.761	0.435	0.199	0.106
5	1	1	0.814	0.406	0.219	0.127	1.607	0.432	0.214	0.108
5	1	2	0.804	0.418	0.222	0.131	1.614	0.429	0.211	0.112
5	2	1	0.794	0.396	0.194	0.127	1.674	0.464	0.222	0.107
5	2	2	0.764	0.397	0.194	0.127	1.674	0.465	0.215	0.112
6	1	1	0.751	0.394	0.197	0.125	1.650	0.457	0.222	0.109
6	1	2	0.736	0.389	0.198	0.127	1.669	0.459	0.220	0.113
6	2	1	0.741	0.402	0.217	0.146	1.632	0.468	0.216	0.111
6	2	2	0.772	0.399	0.218	0.146	1.629	0.474	0.215	0.117
7	1	1	0.769	0.377	0.187	0.119	1.656	0.457	0.212	0.108
7	1	2	0.738	0.373	0.189	0.117	1.681	0.462	0.219	0.108
7	2	1	0.809	0.388	0.209	0.121	1.797	0.464	0.219	0.109
7	2	2	0.777	0.385	0.205	0.121	1.704	0.464	0.219	0.105
Mean			0.808	0.403	0.191	0.124	1.704	0.451	0.215	0.109
s_{CE}^2			$4.4 \cdot 10^{-4}$	$1.4 \cdot 10^{-5}$	$6.7 \cdot 10^{-6}$	$4.1 \cdot 10^{-6}$	$1.0 \cdot 10^{-3}$	$5.3 \cdot 10^{-5}$	$1.1 \cdot 10^{-5}$	$1.2 \cdot 10^{-5}$
s_{sample}^2			$1.7 \cdot 10^{-4}$	$1.8 \cdot 10^{-4}$	$1.2 \cdot 10^{-4}$	$2.9 \cdot 10^{-5}$	$1.0 \cdot 10^{-3}$	$1.8 \cdot 10^{-4}$	$2.3 \cdot 10^{-5}$	$1.5 \cdot 10^{-6}$
s_{time}^2			$2.9 \cdot 10^{-4}$	$1.2 \cdot 10^{-4}$	$1.6 \cdot 10^{-4}$	$5.7 \cdot 10^{-5}$	$5.0 \cdot 10^{-5}$	$3.6 \cdot 10^{-5}$	$6.0 \cdot 10^{-5}$	$3.4 \cdot 10^{-6}$
System repeatability, R.S.D. (%)			2.6	0.9	1.3	1.6	1.9	1.6	1.5	3.1
Method repeatability, R.S.D. (%)			3.1	3.4	5.9	4.6	2.6	3.4	2.7	3.3
Within-lab. reproducibility, R.S.D. (%)			3.7	4.4	8.9	7.6	4.9	3.6	4.5	3.7

[a] s_{CE}^2 = variance due to CE system; s_{sample}^2 = variance due to sample preparation; s_{time}^2 = variance due to time.

3.4. Stability of the capillary

The capillary could be used for at least 400 injections without a significant change in performance.

3.5. Tea analysis

Fig. 3 shows an electropherogram of the 50-fold dilution of a tea digest. Baseline separation was achieved for K^+, Na^+, Ca^{2+}, Mg^{2+} and

Fig. 3. Electropherograms of reference material and tea digests (50-fold dilution). Peaks: 1 = K^+; 2 = Na^+; 3 = Ca^{2+}; 4 = Mg^{2+}; 5 = Mn^{2+}; 6 = Zn^{2+}; 7 = H^+ and NH_4^+; 8 = unidentified. Experimental conditions: hydrostatic injection from 10 cm for 20 s, applied voltage, +20 kV; $I = \pm5.4$ μA; background electrolyte, 5 mM imidazole–6.5 mM HIBA–0.55 mM 18-crown-6–20% methanol (pH 4.5).

Mn^{2+}. Mn^{2+} was determined because tea is rich in this element [24,25]. The concentrations of the metals in teas with different geological origins (China, Sri Lanka, India and Japan) were determined by direct calibration with standard solutions and the results are given in Table 3. For each of the tea samples, the concentration was obtained by analysing two digestions, for each of which duplicate injections were performed. As can be seen from the results in Table 3 and Fig. 3, tea contains relatively large concentrations of micronutrients such as K^+, Mg^{2+}, Ca^{2+} and Mn^{2+} and a relatively small amount of Na^+. Tea is known to be a suitable beverage for people requiring a low-sodium diet [24].

4. Conclusions

The proposed method allows the rapid determination of some inorganic cations in natural products. Accurate results can be obtained by direct calibration with standard solutions. No further sample treatment is needed for the analysis of a variety of natural products. The time-corrected peak area is a suitable response parameter owing to its stability.

The high ionic strength of the sample, caused by the excess of acid in the samples, remains a limitation. Dilution is a solution to this problem, but it decreases the detectability. Analysis of low-concentration samples is therefore impossible with the present technique. The use of less nitric acid and more H_2O_2 in the digestion has been investigated, and showed some promise. However, the ratio of the amount of HNO_3 to the amount of H_2O_2 is limited because of safety considerations, especially in closed-vessel digestions. Membrane-based solid-phase extraction (SPE) [26–28] to eliminate the excess of NO_3^- from the measurement solution might be an alternative solution. It was recently demonstrated to be useful as a sample clean-up technique prior to CE of various anions [27]. It has also been shown to be an effective preconcentration technique for the determination of organic ions by capillary electrophoresis [28].

Table 3
Concentrations of K, Ca, Mg and Mn in teas of different geological origins obtained with CE

Tea	Origin	CE results (%, w/w)[a]			
		K	Ca	Mg	Mn (μg/g)
1	China	2.17 ± 0.03 (1.4)	0.339 ± 0.008 (2.4)	0.197 ± 0.004 (2.0)	741 ± 43.5 (5.9)
2	China	1.99 ± 0.10 (5.0)	0.468 ± 0.001 (0.2)	0.217 ± 0.008 (3.7)	1178 ± 21.5 (1.8)
3	Sri Lanka	2.36 ± 0.15 (6.4)	0.457 ± 0.009 (1.9)	0.191 ± 0.004 (2.1)	362 ± 9.9 (2.7)
4	Sri Lanka	2.17 ± 0.19 (8.8)	0.505 ± 0.002 (0.4)	0.193 ± 0.007 (3.7)	319 ± 24.3 (7.6)
5	India	1.62 ± 0.03 (1.9)	0.486 ± 0.006 (1.2)	0.160 ± 0.001 (0.9)	423 ± 53.5 (12.7)
6	India	2.16 ± 0.08 (3.7)	0.361 ± 0.000 (0.0)	0.206 ± 0.003 (1.4)	591 ± 4.6 (0.8)
7	Japan	1.89 ± 0.01 (0.5)	0.669 ± 0.028 (4.1)	0.238 ± 0.008 (3.2)	869 ± 18.3 (2.1)

[a] Mean ± S.D., with R.S.D. (%) in parentheses. The results were obtained from the analysis of two independent digests measured in duplicate injections within one day. The S.D. is equal to the range of the two digestion means divided by 1.42 [20]. Experimental conditions as in Table 1.

Acknowledgements

References

[1] Q. Yang, M. Jimidar, T. Hamoir, J. Smeyers-Verbeke and D.L. Massart, J. Chromatogr. A, 673 (1994) 275.

[2] Q. Yang, J. Smeyers-Verbeke, W. Wu, M.S. Khots and D.L. Massart, J. Chromatogr. A, 688 (1994) 339.

[3] Q. Yang, Y. Zhuang, J. Smeyers-Verbeke and D.L. Massart, J. Chromatogr. A, 706 (1995) 503.

[4] K. Saitoh, C. Kiyohara and N. Suzuki, J. High. Resolut. Chromatogr., 14 (1991) 245.

[5] W. Beck and H. Engelhardt, Chromatographia, 33 (1992) 313.

[6] D.F. Swaile and M.J. Sepaniak, Anal. Chem., 63 (1991) 179.

[7] H. Shi, R. Zhang, G. Chandrasekher and Y. Ma, J. Chromatogr. A, 680 (1994) 653.

[8] S.A. Oehrle, R.D. Blanchard, C.L. Stumpf and D.L. Wulfeck, J. Chromatogr. A, 680 (1994) 645.

[9] H.M. Kingston and L.B. Jassie (Editors), Introduction to Microwave Sample Preparation, Theory and Practice, American Chemical Society, Washington, DC, 1988, Ch. 1–3.

[10] Q. Yang, W. Penninckx and J. Smeyers-Verbeke, J. Agric. Food Chem., 42 (1994) 1948.

[11] J. Morawski, P. Alden and A. Sims, J. Chromatogr., 640 (1993) 359.

[12] H. Kajiwara, A. Sato and S. Kaneko, Biosci. Biotechnol. Biochem., 57 (1993) 1010.

[13] H.J. Issaq, I.J. Aamna, G.M. Muschik and G.M. Janini, Chromatographia, 32 (1991) 115.

[14] M. Korman, J. Vindevogel and P. Sandra, in P. Sandra and G. Devos (Editors), Proceedings of the 5th International Symposium on Capillary Chromatography, Riva del Garda, Italy, May 24–37, 1993, Vol. 2, p. 1526.

[15] J.M. Riviello and M.P. Harrold, J. Chromatogr. A, 652 (1993) 385.

[16] D.L. Massart, B.G.M. Vandeginste, S.N. Deming, Y. Michotte and L. Kaufman, Chemometrics: A Textbook (Data Handling in Science and Technology, Vol. 2), Elsevier, Amsterdam, 1988, Ch. 5, p. 84.

[17] B.G. Cooper, Statistics for Experimentalists, Pergamon Press, Oxford, 1969, p. 225.

[18] D.L. Massart, J. Smeyers-Verbeke and F.X. Rius, Trends Anal. Chem., 8 (1989) 49.

[19] G.L. Long and J.D. Winefordner, Anal. Chem., 55 (1983) 712.

[20] C. Lang-Michaut, Pratique des Tests Statistiques, Dunod, Paris, 1990, Ch. 3, p. 29.

[21] R.R. Sokal and F. James Rohlf, Biometry, Freeman, San Francisco, 1981, Ch. 10, p. 271.
[22] G. Wernimont, Anal. Chem., 23 (1951) 1572.
[23] Stratgraphics Plus, Version 6, Manugistics, Rockville, MD.
[24] B.A. Fox and A.G. Cameron, Food Science—A Chemical Approach, University of London Press, London, 1972, p. 231.
[25] J. Chu, Environ. Chem., 8 (1989) 80.
[26] Z. Zhang, M.J. Yang and J. Oawliszyn, Anal. Chem., 66 (1994) 845R.
[27] R. Saari-Nordhaus and J.M. Anderson, Jr., J. Chromatogr. A, 706 (1995) 563.
[28] M.W.F. Nielen, Trends Anal. Chem., 12 (1993) 345.

Author Index Vols. 716 and 717

Chromatography in the Petroleum Industry

Edited by E.R. Adlard

Journal of Chromatography Library, Volume 56

Petroleum mixtures consist primarily of relatively unreactive complex hydrocarbons covering a wide boiling range. Such mixtures are difficult to separate by most analytical techniques. Therefore, the petroleum industry has for many years played a leading role in the development of chromatographic methods of analysis. Since the last book specifically concerned with chromatographic analysis of petroleum appeared 15 years ago, numerous advances have been made including developments in liquid and supercritical fluid chromatography, the advent of silica capillary columns with bonded stationary phases and the commercial availability of new selective detectors.

The current book contains chapters written by experts concerning the analysis of mixtures ranging from low boiling gases to waxes and crude oils.

Although the volume is specifically aimed at the petroleum analyst, there is much information of general interest which should be of benefit to a very wide readership.

Contents:

©1995 452 pages Hardbound
Price: Dfl. 435.00 (US$ 255.75)
ISBN 0-444-89776-3

ORDER INFORMATION

ELSEVIER SCIENCE
Customer Service Department
P.O. Box 211
1000 AE Amsterdam
The Netherlands
Fax: +31 (20) 485 3432

For USA and Canada:
ELSEVIER SCIENCE
Customer Service Department
P.O. Box 945, New York
NY 10159-0945
Fax: +1 (212) 633 3764

US$ prices are valid only for the USA & Canada and are subject to exchange rate fluctuations; in all other countries the Dutch guilder price (Dfl.) is definitive. Customers in the European Union should add the appropriate VAT rate applicable in their country to the price(s). Books are sent postfree if prepaid.

ELSEVIER
An imprint of Elsevier Science

THE DATA ANALYSIS HANDBOOK

By I.E. Frank and R. Todeschini

Data Handling in Science and Technology Volume 14

Analyzing observed or measured data is an important step in applied sciences. The recent increase in computer capacity has resulted in a revolution both in data collection and data analysis. An increasing number of scientists, researchers and students are venturing into statistical data analysis; hence the need for more guidance in this field, which was previously dominated mainly by statisticians.

This handbook fills the gap in the range of textbooks on data analysis. Written in a dictionary format, it will serve as a comprehensive reference book in a rapidly growing field. However, this book is more structured than an ordinary dictionary, where each entry is a separate, self-contained entity. The authors provide not only definitions and short descriptions, but also offer an overview of the different topics. Therefore, the handbook can also be used as a companion to textbooks for undergraduate or graduate courses.

Approximately 1700 entries are given in alphabetical order grouped into 20 topics and each topic is organized in a hierarchical fashion. Additional specific entries on a topic can be easily found by following the cross-references in a top-down manner. Several figures and tables are provided to enhance the comprehension of the topics and a list of acronyms helps to locate the full terminologies. The bibliography offers suggestions for further reading.

©1994 386 pages Hardbound
Price: Dfl. 325.00
US$ 185.50
ISBN 0-444-81659-3

ELSEVIER
An imprint of Elsevier Science

INFORMATION FOR AUTHORS

(Detailed *Instructions to Authors* were published in *J. Chromatogr. A*, Vol. 657, pp. 463–469. A free reprint can be obtained by application to the publisher, Elsevier Science B.V., P.O. Box 330, 1000 AH Amsterdam, Netherlands.)

Types of Contributions. The following types of papers are published: Regular research papers (full-length papers), Review articles, Short Communications, Discussions and Letters to the Editor. Short Communications are usually descriptions of short investigations, or they can report minor technical improvements of previously published procedures; they reflect the same quality of research as full-length papers, but should preferably not exceed five printed pages. Discussions (one or two pages) should explain, amplify, correct or otherwise comment substantively upon an article recently published in the journal. Letters to the Editor (max. two printed pages) bring up ideas, comments, opinions, experiences, advice, disagreements, insights, etc. For Review articles, see inside front cover under Submission of Papers.

Submission. Every paper must be accompanied by a letter from the senior author, stating that he/she is submitting the paper for publication in the *Journal of Chromatography A*.

Manuscripts. Manuscripts should be typed in **double spacing** on consecutively numbered pages of uniform size. The manuscript should be preceded by a sheet of manuscript paper carrying the title of the paper and the name and full postal address of the person to whom the proofs are to be sent. As a rule, papers should be divided into sections, headed by a caption (*e.g.*, Abstract, Introduction, Experimental, Results, Discussion, etc.). All illustrations, photographs, tables, etc., should be on separate sheets. Manuscripts should be accompanied by a 5.25- or 3.5-in. disk. Your disk and **(exactly matching)** printed version (printout, hardcopy) should be submitted together to the accepting editor or Editorial Office **according to their request**. Please specify the type of computer and word-processing package used (do not convert your textfile to plain ASCII). Ensure that the letter "l" and digit "1" (also letter "O" and digit "0") have been used properly, and format your article (tabs, indents, etc.) consistently. Characters not available on your word processor (Greek letters, mathematical symbols, etc.) should not be left open but indicated by a unique code (*e.g.* gralpha, @,#, etc., for the Greek letter α). Such codes should be used consistently throughout the entire text. Please make a list of such codes and provide a key. Do not allow your word processor to introduce word splits and do not use a "justified" layout. Please adhere strictly to the general instructions on style/ arrangement and, in particular, the reference style of the journal. Further information may be obtained from the Publisher.

Abstract. All articles should have an abstract of 50–100 words which clearly and briefly indicates what is new, different and significant. No references should be given.

Introduction. Every paper must have a concise introduction mentioning what has been done before on the topic described, and stating clearly what is new in the paper now submitted.

> **Experimental conditions** should preferably be given on a *separate* sheet, headed "Conditions". These conditions will, if appropriate, be printed in a block, directly following the heading "Experimental".

Illustrations. The figures should be submitted in a form suitable for reproduction, drawn in Indian ink on drawing or tracing paper. Each illustration should have a caption, all the *captions* being typed (with double spacing) together on a *separate sheet.* If structures are given in the text, the original drawings should be provided. Coloured illustrations are reproduced at the author's expense. The written permission of the author and publisher must be obtained for the use of any figure already published. Its source must be indicated in the legend.

References. References should be numbered in the order in which they are cited in the text, and listed in numerical sequence on a separate sheet at the end of the article. Please check a recent issue for the layout of the reference list. Abbreviations for the titles of journals should follow the system used by *Chemical Abstracts.* Articles not yet published should be given as "in press" (journal should be specified), "submitted for publication" (journal should be specified), "in preparation" or "personal communication".

> Vols. 1–651 of the *Journal of Chromatography*; *Journal of Chromatography, Biomedical Applications* and *Journal of Chromatography, Symposium Volumes* should be cited as *J. Chromatogr.* From Vol. 652 on, *Journal of Chromatography A* should be cited as *J. Chromatogr. A* and *Journal of Chromatography B: Biomedical Applications* as *J. Chromatogr. B.*

Dispatch. Before sending the manuscript to the Editor please check that the envelope contains four copies of the paper complete with references, captions and figures. One of the sets of figures must be the originals suitable for direct reproduction. Please also ensure that permission to publish has been obtained from your institute.

Proofs. One set of proofs will be sent to the author to be carefully checked for printer's errors. Corrections must be restricted to instances in which the proof is at variance with the manuscript.

Reprints. Fifty reprints will be supplied free of charge. Additional reprints can be ordered by the authors. An order form containing price quotations will be sent to the authors together with the proofs of their article.

Advertisements. The Editors of the journal accept no responsibility for the contents of the advertisements. Advertisement rates are available on request. Advertising orders and enquiries may be sent to: Elsevier Science, Advertising Department, The Boulevard, Langford Lane, Kidlington, Oxford, OX5 1GB, UK; Tel: (+44) (0) 1865 843565; Fax (+44) (0) 1865 843952. *USA and Canada*: Weston Media Associates, Dan Lipner, P.O. Box 1110, Greens Farms, CT 06436-1110, USA; Tel (203) 261 2500; Fax (203) 261 0101. *Japan*: Elsevier Science Japan, Ms Noriko Kodama, 20-12 Yushima, 3 chome, Bunkyo-Ku, Tokyo 113, Japan; Tel (+81) 3 3836 0810; Fax (+81) 3 3839 4344.

0021-9673(19951124)717:1:2;1–1